The structure and bioactivity of ulvan, a sulfated polysaccharide from *Ulva* (chlorophyta)

Thesis submitted by

Joel Thomas Kidgell *BSc (Hons)*

in April 2021

for the degree of

Doctor of Philosophy in Natural and Physical Science

within the Centre for Macroalgal Resources and Biotechnology

and the College of Science and Engineering,

James Cook University, Townsville,

Queensland, Australia

Acknowledgments

It takes a village to raise a child. And this child is deeply appreciative of his village. Well, villages. This PhD has only been possible through the welcoming collaboration of wonderful researchers in multiple research groups and universities spread across the Tasman sea.

My first acknowledgement goes to the captain of my odyssey, Rocky de Nys. Your broad scale perspective of the project and boundless enthusiasm always kept me on course, no matter the winds. Thank you to my primary and secondary advisors, Marie Magnusson and Chris Glasson, for your support not only in my PhD but also for warmly accommodating me whenever I visited Tauranga. A special thank you to Chris for all your assistance helping me edit and publish my papers. I would especially like to thank Aya Taki for all her assistance during the cell culture and immunology work. I learned so much from your excellent tutelage and endless patience. I would also like to thank Andreas Lopata for lending his expertise and lab space to my PhD. And finally, to Susie Carnachan, whom I have learned so much from, thank you for teaching me about the analysis of carbohydrates and entertaining my incessant questions as you did. These six advisors have been the driving force behind the thesis, but no advisor is an island entire of itself.

I would like to extend a thank you to all the research groups that I have been involved with - I found each to be a welcoming port. From my Honours to the first years of my PhD the MACRO group was a constant source of support and inspiration. I would like to thank Maria Martinez and Joel Lenton for their assistance in the lab during this time. I would like to express a special thank you to Kunal Pratap and Sandip Kamath from the Molecular Allergy Research Laboratory for their invaluable assistance in a field very foreign to me. Although I only ended up staying for about three months, the nascent Magnusson lab in Tauranga, New Zealand was a delight to be a part of. Special thank you to Peter Randrup and Ari Brandenburg for their work in cultivation of *Ulva* and extraction of ulvan. And finally, to the Ferrier Institute for adopting me and providing such a stimulating research environment; thank you to Tracey, Alison, Ian, Simon, Norm, Cara, Liam, Pete, Jono, and the whole group, I have learnt so much in my time with you.

This PhD has only been possible with the support of a number of funding bodies and institutions. The generous APA scholarship and top up provided by the Australian Government and JCU enabled me to embark on my PhD journey. The funding from the partnership between JCU and Pacific Biotechnologies has been instrumental in keeping me afloat throughout my PhD, and I thank them for that. I would also like to particularly thank the University of Waikato and the Ferrier Institute of Victoria University of Wellington for assisting in the funding for the latter stages of my PhD.

Thank you to all the anonymous reviewers whose comments, criticisms, and expertise in their respective fields improved each one of the manuscripts published from this thesis.

Finally, I would like to thank my friends and family - the unsung heroes keeping me on an even keel. Thank you to Zoe, Erin, Kayler, Kay, Nico, Max, and Sarah for being there to chat to when I needed it. And thank you to my family, Paul, Judy, Nat, Erin, Florence, Anna, and Giorgio for their unending support, even when this PhD takes me far from home.

Statement on the contribution of others

Financial support for this research was provided by the College of Science and Engineering at James Cook University (JCU); Pacific Biotechnologies, Australia (previously MBD Industries Ltd.) as part of the Research and Development program for Integrated Production of Macroalgae; the University of Waikato and the Tertiary Education Commission as part of the Entrepreneurial Universities Macroalgal Biotechnologies Programme; and the Ferrier Institute of the Victoria University of Wellington. Stipend support was provided by the Australian Government and JCU through a Research Training Program Scholarship.

My primary advisor Marie Magnusson (University of Waikato, Tauranga, New Zealand), secondary advisor Chris Glasson (University of Waikato, Tauranga, New Zealand), and advisor mentor Rocky de Nys (JCU, Townsville, Queensland, Australia) provided principal guidance, financial support and editorial assistance throughout my thesis. Secondary and external advisors Susan Carnachan (Victoria University, Wellington, New Zealand), Aya Taki (Melbourne University, Melbourne, Australia), and Andreas Lopata (JCU, Townsville, Queensland, Australia) provided specialised technical guidance and editorial support.

The work involving cell culture and immunological assessment was carried out under the guidance of Aya Taki and Andreas Lopata in the Molecular Allergy Research Laboratory, College of Public Health, Medical and Veterinary Sciences, JCU (Chapter 5). Ian Sims and Simon Hinkley (Victoria University, Wellington, New Zealand) provided editorial support (Chapters 3, 4, and 5). Rebecca Lawton (University of Waikato, Tauranga, New Zealand) assisted in the genetic analysis of samples (Chapter 3). Analysis of elemental composition of samples was conducted by OEA Laboratories, Exeter, United Kingdom.

Contribution of authors to each chapter:

Chapter 2:

Joel T. Kidgell: Conceptualisation, investigation, data curation, visualisation, writing – original draft.

Marie Magnusson: Writing – review and editing

Rocky de Nys: Conceptualisation, resources, supervision, writing – review and editing

Christopher R.K. Glasson: Conceptualisation, writing – original draft

Chapter 3:

Joel T. Kidgell: Conceptualisation, investigation, data curation, visualisation, writing – original draft.

Christopher R.K. Glasson: Conceptualisation, investigation, supervision, methodology, writing – original draft

Susan M. Carnachan: Investigation, supervision, writing – original draft

Marie Magnusson: Conceptualisation, resources, funding, writing – review and editing

Rebecca Lawton: Investigation (algal cultivation), writing – original draft

Ian M. Sims: Investigation, writing – original draft

Simon F.R. Hinkley: Resources, supervision, writing – review and editing

Rocky de Nys: Conceptualisation, resources, funding, supervision, writing – review and editing

Chapter 4:

Joel T. Kidgell: Conceptualisation, investigation, data curation, visualisation, writing – original draft.

Ian M. Sims: Conceptualisation, methodology, writing – review and editing

Christopher R.K. Glasson: Investigation, supervision, methodology, writing – review and editing

Marie Magnusson: Resources, funding, writing – review and editing

Simon F.R. Hinkley: Resources, supervision

Rocky de Nys: Resources, funding, supervision, writing – review and editing

Susan M. Carnachan: Conceptualisation, investigation, methodology, supervision, writing – review and editing

Chapter 5:

Joel T. Kidgell: Conceptualisation, investigation, data curation, visualisation, writing – original draft.

Christopher R.K. Glasson: Methodology, writing – original draft

Marie Magnusson: Writing – review and editing

George Vamvounis: Investigation

Ian M. Sims: Investigation, writing – original draft

Susan M. Carnachan: Investigation, writing – original draft

Simon F.R. Hinkley: Investigation, writing – original draft

Andreas L. Lopata: Conceptualisation, resources, supervision

Rocky de Nys: Conceptualisation, resources, supervision, writing – review and editing

Aya C. Taki: Conceptualisation, methodology, writing – original draft

Abstract

Ulvan is a complex sulfated polysaccharide with potential rheological, biomaterial, agricultural, and human health applications. It is found within species of the prolific green seaweed *Ulva* and is generally comprised of four principal monosaccharides: rhamnose, glucuronic acid, xylose, and iduronic acid. The structural complexity of ulvan, high density of charged residues, and the glycosidic linkages between the four monosaccharides present a challenge for concise characterisation. Consequently, the purported bioactivities of ulvan, and the physicochemical aspects of the polysaccharide responsible, are ambiguous.

The principal objective of this thesis was to investigate the chemical structure and bioactivities of ulvan from species of *Ulva*, under the broader context of this seaweed being utilised in aquaculture. There were four research aims within this objective. The aim of the first data chapter (Chapter 2) was to synthesise the available literature on ulvan and identify research areas that could be strengthened. Informed by the literature review, the second data chapter (Chapter 3) critically compared the composition of multiple ulvans using standardised methods. The third data chapter (Chapter 4) followed directly from Chapter 3, critically comparing the fine-scale structure of four of the ulvans previously characterised. The final data chapter (Chapter 5) assessed the bioactivity of a highly purified ulvan sourced from aquaculture-produced biomass.

In Chapter 2 the state of ulvan research is synthesised through a systematic meta-analysis and literature review on all available publications from Scopus and Web of Knowledge. This comprehensive review discusses and provides recommendations for the extraction and characterisation of ulvan, in addition to a critical review of the purported bioactivities of the sulfated polysaccharide. The meta-analysis data established characteristic median constituent sugar proportions for ulvan and highlighted the wide variation in extraction procedures and ulvan compositions reported. Several knowledge gaps in the literature were also identified, most notably, characterisation of highly purified ulvan. For example, high contents of protein and glucose are frequently reported despite neither of these being considered part of ulvan. Furthermore, the vast majority of characterisation and bioactivity studies were conducted on ulvan extracted from *Ulva* with a blade morphology. There was a paucity of ulvans assessed that had been isolated from filamentous species of

Ulva. I concluded that further research into ulvan should focus on (i) highly purified and well characterised ulvans, (ii) using standardised methods to control for analytical variability, and (iii) with ulvans from representative morphologies of *Ulva*. These three conclusions formed the basis of the aims for the subsequent chapters of the thesis.

Chapter 3 examined the chemical composition, structure, and rheological properties of eleven ulvans from blade (*U. australis*, *U*. *rigida*, *U*. sp. B, and *Ulva* sp.) and filamentous (*U*. *flexuosa*, *U*. *compressa*, *U*. *prolifera*, and *U*. *ralfsii*) species of *Ulva* collected from the Bay of Plenty, Aotearoa New Zealand. The structure, composition, and rheology of purified ulvan from these species were quantified using a set of standardised protocols to control for analytical error. The results were analysed in a multivariate context which demonstrated significant groupings of differentiated ulvans from blade and filamentous species. Ulvan isolated from blade species had higher yields (14.0-19.3 %) and iduronic acid content (IdoA = 7-18 mol%), and lower molecular weight (Mw = 190-254 kDa) and storage moduli (G' = 0.1-6.6 Pa) than filamentous species (yield = 7.2-14.6 %; IdoA = 4-7 mol%; Mw = 260-406 kDa; G' = 22.7-74.2 Pa). This chapter is the most comprehensive comparison of ulvans from multiple species of *Ulva* performed to date, and the first time that consistent differences have been detected between ulvans from different morphologies of *Ulva*. Therefore, for the next chapter, the structure of ulvans from two blade and two filamentous species were analysed in detail to explore differences in the molecular structure of ulvan related to morphology.

Chapter 4 utilised glycosyl linkage analysis to assess the fine-scale structure and sulfate ester substitution of four ulvans from Chapter 3, two from blade species (*U*. *rigida* and *U*. sp. B) and two from filamentous species (*U*. *prolifera*, and *U*. *ralfsii*). The four ulvans were desulfated at two different temperatures to monitor the loss of sulfate groups. Glycosyl linkages were determined through methylation analysis of the ulvans and desulfated derivatives. Ulvans from blade species of *Ulva* were simpler in structure, mostly composed of the 1,4-linked rhamnose 3-sulfate and 1,4-linked glucuronic acid. Ulvans from filamentous species had higher proportions of branched monosaccharides and a greater variety of sulfate ester substitution positions, confirming a more complex structure. In ulvan from both morphologies, rhamnose was extensively sulfated at *O*-3, as were a minor proportion of xylose at *O*-2. Ulvans from filamentous species also contained glucuronic acid with minor proportions of *O*-2 sulfation. Additionally, ulvans from filamentous species displayed high

proportions of branching on *O*-2 of 1,4-linked rhamnose-3S. These results support the hypothesis that ulvans from filamentous species of *Ulva* have a more complex structure than those from blade species and supports the conclusions of Chapter 3.

Chapter 5 assessed the effect that the molecular weight of a highly purified ulvan had upon the inflammatory response of murine macrophages. This chapter utilised the research framework developed from Chapters 2-4 to test a purified and characterized ulvan in a targeted bioassay to determine the fundamentals of a structure-activity relationship. Ulvan extracted from *Ulva ohnoi* was purified to remove traces of contaminating polymers and proteins before being depolymerised into several size fractions (M_w 7, 9, 13, 21, 209 kDa) and characterised. Ulvan fractions contained 48.8-54.7 mol% rhamnose, 32.5-35.9 mol% glucuronic acid, 4.5-7.3 mol% iduronic acid, and 3.3-5.6 mol% xylose. The effect that these ulvans had upon the inflammatory cytokines released by stimulated murine macrophages was then quantified. All ulvan fractions showed no toxicity on RAW264.7 cells at concentrations below 100 μg mL^{-1} over 48 h. Secreted interleukin-10 and prostaglandin E_2 demonstrated an anti-inflammatory effect by higher molecular weight ulvan fractions at 100 μg mL^{-1}. To a lesser extent, these fractions also enhanced the LPS-induced inflammation through minor increases of IL-1β and IL-6. This study confirms that ulvan from *U. ohnoi* has a mild in vitro immunomodulatory effect.

The data presented in this thesis established that ulvans from blade and filamentous species of *Ulva* are significantly different, and that the structure of ulvan drives its biological activity. These patterns were identified through a systematic research framework using highly purified, thoroughly characterised ulvans. Utilisation of a similar framework promoting collaboration between the intersecting fields of ulvan research, from biomass production, to analytical chemistry, to bioactivity assessment, will accelerate ulvan research.

Abbreviations

2,3,4-tri-*O*-methyl-rhamnitol – 1,5,6-tri-*O*-acetyl-2,3,4-tri-*O*-methyl-rhamnopyranose; other derivatives are similarly abbreviated.

A_{3S} – ulvanobiuronic acid 3-sulfate type A

Ac – acetyl substituent

AEC – anion-exchange chromatography

B_{3S} – ulvanobiuronic acid 3-sulfate type B

C – cultivated *Ulva* biomass

Con – control

CR – carboxyl reduced ulvan

CV – column volume

Đ – dispersity (of molecular weight)

DCM – dichloromethane

DEAE – diethylaminoethyl

Dex – dexamethasone

DMEM – Dulbecco's modified eagle medium

DMF – anhydrous N,N-dimethylformamide

DMSO – dimethyl sulfoxide

DS100 – desulfated at 100 °C, then carboxyl reduced ulvan

DS80 – desulfated at 80 °C, then carboxyl reduced ulvan

EDTA – Ethylenediaminetetraacetic acid

ELISA – enzyme-linked immunosorbent assay

FBS – foetal bovine serum

FTIR – Fourier transform infrared spectroscopy

Fuc – fucose

G' – storage modulus (rheology)

GAG – glycosaminoglycan

Gal*p* – galactopyranose

GC – gas chromatography

GC-MS – gas chromatography-mass spectrometry

Glc*p* – glucopyranose

Glc*p*A – glucuronopyranosic acid

h – hour

HPAEC – high performance anion-exchange chromatography

HPAEC-PAD – high performance anion-exchange chromatography with pulsed amperometric detector

HPLC – high performance liquid chromatography

HSQC – heteronuclear single quantum coherence

Ido*p*A – iduronopyranosic acid

IL – interleukin

LPS – lipopolysaccharide

LVR – linear viscoelastic region (rheology)

MDS – multidimensional scaling

Me – methyl substituent

Mn – number average molecular weight

Mw – weight average molecular weight

MWCO – molecular weight cut-off

MWD – molecular weight distribution

NMR – nuclear magnetic resonance

NMWC – nominal molecular weight cut-off

NO – nitric oxide

OD – optical density

PAMP – pathogen-associated molecular patterns

PBS – Phosphate buffered saline

PERMANOVA – permutational multivariate analysis of variance

PGE_2 – prostaglandin E_2

pI – isoelectric point

PMAA – partially methylated alditol acetate

RFU – relative fluorescence units

Rha*p* – rhamnopyranose

Rha*p*3S – rhamnopyranose-3-sulfate

RI – refractive index (SEC)

SAR – structure-activity relationship

SEC – size-exclusion chromatography

SEC-MALLS – size exclusion chromatography with multi-angle laser light scattering detector

TFA – trifluoroacetic acid

TLR – Toll-like receptor

TMS – trimethylsilyl

TNF-α – tumour necrosis factor alpha

U – ulvanobiose

Vas – asymmetric stretching (FTIR)

VISC – viscosity

Vs – symmetrical stretching (FTIR)

W – wild harvested *Ulva* biomass

Xyl*p* – xylopyranose

Table of contents

List of figures

List of tables

Chapter 1:
General introduction

1.1 Biology of seaweeds

Marine macroalgae, or seaweeds, are a polyphyletic grouping of autotrophic multicellular organisms with extensive biological variation. While lacking a formal taxonomic definition, "seaweeds" are generally accepted as macroscopic multicellular marine algae, which encompasses more than 10,000 species (Brodie & Lewis, 2007; Guiry & Guiry, 2021). Seaweeds are broadly classified into three groups based on the photosynthetic pigment present, as reflected by their common names: brown algae or Phaeophyceae, red algae or Rhodophyta, and green algae or Chlorophyta. The life cycles of seaweeds are complex and diverse, involving combinations of sexual and asexual reproduction across annual and perennial life histories, sometimes with alternation of generations (Roesijadi, Jones, Snowden-Swan, & Zhu, 2010). A notable example of alternation of generations is the distinct heteromorphic variation between the sexual gametophyte and asexual tetrasporophyte stages of the red seaweeds *Asparagopsis taxiformis* and *A. armata* (Chualáin, Maggs, Saunders, & Guiry, 2004). Indeed, the asexual tetrasporophyte of these species were, until relatively recently, considered a different species to the gametophyte due to the stark morphological difference (Bonin & Hawkes, 1987). The majority of seaweeds thrive in shallow coastal environments, utilising the higher light intensity, better access to nutrient run off/upwelling, and convenient substrate compared to deeper locations. When the conditions are right seaweeds can grow prolifically, out-growing competitors like corals and sponges (Chadwick & Morrow, 2011; Gonzalez-Rivero *et al.*, 2016; Gonzalez-Rivero, Ferrari Legorreta, Schoenberg, & Mumby, 2012; McCook, Jompa, & Diaz-Pulido, 2001; Ye *et al.*, 2011). In fact, seaweeds can have higher productivities than cultivated terrestrial crops (Mata, Magnusson, Paul, & de Nys, 2016; Velimirov, Field, Griffiths, & Zoutendyk, 1977). Even when the conditions are sub-optimal, many seaweeds can still proliferate due to a high tolerance to environmental stressors (Taylor, Fletcher, & Raven, 2001). The rapid growth rate of seaweeds is due, in part, to their relatively simplistic and undifferentiated morphology which can

maximise photosynthetically active regions by not contributing resources to rigid structures found in corals (skeleton), sponges (spicules), and terrestrial plants (lignocellulose).

Seaweeds maintain structural integrity predominantly through cell wall and extracellular polysaccharides (i.e., carbohydrates). Multicellular algae, and indeed all photosynthetic eukaryotes, produce a polysaccharide-rich extracellular matrix on the plasma membrane of each cell. The extracellular matrix, which is analogous in structure to a woven cloth, expands and chemically coordinates (weaves) with neighbouring cells. The matrix structure is a mesh-like composite of fibrillar (generally cellulose-based) polysaccharides connected (woven) by multiple hemicellulosic and sulfated polysaccharides (see Lahaye and Robic (2007) for example illustration). Insoluble cellulose is the most common fibrillar skeleton found in seaweed cell walls, but xylan and mannan have also been reported in green algae (Stiger-Pouvreau, Bourgougnon, & Deslandes, 2016). The embedding matrix of the brown seaweeds is most commonly composed of alginates with smaller amounts of fucoidan, while the matrix of red seaweeds often contains a number of sulfated galactans, including agar, carrageenan and porphyran. Green seaweeds are more varied in the composition of both the fibrillar and matrix polymers. As an example, the Ulvophyceae (which includes the genus *Ulva*) utilise cellulose and xyloglucan for fibrillar structure, and glucuronan and the sulfated polysaccharide ulvan as the major components of the embedding matrix (Ciancia, Fernández, & Leliaert, 2020; Stiger-Pouvreau *et al.*, 2016). Within each alga there are many polysaccharides working in concert to provide structural support, flexibility, and resistance to environmental factors such as abrasion and desiccation.

The carbohydrates listed above include sulfated polysaccharides, polymers that are predominantly found in seaweeds, bacteria and animals but are conspicuously absent from terrestrial plants (Popper *et al.*, 2011). Each of the seaweed groups has a predominant sulfated polysaccharide. Brown seaweeds have fucoidan, a polymer of generally 1,3-linked L-fucose with 4-linked sulfate esters (Figure 1.1) (Li, Lu, Wei, & Zhao, 2008) that has intriguing biological activities, including anti-coagulant, anti-viral, immunomodulatory, anti-inflammatory, and antioxidant capacities (Li *et al.*, 2008). Red seaweeds often contain carrageenans as the major sulfated polysaccharide, comprised of alternating 1,4- and 1,3-linked galactose and 3,6-anhydro-galactose both sulfated at various positions (Figure 1.1). The major carrageenans are differentiated by the content of 3,6-anhydro-galactose and the

degree of sulfation, with higher proportions of sulfate generally reducing gelling capacity (Campo, Kawano, da Silva, & Carvalho, 2009). Carrageenans are extensively exploited by the food industry as gelling and thickening agents, in addition to having bioactive applications related to the inflammation and immune response. Ulvophyceaen green seaweeds contain ulvan, a heteropolysaccharide comprised predominantly of 1,4-linked rhamnose, glucuronic acid, xylose, and iduronic acid (Lahaye & Robic, 2007) (Figure 1.1). Like fucoidan and carrageenan, ulvan has a range of bioactivities including immunomodulating, antiviral, antioxidant, antihyperlipidemic, and anticancer (Alves, Sousa, & Reis, 2013b). However, ulvan has been far less extensively studied (Kidgell, Magnusson, de Nys, & Glasson, 2019). The combination of high growth rates, high environmental tolerance, and possession of useful bioactive polysaccharides make seaweeds ideal candidates for intensive aquaculture.

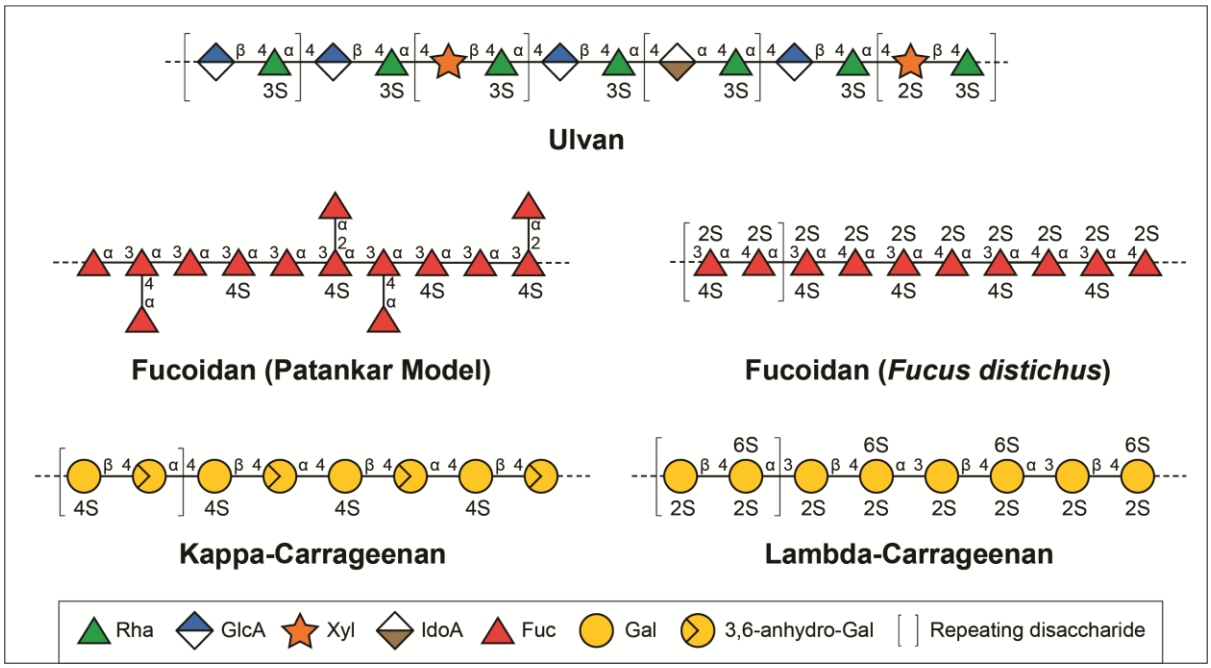

Figure 1.1: Simplified structural representations of some sulfated polysaccharides found in seaweeds. The actual ordering of monosaccharides in ulvan is unknown beyond the repeating disaccharides (Lahaye & Robic, 2007); the order presented here is arbitrary. The Patankar model is a generalised model for fucoidan (Patankar, Oehninger, Barnett, Williams, & Clark, 1993) whereas the more highly sulfated fucoidan presented here was extracted and characterised from *Fucus distichus* (Bilan *et al.*, 2004). The structure of the various carrageenans, including lambda and kappa, is well documented (Campo *et al.*, 2009). Rha = rhamnose; GlcA = glucuronic acid; Xyl = Xylose; IdoA = iduronic acid; Fuc = fucose; Gal = galactose.

1.2 Aquaculture of seaweeds

Aquaculture is currently the major source of seaweeds for commercial applications, with global production totalling 32.4 million tonnes in 2018 - more than triple the production from 2000 (FAO, 2020). Most seaweed is produced as food for human consumption and the production of hydrocolloids (a material that forms a gel-like substance in water). The production Japanese kelp (*Saccharina japonica*), grown for human consumption, represents 35 % of global seaweed aquaculture volume. Production of red seaweeds such as *Eucheuma* spp., G*racilaria* spp., and *Kappaphycus alvarezii*, grown to extract the hydrocolloids carrageenan and agar, account for another 44 % of the total seaweed production (FAO, 2020). Seaweeds are most commonly cultivated in shallow coastal sites by seeding long ropes or nets with algal spores or fragments of biomass and allowing the seaweed to grow to maturity before harvesting (Crawford, 2002). Cultivation of seaweeds in the ocean does carry inherent risk, however. Production is related to the environment with respect to temperature, nutrient availability, and light intensity. Additionally, there is risk of stock loss from extreme weather or line/net breakage, and the stock can be contaminated with undesirable (fouling) organisms such as a competitive seaweed. For example, the net-based cultivation of *Pyropia* sp. (grown for nori in sushi) is often fouled with *Ulva* spp., the removal of the latter is proposed as one of the causal factors of major *Ulva* blooms in the Yellow Sea, China (Ye *et al.*, 2011). Many of these risks can be mitigated through seaweed production in tanks or ponds on land, particularly for more valuable seaweed species or those that can be integrated with other industries for supplementary benefits.

The intensive land-based production of seaweeds can maximise productivity through fine-scale control over the cultivation parameters (e.g., temperature, nutrients, pH, water movement, light intensity). Land-based systems also have the capacity to operate on non-arable land and integrate with other industries, supporting a sustainable circular economy and remediating point source waste streams (Bolton, Robertson-Andersson, Shuuluka, & Kandjengo, 2009; de Paula Silva, McBride, de Nys, & Paul, 2008). For example, seaweeds can take up the nutrients (e.g., nitrogen and phosphorus) from wastewater streams produced by finfish and crustacean aquaculture ponds (Bolton *et al.*, 2009; de Paula Silva *et al.*, 2008). This form of nutrient bioremediation has been applied at scale at Pacific Reef Fisheries in Queensland, Australia, where the green seaweed *Ulva ohnoi* is cultivated in the nutrient-

laden effluent produced by the prawn aquaculture ponds. By growing *U. ohnoi* in high-rate algal ponds (HRAPs) and continuously pumping in the prawn effluent stream, the seaweed remediates the nutrients as it grows. Harvesting of the seaweed biomass removes the assimilated nutrients from the aquaculture system, allowing the treated water to be safely discharged, while also producing *U. ohnoi* as a secondary marketable product (Lawton, Mata, de Nys, & Paul, 2013). Tank or HRAP-based aquaculture maintains a high-quality monoculture free of undesirable species of algae, which reduces post-harvest processing and maximises the yield of valuable bioproducts from the seaweeds.

Seaweed biomass has a wide variety of end use applications, from using the whole biomass as food, feed, or fertiliser to highly technical extraction and purification of high value proteins and polysaccharides. As discussed earlier, over 11 million tonnes (live weight) of Japanese kelp (*Saccharina japonica*) is cultivated for human consumption annually and almost half of the global production of seaweed aquaculture is red seaweeds for the commercial production of hydrocolloids agar and carrageenan (FAO, 2020). Seaweeds are also utilised as animal feeds in marine and terrestrial agriculture. For example, a combination of cultivated green, red, and brown seaweeds, *Ulva lactuca*, *Gracilaria gracilis*, and *Ecklonia maxima*, results in higher growth rates of abalone compared to a formulated feed (Naidoo, Maneveldt, Ruck, & Bolton, 2007). Seaweeds have also been incorporated as animal feed supplements for rainbow trout, laying hens, cattle, and other animal production systems (Evans & Critchley, 2014; Kinley *et al.*, 2020; Kulshreshtha *et al.*, 2017; Soler-Vila, Coughlan, Guiry, & Kraan, 2009). Similarly, seaweeds are used as fertilisers and plant bio-stimulants (Battacharyya, Babgohari, Rathor, & Prithiviraj, 2015; Cole, Roberts, Garside, de Nys, & Paul, 2016; Khan *et al.*, 2009; Rathore *et al.*, 2009; Sivasankari, Venkatesalu, Anantharaj, & Chandrasekaran, 2006). Due to the rapid growth rate and high content of carbohydrates, seaweeds are also excellent feed biomass for conversion to bioethanol and biocrude (Kraan, 2013; Neveux *et al.*, 2014). The end use of seaweed biomass may be affected by the composition of the biomass and/or the remediation target for which the seaweed was cultivated. For example, over 90 % of the global shrimp (prawn) supply is produced in land-based marine and brackish aquaculture facilities (FAO, 2020). These facilities produce huge volumes of nutrient-rich wastewater that is detrimental to the local environment if released without treatment (Coldebella *et al.*, 2018). The green seaweed *Ulva* represents the most appropriate genus for

point source remediation of the high-nutrient marine and brackish water from these facilities, due to high growth rates and the tolerance to variable salinity and temperature displayed by species of this genus (de Paula Silva *et al.*, 2008; Pedersen & Borum, 1997; Taylor *et al.*, 2001)

1.3 *Ulva* and ulvan

Widely dispersed throughout intertidal regions and commonly called "sea lettuce", the cosmopolitan green seaweeds of the genus *Ulva* are remarkably resilient, making them ideal candidates for aquaculture. Species of *Ulva* are also responsible for "green tide" algal blooms that occur around the world (Ye *et al.*, 2011). Indeed the characteristics that promote green tides are the very same that make *Ulva* desirable for bioremediation, in particular rapid growth rates, broad environmental tolerances, and the capacity to assimilate and use multiple sources of nitrogen (de Paula Silva *et al.*, 2008; Pedersen & Borum, 1997; Taylor *et al.*, 2001). Species of *Ulva* tolerate salinity from 5 to 45 ppm and even excel (growth rate >20 % day^{-1}) under extreme salinity and nutrient conditions (45 ppm and 700 µmol L^{-1} total ammonia nitrogen) (de Paula Silva *et al.*, 2008; Taylor *et al.*, 2001). Additionally, tropical species of *Ulva* have been shown to maintain high growth rates (11.2-20.4 % day^{-1}) across a broad range of temperatures (17.5-28.5 °C) (Lawton *et al.*, 2013), while temperate species can maintain a growth rate >10 % day^{-1} even at 10 °C (Taylor *et al.*, 2001). When assessed in an aquaculture context, *Ulva ohnoi* has been shown to maintain an average biomass productivity of 37.7 g dw m^{-2} day^{-1} (i.e. dry weight grams of algae produced per square meter of water surface per day), with a weekly productivity of up to 46 g dw m^{-2} day^{-1} (Mata *et al.*, 2016). The physiology of *Ulva* facilitates such high productivities – *Ulva* is only two cells thick and has minimal anchoring structures, effectively allowing the entire organism to photosynthesise (Wichard *et al.*, 2015). *Ulva* occurs in two distinct morphologies: a flat sheet-like blade form and a tubular filamentous form. Given the remarkably simple morphology of *Ulva*, the cell wall and extracellular carbohydrates provide the structural integrity of the organism.

Ulva contains four major polysaccharides: cellulose, hemicelluloses glucuronan and xyloglucan, and the sulfated polysaccharide ulvan. These four polysaccharides work in concert to support and protect the cells within *Ulva* from environmental fluctuations. For example, desiccation (a common dehydration issue for intertidal organisms) induces structural changes in *Ulva compressa* where the inner cell wall structures shrink with the cytoplasm, while the

outer weave of fibrillar and matrix layers, which includes ulvan, maintain the cell position within the extracellular matrix of the organism (Holzinger, Herburger, Kaplan, & Lewis, 2015). Indeed, a major role of ulvan is the prevention of desiccation in *Ulva* by performing the roles of a hygroscopic material to retain water, an anionic electrolyte to maintain the ionic equilibrium within the cells, and forming a protective gel around the cells to mitigate mechanical damage (Kloareg & Quatrano, 1988; Percival, 1979; Stiger-Pouvreau *et al.*, 2016). The sulfated polysaccharides carrageenan and fucoidan likely perform similar roles within red and brown seaweeds, respectively. However, despite their similar roles, ulvan is remarkably different from these other sulfated polysaccharides.

Ulvan has a high level of structural complexity which hinders precise characterisation of the polysaccharide. For example, while carrageenan and fucoidan are both predominately comprised of a single monosaccharide (galactose and fucose, respectively), ulvan has four principal monosaccharides: rhamnose, glucuronic acid, xylose, and iduronic acid. The linkage of acidic and neutral monosaccharides (e.g. glucuronic acid to rhamnose) creates a highly acid-resistant glycosidic bond (BeMiller, 1967), necessitating a strong acid to hydrolyse. However, such a strong acid would concomitantly degrade the liberated iduronic acid and xylose monosaccharides, which are highly acid labile (Conrad, 1980; Quemener, Lahaye, & Bobin-Dubigeon, 1997). Despite the inherent challenges in analysing ulvan, there has been a plethora of bioactivities reported in the literature including immunomodulating, antiviral, antioxidant, antihyperlipidemic and anticancer (Alves *et al.*, 2013b; Holdt & Kraan, 2011; Jiao, Yu, Zhang, & Ewart, 2011; Kidgell *et al.*, 2019). However, many purported bioactivity efficacies are inconsistent or contradictory, as are many reports of ulvan composition and structure. The overall aim for this thesis was, therefore, to investigate the chemical structure and bioactivities of ulvan from species of *Ulva*, under the broader context of these seaweeds being utilised in aquaculture, including for bioremediation.

1.4 Aims and chapter summaries

The specific aims of this thesis centre around the elucidation of ulvan structure and bioactivity as outlined in detail below. A systematic literature review and meta-analysis was conducted for Chapter 2. The overall conclusion of this review was that the extent of purification and compositional analysis of ulvan is highly variable and accompanying

bioactivity data of ulvan are often inconsistent. Furthermore, there is a paucity of assessments of highly purified ulvan(s) using standardised methods, without which the variation between ulvans and variation due to analytical error are inextricable. The outcomes of the literature review provided the basis for Chapters 3, 4, and 5 to respectively compare the composition of multiple ulvans using standardised methods, critically compare the structure of multiple ulvans using standardised methods, and finally assess the bioactivity of a highly purified ulvan. As the focus of this thesis is specifically on the ulvan polysaccharide, effort was made to study the ulvan polymer in isolation and maintain the polysaccharide integrity throughout experiments (except where intentionally depolymerised). In this regard, the experiments within this thesis reflect the composition and bioactivity of the isolated ulvan polymer as it has been removed from *Ulva* biomass, without manipulation or alteration.

Chapter 2 synthesised the state of ulvan research by performing a systematic meta-analysis and literature review of all the available research on ulvan. Scopus and Web of Knowledge were both searched for all publications relevant to ulvan or sulfated polysaccharides from *Ulva*. Details of the extraction, composition, and bioactivities of the ulvans from these publications were tabulated and analysed. As this was the first meta-analysis of ulvan, it provided some unique insights into trends in the literature. The most important of these was the degree of variation in the composition and bioactivity results reported for ulvan. Despite the variation, the assimilated meta-analysis data established characteristic median constituent sugar proportions for ulvan. The review thoroughly discusses the extraction and characterisation of ulvan and provides suggestions on effective methods. Each of the major bioactive applications of ulvan are then discussed in detail. From this literature review, I concluded that further research into ulvan should focus on (i) highly purified and well characterised ulvans, (ii) using standardised methods to control for analytical variability, and (iii) with ulvans from representative morphologies of *Ulva*. These three conclusions formed the basis of the aims for the subsequent chapters of the thesis.

Chapter 3 examined the chemical composition, structure, and rheological properties of eleven ulvans from blade (*U. australis*, *U*. *rigida*, *U*. sp. B, and *Ulva* sp.) and filamentous (*U*. *flexuosa*, *U*. *compressa*, *U*. *prolifera*, and *U*. *ralfsii*) species of *Ulva* collected from the Bay of Plenty, Aotearoa New Zealand. The cultivation of the biomass and extraction, characterisation, and rheological assessment of the ulvans was performed using standardised

techniques to control for analytical error. The results were analysed in a multivariate context which demonstrated significant groupings of differentiated ulvans from blade and filamentous species. This is the first time that consistent differences have been detected between ulvans from different morphologies of *Ulva*. Therefore, for the next chapter, the structure of ulvans from two blade and two filamentous species were analysed in detail to further explore the differences in the molecular structure of ulvans from different morphologies of *Ulva*.

Chapter 4 assessed the structure and sulfation of ulvans from two blade (*U*. *rigida* and *U*. sp. B) and two filamentous (*U*. *prolifera*, and *U*. *ralfsii*) species of *Ulva* through glycosyl linkage analysis. The four ulvans were desulfated at two different temperatures to monitor the loss of sulfate groups. Glycosyl linkages were determined through methylation analysis of the ulvans and desulfated derivatives. Sulfate substitution positions were then inferred by comparison of the glycosyl linkage composition of native ulvan to its desulfated counterpart. The results of this chapter confirmed the distinction of ulvans from different morphologies of *Ulva* and highlights that ulvans of filamentous species are more complex. The glycosyl linkage compositions of individual ulvans are discussed.

Chapter 5 assessed the effect that the molecular weight of a highly purified ulvan had upon the inflammatory response of a murine macrophage. It utilised the research framework developed from Chapters 2-4 to test a highly purified and characterized ulvan in a targeted bioassay to determine the fundamentals of a structure-activity relationship. Ulvan extracted from *Ulva ohnoi* was purified to remove traces of contaminating polymers and proteins before being depolymerised into several size fractions and thoroughly characterised. Knowing that the fractions were purified ulvan and only differed in molecular weight, the effect that these ulvans had upon the inflammatory cytokines released by stimulated murine macrophages was quantified. The cytotoxicity and the interaction of molecular weight with immunomodulating capacity of these ulvans are discussed.

Chapter 6 presents a summary and discussion of the results of the thesis and how these results fit into the broader research directions for seaweed aquaculture and applications for ulvan.

Chapter 2:

Literature review and meta-analysis[1]

2.1 Introduction

Species of green seaweed from the genus *Ulva* have high growth rates and productivities across diverse geo-climatic conditions, with highly exploitable biochemical profiles (Angell, Mata, de Nys, & Paul, 2014; Glasson, Sims, Carnachan, de Nys, & Magnusson, 2017; Magnusson, Carl, Mata, de Nys, & Paul, 2016; Mata *et al.*, 2016). As a consequence, species of *Ulva* can result in the formation of problematic "green tides" (Blomster *et al.*, 2002; Coat *et al.*, 1998; Hiraoka, Shimada, Uenosono, & Masuda, 2004; Kong, Mao, Cui, Zhang, & Gao, 2011; Largo, Sembrano, Hiraoka, & Ohno, 2004). Therefore, they are well suited for cultivation, in particular for use in the bioremediation of nutrient rich wastewater from intensive land-based aquaculture (de Paula Silva *et al.*, 2008; Lawton *et al.*, 2013; Nardelli, Chiozzini, Braga, & Chow, 2019). Importantly, cultivation, as opposed to natural harvesting, can produce a high-quality monoculture of *Ulva* biomass, which can then generate high-quality bioproducts of consistent composition. One of the major bioproducts of interest from *Ulva* is the sulfated polysaccharide known as ulvan.

Ulvan is a cell wall polysaccharide that contributes from 9-36 % dry weight of the biomass of *Ulva* and is mainly composed of sulfated rhamnose, uronic acids (glucuronic acid and iduronic acid) and xylose (Abdel-Fattah & Edrees, 1972; Brading, Georg-Plant, & Hardy, 1954; Gosselin, Holt, & Lowe, 1964; Lahaye & Axelos, 1993; Lahaye & Robic, 2007; McKinnell & Percival, 1962a; Percival & Wold, 1963; Quemener *et al.*, 1997; Ray & Lahaye, 1995b). Species of *Ulva* have three other cell wall polysaccharides (cellulose, xyloglucan, and glucuronan), which with ulvan collectively account for up to 45 % of the dry weight biomass (Lahaye & Kaeffer, 1997). Like ulvan, xyloglucan and glucuronan are also soluble polysaccharides but are only relatively minor constituents of the cell wall polysaccharides (Lahaye, Brunel, & Bonnin, 1997; Lahaye & Ray, 1996; Ray & Lahaye, 1995a, 1995b).

[1] Published as: Kidgell *et al.* (2019) Ulvan: A systematic review of extraction, composition and function. Algal Research 39:101422

Interestingly, of the four cell wall polysaccharides present within Ulva, ulvan is the only one to contain both rhamnose and iduronic acid (Quemener *et al.*, 1997). Rhamnose is of interest for its effect on biosynthetic pathways in the dermis (Adrien *et al.*, 2017a; Andrès *et al.*, 2006; Faury *et al.*, 2008) and on plant immunity (Jaulneau *et al.*, 2010; Stadnik & de Freitas, 2014; Trouvelot *et al.*, 2014). Uronic acids (glucuronic and iduronic acids) and their sulfate esters are important constituents in mammalian glycosaminoglycans (GAGs) (e.g., heparin, heparan sulphate, and dermatan sulfate). Like GAGs, ulvan has a repeating disaccharide structure predominantly comprised of a uronic acid linked to a sulfated neutral sugar and is, therefore, a candidate for the modulation of processes and functions carried out by mammalian polysaccharides (Fransson, 1985; Lahaye *et al.*, 1999; Quemener *et al.*, 1997). In this regard, ulvan has potential applications in biomaterial science (wound dressings, tissue engineering, biofilm prevention, and excipients), nutraceuticals (antiviral, antioxidant, antihyperlipidemic, anticancer and immunostimulatory), functional foods and agriculture, as outlined in reviews by Venkatesan *et al.* (2015), Cunha and Grenha (2016), Alves *et al.* (2013b), Lahaye and Robic (2007), and Wijesekara, Pangestuti, and Kim (2011). The biological activities of polysaccharides, including ulvan, are directly related to their chemical structure. It is, therefore, important to understand how extraction, isolation and purification procedures affect the chemical structure of the extracted polysaccharide, and as a consequence, its biological activity.

This review evaluates research on ulvan with a focus on extraction and purification methods, and its biological activity and potential applications. In preparing this comprehensive, systematic review, a meta-analysis was conducted on publications identified from the search string "(Ulvan* OR ((sulfate* OR sulphate*) AND polysaccharide* AND (*Ulva* OR *Enteromorpha*)))" through Scopus and Web of Science on 13th of December 2017 (see supplementary material for methods and full access to metadata). This analysis provides a summary of the chemical structures of ulvans from different sources and the methods used to assess them, as well as providing the biological activity of ulvan, and, where possible, their relative efficacies and mechanisms of action. As a consequence, the review is divided into two major sections. Section 2 describes in detail the chemistry of ulvan, providing an overview of its physicochemical properties, extraction and purification techniques and recommended characterisation for biological activity studies. Section 3 then provides an overview of the

biological activities of ulvans with a focus on the mechanistic and structural features involved. Note that in line with current nomenclature convention Enteromorpha is referred to as *Ulva* throughout the review (Hayden *et al.*, 2003).

2.2 Chemistry of ulvans

2.2.1 Chemical structure of ulvans

The macromolecular properties (e.g., conformation) of polysaccharides are influenced by their primary structure, which is determined by their sugar constituents and the order in which they occur, their glycosidic linkages, degree of branching, molecular weights, and the presence of functional groups, such as sulfate esters, methyl ethers, amides and amines. These structural features then determine the physicochemical properties and the biological activities of the polysaccharide. In this regard, ulvans are polyanionic heteropolysaccharides with sugar compositions that are predominantly rhamnose (45.0 mol%), glucuronic acid (22.5 mol%), iduronic acid (5.0 mol%), and xylose (9.6 mol%) (Median values, see Table 2.1). There is, however, a broad range in the composition of ulvan sugars reported for rhamnose (5.0-92.2 mol%), glucuronic acid (2.6-52.0 mol%), iduronic acid (0.6-15.3 mol%) and xylose (0.0-38.0 mol%) (Table 2.1; App. 7.1.2). The composition of ulvan depends on the source species, eco-physiology, and processing procedures used to prepare both biomass and ulvan (see Table 2.1). Compositional variation due to eco-physiological factors can then be magnified by different extraction and analytical techniques. Other monosaccharides are often reported in compositional data (e.g., glucose, galactose, arabinose, and mannose), however, their presence as a component of / or contaminant of ulvan is unclear.

Table 2.1: Ulvan monosaccharide composition (median, minimum, and maximum in mol%) for each species of *Ulva* (1954-2018). Median only reported where n=1.

	Rhamnose			Glucuronic Acid			Xylose			Iduronic Acid			Glucose			Galactose			Uronic Acids			
Species	**Med.**	**Min**	**Max**	**Med.**	**Min**	**Max**	**Med.**	**Min**	**Max**	**Med.**	**Min**	**Max**	**Med.**	**Min**	**Max**	**Med.**	**Min**	**Max**	**Med.**	**Min**	**Max**	**Ref[1]**
U. arasakii	33.2						11.0												46.7			
U. armoricana	51.6	41.9	60.0	21.3	15.2	27.5	7.5	3.7	10.1	7.0	3.8	15.3	10.0	0.0	26.2	3.1	1.0	5.1	13.4	12.6	16.5	
U. clathrata	10.7			4.0												4.8						
U. compressa	13.0	5.0	62.0				17.0	15.0	35.0				40.0	5.7	70.0	9.0	4.0	15.0	18.3			
U. conglobata	67.8	57.0	72.3	6.0			1.5	1.0	20.0				17.1	12.0	22.0	2.4	1.2	5.0				
U. fasciata	57.4	8.2	92.2	14.7			26.1	1.5	36.3				7.7	0.7	22.8	1.9	1.6	2.2				
U. gigantea	42.1			15.4			28.8			3.6			7.9			2.3						
U. intestinalis	37.2	30.2	61.0				10.9	8.5	14.2				40.0	2.3	48.4	11.4	7.7	15.8				
U. lactuca	33.5	8.2	60.8	22.5	2.6	52.0	7.3	0.0	35.4	6.0	5.0	6.0	28.6	2.0	87.2	1.6	0.0	1.9	16.8	16.8	47.1	
U. linza	61.6	60.7	62.5	22.6	17.2	27.9	10.5	9.6	11.3				10.9									
U. meridionalis	39.0						17.0						6.0			6.0			28.0			
U. ohnoi	47.1	41.1	53.1	28.6	27.8	29.4	5.5	5.3	5.7	8.8	7.4	10.1	2.5	1.5	3.5	2.6	1.2	4.0				
U. olivascens	53.8			16.7			15.1			3.8			7.6			3.0						
U. pertusa[2]	25.3	15.2	80.7	27.0			7.7	2.7	21.0				4.7	1.0	27.4	0.0						
U. prolifera	67.8	57.1	87.6				3.8	2.4	8.8				31.9	3.6	67.8	4.0						
U. rigida	26.9	10.7	58.3	31.7	19.0	37.0	10.8	4.3	38.0	6.0	2.5	7.0	7.6	1.6	46.1	0.9	0.3	1.7	18.3	10.3	46.0	
U. rotundata	46.8	7.2	55.0	22.5	15.0	28.9	15.0	4.4	25.0	4.0	0.6	9.0	5.3	0.0	62.8	3.0	0.0	4.5				
U. scandinavica	42.2			11.6			9.6			4.0			30.7			2.0						
***U.* sp.**	33.0	27.9	54.8	13.4	11.3	21.5	12.4	1.7	16.9	3.7	3.3	5.9	5.6	0.1	38.1	1.0	0.0	2.1				
***U.* spp.**	28.2						3.2						5.9			1.3			19.3			
Pooled Total[3]	45.0	5.0	92.2	22.5	2.6	52.0	9.6	0.0	38.0	5.0	0.6	15.3	9.5	0.0	87.2	2.1	0.0	15.8	17.1	10.3	47.1	

[1]See published table for references (App. 7.4)

[2]*pertusa* is currently regarded as a synonym of *australis*

[3]Ulvan composition pooled across species

The ulvan backbone is most commonly made up of α- and β- (1,4)-linked monosaccharides (rhamnose, xylose, glucuronic acid and iduronic acid) with characteristic repeating disaccharide units. (Lahaye, 1998; Lahaye & Robic, 2007; Paradossi, Cavalieri, Pizzoferrato, & Liquori, 1999; Percival & McDowell, 1967). The two major disaccharide repeating units are aldobiuronic acids, referred to as ulvanobiuronic acid (types A and B); minor disaccharide aldobioses, referred to as ulvanobioses (type U), are also found in ulvan (Figure 2.1). Type A and B are far more common than U (Lahaye & Robic, 2007). Ulvanobiuronic acid type A_{3s}, one of the most common disaccharide units, consists of β-D-glucuronic acid (1,4)-linked to α-L-rhamnose 3-sulfate, while in type B_{3s} α-L-iduronic acid (a C-5 epimer of glucuronic acid) is (1,4)-linked to α-L-rhamnose 3-sulfate (Lahaye, 1998; Lahaye & Robic, 2007; Pengzhan *et al.*, 2003b; Percival & McDowell, 1967). Ulvanobiose U_{3s} consists of β-D-xylose (1,4)-linked to α-L-rhamnose 3-sulfate, while type $U_{2's,3s}$ consists of β-D-xylose 2-sulfate (1,4)-linked to α-L-rhamnose 3-sulfate (Lahaye, 1998; Lahaye & Robic, 2007). While (1,4)-glycosidic linkages are the predominant bonds, (1,2)- and (1,3)-glycosidic linkages also occur (Lahaye, 1998; Lahaye & Ray, 1996). In this regard, minor branching has been associated with glucuronic acid (1,2)-linked to the rhamnose residue of the ulvanobiuronic acid type A_{3s} (Lahaye & Ray, 1996; Lahaye & Robic, 2007). However, there are indications that greater diversity in the structure of ulvan is likely (Tabarsa *et al.*, 2018; Tako, Tamanaha, Tamashiro, & Uechi, 2015). For structural comparisons, a useful list of fully characterised ulvan oligosaccharides can be found in Lahaye and Ray (1996); Lahaye and Robic (2007).

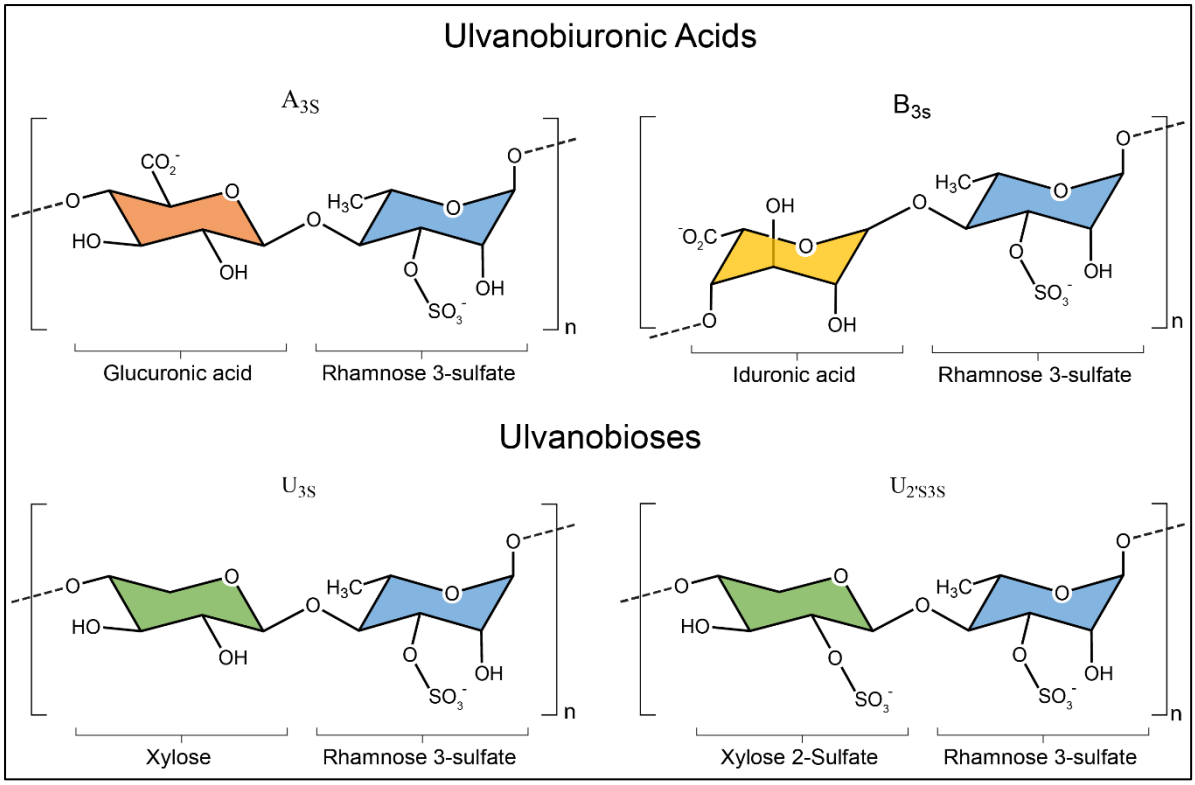

Figure 2.1: Nomenclature and structure of the major repeating disaccharide units that comprise ulvan. Ulvanobiuronic acid A_{3s} contains glucuronic acid (orange) attached to rhamnose 3-sulfate (blue), while the similar B_{3s} also contains rhamnose 3-sulfate but has iduronic acid (yellow) in the place of glucuronic acid. Ulvanobioses are comprised of rhamnose 3-sulfate attached to xylose (green). Xylose can contain a sulfate group, as seen in $U_{2's,3s}$.

The conformation of ulvan in solutions is in part determined by composition and has been described using both molecular modelling and empirical evidence. Predictions of the conformation of ulvan using molecular modelling are impeded by the limited knowledge of the sequencing of the polysaccharide backbone, beyond the presence of its repeating disaccharide units, and the few longer oligosaccharides described (Lahaye, 1998; Lahaye, Inizan, & Vigouroux, 1998; Lahaye & Ray, 1996; Lahaye & Robic, 2007; Tako *et al.*, 2015). However, theoretical calculations have determined that domains with repetitive sequences of any of the major disaccharide units (e.g., chains of A_{3s} or B_{3s}) can adopt secondary helical structures (Paradossi *et al.*, 2002). In practice, the conformation of ulvan in solution is pH dependent and is also influenced by the presence of counter-ions. Due to the relative hydrophobicity of rhamnose and its overall effect on the solubility of ulvan in neutral and low pH aqueous solutions, ulvan folds into a condensed bead-like conformation (Robic, Gaillard,

Sassi, Lerat, & Lahaye, 2009b). In the presence of salts (e.g., NaCl) these beads aggregate. The bead conformation of ulvan reduces its intermolecular interactions, resulting in the low viscosity of its solutions, as well as influencing gel strength and activity. In contrast, in high pH solutions (~13) ulvan has a more open conformation increasing the intermolecular interactions that give higher viscosities and greater gel strengths. The influence of pH over the solution properties of ulvans is a convenient mechanism by which to fine-tune its rheology to suit specific applications. Further discussion of gelling properties can be found in Lahaye and Robic (2007).

While the mole ratio of constituent sugars in ulvan from a particular source and batch are defined, the molecular structure can be altered through depolymerisation and removal or addition of functional groups (e.g., sulfate esters). In this regard, molecular weights (1 -> 2000 kDa, Figure 2.2 b, d, f) and degree of sulfation (2.3-40 %, App. 7.1.3) of ulvan extracts vary widely and have a large influence on physicochemical properties and biological activities. These structural features are also relatively easily manipulated and provide convenient methods for the investigation of structure-function relationships. Depolymerisation can be achieved through chemical (Adrien *et al.*, 2017a; Pengzhan, Quanbin, Hong, Xizhen, & Zhien, 2004; Qi *et al.*, 2005b; Shi *et al.*, 2017a; Zhang, Wang, Zhao, Yu, & Qi, 2013) and enzymatic hydrolysis with ulvan lyases (El Modafar *et al.*, 2012; Lahaye *et al.*, 1997; Reisky *et al.*, 2018; Robic *et al.*, 2009c). The degree of sulfation can be altered by addition of sulfate esters (de Freitas *et al.*, 2015; Qi *et al.*, 2012a; Qi *et al.*, 2005a) or removal of sulfate esters by solvolysis of the ulvan pyridinium salt (de Carvalho *et al.*, 2018; Kaeffer, Benard, Lahaye, Blottiere, & Cherbut, 1999; Leiro *et al.*, 2007; Tsubaki *et al.*, 2014) or through base hydrolysis (El Modafar *et al.*, 2012). Charge can be altered through manipulation of the degree of sulfation and by derivatisation of the carboxylic acid groups (e.g., esterification and amide formation) (Qi, Liu, Ma, Zhang, & Li, 2010; Qi *et al.*, 2006). Both the charge and the mole ratio of constituent sugars can be varied by reduction of glucuronic acid and iduronic acid to glucose and idose, respectively (Kaeffer *et al.*, 1999). Indeed, covalent cross-linking groups can also be added to enhance gel formation and gel strength (Kanno *et al.*, 2014; Morelli *et al.*, 2016a).

2.2.2 Extraction of ulvan

The quantitative yield and the quality of ulvan can vary significantly depending on the applied extraction and purification processes, the source of the biomass (species (Table 2.2),

source as wild or cultivated, location) (Alves *et al.*, 2013b), storage of collected biomass, and pre-extraction processing (Robic, Sassi, & Lahaye, 2008). In this regard, extraction conditions vary widely in the literature, as does the yield and quality of ulvan produced (Table 2.2, App. 7.1.3). The choice of extraction conditions is generally based around the physicochemical properties of the ulvan molecule and its specific interactions with other components of the plant cell wall (Robic *et al.*, 2009c). Less consideration is given to the capacity for the extraction conditions to degrade ulvan or co-extract impurities such as proteins, other polysaccharides (starch, cellulose, xyloglucan, and glucuronan), and to a lesser extent lipids and pigments. Depending on the intended application of the ulvan extract, co-extraction of impurities can lead to more intensive down-stream purification procedures. I use three criteria to determine optimal conditions for the extraction of ulvan: 1. High yield; 2. High selectivity; and 3. Low degradation (i.e. ulvan is extracted without extensive hydrolysis). To address these criteria, I review the physicochemical properties of the predominant macromolecules in *Ulva*, and then review the literature and provide recommendations on the best practices for the extraction of ulvan, focusing on applications.

Table 2.2: Ulvan extract median, minimum, and maximum yield (% algal dry weight) and composition (% w/w) for each species of *Ulva* (1954-2018). Median only reported where n=1. For additional detail, see supplementary data set, sheet 2 "Meta-Table", and search by the "In-text reference" column.

	Yield			Total Carbohydrate			Protein			Ash			Sulfate			
Species	**Median**	**Min**	**Max**	**Median**	**Min**	**Max**	**Median**	**Min**	**Max**	**Median**	**Min**	**Max**	**Median**	**Min**	**Max**	**Ref.[1]**
U. arasakii				54.9	54.9	54.9							0.4			
U. armoricana	40.0	7.0	90.0	48.7	31.2	78.0	7.3	1.5	13.9	17.0	2.9	18.6	14.4	2.7	19.1	
U. clathrata	6.8	0.6	61.9	31.3	26.7	44.6	8.2	0.4	15.3	19.0			10.6	5.6	35.8	
U. compressa	9.0	0.7	23.0	42.0	23.5	54.0	12.0	8.0	27.8	19.2	10.0	40.0	6.7	3.0	13.0	
U. conglobata	1.1	0.9	1.3				3.9	3.8	4.5	16.3	15.4	18.5	23.2	11.9	35.2	
U. fasciata	13.0	0.5	40.0	48.8	1.4	84.7	4.2	0.2	11.8	14.9	12.4	20.9	18.6	2.3	27.5	
U. flexuosa	2.7															
U. gigantea				79.6			5.8						11.9			
U. intestinalis	12.0	2.2	59.1	39.0	4.9	92.2	5.1	0.0	15.0	21.6	12.5	29.4	29.8	2.9	40.0	
U. lactuca	16.6	1.0	36.4	37.7	4.5	84.1	2.9	0.0	33.1	15.7	0.8	47.2	14.3	5.8	32.2	
U. linza	9.8	6.5	15.1	51.0	47.9	60.0	1.9	0.5	3.2				17.7	12.5	21.3	
U. meridionalis	18.7						6.8	4.0	9.5	12.9			10.0			
U. ohnoi	6.3	4.3	8.2	54.7	42.3	67.0	2.8	0.4	5.1	25.9	23.3	28.5	14.1	11.5	15.7	
U. olivascens				63.4			4.9	4.9	4.9				13.8			
***U. pertusa*[2]**	22.5	1.9	43.4	60.7	33.4	72.3	3.4	1.4	4.8	26.3	22.6	29.9	17.1	11.6	24.0	
U. prolifera	20.3	0.6	46.7	56.1	49.2	93.3	1.9	0.0	13.9				16.8	7.7	22.0	
U. reticulata	4.5	1.2	8.3	35.7	20.1	46.1	10.1	9.4	20.8	19.5	19.3	19.7	14.6	10.1	17.8	
U. rigida	10.9	1.3	38.5	59.5	39.8	75.6	10.0	0.2	25.9	18.1	8.1	25.0	19.8	14.3	37.3	
U. rotundata	8.0	0.1	27.5	35.9	22.3	70.8	12.6	1.0	35.5				11.4	2.4	17.3	
U. scandinavica				56.3									13.1			
***U.* sp.**	9.7	5.0	14.4	72.0	25.6	91.9	7.8	4.0	11.6	20.8	6.6	23.0	13.9	7.8	18.5	
***U.* spp.**	12.2	12.2	12.2	41.7			4.3	4.3	4.3	23.7			15.8			
Pooled Total[3]	12.0	0.1	90.0	46.1	1.4	93.3	6.6	0.0	35.5	17.1	0.8	47.2	15.5	0.4	40.0	

[1]See published table for references (App. 7.4)

[2]*pertusa* is currently regarded as a synonym of *australis*

[3]Ulvan yield and composition pooled across species

The extraction yield of ulvan is affected by the properties of the biomass and its pre-treatment, extraction temperature, extractants, extractant to biomass ratio, biomass particle size, and duration of extraction (Figure 2.2). The physicochemical properties of ulvan that influence its extraction yield include its relatively low solubility in aqueous conditions and its stabilisation in the plant cell wall, predominantly through its interaction with divalent cations (e.g., Ca^{2+}), borate, hydrogen bonding, and entanglement. The solubility of ulvan and its intermolecular interaction are pH dependent. Extraction solutions at pH > pKa of both uronic acids (~3.28) and sulfate esters (~2.0) promote a high charge density on ulvan and theoretically an increase in its solubility. Conversely, extraction solutions at pH < pKa of both uronic acids and sulfate esters theoretically reduce its solubility. In practice, the bead-like conformation of ulvan leads to formation of aggregates at neutral to acid pH, and these aggregates disperse at pH < pKa of the uronic acids allowing for greater solubility of ulvan (Robic *et al.*, 2009c). The solubility of glucuronan, a homopolysaccharide consisting of repeating (1,4)-linked glucuronic acids, is also pH dependent with expected enhancement in its solubility above the pKa of glucuronic acid. In this regard, both glucuronan and xyloglucan are more soluble in alkaline solutions. The solubility of water soluble protein is also pH dependent. Extraction solutions with pH equal to the isoelectric point (pI) of the protein result in its reduced aqueous solubility. In this regard, the pI for aqueous and alkaline soluble proteins from macroalgae is generally between pH 3-4 (Harnedy & FitzGerald, 2015). However, lower pI values for soluble proteins from *Ulva* (pI = 2.25) occur (Angell, Paul, & de Nys, 2017). Given these physicochemical properties of macromolecules in *Ulva*, an informed decision of extraction conditions can be made to enhance the efficiency and selectivity of ulvan extraction, while limiting degradation.

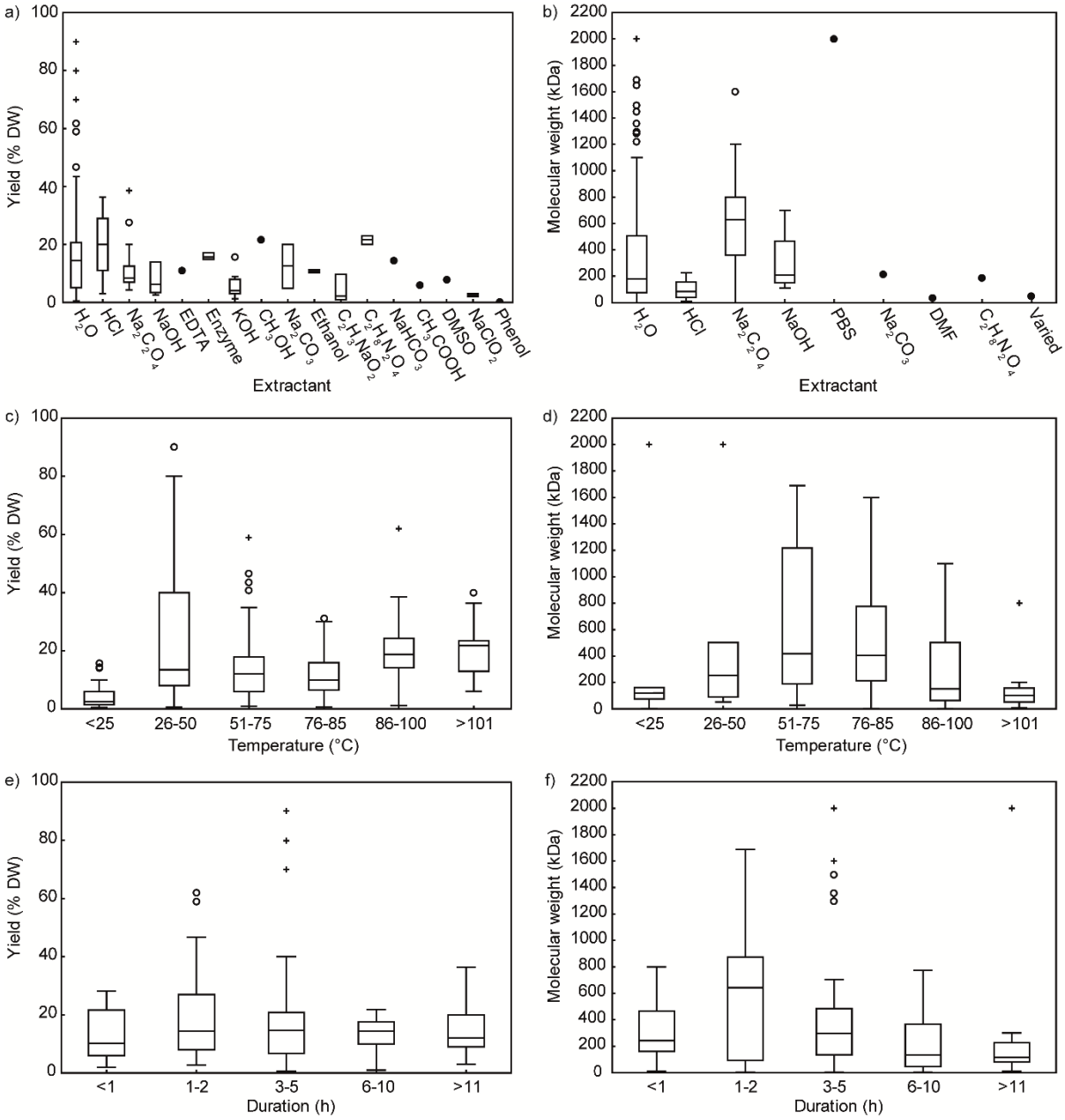

Figure 2.2: Box plots of the median and variability in ulvan yield (a,c,e) and average molecular weight (b,d,f) resulting from extractant applied (a,b), temperature (c,d) and duration (e,f) of the extraction procedure. Yield is presented as % of dry weight; average molecular weight in kDa. "PBS" = Phosphate buffered saline; "DMF" = anhydrous N,N-dimethylformamide; "Varied" = multiple extractants. Boxes represent the interquartile range (IQR) with the mean as a line within the box; whiskers represent the limits of non-outlier data; open circles are outliers, calculated by ±1.5*IQR; crosses are extreme values, calculated by ±3*IQR; closed circles represent values for which n=1

Extraction yield can vary significantly between populations of *Ulva* due to eco-physiological variation (light, temperature) (Robic *et al.*, 2009d), and, therefore, comparisons of extraction yields should be evaluated on a single harvest of biomass. In terms of biomass

pre-treatment, the reduction of salt in the biomass by warm water extraction enhances the extraction efficiency of ulvan (Glasson *et al.*, 2017). The mechanism here is twofold, the reduction of salt reduces the aggregation properties of ulvan, and osmotic shock increases the exposure of cell wall components to the extractant. Other pre-treatments, such as pigment and lipid removal, have no effect on either extraction efficiency or the quality of ulvan extracted and for this reason are considered unnecessary, unless they are targeted products. Finally, to increase the interaction of extractant and biomass cell wall, and, therefore, enhance extraction efficiency, biomass is dried and finely milled.

The solubility of ulvan in aqueous solutions is enhanced by extraction at high temperatures (80-90 °C). The temperature is usually capped below the boiling point of water for convenience and to prevent higher temperatures promoting degradation (e.g., depolymerisation and desulfation) (Tsubaki, Oono, Hiraoka, Onda, & Mitani, 2016). However, high temperature extractions in water generally have low extraction yields due to the interactions of ulvan with other cell wall components (Robic *et al.*, 2009c). As a result, extractants, such as chelators and acids, are used to overcome the structural integrity of the plant cell wall, thus, enhancing the extraction efficiency of ulvan. Chelators, such as oxalates and EDTA, remove divalent cations (e.g., Ca^{2+}) that promote the cross-linking of ulvan in the cell wall. Extractions using chelators are generally conducted at or near neutral pH and at high temperatures (80-90 °C). Reported yields vary widely (see Figure 2.2), but the extraction efficiency (and selectivity) is improved when the pH is adjusted to 4.5 (Robic *et al.*, 2009c). In this regard, extractions in strong acid (e.g., HCl; Figure 2.2) generally produce higher extraction yields (Glasson *et al.*, 2017; Hernández-Garibay, Zertuche-González, & Pacheco-Ruíz, 2011; Robic *et al.*, 2009c). Mechanistically, extractions at pH below the pK_a of glucuronic acids disperse ulvan aggregates, facilitating its extraction. Notably, high temperatures (80-90 °C) are still required to facilitate high extraction efficiencies at low pH, however, isolation methods influence yields (see section 2.2.3). Extraction pH also plays a significant role in the selectivity of ulvan over other macromolecules, as discussed above.

The physicochemical properties of the macromolecular constituents of *Ulva* support extraction pH as an important factor in the selectivity of the extraction process for ulvan. At pH below the pKa of uronic acids (~3.28) the extraction of ulvan is enhanced (see rationale

above), and the solubilities of other macromolecules, such as glucuronan, xyloglucan, and soluble protein, are minimised (Glasson *et al.*, 2017; Hernández-Garibay *et al.*, 2011; Robic *et al.*, 2009c; Yaich *et al.*, 2013). For example, HCl extracts of fresh *U. ohnoi* had superior selectivity for ulvan (306-333 µg rhamnose / mg extract) over protein (4-7 µg protein / mg extract), when compared with sodium oxalate extracts (114-162 µg rhamnose / mg extract and 41 – 59 µg protein / mg extract) (Glasson *et al.*, 2017). The selectivity for ulvan over other polysaccharides can also be inferred by comparing the molar ratios between rhamnose (an ulvan specific monosaccharide), and uronic acids or xylose (both of which are constituents of multiple polysaccharides) of extracts obtained using different extractants (Glasson *et al.*, 2017; Robic *et al.*, 2009c). For example, ulvan extracted from *Ulva ohnoi* had a molar ratio of 1:0.71 for rhamnose to uronic acids when HCl was used as the extractant, and 1:0.88 when oxalate was used as the extractant, demonstrating increased co-extraction of glucuronan in the latter (Glasson *et al.*, 2017). Similarly, the mole ratio of rhamnose to uronic acids for ulvan extracted from *Ulva rotundata* with 0.05 M HCl (pH 1.3) was 1:0.83 compared to 1:0.99 when extracted with 0.02 M ammonium oxalate (adjusted to pH 4.6) (Robic *et al.*, 2009c). These latter studies indicate a quantitative measure of selectivity can be provided using pH, resulting in a more accurate composition of the ulvan attained. It is, however, important to note that while selectivity for ulvan over other macromolecules was enhanced at low pH, significant degradation of its structure also occurred.

Degradation of the structure of ulvan during the extraction procedure may reduce or enhance its functionality depending on the intended application. This review focuses on the versatility of the ulvan extract, and as ulvan can be readily degraded after its extraction using chemical and enzymatic approaches (see above), an ulvan sample with minimal degradation is considered the most versatile product. There are two structural features that are most susceptible to degradation during the extraction of ulvan; its degree of polymerisation and degree of sulfation. In this regard, depolymerisation of the polysaccharide is more facile than desulfation of the polysaccharide under the range of extraction conditions used to extract ulvan. Extraction parameters that influence the degree of depolymerisation include pH, temperature, and duration (Figure 2.2 d, f). In this regard, high temperature (80-90 °C) extractions at low pH (~1.3-1.5) lead to significantly higher levels of depolymerisation than extractions at higher pH (with or without an added extractant) (Glasson *et al.*, 2017; Robic *et*

al., 2009c; Yaich *et al.*, 2014; Yaich *et al.*, 2013). However, small changes in pH, temperature, and duration all have a significant effect on the degree of depolymerisation (Robic *et al.*, 2009c; Tsubaki *et al.*, 2016; Yaich *et al.*, 2014; Yaich *et al.*, 2013). For example, ulvan was extracted from *U. lactuca* using a factorial experimental design that varied temperature (80 °C or 90 °C), pH (pH 1.5 or 2), and time (1-3 hours) (Yaich *et al.*, 2013). The harshest extraction condition (90 °C at pH 1.5 for 3 h) resulted in higher yield at the cost of significantly greater depolymerisation than the milder extraction (80 °C at pH 2 for 1 h). Furthermore, at pH 1.5 for 1 and 2 hours, significantly higher depolymerisation occurred for extractions conducted at 90 °C than at 80 °C, but a higher yield was also obtained. The same temperature dependence was present for 2 and 3 h extractions at pH 2.

The combination of extraction temperature, solvent pH and extraction duration interact to influence extraction yield and quality (e.g., purity and molecular integrity). Higher extraction temperatures enable greater solubilisation of ulvan (Figure 2.2 c), low pH improves the selectivity for ulvan, and increased extraction duration can increase ulvan yield. However, compromises must be made to protect the integrity of the ulvan structure. For example, while high temperature results in higher yields, a combination of high temperature, low pH and long extraction duration lead to significant depolymerisation (Figure 2.2 d, f). However, small adjustments in pH have a large influence on depolymerisation, while small changes in temperature do not. Therefore, using the data available in the literature, the following extraction conditions are recommended based on the criteria listed above: 1. High extraction yield; 2. High selectivity; and 3. Low degradation:

- Temperature: 80-90°C
- pH range: 2 - 4.5
- Duration: 1 - 3 h

2.2.3 Isolation and Purification

Methods for the isolation and purification of ulvan vary significantly and are linked to both the availability of resources and the focus of the study. In this review, isolation is regarded as the separation of the extract from residual biomass and the removal of solvent, and purification as the separation of ulvan from other solutes (e.g., salts and other macromolecules). In practice, these steps are not mutually exclusive. It is also important to

note that isolation and purification methods influence the physicochemical properties and biological activities of ulvan. I briefly review commonly used methods for the isolation and purification of ulvan that yield two desirable outcomes, 1. High recovery, and 2. Pure product. Methods for the isolation and purification, both chemical and enzymatic, of polysaccharides have been comprehensively reviewed (Shi, 2016); here the focus is to briefly review commonly used isolation and purification methods for ulvan, and comment on their effectiveness.

Following the extraction of ulvan, the extract is separated from the residual biomass by filtration and/or centrifugation prior to the isolation of ulvan by precipitation, evaporation, or concentration by ultrafiltration followed by lyophilisation. For industry, spray drying is another efficient process (Barbosa *et al.*, 2015). Precipitation of ulvan with ethanol is by far the most common isolation method used in the laboratory. Typically, addition of ethanol (e.g. 70-96 %) to a concentrated extract is adequate to precipitate ulvan, while ethanol-soluble compounds, such as pigments and metabolites, remain in solution (Béress *et al.*, 1993). Although ethanol precipitation is a convenient method, it is limited by the low solubility of salts and higher solubility of low molecular weight ulvan in ethanol-water mixtures. Precipitation methods are also particularly difficult to replicate and in the absence of dialysis or ultrafiltration can lead to high levels of salt in the ulvan extracts (Costa *et al.*, 2012; Yaich *et al.*, 2013). Consequently, precipitation can lead to incorrect interpretations of yields, physicochemical properties, and biological activities. Efficient desalting of ulvan extracts can be achieved by dialysis, ultrafiltration, or even chromatography.

Dialysis and ultrafiltration allow for the reduction (removal) of excess salts and small molecules contaminating ulvan extracts. Dialysis is highly effective in the removal of excess salt from analytical samples and for other applications that require very low residual ash. Ultrafiltration is generally employed as a two-step process; concentration (volume reduction) followed by diafiltration (washing or buffer exchange). Both dialysis tubing and membrane filters for ultrafiltration are available with a variety of pore sizes (or molecular weight cut-off (MWCO)). The range of MWCOs used for ulvan generally fall between 3.6-12 kDa (Qi *et al.*, 2005a; Siddhanta *et al.*, 2001). For dialysis, pore size selection is based around the retention of ulvan, however, for ultrafiltration pore size selection is based on both the retention of ulvan and the rate of permeate flow (which decreases as pore size decreases). The latter extends

the time associated with the ultrafiltration processes. The balance between ulvan retention and time efficiency is optimised at ~10 kDa MWCO (Glasson *et al.*, 2017; Robic *et al.*, 2008; Yaich *et al.*, 2014).

Given the high level of impurities in many ulvan extracts, it is surprising that chromatographic techniques are not applied more widely for purification prior to characterising the physicochemical properties and biological activities of ulvan. In this regard, the polyanionic and polydisperse nature of ulvan lends itself to anion-exchange chromatography (AEC) and size-exclusion chromatography (SEC), respectively. AEC is effective for the removal of proteins and neutral polysaccharide impurities from ulvan samples. Both weak anion-exchangers (e.g., diethylaminoethyl (DEAE) or tertiary amine functionalised media) (Ray & Lahaye, 1995a; Siddhanta *et al.*, 2001) and strong anion-exchangers (e.g., quaternary (Q) amine functionalised media) (Robic *et al.*, 2009c) have been successfully employed to purify ulvan. SEC is widely used as an analytical technique for determining molecular weights and molecular weight distributions (see section 2.2.4), however, it has wider applications. For example, SEC can be used to fractionate oligosaccharides and polysaccharides for the elucidation of fine structure (Lahaye *et al.*, 1997), and to generate size classes for structure-function relationships (Jaulneau *et al.*, 2010; Zhang *et al.*, 2008). With regards to the former, SEC has been used to fractionate ulvan oligosaccharides for fine structure analysis using NMR techniques (Lahaye, 1998). A large range of size exclusion media is available targeting different molecular size ranges. Media commonly used for purification of ulvan samples are Sepharose CL-6B (Jaulneau *et al.*, 2010), Sephacryl S-400/HR (Zhang *et al.*, 2008), Sephacryl S-1000 (Ghosh *et al.*, 2004), and Sephadex G-200 (Ray, 2006).

In summary, ideally the choice of extraction techniques will limit the co-extraction of macromolecular impurities (see section 2.2.2) and reduce the necessity for intensive purification techniques. However, due to salt content (introduced by extractants and inherent in marine species) and similarities in the physical properties of ulvan and contaminating polysaccharides and proteins, purification is necessary. In general, salt is the most significant impurity and is most effectively removed by dialysis or ultrafiltration techniques. Depending on the extraction process employed, protein may also need to be actively removed, either by

chemical or enzymatic approaches (Alves *et al.*, 2013b; Shi, 2016), or using chromatographic techniques. The latter is more reproducible and allows for highly purified fractions of ulvan. In practice, a strategic selection of extraction procedures, and isolation and purification procedures should be made based on the available resources. For example, in a resource limited situation one might select a more selective acid extraction, concentrate by evaporation, purify using dialysis, and isolate by precipitation. In a resource rich situation, a selective acid extraction is ideal, although a less selective extraction process can be tolerated, with concentration and diafiltration with ultrafiltration. Subsequent purification by anion-exchange chromatography, and lyophilisation or spray drying to isolate the purified ulvan can be applied.

2.2.4 Characterisation

In general, the elucidation of polysaccharide structures is often complicated by the presence of multiple monosaccharide constituents, which may include neutral, acidic and amino sugars, a variety of glycosidic linkages, high molecular weights, branching of constituent sugars, a variable degree of sulfation and substitution patterns, and complex macromolecular properties (e.g., aggregation). The presence of contaminating polysaccharides further complicates structural elucidation of a particular polysaccharide. Therefore, it is important to start with as pure a sample as possible, and even then, full structural elucidation is challenging - 'Structural characterisation' is a more fitting term. Adequate structural characterisation of an ulvan sample is essential for interpreting its physicochemical properties and biological activities. To achieve this, a measurement of composition (e.g., total carbohydrate content, protein content and ash) and the identifying structural features of ulvan (e.g., sugar composition, glycosidic linkages, degree of sulfation) are required. Comprehensive reviews of the techniques used to elucidate the chemical structure and macromolecular properties of bioactive polysaccharides are provided elsewhere (Pettolino, Walsh, Fincher, & Bacic, 2012; Sims, Carnachan, Bell, & Hinkley, 2018; Yang & Zhang, 2009). In this review I focus on the methods used to characterise ulvan and propose the minimum analysis and characterisation required to progress beyond bioprospecting.

The analysis of the chemical structure of ulvan is fundamentally based on the quantitative determination of the major constituent monosaccharides (rhamnose, xylose,

glucuronic acid and iduronic acid) and degree of sulfation. The latter is most commonly carried out using a turbidimetric assay (Craigie, Wen, & van der Meer, 1984) but can be measured using ion chromatography, high performance liquid chromatography (HPLC) coupled with conductivity (Lahaye & Axelos, 1993), elemental analysis, or Fourier transform infrared spectroscopy (FTIR) (Robic, Bertrand, Sassi, Lerat, & Lahaye, 2009a). Constituent monosaccharides are predominantly quantified using chromatography techniques, in particular gas chromatography (GC) (Costa *et al.*, 2012; de Freitas *et al.*, 2015; Lahaye & Axelos, 1993; Leiro *et al.*, 2007; Mao *et al.*, 2006), HPLC (Cho *et al.*, 2010; Tsubaki *et al.*, 2014), and high-performance anion-exchange chromatography (HPAEC) (Glasson *et al.*, 2017; Lahaye *et al.*, 1999). Depending on the chromatographic technique employed, the sample is subjected to pre-treatments. Primarily, accurate quantification of constituent monosaccharides requires complete hydrolysis of ulvan. However, due to the resistance of the aldobiuronic glycosidic linkage to hydrolysis (BeMiller, 1967; McKinnell & Percival, 1962a; Quemener *et al.*, 1997), and the susceptibility of rhamnose, glucuronic acid, iduronic acid and xylose to degradation in concentrated strong acids (e.g., Saeman hydrolysis) (Conrad, 1980; Fransson, Roden, & Spach, 1968), traditional acid hydrolysis methods, such as with trifluoroacetic acid (TFA), are both ineffective and degradative. A traditional acid hydrolysis will not cleave all of the aldobiuronic linkages and, as a result, the neutral and uronic acid residues involved in these linkages will not be detected. As ulvan is predominately comprised of repeating aldobiuronic acid disaccharides, a traditional acid hydrolysis will inaccurately characterise ulvan. However, hydrolysis of ulvan using traditional methods is ubiquitous in the literature. A two-step hydrolysis in methanolic HCl followed by aqueous trifluoroacetic acid is an effective alternative to reduce the hydrolysis-induced damage to constituent monosaccharides (de Ruiter, Schols, Voragen, & Rombouts, 1992; Glasson *et al.*, 2017). A chemo-enzymatic degradation involving hydrolysis with a mild acid followed by β-D-glucuronidase cleavage of aldobiuronic acid is also an effective solution (Lahaye & Robic, 2007; Quemener *et al.*, 1997). Both HPLC (Cho *et al.*, 2010; Tsubaki *et al.*, 2014; Zhang *et al.*, 2013) and HPAEC (Glasson *et al.*, 2017; Lahaye *et al.*, 1999) methods are used to quantify the monosaccharides in the hydrolysis samples without further derivatisation. HPLC methods generally provide less resolution than HPAEC methods (Templeton, Quinn, Van Wychen, Hyman, & Laurens, 2012), but both allow the assessment of the effectiveness of the hydrolysis

method employed (de Ruiter *et al.*, 1992). HPAEC-PAD (pulsed amperometric detection) of methanolic-HCl/TFA hydrolysates also has the major advantage of separating and quantifying acidic and neutral sugars (and amino sugars) in a single run, without further derivatisation (de Ruiter *et al.*, 1992). GC analysis requires that the constituent sugars be converted to volatile derivatives, such as alditol acetates (de Freitas *et al.*, 2015; Lahaye & Axelos, 1993; Leiro *et al.*, 2007; Pengzhan *et al.*, 2003b) and trimethylsilyl (TMS) ethers (Costa *et al.*, 2012). For the former, reduction of monosaccharide C1-aldehyde is conducted prior to the preparation of alditol acetate. In general, C6-carboxylic acids are not reduced under the conditions employed to reduce aldehydes and, therefore, are not converted to alditol acetates. However, GC-MS analysis of alditol acetates, prepared from ulvan hydrolysates that included the pre-hydrolysis reduction of C6-carboxylic acids with sodium borodeuteride ($NaBD_4$) to generate 6,6'-dideuterio-sugars, allows for the determination of the total uronic acid content (Pettolino *et al.*, 2012). Studies that do not include this conversion generally measure uronic acid content using colourimetric assays (Blumenkrantz & Asboe-Hansen, 1973; Radhakrishnamurthy & Berenson, 1963). Alternatively, TMS ethers of sugars can be prepared using reagents such as N,O-bis(trimethylsilyl)trifluoroacetamide, allowing for the quantification of both neutral and acidic sugars (Costa *et al.*, 2012). However, TMS derivatisation of un-reduced sugar residues can yield several peaks in the GC chromatogram corresponding to different pyranose anomers, which complicates interpretation. A solution to this problem is to follow the preparation of alditol acetate derivatives with reduction to the alditol prior to preparation of the TMS derivative. For sample preparation, HPAEC methods (e.g., HPAEC-PAD) provide the simplest and most comprehensive route for sugar constituent analysis; however, excellent results can also be obtained using either GC or HPLC methods.

While sugar constituents are important in determining the physicochemical properties and biological activities of a polysaccharide, glycosidic linkages and functional group substitution patterns, and sugar sequence are arguably more important. Glycosidic linkage (methylation) analysis is generally conducted using GC-MS methods (Cassolato *et al.*, 2008; Ray & Lahaye, 1995a; Sims *et al.*, 2018) and provides information on the linkage positions and substitution patterns of constituent sugars. Briefly, methylation analysis involves the preparation of partially methylated alditol acetates followed by quantitative analysis using GC-MS. To achieve this effectively, the uronic acid components of ulvan are reduced prior to

the methylation step (Pettolino *et al.*, 2012; Sims *et al.*, 2018). Determination of glycosidic linkages and sugar sequence can then be achieved using 2D NMR techniques on hydrolysed ulvan fragments (disaccharides and oligosaccharides) (Cheng & Neiss, 2012; Duus, Gotfredsen, & Bock, 2000; Lahaye & Ray, 1996; Synytsya *et al.*, 2015; Yang & Zhang, 2009). In many cases, ^{1}H and ^{13}C resonances characteristic of ulvan structures (e.g., repeat disaccharide units) can be assigned by comparison with published data (de Freitas *et al.*, 2015; Glasson *et al.*, 2017; Kopel *et al.*, 2016; Robic *et al.*, 2009c; Tako *et al.*, 2015; Thanh *et al.*, 2016; Yaich *et al.*, 2017). In addition, the anomeric configuration and position of substituents (e.g., sulfate groups) can be inferred by location of both ^{1}H and ^{13}C resonances (Duus *et al.*, 2000; Yang & Zhang, 2009).

The physicochemical properties and biological activities of polysaccharides are also fundamentally linked to molecular weight. Therefore, a measure of average molecular weight (M_w) and molecular weight distribution (MWD) is integral to the characterisation of polysaccharides. In this regard, size exclusion chromatographic (SEC) methods are the most commonly employed as they allow a measure of both M_w and MWDs. Firstly, as a minimum requirement for the determination of average M_w and MWDs, SEC is coupled to a concentration dependent (CD) detector, most commonly refractive index and UV. For ulvan, calibration of these setups is usually achieved with narrow polydispersity polymer standards (e.g., dextrans (Adrien *et al.*, 2017a; Li *et al.*, 2018c; Li *et al.*, 2018d; Pengzhan *et al.*, 2003a; Qi *et al.*, 2005b; Yaich *et al.*, 2013), pullulans (Costa *et al.*, 2012; Morelli, Betti, Puppi, & Chiellini, 2016b; Tsubaki *et al.*, 2016) and polyethylene oxides (Barros *et al.*, 2013)). However, due to difference in the macromolecular properties, commonly used calibration standards are unlikely to yield accurate results, and accurate measurements of ulvan (and other complex polymers) M_w and MWDs require online molecular weight detectors (e.g., multiangle laser light scattering (MALLS) and viscosity (VISC)) (Barros *et al.*, 2013; Glasson *et al.*, 2017; Robic *et al.*, 2009b; Tabarsa *et al.*, 2018; Thanh *et al.*, 2016). Both SEC-MALLS and SEC-VISC also allow analysis of macromolecular properties, such as aggregation behaviour (Robic *et al.*, 2009b; Striegel, 2005). Comprehensive reviews on the theory and variety of detection methods in SEC analysis are provided by Kostanski, Keller, and Hamielec (2004) and Striegel (2005).

These methods for the characterisation of ulvan can represent a significant investment in both equipment and experimental time. However, high-throughput determination of the composition of ulvan extracts is desirable in some applications (e.g., bioprospecting studies, ulvan composition comparisons, and for quality control in industry) and requires an alternative approach. The rapid determination of ulvan in samples is commonly carried out using colourimetric assays that probe sugar constituents (e.g., uronic acids, rhamnose, and xylose) and protein content (Bradford, 1976; Lowry, Rosebrough, Farr, & Randall, 1951), and a turbidimetric assay for determination of sulfate ester content (Craigie *et al.*, 1984). Common and relatively accurate colourimetric methods for uronic acid determination include the carbazole/sulfuric acid (Radhakrishnamurthy & Berenson, 1963) and sulfamate/m-hydroxydiphenyl techniques (Blumenkrantz & Asboe-Hansen, 1973). However, due to a lack of specificity for targeted sugars, chemical colourimetric methods for quantitative measurements of neutral sugars (e.g., rhamnose and xylose) are hampered by interference. In this regard, highly specific enzymatic assays for monosaccharides typically present in ulvan including rhamnose (Pittner & Turecek, 1987), xylose (Gong *et al.*, 2016) and uronic acids (Moon, Yoon, Tsang Mui Ching, Lanza, & Prather, 2009) are available. However, to gain an understanding of composition, multiple characterisation assays are necessary, resulting in little time savings. In this regard, a truly high-throughput method would require only a single measurement on an un-degraded sample with minimal preparation.

Chemometric methods coupled with spectral analysis, such as IR, Raman, NIR, and NMR, are effective for the rapid (single measurement) compositional analysis of polysaccharides (Robic *et al.*, 2009a; Salomonsen, Jensen, Stenbæk, & Engelsen, 2008). For example, FT-IR spectra in the range of 1770-600 cm^{-1} coupled with the multivariate analysis method of partial least squares (PLS) analysis was used to develop calibrated FT-IR-PLS-models that allowed the sulfate content and the content of the major monosaccharides in ulvan hydrolysates to be determined (Robic *et al.*, 2009a). The key ulvan spectral features used for the development of FT-IR-PLS-models were the uronic acid carboxylic groups (1650-1600 cm^{-1} (V_{as} C=O); 1425-1400 cm^{-1} (V_s C=O)) (Robic *et al.*, 2009a; Yaich *et al.*, 2017), sulfate ester groups (1260-1215 cm^{-1} (V_{as} S=O); 850-835 cm^{-1} and 795-785 cm^{-1} (C-O-S)) (Pengzhan *et al.*, 2003b; Ray & Lahaye, 1995a; Yaich *et al.*, 2017), and sugar ring side groups and glycosidic linkages (1055-1030 cm^{-1} (C-O-C)) (Robic *et al.*, 2009a). While the broader application of the

FT-IR-PLS-models for ulvans is untested, this analytical approach represents a rapid characterisation method for ulvan.

Ulvan has a broad range of biological activities; however, the characterisation of ulvan is often of low resolution, leading to uncertainty in the origin of the activities tested. At the research level, total characterisation methods are essential in understanding structure-activity relationships. The minimum characterisation data recommended is sugar constituent analysis (preferably suitable for the detection of neutral and acidic sugars), molecular weight analysis, and measures of contaminants, such as protein and ash. To obtain further insight into structure-activity relationships, glycosidic linkage analysis should also be conducted. In the next section I review the biological activities of ulvans and comment on the structural attributes that influence its efficacy.

2.3 Biological activities of ulvans

2.3.1 Overview

Ulvan has demonstrated significant biological activities in both animal and plant systems in in vitro and in vivo studies (Table 2.3). In animals, sulfated polysaccharides, such as free glycosaminoglycans (GAGs) and proteoglycans (protein linked GAGs), are intricately involved in a broad range of biological processes and have significant structural similarities with ulvan (Handel, Johnson, Crown, Lau, & Proudfoot, 2005; Scharnweber *et al.*, 2015). Therefore, the capacity of ulvan to mimic GAGs is a logical link. Sulfated polysaccharides are absent in terrestrial plants and the rationale for the biological activity of ulvans towards plants is less clear; however, ulvan has structural similarities with plant rhamnogalacturonans (Varnier *et al.*, 2009) and rhamnolipids from phytopathogenic bacteria (Vatsa, Sanchez, Clement, Baillieul, & Dorey, 2010), providing an insight to its activity. Importantly, the structural features of ulvan (e.g., molecular weight, degree of sulfation, sulfation pattern, constituent sugars, linkages, isomers, and degree of branching) influence its bioactivity. Therefore, ulvan obtained from different species of *Ulva*, and species from different environments, display significantly varied bioactivity profiles. I review the biological activities attributed specifically to ulvan, focusing on activities with potential biomedical applications and the developing body of technologies in plant physiology, horticulture, and agriculture.

Table 2.3: The number of publications that assessed ulvan bioactivities in addition to detailing the extraction procedure and/or characterisation of the polysaccharide (1954-2018). See published version of table (App. 7.4) for further details on the publications.

Species	Bioactive							Other	
	Anti-coagulant	Immuno-modulating	Anti-Cancer	Anti-oxidant	Anti-viral	Anti-hyperlipidemic	Biomaterial	Plant Defence	Various[2]
U. arasakii									
U. armoricana		2		1	1			1	2
U. clathrata	3	1			1				1
U. compressa	1				1		1		2
U. conglobata	1								
U. fasciata	3	2	2	5		3		4	2
U. flexuosa									
U. gigantea									
U. intestinalis		5	4	4	2	1			1
U. lactuca	3	3	5	10	3	2	2	2	5
U. linza	1	1		3					
U. meridionalis									
U. nematoidea	1								
U. ohnoi		1							
U. olivascens									
U. pertusa[1]		2	1	4	1	6			2
U. prolifera		2	1	4		2			3
U. reticulata	1			1					1
U. rigida		2		1					
U. rotundata							1		1
U. scandinavica							1		
***U.* sp.**	1	1							2
***U.* spp.**								1	
Total publications	11	21	13	31	9	14	4	8	20

[1]*pertusa* is currently regarded as a synonym of *australis*

[2]Various bioactive properties not otherwise listed on the table. See published version of table (App. 7.4) for further details.

2.3.2 Cytotoxicity

Cytotoxicity of supplements, nutraceuticals, therapeutic agents or adjuvants, and biomedical materials is a critical consideration for product development, including a natural product such as ulvan. In this regard, the cytotoxicity of ulvan has been investigated by dosing a range of macrophage cell lines (e.g., RAW 264.7, J774A.1, and peritoneal) (Cho *et al.*, 2010; Peasura *et al.*, 2016; Tabarsa *et al.*, 2012a; Tabarsa *et al.*, 2018), gut cells (e.g., IPEC-1) (Berri *et al.*, 2017; Berri *et al.*, 2016; Roselli *et al.*, 2007), fibroblast cells (e.g., mouse C3H [L929]) (Alves, Sousa, & Reis, 2013a), Vero cells (Morán-Santibañez *et al.*, 2016), Swiss mice and Wistar rats (de Araújo *et al.*, 2016). Ulvan is largely non-toxic, with ulvan fractions from *U. pertusa* (Tabarsa *et al.*, 2012a; Tabarsa *et al.*, 2018), *U. intestinalis* (Jiao *et al.*, 2009; Peasura *et al.*, 2016), *U. armoricana* (Berri *et al.*, 2017; Berri *et al.*, 2016), *U. lactuca* (Alves *et al.*, 2013a; Alves *et al.*, 2012b; de Araújo *et al.*, 2016), *U. clathrata* (Aguilar-Briseño *et al.*, 2015), *U. compressa* (Lopes *et al.*, 2017) and *U. prolifera* (Cho *et al.*, 2010; Kim, Cho, Karnjanapratum, Shin, & You, 2011) having greater than 50 % cell viability for cell cultures dosed with ≥ 500 µg mL^{-1} of sample.

2.3.3 Immunomodulating activity

Molecules that influence the immune system are known as immunomodulators and often act by influencing inflammation. The inflammatory effects of ulvan have been investigated in vitro using macrophage cell types (e.g., RAW 264.7, mouse peritoneal (Jiao *et al.*, 2009), J77A.1 (Peasura *et al.*, 2016) and fish head kidney (Castro *et al.*, 2004)), tissues (e.g., intestinal epithelial cells (Berri *et al.*, 2017; Berri *et al.*, 2016)), and in vivo using animal models (e.g., Wistar rats (Abd-Ellatef *et al.*, 2017), mice (Song *et al.*, 2016; Wei *et al.*, 2014), and chickens (Hong *et al.*, 2011)). Inflammation is dependent on cytokine production and is largely the result of the activation of NF-kB (a protein complex that controls transcription) by pathogen-associated molecular patterns (PAMPs) on Toll-Like Receptors (TLRs) (Berri *et al.*, 2017; Moynagh, 2003; Rang, Ritter, Flower, & Henderson, 2016). Lipopolysaccharides (LPS) on the cell wall of gram-negative bacteria are potent activators of TLRs and are the most commonly employed PAMP class in immunomodulation studies. Activated NF-kB induces transcription of genes coding for cytokines, thus, initiating an inflammatory response (Rang *et al.*, 2016). Evaluation of the influence of ulvan on inflammation has been conducted using

a number of probes, including signalling molecules (e.g., cytokines; TNF-α, IL1, IL2, IL6, IL10, IL12, CXCL1, CXCL12, CXCL14 and CCL22), active metabolites (e.g., PGE_2, NO, HOCl), immunoglobulins (e.g., IgM, ICAM and VCAM-1), enzymes (e.g., COX-2, iNOS-2, HO-1 and MPO) and transcription related molecules (e.g., NF-kB, mRNA) (Berri *et al.*, 2016; Cho *et al.*, 2010; Fernández-Díaz *et al.*, 2017; Jiao *et al.*, 2009; Kim *et al.*, 2011; Leiro *et al.*, 2007; Peasura *et al.*, 2016; Tabarsa *et al.*, 2012a; Tabarsa *et al.*, 2018; Wei *et al.*, 2014). A pro-inflammatory response is initiated by immune cells (e.g., macrophages) through the release of cytokines (e.g., IL-1, IL-2 IL-6, IL-18, IL-12, prostaglandin E_2 (PGE_2), and tumour necrosis factor alpha (TNF-α) (Cavaillon, 2001). Anti-inflammatory cytokines, such as IL-4, IL-10, IL-11, and IL-13, can inhibit the release of pro-inflammatory cytokines to prevent damage from excessive macrophage activation. This simplistic representation of the roles of immune cells and cytokines is useful but cytokine activity is complicated, involving multiple effects and interacting pathways (Cavaillon, 2001).

Macrophage cells (e.g., RAW 264.7, mouse peritoneal, J77A.1, and fish head kidney) are often used to study the effect that ulvan (and other bio-actives) have on the inflammatory response (Castro *et al.*, 2006; Fernández-Díaz *et al.*, 2017; Jiao *et al.*, 2009; Kim *et al.*, 2011; Leiro *et al.*, 2007; Peasura *et al.*, 2016; Rahimi *et al.*, 2016; Tabarsa *et al.*, 2012a; Tabarsa *et al.*, 2018). For example, RAW264.7 cells exposed to 50 μg mL^{-1} of purified ulvan from *U. intestinalis* upregulated the production of pro-inflammatory cytokines (TNF-α, IL-1β, IL-6, and IL-12), the anti-inflammatory cytokine IL-10 and enzymes (e.g., iNOS and COX-2) and their products (e.g., NO and PGE_2); a response of equivalent magnitude to the LPS (1 μg mL^{-1}) positive control (Tabarsa *et al.*, 2018). Importantly IL-10 inhibits pro-inflammatory cytokines (including, TNF-α, IL-1β, IL-6, and IL-12), which might act to limit any potential harmful repercussions from an over-stimulated inflammatory response. Ulvan isolated from *U. pertusa* (Tabarsa *et al.*, 2012a) *U. rigida* (Kim *et al.*, 2011; Leiro *et al.*, 2007) and *U. prolifera* (Cho *et al.*, 2010) also activate RAW 264.7 cells, upregulating the production of cytokines (e.g., TNF-α, IL-1β, IL-6, IL10), enzymes (e.g., iNOS and COX-2) and their products (e.g., NO and PGE_2). Consistent with RAW 264.7, macrophage J774A.1 cells treated with 200 μg mL^{-1} crude ulvan extracted from *U. intestinalis* stimulated the production of pro-inflammatory cytokines TNF-α and IL-1β to a similar degree as the LPS (1 μg mL^{-1}) positive control (Peasura *et al.*, 2016). A similar pro-inflammatory response was also recorded when peritoneal macrophages

from male ICR mice were treated with crude ulvan (100-400 µg mL^{-1}) from *U. intestinalis* (Jiao *et al.*, 2009). Ulvan from *U. ohnoi* also stimulated head kidney macrophages from *Solea senegalensis* (sole fish) (Fernández-Díaz *et al.*, 2017). Overall, ulvans induce a pro-inflammatory response in animal macrophages with potential for application in animal and human supplements as non-specific immunostimulants.

The effect of ulvan on the immune response has also been investigated in fish (Castro *et al.*, 2006; Fernández-Díaz *et al.*, 2017), porcine (pig) intestinal epithelial cells (Berri *et al.*, 2017; Berri *et al.*, 2016), rats (Abd-Ellatef *et al.*, 2017; de Araújo *et al.*, 2016), mice (de Araújo *et al.*, 2016; Jiao *et al.*, 2009; Wei *et al.*, 2014; Zhu *et al.*, 2017) and chickens (Hong *et al.*, 2011). Despite the range of organisms assessed and extraction techniques applied, ulvan is consistently reported to increase mRNA expression (Berri *et al.*, 2017; Berri *et al.*, 2016; Castro *et al.*, 2006) and promote the release of immunomodulating cytokines or enzymes (Abd-Ellatef *et al.*, 2017; Fernández-Díaz *et al.*, 2017; Wei *et al.*, 2014). For example, a porcine intestinal epithelial (IPEC-1) cell line treated with purified low molecular weight (4.4 kDa) ulvan (5-500 µg mL^{-1}) from *U. armoricana* increased the mRNA and the protein expression of cytokines (e.g., CCL20, IL-8 and TNF-α) (Berri *et al.*, 2017). In mechanistic studies conducted by incubating human embryonic kidney (HEK) 293 cells with ulvan (500 µg mL^{-1}), ulvan primarily stimulated TLR4, with a subsequent increase in protein kinase B (Akt) phosphorylation, which activates NF-kB leading to the production of inflammatory cytokines. A similar response was recorded for LPS-treated (100 ng mL^{-1}) cells. Increased production of NF-kB was also reported in thymus and spleens of mice (Kunming) treated with ulvan from *U. prolifera* (Wei *et al.*, 2014). These mechanistic insights are an important consideration in the development of new supplement (nutraceutical or therapeutic) products for animal and human use.

The immunomodulating activity and potency of ulvan varies significantly between studies of the same species, and between different species. While there is evidence that this variability is due to structural features, some is related to sample purity. In this regard, a significant increase in the potency of the immunomodulatory activity of ulvan from *U. intestinalis* occurs following purification of a crude extract (Jiao *et al.*, 2009; Peasura *et al.*, 2016; Tabarsa *et al.*, 2018). However, the structural features of ulvan (e.g., molecular weight

and sulfation) also influence potency. For example, the molecular weight of purified ulvan extracted from *U. pertusa* is an important determinant for RAW 264.7 macrophage activation, with higher molecular weight fractions (1450 kDa and 1690 kDa) leading to >2-fold increase in macrophage activation compared to a lower molecular weight fraction (365 kDa) (Tabarsa *et al.*, 2012a). An even more pronounced decrease in head kidney macrophages stimulation was measured for low molecular weight (5.92 kDa) ulvan from *U. ohnoi* over high molecular weight ulvan (698 kDa) (Fernández-Díaz *et al.*, 2017). However, a study with ulvan from *U. intestinalis* gave contradictory results with a lower molecular weight sample (28.7 kDa) having significantly higher immunomodulatory activity than a higher molecular weight sample (87.2 kDa). This highlights the importance of the interaction of the structural features of ulvan, such as the molecular weight and degree of sulfation, in determining bioactivity (Tabarsa *et al.*, 2018). Although molecular weight is considered a major factor affecting immunomodulatory activity, there is also an effect of the degree of sulfation between the high (24.5 % w/w) and low (6.25 % w/w) molecular weight samples (Tabarsa *et al.*, 2018). The level of sulfation is often positively correlated with activity in ulvan and related sulfated polysaccharides (e.g., λ-carrageenan and fucoidan). For example, de-sulfation (partial sulfate ester removal) of ulvan from *U. rigida* resulted in an ~50 % reduction in its immunomodulatory effect on RAW 264.7 macrophages (Leiro *et al.*, 2007) and Turbot peritoneal leucocytes (Castro *et al.*, 2006), when compared to native ulvan. So far, the studies that have investigated the influence of the structural features of ulvan on its effect on inflammation show that structure-activity correlations are species specific and further studies investigating the structure-activity relationships of ulvans across species are required to elucidate the key structural features driving activity. The latter informs the selection of species for cultivation, extraction procedures of ulvan, and post-extraction modifications, with a focus of enhancing activity as a non-specific immunomodulatory agent.

2.3.4 Antioxidant activity

Reactive Oxygen Species (ROS) and Reactive Nitrogen Species (RNS) are constantly formed in vivo in living tissue by aerobic biogenesis or by oxidative enzymes (e.g., in response to foreign organisms) (Birben, Sahiner, Sackesen, Erzurum, & Kalayci, 2012; Nimse & Pal, 2015). These highly reactive species attack all major classes of biomolecules, including lipids, DNA, proteins, and sugars. Oxidative stress has been implicated in a host of disorders

including inflammatory diseases, neurodegenerative diseases, cancer, cardiovascular diseases, and aging processes. The body has several endogenous enzymatic antioxidant systems to overcome excessive ROS/RNS-mediated damage, including superoxide dismutase (SOD), catalase (CAT), glutathione peroxidase (GSH-Px), glutathione reductase and glucose-6-dehydrogenase, and non-enzymatic antioxidants including glutathione, uric acid, lipoic acid, NADPH, coenzyme Q, albumin, and bilirubin (Bouayed & Bohn, 2010). There are also exogenous antioxidants, including vitamins C and E, carotenoids, phenolic compounds, and trace elements (e.g., zinc and selenium) that play an essential role as antioxidants in living organisms. Food-based protein and polysaccharides also contribute to the antioxidant capacity of organisms, by acting as exogenous antioxidants and enhancing endogenous antioxidants (Forman, Davies, & Ursini, 2014). In this regard, the antioxidant capacity of ulvan is mediated by radical scavenging and subsequent inhibition of lipid peroxidation, and the enhancement of antioxidant enzyme (e.g., SOD, CAT and GSH-Px) activities.

The exogenous anti-oxidant capacity of ulvan has been extensively assessed with in vitro assays using 1,1-diphenyl-2-picryl hydrazil (DPPH) radical scavenging, superoxide scavenging, ferric reducing antioxidant power (FRAP), hydroxyl radical scavenging, and lipid peroxide inhibition. Sulfate content and molecular weight have a significant effect on the anti-oxidant effect of sulfated polysaccharides from macroalgae (Wijesekara *et al.*, 2011). In this regard, chemically over-sulfated (32.8 % w/w sulfate) ulvan from *U. pertusa* had ~90 % hydroxyl radical scavenging at 2.0 mg mL^{-1} compared to ~45 % at 2.0 mg mL^{-1} of native ulvan (19.5 % w/w sulfate) (Qi *et al.*, 2005a). Similarly, radical scavenging is higher for over-sulfated ulvan from *U. linza* compared to its native form (Zhang *et al.*, 2011). Low molecular weight ulvan also has higher antioxidant capacity relative to higher molecular weight fractions (Qi *et al.*, 2005b; Zhang *et al.*, 2013). For example, a negative correlation was recorded between hydroxyl radical scavenging (~50-90 %) and the molecular weight of ulvan (18.2-100.5 kDa) (Zhang *et al.*, 2013). This correlation may not be a general trend (Yaich *et al.*, 2017), however, and highlights that comparative extraction conditions, purification protocols, and test protocols are necessary before concluding an overall and consistent structure-activity trend for the anti-oxidant activity of ulvan.

Although ulvan has direct ROS/RNS scavenging activity, it is its capacity to enhance the expression of the enzymatic components of the endogenous antioxidant system that affects animal health the most by ameliorating the propagation of diseases relating to oxidation. Determination of the antioxidant effects of ulvan in vivo has been made by measuring enzymatic antioxidant activities (e.g., SOD, CAT, and GSH-Px) and oxidation products (e.g., malondialdehyde (MDA) as a product of the peroxidation of polyunsaturated fatty acids; GSSH; oxidised glutathione). In this regard, ulvan from *U. lactuca* (Abd-Ellatef *et al.*, 2017; Hussein *et al.*, 2015; Sathivel *et al.*, 2014), *U. pertusa* (Hong *et al.*, 2011; Li *et al.*, 2018c; Qi & Sun, 2015), *U. armoricana* (Berri *et al.*, 2017), *U. fasciata* (Rizk *et al.*, 2016a; Rizk *et al.*, 2016b) and *U. prolifera* (Wei *et al.*, 2014) mitigate the production of oxidation products and enhance antioxidant enzyme activity in vitro and in vivo. For example, treatment of hyperlipidemic Kunming mice with ulvan from *U. pertusa* resulted in a reduction of MDA (29.2 %) and increases in SOD (35.4 %) and CAT (43.6 %) relative to untreated mice (Li *et al.*, 2018c). Interestingly, a fraction with a molecular weight of 83 kDa exhibited higher antioxidant activity than higher molecular weight fractions (e.g., 190 kDa and 201 kDa). These findings were corroborated in a study of the effect of ulvan on egg quality and the health of laying hens (Li *et al.*, 2018b). Hens fed a diet supplemented with 1 % ulvan showed significantly reduced serum MDA levels and increases in CAT and SOD. Ulvan treated hen groups also had increased levels of cytokines IL-6 and IFN-γ indicative of the close link between the expression of antioxidant enzymes and immune system responses. A single study demonstrated that oversulfated ulvan from *U. pertusa* had a greater capacity to influence antioxidant defence system markers (e.g., MDA, SOD, GSH-Px and CAT) in hyperlipidemic rats relative to native ulvan (Qi & Sun, 2015). Tentatively, ulvans with high sulfate content and lower molecular weights are most effective at ameliorating oxidative stress in vivo.

The mechanistic rationale for these findings is generally due to radical scavenging activity (Hussein *et al.*, 2015; Li *et al.*, 2018d; Qi & Sun, 2015; Sathivel *et al.*, 2014). However, the capacity for exogenous antioxidants to significantly contribute to radical scavenging in vivo and, therefore, act as an antioxidant endogenously, has been questioned (Forman *et al.*, 2014). Furthermore, it was suggested that food-derived antioxidants, like ulvan, act by influencing signalling pathways that lead to the expression of the enzymes involved in the antioxidant defence system. Notably, phytochemicals, including ulvan (Li *et al.*, 2018c; Qi &

Sun, 2015), porphyran (Zhang *et al.*, 2003), and fucoidan (Phull & Kim, 2017), have demonstrated their capacity to regulate antioxidant enzyme expression (Lei *et al.*, 2016). Ulvan is most likely to enhance antioxidant enzyme activity by activating the transcription enzymes (e.g., Nrf2, NF-kB, AP-1, AP-2, Sp1 and C/EBP) involved in the expression of antioxidant enzymes (Forman *et al.*, 2014; Miao & St Clair, 2009). For example, ulvan from *U. armoricana* stimulates the TLR4 receptor in vitro, which results in the activation of NF-kB and the subsequent upregulation of TNF-α (Berri *et al.*, 2017), a cytokine that modulates the expression of SOD (Miao & St Clair, 2009). However, further research on the mechanism(s) by which ulvan influences the expression of antioxidant enzymes is required to identify the signalling pathway(s) involved. In summary, the capacity of ulvans to boost the endogenous antioxidant system protects the body against toxic oxidation products that cause disease, such as chronic inflammation and cancer.

2.3.5 Anticancer

The development of cancer is a multistep process initiated by endogenous and exogenous factors, which often lead to oxidative attack on DNA, resulting in mutations that disrupt the normal regulatory pathways between cell proliferation, differentiation, and apoptosis (Valko, Izakovic, Mazur, Rhodes, & Telser, 2004). There are a growing number of studies showing that ulvan acts as an anti-proliferation agent and promotes apoptosis in cancerous cells. Ulvans from *U. lactuca* (Abd El-Baky *et al.*, 2009; Ahmed & Ahmed, 2014; Hussein *et al.*, 2015; Kaeffer *et al.*, 1999; Thanh *et al.*, 2016), *U. intestinalis* (Jiao *et al.*, 2009; Matloub *et al.*, 2016; Matloub *et al.*, 2018; Wang *et al.*, 2014b), *U. pertusa* (Tabarsa *et al.*, 2012a), *U. prolifera* (Cho *et al.*, 2010), U*. tubulosa* (Hu, Hong, Cheng, Liao, & Li, 2018) and *U. fasciata* (Shao *et al.*, 2013b; Shao *et al.*, 2014a) all demonstrate anticancer activities for a range of cancer models with murine sarcoma cancer cell line S180 (Jiao *et al.*, 2009), human cancer cell lines (e.g., HepG2 (hepatocellular carcinoma) (Abd El-Baky *et al.*, 2009; Ahmed & Ahmed, 2014; Kaeffer *et al.*, 1999; Thanh *et al.*, 2016; Wang *et al.*, 2014b), MCF7 (human breast cancer) (Hu *et al.*, 2018; Thanh *et al.*, 2016), HeLa (cervical cancer) (Thanh *et al.*, 2016), AGS (human gastric carcinoma) (Cho *et al.*, 2010; Tabarsa *et al.*, 2012a), MKN45 (human gastric cancer) (Shao *et al.*, 2013b), HT-29 (human colon carcinoma) (Ahmed & Ahmed, 2014; Kaeffer *et al.*, 1999), HCT-116 (human colon carcinoma), Caco-2 (human colon carcinoma)

(Ahmed & Ahmed, 2014; Kaeffer *et al.*, 1999), DLD1 (human colon carcinoma) (Cho *et al.*, 2010; Shao *et al.*, 2013b; Shao *et al.*, 2014a)) and some cancers in animal models (e.g., rats (Abd-Ellatef *et al.*, 2017; Hussein *et al.*, 2015; Matloub *et al.*, 2016), mice (Jiao *et al.*, 2009)). However, no clinical human trials have yet been conducted.

The anticancer activity of ulvan from different sources is highly variable. For example, ulvan from *U. lactuca* has significant cytotoxic activity against a number of human cancer cell lines including HepG2 (hepatocellular carcinoma), MCF7 (breast cancer), and HeLa (cervical cancer) (Thanh *et al.*, 2016). Ulvan at a concentration of 100 μg mL^{-1} reduced the in vitro cell viability of all three cancer cell lines to 0 %. Although a mechanism of action was not proposed, similar studies of anti-tumour effects of ulvan on HepG2 and MCF-7 cell-lines noted the increased expression of the pro-apoptotic tumour suppressor p53, and reduced expression of anti-apoptotic protein Bcl-2, supporting the conclusion that ulvan promotes programmed cell death (apoptosis) (Abd-Ellatef *et al.*, 2017; Ahmed & Ahmed, 2014; Wang *et al.*, 2014b). The antiproliferation activity of ulvan from *U. lactuca* also reduces levels of proliferating cell nuclear antigen (PCNA) in rat hepatocytes which is indicative of the reduced DNA replication associated with lower proliferation (Hussein *et al.*, 2015). It is also important to note that many studies have registered only very low to moderate cytotoxic activity relative to traditional chemotherapy drugs (Cho *et al.*, 2010; Jiao *et al.*, 2009; Matloub *et al.*, 2016; Shao *et al.*, 2013b; Tabarsa *et al.*, 2012a). For example, ulvan from *U. prolifera* only had low anticancer activity on human gastric carcinoma (AGS) and human colon cancer (DLD-1) cell lines, with dose dependent inhibition of AGS cell proliferation of 10-26 % with concentrations of 200-1000 μg mL^{-1} (Cho *et al.*, 2010). These results do not necessarily preclude the relevance of ulvan in anticancer therapies. For example, ulvan from *U. intestinalis* also had no cytotoxic effects on sarcoma 180 tumour cells in vitro at 50-800 μg mL^{-1}, but reduced sarcoma 180 tumour weight in vivo by 61 -71 % in mice dosed with 100-400 mg kg^{-1} (Jiao *et al.*, 2009). In combination with the latter, important immune organs (e.g., thymus and spleen) were enlarged in ulvan treated mice, supporting the suggestion that the antitumour activity of this polysaccharide originates from its immunomodulatory activity. In summary, the anticancer activity of ulvan appears to operate through one or more of a number of pathways, including the promotion of cancer cell apoptosis, reduction in cancer cell proliferation, and stimulation

of the innate immune response. Furthermore, the pathways affected are dependent on the source and/or structure of the ulvan.

There are preliminary results suggesting that both molecular weight and degree of sulfation influence the anticancer activity of ulvan (Cho *et al.*, 2010; Kaeffer *et al.*, 1999; Matloub *et al.*, 2016; Shao *et al.*, 2014a). However, at this point there are no conclusive interpretations that can be made with respect to the effect of the structure of ulvan on its anticancer activity. The generally low anti-proliferation activity of ulvan means that ulvan is unlikely to replace established chemotherapy drugs but might find application as a co-treatment, due to its broad-spectrum chemopreventative activities (e.g., immunomodulatory, antioxidant, and anticancer) (Abd-Ellatef *et al.*, 2017; Gerhauser *et al.*, 2002). There are also interesting potential applications for ulvan in cancer therapy. For example, as nanoparticle drug delivery systems for hydrophobic anti-tumour drugs (Li *et al.*, 2018a), selenium enriched polysaccharide-protein complexes for cancer treatment (Sun, Zhong, Luo, & Yang, 2017), and pH responsive polysaccharide nanosystems that inhibit angiogenesis (Yang, Fang, Jiang, & Chen, 2017). However, before ulvan can find applications as a co-treatment or adjunct in anticancer technologies, there is a need to ascertain the bioavailability of ulvan and whether ulvan influences the efficacy of traditional chemotherapy drugs in combination therapies.

2.3.6 Anticoagulant activity

The coagulation cascade is activated by two pathways, the intrinsic and extrinsic pathway, both culminating in the production of thrombin through a final, common pathway (Rang *et al.*, 2016). Briefly, this process involves the progressive activation and amplification of serine proteases (e.g., XIII, XII, XI, IX, X and VII) and glycoproteins, collectively termed “factors”, present within the blood. The intrinsic activation pathway is initiated when factor XII is activated by contact with an anionic surface, while activation of the extrinsic pathway occurs when factor XIII binds with tissue factor (a transmembrane receptor) released from damaged cells. Both intrinsic and extrinsic pathways lead to the activation of factor X, mobilising the common pathway and catalysing the conversion of prothrombin to thrombin, and subsequently soluble fibrinogen to insoluble fibrin that facilitates a clot. Anticoagulant compounds can inhibit all three of the above-mentioned pathways. For example, ulvan

generally inhibits coagulation through the intrinsic and/or common pathways (Adrien *et al.*, 2017b; Cui *et al.*, 2018; Faggio *et al.*, 2016; Guerra-Rivas *et al.*, 2011; Mao *et al.*, 2006; Qi *et al.*, 2012a; Qi *et al.*, 2013b; Synytsya *et al.*, 2015; Wang *et al.*, 2013b), while heparin can inhibit intrinsic, extrinsic, and common pathways. Mechanistic details regarding the anticoagulant activity of ulvans, and other potential anticoagulants, are commonly elucidated using three tests, the activated partial thromboplastin time (aPTT), thrombin time (TT) and prothrombin time (PT), which determine if inhibition acts on the intrinsic and/or common pathways, common pathway, and extrinsic pathway, respectively.

Ulvan extracts from *U. clathrata* (Qi *et al.*, 2012a), *U. lactuca* (Adrien *et al.*, 2017b; Shanmugam *et al.*, 2001), *U. prolifera* (Cui *et al.*, 2018), *U. fasciata* (Faggio *et al.*, 2016; Shanmugam *et al.*, 2001), *U. nematoidea* (Guerra-Rivas *et al.*, 2011) *U. conglobata* (Mao *et al.*, 2006), *U. linza* (Qi *et al.*, 2013b; Wang *et al.*, 2013b), *U. reticulata* (Shanmugam *et al.*, 2001) and *Capsosiphon fulvescens* (Synytsya *et al.*, 2015) have demonstrated anticoagulant activity. For example, ulvan from *U. linza* led to a 3.3-6.2-fold increase in aPTT times relative to normal clotting times, and is dependent on the degree of sulfation and molecular weight (Wang *et al.*, 2013b). With regards to the latter, a hydrolysed ulvan sample (M_w = 11 kDa; SO_4^{2-} = 20.1 %) increased aPTT by 63 % compared to the native ulvan extract (M_w = 108 kDa; SO_4^{2-} = 21.3 %), while oversulfation of the hydrolysed sample (SO_4^{2-} = 34.4 %) led to a further 20 % increase in aPTT. While similar structure-activity relationships occur for TT, there is minimal PT activity reported. However, data from a study aiming to optimise the enzymatic extraction of ulvan from *U. prolifera* with the intent to optimise anticoagulant activity demonstrated an interaction between degree of sulfation and molecular weight (Cui *et al.*, 2018). Namely, increasing sulfation led to high anticoagulant activity until a molecular weight threshold (<200 kDa) was reached, after which there was a complete loss of activity (Cui *et al.*, 2018). In summary, the anticoagulant activity of ulvan is dependent on degree of sulfation and molecular weight (Cui *et al.*, 2018; Mao *et al.*, 2006; Qi *et al.*, 2013b; Qi *et al.*, 2012c; Wang *et al.*, 2013b), with a higher degree of sulfation enhancing anticoagulant activity. The relationship between molecular weight and anticoagulant activity remains unclear, and this may also be dependent on the source of the ulvan.

The potency of the anticoagulant activity of ulvan is dependent on species and ecophysiological factors, which directly affect the structure of ulvan (Mao *et al.*, 2006; Qi *et*

al., 2013b). The anticoagulant activities for ulvan isolated from different biomass sources are between ~2-40 times less active than heparin. For example, one of the better performers was a highly sulfated ulvan fraction (SO_4^{2-} = 35.2 %) isolated from *U. conglobata* (Mao *et al.*, 2006). This sample at 2 µg mL^{-1} yielded a 2.5-fold increase in aPTT compared to a 6.2-fold increase in aPTT for 2 µg mL^{-1} of heparin. While the latter highlights the potential of ulvan as an anticoagulant, the overall efficacy of ulvan relative to commercial drugs, like heparin, is less than these previous results indicate, as it only acts on two of the three coagulation pathways. This does not diminish the relevance of the anticoagulant activity of ulvan or its capacity to be used in the preparation of anticoagulants. For example, ulvan acts on the intrinsic pathway, which activates multiple pro-inflammatory, pro-coagulant, and immunomodulating pathways (Long, Kenne, Jung, Fuchs, & Renné, 2016).

2.3.7 Antihyperlipidemic

The human body has a sophisticated lipoprotein transport system that utilises triglyceride (TG) rich, very low-density lipoprotein-cholesterol (VLDL) to shuttle fatty acids to adipocytes and muscle, resulting in cholesterol rich, low-density lipoprotein-cholesterol (LDL-C) that distributes cholesterol for steroidogenesis and cell membranes (Lee, Olson, & Evans, 2003). Excess cholesterol is transported back to the liver by high-density lipoprotein-cholesterol (HDL-C) for recycling or conversion to bile acids (BA) followed by its removal from the body. Imbalances in the lipoprotein transport system are linked to metabolic syndrome. Patients with metabolic syndrome are often hyperlipidaemic, a condition characterised by abnormally high blood levels of lipid(s) and lipoprotein(s), which can lead to cardiovascular diseases, such as coronary artery disease and atherosclerosis. Importantly, the consumption of macroalgae and the associated sulfated polysaccharides, including ulvan, has demonstrated antihyperlipidemic activity in vivo (Jiao *et al.*, 2011; Mohamed, Hashim, & Rahman, 2012; Wang, Wang, Wu, & Liu, 2014a).

To measure the antihyperlipidemic activity of foods and supplements, such as sulfated polysaccharides, the serum total cholesterol (TC), TG, HDL-C and LDL-C of hyperlipidemic rat and mice models are commonly assessed (Hassan *et al.*, 2011; Pengzhan *et al.*, 2003a; Pengzhan *et al.*, 2003b; Qi *et al.*, 2012a; Qi & Sheng, 2015; Qi *et al.*, 2012b; Rizk *et al.*, 2016a). Using these parameters ulvan from *U. pertusa* (Li *et al.*, 2018c; Li *et al.*, 2018d; Pengzhan *et*

al., 2003a; Pengzhan *et al.*, 2003b; Qi *et al.*, 2012a; Qi *et al.*, 2013a; Qi & Sheng, 2015; Qi *et al.*, 2012b; Qi & Sun, 2015), *U. fasciata* (Borai *et al.*, 2015; Matloub *et al.*, 2015; Rizk *et al.*, 2016a; Rizk *et al.*, 2016b), *U. lactuca* (Hassan *et al.*, 2011; Sathivel *et al.*, 2008), *U. prolifera* (Ren *et al.*, 2017; Teng *et al.*, 2013) and *Monostroma nitidum* (Hoang, Kim, Lee, You, & Lee, 2015) have significant antihyperlipidemic activity, reducing or maintaining low levels of TC, TG, LDL-C, and increasing or maintaining a high level of HDL-C. Both molecular weight and degree of sulfation influence this activity. For example, Wistar rats fed a high starch feed supplemented with native ulvan (151.6 kDa) from *U. pertusa* had significant reductions in serum TC (45 %) and LDL-C (54 %), with no significant effect on TG and HDL-C compared to control rats fed the same high starch diet (Pengzhan *et al.*, 2003a). However, rats fed high starch diets with low molecular weight ulvan (28.2 kDa) showed no effect on either TC or LDL-C but significantly reduced TG (78 %) and raised HDL-C (61 %) relative to control fed rats, the mechanisms of which are discussed below (Li *et al.*, 2018c). There is some early evidence that a higher degree of sulfation may enhance the antihyperlipidemic activity (Qi & Sheng, 2015). For example, the serum TC of female rats treated with native ulvan (SO_4^{2-} = 22.5 %) at 250 mg kg^{-1} was reduced by 28 %, while treatment with oversulfated ulvan (SO_4^{2-} = 40.6 %) reduced serum TC by 44 % relative to the hyperlipidemic control group (Qi & Sheng, 2015). Derivatisation of native ulvan (e.g., acetylation) also influences antihyperlipidemic activity (Qi *et al.*, 2012b). However, interactions between the degree of substitution and molecular weight are unclear and need to be understood to optimise structures that affect higher antihyperlipidemic activity.

The effect of molecular weight on the parameters used to assess antihyperlipidemic activity supports the conclusion that several mechanisms are operating in parallel. It has been proposed that reduction in serum TC and LDL-C in ulvan supplemented hyperlipidemic rats results in LDL-C conversion to bile acid in the liver followed by excretion (Pengzhan *et al.*, 2003a). This is further supported by an increase in faecal bile acid concentrations in ulvan supplemented hyperlipidemic rats. In contrast, supplementation of hyperlipidemic rats with lower molecular weight ulvan (28.2 kDa) had no effect on either TC or LDL-C but had elevated faecal bile acids and reduced TG and raised HDL-C relative to control fed rats (Pengzhan *et al.*, 2003a), suggesting that other mechanisms, such as the upregulation of the synthesis of cholesterol in the liver, are also important. Treatment of lipid-loaded hepatocytes with an

ulvan-like polysaccharide from *Monostroma nitidum* resulted in lower lipid concentrations accompanied with downregulation of the cholesterol synthesis gene for 3-hydroxy-3-methyl-glutaryl-CoA (HMG-CoA) reductase, upregulation of the cholesterol catabolism gene for cholesterol-7-α-hydroxylase (CYP7A1), and LDL uptake gene for LDL-receptor (Hoang *et al.*, 2015). To corroborate these results, reduced serum TC concentrations measured in ulvan (*U. prolifera*) treated rats downregulated HMG-CoA reductase and the cholesterol regulating transcription factor sterol regulatory element binding protein 2 (SREBP-2) (Ren *et al.*, 2017). In a later study, reduced serum TG concentrations measured in ulvan treated rats were accompanied by downregulation of acetyl-CoA carboxylase (ACC) and its regulating transcription factor, SREBP-1c (regulates fatty acid synthesis) (Ren *et al.*, 2018). In theory, structurally different ulvan fractions may influence the regulatory genes (SREBP-1c and SREBP-2) to varying degrees, helping to explain the contradictory results obtained by Pengzhan *et al.* (2003a). Evidence for another alternative or additional mechanism suggests that antioxidant effects may contribute to the antihyperlipidemic effects of polysaccharides (Ali & Agha, 2009; Gesquière, Loreau, Minnich, Davignon, & Blache, 1999). In this mechanism, molecules with high antioxidant capacity (or those that can upregulate the endogenous antioxidant system) limit lipid oxidation by ROS, which leads to the accumulation of cholesterol due to changes in its biosynthesis and metabolism. In summary, the antihyperlipidemic activity of ulvan appears to operate by multiple mechanisms in parallel, the balance of which depends on the structural features of ulvan. This provides opportunity to optimise antihyperlipidemic supplements for more targeted applications.

2.3.8 Anti-viral

Viral treatments target the multiple steps in the viral replication cycles, which may be broadly thought of as entry, replication, shedding, and latency. Sulfated polysaccharides derived from marine algae, including ulvan, have promising antiviral activities (Damonte, Matulewicz, & Cerezo, 2004; Shi *et al.*, 2017b; Witvrouw & De Clercq, 1997). Ulvans from *U. compressa* (Lee, Hayashi, Maeda, & Hayashi, 2004; Lopes *et al.*, 2017) *U. lactuca* (Abd El-Baky *et al.*, 2009; Chiu *et al.*, 2012; Jiao *et al.*, 2012), *U. clathrata* (Aguilar-Briseño *et al.*, 2015), *U. intestinalis* (Morán-Santibañez *et al.*, 2016), *U. armoricana* (Hardouin *et al.*, 2016) and *U. pertusa* (Song *et al.*, 2016) all have antiviral activity. The antiviral activity of ulvan extends to

the enveloped viruses of herpes simplex virus (HSV) (Hardouin *et al.*, 2016; Lee *et al.*, 2004; Lopes *et al.*, 2017), Newcastle disease virus (NDV) (Aguilar-Briseño *et al.*, 2015), Japanese encephalitis virus (JEV) (Chiu *et al.*, 2012), dengue virus (DENV) (Chiu *et al.*, 2012), yellow fever virus (YFV) (Chiu *et al.*, 2012), West Nile virus (WNV) (Chiu *et al.*, 2012), influenza (H1N1) (Jiao *et al.*, 2012), avian influenza virus (AIV) (Song *et al.*, 2016) and measles virus (MeV) (Morán-Santibañez *et al.*, 2016). Examination of the antiviral activity of ulvan has been conducted in vitro using human larynx epithelial carcinoma cells (Hep-2) (Lopes *et al.*, 2017), African green monkey cells (Vero) (Abd El-Baky *et al.*, 2009; Aguilar-Briseño *et al.*, 2015; Hardouin *et al.*, 2016; Morán-Santibañez *et al.*, 2016), canine kidney cells (MDCK) (Jiao *et al.*, 2012), and in vivo using mouse models (Chiu *et al.*, 2012; Song *et al.*, 2016).

The antiviral effects of native ulvans against viral targets (measured as 50 % Inhibitory Concentration [IC_{50}], the concentration of ulvan required to inhibit viral yield by 50 %) are mixed ranging from weak (IC_{50} > 150 µg mL^{-1} (Jiao *et al.*, 2012; Lopes *et al.*, 2017)) to significant (IC_{50} = 0.1 – 30 µg mL^{-1} (Aguilar-Briseño *et al.*, 2015; Chiu *et al.*, 2012; Morán-Santibañez *et al.*, 2016)). There are some interesting results supporting the use of ulvan in antiviral therapies. Ulvan from *U. clathrata* is an effective anti-viral for NDV, a fatal virus found in chickens, causing large anthropogenic food losses (Aguilar-Briseño *et al.*, 2015). Treatment with ulvan provided a concentration-dependent inhibition of NDV entry into Vero cells with an IC_{50} of 0.1 µg mL^{-1}. The activity was related to inhibition of an entry protein known as NDV fusion protein F. Although ulvan from *U. pertusa* had only moderate antiviral activity (40 % inhibition at 100 µg mL^{-1}) against AIV-H9N2, it had a beneficial effect in a test relevant to immunisation (Song *et al.*, 2016), where AIV-H9N2 vaccination combined with ulvan treatment (50 mg kg^{-1}) led to an ~100 % increase in antibody titre relative to the vaccination alone. This effect was attributed to the enhancement of the humoral immune response, due to the immunomodulatory effects of ulvan.

Variations in the antiviral activity of ulvan from different sources indicate a significant effect of structure; however, there are only a limited number of studies that probe the antiviral activity of ulvan and, consequently, the understanding of its structure-activity relationships is limited. However, the required structural features of ulvan are essentially similar to other sulfated polysaccharide antivirals, where activity is optimised by a high degree of sulfation and high molecular weight (Ghosh *et al.*, 2009; Witvrouw & De Clercq, 1997). In

this regard, treatment of HSV infected Hep-2 cells with a highly sulfated (SO_4^{2-} = 22 %) ulvan fraction from *U. compressa* resulted in 100 % HSV inhibition at 100 µg mL^{-1} and had an IC_{50} of 28.2 µg mL^{-1}, compared to 153 µg mL^{-1} for native ulvan (SO_4^{2-} = 6 %) (Lopes *et al.*, 2017). Furthermore, ulvan with higher molecular weights (34 kDa) had 2-5 times the antiviral activity of low molecular weight ulvan (<5 kDa). However, further studies are required to verify the generality of these results. In summary, the investigation of ulvan as an antiviral is in its infancy and at this point ulvan has variable antiviral activity against specific targets, with promise as an immunostimulant co-treatment for vaccinations.

2.3.9 Plant defence

More recently, ulvans have been found to also influence the signalling pathways involved in plant immunity. The effect that ulvans have on plant immunity has been investigated *in vitro* with cell cultures (e.g., wheat and rice) (Paulert *et al.*, 2010) and in vivo with various non-cropping (e.g., thale cress) and cropping (e.g., apples, beans, wheat and barley) plant species (Araujo, Goncalves, & Stadnik, 2014; Castellanos-Barriga, Santacruz-Ruvalcaba, Hernández-Carmona, Ramírez-Briones, & Hernández-Herrera, 2017; Cluzet *et al.*, 2004; de Freitas *et al.*, 2015; de Freitas & Stadnik, 2012; Delgado, de Freitas, & Stadnik, 2013; El Modafar *et al.*, 2012; Jaulneau *et al.*, 2010; Paulert *et al.*, 2010; Paulert *et al.*, 2009). Ulvans from *U. fasciata* (Araujo *et al.*, 2014; de Freitas *et al.*, 2015; de Freitas & Stadnik, 2012; Delgado *et al.*, 2013; Paulert *et al.*, 2010; Paulert *et al.*, 2009), *U. lactuca* (Castellanos-Barriga *et al.*, 2017; El Modafar *et al.*, 2012) and *U. armoricana* (Cluzet *et al.*, 2004; Jaulneau *et al.*, 2010) all enhance the inducible defences of plants, a phenomenon known as “priming”. Inducible plant defences operate by the initial recognition of microbe/pathogen-associated molecular patterns (MAMPs/PAMPs), or elicitors, by plant cell membrane bound pattern-recognition receptors (PRRs), known as MAMP/PAMP-triggered immunity (MTI/PTI). Plants also have resistance (R) genes that encode cytoplasmic receptors that recognise pathogen effector molecules designed to suppress PTI, known as Effector-Triggered Immunity (ETI) (Jones & Dangl, 2006; Robert-Seilaniantz, Grant, & Jones, 2011). Plant immune responses downstream of MTI/PTI and ETI include the production of pathogenesis-related proteins that hydrolyse pathogen cell wall constituents, plant cell wall fortification through synthesis of lignin and callose, and the production of antimicrobial secondary metabolites (Burketova,

Trda, Ott, & Valentova, 2015; Pieterse, Leon-Reyes, Van der Ent, & Van Wees, 2009). An additional response unique to ETI is the Hypersensitive Response (HR), which is instigated by a pulse in the production of Reactive Oxygen Species (ROS), triggering localised cell death at the site of infection. MTI/PTI and ETI also trigger Systemic Acquired Resistance (SAR), where the defence alert is transferred from the site of pathogen ingress to distal plant tissues leading to an alert (or primed) state that is more responsive to subsequent pathogen attacks (Conrath *et al.*, 2006). These plant immune responses are orchestrated by a complex balance of phytohormones (e.g., salicylic acid, jasmonic acid, ethylene and abscisic acid, cytokinins, auxins, brassinosteroids, and gibberellins) dependent on the identity of the pathogen and its trophic lifestyle (i.e., biotrophic *vs.* necrotrophic) (Robert-Seilaniantz *et al.*, 2011). Therefore, a great deal of information can be found by studying how the balance of molecules involved in the plant immune response is affected by treatment with potential priming agents, such as ulvan.

The effect of ulvan treatment on plant immunity has been investigated using pathogen and plant based measures including pathogen growth and development, plant health measures, such as growth, spotting and wilting, and molecular probes/profiles, such as hormones, proteins, and DNA. Ulvan from *U. fasciata* inhibits a key stage (appressoria differentiation) in the pathogenic cycle of the anthracnose causing fungi *Colletotrichum gloeosporioides* (Araujo *et al.*, 2014). Consistent with a priming effect in vivo, tests on ulvan pre-treatment on apple leaves reduced disease severity by as much as 50 % over control plants. Similar results were obtained when ulvan (from *U. fasciata*) treated *Arabidopsis thaliana* (thale cress) was inoculated with either *Alternaria brassicicola* (black spot fungi) or *Colletotrichum higginsianum* (anthracnose fungi) (de Freitas *et al.*, 2015). Interestingly, the degree of sulfation did not influence pathogenesis. However in another study, desulfation of ulvan from *U. lactuca* significantly reduced its capacity to induce the production of the defence enzyme, phenylalanine ammonia-lyase (PAL) (El Modafar *et al.*, 2012). In this study, a >2-fold increase in the activity of PAL occurred when tomato plants were treated with ulvan oligomers relative to native ulvan (El Modafar *et al.*, 2012). Increased PAL activity was accompanied by an increase in salicylic acid. Therefore, in this case induction of SAR appears to be salicylic acid dependent. However, a study using transcriptomics combined with hormone profiling and enzyme activity measurements found that ulvan from *U. armoricana*

induced plant immunity via the jasmonic acid signalling pathway in *Medicago truncatula* (Fabaceae), *Nicotianae tabacum* (Solanaceae), and *Arabidopsis thaliana* (Brassicaceae) (Jaulneau *et al.*, 2010). Salicylic acid concentrations were unaffected by ulvan treatment, while jasmonic acid concentrations increased relative to control plants. Furthermore, the mode of action of ulvan was verified by its capacity to induce the expression of jasmonic acid-dependent genes (e.g., PDF1.2 defensin and lipoxygenase NtLOX1 promoter), while failing to induce the expression of salicylic acid-dependent genes (e.g., PR1a and PR5). Regardless of the signalling pathways responsible, ulvan demonstrates significant activity as a bio-elicitor and capacity to act as a priming agent enhancing both plant health and productivity.

According to the current understanding of plant immunity the capacity of ulvan to elicit plant defences requires that it is first recognised by the plant (either directly or indirectly), probably during primary signalling events (e.g., PTI or ETI). Therefore, the assumption that ulvan has analogous structural features to existing MAMPs/PAMPs is a logical conclusion and molecules that have structural similarities with ulvan such as plant rhamnogalacturonan I and rhamnolipids from phytopathogenic bacteria (Varnier *et al.*, 2009; Vatsa *et al.*, 2010) also trigger defence responses. Typically, these latter examples contain rhamnose and uronic acids (but not sulfate esters), and these moieties may be important for ulvan's activity. Notably, the presence of rhamnose (in ulvan) was required to induce immune defence responses in tomato plants, while glucuronic acid (in glucuronan) had no effect (El Modafar *et al.*, 2012). In terms of molecular weight, tomato plants treated with ulvan oligomers had up to twice the PAL activity than control plants. Conclusions regarding the degree of sulfation remain unclear, with one report indicative of a positive correlation and another indicative of no effect. Clearly the optimisation of ulvan products for use as bio-elicitors is in its infancy; however, its capacity to elicit plant immune responses is promising for reducing agricultural reliance on traditional pesticide treatments.

2.4 Conclusion

Research into the structural and biological properties of ulvan remain in its early stages relative to those of the other marine-derived sulfated polysaccharides carrageenan and fucoidan. However, ulvan has the potential to find widespread application, including in agriculture, human health, and biomaterials. General trends in physicochemical properties

and biological activities of ulvan relative to its structural features remain ambiguous, and this is due to the limited number of systematic studies on the structure-function properties of highly refined and well characterised ulvan against highly defined target activities. Additionally, the pharmacokinetics and bioavailability of such a complicated macromolecule will require thorough investigation prior to any application in a therapeutic capacity. The structurally distinct features of ulvans across biomass sources also contributes to this ambiguity and highlights the need for a focus on highly characterised refined ulvan of a single origin, or refining process. This will then clarify the structural requirements for specific biological activities, supporting informed decisions about the selection of species for cultivation and processing for specific target applications.

Chapter 3:

Are all ulvans equal? A comparative assessment of the chemical and gelling properties of ulvan from blade and filamentous *Ulva*[2]

3.1 Introduction

Green seaweeds of the genus *Ulva* occur in two distinct morphologies: a flat sheet-like blade form (occasionally in thin ribbons) and a tubular filamentous form (Figure 3.1). Filamentous species of *Ulva* were historically considered a separate genus, *Enteromorpha*, until genetic barcoding concluded that these two genera were not distinct evolutionary entities and were, therefore, consolidated into a single genus, *Ulva* (Hayden *et al.*, 2003). Both morphologies flourish under high nutrient conditions, resulting in blooms or 'green tides' in extreme cases (Ye *et al.*, 2011). Rapid and resilient growth make species of *Ulva* ideal candidates for the bioremediation of nutrient-rich wastewater, such as that produced by land-based aquaculture of shellfish and finfish (Bolton *et al.*, 2009; Lawton *et al.*, 2013; Nardelli *et al.*, 2019). Applied at a large scale, *Ulva* bioremediation produces a high-quality monoculture of biomass with a biochemical profile that is suitable for the development of valuable bio-products (Glasson *et al.*, 2017). Notably, both blade and filamentous *Ulva* are established food products sold as "Aosa" and "Aonori", respectively (Holdt & Kraan, 2011; McHugh, 2003; Ohno, 1993). A key feature of *Ulva* is the high content of soluble fibre predominantly as the cell wall sulfated polysaccharide ulvan, with desirable biological activities and rheological properties (Alves *et al.*, 2013b; Kidgell *et al.*, 2019; Lahaye & Robic, 2007).

[2] Published as: Kidgell *et al.* (2021) Are all ulvans equal? A comparative assessment of the chemical and gelling properties of ulvan from blade and filamentous *Ulva*. Carbohydrate Polymers 264:118010

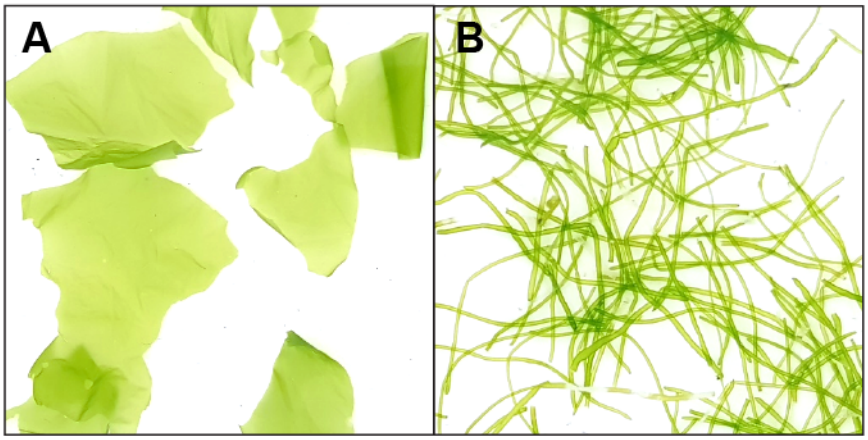

Figure 3.1: Characteristic blade (**A**) and filamentous (**B**) morphologies of *Ulva* collected from the Bay of Plenty, Aotearoa New Zealand.

Ulvan is a heterogeneous rhamnose-rich sulfated polysaccharide that forms weak gels (Haug, 1976; Lahaye & Axelos, 1993). The polysaccharide is characterised by repeat disaccharides of 3-sulfated rhamnose 1,4-linked to either glucuronic acid (ulvanobiouronic acid, A_{3S}), iduronic acid (ulvanobiouronic acid, B_{3S}), or xylose (ulvanobioses, U_{3S}) (Lahaye & Robic, 2007). These assignments, and indeed the majority of research on ulvan, has been conducted on species with the blade morphology (see: (Alves *et al.*, 2013b; Kidgell *et al.*, 2019; Lahaye & Robic, 2007)), while research into the detailed structure of ulvans from filamentous species of *Ulva* is lacking (notable exceptions include: (Chattopadhyay *et al.*, 2007; Qi *et al.*, 2012c; Tabarsa *et al.*, 2018; Yu *et al.*, 2017)). In particular, publications characterising ulvans from filamentous species of *Ulva* rarely quantify iduronic acid content (Zhong *et al.*, 2020), limiting the extent to which the composition of these ulvans can be compared to those from blade species or between filamentous species (Kidgell *et al.*, 2019). In any case, the structure and composition of ulvan, that is, the constituent sugars, the molecular weight and dispersity, the degree of sulfation, and the content of ulvan within individual *Ulva* samples, varies substantially in the literature (Kidgell *et al.*, 2019).

Variation in the composition and structure of ulvans is due to biological (e.g. *Ulva* species (Shanmugam *et al.*, 2001), holobiont (microbial) community structure (Singh & Reddy, 2014)), environmental (e.g. location (Lahaye *et al.*, 1999), seasonal (Robic *et al.*, 2009d)), and methodological factors (Glasson *et al.*, 2017; Kidgell *et al.*, 2019; Robic *et al.*, 2008; Yaich *et al.*, 2013). These sources of variation in turn influence the bioactivity and physical properties (e.g., rheology) of the extracted polysaccharide. While the natural variations due to biological

and environmental factors are difficult to control, except through controlled cultivation, variability due to methodology can be minimised through the use of standardised procedures. Therefore, the current study used an optimised extraction protocol (Glasson *et al.*, 2019), industry-standard analytical techniques (Pettolino *et al.*, 2012) and an optimised rheology protocol (Lahaye & Axelos, 1993; Lahaye, Ray, Baumberger, Quemener, & Axelos, 1996) to compare the yield, composition and structure, and rheological properties of ulvan from *Ulva* species collected and/or cultivated in the Bay of Plenty, Aotearoa New Zealand. My working hypothesis was that; as ulvan is a structural polysaccharide, the physicochemical properties of ulvan will differ between structurally distinct *Ulva* morphologies.

This study was conducted with the broader aim of selecting target species of *Ulva* for cultivation based on the physicochemical properties of the bioactive polysaccharide ulvan. To achieve this goal, the physicochemical properties of ulvan isolated from different *Ulva* species and morphologies were compared. I determined the yield, constituent sugars, content of sulfate esters, molecular weight distribution, and the rheological properties of ulvans from blade (*U. australis*, *U. rigida*, *U.* sp. B and *U.* sp.) and filamentous (*U. compressa*, *U. flexuosa*, *U. prolifera*, and *U. ralfsii*) *Ulva* species. FTIR and NMR spectroscopy were used to confirm the presence of characteristic ulvan functionality and disaccharides, respectively. Multivariate techniques were then applied to distinguish groupings of similar ulvans based on physicochemical properties of the ulvan from different species and morphologies.

3.2 Methods

3.2.1 Materials

The following were purchased from Sigma-Aldrich: glucuronic acid (>98 %, #G5269), sodium tetraborate (99.998 %, #229946), *m*-hydroxydiphenyl (85 %, #262250), concentrated sulfuric acid (ACS, 95-98 %, #258105), boric acid (#B6768), calcium chloride (>99 %, #223506), sodium nitrate (>99.0 %, #S5506), sodium azide (>99 %, #S2002), methanolic HCl (#90964), L-fucose (#F2252), L-rhamnose (#3875), L-arabinose (#10839), D-galactose (#0750), D-glucose (#8270), D-glucosamine (#G4875), D-mannose (#2069), D-xylose (#95729), D-ribose (#7500), D-galacturonic acid (#73960), and D-glucuronic acid (#5269). Other reagents were sourced as follows: trifluoroacetic acid (Synthesis grade, Scarlau, Spain, #AC31420100), sodium chloride (AJAX FineChem, ThermoFisher Scientific, New Zealand, #AJA465), sodium hydroxide (50 %

w/w, Fisher Scientific, Thermo Fisher Scientific, New Zealand, #SS254), anhydrous sodium acetate (Carlo Erba, France, #366377), deuterium oxide (99.9 %, Cambridge Isotope Laboratories, USA, #DLM-4), and L-iduronic acid (Carbosynth, UK, #MI08102).

3.2.2 Extraction and purification of ulvan

3.2.2.1 Algae collection & cultivation

Nine morphologically distinct blade and filamentous *Ulva* samples were collected between October 2018 and April 2019 from the Bay of Plenty region, Aotearoa New Zealand (37°42'S, 176°18'E; App. 7.2.1; See online dataset for details) under Ministry for Primary Industries University of Waikato Special Permit 560. Samples were identified to species level by DNA barcoding by Lawton *et al.* (Lawton, Sutherland, Glasson, & Magnusson, Under review), and found to consist of seven distinct species (*Ulva australis*, *U. rigida*, *U.* sp. B, *U. compressa*, *U. flexuosa*, *U. prolifera*, *U. ralfsii* [syn. *U.* sp. 5]) and one sample that did not amplify successfully so is referred to as "*Ulva* sp.".

The nine *Ulva* samples were cleaned of epiphytes and rinsed in salt water before being cultivated or extracted. Cultivation was attempted on all nine *Ulva* samples to increase biomass for ulvan extraction; however, *Ulva* sp. was unable to be cultivated. Three of the *Ulva* samples (*U.* sp. B, *U.* sp., *U. ralfsii*) had sufficient wild harvested biomass to extract ulvan after some biomass was taken for cultivation. *Ulva* was cultivated as previous reported (Lawton *et al.*, Under review). Briefly, cultivation was carried out in 20 L buckets at a density of 1 g fresh weight L^{-1} and a temperature of 18-20°C under bright white LED (1200mm J Series T8 LED tubes producing 1800 lm of 4000-4500K light) lights on a cycle of 12 h/12 h light/dark in sea water with the addition of F/2 nutrients (Cell-Hi F2P, Varicon Aqua Solutions UK, 0.1 g L^{-1}). Biomass was harvested every 7 days and spun to remove excess water. After restocking, excess biomass was frozen at -18 °C until a sufficient supply was produced for ulvan extraction. Frozen biomass was freeze-dried, milled using a domestic blender, and stored over silica gel until extraction.

3.2.2.2 Ulvan extraction

Ulvan was extracted using an optimised extraction procedure (Glasson *et al.*, 2019). A stirred suspension of milled *Ulva* biomass (40 g dry weight) in dilute H_2SO_4 (1 L, pH 2.92)

was heated at 90 °C for 90 min. The extract was then separated from the biomass by filtration through 50 µm mesh followed by centrifugation (20 min, 3000 g) to remove ultrafine particulate material prior to neutralisation with 2M NaOH. The extract was then concentrated (10x) by ultrafiltration (ÄKTA flux 6 fitted with a Xampler 10,000 Da NMWC cartridge filter), diafiltered with Type 1 water until the permeate conductivity was ≤20 µS cm^{-1} and freeze dried to yield "crude ulvan" (App. 7.2.2).

These crude ulvans containing residual protein and other polysaccharides were characterised in the same manner as the purified ulvan (App. 7.2.2, App. 7.2.5). However, four samples (*U. ralfsii* (wild), *U. rigida, U. australis*, and *U. flexuosa)* had insufficient quantities of crude ulvan for characterisation of both crude and purified material. Therefore, only the characterisation of the purified ulvans is explored in detail in the results and discussion.

3.2.2.3 Purification & fractionation

Crude ulvan was dissolved overnight in Type 1 water at a concentration of 1 % w/w and filtered by vacuum filtration (Filtech, 453) prior to purification by anion exchange chromatography (AEC) using an ÄKTA pure 150 L coupled with a single wavelength (280 nm) UV detector and fraction collector. The ulvan solution (~350 mL) was loaded onto an equilibrated (Type 1 water, 5 column volumes (CV); 2M NaCl, 5 CV; Type 1 water, 5 CV) XK 50/30 column (GE Healthcare Life Sciences) packed with Q Sepharose XL media (bed height = 24.5 cm). The column was eluted using a stepwise gradient of NaCl (0 M, 2 CV; 0 – 1 M, 4 CV; 1 – 2 M, 1.2 CV; 2 M, 3 CV) at a flow rate of 20 mL min^{-1}. A chromatogram was produced by colourimetric analysis of collected fractions (13 mL) for uronic acid using the *m*-phenyl phenol method with glucuronic acid as standard (van den Hoogen *et al.*, 1998). Fractions containing uronic acid that did not overlap the major peak in the UV trace (attributed to protein and other chromophore containing impurities) were pooled and concentrated by diafiltration with Type 1 water (ÄKTA flux 6 system fitted with a 10,000 Da NMWC filter, UFP-10-E-4X2MA) until permeate conductivity was <5 µS cm^{-1} and then freeze dried to yield "purified ulvan".

Ulvan was successfully extracted and purified from eight cultivated samples and from the wild harvested biomass of three samples (*U.* sp. B, *U.* sp., *U. ralfsii*), resulting in a total of eleven purified ulvans (Table 3.1). *Ulva* sp. B and *U. ralfsii* both had ulvans extracted and

purified from wild harvested and cultivated biomass (Table 3.1). Two of the *Ulva* samples collected and cultivated were later identified as *U.* sp. B, so were named "*U.* sp. B (cult.A)" and "*U.* sp. B (cult.B)".

3.2.3 Chemical composition

3.2.3.1 Elemental characterisation

Elemental analysis (% C, H, N, S; n=1) and ash content (% w/w) of ulvans were measured commercially by OEA labs (www.oealabs.com, Callington, UK). Percent oxygen was calculated as % O = 100 – Σ(C, H, N, S, ash), where C, H, N, S, and ash are expressed as a percentage of the total mass. Sulfate content was measured using the turbidimetric assay (Craigie *et al.*, 1984). Protein content was estimated from the N content using the nitrogen-to-protein conversion factor of 5 (% N x 5) (Angell, Mata, de Nys, & Paul, 2016).

3.2.3.2 Constituent sugar composition

Constituent sugar composition was determined by high-performance anion-exchange chromatography with pulsed amperometric detection (HPAEC-PAD) after hydrolysis of the polysaccharides to their component monosaccharides based on the methodology of Nep *et al.* (2016), but with a modified eluant gradient. This methodology was based on the protocol optimised by de Ruiter *et al.* (1992) for the analysis of water-soluble uronic acid-containing polysaccharides. Briefly, samples (1 mg) were hydrolysed in duplicate with methanolic HCl (3 M, 500 µL, 80 °C, 18 h), followed by aqueous trifluoroacetic acid (TFA, 2.5 M, 500 µL, 120 °C, 1 h). The resulting hydrolysates were dried, redissolved in Type 1 water (1 mL), and diluted to 50 µg mL^{-1}. Aliquots (20 µL) of the hydrolysates were analysed on a CarboPac PA-1 (4 x 250 mm) column equilibrated in 20 mM NaOH and eluted with a simultaneous gradient of NaOH (20 mM from 0 to 25 min, 20 to 100 mM from 25-30 min, 100 to 200 mM from 30 to 50 min, then held to 60 min) and NaOAc (0 mM until 30 min, 0 to 500 mM from 30 to 50 min, 500 to 1000 mM from 50 to 52 min, then held until 60 min) at 30 °C and a flow rate of 1 mL min^{-1}. The sugars were identified from their elution times relative to a standard sugar mix (L-fucose, L-rhamnose, L-arabinose, D-galactose, D-glucose, D-glucosamine, D-mannose, D-xylose, D-ribose, D-galacturonic acid, D-glucuronic acid, and L-iduronic acid), quantified from response calibration curves of each sugar and expressed as µg of the anhydro-sugar (as this is the form

of sugar present in a polysaccharide) per mg of sample; the normalised mol% of each anhydro-sugar was also calculated.

3.2.4 Structural characterisation

3.2.4.1 NMR & FTIR spectroscopy

Samples of ulvan were dissolved in D_2O at 25 mg mL^{-1}. Acetone (0.4 % v/v) was added as an internal standard to all samples and assigned as the reference peak (31.45 ppm for ^{13}C and 2.225 ppm for ^{1}H). NMR data was collected on a Bruker Avance III 500 operating at a proton frequency of 499.843 MHz running Topspin 2.1 software. Data was collected on a Bruker two channel 5-mm broadband observe nuclei probe (31P-109 Ag) equipped with actively shielded Z-axis gradient coil (303 K). Proton NMR spectra were recorded with a spectral width of 20 ppm, 65,536 complex data points, 30-degree excitation pulse, each with a 1-second delay time and an acquisition time of 3.18 s. Heteronuclear single quantum coherence (HSQC) experiments were carried out using pulse programs supplied with the Bruker manual. The superimposed HSQC plots were calibrated by standardising the intensity of the acetone (0.4 % v/v) resonance between ulvan spectra. Spectra were processed with a standard exponential weighting function of 0.3 Hz line broadening prior to Fourier transformation. NMR spectra were analysed and processed in Mestranova (Ver. 14.1.1).

FTIR spectra of ulvans were recorded on a Shimadzu IRSpirit with a QATR-detector between wavenumbers 400 and 4000 cm^{-1} with an average of 32 scans. Data were processed in LabSolutions IR software using the built-in smoothing function followed by ATR correction, baseline correction and normalisation around the significant peaks for C-O stretching (~1050 cm^{-1}).

3.2.4.2 Molecular weight

Molecular weight distributions were determined using size-exclusion chromatography coupled with multi-angle laser light scattering (SEC-MALLS). Samples (5 mg mL^{-1} in 0.1 M $NaNO_3$) were dissolved by heating at 80 °C and then standing at room temperature overnight (~20 h). Soluble material was separated on three columns (TSK-Gel G5000PW_{XL}, G4000PW_{XL}, and G3000PW_{XL}, 300 x 7.8 mm, Tosoh Corp., Tokyo, Japan) connected in series, with a void volume (V_0) of 15 mL and total volume (V_t) of 32 mL, eluting with 0.1 M $NaNO_3$ with 0.02 %

NaN_3 (0.5 mL min^{-1}, 60 °C). The eluted material was detected using a variable wavelength detector (280 nm), an SDL7000 MALLS detector (PSS Polymer Standards Service GmbH, Mainz, Germany) and a refractive index monitor. Weight-average molecular weight (M_w), number-average molecular weight (M_n), and dispersity (Đ) were calculated using Win GPC Unichrom software (v8.2.1, PSS Polymer Standards Service) using a refractive index increment, dn/dc, of 0.146 mL g^{-1} (Robic *et al.*, 2008). The angular dependence of light scattering was fitted using a linear Debye plot and molecular weight data fitted using linear regression.

3.2.5 Rheology

Gelling properties of ulvan from *Ulva* species were determined through dynamic rheological measurements performed using a TA Instruments DHR-1 single-head hybrid rheometer with a temperature-controlled Peltier plate and a steel cone geometry (60 mm diameter, 1° angle). Rheological data were collected using TA TRIOS software (ver. 4.3.0.38388). Experiments were conducted at 20 °C with a solvent trap over the geometry to reduce evaporation. Viscosity was measured on a 2 % w/v ulvan solutions (prior to addition of gel-inducing reagents) with a logarithmic flow sweep using a shear rate range of 500 to 1 s^{-1}. For the gelling experiments, the 2 % ulvan solution was pH-adjusted to 7.5 and heated to 75 °C prior to addition of $CaCl_2$ and H_3BO_3 to final concentrations of 7 and 33 mM, respectively, resulting in a final ulvan concentration of 1.6 % (Lahaye & Axelos, 1993; Lahaye *et al.*, 1996). To prevent the gel from forming prior to starting measurements, H_3BO_3 was added immediately prior to transferring the ulvan solution to the rheometer plate, and the plate was held at 40 °C while the rheometer geometry (rotating at 1 rad s^{-1}) was lowered onto the ulvan solution. Finally, the geometry movement was stopped, the solvent trap was added, and the temperature adjusted to 20 °C prior to beginning any experiments.

The linear viscoelastic region (LVR) was determined with a constant angular frequency of 1 rad s^{-1} across a displacement of $5x10^{-5}$ to 0.5 rad and indicated that ulvan gels could not withstand an oscillation displacement (strain) greater than 0.01 rad. A displacement of 0.003 rad was selected for subsequent experiments. Ulvan gel formation was monitored by recording the storage modulus resulting from a constant angular frequency of 1 rad s^{-1} with a displacement of 0.003 rad for 30 min. Mechanical spectra (storage and loss moduli, tan δ, complex viscosity) were recorded once gel formation was complete using a constant strain of

0.003 rad displacement over an angular frequency range of 0.03 to 100 rad s^{-1}, a range which maintained a raw phase angle of ≤ 175° and therefore did not allow inertial forces to dominate the measurements.

3.2.6 Data & statistical analysis

The effect of the morphology of *Ulva* on chemical and rheological properties of the extracted ulvan was analysed with a one-factor permutational analysis of variance (PERMANOVA) (Anderson, Gorley, & Clarke, 2008). Morphology was treated as a fixed factor. The PERMANOVA was conducted with 9,999 unrestricted permutations and type III sum of squares. Homogeneity of multivariate dispersions was confirmed with the PERMDISP function. Complete linkage cluster analysis was performed with an associated SIMPROF test using a significance level of 5 %, 20,000 permutations to generate the mean profile, and 9,999 permutations to calculate the statistic. Permutational statistical analyses were performed in Primer v6 (Primer-E Ltd., UK) using a Bray-Curtis similarity matrix on square-root transformed data. Correlation matrices were produced in Statistica for Windows (Ver. 12, Statsoft Inc.). Figures were generated using relevant specialised software listed above, R, or Microsoft Excel 2016 and prepared for publication in Adobe Illustrator (Ver. 24).

3.3 Results and discussion

The physicochemical properties of eleven ulvans isolated and purified from either blade (*U. australis*, *U*. *rigida*, *U*. sp. B, and *Ulva* sp.) or filamentous (*U*. *flexuosa*, *U*. *compressa*, *U*. *prolifera*, and *U*. *ralfsii*) *Ulva* species were assessed. The composition of characteristic ulvan sugars (rhamnose, xylose, glucuronic acid, and iduronic acid) conformed to the expected stoichiometry (~1:1 for [Rha]:[GlcA+IdoA+Xyl]) for all ulvans, except those from *U. flexuosa* (1.3:1) and *U. prolifera* (1.5:1), which had 56 and 60 mol% rhamnose, respectively. In general, blade species of *Ulva* had higher yields of ulvan (14.0-19.3 %) containing a higher iduronic acid content (IdoA = 7-18 mol%), lower average molecular weights (M_w = 190-254 kDa), and lower storage moduli (i.e., gel strength, G' = 0.1-6.6 Pa) than ulvan isolated from filamentous species (yield = 7.2-14.6 %; IdoA = 4-7 mol%; M_w = 260-406 kDa; G' = 22.7-74.2 Pa). The above compositional, structural, and rheological data were assessed in a multivariate context which identified a significant difference between ulvans isolated from filamentous and blade species of *Ulva* (PERMANOVA, pseudo-$F_{1,9}$ = 18.0, $p<0.005$). The current research highlights the

variability of the composition and structure of ulvans from different *Ulva* species, and confirms my hypothesis that the physicochemical properties of ulvans differ between *Ulva* morphologies.

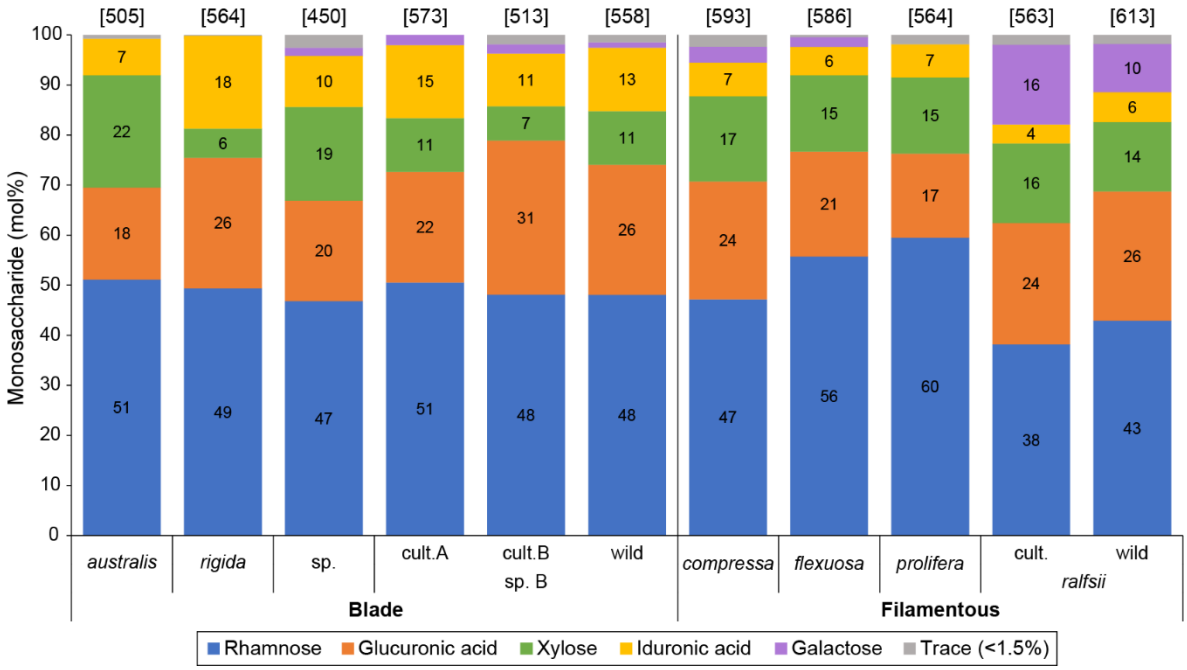

Figure 3.2: Constituent monosaccharide composition (mol%) of purified ulvans, categorised by *Ulva* morphology, species, and, for *U.* sp. B and *U. ralfsii*, biomass source. For visual clarity, monosaccharides less than 1.5 mol% were grouped as 'Trace' – full data in App. 7.2.4. The total sugar content (µg mg^{-1}) of each ulvan is presented at the top of the respective column in square brackets [].

3.3.1 Yield and composition

There are very few studies in the literature that systematically assess the yield and composition of ulvan from a range of *Ulva* species (Shanmugam *et al.* (2001) and Lahaye *et al.* (1999) are notable exceptions), and none that systematically compare ulvans isolated from blade and filamentous growth forms. In this regard, an average yield of 13.4 ± 4.3 % w/w ulvan was extracted from the *Ulva* biomass (App. 7.2.2), with an average recovery after purification of 48.3 ± 7.1 % w/w (Table 3.1) In general, higher yields of purified ulvans were recorded for blade species (7.4 ± 1.4 %) than for filamentous species (5.1 ± 1.7 %) (Table 3.1). The crude yields of ulvan (16.5 ± 2.0 % for blade species and 9.8 ± 3.1 % for filamentous species; App. 7.2.2) fall within the range of median crude yields (median 12.0, interquartile range = 6.0-20.0) reported in a recent meta-analysis of ulvans (Kidgell *et al.*, 2019), and indicate that blade *Ulva* species have higher contents of ulvan compared to filamentous

species. The elemental composition of the ulvans was consistent with previous reports (App. 7.2.2, App. 7.2.3) (Glasson *et al.*, 2017; Kidgell *et al.*, 2020; Shanmugam *et al.*, 2001). Ulvans isolated from blade species had a higher content of sulfate esters than filamentous species with 13.7 ± 2.9 % compared to 9.3 ± 1.8 %, respectively. The degree of sulfation in ulvan has previously been correlated with anticoagulant (Wang *et al.*, 2013b), antihyperlipidemic (Qi & Sheng, 2015), and anti-viral (Lopes *et al.*, 2017) activity. These results suggest that ulvans isolated from blade and filamentous species of *Ulva* may have different bioactivities (Leiro *et al.*, 2007; Qi *et al.*, 2012a; Shao *et al.*, 2014a; Wang *et al.*, 2013b). The degree of sulfation is also likely to affect the solution properties of ulvan (e.g. rheology) (Lahaye *et al.*, 1996). Importantly, the protein content of the ulvans in this study is low and there is negligible difference in protein content between samples from blade (0.7 ± 0.3 %) and filamentous (1.0 ± 0.4 %) *Ulva* species, as this is another factor that could drive rheological differences (Robic *et al.*, 2009d).

Table 3.1: Purified ulvan composition: details of the *Ulva* biomass from which ulvan was extracted and purified, the yield (of purified ulvan) obtained, the sulfate and protein content and the ratio of rhamnose to the sum of glucuronic acid, iduronic acid and xylose.

***Ulva* details**			**Yield**	**Composition**		
***Ulva* species**	**Biomass source**	**Morphology**	**Ulvan (% dw)** [a]	**% SO_4^{2-}** [b]	**% Protein** [c]	**[Rha]: [GlcA+IdoA+Xyl]** [d]
australis	Cultivated	Blade	6.5	16.9 ± 1.1	0.8	1.0
rigida	Cultivated	Blade	5.7	15.2 ± 0.3	0.6	1.1
sp.	Wild harvest	Blade	6.3	16.5 ± 0.7	1.3	1.0
sp. B (cult.A)	Cultivated	Blade	9.5	9.9 ± 0.9	0.7	1.0
sp. B (cult.B)	Cultivated	Blade	8.3	10.4 ± 0.5	0.5	1.1
sp. B (wild)	Wild harvest	Blade	8.0	13.1 ± 1.1	0.3	1.0
compressa	Cultivated	Filamentous	3.3	7.5 ± 0.8	1.2	1.0
flexuosa	Cultivated	Filamentous	7.3	12.2 ± 0.5	1.5	1.3
prolifera	Cultivated	Filamentous	6.6	9.4 ± 0.5	0.7	1.5
ralfsii (cult.)	Cultivated	Filamentous	4.1	7.7 ± 0.4	0.9	0.9
ralfsii (wild)	Wild harvest	Filamentous	4.3	9.8 ± 0.4	0.7	0.9

[a] % dry weight (dw) biomass

[b] Average of triplicate (±S.D.)

[c] Estimated from conversion factor of 5 (%N x 5)

[d] Ratio of mol% of rhamnose to sum of glucuronic acid, iduronic acid and xylose

The constituent sugar compositions of all purified ulvans broadly conformed to the literature definition of ulvan (Kidgell *et al.*, 2019; Lahaye & Robic, 2007). The ulvans were comprised of 38-60 mol% rhamnose, 17-31 mol% glucuronic acid, 6-22 mol% xylose and 4-18 mol% iduronic acid (Figure 3.2, App. 7.2.4, App. 7.2.6, App. 7.2.7). Additionally, a large proportion of galactose (10-16 mol%) was present in ulvans from *U. ralfsii*, and as a minor component in all other ulvans (Figure 3.2, App. 7.2.4). Notably, ulvans from filamentous species had a lower proportion of acidic to neutral monosaccharides (~0.4:1) compared to those isolated from blade species (~0.6:1). Of particular note is the low proportion of iduronic acid in ulvans isolated from filamentous species (6 ± 1 mol%) relative to ulvans isolated from blade species (12 ± 4 mol%) (Figure 3.2). Within this study, ulvan from *U. rigida* had the highest iduronic acid content with 18 mol%, closely followed by ulvans from *U.* sp. B with 11-15 mol% (Figure 3.2). An iduronic acid content of 18 mol% (116 µg mg^{-1}; App. 7.2.4) is the highest recorded for ulvan in the literature to date (Kidgell *et al.*, 2019). High contents of iduronic acid in ulvans extracted from other blade *Ulva* species, *U. armoricana* (15 mol% (Paradossi *et al.*, 2002) and ~11 mol% (Robic *et al.*, 2009d)), and *U. ohnoi* (10 mol% (Glasson *et al.*, 2017)) have also been reported. While the effect that iduronic acid content has on ulvan and its function as a cell wall polysaccharide is unclear, high contents are associated with *Ulva* species with blade morphology.

There were several ulvans with sugar compositions that substantially deviate from median literature values (Kidgell *et al.*, 2019). Specifically, ulvans isolated from *U. flexuosa* and *U. prolifera* had high proportions of rhamnose (56 and 60 mol%, respectively), and ulvans from *U. ralfsii* contained high proportions of galactose (10 and 16 mol%) (Figure 3.2, App. 7.2.4). The high content of rhamnose in *U. flexuosa* and *U. prolifera* is an interesting result as ulvan is considered to be comprised of rhamnose-containing disaccharides (Lahaye & Robic, 2007). Based on this assumption, the ratio of rhamnose to the sum of glucuronic acid, iduronic acid and xylose (i.e. Rha:[GlcA+IdoA+Xyl]) is theoretically 1:1. Indeed, this ratio is consistent for almost all of the ulvans in this study (ranging from 0.9-1.1:1), however, ulvans from *U. flexuosa* and *U. prolifera* had ratios of 1.3:1 and 1.5:1, respectively (Table 3.1). The excess rhamnose present in these samples may exist as repeat units interspaced between conventional disaccharides, as branching chains, or possibly as a separate repeating rhamnan, related to those found in green seaweeds of the order Ulotrichales, *Gayralia oxsperma* and

Monostroma latissimum (Cassolato *et al.*, 2008; Lee, Yamagaki, Maeda, & Nakanishi, 1998; Li *et al.*, 2011). Interestingly, despite the high proportions of galactose found in ulvans from filamentous *U. ralfsii*, the Rha:[GlcA+IdoA+Xyl] ratio for both was 0.9:1 (Table 3.1). This ratio is consistent with galactose being either interspaced between the conventional disaccharides of ulvan, as branching chains, or as part of a separate galactan (Castro *et al.*, 2009; Farias *et al.*, 2008). Further structural investigation via linkage analysis and NMR spectroscopy is required to ascertain the origin of the excess rhamnose and high galactose detected in the sugar analysis of ulvans from *U. flexuosa* and *U. prolifera*, and *U. ralfsii*, respectively.

3.3.2 Structure and rheology

3.3.2.1 NMR spectroscopy

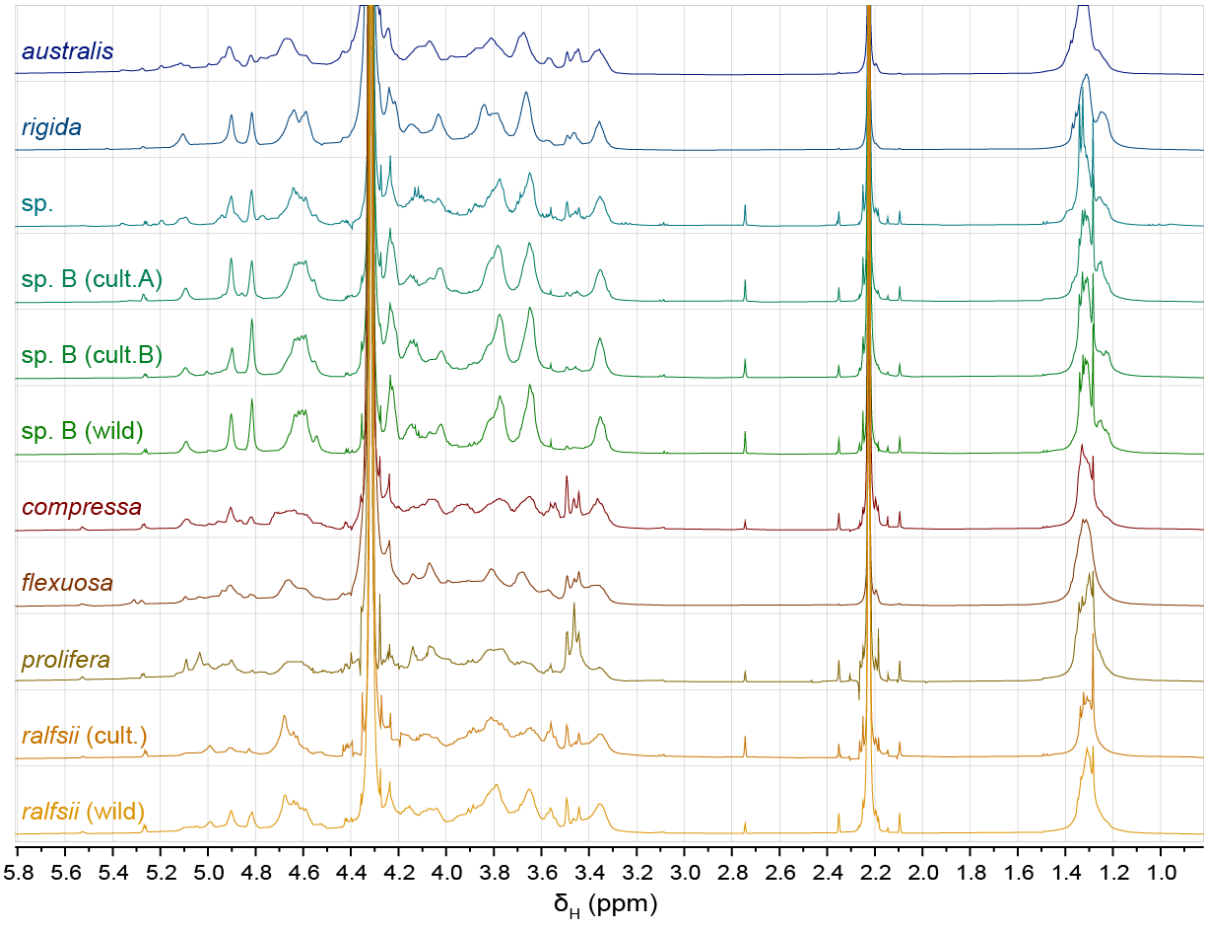

Figure 3.3: ^{1}H spectrum of purified ulvans from blade (blue-green) and filamentous (red-yellow) *Ulva* species. Chemical shifts relative to acetone at 2.225 ppm.

The ^{1}H and ^{1}H-^{13}C HSQC spectra of purified ulvans from blade and filamentous species of *Ulva* suggest structural differences between the morphologies (Figure 3.3, Figure 3.4, Figure 3.5). Ulvans from blade species have fewer and more highly resolved peaks compared to ulvans from filamentous species. This pattern in the ^{1}H NMR may be explained by ulvans isolated from blade species of *Ulva* containing a high proportion of repeating saccharide structural-moieties, while ulvans from filamentous species are more heterogeneous in structure displaying greater signal complexity (Figure 3.3). Almost all the peaks from ulvans of blade species can be identified by comparison with the literature (Table 3.2). Within the anomeric region (^{13}C ~95-105 ppm/^{1}H ~4.6-5.1, ppm), there are resonances consistent with A_{3S} and U_{3S} disaccharides in ulvans from both blade and filamentous species (Figure 3.4, Table 3.2). Resonances for B_{3S} disaccharides are also detected in ulvans from blade species (Figure 3.4 A), but not in the spectra of ulvans from filamentous species (Figure 3.4 B). A lack of anomeric resonances associated with the B_{3S} disaccharide is consistent with the lower content of iduronic acid detected in ulvans from filamentous species (See section 3.3.1). Individual HSQC plots further support the constituent sugar analysis (App. 7.2.10 to App**.** 7.2.15). For example, strong resonances are detected for R"1 and R'1 for ulvans high in xylose (*U. australis*, App. 7.2.10 A) and iduronic acid (*U. rigida*, App. 7.2.10 B), respectively. There are also a series of unassigned resonances detected in ulvans isolated from filamentous species in the region of ^{13}C 100-103 ppm/^{1}H 5.0-5.1 ppm that are absent in those isolated from blade species (Figure 3.4, Table 3.2). Some of these resonances could result from deshielding of the xylose or glucuronic acid anomeric carbons due to the presence of a 2-sulfate (Lahaye *et al.*, 1999), however, further research is required for conclusive assignment. The greater complexity in resonances of ulvans isolated from filamentous species is also detected in the non-anomeric region.

Within the non-anomeric region of the ^{1}H-^{13}C HSQC, the resonances for the A_{3S} and U_{3S} disaccharides can be identified in the spectra of ulvans from both blade and filamentous species of *Ulva* (Table 3.2). Similar to the anomeric region, resonances for the B_{3S} disaccharide are detected in ulvans from blade species (Figure 3.5 A) yet are not detected for ulvans from filamentous species (Figure 3.5 B). Furthermore, a series of resonances between ^{13}C 70-75 ppm/^{1}H 3.4-3.6 ppm are present in the spectra of ulvans from filamentous but not blade species, and do not appear to be identified in the ulvan literature. In the spectra of the

galactose-rich ulvans isolated from *U. ralfsii* there are two unidentified resonances at ^{13}C 62.5/^{1}H 3.75 ppm and ^{13}C 62.5/^{1}H 3.85 ppm (Figure 3.5 B; App. 7.2.14). These resonances are in a similar region to previous assignments made for the C6/H6,6' for a galactan isolated from a green alga (Farias *et al.*, 2008) and a sea urchin (Castro *et al.*, 2009). In addition, there are three resonances centred at ~^{13}C 57/^{1}H 3.4 ppm that are more intense in ulvans isolated from filamentous species than blade species (Figure 3.5). These resonances likely correspond to a methoxy substituent on one of the sugars, such as 3-O-Me rhamnose (Gosselin *et al.*, 1964; McKinnell & Percival, 1962a; Ogawa, Yamaura, & Maruyama, 1997). The greater complexity of resonances throughout the ^{1}H-^{13}C HSQC NMR spectra for ulvans isolated from filamentous species supports a higher level of structural complexity in these polysaccharides. However, further structural investigation via linkage analysis is required to elucidate the structural differences between ulvans isolated from blade and filamentous species of *Ulva*.

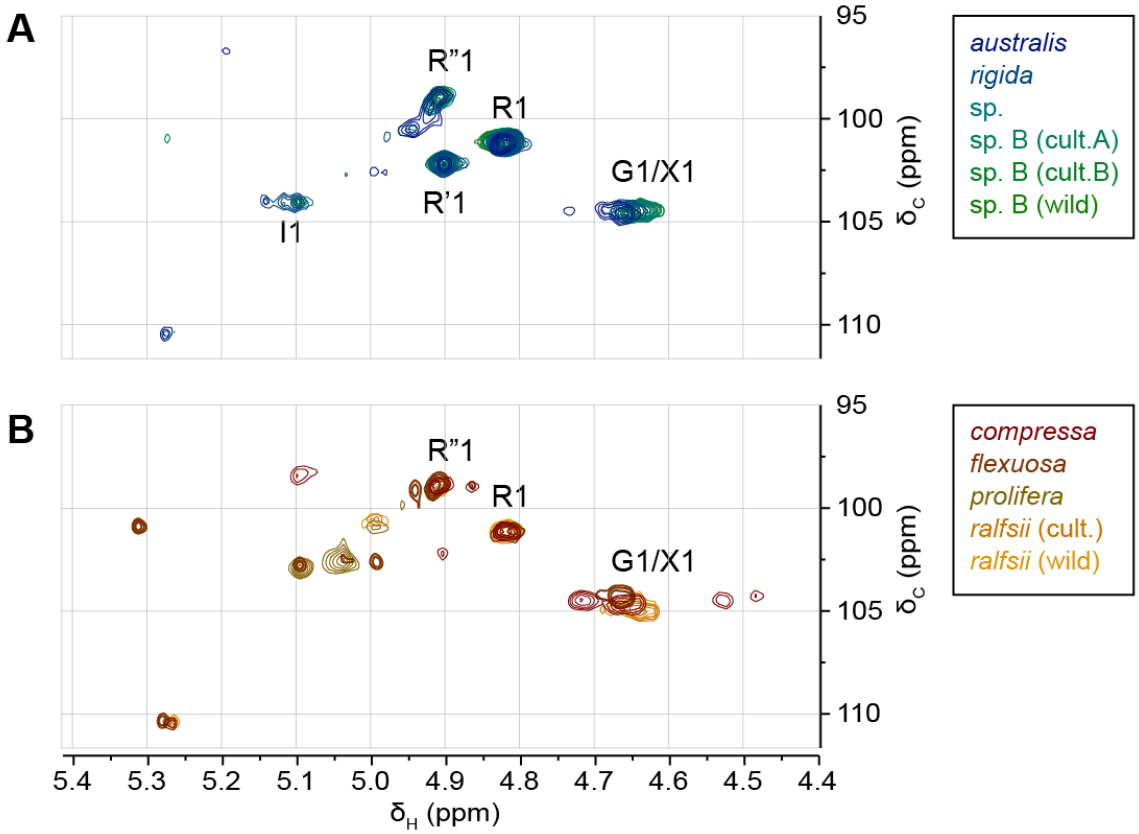

Figure 3.4: The anomeric region of superimposed ^{1}H-^{13}C HSQC spectra highlighting the structural difference of ulvans from (**A**) blade and (**B**) filamentous *Ulva* species. Chemical shifts relative to acetone at 31.45 and 2.225 ppm for ^{13}C and ^{1}H, respectively. Labels and numbers correspond to carbon/proton coupling pair of ulvan units outlined in Table 3.2.

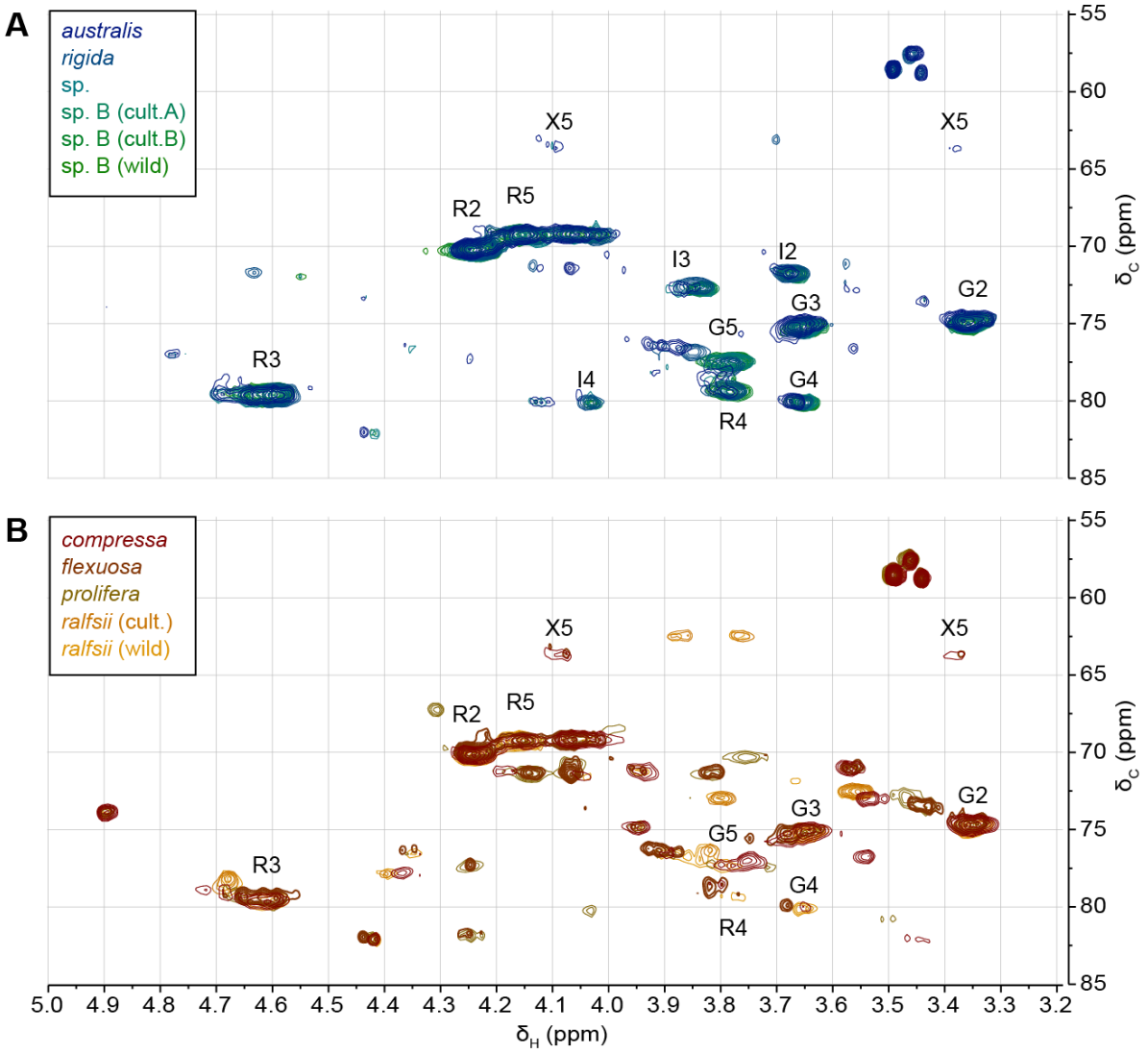

Figure 3.5: Non-anomeric region of superimposed ^{1}H-^{13}C HSQC spectra highlighting the structural difference of ulvans from (**A**) blade and (**B**) filamentous *Ulva* species. Chemical shifts relative to acetone at 31.45 and 2.225 ppm for ^{13}C and ^{1}H, respectively. Labels and numbers correspond to carbon/proton coupling pair of ulvan units outlined in Table 3.2 – note that many resonances from B_{3S} and U_{3S} overlap with A_{3S} so are not specifically listed.

Table 3.2: Ulvan disaccharide units, assigned labels, and approximate chemical shifts based on references indicated; rounded chemical shift values are given as peaks from different ulvans vary.

			Chemical shift (ppm)[b]						
Diads[a]	**Units**	**Label**	**C1/H1**	**C2/H2**	**C3/H3**	**C4/H4**	**C5/H5**	**C6/H6**	**Ref.**
A_{3S}	[→4)-*β*-D-Glc*p*A-(1→	G	104.5/4.65	75.0/3.35	75.0/3.65	80.0/3.65	77.0/3.80	-	(de Carvalho *et al.*, 2018; de Freitas *et al.*, 2015; Lahaye *et al.*, 1998)
	4)-*α*-L-Rha*p*3S-(1→]	R	101.0/4.80	70.0/4.25	79.0/4.60	79.0/3.80	69.0/4.15	18.0/1.30	(de Carvalho *et al.*, 2018; de Freitas *et al.*, 2015; Lahaye *et al.*, 1998)
B_{3S}	[→4)-*β*-D-Ido*p*A-(1→	I	104.0/5.10	72.0/3.70	73.0/3.85	80.0/4.00	-	-	(de Carvalho *et al.*, 2018; Lahaye *et al.*, 1998)
	4)-*α*-L-Rha*p*3S-(1→]	R’	102.0/4.90	70.0/4.25[c]	79.0/4.60[c]	79.0/3.80[c]	69.0/4.15[c]	-	(Adrien *et al.*, 2017a; de Carvalho *et al.*, 2018; Lahaye *et al.*, 1998)
U_{3S}	[→4)-*β*-D-Xyl-(1→	X	104.5/4.65	75.0/3.35[d]	75.0/3.65[d]	75.0/3.65[d]	64.0/3.40 64.0/4.10	-	(de Carvalho *et al.*, 2018; de Freitas *et al.*, 2015; Lahaye *et al.*, 1998)
	4)-*α*-L-Rha*p*3S-(1→]	R”	99.0/4.90	70.0/4.25[c]	79.0/4.60[c]	79.0/3.80[c]	69.0/4.15[c]	-	(de Carvalho *et al.*, 2018; de Freitas *et al.*, 2015; Lahaye *et al.*, 1998)

[a] Nomenclature for disaccharide units follows Lahaye and Robic (2007)

[b] Chemical shifts relative to acetone at 31.45 and 2.225 ppm for ^{13}C and ^{1}H, respectively.

[c] Resonance peaks overlap with R

[d] Resonance peaks overlap with G

3.3.2.2 FTIR spectroscopy

Ulvan has a unique FTIR fingerprint region in the range of 1770-600 cm^{-1} due to the presence of absorptions by carboxylic groups (V_{as} C=O, 1650-1600cm^{-1}; V_s C=O, 1425-1400 cm^{-1})(Robic *et al.*, 2009a; Yaich *et al.*, 2017), sulfate ester groups (V_{as} S=O, 1260-1215 cm^{-1}; C-O-S, 850-835 cm^{-1} and 795-785 cm^{-1})(Pengzhan *et al.*, 2003b; Ray & Lahaye, 1995a; Yaich *et al.*, 2017), and sugar ring side groups and glycosidic linkages (C-O-H, C-O-C, ~1055 cm^{-1})(Pengzhan *et al.*, 2003b; Robic *et al.*, 2009a; Zhang *et al.*, 2010). The ulvans assessed in this study consistently displayed absorption profiles characteristic of ulvan within the above-mentioned fingerprint region, with minor variations between ulvans detected (App. 7.2.8, App. 7.2.9). In general, the intensities of the sulfate ester (C-O-S, 850-835 cm^{-1} and 795-785 cm^{-1}) absorptions (relative to absorptions not related to these groups) were higher for ulvans isolated from blade species than ulvans from filamentous species. This pattern is consistent with the higher content of sulfate esters in ulvans from blade species of *Ulva* (See section 3.3.1). The absorption pattern in the region commonly associated with glycosidic linkages and other pyranose vibrational modes (~1160-900 cm^{-1}) differed between ulvans isolated from blade and filamentous species of *Ulva*. Specifically, the absorbance at ~980 cm^{-1} had a lower intensity relative to the absorbance at ~1040 cm^{-1} in ulvans isolated from filamentous *Ulva*. While the absorption band at 980 cm^{-1} remains unassigned, the feature corresponds with a lower content of sulfate esters in filamentous samples relative to blade samples and thus may arise due to a vibrational mode associated with the presence of sulfate esters. Indeed, desulfation of ulvan isolated from *U. rigida* also resulted in the disappearance of this peak in two independent studies (Castro *et al.*, 2006; Ray & Lahaye, 1995a). However, such an assignment needs further confirmation.

3.3.2.3 Molecular weight

It is difficult to compare molecular weight profiles of polysaccharides between studies as each step leading to quantification (e.g. biomass collection/cultivation/pre-treatment, extraction, isolation, and measurement method employed) affects the molecular weight measured (de Reviers & Leproux, 1993; Glasson *et al.*, 2017; Robic *et al.*, 2009d; Robic *et al.*, 2008; Shanmugam *et al.*, 2001; Yaich *et al.*, 2014). For example, in a study where ulvans were extracted from a single source of *U. ohnoi* (a blade species) using different biorefinery pre-

treatments and extractants, the weight average molecular weight (M_w) of the isolated ulvan varied from 10.5 to 312 kDa (Glasson *et al.*, 2017). Other studies have reported widely varying molecular weights for ulvans (e.g. 2000 kDa from blade *U. armoricana* (Hardouin *et al.*, 2016), 194 kDa from filamentous *U. intestinalis* (Tabarsa *et al.*, 2018), and 1218 kDa from filamentous *U. prolifera* (Cho *et al.*, 2010)). The use of standardised protocols such as those employed in the current study overcomes the issues of extraction and measurement variability, producing ulvans that only differ on the basis of source biomass (i.e., species/morphology/wild harvest/cultivation).

The M_w of purified ulvans assessed in the current study ranged from 190 to 406 kDa, with ulvans from filamentous species (338 ± 52 kDa) being approximately 50 % larger than those from blade species (225 ± 23 kDa). (Table 3.3, App. 7.2.16, App. 7.2.17). Similarly, the number average molecular weight (M_n) of ulvans from filamentous species (216 ± 27 kDa) was over double that of ulvans from blade species (102 ± 24 kDa; Table 3.3). Variation in molecular weight was detected for ulvans extracted from different biomass sources (cultivated vs. wild harvest) of the same *Ulva* species. Ulvans isolated from blade *U*. sp. B only had a minor variation of 36 kDa (218-254 kDa) while ulvans from filamentous *U*. *ralfsii* varied by 78 kDa (328-406 kDa). The ulvans with highest molecular weight from both species were isolated from the cultivated biomass. This variation highlights the importance of species selection and cultivation conditions on the quality of ulvan products.

Table 3.3: Purified ulvan molecular weight, rheological properties, and details of the *Ulva* biomass from which ulvan was extracted. Including weight average (M_w) and number average (M_n) molecular weight, dispersity (Đ), the storage modulus and tan δ of the ulvan gel, and the viscosity of 2 % w/v ulvan solution.

***Ulva* details**		**Molecular Weight**			**Rheology**		
***Ulva* species**	**Morphology**	**M_w (kDa)**	**M_n (kDa)**	**Đ**	**Storage Modulus (Pa)[a]**	**Tan δ**	**Viscosity (mPa s^{-1})[b]**
australis	Blade	214	82	2.6	0.4 ± 0.1	1.6	8
rigida	Blade	190	66	2.9	0.1 ± 0.0	4.3	10
sp.	Blade	245	104	2.4	1.3 ± 0.2	0.8	9
sp. B (cult.A)	Blade	218	126	1.7	0.1 ± 0.0	3.8	14
sp. B (cult.B)	Blade	254	114	2.2	2.2 ± 0.1	0.7	13
sp. B (wild)	Blade	229	120	1.2	6.6 ± 1.4	0.3	14
compressa	Filamentous	346	208	1.7	22.7 ± 2.0	0.1	7
flexuosa	Filamentous	352	218	1.6	34.2 ± 1.8	<0.1	10
prolifera	Filamentous	260	185	1.4	24.9 ± 3.1	0.1	7
ralfsii (cult.)	Filamentous	406	259	1.6	29.5 ± 4.2	0.1	10
ralfsii (wild)	Filamentous	328	210	1.6	74.2 ± 2.6	<0.1	9

[a] Average of triplicate values (±SD) recorded at an angular frequency of 10 rad s^{-1}

[b] Value recorded at a shear rate of 100 s^{-1}

3.3.2.4 Rheology

Ulvan polysaccharides are capable of forming a weak gel with a storage modulus (i.e., gel strength, G') ranging from 5-600 Pa (Lahaye & Axelos, 1993; Lahaye *et al.*, 1996; Robic *et al.*, 2009d; Sari-Chmayssem *et al.*, 2019; Yaich *et al.*, 2014). The ulvan gels formed in this study were prepared using a standardised method at pH 7.5 with a final concentration of ulvan, $CaCl_2$ and H_3BO_3 of 1.6 % w/v, 7 mM, and 33 mM, respectively. Under these conditions the ulvans that formed stronger gels did so rapidly on addition of the boric acid at room temperature, impeding accurate measurements. To overcome this issue, the thermoreversilibility of the ulvan gels (App. 7.2.18) (Lahaye *et al.*, 1996; Qiao *et al.*, 2016; Shao *et al.*, 2014b; Yaich *et al.*, 2014) was exploited by adding boric acid to the ulvan solution while heated to 75 °C and maintaining the Peltier plate at 40 °C while the geometry was lowered into position for measurement. Using this approach, ulvans isolated from filamentous species of *Ulva* consistently produced gels with a higher storage modulus (G' = 22.7-74.2 Pa) compared to ulvans isolated from blade species (G' = 0.1-6.6 Pa) (Figure 3.6,

Table 3.3). It should be noted that the storage modulus of the ulvan isolated from *Ulva ralfsii* (wild) of 74.2 ± 2.6 Pa is greater than three standard deviations from the storage moduli of other ulvans and so was considered an outlier and excluded from further analysis.

Gels formed by ulvans from filamentous species (G' = 27.8 ± 5.1 Pa, excluding *U. ralfsii* (wild)) held their shape and resisted light pressure, while the gels formed by ulvans from blade species (G' = 1.8 ± 2.5 Pa) were akin to highly viscous liquids. Indeed, half of the gels formed by ulvans from blade species of *Ulva* had a tan δ > 1, indicating that the gel was more viscous than elastic and could not be considered a gel (Table 3.3). The higher content of sulfate in ulvans isolated from blade *Ulva* species could potentially impede intramolecular interactions resulting in lower storage moduli compared to ulvans from filamentous species. However, the relationship between ulvan gel formation and sulfate content is unclear and requires further research. Robic *et al.* (2009d) found that the gels formed by ulvans varied substantially (G' = 5-600 Pa) when assessing ulvans isolated from different batches of wild harvested *U. rotundata* and *U. armoricana*. The authors attributed the variation in storage moduli to the proportion of high molecular weight ulvan, but also acknowledged that the presence of protein (which ranged from 1.2 to 16.4 % in the ulvans assessed) amplified the storage modulus of the resulting gel. In other studies where the protein content is <5 %, the maximum recorded storage modulus is 250 Pa, but is more consistently below 100 Pa (Lahaye & Axelos, 1993; Sari-Chmayssem *et al.*, 2019; Yaich *et al.*, 2014). Yaich *et al.* (2014) also reported a decrease in storage modulus with a decrease in molecular weight of ulvans with <5 % protein, as was observed in the current study. Thus, the storage moduli of ulvan gels recorded in the current study (0.1-34.2 Pa) may be at the low end of the reported range for ulvan (G' = 5-600 Pa) due, in part, to low protein content (i.e., high purity of ulvan). In support of this hypothesis is the higher storage moduli of gels formed by crude ulvans, which had higher protein content than purified counterparts (App. 7.2.2; App. 7.2.19). However, crude ulvans also had higher molecular weights than purified ulvans. Further research into the relationship between the storage modulus of ulvan gels, molecular weight, and protein is needed.

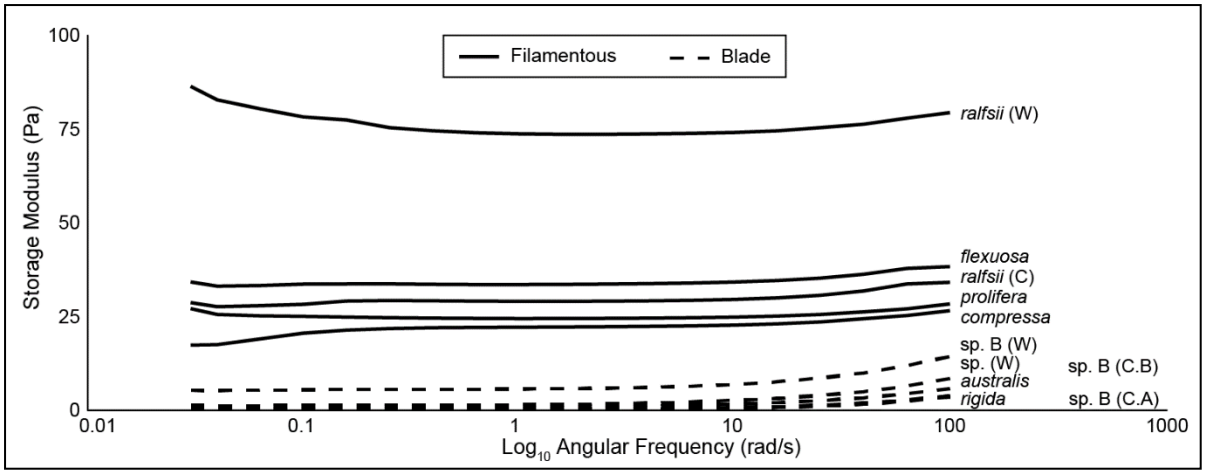

Figure 3.6: Storage modulus (gel strength) of purified ulvans in response to a range of rheometer angular frequencies (deformation). Solid lines and dashed lines represent ulvans from filamentous and blade *Ulva* species, respectively. "W" and "C" following a species name indicates whether the biomass was wild harvested or cultivated, respectively; see Table 3.3 for further details.

3.3.3 Multivariate synthesis of results

When the composition, structure, and rheological data are considered as a whole, ulvans isolated from blade *Ulva* species are significantly different (pseudo-$F_{1,9}$ = 18.0, $p<0.005$) (Figure 3.7) from ulvans isolated from filamentous *Ulva* species. The multivariate dispersions of ulvans from blade and filamentous *Ulva* species did not significantly differ (pseudo-$F_{1,9}$ = 0.444, p = 0.556), indicating that the significant PERMANOVA result above is due to a difference in ulvans from the two *Ulva* morphologies and not heterogeneous multivariate dispersity of the groups. Ulvans from filamentous and blade species separate on the MDS plot (Figure 3.7) predominantly due to the strong positive correlation of large molecular weight and high storage modulus of ulvans of filamentous species, and the high iduronic acid and sulfate content of ulvans from blade species (App. 7.2.21). The clustering of ulvans from different morphologies was also significant with 25 % dissimilarity between the two clusters (SIMPROF, π = 1.85, p = 0.01; App. 7.2.20). The content of glucuronic acid, rhamnose and xylose, and the viscosity of ulvan solutions all had very little effect on the significant distinction of ulvans between *Ulva* morphologies (Figure 3.7). The blade and filamentous species analysed here are dispersed throughout the *Ulva* phylogenetic tree (Hayden *et al.*, 2003), and the ulvan physicochemical properties do not reflect the phylogenetic relationship between species. For example, while the physicochemical

properties of the ulvans from filamentous *U. compressa* and *U. flexuosa* cause these species to tightly cluster on the MDS plot, these two species are more distantly related phylogenetically than filamentous *U. compressa* and blade *U. australis* (Lawton *et al.*, Under review), which are widely dispersed on the MDS plot. These findings demonstrate that morphology is driving the significant difference in ulvans and not phylogeny.

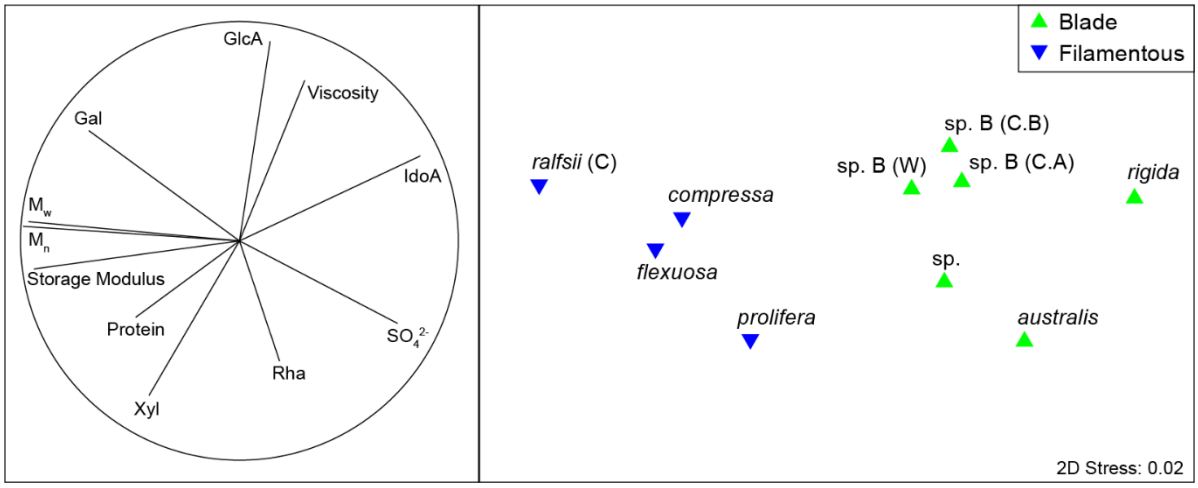

Figure 3.7: Multidimensional scaling (MDS) from a square-root transformed Bray-Curtis similarity matrix of the chemical characteristics of the ten ulvans (excluding *U. ralfsii* (wild) as an outlier). Pearson correlation vectors (left plot) influence the distribution of data points (right plot). "W" and "C" following a species name indicates whether the biomass was wild harvested or cultivated, respectively; see Table 3.3 for further details.

The storage modulus of ulvan is strongly positively correlated ($r^2 = 0.9$) with molecular weight (both M_w and M_n), and strongly negatively correlated with iduronic acid ($r^2 = -0.8$) (App. 7.2.21). And, in turn, iduronic acid content is strongly negatively correlated with molecular weight ($r^2 = -0.8$). A correlation between molecular weight and storage modulus is intuitive, where an increase in the size of a gel-forming polymer will result in an increase in gel strength due to an increase in intermolecular interactions (Yaich *et al.*, 2014). The correlation of iduronic acid, molecular weight, and storage modulus is somewhat more complicated. Iduronic acid is notoriously acid labile (Conrad, 1980) and its presence in a polysaccharide may contribute to the lower M_w of ulvans due to greater rates of depolymerisation during extraction. In contrast, however, is the principal that the glycosidic linkage of uronic acid to neutral residues is highly acid resistant and the presence of these linkages reduces depolymerisation (BeMiller, 1967). How the acid lability of iduronic acid as

a monosaccharide relates to the acid-resistance of its glycosidic linkage is unclear. Iduronic acid also possesses a high degree of conformational freedom (Casu, Petitou, Provasoli, & Sinaÿ, 1988; Hsieh, Thieker, Guerrini, Woods, & Liu, 2016) relative to other monosaccharides (Rees, Morris, Thorn, & Madden, 1982), which may lead to polysaccharide conformations that impede gel formation. Consistent with this hypothesis, ulvans are known to form microbead structures, where the polysaccharide folds back on itself and rolls up into little balls (de Carvalho *et al.*, 2020; Robic *et al.*, 2009b). A spherical structure limits the exposed functional areas of the polymer, impeding the strong intramolecular interactions required for high gel strengths, especially given the proposed weak ionic cross-linking mechanism of ulvan gel formation (Lahaye *et al.*, 1996). Furthermore, models of oligomers of repeat B_{3S} disaccharides (IdoA-Rha3S) have a more helical folded arrangement compared to the more linear structure of oligomers of repeat A_{3S} disaccharides (GlcA-Rha3S) (de Carvalho *et al.*, 2020; Paradossi *et al.*, 2002). The helical arrangement would further limit intramolecular interactions of ulvans rich in B_{3S} disaccharides. Therefore, the sequence and arrangement of disaccharide repeating units in ulvan will likely have a great impact on the gelling capacity of the polymer. Indeed, these studies and my results suggest that the gelling properties of ulvan is diminished in ulvans with high proportions of the B_{3S} disaccharide.

3.4 Conclusion

The multivariate analysis identified an *Ulva* morphology-based division in the physicochemical properties of isolated ulvans, thus confirming my original hypothesis. The data are compelling when assessed in a multivariate context, which is appropriate as the composition and structure of ulvans drive their rheological properties. Although further validation with ulvans from other species is required to generalise this pattern more broadly, the identification of a morphology-based distinction in ulvan is an important step forward in ulvan research. Not only in characterisation of the under-studied ulvans from filamentous species of *Ulva*, but also in the application of ulvan isolated from cultivated *Ulva* biomass. This research identifies a potential to select an *Ulva* morphology for cultivation to target a desirable property or activity in the resulting ulvan. For example, in the context of this study, ulvan from *U. ralfsii* would be suited for rheological applications. However, further understanding of the structure-activity relationships between ulvans isolated from different species and morphologies is required for species selection based on favourable biological

activities. In closing, there is a clear disparity in ulvans from blade and filamentous species of *Ulva*, demonstrating the importance of considering morphology in the selection of *Ulva* species for cultivation with respect to the biotechnical applications of ulvan.

Chapter 4:
Glycosyl linkage and sulfation of ulvans from blade and filamentous species of *Ulva*

4.1 Introduction

The composition and rheology of ulvans from blade and filamentous species of *Ulva* are significantly different (Chapter 3 (Kidgell *et al.*, 2021)). Ulvans from filamentous species of *Ulva* have higher weight average molecular weights (M_w = 260-406 kDa), formed gels with higher storage moduli (G' = 22.7-74.2 Pa), and have less iduronic acid (IdoA = 4-7 mol%) compared to ulvans from blade species (M_w = 190-254 kDa; G' = 0.1-6.6 Pa; IdoA = 7-18 mol%). The NMR spectra of these ulvans indicated there was also fine structure (glycosidic linkage) differences between the ulvans isolated from the different morphologies (Chapter 3 (Kidgell *et al.*, 2021)). NMR spectra of ulvans from filamentous species displayed greater signal complexity, suggesting that these ulvans were more heterogeneous in structure, while the spectra of ulvans from blade species were simpler, indicative of a highly repeating structure. The current chapter aimed to more closely investigate these structural differences using four ulvans from the previous chapter, two from blade species of *Ulva* (*U. rigida* and *U.* sp. B) and two from filamentous species of *Ulva* (*U. prolifera* and *U. ralfsii*). Ulvan isolated from *U. prolifera*, *U. ralfsii* (cult.), and *U. rigida* were chosen as these had higher than median (Kidgell *et al.*, 2019) proportions of rhamnose (60 mol%), galactose (16 mol%), and iduronic acid (18 mol%), respectively. Ulvan isolated from *U.* sp. B (cult. B) was included to represent the more 'conventional' sugar composition of ulvan. These four ulvans were analysed by glycosyl linkage analysis to determine the position of linkages, branches, and sulfate substitutions present on the constituent monosaccharides.

Glycosyl linkage (methylation) analysis is a procedure to identify which carbon atoms of the constituent monosaccharides within a polysaccharide are glycosidically linked with other sugars or *O*-substituted with non-glycosyl groups (e.g., sulfate esters). This knowledge is integral to analytical carbohydrate chemistry. For example, linkage analysis was instrumental in identifying the tetrasaccharide linkage region (GlcA-Gal-Gal-Xyl-) involved in

the initiation of heparan sulfate biosynthesis, facilitating the synthesis of analogues with similar bioactive efficacy (Sugahara & Kitagawa, 2002). Glycosyl linkage analysis of a polysaccharide involves a series of derivatisations to convert the constituent monosaccharides to partially methylated alditol acetates (PMAAs), which can then be analysed using gas-chromatography mass spectrometry (GC-MS) (Figure 4.1) (Ciucanu & Kerek, 1984; Hakomori, 1964; Sims *et al.*, 2018). The exact procedure applied depends on the nature of the polysaccharide but, in general, the methylation analysis involves: (I) methylation of all available -OH groups; (II) complete hydrolysis of the per-*O*-methylated polysaccharide to its constituent partially methylated monosaccharides; (III) reduction of partially methylated pyranose/furanose monosaccharides to alditols; (IV) acetylation of newly available -OH groups resulting from the hydrolysis of glycosidic linkages and reduction procedures; (V) analysis of the PMAA derivatives by GC-MS (Figure 4.1). Methylation analysis of uronic acid-containing sulfated polysaccharides such as ulvan also require (a) desulfation and (b) carboxyl reduction steps as the charged sulfate groups and uronic acid residues can hinder analysis (Figure 4.1).

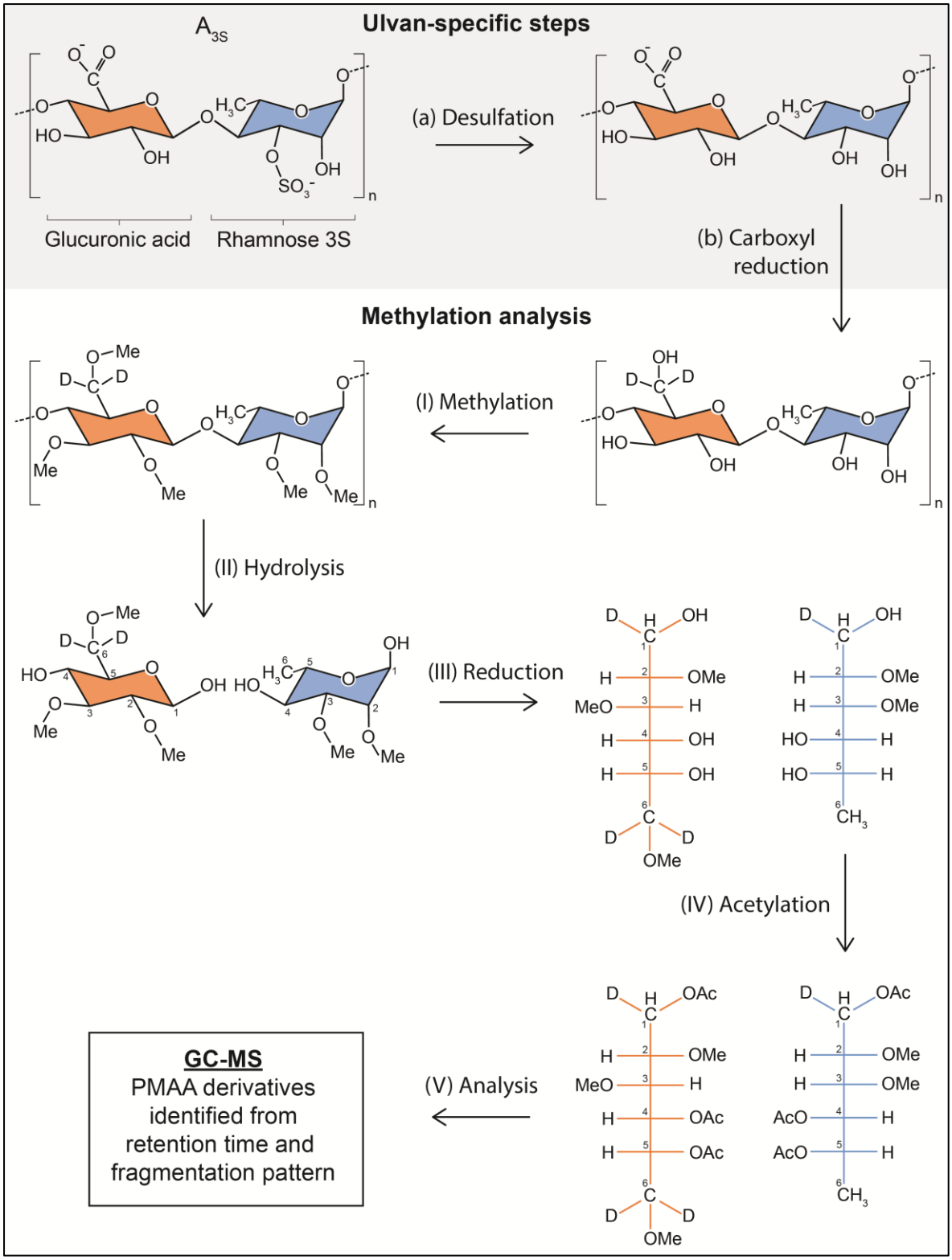

Figure 4.1: Flow chart of the steps involved in methylation analysis of ulvan using a glucuronic acid-rhamnose-3-sulfate diad (A_{3S} disaccharide) as an example. Each step is outlined in detail throughout the introduction.

Sulfate ester substitution patterns of sulfated polysaccharides can be determined through methylation analysis of sulfated and desulfated samples (Figure 4.1 (a)). Derivatisation of a sulfated sugar to a PMAA will result in an *O*-acetyl substitution where the sulfate ester was present (Figure 4.2). Derivatisation of the same sugar that has been desulfated will result in an *O*-methyl substitution where the sulfate ester was present prior to desulfation (Figure 4.2). Therefore, the carbons of constituent sugars that are *O*-acetylated in native samples and *O*-methylated in desulfated samples possess sulfate esters (Figure 4.2). However, desulfation of a complex polysaccharide like ulvan is inherently difficult. Acid hydrolysis of the sulfate esters is not suitable as this method results in concurrent depolymerisation of the polysaccharide and decomposition of acid-labile constituent sugars (e.g., xylose and iduronic acid) (Miller & Blunt, 1998; Quemener *et al.*, 1997; Usov, Adamyants, Miroshnikova, Shaposhnikova, & Kochetkov, 1971). In this regard, the acid-free solvolytic desulfation method, where the pyridinium salt form of the polysaccharide is heated in a mixture of DMSO, methanol, and pyridine, is more suitable. However, depolymerisation remains a problem even using the solvolytic method due to the high temperatures and long reactions times required (Bedini, Laezza, Parrilli, & Iadonisi, 2017; Miller & Blunt, 1998; Nagasawa, Inoue, & Kamata, 1977; Nagasawa, Inoue, & Tokuyasu, 1979; Usov *et al.*, 1971). Any significant depolymerisation of the polysaccharide that occurs during the desulfation procedure could result in erroneous interpretation of the results, as a hydrolysed glycosidic linkage may be misidentified as a sulfate substitution. Therefore, a conservative desulfation procedure well established in the literature, was used in the current chapter to reduce the likelihood of depolymerisation occurring (Nagasawa *et al.*, 1979).

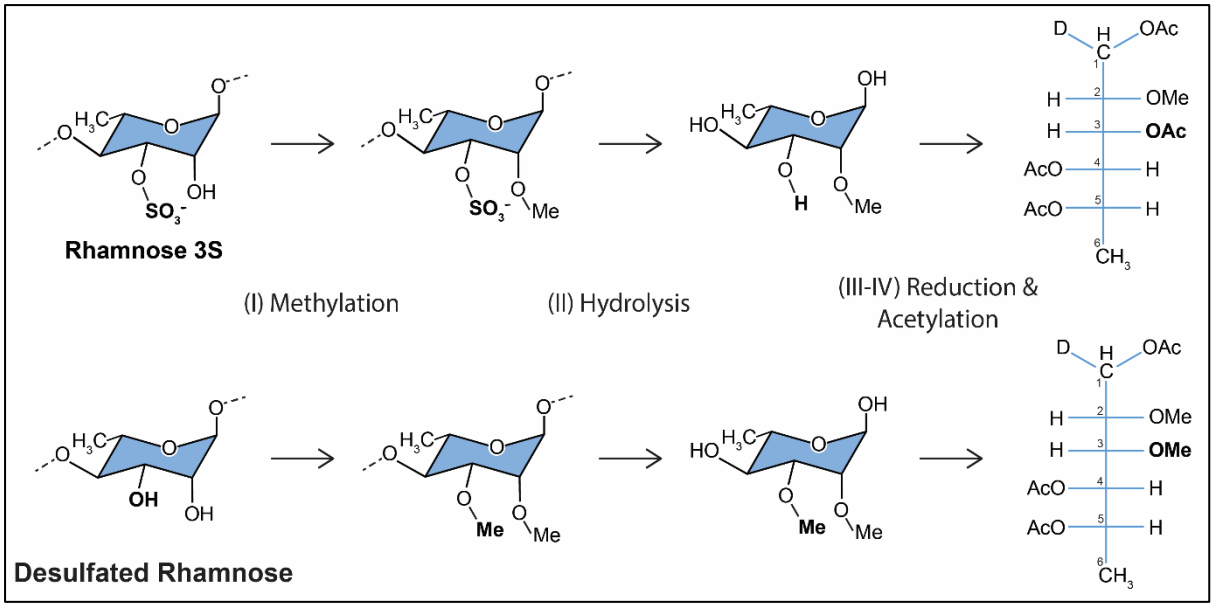

Figure 4.2: Derivatisation of 3-*O*-sulfated and desulfated rhamnose to PMAAs. The presence of a sulfate group in **Rhamnose 3S** will prevent 3-*O*-methylation and the sulfate group will (almost certainly) be lost during hydrolysis, resulting in 3-*O*-acetylation in the PMAA. In the **Desulfated Rhamnose**, the sulfate group is removed prior to methylation, so 3-*O*-methylation can occur and will be present in the PMAA.

Reduction of the carboxyl groups of uronic acids (Figure 4.1 (b)) is an essential derivatisation that facilitates methylation, hydrolysis, and acetylation in glycosyl linkage analysis (Pettolino *et al.*, 2012; Willför *et al.*, 2009). Performing linkage analysis without reducing the uronic acids to their neutral equivalents will result in under representation (or absence) of a uronic acid, as well as any linked neutral sugars, as the glycosidic bond between a uronic acid and neutral sugar is notoriously resistant to acid hydrolysis (BeMiller, 1967). Given that over 40 mol% of ulvan can be uronic acids (Kidgell *et al.*, 2021; Kidgell *et al.*, 2019), the sugar proportions obtained from linkage analysis on the native polysaccharide will be unrepresentative. Therefore, ulvans must be carboxyl reduced for accurate linkage analysis. Carboxyl reduction can be achieved through activation of the carboxyl group with a carbodiimide reagent followed by reduction with a deuterated reductant (sodium borodeuteride) to place two deuterium atoms on the C-6 carbons of uronic acid residues (i.e. reduction of C(=O)OH to CD_2OH). Once the subsequent methylation steps are complete, the PMAA dideuterio derivatives of uronic acids (e.g., glucose-6,6'-D2 from glucuronic acid) produce mass spectra with several fragments showing a characteristic 2 *m/z* increase, enabling the distinction of a reduced uronic acid from a native neutral monosaccharide.

Deuterium labelling is also important during the reduction of the partially methylated monosaccharides to their corresponding alditols (Figure 4.1 (III)). By using sodium borodeuteride as the reducing agent, a deuterium atom is placed on the anomeric carbon (C-1) so that enantiomeric PMAA derivatives can be distinguished (e.g., 3,4-di-*O*-methyl-xylitol (1,2-Xyl*p*) and 2,3-di-*O*-methyl-xylitol (1,4-Xyl*p*)). These derivatives do not separate on most GC columns but can be distinguished by the 1 *m/z* shift in mass fragment patterns due to the anomeric deuterium label. This issue is clearly detailed by Sims *et al.* (2018).

In the current chapter, glycosyl linkage positions and sulfate ester substitutions of each component monosaccharide from four ulvan samples were identified and quantified. The chapter builds on Chapter 3 (Kidgell *et al.*, 2021) with an investigation of the fine scale differences between ulvans isolated from two blade species of *Ulva* (*U. rigida* and *U.* sp. B) and two filamentous species of *Ulva* (*U. prolifera* and *U. ralfsii*). Three derivatised forms of each native ulvan were prepared and analysed:

- CR - carboxyl reduced material
- DS80 - desulfated at 80 °C, then carboxyl reduced material
- DS100 - desulfated at 100 °C, then carboxyl reduced material

Based on the previous chapter, it was hypothesised that ulvans from filamentous species of *Ulva* are more structurally complex than ulvans from blade species. Therefore, the aims were to: (I) identify differences in the monosaccharide linkage compositions of ulvans isolated from blade and filamentous species of *Ulva*; (II) determine the position and extent of sulfation of monosaccharide constituents of ulvans from blade and filamentous species of *Ulva*; and (III) investigate how the rhamnose, galactose, and iduronic acid, present in higher than literature median proportions in *U. prolifera*, *U. ralfsii*, and *U. rigida*, respectively, are linked and/or substituted in the ulvan polymer.

4.2 Methods

4.2.1 Materials

The following were purchased from Sigma-Aldrich: anhydrous pyridine (#270970), anhydrous DMSO (#276855), anhydrous methanol (#322415), HCl (#258148), 2-(N-morpholino) ethanesulfonic acid (MES, #M8250), potassium hydroxide (#221473), N-Cyclohexyl-N'-(2-morpholinoethyl)carbodiimide methyl-*p*-toluenesulfonate (#C106402),

sodium borodeuteride (#205591), Trizma base (#T1503), glacial acetic acid (#695092), triethylamine (#471283), dimethyl sulfoxide (DMSO, #276855), Iodomethane (#289566), ammonium hydroxide (#221228), methanol (#322415), ethyl acetate (#34858), acetic anhydride (#91204), dichloromethane (DCM, #34856), sodium carbonate (#222321), sodium nitrate (>99.0 %, #S5506), sodium azide (>99 %, #S2002),.

Other reagents were sourced as follows: trifluoroacetic acid (synthesis grade, Scarlau, Spain, #AC31420100), NaOH (50 % w/w, Fisher Scientific, Thermo Fisher Scientific, New Zealand, #SS254), perchloric acid (BDH Chemicals, #87003), and acetic acid (Fisher Scientific, #A38S), *myo*-inositol (research grade, Serva, Germany, #26310).

Purified native ulvans prepared for the research described in Chapter 3 (Kidgell *et al.*, 2021) were used.

4.2.2 Derivatisation and linkage analysis

4.2.2.1 Desulfation

Solvolytic desulfation of purified native ulvans was carried out based on methods previously described (Nagasawa *et al.*, 1979; Usov *et al.*, 1971), with some modifications. Ulvans were converted to the pyridinium salt form by dialysis (6-8 kDa tubing) against 10 volumes of 0.1 M pyridine-HCl (pH 7). The pyridine-HCl solution was changed three times, followed by two Type 1 water changes, each for 8-12 h. Once recovered by freeze drying, the pyridinium salt form of ulvan was dissolved (2.5 mg mL^{-1}) in an anhydrous mixture of dimethyl sulfoxide (DMSO)-methanol-pyridine (89:10:1) under an atmosphere of argon in a sealed Kimax tube. The solution was then heated to 80 °C or 100 °C for 4 h in a dry heating block. Once cooled, the solution was dialysed (6-8 kDa) against Type 1 water four times, 8-12 h each, and the desulfated ulvan was recovered by freeze drying. The extent of desulfation was evaluated by Fourier-transform infrared spectroscopy (FTIR, particularly monitoring the S=O bond at ~1250 cm^{-1}). FTIR spectra were recorded on a Bruker Tensor II between wavenumbers 400 and 4000 cm^{-1} with an average of 32 scans. Data were processed in Opus software (Ver. 8.1) using the built-in smoothing function followed by ATR correction, baseline correction and normalisation around the significant peak for S=O (~1250 cm^{-1}).

The molecular weight distributions of native and desulfated ulvans from *U*. sp. B and *U*. *ralfsii* were determined using size-exclusion chromatography coupled with a refractive index detector (SEC-RI) to determine if any depolymerisation had occurred during desulfation. Samples (5 mg mL^{-1} in 0.1 M $NaNO_3$) were separated on three columns (TSK-Gel G5000PWXL, G4000PWXL, and G3000PWXL, 300 x 7.8 mm, Tosoh Corp., Tokyo, Japan) connected in series, with a void volume (V_0) of 15 mL and total volume (V_t) of 32 mL, eluting with 0.1 M $NaNO_3$ with 0.02 % NaN_3 (0.5 mL min^{-1}, 60 °C). The eluted material was detected using a variable wavelength detector (280 nm) and a refractive index monitor. Molecular weight distributions of desulfated ulvans from *U. rigida* and *U. prolifera* were not determined due to lack of material.

4.2.2.2 Carboxyl reduction

The uronic acid constituents of native and desulfated ulvans were reduced using a modified version of a previously described protocol (Sims & Bacic, 1995). Briefly, desulfated and purified native ulvans (5 mg) were dissolved in Type 1 water (2 mL) and the uronic acids were activated with *n*-cyclo-*n*-(2-morpholineoethyl) carbodiimide *metho*-*p*-toluensulfonate (400 µL, 500 mg mL^{-1}) at 30 °C for 3 h using 2-(N-morpholino)ethanesulfonic acid (MES)-KOH (400 µL, pH 4.75) to buffer the reaction. The activated uronic acids were then reduced using sodium borodeuteride ($NaBD_4$; 1 mL, 70 mg mL^{-1} in 0.05 M NaOH) for 18 h at 25 °C buffered with Tris-HCl (1 mL, pH 8.0). After 18 h, excess reductant was neutralised by drop-wise addition of glacial acetic acid prior to samples being dialysed (6-8 kDa tubing) against 10 volumes of Type 1 water for 24 h (three water changes), followed by freeze drying. This carboxyl reduction procedure was repeated 2-3 times until the uronic acid content was reduced to <5 % w/w, as determined by constituent sugar analysis using HPAEC-PAD (Nep *et al.*, 2016).

4.2.2.3 Methylation

Per-*O*-methylation was performed using the method of Ciucanu and Kerek (1984) on the carboxyl reduced ulvans (CR), and desulfated and carboxyl reduced ulvans (DS80, DS100). Prior to methylation, the samples were converted to the triethylammonium salt form (to increase solubility of ulvan in DMSO) by dialysis (6-8 kDa tubing) against 10 volumes of 0.1 M triethylamine-HCl (pH 7.0) involving three solution changes followed by two changes of Type

1 water, each for 8-12 h (Stevenson & Furneaux, 1991). Freeze dried ulvans in the triethylammonium salt form (0.5 mg in duplicate) were dissolved in DMSO (200 µL) overnight at 25 °C before addition of freshly prepared NaOH/DMSO slurry (200 µL; slurry prepared from ~120 mg NaOH pellets ground in 1 mL DMSO). Three aliquots of iodomethane (50 µL) were added with 30, 30, and 60 minutes of sonication and stirring following the addition of each aliquot, respectively. The reaction was completed with addition of Type 1 water (2 mL) and glacial acetic acid (100 µL) prior to dialysis (6-8 kDa tubing) against 10 volumes of Type 1 water with frequent water changes until conductivity was <1 µS cm^{-1}. Permethylated ulvans were recovered by freeze drying and subject to the methylation protocol a second time.

Following methylation, partially methylated alditol acetates (PMAA) were generated. The permethylated polysaccharides were hydrolysed in TFA (200 µL, 2.5 M) for 1 h at 121 °C followed by addition of *myo*-inositol (10 µg) to act as an internal standard. The samples were then reduced using $NaBD_4$ (100 µL, 1 M in 2 M NH_4OH) for 18 h at 25 °C followed by addition of glacial acetic acid (50 µL) to neutralise excess reductant. Two aliquots of acetic acid in methanol (500 µL, 5 % v/v) were added and evaporated under a stream of air until dry after each addition. Finally, methanol (500 µL) was added and evaporated repeatedly (2-4 times) until the sample was crystalline. The partially methylated alditols were acetylated based on the method established by Harris, Henry, Blakeney, and Stone (1984) using a mixture of glacial acetic acid (40 µL), ethyl acetate (200 µL), acetic anhydride (600 µL), and 60 % perchloric acid (23 µL) over 15 min at 25 °C. Type 1 water (2 mL) and 1-methylimidazole (40 µL) were added to quench the reaction. PMAAs were partitioned into dichloromethane (DCM, 2 mL), the samples thoroughly mixed and centrifuged (2000 rpm, 5 min), and the aqueous layer was removed using Pasteur pipettes. The DCM was rinsed with 0.5 M Na_2CO_3 (2 mL) and Type 1 water (2 mL, twice) each time followed by mixing, centrifuging and removal of the aqueous layer. Finally, the DCM was evaporated under a stream of air and the residual partially methylated alditol acetates dissolved in acetone (analytical grade) for analysis.

PMAAs were analysed on an Agilent 8890 GC system coupled with a 5977B mass spectrum detector. Samples (1 µL) were auto-injected at 250 °C using splitless mode into a fused-silica capillary BPX90 (25m x 0.22 mm i.d., 0.25mm film thickness) column at 80 °C with a He flow rate of 1.5 mL min^{-1}. The temperature was held for 1 min, then increased to 130 °C at a rate of 50 °C min^{-1}, then up to 250 °C at a rate of 5 °C min^{-1} with a final hold of 10 min.

The separated derivatives were analysed using an electron impact mass detector (70 eV, source temperature 230 °C, quadrupole temperature 150 °C), scanning from 40-400 *m/z*. Data were processed in Agilent OpenLabs software (Ver. 2.4).

4.2.3 Data analysis

Ulvan PMAA derivatives were identified by GC retention time relative to *myo*-inositol and electron impact mass spectra of the derivative, compared to previously prepared PMAA standards (Doares, Albersheim, & Darvill, 1991). Relative mol% of linkages were then calculated by standardising the peak area of an identified PMAA derivative by its molecular weight. FTIR figures were produced using R from data exported from Opus. Figures produced in propriety software were refined in Adobe Illustrator (Ver. 24).

4.3 Results and discussion

The glycosyl linkages and positions of sulfate substitution of the monosaccharide constituents of four ulvans isolated from blade (*U. rigida* and *U*. sp. B) and filamentous (*U. prolifera* and *U. ralfsii*) species of *Ulva* were quantified. Ulvan isolated from *U. prolifera*, *U. ralfsii* (cult.), and *U. rigida* were chosen as these had higher than median (Kidgell *et al.*, 2019) proportions of rhamnose (60 mol%), galactose (16 mol%), and iduronic acid (18 mol%), respectively (Table 4.1). Ulvan isolated from *U.* sp. B (cult. B) was included to represent the more 'conventional' sugar composition of ulvan (Table 4.1). Native and desulfated ulvans (80 °C and 100 °C) were analysed following carboxyl reduction of the uronic acid constituents, resulting in three derivatised forms, CR, DS80 and DS100, respectively. The sulfate substitution of the monosaccharide constituents was inferred by comparing the glycosyl linkage compositions of CR ulvans with DS80 and DS100 counterparts. The major monosaccharide components of all four ulvans, rhamnose (Rha), glucuronic acid (GlcA), xylose (Xyl), iduronic acid (IdoA) and galactose (Gal) were all predominantly 1,4-linked, consistent with the literature consensus of ulvan containing a 1,4-linked backbone (Chattopadhyay *et al.*, 2007; Lahaye & Robic, 2007; Lopes *et al.*, 2017; McKinnell & Percival, 1962b; Ray & Lahaye, 1995a). Rhamnose and glucuronic acid residues accounted for 68 – 87 mol% of all CR ulvans, with the predominant linkages from ulvans of the blade species being →3,4)-Rha*p*-(1→ and →4)-GlcA*p*-(1→ (Table 4.2). Ulvans from the filamentous species, however, had higher proportions of →2,3,4)-Rha*p*-(1→ than →3,4)-Rha*p*-(1→ and →4)-GlcA*p*-(1→. Varying

degrees of sulfate substitution were detected on *O*-3 of rhamnose and *O*-2 of xylose in all ulvans; ulvans from filamentous species also contained sulfate substitution on *O*-2 of glucuronic acid. These results suggest that the A_{3S} disaccharide, →4)-GlcA*p*-(1→4)-Rha*p*3S-(1→, is the principal repeat unit in all four ulvans (Lahaye & Robic, 2007). However, the predominance of →2,3,4)-Rha*p*-(1→ in ulvans from filamentous species suggests that the majority of rhamnose in these ulvans is also branched on *O*-2. The ulvans from filamentous species had a higher proportion of branched linkages and different sulfate substitution positions compared to ulvans from blade species, confirming the hypothesis that filamentous species of *Ulva* contain ulvan with greater structural complexity.

Table 4.1: Summarised constituent sugar composition (normalised mol%) of purified ulvan from *U. rigida*, *U*. sp. B, *U. prolifera* and *U. ralfsii*. See Chapter 3 (Kidgell *et al.*, 2021) for details.

Ulvan Species	Morphology	Sugars (normalised mol%)[a]				
		Rha	GlcA	Xyl	IdoA	Gal
rigida	Blade	49	26	6	18	tr.[b]
sp. B (cult.B)	Blade	48	31	7	11	2
prolifera	Filamentous	60	17	15	7	tr.
ralfsii (cult.)	Filamentous	38	24	16	4	16

[a] Values are the averages of duplicate analyses

[b] Sugars < 1 mol% are considered trace (tr.)

4.3.1 Ulvan linkage compositions

The ulvans from blade and filamentous species of *Ulva* had distinctly different glycosyl linkage compositions, with ulvans from blade species (*U.* sp. B and *U. rigida*) exhibiting fewer branched and substituted sugars, compared to ulvans from filamentous species (*U*. *ralfsii* and *U. prolifera*) (Table 4.2). CR ulvans of *U.* sp. B and *U. rigida* were predominantly composed of →3,4)-Rha*p*-(1→ and →4)-GlcA*p*-(1→, collectively accounting for 75 and 58 mol% of the total linkages in these ulvans, respectively; suggesting that the A_{3S} disaccharide is the principal repeat unit. High proportions of A_{3S} linkages have also been detected in carboxyl reduced ulvans from other blade species, *U. ohnoi* (68.4 mol%), and *U. rigida* (61.9 mol%) (Luiten *et al.*, Under review; Ray & Lahaye, 1995a). In contrast, the ulvans isolated from the filamentous species of *Ulva* assessed here, *U. ralfsii* and *U. prolifera*, had →2,3,4)-Rha*p*-(1→ as the predominant linkage (23 and 21 mol%, respectively) followed by →3,4)-Rha*p*-(1→ and →4)-

GlcA*p*-(1→. These three linkages collectively accounted for 58 and 48 mol% of the total linkages in these ulvans, respectively. High proportions of →2,3,4)-Rha*p*-(1→ have previously been reported in ulvan isolated from filamentous *U. tepida* (15.7 mol%), and *U. prolifera*[3] (16.8 mol%) (Luiten *et al.*, Under review); smaller proportions were also detected in ulvan from *U. compressa* (1 mol%) (Chattopadhyay *et al.*, 2007). Indeed, →2,3,4)-Rha*p*-(1→ is frequently reported to some degree during ulvan linkage analysis, irrespective of the morphology of *Ulva* (Gosselin *et al.*, 1964; Lopes *et al.*, 2017; Ray & Lahaye, 1995a). However, high proportions of →2,3,4)-Rha*p*-(1→ have only been reported for ulvans from filamentous species of *Ulva*. Another distinguishing glycosyl linkage of the ulvans from filamentous species in this study is →2,4)-GlcA*p*-(1→ (Table 4.2). The same residue was detected in ulvans from filamentous *U. tepida* and *U. prolifera*, but not blade *U. ohnoi* (Luiten *et al.*, Under review). Consistent with constituent sugar analysis, ulvans from blade and filamentous species had higher proportions of iduronic acid and xylose linkages, respectively, both of which were predominately 1,4-linked (Table 4.2). Additionally, there is a higher proportion of →2,4)-Xyl*p*-(1→ in ulvans from filamentous species. The glycosyl linkage analysis of the four CR ulvans assessed here indicates that the ulvans from filamentous species of *Ulva* have higher proportions of branched sugars, suggesting a broader range of sulfate ester substitutions.

[3] The ulvan from *U. prolifera* analysed by Luiten *et al.* (Under review) had a remarkably different chemical composition (constituent sugar composition and glycosyl linkage residue proportions) to the ulvan from *U. prolifera* analysed in this chapter

Table 4.2: Glycosyl linkage composition (relative mol%) of the carboxyl reduced (CR) and 80 °C and 100 °C desulfated, carboxyl reduced ulvans (80DS and 100DS, respectively) isolated from *U. rigida*, *U.* sp. B, *U. prolifera*, *U. ralfsii*. The total mol% of deduced linkages for each monosaccharide is presented in bold. The mol% constituent sugars for each native ulvan, as determined by HPAEC-PAD, are included for reference in bold brackets.

		***U.* sp. B**			***U. rigida***			***U. ralfsii***			***U. prolifera***		
Methylated Derivative	**Deduced Linkage**	**CR**	**80°C DS**	**100°C DS**	**CR**	**80°C DS**	**100°C DS**	**CR**	**80°C DS**	**100°C DS**	**CR**	**80°C DS**	**100°C DS**
2,3,4-Rha[a]	Rha*p*-(1→	1[b]	1	2	2	2	3	3	3	3	17	15	18
2,4-Rha	→3)-Rha*p*-(1→	2	1	-[c]	3	1	-	2	2	2	7	8	8
2,3-Rha	→4)-Rha*p*-(1→	2	10	31	5	11	29	tr.[d]	3	8	3	7	11
3-Rha	→2,4)-Rha*p*-(1→	-	1	3	-	1	3	-	6	16	-	4	11
2-Rha	→3,4)-Rha*p*-(1→	44	34	13	36	32	15	13	9	5	17	13	7
Rha	→2,3,4)-Rha*p*-(1→	6	5	2	10	6	3	23	16	7	21	16	8
	Total Rha	**55 (48)**	**52**	**51**	**56 (49)**	**53**	**53**	**41 (38)**	**39**	**41**	**65 (60)**	**63**	**63**
2,3,4,6-Glc	GlcA*p*-(1→	1	1	1	2	1	tr.	1	1	1	-	-	-
2,3,6-Glc	→4)-GlcA*p*-(1→	31	31	33	22	24	25	22	25	24	10	11	12
3,6-Glc	→2,4)-GlcA*p*-(1→	tr.	tr.	tr.	1	tr.	tr.	4	2	1	5	4	3
2,6-Glc	→3,4)-GlcAp-(1→	tr.	tr.	tr.	tr.	tr.	tr.	tr.	-	-	1	1	1
	Total GlcA	**32 (31)**	**32**	**34**	**25 (26)**	**25**	**25**	**27 (24)**	**28**	**26**	**16 (17)**	**16**	**16**
2,3-Xyl	→4)-Xyl*p*-(1→	4	6	7	5	6	6	10	12	14	6	10	11
3-Xyl	→2,4)-Xyl*p*-(1→	2	-	-	1	-	-	3	2	2	5	3	2
	Total Xyl	**6 (7)**	**6**	**7**	**6 (6)**	**6**	**6**	**13 (16)**	**14**	**16**	**11 (15)**	**13**	**13**
2,3,6-Ido	→4)-IdoA*p*-(1→	6	7	7	9	13	13	-	2	2	2	3	3
3,6-Ido	→2,4)-IdoA*p*-(1→	-	tr.	tr.	tr.	tr.	tr.	1	tr.	tr.	1	1	1
	Total IdoA	**6 (11)**	**7**	**7**	**9 (18)**	**13**	**13**	**1 (4)**	**2**	**2**	**3 (7)**	**4**	**4**
2,3,4,6-Gal	Gal*p*-(1→	-	-	-	-	-	-	1	1	3	-	tr.	tr.
2,3,6-Gal	→4)-Gal*p*-(1→	tr.	tr.	tr.	-	-	-	13	12	9	1	tr.	tr.
2,3,4-Gal	→6)-Gal*p*-(1→	tr.	tr.	tr.	1	1	1	1	2	2	1	2	2
2,3-Gal	→4,6)-Galp-(1→	tr.	-	-	1	tr.	-	2	tr.	tr.	2	1	-
2,6-Gal	→3,4)-Galp-(1→	1	tr.	-	tr.	tr.	-	1	1	-	tr.	tr.	-
	Total Gal	**1 (2)**	**0**	**0**	**2 (0)**	**1**	**1**	**18 (16)**	**16**	**15**	**4 (0)**	**3**	**2**
Others[e]		**0**	**3**	**1**	**2**	**2**	**2**	**1**	**1**	**0**	**1**	**1**	**2**

[a] 2,3,4-Rha = 1,5-di-*O*-acetyl-1-deuterio-2,3,4-tri-*O*-methylrhamnitol etc.

[b] values are the averages of duplicate analyses.

[c] -, not detected.

[d] tr., < 1 mol%

[e] minor linkages; sum of < 1 mol% trace derivatives

4.3.2 Desulfation of ulvans

Ulvans were desulfated at two temperatures (80 °C and 100 °C) as there is evidence to suggest that the higher temperature is more efficient but may degrade the ulvan. At the higher temperature (100 °C) ulvans were desulfated to a greater extent but neither desulfation treatment (80 °C or 100 °C) resulted in removal of all sulfate groups (Figure 4.3). A clear reduction in S=O peak height (~1250 cm^{-1}) is detected on the FTIR spectra between the 80 °C and 100 °C desulfation treatments for all ulvans, suggesting a substantial quantity of sulfate groups were removed at the higher temperature (Figure 4.3). A smaller reduction in peak height is detected between the native and 80 °C desulfation treatment, indicating that at least some sulfate groups were removed at this lower temperature.

To limit degradation of the ulvans but still reduce the sulfate ester content, a conservative desulfation procedure, well established in the literature, was used (Nagasawa *et al.*, 1979). This procedure was initially trialled on ulvans from *U*. sp. B and *U. ralfsii* (due to insufficient material, *U. rigida* and *U. prolifera* were not included in the trial), at two temperatures, 80 °C and 100 °C, to determine the best conditions for desulfating the polymers with minimal degradation. A reaction temperature of 100 °C resulted in removal of more sulfate groups compared to 80 °C for ulvans from both *U*. sp. B and *U. ralfsii* (Figure 4.3; estimated by reduction in intensity of the S=O bond at ~1250 cm^{-1} on FTIR (Lloyd, Dodgson, Price, & Rose, 1961)). However, the 100 °C treatment also resulted in a shift in the molecular weight distribution of both ulvans (Figure 4.4). The SEC-RI chromatograph of ulvan from *U.* sp. B following desulfation at 100 °C displays a distinct shoulder (~22 min) to the right of the major peak (Figure 4.4), while the chromatograph of ulvan from *U. ralfsii* displays the formation of a small well resolved peak (~25 min) to the right of the major peak. Both shifts indicate the presence of lower molecular weight material following 100 °C desulfation, but it is interesting to note that the shift in molecular weight distribution is different for the two ulvans. As a result of this trial, desulfation was performed at both 80 °C and 100 °C for all four ulvans to monitor progressive desulfation and account for possible depolymerisation at 100 °C (Figure 4.3).

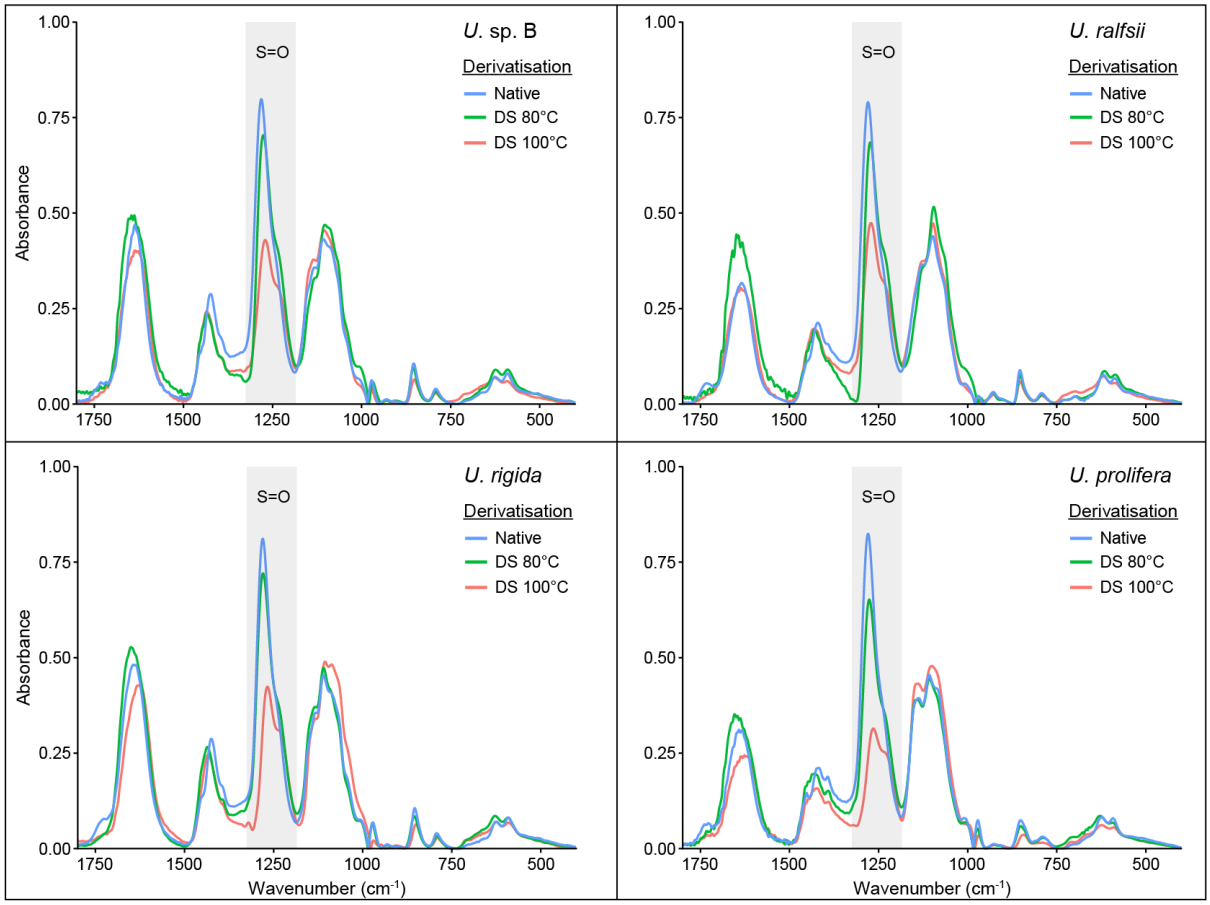

Figure 4.3: FTIR plots of native and desulfated (80 °C and 100 °C treatments) ulvans from four species of *Ulva* (*U.* sp. B, *U. ralfsii*, *U. rigida*, and *U. prolifera*) with the S=O bond around wavenumber 1250 cm^{-1} highlighted.

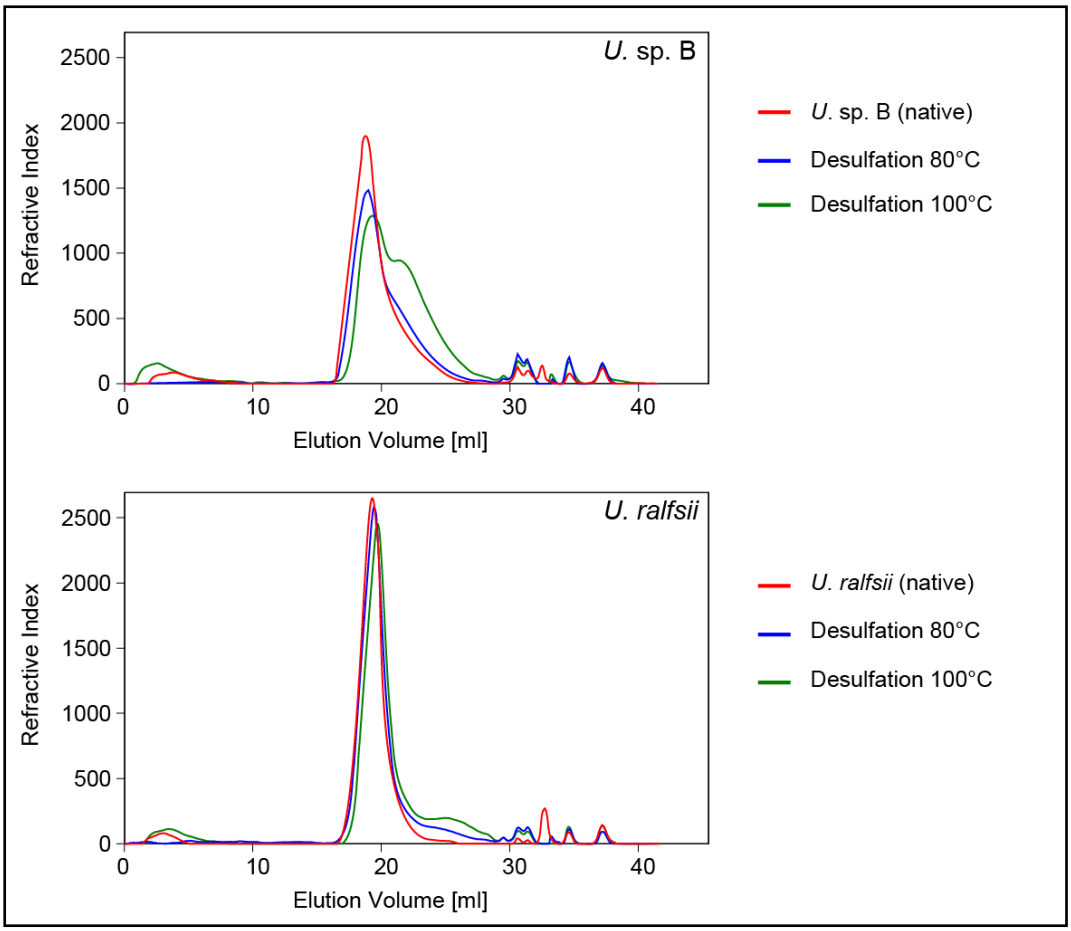

Figure 4.4: The refractive index (RI) trace from size-exclusion chromatography (SEC) of native ulvans isolated from *U.* sp. B and *U.* ralfsii, and the desulfated (80 °C and 100 °C) derivatives of these ulvans.

4.3.3 Sulfate ester substitution of ulvans

Comparison of the glycosyl linkage compositions of CR ulvans with their desulfated counterparts indicates that 1,4-linked rhamnose is predominantly 3-*O*-sulfated in all four ulvans (Table 4.2), which is consistent with the literature (Chattopadhyay *et al.*, 2007; Lahaye & Robic, 2007; Ray & Lahaye, 1995a). Additionally, the linkage analysis suggests that some 1,4-linked xylose is 2-*O*-sulfated in all four ulvans, and that minor proportions of 1,4-linked glucuronic acid may be 2-*O*-sulfated in the ulvans from filamentous species. For rhamnose, the various derivatised ulvans from *U*. sp. B show the progressive loss of 3-*O*-sulfate esters clearly: the proportion of →3,4)-Rha*p*-(1→ (i.e., 2-*O*-Me-Rha) successively reduces from 44, to 34, to 13 mol% between CR, DS80, and DS100, respectively, with a simultaneous increase in the proportion of →4)-Rhap-(1→ (i.e., 2,3-*O*-Me_2-Rha) from 2, to 10, to 31 mol% through the same derivatisations. And, importantly, the combined mol% of →3,4)-Rha*p*-(1→ and →4)-

Rha*p*-(1→ remains almost unchanged in each of these derivatisations (46, 44, and 44 mol% for CR, DS80, and DS100, respectively). Therefore, the only difference between these derivatives is the loss of an *O*-3 sulfate ester in DS80 and DS100 ulvans, as evidenced by the progressive reduction in 3-*O*-acetyl substitutions and simultaneous increase in 3-*O*-methyl substitutions in the PMAA derivatives. The same pattern is present in the other three ulvans, however, the higher proportion of →2,3,4)-Rha*p*-(1→ in these ulvans complicates interpretation. A similar inverse change in proportions is detected for →2,4)-Xyl*p*-(1→ to →4)-Xyl*p*-(1→ for all ulvans and →2,4)-GlcA*p*-(1→ to →4)-GlcA*p*-(1→ for ulvans from filamentous species, albeit in much lower proportions of linkages compared to rhamnose. These changes in proportions suggest the presence of *O*-2 sulfate esters, but it is a tentative conclusion due to the minor quantity of these linkages.

In the four ulvans assessed, the pattern of rhamnose substitution is clear when the percentage of 1,4-linked rhamnose residues that also contain a linkage or substitution at *O*-2 or *O*-3 (i.e., are 2-*O*- or 3-*O*-acetylated) is considered (Figure 4.5). For example, the percentage of 1,4-linked rhamnose residues that contains an *O*-3-acetyl group: ([3,4-Rha + 2,3,4-Rha]/[4-Rha + 2,4-Rha + 3,4-Rha + 2,3,4-Rha])*100. This comparison effectively provides the percentage of rhamnose residues that are 1,4-linked in the backbone of ulvan while also containing either a sugar branch or sulfate on *O*-2 or *O*-3. Figure 4.5 clearly identifies that in all four ulvans the percentage of 3-*O*-acetyl substitution progressively reduces from 91-99 % in the CR ulvan, to 72-78 % in DS80, and finally 30-40 % in DS100 - conclusive evidence of the loss of sulfate esters at *O*-3 of rhamnose. These percentages correlate with the reduction in the peak height of the S=O absorbance on the FTIR, where the peak from DS100 ulvans was approximately 1/2 to 1/3 the height of the peak from CR ulvans (Figure 4.3). Therefore, in the four ulvans assessed, the vast majority of 1,4-linked rhamnose occurred as rhamnose-3-sulfate in the native polysaccharide. Presenting the data in this way also highlights the percentage of 1,4-linked rhamnose residues that are substituted at *O*-2: 10-20 % for ulvans from blade species of *Ulva*, and 51-64 % for ulvans from filamentous species (Figure 4.5). The same percentage (20 %) of *O*-2 branching on 1,4-linked rhamnose residues has previously been reported for ulvan from blade *U. rigida* (Ray & Lahaye, 1995a). As the presence of this substitution does not change with desulfation treatments, the substituent at *O*-2 is concluded to be a branching point or substituted with another group.

Ulvan	Carboxyl Reduced (CR)	80°C Desulfated (DS80)	100°C Desulfated (DS100)
U. sp. B (blade)	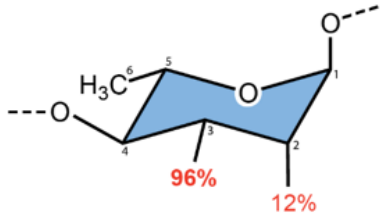	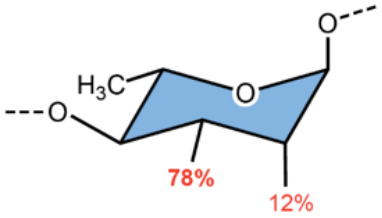	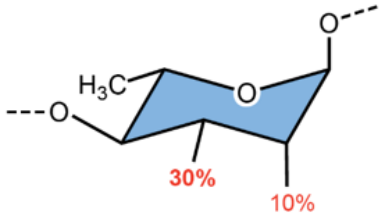
U. rigida (blade)	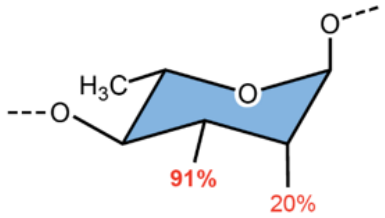	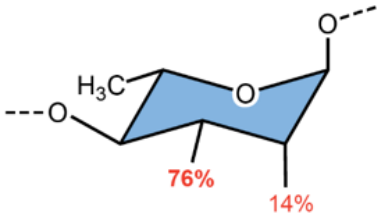	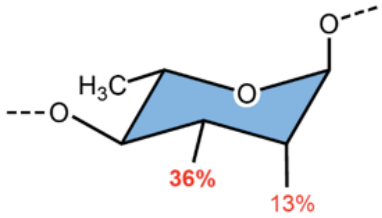
U. ralfsii (filamentous)	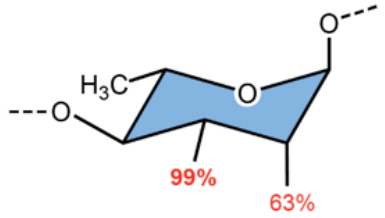	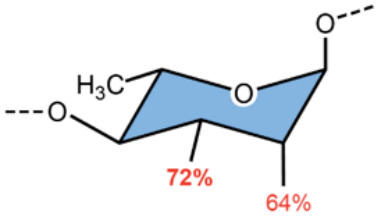	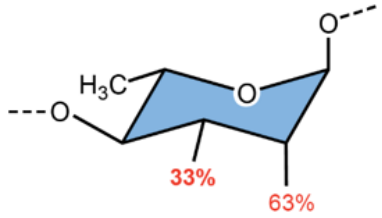
U. prolifera (filamentous)	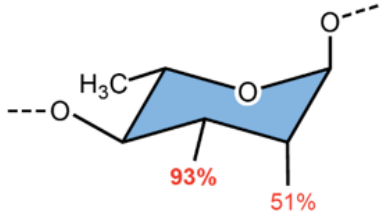	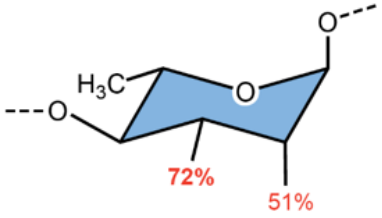	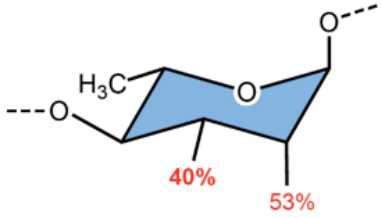

Figure 4.5: The percentage of 2- or 3-*O*-acetyl substitution of 1,4-linked rhamnose PMAA residues for carboxyl reduced and desulfated ulvans from *U*. sp. B, *U. rigida*, *U. ralfsii*, and *U. prolifera*. These percentages indicate how often rhamnose in the backbone of ulvan contains a 2- or 3- linkage to a sugar or sulfate.

4.3.4 Substitution of 1,4-linked rhamnose

The unidentified *O*-2 substitution of 1,4-linked rhamnose-3S could potentially be a glucuronic acid branch, as has been previously reported (Lahaye & Ray, 1996). A branch to glucuronic acid, or any other sugar, would need to be capped with a terminal sugar. In the linkage proportions detected, there are not enough terminal sugars to account for the number of *O*-2 branches present, except for the ulvan from *U. prolifera* (discussed in 4.3.5). For the other three ulvans, it is possible that the 1,4-linked rhamnose-3-sulfate residues may contain a glucuronic acid branch at *O*-2, however, the terminal sugar on such a branch would remain unaccounted for.

An excess of branch points in the linkages detected and the presence of fully acetylated sugars, such as →2,3,4)-Rha*p*-(1→, are characteristic signs that undermethylation has occurred (Biermann & McGinnis, 1989). However, the success of the methylation step in the current study is evidenced by the comparison of the linkages between CR, DS80, and DS100 PMAA derivatives (Table 4.2, Figure 4.5) indicating a near stoichiometric shift of the *O*-3 substitution of rhamnose from *O*-acetyl (sulfated) to *O*-methyl (desulfated) as the degree of desulfation increased. Additionally, the concurrent increase in →2,4)-Rha*p*-(1→ indicates that *O*-2 of rhamnose is not sulfated and that undermethylation at this position due to steric hinderance from *O*-3 sulfate esters in CR ulvans is not occurring. The *O*-2 substitution of 1,4-linked rhamnose-3S could also be to an unidentified substituent that was lost during sample preparation, such as a highly volatile sugar alcohol (Biermann & McGinnis, 1989). However, there is no evidence for losses of monosaccharide constituents during linkage analysis which could account for the *O*-2 branch. Both the constituent sugar analysis (HPAEC-PAD) and linkage analysis (GC-MS) report similar proportions of sugars. Furthermore, accounting for the total sugars (% w/w) detected by constituent sugar analysis combined with the sulfate and ash content determined in Chapter 3 (Kidgell *et al.*, 2021), 85-96 % of the ulvan is accounted for. Further investigation of enzymatically hydrolysed ulvans from filamentous species of *Ulva*, particularly through more in-depth 2D NMR analyses (e.g., HMBC, HSQC-TOCSY) supported by linkage analysis and high-resolution mass spectrometry (LCMS) would be beneficial in identifying this unknown *O*-2 substituent on rhamnose.

4.3.5 The linkages of ulvan constituent sugars present in higher-than-median proportions

The ulvan isolated from *U. prolifera* was chosen for linkage analysis due to the high proportion of rhamnose identified by constituent sugar analysis, 60 mol%, compared to the literature median of 45 mol% (Chapter 3 (Kidgell *et al.*, 2019)). The linkage analysis determined that the structure of this ulvan was highly complex with multiple representative rhamnose glycosyl residues, including considerable amounts of →3)-Rha*p*-(1→ (7-8 mol%), and terminal rhamnose (Rha*p*-(1→, 15-18 mol%, Table 4.2) – the highest proportion of terminal sugar (of any monosaccharide) detected in the ulvan literature. Generally, only lesser quantities of terminal glucuronic acid (1-8 mol%) and terminal rhamnose (1-3 mol%) are reported for ulvans (Chattopadhyay *et al.*, 2007; Gosselin *et al.*, 1964; Luiten *et al.*, Under review; Ray & Lahaye, 1995a). A general rule when interpreting glycosyl linkage analysis from (non-sulfated) polysaccharides is that for each branch point on a sugar there should be a terminal sugar to cap the branch (Pettolino *et al.*, 2012). However, the presence of sulfate esters, particularly coupled with incomplete desulfation, muddles this neat relationship between branch points and terminal sugars. For simplicity, in the following comparison of DS100 ulvans it has been assumed that all *O*-3 substituents on 1,4-linked rhamnose moieties are sulfate esters. The high proportion of terminal rhamnose in DS100 ulvan from *U. prolifera* (18 mol%) almost completely accounts for the branched linkages for this ulvan (21 mol%: 11 mol% →2,4)-Rha*p*-(1→; 8 mol% →2,3,4)-Rha*p*-(1→; 1 mol% →3,4)-GlcA*p*-(1→; 1 mol% →2,4)-IdoA*p*-(1→). In contrast, the terminal sugars of the other three DS100 ulvans only account for 1/3 to 1/2 of the branches present (Table 4.2). Two other studies have found agreement in the ratio of terminal to branched sugars of desulfated, carboxyl reduced ulvans (Chattopadhyay *et al.*, 2007; Ray & Lahaye, 1995a). However, it should be noted that a second ulvan assessed in one of these studies also had an excess of branched linkages (Ray & Lahaye, 1995a).

The ulvan from *U. rigida* was specifically chosen for linkage analysis because it contained considerably more iduronic acid (18 mol%) than the other ulvans assessed (Chapter 3 (Kidgell *et al.*, 2021)). The major iduronic acid linkage detected for *U. rigida*, and indeed all the ulvans assessed, was →4)-IdoA*p*-(1→, with minor proportions of →2,4)-IdoA*p*-(1→ also detected. The presence of →4)-IdoA*p*-(1→ is indicative of the aldobiuronic acid B_{3S}, →4)-IdoA*p*-(1→4)-Rha*p*3S-(1→ (Lahaye & Robic, 2007). The results reported here are supported

by the only other study of ulvans to detect and quantify linkages for iduronic acid, where ulvans from *U. ohnoi* (7.6 mol% IdoA), *U. tepida* (3.1 mol% IdoA), and *U. prolifera* (3.1 mol% IdoA) contained →4)-IdoA*p*-(1→, with minor proportions of →2,4)-IdoA*p*-(1→ also found in *U. tepida* (Luiten *et al.*, Under review). Indeed, the identification of iduronic acid through linkage analysis in the current study is only possible due to pioneering work in preparing a standard mixture of partially methylated alditol acetates of idose (Luiten *et al.*, Under review). Another similarity between the paper by Luiten *et al.* and the current chapter is that iduronic acid is underrepresented in the results from glycosyl linkage analysis (GC-MS, Table 4.2) compared to the results from constituent sugar analysis (HPAEC-PAD, Table 4.1). The underrepresentation of iduronic acid by linkage analysis is particularly noticeable for the CR ulvan from *U. rigida*, where the iduronic acid content is half that determined by constituent sugar analysis (9 and 18 mol%, respectively) (Table 4.2; Chapter 3 (Kidgell *et al.*, 2021)). It is possible that the multiple derivatisation steps involved in glycosyl linkage analysis could result in the destruction of some of the iduronic acid, as the monosaccharide is notoriously acid labile (Conrad, 1980). Alternatively, the various conformations of iduronic acid (Casu *et al.*, 1988; Hsieh *et al.*, 2016) may have different susceptibility to carboxyl reduction. However, this is unlikely as the carboxyl reduction was confirmed to have reduced >90 % of the uronic acids by HPAEC-PAD. Variable representation of sugar proportions from different analyses, exemplified by iduronic acid here, highlights the inherent complexity of carbohydrate analysis.

The ulvan isolated from *U. ralfsii* was chosen for linkage analysis due to the unusually high proportion of galactose (16 mol%; Table 4.2; Chapter 3 (Kidgell *et al.*, 2021)), compared to the literature median of 2.1 mol% (Kidgell *et al.*, 2019). The galactose in this ulvan was present predominantly as →4)-Gal*p*-(1→, with minor proportions of Gal*p*-(1→, →6)-Gal*p*-(1→, →3,4)-Gal*p*-(1→, and →4,6)-Gal*p*-(1→ (Table 4.2). Similarly, the high proportion of galactose within ulvans from filamentous *U. tepida* (13.8 mol%) and *U. prolifera* (27.1 mol%) resulted in a wide range of glycosyl residues, the most common being →4)-Gal*p*-(1→ and →3,4)-Gal*p*-(1→ (Luiten *et al.*, Under review)). Other studies of ulvan from *U. compressa* also found a variety of galactose linkages including →3)-Gal*p*-(1→, →4)-Gal*p*-(1→, and →6)-Gal*p*-(1→ (Chattopadhyay *et al.*, 2007; Lopes *et al.*, 2017). Despite not being considered a major constituent of ulvan, high proportions (7-18 mol%) of galactose are commonly detected in

ulvans from filamentous species of *Ulva* (e.g., *U. compressa*, *U. intestinalis*, and *U. linza*) (Chattopadhyay *et al.*, 2007; Matloub *et al.*, 2016; Qi *et al.*, 2013b; Ray, 2006; Tabarsa *et al.*, 2018). These high proportions of galactose are well in excess of the literature median of 2.1 mol% (Kidgell *et al.*, 2019). However, it is important to note that this median is produced from literature where over 75 % of the data is related to ulvans from blade species of *Ulva*. Ulvans from blade species consistently report low proportions of galactose. For example, assessment of the composition of 19 ulvans from five bladed species (*U. armoricana, U. rigida, U. rotundata, U. scandinavica,* and *U. olivascens*) collected at different times and locations found that galactose ranged from 1.0-3.1 mol% (Lahaye *et al.*, 1999). The ulvan isolated from *U. ralfsii*, which contained 10-16 mol% galactose (Table 4.1, Table 4.2; (Kidgell *et al.*, 2021)), was originally collected high in the intertidal region where high UV, salinity, and desiccation risk are present. The galactose may be present in response to the environmental stress to enhance the structural support provided by ulvan. Whether this galactose is a separate polymer entrained with ulvan or an additional constituent sugar of ulvan itself is unclear. Further research is needed to determine the role of galactose in ulvan. However, based on the literature and the data collected within this thesis, it appears that high proportions of galactose are a unique, yet not ubiquitous, component (or co-polymer) of ulvans from filamentous species of *Ulva*.

4.4 Conclusion

The glycosyl linkage compositions of the four ulvans assessed confirm that these ulvans are predominately 1,4-linked with high proportions of repeat A_{3S} disaccharides and that the vast majority of rhamnose is 3-*O*-sulfated. In particular, the ulvans from blade species of *Ulva* (*U*. sp. B and *U. rigida*) closely resembled the literature definition of ulvan structure (Lahaye & Robic, 2007). Additionally, high proportions of 1,4-linked xylose and iduronic acid detected in ulvans from the filamentous and blade species, respectively, indicates the presence of U_{3S} and B_{3S} disaccharides. There were multiple other distinct differences between the ulvans from blade and filamentous species of *Ulva*, with ulvan from filamentous species exhibiting a more branched structure and a greater number of sulfate ester substitution positions. The predominance of →2,3,4)-Rha*p*-(1→ in ulvans from filamentous species suggests extensive *O*-2 branching, likely to rhamnose side chains in ulvan from *U. prolifera* and an unknown substituent (possibly galactose) in ulvan from *U. ralfsii*. Additionally, minor

proportions of sulfate esters detected on *O*-2 of 1,4-linked glucuronic acid for ulvans from filamentous species further highlight the differences between ulvans of different morphologies of *Ulva*. These results support the hypothesis that ulvans from filamentous species of *Ulva* have a more complex structure than those from blade species and supports the conclusions of Chapter 3.

Possible structures for the ulvans assessed in this chapter are presented in Figure 4.6. Ulvans from blade species (*U*. sp. B and *U*. *rigida*) predominately contained A_{3S} and B_{3S} disaccharides, in addition to minor *O*-2 substitution on 1,4-linked rhamnose-3S potentially to terminal rhamnose or glucuronic acid. However, as there are not enough terminal sugars to account for the branch points in these ulvans, the *O*-2 substituents of 1,4-linked rhamnose-3S are speculative. Ulvan from *U. prolifera* contains higher proportions of 2-*O*-sulfated xylose and glucuronic acid in addition to higher proportions of *O*-2 substituted 1,4-linked rhamnose-3S. Given the approximately equal ratio of branch to terminal sugars for this ulvan, the *O*-2 substitutions of rhamnose could be branches to terminal rhamnose, possibly interspaced with short 3-linked chains of the same sugar. The ulvan from *U. ralfsii* is similar to ulvan from *U. prolifera* in that it has a lot of branch positions, however, due to the lack of terminal sugars detected in the ulvan from *U. ralfsii*, the identity of the *O*-2 substituent on 1,4-linked rhamnose-3S is more speculative. The galactose in this ulvan could potentially occur as a branch on O-2 of rhamnose as a short side chain with a terminal galactose. However, the galactose could also occur in the ulvan backbone interspaced between the conventional disaccharide or as a separate polymer as depicted (Figure 4.6).

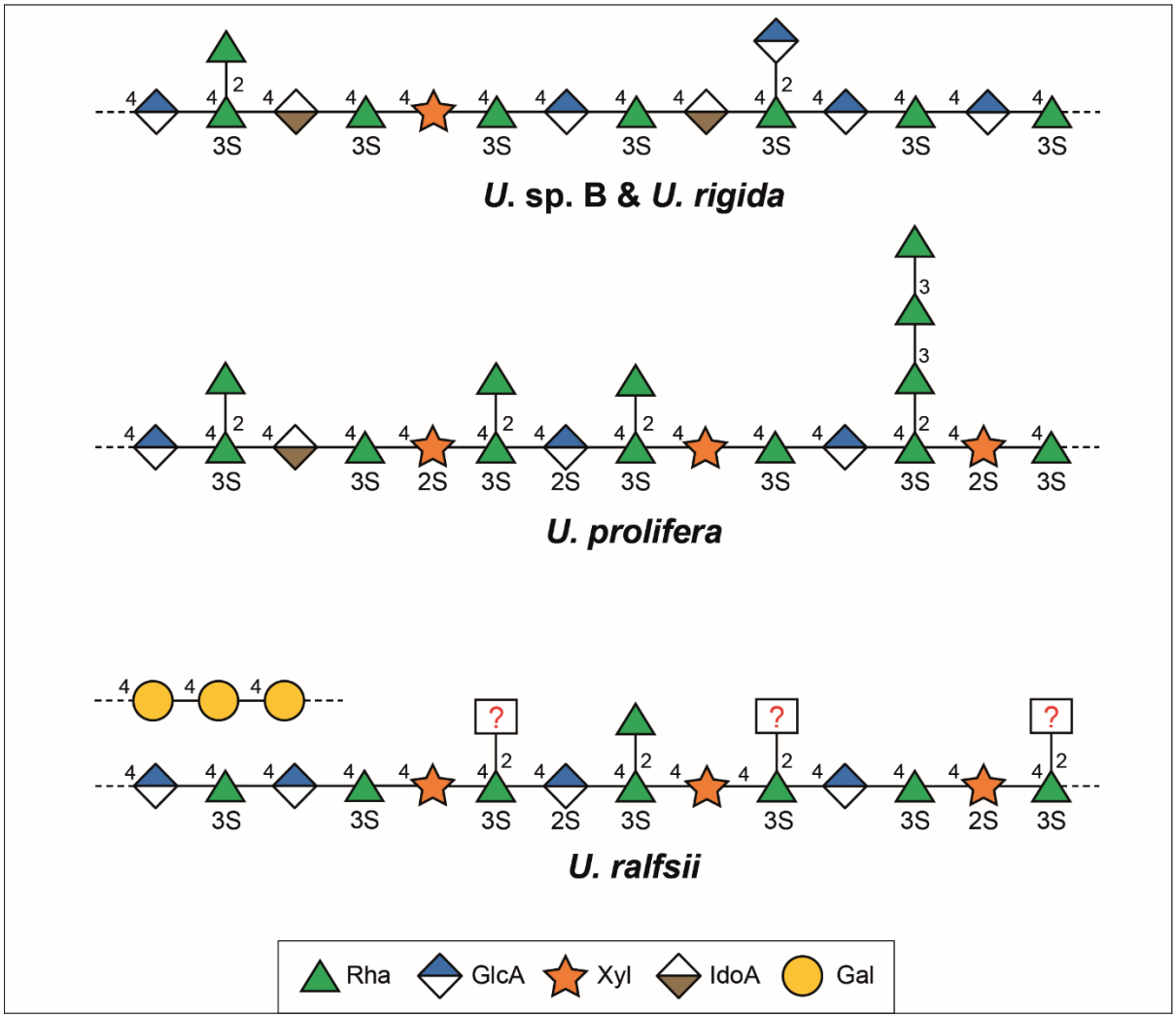

Figure 4.6: The speculative structures of the ulvans assessed in this chapter based on the linkage data obtained. There is a large degree of uncertainty around each of these speculative structures. The identity of the *O*-2 substituent of 1,4-linked rhamnose-3S is uncertain and has been represented by a question mark where a reasonable substituent cannot be suggested. Galactose in ulvan from *U. ralfsii* may be a constituent of ulvan as a side chain or as part of the backbone, or may be a separate polymer as depicted. Rha = rhamnose; GlcA = glucuronic acid; Xyl = xylose; IdoA = iduronic acid; Gal = galactose.

Chapter 5:

The molecular weight of ulvan affects the in vitro inflammatory response of a murine macrophage[4]

5.1 Introduction

Sulfated polysaccharides are complex, bioactive macromolecules featuring sugar residues with sulfate esters (Wijesekara *et al.*, 2011). In mammals, sulfated polysaccharides modulate a range of biological functions including blood coagulation, cell adhesion, and cell growth; in addition to contributing structural support to the extracellular matrix and cartilage (Blondin, Fischer, Boisson-Vidal, Kazatchkine, & Jozefonvicz, 1994; Shriver, Capila, Venkataraman, & Sasisekharan, 2012; Wight, Kinsella, & Qwarnstrom, 1992). Sulfated polysaccharides containing the monosaccharide rhamnose induce a host of immunostimulating reactions in human skin (Andrès *et al.*, 2006). Rhamnose is uncommon in nature; only being found in bacterial exopolysaccharides, plant pectic (non-sulfated) polysaccharides, and ulvan - a sulfated polysaccharide from green marine algae of the genus *Ulva* (Lahaye & Ray, 1996). Ulvan is composed predominantly of sulfated rhamnose, uronic acids (glucuronic and iduronic), and xylose. Featuring a rare bioactive monosaccharide and exhibiting a wide range of bioactive properties ulvan has potential for human health applications (Alves *et al.*, 2013b; Jiao *et al.*, 2011; Kidgell *et al.*, 2019; Lahaye & Robic, 2007).

To assess the impact of ulvan on human health, ulvan (or extracts containing ulvan) has been tested for the capacity to alter the inflammatory response both in vitro using macrophages (e.g. RAW264.7 cells) (Cho *et al.*, 2010; Jiao *et al.*, 2010; Kim *et al.*, 2011; Leiro *et al.*, 2007; Leiro *et al.*, 2010; Peasura *et al.*, 2016; Tabarsa *et al.*, 2012a; Tabarsa *et al.*, 2018) and in vivo using animal models (Abd-Ellatef *et al.*, 2017; Song *et al.*, 2016; Wei *et al.*, 2014). in vitro assessment of the effect of ulvan on inflammatory responses is often evaluated by quantifying the levels of inflammatory cytokines secreted from macrophages such as

[4] Published as: Kidgell *et al.* (2020) The molecular weight of ulvan affects the in vitro inflammatory response of a murine macrophage. International Journal of Biological Macromolecules 150:839-848

interleukin (IL)-1β, 4, 5, 6, 10, 12, 18, and tissue necrosis factor alpha (TNF-α), and other inflammation markers such as prostaglandin E_2 (PGE_2) and nitric oxide (NO) (Kim *et al.*, 2011; Leiro *et al.*, 2007). Despite the increasing number of reports on the immunomodulating properties of ulvan, little is known about the structure-activity relationships of this class of sulfated polysaccharide. However, molecular weight is known to be critical to the efficacy of bioactive polysaccharides (Jiao *et al.*, 2011; Kidgell *et al.*, 2019; Leiro *et al.*, 2007; Qi *et al.*, 2005b; Shriver *et al.*, 2012; Wijesekara *et al.*, 2011). Ulvan extracts naturally exhibit a high level of polydispersity (which may be exacerbated by the extraction conditions employed) (Glasson *et al.*, 2019), a feature that hinders precise assignment of immunomodulating activity.

The aims of this study were, therefore, to elucidate the effect of the molecular weight of purified ulvan, extracted from *Ulva ohnoi*, on the inflammatory response of RAW264.7 murine macrophages. To achieve these aims, I (i) characterised 'native' and depolymerised ulvan from *U. ohnoi*; (ii) assessed toxicity of ulvan on murine macrophages; (iii) assessed the effect of 'native' *U. ohnoi* ulvan on the inflammatory response of murine macrophages; and (iv) assessed the effect that the molecular weight of ulvan has on the inflammatory response of murine macrophages.

5.2 Methods

5.2.1 Materials

The following were purchased from Fisher Scientific, Thermo Fisher Scientific, Australia: H_2O_2 (ACS, 30 %, #H325) and NaCl (ACS, #S271). The following were purchased from Sigma-Aldrich, Australia: Glucuronic acid (>98 %, #G5269), sodium tetraborate (99.998 %, #229946), *m*-hydroxydiphenyl (85 %, #262250), concentrated sulfuric acid (ACS, 95-98 %, #258105), dimethyl sulfoxide (>99.9 %, #276855), Na_2CO_3 (ACS, >99.5 %, #222321), $NaHCO_3$ (ACS >99.7 %, #S6014), K_2SO_4 (>99.0 %, #P0772), and sodium nitrite (ACS >97 %, #237213). The following were purchased from Sigma-Aldrich, New Zealand: $NaNO_3$ (>99.0 %, #S5506), NaN_3 (>99 %, #S2002), methanolic HCl (#90964), L-fucose (#F2252), L-rhamnose (#3875), L-arabinose (#10839), D-galactose (#0750), D-glucose (#8270), D-mannose (#2069), D-xylose (#95729), D-ribose (#7500), D-galacturonic acid (#73960), and D-glucuronic acid (#5269). Other reagents were sourced as follows: trifluoroacetic acid (Synthesis grade, Scarlau, Spain,

#AC31420100), NaOH (50 % w/w, Fisher Scientific, Thermo Fisher Scientific, New Zealand, #SS254), anhydrous NaOAc (Carlo Erba, France, #366377), D_2O (99.9 %, Cambridge Isotope Laboratories, USA, #DLM-4), and L-iduronic acid (Carbosynth, UK, #MI08102).

5.2.2 Ulvan preparation

5.2.2.1 Algal cultivation & ulvan extraction

Ulva ohnoi (Gen-bank accession number KF195509, strain JCU 1 (Lawton *et al.*, 2013)) was cultivated and supplied by Pacific Biotechnologies ABA facility, a land-based aquaculture facility near Ayr, Queensland, Australia (19°29'S, 147°28E). Crude ulvan was extracted using a proprietary extraction procedure (Marinova Pty. Ltd.) and purified as described below.

5.2.2.2 Purification & fractionation

Crude ulvan (2 g L^{-1}) was dissolved in Type 1 water prior to vacuum filtration (Filtech, 453) and diafiltration (ÄKTA flux 6 system fitted with a 10,000 NMWC filter, UFP-10-E-4X2MA) with five volumes of Type 1 water. Protein was separated from the diafiltered retentate via anion exchange chromatography (AEC) using an ÄKTA pure 150 L coupled with a single wavelength (280nm) UV detector. The retentate (400 mL) was loaded onto an equilibrated (Type 1 water, 5 column volumes (CV); 2 M NaCl, 5 CV; Type 1 water, 5 CV) XK 50/30 column (GE Healthcare Life Sciences) packed with Q Sepharose XL media (bed height = 24.5 cm). The column was eluted using a stepwise gradient (0 M NaCl, 2 CV; 0 – 0.5 M NaCl, 2 CV; 0.5 – 1 M, 2 CV; 1 – 1.75 M NaCl, 3 CV; 1.75 – 2 M NaCl, 5 CV) at a flow rate of 20 mL min^{-1}. A chromatogram was produced by analysing collected fractions (13 mL) for uronic acid colourimetrically using the *m*-phenyl-phenol method with glucuronic acid as standard (van den Hoogen *et al.*, 1998). Fractions containing uronic acid that did not overlap the major peak in the UV trace (attributed to protein) were pooled and concentrated by diafiltration with Type 1 water until permeate conductivity was < 5 µS cm^{-1}. The purified ulvan was recovered via lyophilisation – this is referred to as 'native' ulvan.

5.2.2.3 Ulvan hydrolysis

The hydrolysis method was modified from Zhang *et al.* (2008) so that time was the only variable parameter. Native ulvan solution (1 % w/v in Type 1 water) was heated to 50 °C under constant stirring before H_2O_2 was added to a final solution concentration of 2.5 % v/v.

The hydrolysis reaction was held at 50 °C for 1, 2, 5, or 7 h before being quenched in an ice bath. The cold solution was diafiltered (Amicon Ultra-15, 10 kDa NMWC) with five volumes of Type 1 water prior to recovery by lyophilisation. The permeates from hydrolysed ulvan samples were collected, combined, and lyophilised. The 5 and 7 h treatments were combined due to low yield of hydrolysed ulvan and comparable molecular weight profiles. Table 5.1 assigns sample labels used throughout the text.

Table 5.1: Sample labels used through the text for hydrolysed ulvan fractions

Sample ID	Hydrolysis time (h)
U209	0 (native ulvan)
U21	1
U13	2
U9	5 + 7
U7	Permeate

5.2.3 Chemical characterisation

5.2.3.1 Elemental characterisation

Elemental analysis (% C, H, N, S; n=1) and ash content (% w/w) of ulvan samples were measured commercially by OEA labs (www.oealabs.com, Callington, UK). Percent oxygen was calculated as % O = 100 – Σ(C, H, N, S, ash), where C, H, N, S, and ash are expressed as a percentage of the total mass. Sulfate content was quantified by ion chromatography (Metrohm 930 Compact IC Flex fitted with a Metrosep A Supp 5, 150 × 4.0 mm column and a Metrosep RP 2 Guard 3.5 mm guard column) by elution at 0.7 mL min^{-1} with 3.2 mmol L^{-1} Na_2CO_3 and 1.0 mmol L^{-1} $NaHCO_3$ using K_2SO_4 as a standard. Protein content was estimated using the nitrogen-to-protein conversion factor of 5 (% N x 5) (Angell *et al.*, 2016).

5.2.3.2 Molecular weight

Molecular weight distributions were determined using size-exclusion chromatography coupled with multi-angle laser light scattering (SEC-MALLS). Samples (5 mg mL^{-1} in 0.1 M $NaNO_3$) were dissolved by heating at 80 °C and then standing at room temperature overnight (~20 h). Soluble material was separated on three columns (TSK-Gel G5000PW_{XL}, G4000PW_{XL} and G3000PW_{XL}, 300 x 7.8 mm, Tosoh Corp., Tokyo, Japan) connected in series, eluted with

0.1 M $NaNO_3$ with 0.02 % NaN_3 (0.5 mL min^{-1}, 60 °C). The eluted material was detected using a variable wavelength detector (280 nm), a SDL7000 MALLS detector (PSS Polymer Standards Service GmbH, Mainz, Germany) and a refractive index monitor. The data for molecular weight determination were analysed using Win GPC Unichrom software (v8.2.1, PSS Polymer Standards Service) using a refractive index increment, dn/dc, of 0.146 mL g^{-1} (Robic *et al.*, 2008).

5.2.3.3 Constituent sugar composition

Constituent sugar composition was determined by high-performance anion-exchange chromatography with pulsed amperometric detection (HPAEC-PAD) after hydrolysis of the polysaccharides present to their component monosaccharides. Samples (1 mg) were hydrolysed and analysed in duplicate with methanolic HCl (3 M, 500 µL, 80 °C, 18 h), followed by aqueous trifluoroacetic acid (TFA, 2.5 M, 500 µL, 120 °C, 1 h). The resulting hydrolysates were dried and redissolved in Type 1 water (1 mL). An aliquot of hydrolysate was then diluted with Type 1 water (to 50 µg mL^{-1}) and analysed on a CarboPac PA-1 (4 x 250 mm) column equilibrated in 20 mM NaOH and eluted with a simultaneous gradient of NaOH and NaOAc at 30 °C and a flow rate of 1 mL min^{-1}. The sugars were identified from their elution times relative to a standard sugar mix, quantified from response calibration curves of each sugar and expressed as µg of the anhydro-sugar (as this is the form of sugar present in a polysaccharide) per mg of sample; the normalised mol% of each anhydro-sugar was also calculated.

5.2.3.4 NMR spectroscopy

Ulvan samples were dissolved in D_2O at 25 mg mL^{-1}. NMR data was collected on a Bruker Avance III 500 operating at a proton frequency of 499.843 MHz and 125.698 MHz for ^{13}C running Topspin 2.1 software.

Data was collected on a Bruker two channel 5-mm broadband observe nuclei probe (^{31}P-^{109}Ag) equipped with actively shielded Z-axis gradient coil (303 K). Typical high-power 90º-pulse widths for proton observation were 10.5 µs and 11 µs for ^{13}C. Proton NMR spectra were recorded with a spectral width of 20 ppm, 65,536 complex data points, 30-degree excitation pulse, each with a 1-second delay time and an acquisition time of 3.18 s. The residual solvent peak was assigned as the reference peak for proton NMR. Carbon-13 NMR

spectra were recorded using a spectral width of 240 ppm, 65,536 data points, 30-degree excitation pulse, with a 0.5-second recycle delay, an acquisition time of 1.0486 s with low power WALTZ-16 proton composite pulse decoupling (CPD) with power levels corresponding to a proton 90 degree r.f. pulse width of 68 µs. TMS was defined as 0 ppm for ^{13}C NMR. Spectra were processed with a standard exponential weighting function of 0.3 Hz (^{1}H) or 3 Hz (^{13}C) line broadening prior to Fourier transformation.

5.2.4 Immunomodulating activity

5.2.4.1 Cell culture

RAW264.7 murine macrophages were purchased from The European Collection of Authenticated Cell Cultures (ECACC) (Sigma-Aldrich, Australia, #85062803) and maintained in a clean culture of Dulbecco's modified eagle medium (DMEM, #LTS10566016) with GLUTAMAX with the addition of 0.5 M HEPES buffer (HEPES, #83264) (Gibco, Thermo Fisher scientific, Australia) and 10 % foetal bovine serum (FBS) (Bovogen, Interpath Services, Australia, #SFBS-FR). Cells were cultured in T75 flasks at 37 °C in an atmosphere of 5 % CO_2 with 100 % humidity until reaching 80-90 % confluence before passage with cell scraper to dislodge cells. RAW264.7 cells were regularly screened for mycoplasma.

5.2.4.2 Cell viability assay

Toxicity of 2 to 2000 µg mL^{-1} of ulvan fractions was assessed over 48 h. Cells were seeded into a 96-well plate at a density of $3x10^5$ cells/well in DMEM supplemented with FBS, HEPES, 100 U penicillin/100 µg mL^{-1} streptomycin (pen/strep) (Gibco, Thermo Fisher scientific, Australia, #LTS15140148), and allowed to adhere for 16 h. Ulvan (dissolved in DMEM containing HEPES and pen/strep) was added through a media change in concentrations from 2 to 2000 µg mL^{-1}. The cells were then incubated for 6, 24 or 48 h. Following incubation, PrestoBlue™ reagent (Invitrogen, Thermofisher scientific, Australia) was added to the wells to 10 % v/v. The cells were incubated for a further 60 min before fluorescence was measured (excitation, 544 nm; emission 620 nm) on a BMG POLARstar Omega microplate reader. The relative fluorescence units (RFU) were used to calculate macrophage viability by: viability % = RFU_t/RFU_c x 100, where RFU_t and RFU_c are the intensity of test and control groups, respectively. Ulvan concentrations were log_{10}-transformed, fitted using a variable slope four-

parameter equation with the top value constrained to 100 % using a least squares (ordinary) fit model in GraphPad Prism (v. 8.1.0).

5.2.4.3 Lipopolysaccharide (LPS) stimulation assay

The immunomodulating effect of ulvan fractions was assessed in lipopolysaccharide (LPS)-stimulated RAW264.7 cells by measuring the concentrations of secreted cytokines (IL-1β, IL-6, IL-10, IL-12, and TNFα) and PGE_2 in the cell culture supernatant by enzyme-linked immunosorbent assay (ELISA) (Figure 5.1). RAW264.7 cells were seeded into 24-well plates at a density of $1x10^5$ cells/well in 1000 µL of DMEM supplemented with FBS, HEPES, and pen/strep; cells were allowed to adhere for 16 h. Ulvan fractions (dissolved in DMEM supplemented with FBS, HEPES, pen/strep, and absent phenol red) in concentrations of 1, 10 or 100 µg mL^{-1} were added through a media change. It was determined during optimisation that FBS is required for the release of cytokines by LPS-stimulated RAW264.7 cells (App. 7.3.1). Dexamethasone (1 µg mL^{-1}; Sigma-Aldrich, Australia, #D4902) served as a positive control; wells without the addition of ulvan served as negative controls.

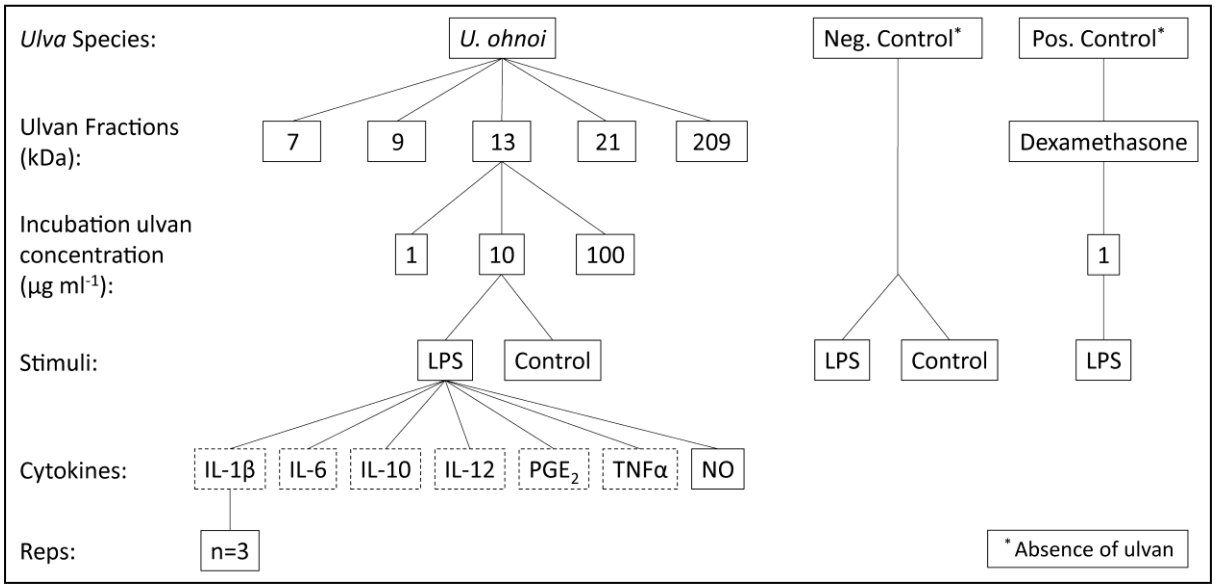

Figure 5.1: Experimental design of lipopolysaccharide (LPS) stimulation assay. "Cytokines" collectively refers to cytokines and other immunological markers such as prostaglandin E_2 (PGE_2) and nitric oxide (NO). Cytokines with dashed borders were quantified by ELISA; NO was quantified through the Griess test.

Cells were pre-treated with ulvan or dexamethasone for 2 h before LPS from *Escherichia coli* (0111:B4; Sigma-Aldrich, Australia, #L4391) was added to a final concentration of 1 µg mL^{-1}. There were an equal number of wells across all treatments that did not receive LPS-stimulation to act as internal controls. Cells were incubated for 46 h (48 h was necessary for secretion of IL-1β – see App. 7.3.3 B), after which the supernatant was collected and stored at 4 °C. The concentration of cytokines in the cell culture supernatant was analysed using respective ELISA kits within 6 hours of separation from cells by following the manufacturer's instructions (Abcam, UK: ab208348, 1:10 dilution; ab197742, 1:2 dilution; ab46103, 1:2 dilution; ab222503, 1:50 dilution; ab136949, 1:1 dilution; ab236717, 1:2 dilution). The optical density (OD) or relative fluorescence units (RFU) for each of the cytokine assays was read on a BMG POLARstar Omega microplate reader at the wavelength recommended by the assay manufacturer.

5.2.4.4 Nitric oxide assay

Nitric oxide (NO) secretion was estimated through quantification of its decomposition product, nitrite (NO_2^-) (Figure 5.1). The concentration of NO_2^- in cell supernatant was determined using the Griess reagent (modified) (Sigma-Aldrich, Australia, #G4410). Cell supernatant collected as outlined in section 5.2.4.3 (above) was mixed with equal volumes of Griess reagent (modified). The absorbance was read at 540 nm after 15 min on a BMG POLARstar Omega microplate reader. Concentration of nitrite in cell supernatant was calculated from 0-100 µM sodium nitrite standards.

5.2.5 Data & statistical analysis

Cytokine concentrations were calculated by using either 4-parameter logistic regressions or linear regressions derived from the assay standards. The fit with the highest r^2 value was used. Recorded sample OD values less than three standard deviations of the mean ELISA assay blank OD value were considered to have a concentration of zero. In the rare occurrence that a treatment OD was outside the standard range of the 4-parameter fit, linear regression was used to estimate a corresponding concentration. Prior to statistical analysis, cytokine, PGE_2, and NO_2^- concentrations were normalised to a percent of the respective ulvan-free control for each plate.

The effects of ulvan molecular weight and concentration on RAW264.7 cells were analysed with two-factor permutational analysis of variance (PERMANOVA) (Anderson *et al.*, 2008). Molecular weight and ulvan concentration were treated as fixed factors. Cytotoxicity of ulvan on RAW264.7 cells was analysed by a three-factor PERMANOVA with ulvan molecular weight, ulvan concentration, and exposure time as fixed factors. All analyses were performed in Primer v6 (Primer-E Ltd., UK) using Euclidian distance similarity and 9,999 unrestricted permutations of the raw data. *a posteriori* pair–wise comparisons were used to determine the contribution of factors to significant results. Monte Carlo P-values were used in pair-wise comparisons with less than 100 unique permutations (Anderson *et al.*, 2008).

5.3 Results

5.3.1 Chemical characterisation

5.3.1.1 Elemental analysis

Ulvan elemental composition, ash, sulfate ester and protein contents are presented in Table 5.2. The ratio for C, H, O, N, and S are similar between samples, with significantly lower contents of N (and protein) in the chromatographed samples compared to the crude extract (data not shown). Variations in the content of ash account for the absolute content of C, H, O, N, and S. Sulfate content was the same for the native, unhydrolysed sample (U209) and for samples hydrolysed for up to 2 h (U21, U13), reducing after 5 to 7 hours of hydrolysis (U9), and higher in crude ulvan (data not shown) and the permeate sample (U7).

Table 5.2: Elemental analysis of native and hydrolysed ulvan. Average % w/w (± S.D, where applicable). Protein content calculated from % N.

Sample ID	%C	%H	%O	%N	%S	%Ash	%Sulfate	%Protein[1]
U209 (native)	25.9	4.8	42.1	0.1	5.5	21.7	16.4 ± 0.5	0.5
U21	26.7	4.8	41.3	0.1	5.7	21.5	16.3 ± 0.7	0.5
U13	26.2	4.9	42.7	0.1	5.4	20.8	16.3 ± 0.6	0.5
U9	29.7	5.0	43.9	0.3	5.9	15.1	13.7 ± 3.8	1.7
U7	26.5	4.2	35.4	0.1	6.3	27.5	22.4 ± 1.7	0.5

[1]Based on % N x 5

5.3.1.2 Molecular weight

Native ulvan (U209) had a weight average molecular weight (M_w) of 209 kDa (Table 5.3). Both the M_w and dispersity of the hydrolysed ulvans decreased with increasing time of hydrolysis (Table 5.3, App. 7.3.2).

Table 5.3: The duration of hydrolysis applied to native ulvan, resulting weight average molecular weight (M_w) and dispersity (Đ).

Sample ID	Hydrolysis time (h)	M_w (kDa)	Dispersity (Đ)
U209 (native)	0	208.9	2.2
U21	1	21.3	1.7
U13	2	13.4	1.4
U9	5 + 7	8.9	1.4
U7	Permeate	6.8	1.3

5.3.1.3 Constituent sugar composition

The total sugar content of the ulvan fractions ranged from 367 to 486 µg mg^{-1} of sample (Table 5.4). Native ulvan had the highest total sugar content (486 µg mg^{-1} sample) with the three partially hydrolysed ulvans having similar total sugar contents (453 – 478 µg mg^{-1} sample). U7 had the lowest total sugar content (367 µg mg^{-1} sample).

The ulvan fractions contained 48.8-54.7 mol% rhamnose, 32.5-35.9 mol% glucuronic acid, 4.5-7.3 mol% iduronic acid, and 3.3-5.6 mol% xylose (Table 5.5). Smaller amounts of other sugars including fucose, arabinose, galactose, glucose, and mannose were also present in all fractions. U9 had the highest content of rhamnose (54.7 mol%), with the lowest content of xylose (3.3 mol%), glucuronic acid (32.5 mol%), iduronic acid (4.5 mol%), in addition to the highest content of fucose, arabinose, galactose, glucose, and mannose.

Table 5.4: Constituent sugar composition and total sugar content (µg mg^{-1} sample) of purified, native ulvan, partially hydrolysed fractions and the permeate.

Sample ID	Sugars (µg mg^{-1} sample)[a]									
	Rha	Xyl	GlcA	IdoA	Fuc	Ara	Gal	Glc	Man	Total
U209 (native)	218.6	22.5	194.0	38.7	0.5	0.2	10.3	1.2	tr.	486.1
U21	223.2	21.9	183.6	36.5	0.5	0.2	10.1	1.5	0.5	478.1
U13	213.1	18.4	176.7	31.7	0.6	0.2	9.9	1.6	0.4	452.6
U9	233.4	12.7	167.1	22.9	2.1	0.6	14.8	4.3	1.7	459.5
U7	178.3	15.1	137.0	29.8	0.1	0.2	4.7	0.7	1.1	367.0

[a] Values are the averages of duplicate analyses
Sugars < 0.1 µg mg^{-1} are considered trace (tr.)

Table 5.5: Constituent sugar composition (normalised mol%) of purified, native ulvan, partially hydrolysed fractions and the permeate.

Sample ID	Sugars (normalised mol%)[a]								
	Rha	Xyl	GlcA	IdoA	Fuc	Ara	Gal	Glc	Man
U209 (native)	48.8	5.6	35.9	7.2	0.1	0.1	2.1	0.2	tr.
U21	50.5	5.5	34.5	6.9	0.1	tr.	2.1	0.3	0.1
U13	51.0	4.9	35.1	6.3	0.1	0.1	2.1	0.3	0.1
U9	54.7	3.3	32.5	4.5	0.5	0.1	3.1	0.9	0.4
U7	52.5	4.9	33.5	7.3	tr.	0.1	1.2	0.2	0.3

[a] Values are the averages of duplicate analyses
Sugars < 0.1 mol% are considered trace (tr.)

5.3.1.4 NMR spectroscopy

Both ^{13}C and ^{1}H NMR spectra recorded were consistent with data reported for ulvan polysaccharides (Costa *et al.*, 2012; Glasson *et al.*, 2017; Lahaye *et al.*, 1995; Lahaye & Robic, 2007; Robic *et al.*, 2009b; Robic *et al.*, 2009c; Tabarsa, Lee, & You, 2012b; Thanh *et al.*, 2016;

Tran *et al.*, 2018). Spectra from native and partially hydrolysed ulvan samples were recorded in D_2O (Figure 5.2, Figure 5.3).

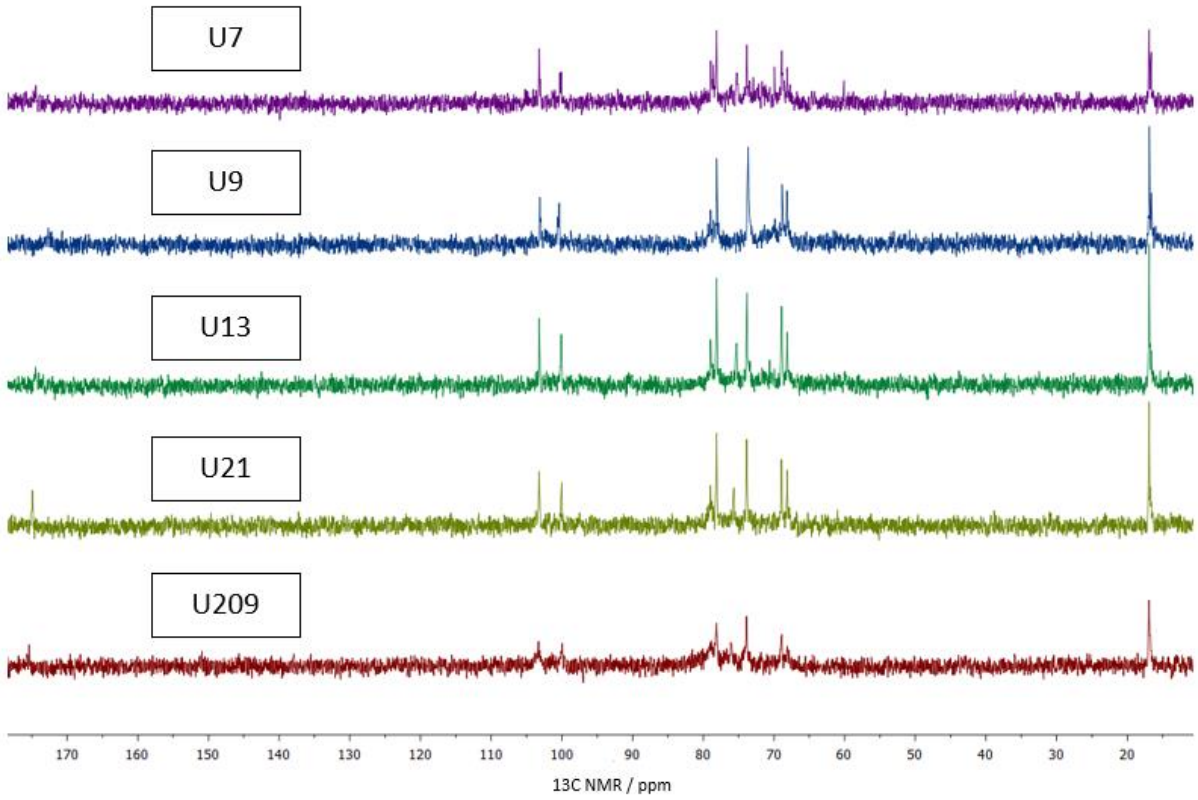

Figure 5.2: ^{13}C NMR data of native and hydrolysed ulvan samples (25 mg mL^{-1}, D_2O, 25 °C, 125 MHz).

The ^{13}C NMR displayed signals characteristic of those reported (Tabarsa *et al.*, 2012b) for anomeric resonances assigned to glucuronic acid (104 ppm) and rhamnose (100 ppm) (Figure 5.2). The relative intensity of these resonances was consistent with ulvan predominantly containing the named disaccharide, A_{3S} (→4)-GlcA*p*-(1→4)-Rha*p*3S-(1→) (Lahaye *et al.*, 1998). Further evidence for this assignment is the uronic acid carboxyl resonance at δ 176 ppm and the rhamnose methyl peak at δ 17 ppm (Tran *et al.*, 2018). Intense signals for rhamnose C5, C2, and C3/C4 from A_{3S} are also observed resonating at 68, 69, and 78 ppm, respectively. A strong signal recorded at 74 ppm is consistent with the C3/C2 of glucuronic acid in A_{3S}, with the remaining uronic acid detected at 76 ppm (C5) and 79 ppm (C4) (Lahaye & Robic, 2007; Tran *et al.*, 2018). The minor peak at ~71 ppm, readily identified in the U13 spectra, is consistent with overlapping C2/C5 resonances that can be assigned to iduronic acid, indicating the presence of another known ulvan disaccharide, B_{3S} (→4)-IdoA*p*-(1→4)-Rha*p*3S-(1→) (Lahaye *et al.*, 1998; Tran *et al.*, 2018).

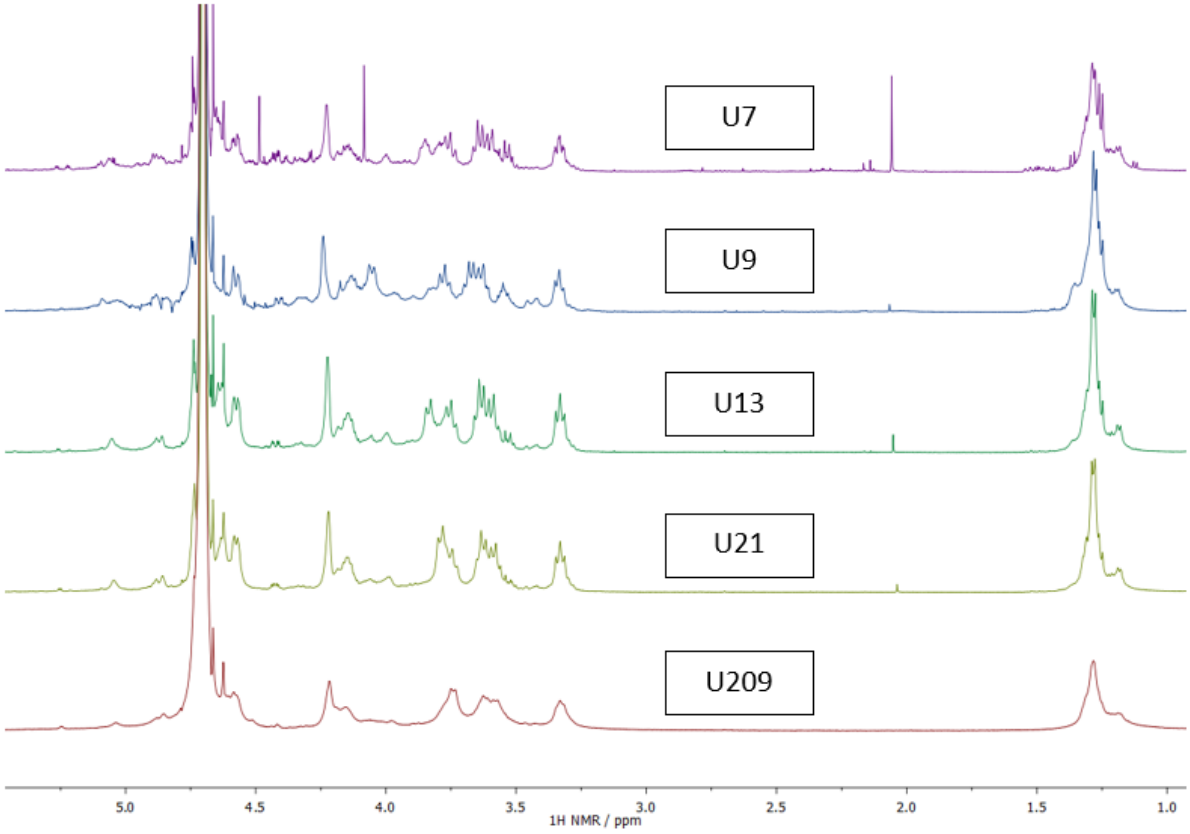

Figure 5.3: ^{1}H NMR data of native and hydrolysed ulvan samples (25 mg mL^{-1}, D_2O, 25 °C, 500 MHz, HDO peak not suppressed).

Proton NMR data supports the ^{13}C assignments outlined above (Figure 5.3). A strong ^{1}H resonance at δ 1.3 ppm may be attributed to the protons of the rhamnose methyl group (C6). The ^{1}H NMR peaks at 3.3 ppm and 3.7 ppm are consistent with H2 and H3/H4 of glucuronic acid, respectively (Lahaye & Robic, 2007; Tran *et al.*, 2018). Proton resonances at 3.8-3.9 ppm are likely a combination of a H4 peak from rhamnose and H5 peak of glucuronic acid (Lahaye & Robic, 2007; Tran *et al.*, 2018); these peaks are more highly resolved and separated in the U13 and U7 spectra. The major peak at 4.2 ppm is consistent with the data reported for the H2 of rhamnose, and H5 is recorded resonating at 4.1 ppm (Lahaye & Robic, 2007; Tran *et al.*, 2018).

5.3.2 Immunomodulating activity

5.3.2.1 Ulvan cytotoxicity

All ulvan fractions showed no toxicity on RAW264.7 cells at concentrations below 100 µg mL^{-1} over 48 h (Figure 5.4). The cytotoxic effect of U9, U13, U21, and U209 increased with

time for concentrations > 100 µg mL^{-1}, while the lowest M_w ulvan, U7, showed no cytotoxicity at any concentration up to 48 h (Figure 5.4 A, B, C). This deviation in cytotoxicity with ulvan M_w, ulvan concentration and exposure time produced a significant three-way interaction (pseudo-$F_{88,360}$ = 13.15 P < 0.01).

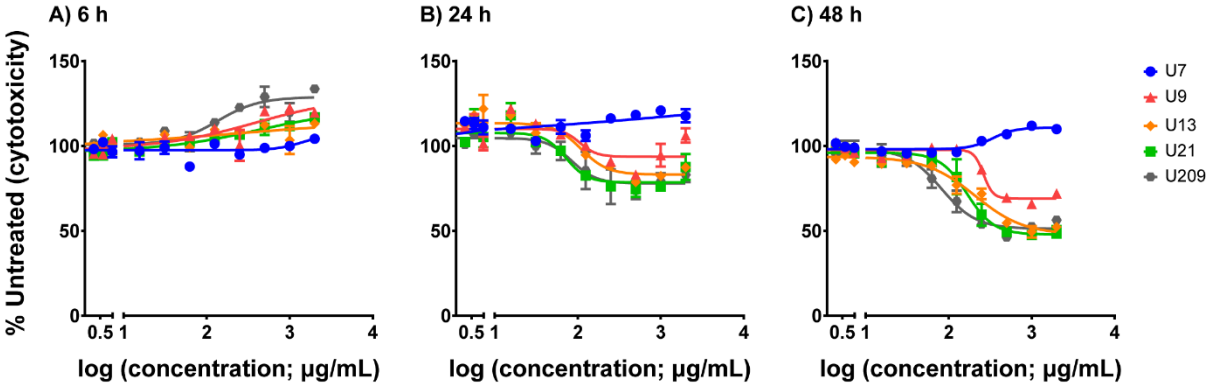

Figure 5.4: Effect of ulvan fractions on RAW264.7 cell viability. Cell proliferation was measured after incubation with ulvan of differing molecular weights (U7, U9, U13, U21, and U209) at concentrations of 2-2000 µg mL^{-1} for (A) 6 h, (B) 24 h and (C) 48 h.

After 6 h, > 100 µg mL^{-1} of ulvan induced cell proliferation, with up to 33 % increase in cell viability induced by 2000 µg mL^{-1} of U209 (Figure 5.4 A). After 24 h, all ulvan fractions decreased cell viability at higher concentrations, except for U7. The lowest 24 h viability observed was 75 % by 500 µg mL^{-1} of U21 and U209 ulvan (Figure 5.4 B). With the exception of U7, the reduction in cell viability by ulvan became pronounced ≥ 100 µg mL^{-1} (Figure 5.4 C). 500 µg mL^{-1} of ulvan was sufficient to reduce cell viability to 70 % for U9 and to 50 % for larger M_w ulvans (U12, U21, and U209); these reduced viabilities respectively remained at 70 % and 50 % up to the highest concentration of ulvan tested (2000 µg mL^{-1}). The dose-dependent increase in cytotoxic effect of high concentration (100-500 µg mL^{-1}) ulvan through time was also confirmed during pilot assays (App. 7.3.4). The presence of 1 µg mL^{-1} LPS had low toxicity to RAW264.7 cell (85 % viable at 24 h) (App. 7.3.5), therefore this concentration was selected for further experiments.

5.3.2.2 Effect of ulvan in modulating inflammatory response

5.3.2.2.1 Inflammatory cytokines

High concentration of the two highest M_w fractions consistently resulted in the greatest levels of IL-1β, IL-6, IL-10 and IL-12 from RAW264.7 cells (Figure 5.5 A-D). For IL-10,

each concentration of U21 and U209 (1, 10, and 100 µg mL^{-1}) produced significantly higher levels of IL-10 compared to ulvan-absent controls (pseudo-$F_{13,42}$ = 4.28, P < 0.001), while the lower M_w fractions resulted in no change or a reduction in levels of IL-10 (Figure 5.5 A).

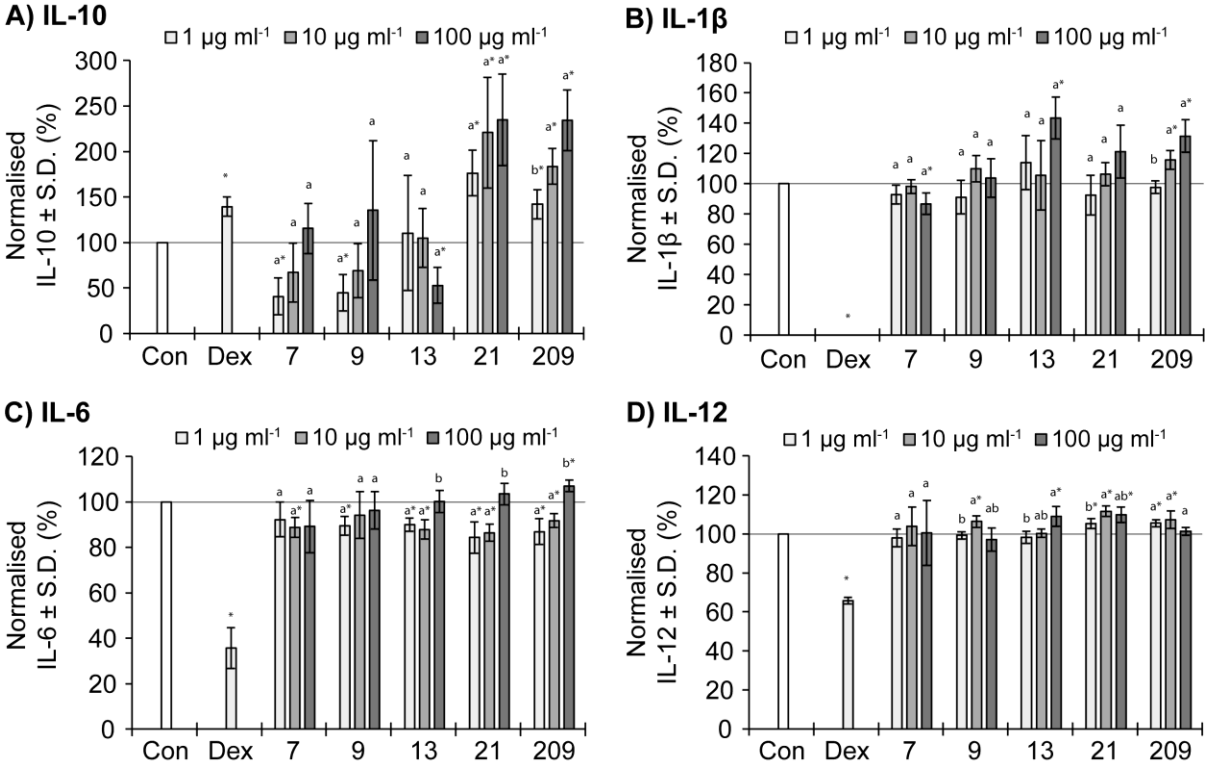

Figure 5.5: Percent normalised concentrations of interleukins (IL) (A) IL-10, (B) IL-1β, (C) IL-6, and (D) IL-12 (±S.D., n=3) measured in RAW264.7 cell supernatant following exposure to ulvan of differing molecular weights (7, 9, 13, 21, 209 kDa) at 1, 10 and 100 µg mL^{-1} in the presence of 1 µg mL^{-1} LPS. 1 µg mL^{-1} Dexamethasone (Dex) used as a positive control. Control (Con) contained 1 µg mL^{-1} LPS in the absence of ulvan or dexamethasone. Superscript letters (a, b) indicate significant difference between concentrations within a molecular weight fraction; Asterisk (*) indicates significant difference from control.

High M_w ulvan fractions at high concentrations increased the secretion of IL-1β, IL-6, and IL-12 above that of ulvan-absent controls. The level of IL-1β was increased by 44 and 32 % in treatments with 100 µg mL^{-1} of U13 and U209, respectively (Figure 5.5 B) (pseudo-$F_{13,46}$ = 15.52, P < 0.001). Additionally, 100 µg mL^{-1} of U209 also increased the level of IL-6 by 7 % - the only treatment to significantly increase the level of IL-6 above the ulvan-absent control (Figure 5.5 C) (pseudo-$F_{13,46}$ = 12.88, P < 0.001). As with IL-6, significantly more IL-12 was

produced in treatments with 100 µg mL^{-1} of U13 and U21 (pseudo-$F_{13,46}$ = 7.95, P < 0.001). However, lower concentrations of high M_w ulvan also increased IL-12 levels (Figure 5.5 D).

Low concentrations of ulvan, often combined with low molecular weights, resulted in the lowest levels of cytokine production. For example, IL-10 was reduced by 59 and 55 % from 1 µg mL^{-1} of U7 and U9, respectively (Figure 5.5 A) (pseudo-$F_{13,42}$ = 4.28, P < 0.001). Levels of IL-6 were also reduced by low concentrations: by 10-15 % for U13, U21, and U209 (pseudo-$F_{13,46}$ = 12.88, P < 0.001) (Figure 5.5 C). Contrary to IL-6 and IL-10, the lowest level of IL-1β (13 % lower than the ulvan-absent control) was at a high concentration (100 µg mL^{-1}) of low M_w ulvan (U7) (Figure 5.5 B) (pseudo-$F_{13,46}$ = 15.52, P < 0.001).

Dexamethasone (1 µg mL^{-1}) significantly reduced the level of IL-1β, IL-6, and IL-12 to a greater extent than any ulvan treatment (Figure 5.5 B-D). Conversely, dexamethasone significantly increased IL-10 level by 40 % (Figure 5.5 A). These effects of dexamethasone are consistent with the literature (Franchimont *et al.*, 1999; Gewert, Svensson, Andersson, Holst, & Sundler, 1999). Basal expression (cytokine levels in the absence of LPS) of IL-1β, IL-6, and IL-12 were, on average, 98 %, 99 %, and 98 % lower than LPS-treated cells, respectively. Further, basal IL-10 levels were 35 % lower, on average, in the absence of LPS compared to LPS treated cells and showed no effect of M_w or concentration.

TNFα was released in concentrations far exceeding that recorded during optimisation trials (App. 7.3.3). The levels of TNFα for all LPS treatments in the LPS stimulation assay were above the OD detection limit for the microplate reader, resulting in unusuable data. No basal TNFα levels were recorded.

5.3.2.2.2 PGE_2 and NO_2^-

The levels of PGE_2 were consistently reduced when ulvan was applied to RAW264.7 cells stimulated by LPS; further reductions occurred at higher concentrations of ulvan (Figure 5.6 A). A dose-dependent reduction in PGE_2 occurred when averaged across ulvan molecular weights (pseudo-$F_{3,45}$ = 8.21, P < 0.001), culminating with 100 µg mL^{-1} of U9, U21, and U209 inducing reductions of 24, 29, and 39 %, respectively. The proportional reduction in PGE_2 induced by 100 µg mL^{-1} of U209 (39 %) was very close to the 42 % reduction induced by 1 µg mL^{-1} of dexamethasone. In contrast, lower concentrations of ulvan resulted in reduced concentrations of nitrite (NO_2^-), on average (Figure 5.6 B). 1 and 10 µg mL^{-1} of ulvan resulted

in significantly lower nitrite levels compared to either ulvan-absent controls or 100 µg mL^{-1} of ulvan (pseudo-$F_{3,46}$ = 7.18, P < 0.001). There was no significant difference between 100 µg mL^{-1} of ulvan and the ulvan-absent controls.

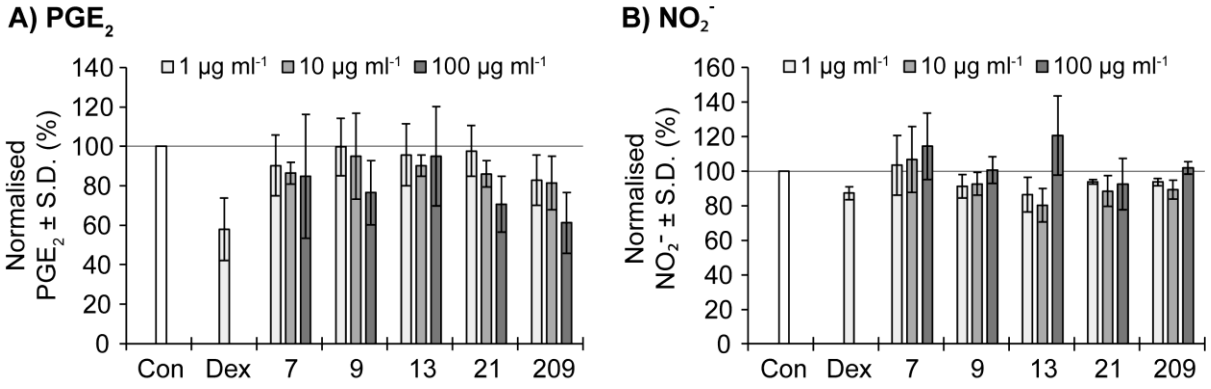

Figure 5.6: Percent normalised concentration of (A) prostaglandin E_2 (PGE_2) and (B) nitrite (NO_2^-) (± S.D., n=3) measured in RAW264.7 cell supernatant following exposure to ulvan of differing molecular weights (7, 9, 13, 21, 209 kDa) at 1, 10 and 100 µg mL^{-1} in the presence of 1 µg mL^{-1} LPS. Nitrite measured with Griess reagent using $NaNO_2$ (0-100 µM) as standard. 1 µg mL^{-1} Dexamethasone (Dex) used as a positive control. Control (Con) contained 1 µg mL^{-1} LPS in the absence of ulvan or dexamethasone. Statistical analysis not possible due to lack of interaction between ulvan concentration and M_w.

Dexamethasone (1 µg mL^{-1}) significantly reduced secretion of PGE_2, but had no significant effect on nitrite secretion. On average, dexamethasone produced significantly less PGE_2 than 9, 13 and 21 kDa ulvan (pseudo-$F_{5,45}$ = 3.39, P < 0.05).

The nitrite level in the absence of LPS was on average 84 % lower than LPS treatments. However, in the absence of LPS the nitrite level was 2-8 times higher from 100 µg mL^{-1} of 9, 13, 21 and 209 kDa ulvan compared to any other respective concentration. No PGE_2 was detected in the absence of LPS.

5.4 Discussion

Ulvan from *Ulva ohnoi* was depolymerised into fractions of 7, 9, 13, 21, and 209 kDa (named U7, U9, U13, U21, and U209, respectively). These fractions were chemically characterised and their cytotoxic and immunomodulating effect on RAW264.7 murine macrophages assessed. No ulvan fraction showed toxicity to RAW264.7 cells at

concentrations up to 100 μg mL^{-1} over 48 h. Higher molecular weight fractions of ulvan elicited a greater immunomodulatory response at 100 μg mL^{-1} (by increasing IL-10, IL-1β and IL-6, and decreasing PGE_2) compared to lower M_w ulvan fractions. Ulvan extracted from *Ulva ohnoi* is non-cytotoxic and has a mild anti-inflammatory capacity.

5.4.1 Chemical characterisation

Minor variation in elemental composition, ash, and sulfate ester content confirmed only small changes in the composition between ulvan fractions. The ash content for ulvan fractions ranged from 15-21 % ash for U9-U209, while U7 had an ash content of 27 %. The latter was due to the ulvan being analysed and tested without desalting. The sulfate ester content ranged from 13.7-22.4 %, which is consistent with previously analysed ulvan from *U. ohnoi* (7.1 to 15.7 %) (Fernández-Díaz *et al.*, 2017; Glasson *et al.*, 2017) and the median from the ulvan literature (15.5 %) (Kidgell *et al.*, 2019). Depolymerisation had no effect on sulfate ester content for ulvan hydrolysed for 0-2 h (U209, U21, and U13), however a lower content was measured for U9 which was hydrolysed for 5-7 h. The apparent low sulfate content detected for U9 could be a result of the high variability in the sulfate measurement. In support of this, the S content for U9-U209 is consistent, reinforcing no change in sulfate ester content in ulvan fractions over the full 0-7 h hydrolysis period.

Chemical depolymerisation of ulvan with H_2O_2 was the chosen method as it has been used to selectively depolymerise related algal sulfated polysaccharides (Fernández-Díaz *et al.*, 2017; Zhang *et al.*, 2008). In this study, SEC-MALLS measurements confirmed that H_2O_2 successfully depolymerised native ulvan affording five different molecular weight fractions ranging from 7 to 209 kDa, depending on the duration of treatment. ^{1}H and ^{13}C NMR spectra of the fractions were both dominated by resonances consistent with ulvan samples that were rich in the disaccharide A_{3s}. The extent to which the spectra from the native and hydrolysed ulvan variants overlap in both ^{1}H and ^{13}C NMR indicate that the only major chemical modification observed was depolymerisation at the anomeric centre. However, further chemical characterisation of these fractions detected minor differences in composition; in particular, small variations in the amount of labile constituent sugars were detected.

Constituent sugar analysis confirmed that the native, sulfated polysaccharide extracted here from *U. ohnoi* and its hydrolysed products were consistent with the broader

literature definition of ulvan (Glasson *et al.*, 2017; Kidgell *et al.*, 2019). Furthermore, a high content of both rhamnose and glucuronic acid confirmed the NMR finding that ulvan from *U. ohnoi* is rich in the disaccharide A_{3s}. However, sugar constituent analysis also detected incremental degradation of xylose and iduronic acid, with concomitant increase in the content of rhamnose, as the duration of hydrolysis was increased. This is consistent with previous reports that xylose and iduronic acid are the most labile of the ulvan constituents (Quemener *et al.*, 1997). The small changes in rhamnose and glucuronic acid (the two major constituent sugars) indicate only minor variations in constituent sugars between fractions, particularly relative to the differences in molecular weight.

Thus, in terms of cytotoxicity and immunomodulation, the composition of ulvan is considered to be equal between hydrolysed fractions. Differences in the bioactivity of these fractions are therefore interpreted on the basis of concentration and molecular weight.

5.4.2 Cytotoxicity and immunomodulating activity

All ulvan M_w fractions showed no cytotoxic effects on RAW264.7 cells after 48 h of exposure with < 100 µg mL^{-1}. Furthermore, for all fractions, cell viability was only reduced to 50 % with a 5- to 20-fold increase in ulvan concentration. These results are consistent with previous cytotoxic assessments of ulvan-containing extracts on murine macrophages and cancer cells (Cho *et al.*, 2010; Kim *et al.*, 2011; Peasura *et al.*, 2016; Tabarsa *et al.*, 2012a; Tabarsa *et al.*, 2018). In the present study, the lowest M_w ulvan (U7) displayed no cytotoxicity over 48 h (up to and including the highest concentration tested, 2000 µg mL^{-1}) and instead increased cell proliferation by 10 %; by 18 % from the same concentration over 24 h. A similar 20 % increase in cell proliferation is also observed for the lowest molecular weight ulvan fraction (29 kDa) from *U. intestinalis* (Tabarsa *et al.*, 2018). The low cytotoxicity of all ulvan M_w fractions allowed the immunomodulation capacity of ulvan to be assessed on RAW264.7 cells with an upper concentration limit of 100 µg mL^{-1}. Additionally, as neither 100 µg mL^{-1} ulvan nor 1 µg mL^{-1} LPS are significantly toxic to RAW264.7 cells, differences in cytokine release are interpreted on the basis of ulvan concentration and molecular weight.

Immunomodulatory effects have been reported for ulvan samples from *U. armoricana* (Berri *et al.*, 2017; Berri *et al.*, 2016), *U. clathrata* (del Rocío Quezada-Rodríguez & Fajer-Ávila, 2017), *U. fasciata* (Rizk *et al.*, 2016a; Rizk *et al.*, 2016b), *U. intestinalis* (Jiao *et al.*, 2010; Jiao

et al., 2009; Peasura *et al.*, 2016; Tabarsa *et al.*, 2018), *U. lactuca* (Abd-Ellatef *et al.*, 2017; Chiu *et al.*, 2012; de Araújo *et al.*, 2016), *U. linza* (Zhang *et al.*, 2013), *U. ohnoi* (Fernández-Díaz *et al.*, 2017), *U. australis* (Song *et al.*, 2016; Tabarsa *et al.*, 2012a), *U. prolifera* (Cho *et al.*, 2010; Wei *et al.*, 2014), and *U. rigida* (Castro *et al.*, 2004; Leiro *et al.*, 2007). In this study, ulvan from *U. ohnoi* had immunomodulatory effects on RAW264.7 cells that were both concentration dependent and influenced by M_w.

Increased levels of IL-10 and IL-1β, and to a lesser extent IL-6 and IL-12, were observed at high concentrations of the high molecular weight fractions (U21 and U209), a response that is consistent with the literature (Jiao *et al.*, 2009; Kim *et al.*, 2011; Leiro *et al.*, 2007; Peasura *et al.*, 2016; Tabarsa *et al.*, 2012a). IL-10, a predominately anti-inflammatory cytokine that inhibits cytokine production and down-regulates inflammation, had the largest magnitude of change, increasing by 135 % from the treatment of U209 at 100 μg mL^{-1}, suggesting an anti-inflammatory effect of ulvan. PGE_2 is a principal protagonist in the inflammatory response due to its hyperalgesic, pyrogenic, and potent vasodilator capacities (Rang *et al.*, 2016). The dose-dependent reduction of PGE_2 levels below the control (up to 40 % reduction with 100 μg mL^{-1} of U209) also suggests an anti-inflammatory response. The reduction in PGE_2 is particularly notable as in a similar study on RAW264.7 cells, ulvan from *U. rigida* stimulated a dose-dependent increase in PGE_2 levels from < 10 pg mL^{-1} up to ~270 pg mL^{-1} (a 2700 % increase) in treatments of 0 to 100 μg mL^{-1} of polysaccharide (Leiro *et al.*, 2007). However, increased levels of the pro-inflammatory cytokines IL-1β, IL-6, and IL-12 detected in the current study contradict the anti-inflammatory response of IL-10 and PGE_2. The precise immunomodulatory nature of ulvan in vivo cannot be conclusively predicted from this study alone, however, these in vitro results support previous findings that ulvan possesses immunomodulating activity (Kim *et al.*, 2011; Leiro *et al.*, 2007; Peasura *et al.*, 2016; Tabarsa *et al.*, 2012a; Tabarsa *et al.*, 2018).

Although the mechanism of interaction between ulvan and LPS on RAW264.7 cells cannot be determined from the current data, molecular weight evidently plays a role in the cytotoxicity and immunomodulating capacity of ulvan. However, the apparent effect of ulvan M_w in the literature is contradictory, with some studies finding comparatively enhanced immunomodulating activity from higher M_w ulvan (Fernández-Díaz *et al.*, 2017; Kim *et al.*, 2011; Tabarsa *et al.*, 2012a) while others found comparatively higher activity with lower M_w

ulvan (Jiao *et al.*, 2010; Peasura *et al.*, 2016; Tabarsa *et al.*, 2018). Due to the wide range of M_w reported, and methods of determining immunomodulating activity, it is difficult to directly compare these studies. It is important to note that while these studies did use similar dose concentrations of ulvan, they did not study the effect of ulvan M_w in isolation; variation in the proportions of constituent sugars, proteins, and sulfate esters could affect immunomodulating activity. In the current study, I assessed the effect of ulvan M_w in isolation, having shown that all the ulvan fractions had similar chemical compositions. The fact that the native (i.e., unhydrolysed) ulvan had the greatest immunomodulating effect is ideal for future studies and potential future commercial applications as minimal processing reduces production costs and time.

The mild immunomodulating activity and enhanced cell proliferation effects of ulvan, coupled with the capacity of mammalian skin fibroblast and keratinocyte cells to directly recognise and respond to rhamnose (Andrès *et al.*, 2006; Cerdan, Grillon, Monsigny, Redziniak, & Kieda, 1991; Condaminet, Redziniak, Monsigny, & Kieda, 1997), suggest that ulvan may be applicable for topical treatments (e.g. wound dressing). However, while the in vitro results presented here are encouraging, in vivo assessment of ulvan will provide a more complete picture of ulvan immunomodulatory effects, and related anti-cancer (Hussein *et al.*, 2015; Thanh *et al.*, 2016), anti-oxidant (Qi *et al.*, 2005b; Zhang *et al.*, 2013), and antihyperlipidemic (Kumar, Magnusson, Ward, Paul, & Brown, 2015; Li *et al.*, 2018d; Pengzhan *et al.*, 2003a) effects.

5.5 Conclusion

The influence of the molecular weight of ulvan, extracted from *Ulva ohnoi*, on cytotoxicity and immunomodulatory activity was assessed. Ulvan M_w and concentration interacted to influence the cytotoxicity in RAW264.7 murine macrophages, and level of signalling molecules released. Depolymerisation appears to make the ulvan more benign; the unhydrolysed 'native' ulvan was the most bio-active, particularly at high concentrations. However, low molecular weight ulvan enhanced cell proliferation with little to no detectable immunomodulation activity. To summarise, due to the promotion of cell viability, low cytotoxicity at low concentrations, a moderate immunomodulating activity, and innate

capacity to interact with human skin immunomodulatory cells, ulvan has multiple characteristics ideal for applications targeting the treatment of dermal diseases and wounds.

Chapter 6:
General discussion

Ulvan is a complex and underutilised sulfated polysaccharide that has potential applications as an immunomodulating, antiviral, antioxidant, antihyperlipidemic, and anticancer agent (Alves *et al.*, 2013b; Jiao *et al.*, 2011; Lahaye & Robic, 2007; Venkatesan *et al.*, 2015; Wijesekara *et al.*, 2011). However, the complexity of ulvan impedes literature consensus on the composition, structure, and potential applications of the polysaccharide (Kidgell *et al.*, 2019). This thesis examined several contentious areas of ulvan research with a focus on using highly purified, thoroughly characterised ulvan to ensure validity of the results. Specifically, (I) the composition and rheology of multiple ulvans was critically assessed using standardised methods for extraction and analysis, (II) the structure of a subset of these ulvans was investigated in detail using glycosyl linkage analysis, and (III) the immunomodulating capacity of an ulvan produced at industrial scale was assessed. Through this approach I have clearly demonstrated that ulvans from different species of *Ulva* have distinct physicochemical properties and that the structure of ulvan drives the biological activity. Notably, I identified a morphology-based division of the physicochemical properties of ulvan within the genus *Ulva*.

A central finding of this thesis was that the physicochemical properties of ulvans isolated from blade and filamentous species of *Ulva* from Aotearoa New Zealand were significantly different. Analysis of the constituent sugars, molecular weights, NMR spectra and glycosidic linkages demonstrated that ulvans from blade species of *Ulva* are simpler in structure than ulvans from filamentous species. Notably, ulvans from blade species had higher proportions of iduronic acid, lower molecular weights, and a near absent capacity to gel. In direct contrast, ulvans from filamentous species of *Ulva* had molecular weights approximately double that of ulvans from blade species, and consistently formed gels. NMR spectra of ulvans from blade species were characteristic of highly repeating saccharide structural moieties, supporting the linkage analysis conclusion that these ulvans had a consistent repeating structure, with at least two thirds of the ulvan comprised of repeat units of ulvanobiuronic acid disaccharides A_{3S} and B_{3S}. Ulvans from filamentous species were far

more heterogeneous in structure as evidenced by lower proportions of linear A_{3S} and B_{3S} disaccharides (only one third of the ulvans), greater proportions of branched sugars, and a greater diversity of NMR resonances detected. This variation in physicochemical properties of ulvans from blade and filamentous species of *Ulva* may account for some of the variance in composition, structure, and function of ulvan reported in the literature (Kidgell *et al.*, 2019). For example, despite a literature median of 2.1 mol% galactose, there are sporadic reports of high proportions (7-16 mol%) of galactose in ulvans (Chattopadhyay *et al.*, 2007; Kidgell *et al.*, 2021; Matloub *et al.*, 2016; Qi *et al.*, 2013b; Ray, 2006; Tabarsa *et al.*, 2018), all of which were extracted from filamentous species of *Ulva*. Galactose occurring as a component (or co-polymer) of ulvan from some filamentous species of *Ulva*, as suggested in this thesis, would account for such sporadic reports. However, although the morphology-based divisions in composition and physicochemical properties of ulvans are compelling, additional validation through analysis of ulvans from a broader range of blade and filamentous species of *Ulva* would be beneficial.

The biological activity/function of a natural product such as ulvan is inextricably linked to its structure. Thorough investigation of the bioactivity of a natural product with known variations to its structure can facilitate the identification of a structure-activity relationship (SAR). During this thesis I have contributed initial results towards the identification of molecular weight-based SARs by investigating the effect that the molecular weight of ulvan has upon its rheological and immunomodulating properties. I established that ulvans from the filamentous species *U. ralfsii* and *U. flexuosa* have the highest molecular weights (406 kDa and 352 kDa, respectively) and gelling capacity (storage moduli of 29.5 ± 4.2 Pa and 34.2 ± 1.8 Pa, respectively) in contrast to the lower molecular weight (190-254 kDa) and gelling capacity (0.1-6.6 Pa) of ulvans from blade species of *Ulva*. Similarly, the molecular weight of ulvan from the blade species *Ulva ohnoi* influences the immunomodulating capacity of this ulvan with larger molecular weights having the greatest magnitude of effect. Considering the positive correlation between molecular weight and immunomodulating capacity, and the larger molecular weight of ulvans from filamentous species compared to blade species, ulvan from filamentous species may be better suited to applications where immunomodulation is required. However, it is important to note that these results constitute only the beginning of the identification of SAR(s) and cannot be generalised to ulvans from other sources without

further assessment. Indeed, the lack of SARs is an acknowledged gap in ulvan research often emphasised in reviews of the field (Jiao *et al.*, 2011; Kidgell *et al.*, 2019; Tziveleka, Ioannou, & Roussis, 2019; Venkatesan *et al.*, 2015). Further progress of SARs with comprehensive assessments of ulvan can be achieved through use of a more broadly encompassing research framework, such as the one developed during this thesis.

The experiments performed in Chapters 3, 4, and 5 in this thesis crossed the fields of analytical chemistry and immunology and required an understanding of physical chemistry and seaweed aquaculture. The breadth of these fields, in conjunction with the literature review and meta-analysis performed at the start of this thesis, provided insight into each step of ulvan research, from the production of *Ulva* to the application of the isolated polysaccharide. From this insight, a broadly encompassing framework for future research on ulvan can be proposed to advance the field in a systematic and comparative manner (Figure 6.1). The framework developed throughout this thesis can act as a guide for researchers to systematically test ulvans from a variety of species from different sources (wild/aquaculture) for different applications and, importantly, compare results between these studies.

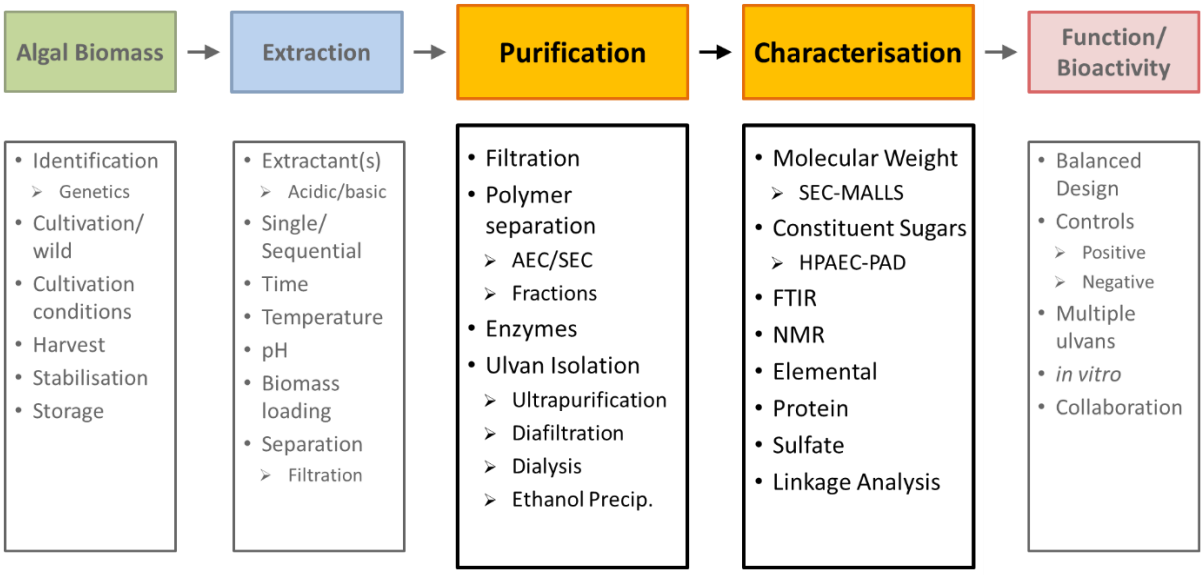

Figure 6.1: A framework for ulvan research involving five major stages: algal biomass, extraction, purification, characterisation, and function. The purification and characterisations steps have been highlighted as these are of particular importance to the identification of structure-activity relationships. Each stage has several important considerations to ensure research is specific to ulvan and comparable to other studies. These considerations are by no means an exhaustive list, nor are each going to be discussed in detail in this thesis.

Progress in the identification of structure-activity relationships for ulvan can be greatly accelerated using a research framework with a focus on the isolation of highly purified, thoroughly characterised ulvan(s) prior to any function or bioactivity assessments (Figure 6.1). Such a framework would provide more certainty around the bioactivity of ulvan, promoting the formation of structure-activity relationships. Importantly, it will also enable comparisons between ulvans from different studies. Indeed, the issues in the literature identified from my review and meta-analysis (Kidgell *et al.*, 2019), notably: defined structure-activity relationships; studies on highly purified ulvans; and assessment of multiple ulvans using standardised methods, could all be strengthened using a more broadly encompassing research framework in the future. The research framework suggested here is broken down into five steps, each of which has a number of considerations to address to ensure results are accurate. These steps are algal biomass, extraction, purification, characterisation, and function/bioactivity. Each step is described further below, with emphasis on the critical steps required for accurate comparisons of ulvans and identification of SARs, namely purification and characterisation.

Detailed accounting of the source of **algal biomass** is critical for comparison of ulvans (between different species, locations, seasons, etc.). Accurate identification of the species of *Ulva* is key to future intra- and interspecific comparisons between extracted ulvans. Due to the high morphological plasticity of *Ulva* species, the best method of identification is genetic barcoding (See (Lawton *et al.*, Under review)). How the seaweed biomass is produced (cultivation or wild harvest), harvested, stabilised, and stored prior to extraction, are also important considerations that could affect the ulvan within (Jmel *et al.*, 2017; Magnusson *et al.*, 2016; Robic *et al.*, 2008). If the biomass is wild harvested, it is important to record time, season, and location for future comparisons as seasonality and local environment conditions can affect the ulvan. If the biomass is cultivated, the cultivation parameters (i.e. light, temperature, biomass loading, nutrients, harvest schedule, etc.) must be recorded, and ideally standardised, to be replicated in the future (See (Carl, Magnusson, Paul, & de Nys, 2016; Lawton *et al.*, Under review; Mata *et al.*, 2016)). The **extraction** stage of the framework is the one that will have the most flow-on effects for latter stages. It is critical that the extraction be standardised for comparison of ulvans. The extractant used can greatly affect the quality of ulvan obtained (Glasson *et al.*, 2017; Haug, 1976; Hernández-Garibay *et al.*,

2011; Jiao *et al.*, 2012; Peasura *et al.*, 2015), and therefore, any bioactivity detected. For example, acidic extractions are more selective for ulvan over co-extracted polysaccharides but can result in depolymerisation, while an alkali extraction yields more material but with a higher degree of co-extracted impurities (e.g. protein) (Glasson *et al.*, 2017). Similarly, the time, temperature, and pH of the extraction solution affects the yield, molecular weight, and proportion of contaminants (de Reviers & Leproux, 1993; Glasson *et al.*, 2019; Peasura *et al.*, 2015; Pezoa-Conte *et al.*, 2017; Yaich *et al.*, 2013). For more details of the extraction stage see the literature review (Kidgell *et al.*, 2019). Both the source of the biomass and the method by which ulvan is extracted are vitally important when comparing one ulvan to another, within and between studies. However, in the context of identifying structure-activity relationships, purification and characterisation of the ulvan obtained are of paramount importance – the agent responsible for bioactivity cannot be ascribed without precisely knowing the identity of the agent.

Purification of ulvan is critical. Without purification of the ulvan polysaccharide following extraction, any characterisation and function/bioactivity studies will be unable to attribute causal effects to ulvan with certainty. Purification starts with post-extraction filtration of solubilised ulvan from the residual biomass, followed by a method to isolate ulvan from co-extracted molecules. Anion-exchange and size exclusion chromatography are appropriate methods to isolate ulvan based on charge and molecular weight, respectively. Both methods separate ulvan from co-extracted protein or other polysaccharides, providing that a suitable assay is chosen to determine the retention of fractions (such as comparison of UV chromatogram with a glucuronic acid or rhamnose colourimetry assay). Identifying the chromatography fractions to retain is a balance between purity and yield. Obtaining highly purified ulvan will often come at the (acceptable) cost of losing some material. Ethanol precipitation is an alternative method for isolating ulvan, however, this method is non-selective and biased for larger molecules. If ethanol precipitation is used, a secondary purification method such as the chromatographic methods discussed above should be employed. Enzymes (e.g., amylase, cellulase) can also be used during purification to degrade co-extracted molecules (e.g., protein, cellulose) and enable their removal as small-molecule hydrolysates (Hardouin *et al.*, 2016; Lahaye *et al.*, 1999; Lahaye & Jegou, 1993; Ray & Lahaye, 1995b; Yaich *et al.*, 2014). Once co-extracted molecules have been separated and/or

degraded, the ulvan-containing fractions must be concentrated. Repetitive diafiltration followed by ultrafiltration is an ideal and robust method. However, dialysis will also provide a similar outcome with more labour and time. The actual methods applied during the purification step will vary based on access to resources and experience. However, the intent of purification is emphasised, namely, to produce an isolated ulvan with no impurities, as certified by thorough characterisation. Purifying and precisely characterising the ulvan polymer is essential to attributing a causal effect during any subsequent functional or bioactivity studies.

Thorough **characterisation** of the purified ulvan is required to ensure what was extracted and isolated is ulvan to the highest degree possible. Detailed characterisation will be instrumental in identifying structure-activity relationships and enable comparison of ulvans between studies. There are many possible methods for the characterisation of polysaccharides, and each has advantages and disadvantages. Characterisation of elemental, protein, and sulfate content provide an excellent insight into the quality of ulvan. Elemental composition (C, H, O, N, S, ash) details the percent (purity) of carbohydrate material in the sample. Additionally, the proportion of N and S supports individual assays for protein and sulfate. It should be noted that sulfate content is difficult to determine accurately – the proportion of S may not correlate with the percentage of sulfate esters determined. A critical assessment of sulfate analysis and desulfation of ulvans would be a valuable contribution to the literature. Constituent sugar analysis is one of the most informative techniques, both for certifying the identity of ulvan and determining the purity of the sample. However, accurate determination of the constituent sugar composition is complicated, given the presence of both uronic acids and acid-labile monosaccharides. HPAEC-PAD following methanolysis and TFA hydrolysis enables quantitation of all the principal ulvan constituent sugars, rhamnose, glucuronic acid, xylose, iduronic acid, and galactose (in ulvans from filamentous species) in minimal reaction steps while achieving optimal hydrolysis and negligible loss of monosaccharides (de Ruiter *et al.*, 1992). Trace quantities of arabinose, fucose, and ribose are also often found. High quantities of glucose, however, suggest contamination with a co-extracted polysaccharide such as xyloglucan or cellulose. Alternatively, constituent sugars can be quantified by GC-MS following derivatisation of hydrolysed sugars. However, the additional derivatisation steps required increases the chance for loss of monosaccharides or

material and can result in highly complicated chromatograms (e.g., from trimethylsilyl (TMS) derivatisation). NMR and FTIR spectroscopy are valuable techniques providing information on the purity and structure of ulvan, although NMR spectra can be difficult to decipher with large complex polymers due to a high level of noise and broad resonances. Depolymerised ulvan oligosaccharides are better suited to NMR analysis. Further elucidation of ulvan structure involves the determination of molecular weight, which is ideally performed with SEC-MALLS as there are no appropriate molecular weight standards available to enable the use of SEC-RI and elution volume alone. Finally, linkage analysis can provide a great deal of information on how the constituent monosaccharides are linked to each other, the sulfate substituent positions, and structure of ulvan, when supported with NMR data (Sims *et al.*, 2018). As with the purification step, the intent of characterisation of ulvan is to understand the polymer composition and structure in such detail that particular structural components of ulvan can be investigated for bioactivity stimulation. Failure to accurately characterise components of ulvan (such as molecular weight or iduronic acid content) or demonstrate through characterisation that the assessed ulvan has been purified, is counter-productive to subsequent bioactivity assessments of the polysaccharide.

Assessment of the **function or bioactivity** of ulvan should only be conducted after the source species of *Ulva* has been accurately identified, the extraction protocol used was suitable and repeatable, and the ulvan has been isolated from other molecules, purified, and thoroughly characterised. The method or assay to determine function/bioactivity will vary widely, but some general considerations follow. Balanced, factorial experimental designs are robust and useful for comparing ulvan functions/bioactivities. For bioactivity assays, judicious use of both positive and negative controls is essential to determine the magnitude of effect. Similarly, at this stage, in vitro assays are likely to be the most applicable to ulvan research as they provide a high level of control over experimental variables. Critically, however, these assays or methods must be completed by, or in consultation with, experts in the relevant field. The essence of the ulvan research framework discussed here is collaboration.

Collaboration between researchers in the fields which the ulvan research framework intersects is essential to progress. An example of the application of this framework can be seen in Chapter 3 of this thesis. The New Zealand species of *Ulva* were collected, identified,

and cultivated with the support of aquaculturists and geneticists. Ulvan was then extracted and isolated using an optimised procedure that was standardised across all samples of *Ulva*. The ulvans were characterised with the support of analytical carbohydrate chemists using standardised, established protocols. And finally, the rheological measurements were collected using specialised equipment with support of experts in the field. Similarly, the fully factorial immunology assays performed in Chapter 5 would not have been possible without the tutelage and support of experienced immunologists. It was only through collaboration that the breadth of this thesis was able to be assailed. And it was only with careful isolation and thorough characterisation that nuanced differences in the composition, structure, and rheology of ulvan were able to be conclusively identified.

6.1 Conclusion

In conclusion, ulvan was assessed in this thesis under the broader context of selecting a species of *Ulva* for land-based aquaculture in New Zealand as part of an overarching platform for the University of Waikato Algal Biotechnology Research Project. In addition to the physicochemical properties of ulvan assessed in this thesis, the growth rate and productivity of candidate species of *Ulva* are key considerations for application in aquaculture. The growth rate of the species of *Ulva* from which ulvan was isolated for Chapters 3 and 4 has been evaluated (Lawton *et al.*, Under review). Selection of a New Zealand species of *Ulva* to target to produce ulvan can therefore be based on the species growth rate in conjunction with the yield and gelling capacity of the extracted ulvan. An assessment of these three critical parameters utilising a matrix approach for the ranking and selection of species investigated in this thesis is presented in Figure 6.2. Of these species, *Ulva ralfsii* had the highest growth rate and the ulvan isolated from this species had the highest storage modulus. However, the yield of ulvan from *U. ralfsii* was comparatively low. *Ulva flexuosa* represents a more balanced option with growth rates similar to *U. ralfsii*, but with approximately double the yield of ulvan, which forms gels with a similar storage modulus to *U. ralfsii* (Figure 6.2). Therefore, *U. flexuosa* represents an excellent candidate for land-based aquaculture to produce gelling ulvans, with *U. ralfsii* as a close second candidate.

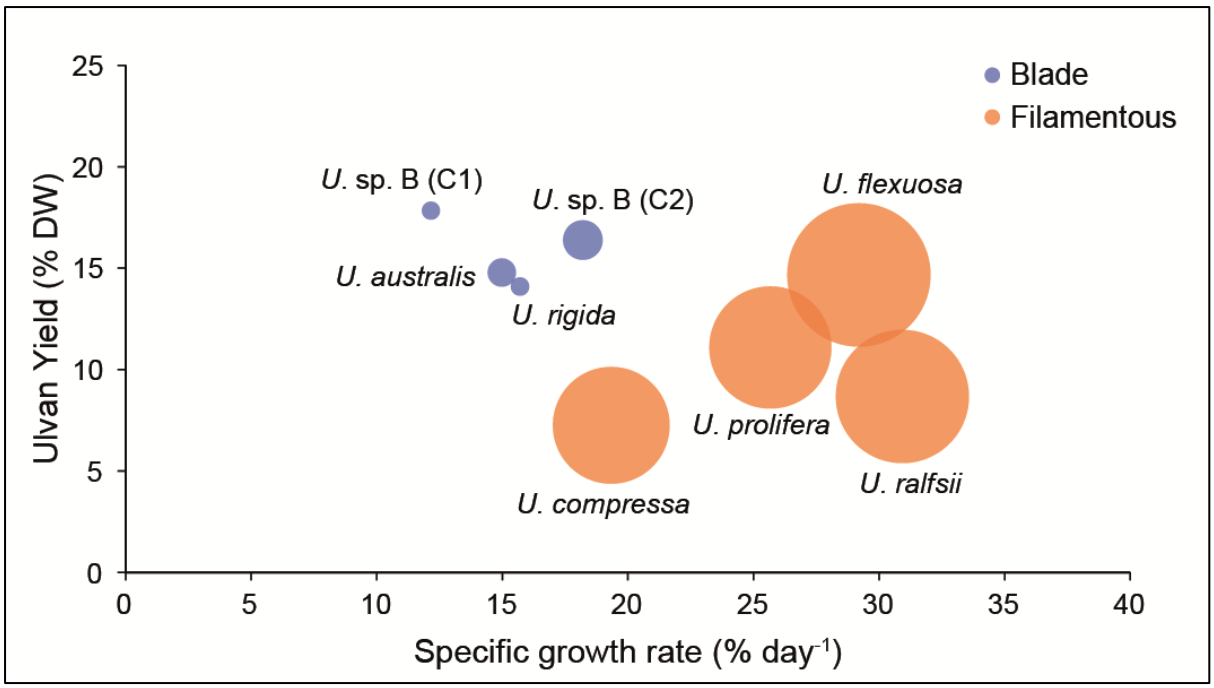

Figure 6.2: The relationship between the specific growth rate (SGR) of an *Ulva* species (as a percent increase in biomass per day), the yield of ulvan extracted from the species (as % of dry weight biomass) and the storage modulus of the gel produced by the ulvan (bubble size, larger is stronger gel). Two samples of *U*. sp. B were cultivated, "C1" and "C2". Refer to Chapter 3 for further details of ulvans.

6.2 Future research

Ulvan holds significant academic and commercial interest with many potential applications. Based on the publications citing the ulvan literature review and meta-analysis published at the start of this thesis (Kidgell *et al.*, 2019), ulvan is currently being investigated for use as various forms of biomaterial (Gajaria *et al.*, 2020; Lakshmi *et al.*, 2020; Moghazy, Labena, Husien, Mansor, & Abdelhamid, 2020; Moon *et al.*, 2020; Tziveleka *et al.*, 2019; Tziveleka *et al.*, 2020) with a focus on porous scaffolds and membranes for applications in bone regrowth, neural implants, and wound dressings. These studies highlight that ulvan is a promising biomaterial candidate due to its capacity to act as a hydrogel, form a thermoreversible gel, and promote cell proliferation. The structure of ulvan, which is similar to mammalian glycosaminoglycans, makes ulvan highly amenable to chemical modification, enabling fine-tuning of the molecule for specific applications. Additionally, the biologically active properties of ulvan as an anti-microbial/viral (Hans, Malik, & Naik, 2021; Ray *et al.*, 2021; Sivakanthan, Rajendran, Gamage, Madhujith, & Mani, 2020), and immunomodulating

agent (Fumanal *et al.*, 2020; Kidgell *et al.*, 2020; Klongklaew, Praiboon, Tamtin, & Srisapoome, 2021; Ponce, Zuasti, Anguís, & Fernández-Díaz, 2020; Pratap, Taki, Johnston, Lopata, & Kamath, 2020) act in synergy with proposed biomaterial applications. For example, ulvan could act as a pharmaceutical-embedded hydrogel that concomitantly acted as an anti-microbial or immunomodulating agent. Alternatively, ulvan could be applied as a hybrid scaffold for bone repair where the highly porous structure and charge promotes adherence of osteogenic cells and deposition of minerals near the site of repair, in addition to ulvan enhancing cell proliferation. There has also been advances in the structural elucidation of ulvan (Chi *et al.*, 2020; Jin *et al.*, 2020; Wahlström *et al.*, 2020; Zhang *et al.*, 2020), and in the aquaculture and cultivation of ulvan-producing seaweeds (García-Poza *et al.*, 2020; López-Pedrouso *et al.*, 2020; Olsson *et al.*, 2020a; Olsson *et al.*, 2020b; White & White, 2020). Future research into ulvan needs to take into consideration the difference in the composition and structure of ulvan from blade and filamentous species of *Ulva*. However, this difference also opens research avenues, such as assessing the bioactive potential of ulvans from filamentous species of *Ulva*. Application of the ulvan research framework outlined in this discussion, notably using highly purified and thoroughly characterised ulvan(s), will support conclusive results and the identification of structure-activity relationships. Most critical, however, is collaboration between specialist researchers in each stage of the ulvan research framework to ensure future investigations are specific to ulvan, representative, and comparable between studies.

References

Abd-Ellatef, G. E. F., Ahmed, O. M., Abdel-Reheim, E. S., & Abdel-Hamid, A. H. Z. (2017). *Ulva lactuca* polysaccharides prevent Wistar rat breast carcinogenesis through the augmentation of apoptosis, enhancement of antioxidant defense system, and suppression of inflammation. *Breast Cancer: Targets and Therapy,* 9, 67-83.

Abd El-Baky, H. H., El Baz, F. K., & El Baroty, G. S. (2009). Potential biological properties of sulphated polysaccharides extracted from the macroalgae *Ulva lactuca* L. *Academic Journal of Cancer Research,* 2(1), 1-11.

Abdel-Fattah, A. F., & Edrees, M. (1972). A study on the polysaccharide content of *Ulva lactuca* L. *Qualitas Plantarum et Materiae Vegetabiles,* 22(1), 15-22.

Adrien, A., Bonnet, A., Dufour, D., Baudouin, S., Maugard, T., & Bridiau, N. (2017a). Pilot production of ulvans from *Ulva* sp. and their effects on hyaluronan and collagen production in cultured dermal fibroblasts. *Carbohydrate Polymers,* 157, 1306-1314.

Adrien, A., Dufour, D., Baudouin, S., Maugard, T., & Bridiau, N. (2017b). Evaluation of the anticoagulant potential of polysaccharide-rich fractions extracted from macroalgae. *Natural Product Research,* 31(18), 2126-2136.

Aguilar-Briseño, J. A., Cruz-Suarez, L. E., Sassi, J. F., Ricque-Marie, D., Zapata-Benavides, P., Mendoza-Gamboa, E*., et al.* (2015). Sulphated polysaccharides from *Ulva clathrata* and *Cladosiphon okamuranus* seaweeds both inhibit viral attachment/entry and cell-cell fusion, in NDV infection. *Marine Drugs,* 13(2), 697-712.

Ahmed, O. M., & Ahmed, R. R. (2014). Anti-proliferative and apoptotic efficacies of ulvan polysaccharides against different types of carcinoma cells in vitro and in vivo. *Journal of Cancer Science and Therapy,* 6(6), 202-208.

Al-Amoudi, O. A., Mutawie, H. H., Patel, A. V., & Blunden, G. (2009). Chemical composition and antioxidant activities of Jeddah corniche algae, Saudi Arabia. *Saudi Journal of Biological Sciences,* 16(1), 23-29.

Alam, S. S., Abd El-Kader, H. A. M., Abd El-Rahim, A. H., Hamed, S. M., & Saber, A. A. (2016). The protective role of *Ulva lactuca* against genotoxic and biochemical effects induced by γ-irradiation in rats. *International Journal of Pharmaceutical Sciences Review and Research,* 37(2), 40-48.

Ali, M. M., & Agha, F. G. (2009). Amelioration of streptozotocin-induced diabetes mellitus, oxidative stress and dyslipidemia in rats by tomato extract lycopene. *Scandinavian Journal of Clinical and Laboratory Investigation,* 69(3), 371-379.

Alipour, H. J., Rezaei, M., Shabanpour, B., & Tabarsa, M. (2018). Effects of sulfated polysaccharides from green alga *Ulva intestinalis* on physicochemical properties and microstructure of silver carp surimi. *Food Hydrocolloids,* 74, 87-96.

Alves, A., Caridade, S. G., Mano, J. F., Sousa, R. A., & Reis, R. L. (2010). Extraction and physico-chemical characterization of a versatile biodegradable polysaccharide obtained from green algae. *Carbohydrate Research,* 345(15), 2194-2200.

Alves, A., Pinho, E. D., Neves, N. M., Sousa, R. A., & Reis, R. L. (2012a). Processing ulvan into 2D structures: Cross-linked ulvan membranes as new biomaterials for drug delivery applications. *International Journal of Pharmaceutics,* 426(1-2), 76-81.

Alves, A., Sousa, R. A., & Reis, R. L. (2013a). In vitro cytotoxicity assessment of ulvan, a polysaccharide extracted from green algae. *Phytotherapy Research,* 27(8), 1143-1148.

Alves, A., Sousa, R. A., & Reis, R. L. (2013b). A practical perspective on ulvan extracted from green algae. *Journal of Applied Phycology,* 25(2), 407-424.

Alves, A., Sousa, R. A., & Reis, R. L. (2013c). Processing of degradable ulvan 3D porous structures for biomedical applications. *Journal of Biomedical Materials Research Part A,* 101(4), 998-1006.

Alves, M. G. D. F., Dore, C. M. P. G., Castro, A. J. G., do Nascimento, M. S., Cruz, A. K. M., Soriano, E. M*., et al.* (2012b). Antioxidant, cytotoxic and hemolytic effects of sulfated galactans from edible red alga *Hypnea musciformis*. *Journal of Applied Phycology,* 24(5), 1217-1227.

Anderson, M. J., Gorley, R. N., & Clarke, R. K. (2008). *Permanova+ for Primer : guide to software and statisticl methods*.

Andrès, E., Molinari, J., Péterszegi, G., Mariko, B., Ruszova, E., Velebny, V*., et al.* (2006). Pharmacological properties of rhamnose-rich polysaccharides, potential interest in age-dependent alterations of connectives tissues. *Pathologie Biologie,* 54(7), 420-425.

Angell, A. R., Mata, L., de Nys, R., & Paul, N. A. (2014). Variation in amino acid content and its relationship to nitrogen content and growth rate in *Ulva ohnoi* (Chlorophyta). *Journal of Phycology,* 50(1), 216-226.

Angell, A. R., Mata, L., de Nys, R., & Paul, N. A. (2016). The protein content of seaweeds: a universal nitrogen-to-protein conversion factor of five. *Journal of Applied Phycology,* 28(1), 511-524.

Angell, A. R., Paul, N. A., & de Nys, R. (2017). A comparison of protocols for isolating and concentrating protein from the green seaweed *Ulva ohnoi*. *Journal of Applied Phycology,* 29(2), 1011-1026.

Araujo, L., Goncalves, A. E., & Stadnik, M. J. (2014). Ulvan effect on conidial germination and appressoria formation of *Colletotrichum gloeosporioides*. *Phytoparasitica,* 42(5), 631-640.

Araújo, L., Stadnik, M. J., Borsato, L. C., & Valdebenito-Sanhueza, R. M. (2008). Potassium phosphite and ulvan in the control of 'Gala' leaf spot on apple. *Tropical Plant Pathology,* 33(2), 148-152.

Badr, H. A., Takahashi, K., Kawakami, R., Oyama, Y., Yokoigawa, K., & Kanemaru, K. (2017). Screening and analysis of edible seaweeds in the ability to adsorb Shiga toxin. *European Food Research and Technology,* 243(12), 2147-2153.

Balaji Raghavendra Rao, H., Sathivel, A., & Devaki, T. (2004). Antihepatotoxic nature of *Ulva reticulata* (Chlorophyceae) on acetaminophen-induced hepatoxicity in experimental rats. *Journal of Medicinal Food,* 7(4), 495-497.

Barbosa, J., Borges, S., Amorim, M., Pereira, M. J., Oliveira, A., Pintado, M. E.*, et al.* (2015). Comparison of spray drying, freeze drying and convective hot air drying for the production of a probiotic orange powder. *Journal of Functional Foods,* 17, 340-351.

Barros, A. A. A., Alves, A., Nunes, C., Coimbra, M. A., Pires, R. A., & Reis, R. L. (2013). Carboxymethylation of ulvan and chitosan and their use as polymeric components of bone cements. *Acta Biomaterialia,* 9(11), 9086-9097.

Battacharyya, D., Babgohari, M. Z., Rathor, P., & Prithiviraj, B. (2015). Seaweed extracts as biostimulants in horticulture. *Scientia Horticulturae,* 196, 39-48.

Bedini, E., Laezza, A., Parrilli, M., & Iadonisi, A. (2017). A review of chemical methods for the selective sulfation and desulfation of polysaccharides. *Carbohydrate Polymers,* 174, 1224-1239.

BeMiller, J. N. (1967). Acid-catalyzed hydrolysis of glycosides. *Advances in Carbohydrate Chemistry and Biochemistry,* 22, 25-108.

Béress, A., Wassermann, O., Bruhn, T., Béress, L., Kraiselburd, E. N., Gonzalez, L. V.*, et al.* (1993). A new procedure for the isolation of anti-HIV compounds (polysaccharides and polyphenols) from the marine alga *Fucus vesiculosus*. *Journal of Natural Products,* 56(4), 478-488.

Berri, M., Olivier, M., Holbert, S., Dupont, J., Demais, H., Le Goff, M.*, et al.* (2017). Ulvan from *Ulva armoricana* (Chlorophyta) activates the PI3K/Akt signalling pathway via TLR4 to induce intestinal cytokine production. *Algal Research,* 28, 39-47.

Berri, M., Slugocki, C., Olivier, M., Helloin, E., Jacques, I., Salmon, H.*, et al.* (2016). Marine-sulfated polysaccharides extract of *Ulva armoricana* green algae exhibits an antimicrobial activity and stimulates cytokine expression by intestinal epithelial cells. *Journal of Applied Phycology,* 28(5), 2999-3008.

Biermann, C. J., & McGinnis, G. D. (1989). *Analysis of carbohydrates by GLC and MS*. Boca Raton, FL 33431: CRC Press Inc.

Bigot, S., Louarn, G., Kébir, N., & Burel, F. (2013). Click grafting of seaweed polysaccharides onto PVC surfaces using an ionic liquid as solvent and catalyst. *Carbohydrate Polymers,* 98(2), 1644-1649.

Bilan, M. I., Grachev, A. A., Ustuzhanina, N. E., Shashkov, A. S., Nifantiev, N. E., & Usov, A. I. (2004). A highly regular fraction of a fucoidan from the brown seaweed *Fucus distichus* L. *Carbohydrate Research,* 339(3), 511-517.

Birben, E., Sahiner, U. M., Sackesen, C., Erzurum, S., & Kalayci, O. (2012). Oxidative stress and antioxidant defense. *World Allergy Organization Journal,* 5(1), 9-19.

Blomster, J., Back, S., Fewer, D. P., Kiirikki, M., Lehvo, A., Maggs, C. A.*, et al.* (2002). Novel morphology in *Enteromorpha* (Ulvophyceae) forming green tides. *American Journal of Botany,* 89(11), 1756-1763.

Blondin, C., Fischer, E., Boisson-Vidal, C., Kazatchkine, M. D., & Jozefonvicz, J. (1994). Inhibition of complement activation by natural sulfated polysaccharides (fucans) from brown seaweed. *Molecular Immunology,* 31(4), 247-253.

Blumenkrantz, N., & Asboe-Hansen, G. (1973). New method for quantitative determination of uronic acids. *Analytical Biochemistry,* 54(2), 484-489.

Bobin-Dubigeon, C., Lahaye, M., Guillon, F., Barry, J.-L., & Gallant, D. J. (1997). Factors limiting the biodegradation of *Ulva* sp. cell-wall polysaccharides. *Journal of the Science of Food and Agriculture,* 75(3), 341-351.

Bolton, J. J., Robertson-Andersson, D. V., Shuuluka, D., & Kandjengo, L. (2009). Growing *Ulva* (Chlorophyta) in integrated systems as a commercial crop for abalone feed in South Africa: a SWOT analysis. *Journal of Applied Phycology,* 21(5), 575-583.

Bonin, D. R., & Hawkes, M. W. (1987). Systematics and life histories of New Zealand Bonnemaisoniaceae (Bonnemaisoniales, Rhodophyta): I. The genus *Asparagopsis*. *New Zealand Journal of Botany,* 25(4), 577-590.

Borai, I. H., Ezz, M. K., Rizk, M. Z., El-Sherbiny, M., Matloub, A. A., Aly, H. F.*, et al.* (2015). Hypolipidemic and anti-atherogenic effect of sulphated polysaccharides from the green alga *Ulva fasciata*. *International Journal of Pharmaceutical Sciences Review and Research,* 31(1), 1-12.

Bouayed, J., & Bohn, T. (2010). Exogenous antioxidants--Double-edged swords in cellular redox state: Health beneficial effects at physiologic doses versus deleterious effects at high doses. *Oxidative Medicine and Cellular Longevity,* 3(4), 228-237.

Bradford, M. M. (1976). A rapid and sensitive method for the quantitation of microgram quantities of protein utilizing the principle of protein-dye binding. *Analytical Biochemistry,* 72(1), 248-254.

Brading, J. W. E., Georg-Plant, M. M. T., & Hardy, D. M. (1954). The polysaccharide from the alga *Ulva lactuca*. Purification, hydrolysis, and methylation of the polysaccharide. *Journal of the Chemical Society (Resumed)*, 319-324.

Brodie, J., & Lewis, J. (2007). *Unravelling the algae: The past, present, and future of algal systematic*.

Burketova, L., Trda, L., Ott, P. G., & Valentova, O. (2015). Bio-based resistance inducers for sustainable plant protection against pathogens. *Biotechnology Advances,* 33(6), 994-1004.

Cai, C., Guo, Z., Yang, Y., Geng, Z., Tang, L., Zhao, M.*, et al.* (2016). Inhibition of hydrogen peroxide induced injuring on human skin fibroblast by *Ulva prolifera* polysaccharide. *International Journal of Biological Macromolecules,* 91, 241-247.

Campo, V. L., Kawano, D. F., da Silva, D. B., & Carvalho, I. (2009). Carrageenans: Biological properties, chemical modifications and structural analysis - A review. *Carbohydrate Polymers,* 77(2), 167-180.

Carl, C., Magnusson, M., Paul, N. A., & de Nys, R. (2016). The yield and quality of multiple harvests of filamentous *Ulva tepida*. *Journal of Applied Phycology,* 28(5), 2865-2873.

Cassolato, J. E., Noseda, M. D., Pujol, C. A., Pellizzari, F. M., Damonte, E. B., & Duarte, M. E. (2008). Chemical structure and antiviral activity of the sulfated heterorhamnan isolated from the green seaweed *Gayralia oxysperma*. *Carbohydrate Research,* 343(18), 3085-3095.

Castellanos-Barriga, L. G., Santacruz-Ruvalcaba, F., Hernández-Carmona, G., Ramírez-Briones, E., & Hernández-Herrera, R. M. (2017). Effect of seaweed liquid extracts from *Ulva lactuca* on seedling growth of mung bean (*Vigna radiata*). *Journal of Applied Phycology,* 29(5), 2479-2488.

Castro, M. O., Pomin, V. H., Santos, L. L., Vilela-Silva, A. C., Hirohashi, N., Pol-Fachin, L.*, et al.* (2009). A unique 2-sulfated beta-galactan from the egg jelly of the sea urchin *Glyptocidaris crenularis*: conformation flexibility versus induction of the sperm acrosome reaction. *Journal of Biological Chemistry,* 284(28), 18790-18800.

Castro, R., Piazzon, M. C., Zarra, I., Leiro, J., Noya, M., & Lamas, J. (2006). Stimulation of turbot phagocytes by *Ulva rigida* C. Agardh polysaccharides. *Aquaculture,* 254(1), 9-20.

Castro, R., Zarra, I., & Lamas, J. (2004). Water-soluble seaweed extracts modulate the respiratory burst activity of turbot phagocytes. *Aquaculture,* 229(1), 67-78.

Casu, B., Petitou, M., Provasoli, M., & Sinaÿ, P. (1988). Conformational flexibility: a new concept for explaining binding and biological properties of iduronic acid-containing glycosaminoglycans. *Trends in Biochemical Sciences,* 13(6), 221-225.

Cavaillon, J. M. (2001). Pro- versus anti-inflammatory cytokines: Myth or reality. *Cellular and Molecular Biology* 47(4), 695-702.

Cerdan, D., Grillon, C., Monsigny, M., Redziniak, G., & Kieda, C. (1991). Human keratinocyte membrane lectins: characterization and modulation of their expression by cytokines. *Biology of the Cell,* 73(1), 35-42.

Chadwick, N. E., & Morrow, K. M. (2011). *Competition Among Sessile Organisms on Coral Reefs*. In Z. Dubinsky & N. Stambler (Eds.), *Coral Reefs: An Ecosystem in Transition* (pp. 347-371). Dordrecht: Springer Netherlands

Chandika, P., Ko, S. C., & Jung, W. K. (2015). Marine-derived biological macromolecule-based biomaterials for wound healing and skin tissue regeneration. *International Journal of Biological Macromolecules,* 77, 24-35.

Chattopadhyay, K., Mandal, P., Lerouge, P., Driouich, A., Ghosal, P., & Ray, B. (2007). Sulphated polysaccharides from Indian samples of *Enteromorpha compressa* (Ulvales, Chlorophyta): Isolation and structural features. *Food Chemistry,* 104(3), 928-935.

Cheng, H. N., & Neiss, T. G. (2012). Solution NMR spectroscopy of food polysaccharides. *Polymer Reviews,* 52(2), 81-114.

Chi, Y., Li, H., Wang, P., Du, C., Ye, H., Zuo, S.*, et al.* (2020). Structural characterization of ulvan extracted from *Ulva clathrata* assisted by an ulvan lyase. *Carbohydrate Polymers,* 229, 115497.

Chiu, Y. H., Chan, Y. L., Li, T. L., & Wu, C. J. (2012). Inhibition of japanese encephalitis virus infection by the sulfated polysaccharide extracts from *Ulva lactuca*. *Marine Biotechnology,* 14(4), 468-478.

Cho, M., Yang, C., Kim, S. M., & You, S. (2010). Molecular characterization and biological activities of water-soluble sulfated polysaccharides from *Enteromorpha prolifera*. *Food Science and Biotechnology,* 19(2), 525-533.

Chualáin, F. N., Maggs, C. A., Saunders, G. W., & Guiry, M. D. (2004). The invasive genus *Asparagopsis* (bonnemaisoniaceae, rhodophyta): molecular systematics, morphology, and ecophysiology of *Falkenbergia* isolates. *Journal of Phycology,* 40(6), 1112-1126.

Ciancia, M., Fernández, P. V., & Leliaert, F. (2020). Diversity of sulfated polysaccharides from cell walls of coenocytic green algae and their structural relationships in view of green algal evolution. *Frontiers in Plant Science,* 11(1452).

Ciucanu, I., & Kerek, F. (1984). A simple and rapid method for the permethylation of carbohydrates. *Carbohydrate Research,* 131(2), 209-217.

Cluzet, S., Torregrosa, C., Jacquet, C., Lafitte, C., Fournier, J., Mercier, L.*, et al.* (2004). Gene expression profiling and protection of *Medicago truncatula* against a fungal infection in response to an elicitor from green algae *Ulva* spp. *Plant, Cell & Environment,* 27(7), 917-928.

Coat, G., Dion, P., Noailles, M. C., de Reviers, B., Fontaine, J. M., Berger-Perrot, Y.*, et al.* (1998). *Ulva armoricana* (Ulvales, Chlorophyta) from the coasts of Brittany (France). II. Nuclear rDNA ITS sequence analysis. *European Journal of Phycology,* 33(1), 81-86.

Coldebella, A., Gentelini, A. L., Piana, P. A., Coldebella, P. F., Boscolo, W. R., & Feiden, A. (2018). Effluents from Fish Farming Ponds: A View from the Perspective of Its Main Components. *Sustainability,* 10(1), 3.

Cole, A. J., Roberts, D. A., Garside, A. L., de Nys, R., & Paul, N. A. (2016). Seaweed compost for agricultural crop production. *Journal of Applied Phycology,* 28(1), 629-642.

Collén, P. N., Sassi, J. F., Rogniaux, H., Marfaing, H., & Helbert, W. (2011). Ulvan lyases isolated from the flavobacteria *Persicivirga ulvanivorans* are the first members of a new polysaccharide lyase family. *Journal of Biological Chemistry,* 286(49), 42063-42071.

Condaminet, B., Redziniak, G., Monsigny, M., & Kieda, C. (1997). Ultraviolet rays induced expression of lectins on the surface of a squamous carcinoma keratinocyte cell line. *Experimental Cell Research,* 232(2), 216-224.

Conrad, H. E. (1980). The acid lability of the glycosidic bonds of L-iduronic acid residues in glycosaminoglycans. *Biochemical Journal,* 191(2), 355-363.

Conrath, U., Beckers, G. J., Flors, V., Garcia-Agustin, P., Jakab, G., Mauch, F.*, et al.* (2006). Priming: Getting ready for battle. *Molecular Plant-Microbe Interactions,* 19(10), 1062-1071.

Costa, C., Alves, A., Pinto, P. R., Sousa, R. A., Borges da Silva, E. A., Reis, R. L.*, et al.* (2012). Characterization of ulvan extracts to assess the effect of different steps in the extraction procedure. *Carbohydrate Polymers,* 88(2), 537-546.

Craigie, J. S., Wen, Z. C., & van der Meer, J. P. (1984). Interspecific, intraspecific and nutritionally-determined variations in the composition of agars from *Gracilaria* spp. *Botanica Marina* (Vol. 27, p. 55).

Crawford, B. (2002). Seaweed farming: An alternative livelihood for small-scale fishers? University of Rhode Island: Coastal Resources Center.

Cui, J., Li, Y., Wang, S., Chi, Y., Hwang, H., & Wang, P. (2018). Directional preparation of anticoagulant-active sulfated polysaccharides from *Enteromorpha prolifera* using artificial neural networks. *Scientific Reports,* 8(1), 3062.

Cunha, L., & Grenha, A. (2016). Sulfated seaweed polysaccharides as multifunctional materials in drug delivery applications. *Marine Drugs,* 14(3).

Damonte, E. B., Matulewicz, M. C., & Cerezo, A. S. (2004). Sulfated seaweed polysaccharides as antiviral agents. *Current Medicinal Chemistry,* 11(18), 2399-2419.

de Araújo, I. W. F., Rodrigues, J. A. G., Quinderé, A. L. G., Silva, J. D. F. T., Maciel, G. D. F., Ribeiro, N. A*., et al.* (2016). Analgesic and anti-inflammatory actions on bradykinin route of a polysulfated fraction from alga *Ulva lactuca*. *International Journal of Biological Macromolecules,* 92, 820-830.

de Carvalho, M. M., de Freitas, R. A., Ducatti, D. R. B., Ferreira, L. G., Gonçalves, A. G., Colodi, F. G*., et al.* (2018). Modification of ulvans via periodate-chlorite oxidation: Chemical characterization and anticoagulant activity. *Carbohydrate Polymers,* 197, 631-640.

de Carvalho, M. M., Noseda, M. D., Dallagnol, J. C. C., Ferreira, L. G., Ducatti, D. R. B., Gonçalves, A. G*., et al.* (2020). Conformational analysis of ulvans from *Ulva fasciata* and their anticoagulant polycarboxylic derivatives. *International Journal of Biological Macromolecules,* 162, 599-608.

de Freitas, M. B., Ferreira, L. G., Hawerroth, C., Duarte, M. E. R., Noseda, M. D., & Stadnik, M. J. (2015). Ulvans induce resistance against plant pathogenic fungi independently of their sulfation degree. *Carbohydrate Polymers,* 133, 384-390.

de Freitas, M. B., & Stadnik, M. J. (2012). Race-specific and ulvan-induced defense responses in bean (*Phaseolus vulgaris*) against *Colletotrichum lindemuthianum*. *Physiological and Molecular Plant Pathology,* 78, 8-13.

de Paula Silva, P. H., McBride, S., de Nys, R., & Paul, N. A. (2008). Integrating filamentous 'green tide' algae into tropical pond-based aquaculture. *Aquaculture,* 284(1), 74-80.

de Reviers, B., & Leproux, A. (1993). Characterization of polysaccharides from *Enteromorpha intestinalis* (L.) link, chlorophyta. *Carbohydrate Polymers,* 22(4), 253-259.

de Ruiter, G. A., Schols, H. A., Voragen, A. G. J., & Rombouts, F. M. (1992). Carbohydrate analysis of water-soluble uronic acid-containing polysaccharides with high-performance anion-exchange chromatography using methanolysis combined with TFA hydrolysis is superior to four other methods. *Analytical Biochemistry,* 207(1), 176-185.

del Rocío Quezada-Rodríguez, P., & Fajer-Ávila, E. J. (2017). The dietary effect of ulvan from *Ulva clathrata* on hematological-immunological parameters and growth of tilapia (*Oreochromis niloticus*). *Journal of Applied Phycology,* 29(1), 423-431.

Delgado, D. Z., de Freitas, M. B., & Stadnik, M. J. (2013). Effectiveness of saccharin and ulvan as resistance inducers against rust and angular leaf spot in bean plants (*Phaseolus vulgaris*). *Crop Protection,* 47, 67-73.

Devaki, T., Sathivel, A., & BalajiRaghavendran, H. R. (2009). Stabilization of mitochondrial and microsomal function by polysaccharide of *Ulva lactuca* on D-Galactosamine induced hepatitis in rats. *Chemico-Biological Interactions,* 177(2), 83-88.

Doares, S. H., Albersheim, P., & Darvill, A. G. (1991). An improved method for the preparation of standards for glycosyl-linkage analysis of complex carbohydrates. *Carbohydrate Research,* 210, 311-317.

Duus, J. Ø., Gotfredsen, C. H., & Bock, K. (2000). Carbohydrate structural determination by NMR spectroscopy: Modern methods and limitations. *Chemical Reviews,* 100(12), 4589-4614.

El Modafar, C., Elgadda, M., El Boutachfaiti, R., Abouraicha, E., Zehhar, N., Petit, E.*, et al.* (2012). Induction of natural defence accompanied by salicylic acid-dependant systemic acquired resistance in tomato seedlings in response to bioelicitors isolated from green algae. *Scientia Horticulturae,* 138, 55-63.

Evans, F. D., & Critchley, A. T. (2014). Seaweeds for animal production use. *Journal of Applied Phycology,* 26(2), 891-899.

Faggio, C., Pagano, M., Dottore, A., Genovese, G., & Morabito, M. (2016). Evaluation of anticoagulant activity of two algal polysaccharides. *Natural Product Research,* 30(17), 1934-1937.

FAO. (2020). *The State of World Fisheries and Aquaculture 2020*. Rome.

Farias, E., Pomin, V., Valente, A., Nader, H., Rocha, H., & Mourão, P. (2008). A preponderantly 4-sulfated, 3-linked galactan from the green alga *Codium isthmocladum*. *Glycobiology,* 18, 250-259.

Faury, G., Ruszova, E., Molinari, J., Mariko, B., Raveaud, S., Velebny, V.*, et al.* (2008). The α-L-Rhamnose recognizing lectin site of human dermal fibroblasts functions as a signal transducer: Modulation of Ca^{2+} fluxes and gene expression. *Biochimica et Biophysica Acta,* 1780(12), 1388-1394.

Fernández-Díaz, C., Coste, O., & Malta, E. J. (2017). Polymer chitosan nanoparticles functionalized with *Ulva ohnoi* extracts boost in vitro ulvan immunostimulant effect in *Solea senegalensis* macrophages. *Algal Research,* 26, 135-142.

Forman, H. J., Davies, K. J., & Ursini, F. (2014). How do nutritional antioxidants really work: Nucleophilic tone and para-hormesis versus free radical scavenging in vivo. *Free Radical Biology & Medicine,* 66, 24-35.

Franchimont, D., Martens, H., Hagelstein, M. T., Louis, E., Dewe, W., Chrousos, G. P.*, et al.* (1999). Tumor necrosis factor alpha decreases, and interleukin-10 increases, the sensitivity of human monocytes to dexamethasone: potential regulation of the glucocorticoid receptor. *Journal of Clinical Endocrinology Metabolism,* 84(8), 2834-2839.

Fransson, L.-A. (1985). *Mammalian Glycosaminoglycans*. In G. O. Aspinall (Ed.), *The Polysaccharides* (pp. 338-415). New York: Academic Press

Fransson, L. A., Roden, L., & Spach, M. L. (1968). Automated ion-exchange chromatography of uronic acids and uronic acid containing oligosaccharides. *Analytical Biochemistry,* 23(2), 317-330.

Fumanal, M., Di Zeo, D. E., Anguís, V., Fernández-Diaz, C., Alarcón, F. J., Piñera, R.*, et al.* (2020). Inclusion of dietary *Ulva ohnoi* 5% modulates *Solea senegalensis* immune response during *Photobacterium damselae* subsp. *piscicida* infection. *Fish and Shellfish Immunology,* 100, 186-197.

Gadenne, V., Lebrun, L., Jouenne, T., & Thebault, P. (2013). Antiadhesive activity of ulvan polysaccharides covalently immobilized onto titanium surface. *Colloids and Surfaces B: Biointerfaces,* 112, 229-236.

Gadenne, V., Lebrun, L., Jouenne, T., & Thebault, P. (2015). Role of molecular properties of ulvans on their ability to elaborate antiadhesive surfaces. *Journal of Biomedical Materials Research Part A,* 103(3), 1021-1028.

Gajaria, T. K., Bhatt, H., Khandelwal, A., Vasu, V. T., Reddy, C. R. K., & Shanthana Lakshmi, D. (2020). A facile chemical cross-linking approach toward the fabrication of a sustainable porous ulvan scaffold. *Journal of Bioactive and Compatible Polymers,* 35(4-5), 301-313.

Gajaria, T. K., Suthar, P., Baghel, R. S., Balar, N. B., Sharnagat, P., Mantri, V. A.*, et al.* (2017). Integration of protein extraction with a stream of byproducts from marine macroalgae: A model forms the basis for marine bioeconomy. *Bioresource Technology,* 243, 867-873.

García-Poza, S., Leandro, A., Cotas, C., Cotas, J., Marques, J. C., Pereira, L.*, et al.* (2020). The evolution road of seaweed aquaculture: Cultivation technologies and the industry 4.0. *International Journal of Environmental Research and Public Health,* 17(18), 1-42.

Gerhauser, C., Alt, A., Heiss, E., Gamal-Eldeen, A., Klimo, K., Knauft, J.*, et al.* (2002). Cancer chemopreventive activity of Xanthohumol, a natural product derived from hop. *Molecular Cancer Therapeutics,* 1(11), 959-969.

Gesquière, L., Loreau, N., Minnich, A., Davignon, J., & Blache, D. (1999). Oxidative stress leads to cholesterol accumulation in vascular smooth muscle cells. *Free Radical Biology and Medicine,* 27(1), 134-145.

Gewert, K., Svensson, U., Andersson, K., Holst, E., & Sundler, R. (1999). Dexamethasone differentially regulates cytokine transcription and translation in macrophages responding to bacteria or okadaic acid. *Cell Signal,* 11(9), 665-670.

Ghosh, P., Adhikari, U., Ghosal, P. K., Pujol, C. A., Carlucci, M. J., Damonte, E. B.*, et al.* (2004). In vitro anti-herpetic activity of sulfated polysaccharide fractions from *Caulerpa racemosa*. *Phytochemistry,* 65(23), 3151-3157.

Ghosh, T., Chattopadhyay, K., Marschall, M., Karmakar, P., Mandal, P., & Ray, B. (2009). Focus on antivirally active sulfated polysaccharides: from structure-activity analysis to clinical evaluation. *Glycobiology,* 19(1), 2-15.

Glasson, C. R. K., Donnet, L., Angell, A., Vucko, M. J., Lorbeer, A. J., Vamvounis, G.*, et al.* (2019). Multiple response optimisation of the aqueous extraction of high quality ulvan from *Ulva ohnoi*. *Bioresource Technology Reports,* 7.

Glasson, C. R. K., Sims, I. M., Carnachan, S. M., de Nys, R., & Magnusson, M. (2017). A cascading biorefinery process targeting sulfated polysaccharides (ulvan) from *Ulva ohnoi*. *Algal Research,* 27, 383-391.

Gong, Z., Zhou, W., Shen, H., Yang, Z., Wang, G., Zuo, Z.*, et al.* (2016). Co-fermentation of acetate and sugars facilitating microbial lipid production on acetate-rich biomass hydrolysates. *Bioresource Technology,* 207, 102-108.

Gonzalez-Rivero, M., Bozec, Y.-M., Chollett, I., Ferrari Legorreta, R., Schoenberg, C., & Mumby, P. (2016). Asymmetric competition prevents the outbreak of an opportunistic species after coral reef degradation. *Oecologia,* 181.

Gonzalez-Rivero, M., Ferrari Legorreta, R., Schoenberg, C., & Mumby, P. (2012). Impacts of macroalgal competition and parrotfish predation on the growth of a common bioeroding sponge. *Marine Ecology Progress Series,* 444, 133-142.

Gosselin, C. C., Holt, A., & Lowe, P. A. (1964). Polysaccharides of *Enteromorpha* species. *Journal of the Chemical Society (Resumed)*, 5877–5880.

Guerra-Rivas, G., Gomez-Gutierrez, C. M., Alarcon-Arteaga, G., Soria-Mercado, I. E., & Ayala-Sanchez, N. E. (2011). Screening for anticoagulant activity in marine algae from the Northwest Mexican Pacific coast. *Journal of Applied Phycology,* 23(3), 495-503.

Guiry, M. D., & Guiry, G. M. (2021). *AlgaeBase*. https://www.algaebase.org: National University of Ireland, Galway.

Hakomori, S. (1964). A rapid permethylation of glycolipid, and polysaccharide catalyzed by methylsulfinyl carbanion in dimethyl sulfoxide. *Journal of Biochemistry,* 55, 205-208.

Handel, T. M., Johnson, Z., Crown, S. E., Lau, E. K., & Proudfoot, A. E. (2005). Regulation of protein function by glycosaminoglycans--as exemplified by chemokines. *Annual Review of Biochemistry,* 74, 385-410.

Hans, N., Malik, A., & Naik, S. (2021). Antiviral activity of sulfated polysaccharides from marine algae and its application in combating COVID-19: Mini review. *Bioresource Technology Reports,* 13.

Hardouin, K., Bedoux, G., Burlot, A.-S., Donnay-Moreno, C., Bergé, J.-P., Nyvall-Collén, P.*, et al.* (2016). Enzyme-assisted extraction (EAE) for the production of antiviral and antioxidant extracts from the green seaweed *Ulva armoricana* (Ulvales, Ulvophyceae). *Algal Research,* 16, 233-239.

Harnedy, P. A., & FitzGerald, R. J. (2015). Extraction and enrichment of protein from red and green macroalgae. *Methods in Molecular Biology,* 1308, 103-108.

Harris, P. J., Henry, R. J., Blakeney, A. B., & Stone, B. A. (1984). An improved procedure for the methylation analysis of oligosaccharides and polysaccharides. *Carbohydrate Research,* 127(1), 59-73.

Hassan, S., El-Twab, S. A., Hetta, M., & Mahmoud, B. (2011). Improvement of lipid profile and antioxidant of hypercholesterolemic albino rats by polysaccharides extracted from the green alga *Ulva lactuca* Linnaeus. *Saudi Journal of Biological Sciences,* 18(4), 333-340.

Haug, A. (1976). The influence of borate and calcium on the gel formation of a sulfated polysaccharide from *Ulva lactuca*. *Acta chemica Scandinavica. Series B: Organic chemistry and biochemistry,* 30(6), 562-566.

Hayden, H. S., Blomster, J., Maggs, C. A., Silva, P. C., Stanhope, M. J., & Waaland, J. R. (2003). Linnaeus was right all along: *Ulva* and *Enteromorpha* are not distinct genera. *European Journal of Phycology,* 38(3), 277-294.

He, J., Xu, Y., Chen, H., & Sun, P. (2016). Extraction, structural characterization, and potential antioxidant activity of the polysaccharides from four seaweeds. *International Journal of Molecular Sciences,* 17(12).

Hernández-Garibay, E., Zertuche-González, J. A., & Pacheco-Ruíz, I. (2011). Isolation and chemical characterization of algal polysaccharides from the green seaweed *Ulva clathrata* (Roth) C. Agardh. *Journal of Applied Phycology,* 23(3), 537-542.

Hernandez-Herrera, R. M., Virgen-Calleros, G., Ruiz-Lopez, M., Zanudo-Hernandez, J., Delano-Frier, J. P., & Sanchez-Hernandez, C. (2014). Extracts from green and brown seaweeds protect tomato (*Solanum lycopersicum*) against the necrotrophic fungus *Alternaria solani*. *Journal of Applied Phycology,* 26(3), 1607-1614.

Hiraoka, M., Shimada, S., Uenosono, M., & Masuda, M. (2004). A new green-tide-forming alga, *Ulva ohnoi* Hiraoka et Shimada sp. nov. (Ulvales, Ulvophyceae) from Japan. *Phycological Research,* 52(1), 17-29.

Hoang, M. H., Kim, J.-Y., Lee, J. H., You, S., & Lee, S.-J. (2015). Antioxidative, hypolipidemic, and anti-inflammatory activities of sulfated polysaccharides from *Monostroma nitidum*. *Food Science and Biotechnology,* 24(1), 199-205.

Holdt, S. L., & Kraan, S. (2011). Bioactive compounds in seaweed: functional food applications and legislation. *Journal of Applied Phycology,* 23(3), 543-597.

Holzinger, A., Herburger, K., Kaplan, F., & Lewis, L. A. (2015). Desiccation tolerance in the chlorophyte green alga *Ulva compressa*: does cell wall architecture contribute to ecological success? *Planta,* 242(2), 477-492.

Hong, J. K., Bong, M. H., Park, J. C., Moon, H. K., Kim, D. W., Lee, S. C.*, et al.* (2011). Antioxidant and immunomodulatory effects of *Ulva pertusa* Kjellman on broiler chickens. *Journal of Animal Science and Technology,* 53(5), 419-428.

Hsieh, P.-H., Thieker, D. F., Guerrini, M., Woods, R. J., & Liu, J. (2016). Uncovering the Relationship between Sulphation Patterns and Conformation of Iduronic Acid in Heparan Sulphate. *Scientific Reports,* 6(1), 29602.

Hu, Z., Hong, P., Cheng, Y., Liao, M., & Li, S. (2018). Polysaccharides from *Enteromorpha tubulosa*: Optimization of extraction and cytotoxicity. *Journal of Food Processing and Preservation,* 42(1), e13373.

Hussein, U. K., Mahmoud, H. M., Farrag, A. G., & Bishayee, A. (2015). Chemoprevention of diethylnitrosamine-initiated and phenobarbital-promoted hepatocarcinogenesis in rats by sulfated polysaccharides and aqueous extract of *Ulva lactuca*. *Integrative Cancer Therapies,* 14(6), 525-545.

Jaulneau, V., Lafitte, C., Corio-Costet, M. F., Stadnik, M. J., Salamagne, S., Briand, X*., et al.* (2011). An *Ulva armoricana* extract protects plants against three powdery mildew pathogens. *European Journal of Plant Pathology,* 131(3), 393-401.

Jaulneau, V., Lafitte, C., Jacquet, C., Fournier, S., Salamagne, S., Briand, X*., et al.* (2010). Ulvan, a sulfated polysaccharide from green algae, activates plant immunity through the jasmonic acid signaling pathway. *Journal of Biomedicine and Biotechnology*, 11.

Jiao, G., Yu, G., Wang, W., Zhao, X., Zhang, J., & Ewart, S. H. (2012). Properties of polysaccharides in several seaweeds from Atlantic Canada and their potential anti-influenza viral activities. *Journal of Ocean University of China,* 11(2), 205-212.

Jiao, G., Yu, G., Zhang, J., & Ewart, H. S. (2011). Chemical structures and bioactivities of sulfated polysaccharides from marine algae. *Marine Drugs,* 9(2), 196-233.

Jiao, L. L., Jiang, P., Zhang, L. P., & Wu, M. J. (2010). Antitumor and immunomodulating activity of polysaccharides from *Enteromorpha intestinalis*. *Biotechnology and Bioprocess Engineering,* 15(3), 421-428.

Jiao, L. L., Li, X., Li, T. B., Jiang, P., Zhang, L. X., Wu, M. J*., et al.* (2009). Characterization and anti-tumor activity of alkali-extracted polysaccharide from *Enteromorpha intestinalis*. *International Immunopharmacology,* 9(3), 324-329.

Jin, W., He, X., Long, L., Fang, Q., Wei, B., Sun, J*., et al.* (2020). Structural characterization and anti-lung cancer activity of a sulfated glucurono-xylo-rhamnan from *Enteromorpha prolifera*. *Carbohydrate Polymers,* 237.

Jmel, M. A., Anders, N., Yahmed, N. B., Schmitz, C., Marzouki, M. N., Spiess, A*., et al.* (2017). Variations in physicochemical properties and bioconversion efficiency of *Ulva lactuca* polysaccharides after different biomass pretreatment techniques. *Applied Biochemistry and Biotechnology*, 1-17.

Jones, J. D. G., & Dangl, J. L. (2006). The plant immune system. *Nature,* 444, 323.

Jose, G. M., & Kurup, M. (2016). In vitro antioxidant properties of edible marine algae *Sargassum swartzii*, *Ulva fasciata* and *Chaetomorpha antennina* of Kerala coast. *Pharmaceutical Bioprocessing,* 4(6), 100-108.

Kaeffer, B., Benard, C., Lahaye, M., Blottiere, H. M., & Cherbut, C. (1999). Biological properties of ulvan, a new source of green seaweed sulfated polysaccharides, on cultured normal and cancerous colonic epithelial tells. *Planta Medica,* 65(6), 527-531.

Kanno, K., Tanigawa, T., Fujita, Y., Ohnaka, N., Kubo, Y., Yoshida, K*., et al.* (2014). Adsorbents for apheresis prepared from polysaccharides of algae that threaten ecosystem services. *Chemistry and Biodiversity,* 11(8), 1140-1150.

Khan, W., Rayirath, U. P., Subramanian, S., Jithesh, M. N., Rayorath, P., Hodges, D. M*., et al.* (2009). Seaweed Extracts as Biostimulants of Plant Growth and Development. *Journal of Plant Growth Regulation,* 28(4), 386-399.

Kidgell, J. T., Carnachan, S. M., Magnusson, M., Lawton, R. J., Sims, I. M., Hinkley, S. F. R*., et al.* (2021). Are all ulvans equal? A comparative assessment of the chemical and gelling properties of ulvan from blade and filamentous *Ulva*. *Carbohydrate Polymers,* 264, 118010.

Kidgell, J. T., Glasson, C. R. K., Magnusson, M., Vamvounis, G., Sims, I. M., Carnachan, S. M., *et al.* (2020). The molecular weight of ulvan affects the in vitro inflammatory response of a murine macrophage. *International Journal of Biological Macromolecules,* 150, 839-848.

Kidgell, J. T., Magnusson, M., de Nys, R., & Glasson, C. R. K. (2019). Ulvan: A systematic review of extraction, composition and function. *Algal Research,* 39, 101422.

Kim, J.-K., Cho, M. L., Karnjanapratum, S., Shin, I.-S., & You, S. G. (2011). In vitro and in vivo immunomodulatory activity of sulfated polysaccharides from *Enteromorpha prolifera*. *International Journal of Biological Macromolecules,* 49(5), 1051-1058.

Kinley, R. D., Martinez-Fernandez, G., Matthews, M. K., de Nys, R., Magnusson, M., & Tomkins, N. W. (2020). Mitigating the carbon footprint and improving productivity of ruminant livestock agriculture using a red seaweed. *Journal of Cleaner Production,* 259.

Kloareg, B., & Quatrano, R. (1988). Structure of the cell walls of marine algae and ecophysiological functions of the matrix polysaccharides. *Oceanography and Marine Biology,* 26, 259-315.

Klongklaew, N., Praiboon, J., Tamtin, M., & Srisapoome, P. (2021). Chemical composition of a hot water crude extract (HWCE) from *Ulva intestinalis* and its potential effects on growth performance, immune responses, and resistance to white spot syndrome virus and yellowhead virus in Pacific white shrimp (*Litopenaeus vannamei*). *Fish and Shellfish Immunology,* 112, 8-22.

Kong, F., Mao, Y., Cui, F., Zhang, X., & Gao, Z. (2011). Morphology and molecular identification of *Ulva* forming green tides in Qingdao, China. *Journal of Ocean University of China,* 10(1), 73-79.

Kong, Q., Dong, S. Y., Gao, J., & Jiang, C. Y. (2016). In vitro fermentation of sulfated polysaccharides from *E. prolifera* and *L. japonica* by human fecal microbiota. *International Journal of Biological Macromolecules,* 91, 867-871.

Kopel, M., Helbert, W., Belnik, Y., Buravenkov, V., Herman, A., & Banin, E. (2016). New family of ulvan lyases identified in three isolates from the alteromonadales order. *Journal of Biological Chemistry,* 291(11), 5871-5878.

Kostanski, L. K., Keller, D. M., & Hamielec, A. E. (2004). Size-exclusion chromatography—a review of calibration methodologies. *Journal of Biochemical and Biophysical Methods,* 58(2), 159-186.

Kraan, S. (2013). Mass-cultivation of carbohydrate rich macroalgae, a possible solution for sustainable biofuel production. *Mitigation and Adaptation Strategies for Global Change,* 18(1), 27-46.

Kulshreshtha, G., Rathgeber, B., MacIsaac, J., Boulianne, M., Brigitte, L., Stratton, G., *et al.* (2017). Feed supplementation with red seaweeds, *Chondrus crispus* and *Sarcodiotheca gaudichaudii*, reduce *Salmonella enteritidis* in laying hens. *Frontiers in Microbiology,* 8(567).

Kumar, S. A., Magnusson, M., Ward, L. C., Paul, N. A., & Brown, L. (2015). Seaweed supplements normalise metabolic, cardiovascular and liver responses in high-carbohydrate, high-fat fed rats. *Marine Drugs,* 13(2), 788-805.

Lahaye, M. (1998). NMR spectroscopic characterisation of oligosaccharides from two *Ulva rigida* ulvan samples (Ulvales, Chlorophyta) degraded by a lyase. *Carbohydrate Research,* 314(1-2), 1-12.

Lahaye, M., & Axelos, M. A. V. (1993). Gelling properties of water-soluble polysaccharides from proliferating marine green seaweeds (*Ulva* spp.). *Carbohydrate Polymers,* 22(4), 261-265.

Lahaye, M., Brunel, M., & Bonnin, E. (1997). Fine chemical structure analysis of oligosaccharides produced by an ulvan-lyase degradation of the water-soluble cell-wall polysaccharides from *Ulva* sp. (Ulvales, Chlorophyta). *Carbohydrate Research,* 304(3-4), 325-333.

Lahaye, M., Cimadevilla, E. A. C., Kuhlenkamp, R., Quemener, B., Lognoné, V., & Dion, P. (1999). Chemical composition and 13C NMR spectroscopic characterisation of ulvans from *Ulva* (Ulvales, Chlorophyta). *Journal of Applied Phycology,* 11(1), 1-7.

Lahaye, M., Gomez-Pinchetti, J.-L., del Rio, M. J., & Garcia-Reina, G. (1995). Natural decoloration, composition and increase in dietary fibre content of an edible marine algae, *Ulva rigida* (Chlorophyta), grown under different nitrogen conditions. *Journal of the Science of Food and Agriculture,* 68(1), 99-104.

Lahaye, M., Inizan, F., & Vigouroux, J. (1998). NMR analysis of the chemical structure of ulvan and of ulvan-boron complex formation. *Carbohydrate Polymers,* 36(2-3), 239-249.

Lahaye, M., & Jegou, D. (1993). Chemical and physical-chemical characteristics of dietary fibres from *Ulva lactuca* (L.) Thuret and *Enteromorpha compressa* (L.) Grev. *Journal of Applied Phycology,* 5(2), 195.

Lahaye, M., & Kaeffer, B. (1997). Seaweed dietary fibres: structure, physico-chemical and biological properties relevant to intestinal physiology. *Sciences Des Aliments,* 17(6), 563-584.

Lahaye, M., & Ray, B. (1996). Cell-wall polysaccharides from the marine green alga *Ulva* "*rigida*" (Ulvales, Chlorophyta) - NMR analysis of ulvan oligosaccharides. *Carbohydrate Research,* 283, 161-173.

Lahaye, M., Ray, B., Baumberger, S., Quemener, B., & Axelos, M. A. V. (1996). Chemical characterisation and gelling properties of cell wall polysaccharides from species of *Ulva* (Ulvales, Chlorophyta). *Hydrobiologia,* 326(1), 473-480.

Lahaye, M., & Robic, A. (2007). Structure and functional properties of ulvan, a polysaccharide from green seaweeds. *Biomacromolecules,* 8(6), 1765-1774.

Lai, M. f., Li, C. F., & Li, C. y. (1994). Characterization and thermal behavior of six sulphated polysaccharides from seaweeds. *Topics in Catalysis,* 8(3-4), 215-232.

Lakshmi, D. S., Sankaranarayanan, S., Gajaria, T. K., Li, G., Kujawski, W., Kujawa, J.*, et al.* (2020). A short review on the valorization of green seaweeds and ulvan: Feedstock for chemicals and biomaterials. *Biomolecules,* 10(7), 1-20.

Largo, D. B., Sembrano, J., Hiraoka, M., & Ohno, M. (2004). Taxonomic and ecological profile of 'green tide' species of *Ulva* (Ulvales, Chlorophyta) in central Philippines. *Hydrobiologia,* 512(1-3), 247-253.

Lawton, R. J., Mata, L., de Nys, R., & Paul, N. A. (2013). Algal bioremediation of waste waters from land-based aquaculture using ulva: selecting target species and strains. *PLOS ONE,* 8(10), e77344.

Lawton, R. J., Sutherland, J. E., Glasson, C. R. K., & Magnusson, M. (Under review). Selection of temperate *Ulva* species and strains for land-based cultivation and biomass applications. *Algal Research*.

Lee, C. H., Olson, P., & Evans, R. M. (2003). Minireview: lipid metabolism, metabolic diseases, and peroxisome proliferator-activated receptors. *Endocrinology,* 144(6), 2201-2207.

Lee, J. B., Hayashi, K., Maeda, M., & Hayashi, T. (2004). Antiherpetic activities of sulfated polysaccharides from green algae. *Planta Medica,* 70(9), 813-817.

Lei, X. G., Zhu, J. H., Cheng, W. H., Bao, Y., Ho, Y. S., Reddi, A. R.*, et al.* (2016). Paradoxical roles of antioxidant enzymes: Basic mechanisms and health implications. *Physiological Reviews,* 96(1), 307-364.

Leiro, J. M., Castro, R., Arranz, J. A., & Lamas, J. (2007). Immunomodulating activities of acidic sulphated polysaccharides obtained from the seaweed *Ulva rigida* C. Agardh. *International Immunopharmacology,* 7(7), 879-888.

Leiro, J. M., Varela, M., Piazzon, M. C., Arranz, J. A., Noya, M., & Lamas, J. (2010). The anti-inflammatory activity of the polyphenol resveratrol may be partially related to inhibition of tumour necrosis factor-α (TNF-α) pre-mRNA splicing. *Molecular Immunology,* 47(5), 1114-1120.

Li, B., Liu, S., Xing, R., Li, K. C., Li, R. F., Qin, Y. K.*, et al.* (2013). Degradation of sulfated polysaccharides from *Enteromorpha prolifera* and their antioxidant activities. *Carbohydrate Polymers,* 92(2), 1991-1996.

Li, B., Lu, F., Wei, X., & Zhao, R. (2008). Fucoidan: structure and bioactivity. *Molecules,* 13(8), 1671-1695.

Li, J., Jiang, F., Chi, Z., Han, D., Yu, L., & Liu, C. (2018a). Development of *Enteromorpha prolifera* polysaccharide-based nanoparticles for delivery of curcumin to cancer cells. *International Journal of Biological Macromolecules,* 112, 413-421.

Li, J. X., Chi, Z., Yu, L. J., Jiang, F., & Liu, C. G. (2017). Sulfated modification, characterization, and antioxidant and moisture absorption/retention activities of a soluble neutral polysaccharide from *Enteromorpha prolifera*. *International Journal of Biological Macromolecules,* 105, 1544-1553.

Li, Q., Luo, J., Wang, C., Tai, W., Wang, H., Zhang, X.*, et al.* (2018b). Ulvan extracted from green seaweeds as new natural additives in diets for laying hens. *Journal of Applied Phycology,* 30(3), 2017-2027.

Li, W., Jiang, N., Li, B., Wan, M., Chang, X., Liu, H.*, et al.* (2018c). Antioxidant activity of purified ulvan in hyperlipidemic mice. *International Journal of Biological Macromolecules,* 113, 971-975.

Li, W., Wang, K., Jiang, N., Liu, X., Wan, M., Chang, X.*, et al.* (2018d). Antioxidant and antihyperlipidemic activities of purified polysaccharides from *Ulva pertusa*. *Journal of Applied Phycology,* 30(4), 2619-2627.

Lin, W. T., Wang, W. X., Liao, D. D., Chen, D. M., Zhu, P. P., Cai, G. X.*, et al.* (2015). Polysaccharides from *Enteromorpha prolifera* improve glucose metabolism in diabetic rats. *Journal of Diabetes Research,* 2015, 1-12.

Lloyd, A. G., Dodgson, K. S., Price, R. G., & Rose, F. A. (1961). I. Polysaccharide sulphates. *Biochimica et Biophysica Acta,* 46(1), 108-115.

Long, A. T., Kenne, E., Jung, R., Fuchs, T. A., & Renné, T. (2016). Contact system revisited: an interface between inflammation, coagulation, and innate immunity. *Journal of Thrombosis and Haemostasis,* 14(3), 427-437.

Lopes, N., Ray, S., Espada, S. F., Bomfim, W. A., Ray, B., Faccin-Galhardi, L. C.*, et al.* (2017). Green seaweed *Enteromorpha compressa* (Chlorophyta, Ulvaceae) derived sulphated polysaccharides inhibit *herpes simplex* virus. *International Journal of Biological Macromolecules,* 102, 605-612.

López-Pedrouso, M., Lorenzo, J. M., Cantalapiedra, J., Zapata, C., Franco, J. M., & Franco, D. (2020). Aquaculture and by-products: Challenges and opportunities in the use of alternative protein sources and bioactive compounds. (Vol. 92, pp. 127-185).

Lowry, O. H., Rosebrough, N. J., Farr, A. L., & Randall, R. J. (1951). Protein measurement with the Folin phenol reagent. *Journal of Biological Chemistry,* 193(1), 265-275.

Luiten, C., Sargison, L., Daines, A. M., Carnachan, S. M., Kidgell, J. T., Hinkley, S. F. R.*, et al.* (Under review). Structural characterisation of ulvans extracted from blade (*Ulva ohnoi*) and filamentous (*Ulva tepida* and *Ulva prolifera*) species of *Ulva*.

Magnusson, M., Carl, C., Mata, L., de Nys, R., & Paul, N. A. (2016). Seaweed salt from *Ulva*: A novel first step in a cascading biorefinery model. *Algal Research,* 16, 308-316.

Mahmoud, H. M., Hussein, U. L., & Hussein, U. L. (2014). Suppression of N-nitrosodiethylamine induced oxidative renal toxicity by sulphated polysaccharide and aqueous extract of *Ulva lactuca* in rats. *International Journal of Pharmacy and Pharmaceutical Sciences,* 6(11), 248-253.

Mao, W., Zang, X., Li, Y., & Zhang, H. (2006). Sulfated polysaccharides from marine green algae *Ulva conglobata* and their anticoagulant activity. *Journal of Applied Phycology,* 18(1), 9-14.

Mata, L., Magnusson, M., Paul, N. A., & de Nys, R. (2016). The intensive land-based production of the green seaweeds *Derbesia tenuissima* and *Ulva ohnoi*: biomass and bioproducts. *Journal of Applied Phycology,* 28(1), 365-375.

Matloub, A. A., Aglan, H. A., Mohamed El Souda, S. S., Aboutabl, M. E., Maghraby, A. S., & Ahmed, H. H. (2016). Influence of bioactive sulfated polysaccharide-protein complexes on hepatocarcinogenesis, angiogenesis and immunomodulatory activities. *Asian Pacific Journal of Tropical Medicine,* 9(12), 1200-1211.

Matloub, A. A., Elsouda, S. S. M., El-Senousy, W. M., Hamed, M., Aly, H., Ali, S. A*., et al.* (2015). In vitro antiviral, cytotoxic, antioxidant and hypolipidemic activites of polysaccharide isolated from marine algae. *International Journal of Pharmacognosy and Phytochemical Research,* 7(5), 1099-1111.

Matloub, A. A., Salama, A. H., Aglan, H. A., AbouSamra, M. M., ElSouda, S. S. M., & Ahmed, H. H. (2018). Exploiting bilosomes for delivering bioactive polysaccharide isolated from *Enteromorpha intestinalis* for hacking hepatocellular carcinoma. *Drug Development and Industrial Pharmacy,* 44(4), 523-534.

McCook, L., Jompa, J., & Diaz-Pulido, G. (2001). Competition between corals and algae on coral reefs: a review of evidence and mechanisms. *Coral Reefs,* 19(4), 400-417.

McHugh, D. J. (2003). A guide to the seaweed industry. *FAO Fisheries Technical Paper. No. 441.* (p. 105). Rome: FAO.

McKinnell, J. P., & Percival, E. (1962a). The acid polysaccharide from the Green Seaweed, *Ulva lactuca*. *Journal of the Chemical Society (Resumed)*(0), 2082-2084.

McKinnell, J. P., & Percival, E. (1962b). Structural investigations on the water-soluble polysaccharide of the green seaweed *Enteromorpha compressa*. *Journal of the Chemical Society (Resumed)*, 3141-3148.

Medcalf, D. G., Lionel, T., Brannon, J. H., & Scott, J. R. (1975). Seasonal variation in the mucilaginous polysaccharides from *Ulva lactuca*. *Botanica Marina,* 18(2), 67-70.

Miao, L., & St Clair, D. K. (2009). Regulation of superoxide dismutase genes: implications in disease. *Free Radical Biology & Medicine,* 47(4), 344-356.

Miller, I. J., & Blunt, J. W. (1998). Desulfation of algal galactans. *Carbohydrate Research,* 309(1), 39-43.

Moghazy, R. M., Labena, A., Husien, S., Mansor, E. S., & Abdelhamid, A. E. (2020). Neoteric approach for efficient eco-friendly dye removal and recovery using algal-polymer biosorbent sheets: Characterization, factorial design, equilibrium and kinetics. *International Journal of Biological Macromolecules,* 157, 494-509.

Mohamed, S., Hashim, S. N., & Rahman, H. A. (2012). Seaweeds: A sustainable functional food for complementary and alternative therapy. *Trends in Food Science & Technology,* 23(2), 83-96.

Moher, D., Liberati, A., Tetzlaff, J., & Altman, D. G. (2009). Preferred reporting items for systematic reviews and meta-analyses: the PRISMA statement. *Ann Intern Med,* 151(4), 264-269, w264.

Moon, H. C., Choi, H., Kikionis, S., Seo, J., Youn, W., Ioannou, E*., et al.* (2020). Fabrication and characterization of neurocompatible ulvan-based layer-by-layer films. *Langmuir,* 36(39), 11610-11617.

Moon, T. S., Yoon, S.-H., Tsang Mui Ching, M.-J., Lanza, A. M., & Prather, K. L. J. (2009). Enzymatic assay of D-glucuronate using uronate dehydrogenase. *Analytical Biochemistry,* 392(2), 183-185.

Morán-Santibañez, K., Cruz-Suárez, L. E., Ricque-Marie, D., Robledo, D., Freile-Pelegrín, Y., Peña-Hernández, M. A.*, et al.* (2016). Synergistic effects of sulfated polysaccharides from Mexican seaweeds against measles virus. *BioMed Research International,* 2016.

Morelli, A., Betti, M., Puppi, D., Bartoli, C., Gazzarri, M., & Chiellini, F. (2016a). Enzymatically crosslinked ulvan hydrogels as injectable systems for cell delivery. *Macromolecular Chemistry and Physics,* 217(4), 581-590.

Morelli, A., Betti, M., Puppi, D., & Chiellini, F. (2016b). Design, preparation and characterization of ulvan based thermosensitive hydrogels. *Carbohydrate Polymers,* 136, 1108-1117.

Moynagh, P. N. (2003). Toll-like receptor signalling pathways as key targets for mediating the anti-inflammatory and immunosuppressive effects of glucocorticoids. *Journal of Endocrinology,* 179(2), 139-144.

Nagasawa, K., Inoue, Y., & Kamata, T. (1977). Solvolytic desulfation of glycosaminoglycuronan sulfates with dimethyl sulfoxide containing water or methanol. *Carbohydrate Research,* 58(1), 47-55.

Nagasawa, K., Inoue, Y., & Tokuyasu, T. (1979). An improved method for the preparation of chondroitin by solvolytic desulfation of chondroitin sulfates. *Journal of Biochemistry,* 86(5), 1323-1329.

Naidoo, K., Maneveldt, G., Ruck, K., & Bolton, J. J. (2007). A comparison of various seaweed-based diets and formulated feed on growth rate of abalone in a land-based aquaculture system. (pp. 211-217). Dordrecht: Springer Netherlands.

Nardelli, A. E., Chiozzini, V. G., Braga, E. S., & Chow, F. (2019). Integrated multi-trophic farming system between the green seaweed *Ulva lactuca*, mussel, and fish: a production and bioremediation solution. *Journal of Applied Phycology,* 31, 847-856.

Nep, E. I., Carnachan, S. M., Ngwuluka, N. C., Kontogiorgos, V., Morris, G. A., Sims, I. M.*, et al.* (2016). Structural characterisation and rheological properties of a polysaccharide from sesame leaves (*Sesamum radiatum* Schumach. & Thonn.). *Carbohydrate Polymers,* 152, 541-547.

Neveux, N., Yuen, A. K. L., Jazrawi, C., Magnusson, M., Haynes, B. S., Masters, A. F.*, et al.* (2014). Biocrude yield and productivity from the hydrothermal liquefaction of marine and freshwater green macroalgae. *Bioresource Technology,* 155, 334-341.

Nimse, S. B., & Pal, D. (2015). Free radicals, natural antioxidants, and their reaction mechanisms. *RSC Advances,* 5(35), 27986-28006.

Ogawa, K., Yamaura, M., & Maruyama, I. (1997). Isolation and identification of 2-*O*-methyl-L-rhamnose and 3-*O*-methyl-L-rhamnose as constituents of an acidic polysaccharide of *Chlorella vulgaris*. *Bioscience, Biotechnology, and Biochemistry,* 61(3), 539-540.

Ohno, M. (1993). *Cultivation of the green algae Monostroma and Enteromorpha "Aonori"*. In M. Ohno & A. T. Critchley (Eds.), *Seaweed cultivation and marine ranching* (pp. 7-16). Jokocuka: Japan International Cooperation Agency

Olsson, J., Raikova, S., Mayers, J. J., Steinhagen, S., Chuck, C. J., Nylund, G. M.*, et al.* (2020a). Effects of geographical location on potentially valuable components in *Ulva intestinalis* sampled along the Swedish coast. *Applied Phycology,* 1(1), 80-92.

Olsson, J., Toth, G. B., Oerbekke, A., Cvijetinovic, S., Wahlström, N., Harrysson, H., *et al.* (2020b). Cultivation conditions affect the monosaccharide composition in *Ulva fenestrata*. *Journal of Applied Phycology*.

Onda, A., Onda, S., Koike, M., Yanagisawa, K., Tsubaki, S., & Hiraoka, M. (2017). Catalytic hydrolysis of polysaccharides derived from fast-growing green macroalgae. *ChemCatChem,* 9(14), 2638-2641.

Padmanaban, V. C., Prashant, K. P., Ranjith, M. V., Aswani, T., & Aswani, M. T. (2013). Comparative analysis of anti-coagulant potential of marine macro algae. *International Journal of Pharmacy and Pharmaceutical Sciences,* 5(SUPPL.1), 334-337.

Pankiewicz, R., Łęska, B., Messyasz, B., Fabrowska, J., Sołoducha, M., & Pikosz, M. (2016). First isolation of polysaccharidic ulvans from the cell walls of freshwater algae. *Algal Research,* 19, 348-354.

Paradossi, G., Cavalieri, F., & Chiessi, E. (2002). A conformational study on the algal polysaccharide ulvan. *Macromolecules,* 35(16), 6404-6411.

Paradossi, G., Cavalieri, F., Pizzoferrato, L., & Liquori, A. M. (1999). A physico-chemical study on the polysaccharide ulvan from hot water extraction of the macroalga *Ulva*. *International Journal of Biological Macromolecules,* 25(4), 309-315.

Patankar, M. S., Oehninger, S., Barnett, T., Williams, R. L., & Clark, G. F. (1993). A revised structure for fucoidan may explain some of its biological activities. *Journal of Biological Chemistry,* 268(29), 21770-21776.

Paulert, R., Ebbinghaus, D., Urlass, C., & Moerschbacher, B. M. (2010). Priming of the oxidative burst in rice and wheat cell cultures by ulvan, a polysaccharide from green macroalgae, and enhanced resistance against powdery mildew in wheat and barley plants. *Plant Pathology,* 59(4), 634-642.

Paulert, R., Talamini, V., Cassolato, J. E. F., Duarte, M. E. R., Noseda, M. D., Smania, A., *et al.* (2009). Effects of sulfated polysaccharide and alcoholic extracts from green seaweed *Ulva fasciata* on anthracnose severity and growth of common bean (*Phaseolus vulgaris* L.). *Journal of Plant Diseases and Protection,* 116(6), 263-270.

Peasura, N., Laohakunjit, N., Kerdchoechuen, O., Vongsawasdi, P., & Chao, L. K. (2016). Assessment of biochemical and immunomodulatory activity of sulphated polysaccharides from *Ulva intestinalis*. *International Journal of Biological Macromolecules,* 91, 269-277.

Peasura, N., Laohakunjit, N., Kerdchoechuen, O., & Wanlapa, S. (2015). Characteristics and antioxidant of *Ulva intestinalis* sulphated polysaccharides extracted with different solvents. *International Journal of Biological Macromolecules,* 81, 912-919.

Pedersen, M. F., & Borum, J. (1997). Nutrient control of estuarine macroalgae: growth strategy and the balance between nitrogen requirements and uptake. *Marine Ecology Progress Series,* 161, 155-163.

Pengzhan, Y., Ning, L., Xiguang, L., Gefei, Z., Quanbin, Z., & Pengcheng, L. (2003a). Antihyperlipidemic effects of different molecular weight sulfated polysaccharides from *Ulva pertusa* (Chlorophyta). *Pharmacological Research,* 48(6), 543-549.

Pengzhan, Y., Quanbin, Z., Hong, Z., Xizhen, N., & Zhien, L. (2004). Preparation of polysaccharides in different molecular weights from *Ulva pertusa* Kjellm (Chorophyta). *Chinese Journal of Oceanology and Limnology,* 22(4), 381-385.

Pengzhan, Y., Quanbin, Z., Ning, L., Zuhong, X., Yanmei, W., & Zhi'en, L. (2003b). Polysaccharides from *Ulva pertusa* (Chlorophyta) and preliminary studies on their antihyperlipidemia activity. *Journal of Applied Phycology,* 15(1), 21-27.

Percival, E. (1979). The polysaccharides of green, red and brown seaweeds: Their basic structure, biosynthesis and function. *British Phycological Journal,* 14(2), 103-117.

Percival, E., & McDowell, R. H. (1967). *Chemistry and enzymology of marine algal polysaccharides*. London: Academic Press.

Percival, E., & Wold, J. K. (1963). The acid polysaccharide from the green seaweed *Ulva lactuca*. Part II. The site of the ester sulphate. *Journal of the Chemical Society (Resumed)*, 5459.

Pettolino, F. A., Walsh, C., Fincher, G. B., & Bacic, A. (2012). Determining the polysaccharide composition of plant cell walls. *Nature Protocols,* 7(9), 1590-1607.

Pezoa-Conte, R., Leyton, A., Baccini, A., Ravanal, M. C., Mäki-Arvela, P., Grénman, H*., et al.* (2017). Aqueous extraction of the sulfated polysaccharide ulvan from the green alga *Ulva rigida* - kinetics and modeling. *Bioenergy Research,* 10(3), 915-928.

Phull, A. R., & Kim, S. J. (2017). Fucoidan as bio-functional molecule: Insights into the anti-inflammatory potential and associated molecular mechanisms. *Journal of Functional Foods,* 38, 415-426.

Pieterse, C. M., Leon-Reyes, A., Van der Ent, S., & Van Wees, S. C. (2009). Networking by small-molecule hormones in plant immunity. *Nature Chemical Biology,* 5(5), 308-316.

Pittner, F., & Turecek, P. L. (1987). The application of immobilized α-L-rhamnosidase and L-rhamnosedehydrogenase in the analysis of L-rhamnose and α-L-rhamnosides. *Applied Biochemistry and Biotechnology,* 16(1), 15-24.

Ponce, M., Zuasti, E., Anguís, V., & Fernández-Díaz, C. (2020). Effects of the sulfated polysaccharide ulvan from *Ulva ohnoi* on the modulation of the immune response in Senegalese sole (Solea senegalensis). *Fish and Shellfish Immunology,* 100, 27-40.

Popper, Z. A., Michel, G., Hervé, C., Domozych, D. S., Willats, W. G. T., Tuohy, M. G*., et al.* (2011). Evolution and diversity of plant cell walls: From algae to flowering plants. *Annual Review of Plant Biology,* 62(1), 567-590.

Pratap, K., Taki, A. C., Johnston, E. B., Lopata, A. L., & Kamath, S. D. (2020). A comprehensive review on natural bioactive compounds and probiotics as potential therapeutics in food allergy treatment. *Frontiers in Immunology,* 11.

Qi, H., Huang, L., Liu, X., Liu, D., Zhang, Q., & Liu, S. (2012a). Antihyperlipidemic activity of high sulfate content derivative of polysaccharide extracted from *Ulva pertusa* (Chlorophyta). *Carbohydrate Polymers,* 87(2), 1637-1640.

Qi, H., Liu, X., Wang, K., Liu, D., Huang, L., Liu, S*., et al.* (2013a). Subchronic toxicity study of ulvan from *Ulva pertusa* (Chlorophyta) in Wistar rats. *Food and Chemical Toxicology,* 62, 573-578.

Qi, H., & Sheng, J. (2015). The antihyperlipidemic mechanism of high sulfate content ulvan in rats. *Marine Drugs,* 13(6), 3407-3421.

Qi, H., Zhang, Q., Zhao, T., Chen, R., Zhang, H., Niu, X.*, et al.* (2005a). Antioxidant activity of different sulfate content derivatives of polysaccharide extracted from *Ulva pertusa* (Chlorophyta) in vitro. *International Journal of Biological Macromolecules,* 37(4), 195-199.

Qi, H., Zhao, T., Zhang, Q., Li, Z., Zhao, Z., & Xing, R. (2005b). Antioxidant activity of different molecular weight sulfated polysaccharides from *Ulva pertusa* Kjellm (Chlorophyta). *Journal of Applied Phycology,* 17(6), 527-534.

Qi, H. M., Liu, X. L., Ma, J., Zhang, Q. B., & Li, Z. E. (2010). In vitro antioxidant activity of acetylated derivatives of polysaccharide extracted from *Ulva pertusa* (Cholorophta). *Journal of Medicinal Plants Research,* 4(23), 2445-2451.

Qi, H. M., Liu, X. L., Zhang, J. B., Duan, Y., Wang, X. L., & Zhang, Q. B. (2012b). Synthesis and antihyperlipidemic activity of acetylated derivative of ulvan from *Ulva pertusa*. *International Journal of Biological Macromolecules,* 50(1), 270-272.

Qi, H. M., & Sun, Y. L. (2015). Antioxidant activity of high sulfate content derivative of ulvan in hyperlipidemic rats. *International Journal of Biological Macromolecules,* 76, 326-329.

Qi, H. M., Zhang, Q. B., Zhao, T. T., Hu, R. G., Zhang, K., & Li, Z. (2006). In vitro antioxidant activity of acetylated and benzoylated derivatives of polysaccharide extracted from *Ulva pertusa* (Chlorophyta). *Bioorganic & Medicinal Chemistry Letters,* 16(9), 2441-2445.

Qi, X. H., Mao, W. J., Chen, Y., Chen, Y. L., Zhao, C. Q., Li, N.*, et al.* (2013b). Chemical characteristics and anticoagulant activities of two sulfated polysaccharides from *Enteromorpha linza* (Chlorophyta). *Journal of Ocean University of China,* 12(1), 175-182.

Qi, X. H., Mao, W. J., Gao, Y., Chen, Y., Chen, Y. L., Zhao, C. Q.*, et al.* (2012c). Chemical characteristic of an anticoagulant-active sulfated polysaccharide from *Enteromorpha clathrata*. *Carbohydrate Polymers,* 90(4), 1804-1810.

Qiao, L. K., Li, Y. P., Chi, Y. Z., Ji, Y. L., Gao, Y., Hwang, H. M.*, et al.* (2016). Rheological properties, gelling behavior and texture characteristics of polysaccharide from *Enteromorpha prolifera*. *Carbohydrate Polymers,* 136, 1307-1314.

Quemener, B., Lahaye, M., & Bobin-Dubigeon, C. (1997). Sugar determination in ulvans by a chemical-enzymatic method coupled to high performance anion exchange chromatography. *Journal of Applied Phycology,* 9(2), 179-188.

Radhakrishnamurthy, B., & Berenson, G. S. (1963). Effect of temperature and time of heating on the carbazole reaction of uronic acids and acid mucopolysaccharides. *Analytical Chemistry,* 35(9), 1316-1318.

Rahimi, F., Tabarsa, M., & Rezaei, M. (2016). Ulvan from green algae *Ulva intestinalis*: optimization of ultrasound-assisted extraction and antioxidant activity. *Journal of Applied Phycology,* 28(5), 2979-2990.

Rang, H. P., Ritter, J. M., Flower, R. J., & Henderson, G. (2016). *Rang & Dale's Pharmacology*: Churchill Livingstone.

Rathore, S. S., Chaudhary, D. R., Boricha, G. N., Ghosh, A., Bhatt, B. P., Zodape, S. T.*, et al.* (2009). Effect of seaweed extract on the growth, yield and nutrient uptake of soybean (*Glycine max*) under rainfed conditions. *South African Journal of Botany,* 75(2), 351-355.

Ray, B. (2006). Polysaccharides from *Enteromorpha compressa*: Isolation, purification and structural features. *Carbohydrate Polymers,* 66(3), 408-416.

Ray, B., & Lahaye, M. (1995a). Cell-wall polysaccharides from the marine green alga *Ulva* "*rigida*" (Ulvales, Chlorophyta). Chemical structure of ulvan. *Carbohydrate Research,* 274, 313-318.

Ray, B., & Lahaye, M. (1995b). Cell-wall polysaccharides from the marine green alga *Ulva* "*rigida*" (ulvales, chlorophyta). Extraction and chemical composition. *Carbohydrate Research,* 274, 251-261.

Ray, B., Schütz, M., Mukherjee, S., Jana, S., Ray, S., & Marschall, M. (2021). Exploiting the amazing diversity of natural source-derived polysaccharides: Modern procedures of isolation, engineering, and optimization of antiviral activities. *Polymers,* 13(1), 1-22.

Rees, D. A., Morris, E. R., Thorn, D., & Madden, J. K. (1982). *Shapes and interactions of carbohydrate chains*. In G. O. Aspinall (Ed.), *The Polysaccharides* (pp. 195-290). New York: Academic Press

Reisky, L., Stanetty, C., Mihovilovic, M. D., Schweder, T., Hehemann, J.-H., & Bornscheuer, U. T. (2018). Biochemical characterization of an ulvan lyase from the marine flavobacterium *Formosa agariphila* KMM 3901T. *Applied Microbiology and Biotechnology,* 102(16), 6987-6996.

Ren, R., Gong, J., Zhao, Y., Zhuang, X., Ye, Y., Huang, F.*, et al.* (2018). Sulfated polysaccharide from *Enteromorpha prolifera* suppresses SREBP-1c and ACC expression to lower serum triglycerides in high-fat diet-induced hyperlipidaemic rats. *Journal of Functional Foods,* 40, 722-728.

Ren, R., Gong, J., Zhao, Y., Zhuang, X., Ye, Y., & Lin, W. (2017). Sulfated polysaccharides from *Enteromorpha prolifera* suppress SREBP-2 and HMG-CoA reductase expression and attenuate non-alcoholic fatty liver disease induced by a high-fat diet. *Food and Function,* 8(5), 1899-1904.

Rizk, M. Z., Aly, H. F., Matloub, A. A., & Fouad, G. I. (2016a). The anti-hypercholesterolemic effect of ulvan polysaccharide extracted from the green alga *Ulva fasciata* on aged hypercholesterolemic rats. *Asian Journal of Pharmaceutical and Clinical Research,* 9(3).

Rizk, M. Z., El-Sherbiny, M., Borai, I. H., Ezz, M. K., Aly, H. F., Matloub, A. A.*, et al.* (2016b). Sulphated polysaccharides (SPS) from the green alga *Ulva fasciata* extract modulates liver and kidney function in high fat diet-induced hypercholesterolemic rats. *International Journal of Pharmacy and Pharmaceutical Sciences,* 8(6), 43-55.

Robert-Seilaniantz, A., Grant, M., & Jones, J. D. G. (2011). Hormone crosstalk in plant disease and defense: more than just jasmonate-salicylate antagonism. *Annual Review of Phytopathology,* 49(1), 317-343.

Robic, A., Bertrand, D., Sassi, J. F., Lerat, Y., & Lahaye, M. (2009a). Determination of the chemical composition of ulvan, a cell wall polysaccharide from *Ulva* spp. (Ulvales, Chlorophyta) by FT-IR and chemometrics. *Journal of Applied Phycology,* 21(4), 451-456.

Robic, A., Gaillard, C., Sassi, J. F., Lerat, Y., & Lahaye, M. (2009b). Ultrastructure of ulvan: A polysaccharide from green seaweeds. *Biopolymers,* 91(8), 652-664.

Robic, A., Rondeau-Mouro, C., Sassi, J. F., Lerat, Y., & Lahaye, M. (2009c). Structure and interactions of ulvan in the cell wall of the marine green algae *Ulva rotundata* (Ulvales, Chlorophyceae). *Carbohydrate Polymers,* 77(2), 206-216.

Robic, A., Sassi, J. F., Dion, P., Lerat, Y., & Lahaye, M. (2009d). Seasonal variability of physicochemical and rheological properties of ulvan in two *Ulva* species (chlorophyta) from the Brittany coast. *Journal of Phycology,* 45(4), 962-973.

Robic, A., Sassi, J. F., & Lahaye, M. (2008). Impact of stabilization treatments of the green seaweed *Ulva rotundata* (Chlorophyta) on the extraction yield, the physico-chemical and rheological properties of ulvan. *Carbohydrate Polymers,* 74(3), 344-352.

Roesijadi, G., Jones, S. B., Snowden-Swan, L. J., & Zhu, Y. (2010). Macroalgae as a biomass feedstock: A preliminary analysis. (p. Medium: ED; Size: PDFN): ; Pacific Northwest National Lab. (PNNL), Richland, WA (United States).

Roselli, M., Britti, M. S., Le Huërou-Luron, I., Marfaing, H., Zhu, W. Y., & Mengheri, E. (2007). Effect of different plant extracts and natural substances (PENS) against membrane damage induced by enterotoxigenic *Escherichia coli* K88 in pig intestinal cells. *Toxicology in Vitro,* 21(2), 224-229.

Salomonsen, T., Jensen, H. M., Stenbæk, D., & Engelsen, S. B. (2008). Chemometric prediction of alginate monomer composition: A comparative spectroscopic study using IR, Raman, NIR and NMR. *Carbohydrate Polymers,* 72(4), 730-739.

Sari-Chmayssem, N., Taha, S., Mawlawi, H., Guégan, J.-P., Jeftić, J., & Benvegnu, T. (2019). Extracted ulvans from green algae *Ulva linza* of Lebanese origin and amphiphilic derivatives: evaluation of their physico-chemical and rheological properties. *Journal of Applied Phycology,* 31(3), 1931-1946.

Sathivel, A., Balavinayagamani, Hanumantha Rao, B. R., & Devaki, T. (2014). Sulfated polysaccharide isolated from *Ulva lactuca* attenuates D-galactosamine induced DNA fragmentation and necrosis during liver damage in rats. *Pharmaceutical Biology,* 52(4), 498-505.

Sathivel, A., Raghavendran, H. R. B., Srinivasan, P., & Devaki, T. (2008). Anti-peroxidative and anti-hyperlipidemic nature of *Ulva lactuca* crude polysaccharide on D-Galactosamine induced hepatitis in rats. *Food and Chemical Toxicology,* 46(10), 3262-3267.

Scharnweber, D., Hubner, L., Rother, S., Hempel, U., Anderegg, U., Samsonov, S. A.*, et al.* (2015). Glycosaminoglycan derivatives: promising candidates for the design of

functional biomaterials. *Journal of Materials Science: Materials in Medicine,* 26(9), 232.

Shanmugam, M., Ramavat, B. K., Mody, K. H., Oza, R. M., & Tewari, A. (2001). Distribution of heparinoid-active sulphated polysaccharides in some Indian marine green algae. *Indian Journal of Marine Sciences,* 30(4), 222-227.

Shao, P., Chen, M., Pei, Y. P., & Sun, P. L. (2013a). In vitro antioxidant activities of different sulfated polysaccharides from chlorophytan seaweeds *Ulva fasciata*. *International Journal of Biological Macromolecules,* 59, 295-300.

Shao, P., Chen, X., & Sun, P. (2013b). In vitro antioxidant and antitumor activities of different sulfated polysaccharides isolated from three algae. *International Journal of Biological Macromolecules,* 62, 155-161.

Shao, P., Pei, Y., Fang, Z., & Sun, P. (2014a). Effects of partial desulfation on antioxidant and inhibition of DLD cancer cell of *Ulva fasciata* polysaccharide. *International Journal of Biological Macromolecules,* 65, 307-313.

Shao, P., Qin, M. P., Han, L. F., & Sun, P. L. (2014b). Rheology and characteristics of sulfated polysaccharides from chlorophytan seaweeds *Ulva fasciata*. *Carbohydrate Polymers,* 113, 365-372.

Shao, P., Shao, J., Han, L., Lv, R., & Sun, P. (2015). Separation, preliminary characterization, and moisture-preserving activity of polysaccharides from *Ulva fasciata*. *International Journal of Biological Macromolecules,* 72, 924-930.

Shi, J. M., Cheng, C. L., Zhao, H. T., Jing, J., Gong, N., & Lu, W. H. (2013). In vivo anti-radiation activities of the *Ulva pertusa* polysaccharides and polysaccharide-iron(III) complex. *International Journal of Biological Macromolecules,* 60, 341-346.

Shi, L. (2016). Bioactivities, isolation and purification methods of polysaccharides from natural products: A review. *International Journal of Biological Macromolecules,* 92, 37-48.

Shi, M. J., Wei, X., Xu, J., Chen, B. J., Zhao, D. Y., Cui, S*., et al.* (2017a). Carboxymethylated degraded polysaccharides from *Enteromorpha prolifera*: Preparation and in vitro antioxidant activity. *Food Chemistry,* 215, 76-83.

Shi, Q., Wang, A., Lu, Z., Qin, C., Hu, J., & Yin, J. (2017b). Overview on the antiviral activities and mechanisms of marine polysaccharides from seaweeds. *Carbohydrate Research,* 453-454(Supplement C), 1-9.

Shriver, Z., Capila, I., Venkataraman, G., & Sasisekharan, R. (2012). Heparin and heparan sulfate: analyzing structure and microheterogeneity. *Handbook of experimental pharmacology*(207), 159-176.

Siddhanta, A. K., Goswami, A. M., Ramavat, B. K., Mody, K. H., & Mairh, O. P. (2001). Water soluble polysaccharides of marine algal species of *Ulva* (Ulvales, Chlorophyta) of Indian waters. *Indian Journal of Marine Sciences,* 30(3), 166-172.

Sims, I. M., & Bacic, A. (1995). Extracellular polysaccharides from suspension cultures of *Nicotiana plumbaginifolia*. *Phytochemistry,* 38(6), 1397-1405.

Sims, I. M., Carnachan, S. M., Bell, T. J., & Hinkley, S. F. R. (2018). Methylation analysis of polysaccharides: Technical advice. *Carbohydrate Polymers,* 188, 1-7.

Singh, R. P., & Reddy, C. R. K. (2014). Seaweed–microbial interactions: key functions of seaweed-associated bacteria. *FEMS Microbiology Ecology,* 88(2), 213-230.

Sivakanthan, S., Rajendran, S., Gamage, A., Madhujith, T., & Mani, S. (2020). Antioxidant and antimicrobial applications of biopolymers: A review. *Food Research International,* 136.

Sivasankari, S., Venkatesalu, V., Anantharaj, M., & Chandrasekaran, M. (2006). Effect of seaweed extracts on the growth and biochemical constituents of *Vigna sinensis*. *Bioresource Technology,* 97(14), 1745-1751.

Soler-Vila, A., Coughlan, S., Guiry, M. D., & Kraan, S. (2009). The red alga *Porphyra dioica* as a fish-feed ingredient for rainbow trout (*Oncorhynchus mykis*): effects on growth, feed efficiency, and carcass composition. *Journal of Applied Phycology,* 21(5), 617-624.

Song, L., Chen, X., Liu, X., Zhang, F., Hu, L., Yue, Y.*, et al.* (2016). Characterization and comparison of the structural features, immune-modulatory and anti-avian influenza virus activities conferred by three algal sulfated polysaccharides. *Marine Drugs,* 14(1).

Spavieri, J., Kaiser, M., Casey, R., Hingley-Wilson, S., Lalvani, A., Blunden, G.*, et al.* (2010). Antiprotozoal, antimycobacterial and cytotoxic potential of some British green algae. *Phytotherapy Research,* 24(7), 1095-1098.

Stadnik, M. J., & de Freitas, M. B. (2014). Algal polysaccharides as source of plant resistance inducers. *Tropical Plant Pathology,* 39(2), 111-118.

Stevenson, T. T., & Furneaux, R. H. (1991). Chemical methods for the analysis of sulphated galactans from red algae. *Carbohydrate Research,* 210, 277-298.

Stiger-Pouvreau, V., Bourgougnon, N., & Deslandes, E. (2016). *Carbohydrates From Seaweeds*. In J. Fleurence & I. Levine (Eds.), *Seaweed in Health and Disease Prevention* (pp. 223-274). San Diego: Academic Press

Striegel, A. M. (2005). Multiple detection in size-exclusion chromatography of macromolecules. *Analytical Chemistry,* 77(5), 104 A-113 A.

Sugahara, K., & Kitagawa, H. (2002). Heparin and heparan sulfate biosynthesis. *IUBMB Life,* 54(4), 163-175.

Sun, X., Zhong, Y., Luo, H., & Yang, Y. (2017). Selenium-containing polysaccharide-protein complex in Se-enriched *Ulva fasciata* induces mitochondria-mediated apoptosis in A549 human lung cancer cells. *Marine Drugs,* 15(7).

Synytsya, A., Choi, D. J., Pohl, R., Na, Y. S., Capek, P., Lattová, E.*, et al.* (2015). Structural features and anti-coagulant activity of the sulphated polysaccharide SPS-CF from a green alga *Capsosiphon fulvescens*. *Marine Biotechnology,* 17(6), 718-735.

Tabarsa, M., Han, J. H., Kim, C. Y., & You, S. G. (2012a). Molecular characteristics and immunomodulatory activities of water-soluble sulfated polysaccharides from *Ulva pertusa*. *Journal of Medicinal Food,* 15(2), 135-144.

Tabarsa, M., Lee, S. J., & You, S. (2012b). Structural analysis of immunostimulating sulfated polysaccharides from *Ulva pertusa*. *Carbohydrate Research,* 361, 141-147.

Tabarsa, M., You, S., Dabaghian, E. H., & Surayot, U. (2018). Water-soluble polysaccharides from *Ulva intestinalis*: Molecular properties, structural elucidation and immunomodulatory activities. *Journal of Food and Drug Analysis,* 26(2), 599-608.

Tako, M., Tamanaha, M., Tamashiro, Y., & Uechi, S. (2015). Structure of ulvan isolated from the edible green seaweed, *Ulva pertusa*. *Advances in Bioscience and Biotechnology,* 6, 645-655.

Tariq, A., Athar, M., Ara, J., Sultana, V., Ehteshamul-Haque, S., & Ahmad, M. (2015). Biochemical evaluation of antioxidant activity in extracts and polysaccharide fractions of seaweeds. *Global Journal of Environmental Science and Management,* 1(1), 47-62.

Taylor, R., Fletcher, R. L., & Raven, J. A. (2001). Preliminary studies on the growth of selected 'green tide' algae in laboratory culture: effects of irradiance, temperature, salinity and nutrients on growth rate. 44(4), 327-336.

Templeton, D. W., Quinn, M., Van Wychen, S., Hyman, D., & Laurens, L. M. L. (2012). Separation and quantification of microalgal carbohydrates. *Journal of Chromatography A,* 1270, 225-234.

Teng, Z. L., Qian, L., & Zhou, Y. (2013). Hypolipidemic activity of the polysaccharides from *Enteromorpha prolifera*. *International Journal of Biological Macromolecules,* 62, 254-256.

Thanh, T. T. T., Quach, T. M. T., Nguyen, T. N., Luong, D. V., Bui, M. L., & Tran, T. T. V. (2016). Structure and cytotoxic activity of ulvan extracted from green seaweed *Ulva lactuca*. *International Journal of Biological Macromolecules,* 93, 695-702.

Thu, Q. T. M., Bang, T. H., Nu, N. T., Luong, D. V., Ly, B. M., Van, T. T. T.*, et al.* (2015). Structural determination of ulvan from green seaweed *Ulva reticulata* collected at central coast of Vietnam. *Chemistry Letters,* 44(6), 788-790.

Tian, H., Yin, X., Zeng, Q., Zhu, L., & Chen, J. (2015). Isolation, structure, and surfactant properties of polysaccharides from *Ulva lactuca* L. from South China Sea. *International Journal of Biological Macromolecules,* 79, 577-582.

Toskas, G., Hund, R. D., Laourine, E., Cherif, C., Smyrniotopoulos, V., & Roussis, V. (2011). Nanofibers based on polysaccharides from the green seaweed *Ulva rigida*. *Carbohydrate Polymers,* 84(3), 1093-1102.

Tran, T. T. V., Huy, B. T., Truong, H. B., Bui, M. L., Thanh, T. T. T., & Dao, D. Q. (2018). Structure analysis of sulfated polysaccharides extracted from green seaweed *Ulva lactuca*: experimental and density functional theory studies. *Chemical Monthly*, 1-9.

Tran, T. T. V., Truong, H. B., Tran, N. H. V., Quach, T. M. T., Nguyen, T. N., Bui, M. L.*, et al.* (2017). Structure, conformation in aqueous solution and antimicrobial activity of ulvan extracted from green seaweed *Ulva reticulata*. *Natural Product Research*, 1-6.

Trouvelot, S., Héloir, M.-C., Poinssot, B., Gauthier, A., Paris, F., Guillier, C.*, et al.* (2014). Carbohydrates in plant immunity and plant protection: roles and potential application as foliar sprays. *Frontiers in Plant Science,* 5, 592.

Tsubaki, S., Hiraoka, M., Hadano, S., Nishimura, H., Kashimura, K., & Mitani, T. (2014). Functional group dependent dielectric properties of sulfated hydrocolloids extracted from green macroalgal biomass. *Carbohydrate Polymers,* 107(1), 192-197.

Tsubaki, S., Oono, K., Hiraoka, M., Onda, A., & Mitani, T. (2016). Microwave-assisted hydrothermal extraction of sulfated polysaccharides from *Ulva* spp. and *Monostroma latissimum*. *Food Chemistry,* 210, 311-316.

Tziveleka, L. A., Ioannou, E., & Roussis, V. (2019). Ulvan, a bioactive marine sulphated polysaccharide as a key constituent of hybrid biomaterials: A review. *Carbohydrate Polymers,* 218, 355-370.

Tziveleka, L. A., Sapalidis, A., Kikionis, S., Aggelidou, E., Demiri, E., Kritis, A.*, et al.* (2020). Hybrid sponge-like scaffolds based on ulvan and gelatin: Design, characterization and evaluation of their potential use in bone tissue engineering. *Materials,* 13(7).

Usov, A. I., Adamyants, K. S., Miroshnikova, L. I., Shaposhnikova, A. A., & Kochetkov, N. K. (1971). Solvolytic desulphation of sulphated carbohydrates. *Carbohydrate Research,* 18(2), 336-338.

Valko, M., Izakovic, M., Mazur, M., Rhodes, C. J., & Telser, J. (2004). Role of oxygen radicals in DNA damage and cancer incidence. *Molecular and Cellular Biochemistry,* 266(1), 37-56.

van den Hoogen, B. M., van Weeren, P. R., Lopes-Cardozo, M., van Golde, L. M., Barneveld, A., & van de Lest, C. H. (1998). A microtiter plate assay for the determination of uronic acids. *Analytical Biochemistry,* 257(2), 107-111.

Varnier, A. L., Sanchez, L., Vatsa, P., Boudesocque, L., Garcia-Brugger, A., Rabenoelina, F.*, et al.* (2009). Bacterial rhamnolipids are novel MAMPs conferring resistance to *Botrytis cinerea* in grapevine. *Plant, Cell & Environment,* 32(2), 178-193.

Vatsa, P., Sanchez, L., Clement, C., Baillieul, F., & Dorey, S. (2010). Rhamnolipid biosurfactants as new players in animal and plant defense against microbes. *International Journal of Molecular Sciences,* 11(12), 5095-5108.

Velimirov, B., Field, J. G., Griffiths, C. L., & Zoutendyk, P. (1977). The ecology of kelp bed communities in the Benguela upwelling system. *Helgoländer wissenschaftliche Meeresuntersuchungen,* 30(1), 495-518.

Venkatesan, J., Lowe, B., Anil, S., Manivasagan, P., Kheraif, A. A. A., Kang, K.-H.*, et al.* (2015). Seaweed polysaccharides and their potential biomedical applications. *Starch - Stärke,* 67(5-6), 381-390.

Violle, N., Rozan, P., Demais, H., Nyvall Collen, P., & Bisson, J. F. (2017). Evaluation of the antidepressant- and anxiolytic-like effects of a hydrophilic extract from the green seaweed *Ulva* sp. in rats. *Nutritional Neuroscience*, 1-9.

Wahlström, N., Nylander, F., Malmhäll-Bah, E., Sjövold, K., Edlund, U., Westman, G.*, et al.* (2020). Composition and structure of cell wall ulvans recovered from *Ulva* spp. along the Swedish west coast. *Carbohydrate Polymers,* 233, 115852.

Wang, J., Jin, W. H., Hou, Y., Niu, X. Z., Zhang, H., & Zhang, Q. B. (2013a). Chemical composition and moisture-absorption/retention ability of polysaccharides extracted from five algae. *International Journal of Biological Macromolecules,* 57, 26-29.

Wang, L., Wang, X., Wu, H., & Liu, R. (2014a). Overview on biological activities and molecular characteristics of sulfated polysaccharides from marine green algae in recent years. *Marine Drugs,* 12(9), 4984-5020.

Wang, X. M., Zhang, Z. S., Yao, Z. Y., Zhao, M. X., & Qi, H. M. (2013b). Sulfation, anticoagulant and antioxidant activities of polysaccharide from green algae *Enteromorpha linza*. *International Journal of Biological Macromolecules,* 58, 225-230.

Wang, X. X., Chen, Y., Wang, J. J., Liu, Z. X., & Zhao, S. G. (2014b). Antitumor activity of a sulfated polysaccharide from *Enteromorpha intestinalis* targeted against hepatoma through mitochondrial pathway. *Tumor Biology,* 35(2), 1641-1647.

Wei, J., Wang, S., Liu, G., Pei, D., Liu, Y., Liu, Y.*, et al.* (2014). Polysaccharides from *Enteromorpha prolifera* enhance the immunity of normal mice. *International Journal of Biological Macromolecules,* 64, 1-5.

White, L. N., & White, W. L. (2020). Seaweed utilisation in New Zealand. *Botanica Marina,* 63(4), 303-313.

Wichard, T., Charrier, B., Mineur, F., Bothwell, J. H., Clerck, O. D., & Coates, J. C. (2015). The green seaweed *Ulva*: a model system to study morphogenesis. *Frontiers in plant science,* 6, 72-72.

Wight, T. N., Kinsella, M. G., & Qwarnstrom, E. E. (1992). The role of proteoglycans in cell adhesion, migration and proliferation. *Current Opinion in Cell Biology,* 4(5), 793-801.

Wijesekara, I., Pangestuti, R., & Kim, S. K. (2011). Biological activities and potential health benefits of sulfated polysaccharides derived from marine algae. *Carbohydrate Polymers,* 84(1), 14-21.

Willför, S., Pranovich, A., Tamminen, T., Puls, J., Laine, C., Suurnäkki, A.*, et al.* (2009). Carbohydrate analysis of plant materials with uronic acid-containing polysaccharides–A comparison between different hydrolysis and subsequent chromatographic analytical techniques. *Industrial Crops and Products,* 29(2), 571-580.

Witvrouw, M., & De Clercq, E. (1997). Sulfated polysaccharides extracted from sea algae as potential antiviral drugs. *General Pharmacology: The Vascular System,* 29(4), 497-511.

Xu, J., Xu, L. L., Zhou, Q. W., Hao, S. X., Zhou, T., & Xie, H. J. (2015). Isolation, purification, and antioxidant activities of degraded polysaccharides from *Enteromorpha prolifera*. *International Journal of Biological Macromolecules,* 81, 1026-1030.

Yaich, H., Amira, A. B., Abbes, F., Bouaziz, M., Besbes, S., Richel, A.*, et al.* (2017). Effect of extraction procedures on structural, thermal and antioxidant properties of ulvan from *Ulva lactuca* collected in Monastir coast. *International Journal of Biological Macromolecules,* 105(Pt 2), 1430-1439.

Yaich, H., Garna, H., Besbes, S., Barthélemy, J.-P., Paquot, M., Blecker, C.*, et al.* (2014). Impact of extraction procedures on the chemical, rheological and textural properties of ulvan from *Ulva lactuca* of Tunisia coast. *Food Hydrocolloids,* 40, 53-63.

Yaich, H., Garna, H., Besbes, S., Paquot, M., Blecker, C., & Attia, H. (2013). Effect of extraction conditions on the yield and purity of ulvan extracted from *Ulva lactuca*. *Food Hydrocolloids,* 31(2), 375-382.

Yamamoto, M. (1980). Physicochemical studies on sulfated polysaccharides extracted from seaweeds at various temperatures. *Agricultural and Biological Chemistry,* 44(3), 589-593.

Yamamoto, M., Imai, H., Mita, K., & Tadokoro, Y. (1980). Physicochemical characterization of sulfated polysaccharides from green seaweeds: *Ulva pertusa* and *Ulva conglobata*. *Agricultural and Biological Chemistry,* 44(4), 723-729.

Yang, F., Fang, X., Jiang, W., & Chen, T. (2017). Bioresponsive cancer-targeted polysaccharide nanosystem to inhibit angiogenesis. *International Journal of Nanomedicine,* 12, 7419-7431.

Yang, L., & Zhang, L.-M. (2009). Chemical structural and chain conformational characterization of some bioactive polysaccharides isolated from natural sources. *Carbohydrate Polymers,* 76(3), 349-361.

Ye, N.-h., Zhang, X.-w., Mao, Y.-z., Liang, C.-w., Xu, D., Zou, J.*, et al.* (2011). 'Green tides' are overwhelming the coastline of our blue planet: taking the world's largest example. *Ecological Research,* 26(3), 477.

Yu, Y., Li, Y. P., Du, C. Y., Mou, H. J., & Wang, P. (2017). Compositional and structural characteristics of sulfated polysaccharide from *Enteromorpha prolifera*. *Carbohydrate Polymers,* 165, 221-228.

Yuan, Y., Xu, X., Jing, C., Zou, P., Zhang, C., & Li, Y. (2018). Microwave assisted hydrothermal extraction of polysaccharides from *Ulva prolifera*: Functional properties and bioactivities. *Carbohydrate Polymers,* 181, 902-910.

Zhang, H.-J., Mao, W.-J., Fang, F., Li, H.-Y., Sun, H.-H., Chen, Y.*, et al.* (2008). Chemical characteristics and anticoagulant activities of a sulfated polysaccharide and its fragments from *Monostroma latissimum*. *Carbohydrate Polymers,* 71(3), 428-434.

Zhang, L., Wang, X., Hua, Q., Wang, J., Liu, J., & Yang, Y. (2020). Synthesis and immunomodulatory activity of the sulfated tetrasaccharide motif of type B ulvanobiuronic acid 3-sulfate. *Organic and Biomolecular Chemistry,* 18(39), 7932-7935.

Zhang, Q., Li, N., Zhou, G., Lu, X., Xu, Z., & Li, Z. (2003). In vivo antioxidant activity of polysaccharide fraction from *Porphyra haitanesis* (Rhodophyta) in aging mice. *Pharmacological Research,* 48(2), 151-155.

Zhang, Z., Wang, X., Zhao, M., Yu, S., & Qi, H. (2013). The immunological and antioxidant activities of polysaccharides extracted from *Enteromorpha linza*. *International Journal of Biological Macromolecules,* 57, 45-49.

Zhang, Z. S., Wang, F., Wang, X. M., Liu, X. L., Hou, Y., & Zhang, Q. B. (2010). Extraction of the polysaccharides from five algae and their potential antioxidant activity in vitro. *Carbohydrate Polymers,* 82(1), 118-121.

Zhang, Z. S., Wang, X. M., Yu, S. C., Yin, L., Zhao, M. X., & Han, Z. P. (2011). Synthesized oversulfated and acetylated derivatives of polysaccharide extracted from *Enteromorpha linza* and their potential antioxidant activity. *International Journal of Biological Macromolecules,* 49(5), 1012-1015.

Zhong, R., Wan, X., Wang, D., Zhao, C., Liu, D., Gao, L.*, et al.* (2020). Polysaccharides from marine *Enteromorpha*: Structure and function. *Trends in Food Science & Technology,* 99, 11-20.

Zhu, C., Zhang, S., Song, C., Zhang, Y., Ling, Q., Hoffmann, P. R.*, et al.* (2017). Selenium nanoparticles decorated with *Ulva lactuca* polysaccharide potentially attenuate colitis by inhibiting NF-κB mediated hyper inflammation. *Journal of Nanobiotechnology,* 15, 20.

Appendices

7.1 Chapter 2 supporting information

Methods

'Ulvan' as a descriptive term is underutilised in the literature. Limiting the search only to papers that had included ulvan in the title, keywords or abstract would have underrepresented the volume of research conducted on sulfated polysaccharides from Chlorophyta. Instead, the search string: "(Ulvan* OR ((sulfate* OR sulphate*) AND polysaccharide* AND (*Ulva* OR *Enteromorpha*)))" was used to include as many articles as possible surrounding the broader subject area of sulfated polysaccharides (which encompasses ulvan) from the two most commonly studied Chlorophyta genera. Web of Science (core collection) and Scopus were both searched using the above string on 13th December 2017. The search was performed on the title, keywords or abstract with no constraints on any other parameters. Combined there were 624 papers retrieved. Additionally, through the process of writing the review 16 other publications were found that were not picked up by the search string, or were published after the search date. After removing duplicates first through the inbuilt function in Endnote X8, then by manual review, 397 original papers remained (**App. 7.1.1**).

Inclusion of a paper and data in a meta-table and subsequent analysis was subject to meeting the criteria stipulated by the search string. The paper must use algae from *Ulva* or *Enteromorpha*, and involve the extraction of sulfated polysaccharides. The paper must also contribute original quantitative data to the extraction procedure, characterisation and/or application of the sulfated polysaccharide. The 398 original papers were then each individually examined by reading the title, abstract, methods and results to exclude articles that did not contribute original data as outlined above. The Preferred Reporting Items for Systematic and Meta-Analyses (PRISMA) Statement was used to record the number of articles included and excluded (See **App. 7.1.1**) (Moher, Liberati, Tetzlaff, & Altman, 2009).

Each of the 154 publications included in the meta-analysis were read and data collected on: (1) the year, first author, first 40 characters of the title, journal of publication; (2) genera and species used along with country and a description of the biomass source; (3)

The extractant applied, and concentration (if applicable), any enzymes applied, along with the temperature and duration of the extraction, and the precipitate if one was used; (4) the yield of polysaccharide (% DW), total carbohydrate, protein, ash, sulfate, uronic acid and neutral sugar content (in % w/w); (5) the average molecular weight; (6) the monosaccharide composition of rhamnose, uronic acids, glucuronic acid, xylose, iduronic acid, glucose and galactose (in mol%, % DW, or molar ratio); and (7) the tests applied to assess the biomedical application of the extracted polysaccharide. This data were recorded in the form and units that it was presented in unless the conversion was simply adjusting the magnitude of the value so that the data were comparable to other values in the table. If a conversion was performed, the cell is outlined in a dotted line and reading the formula will provide detail on the exact conversion applied. Some data were also estimated from figures, these values are also outlined in a dotted line. Where data were provided not in the units used in the table, these points were entered as text values with the corresponding units so as to avoid being included in the meta-analysis.

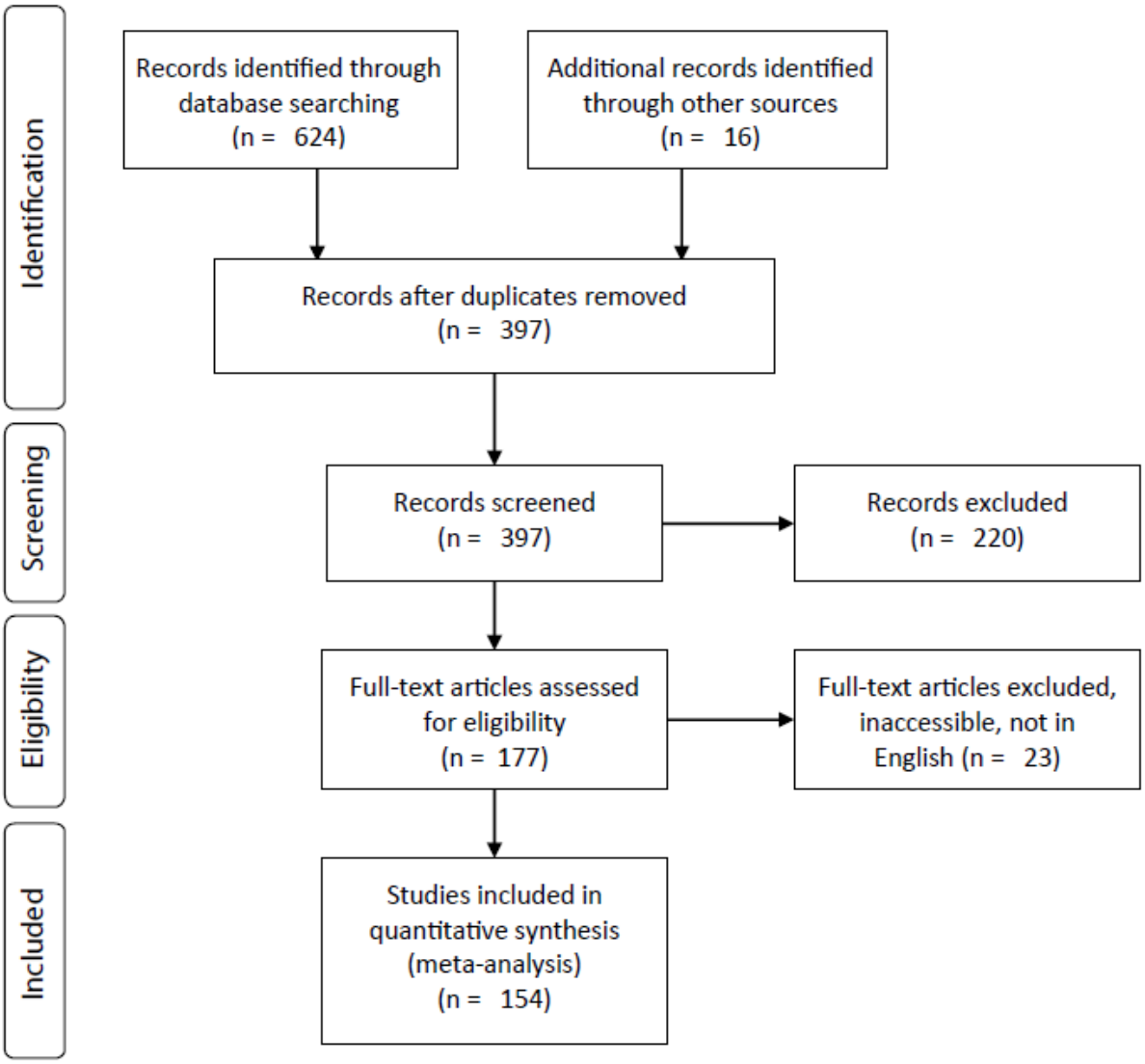

App. 7.1.1: Preferred reporting items for systematic and meta-analyses (PRISMA) flow diagram (Moher *et al.*, 2009) outlining the number of publications screened and included in the meta-analysis.

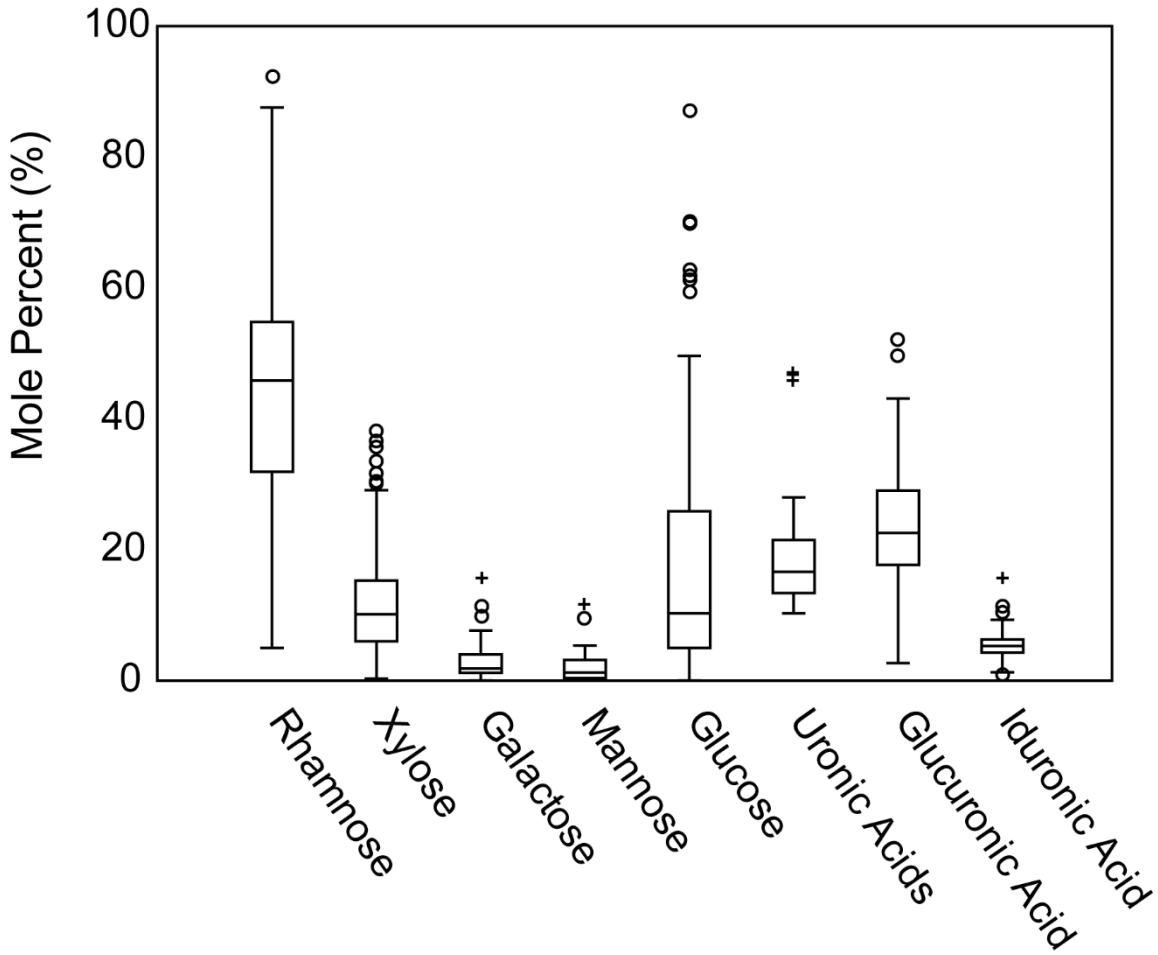

App. 7.1.2: Proportion of most common constituent monosaccharides (in mole percent) reported within ulvan. “Uronic acids” is a combined measurement of all uronic acids, including both iduronic and glucuronic. Boxes represent the interquartile range (IQR) with the mean as a line within the box; whiskers represent the limits of non-outlier data; open circles are outliers, calculated by ±1.5*IQR; crosses are extreme values, calculated by ±3*IQR; closed circles represent values for which n=1.

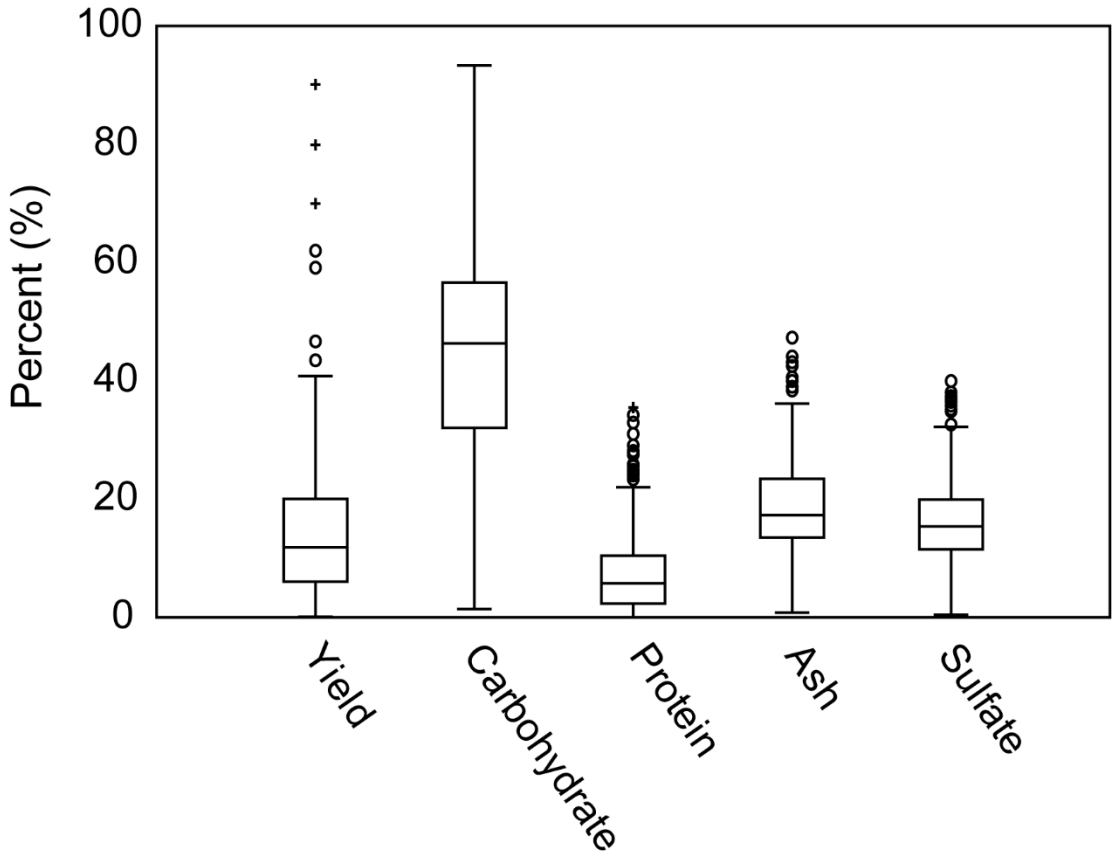

App. 7.1.3: General polysaccharide composition data including ulvan yield (% dry weight of alga), total carbohydrate (% w/w), protein (%), ash (%), and sulfate (%) in polysaccharide extract. Boxes represent the interquartile range (IQR) with the mean as a line within the box; whiskers represent the limits of non-outlier data; open circles are outliers, calculated by ±1.5*IQR; crosses are extreme values, calculated by ±3*IQR; closed circles represent values for which n=1.

7.2 Chapter 3 supporting information

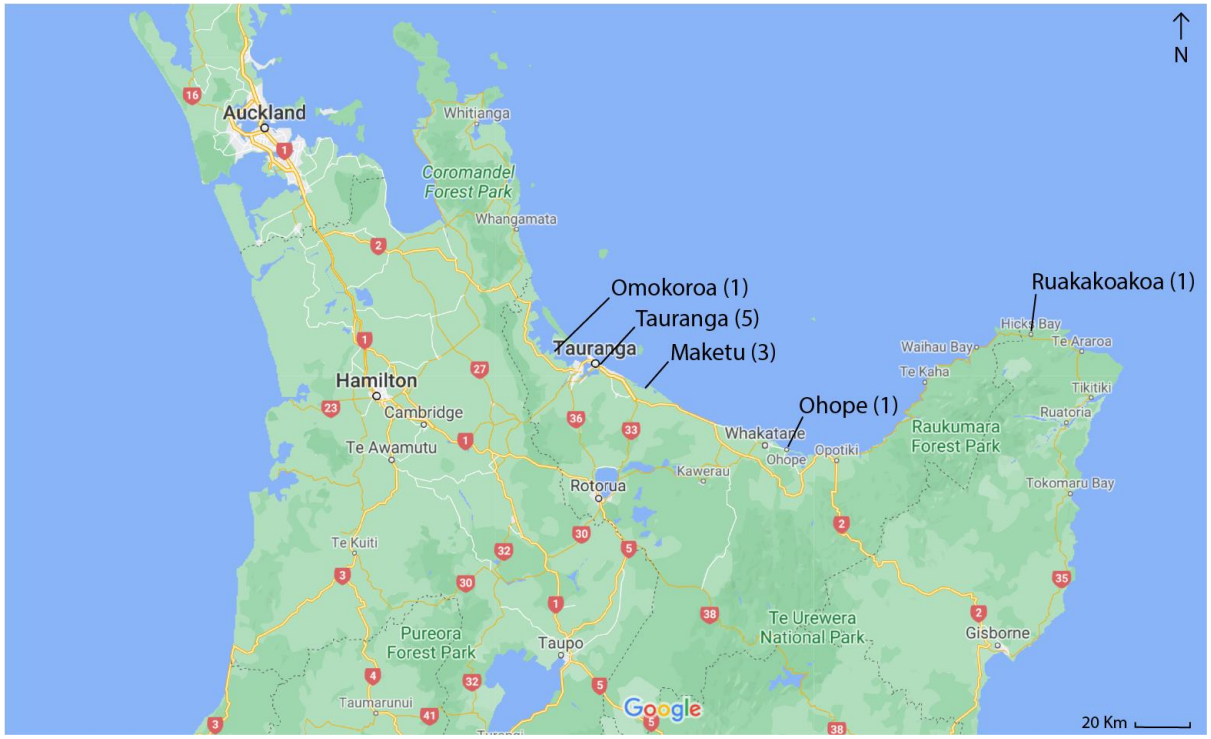

App. 7.2.1: Map of the Bay of Plenty Region, New Zealand with *Ulva* collection sites listed and number of samples collected at each site in brackets. See uploaded data sheet for more detail. Map sourced from Google Maps in Oct. 2020.

App. 7.2.2: Crude ulvan composition: details of the *Ulva* biomass from which ulvan was extracted, the yield obtained, the elemental composition and molecular weight, along with sulfate and protein content. For more details, see data sheet associated with publication.

***Ulva* details**			**Yield**	**Composition (% w/w)**							**Molecular Weight**		
***Ulva* species**	**Biomass source**	**Growth Form**	**Ulvan (% dw)** [a]	**%N** [b]	**%C** [b]	**%H** [b]	**%S** [b]	**%O** [b]	**%Ash** [b]	**%Protein** [c]	**M_w (kDa)**	**M_n (kDa)**	**Đ**
australis	Cultivated	Blade	14.7	n.d.[d]	n.d.	n.d.	n.d.	n.d.	n.d.	n.d.	n.d.	n.d.	n.d.
rigida	Cultivated	Blade	14.01	n.d.	n.d.	n.d.	n.d.	n.d.	n.d.	n.d.	n.d.	n.d.	n.d.
sp.	Wild harvest	Blade	16.72	0.9	27.2	5.1	7.3	40.4	19.2	4.3	363	190	1.9
sp. B (cult.A)	Cultivated	Blade	17.75	0.5	26.9	5.3	6.0	49.1	12.3	2.3	241	125	1.9
sp. B (cult.B)	Cultivated	Blade	16.3	0.4	25.4	5.4	5.7	53.0	10.2	2.1	251	153	1.6
sp. B (wild)	Wild harvest	Blade	19.33	0.4	26.3	5.3	5.8	51.0	11.2	1.8	341	154	2.2
compressa	Cultivated	Filamentous	7.16	1.9	32.4	5.8	4.5	44.4	11.1	9.3	466	264	1.8
flexuosa	Cultivated	Filamentous	14.59	n.d.	n.d.	n.d.	n.d.	n.d.	n.d.	n.d.	n.d.	n.d.	n.d.
prolifera	Cultivated	Filamentous	11.01	1.5	32.1	5.7	5.5	44.7	10.6	7.3	281	200	1.4
ralfsii (cult.)	Cultivated	Filamentous	8.59	1.2	27.9	5.3	5.6	48.9	11.1	5.9	455	284	1.6
ralfsii (wild)	Wild harvest	Filamentous	7.38	n.d.	n.d.	n.d.	n.d.	n.d.	n.d.	n.d.	n.d.	n.d.	n.d.

[a] % dry weight (dw) biomass

[b] Average of duplicates (S.D.<0.01 for N; <0.3 for C, H, S, O, Ash)

[c] Estimated from conversion factor of 5 (%N x 5)

[d] n.d. = not determined; sample unavailable for analysis.

App. 7.2.3: Purified ulvan elemental composition: details of the *Ulva* biomass from which ulvan was extracted and purified, and the elemental composition of each ulvan

***Ulva* details**			**Elemental composition (%w/w)**					
***Ulva* species**	**Biomass source**	**Morphology**	**%N** [a]	**%C** [a]	**%H** [a]	**%S** [a]	**%O** [a]	**%Ash** [a]
australis	Cultivated	Blade	0.2	26.8	4.9	7.2	38.7	22.3
rigida	Cultivated	Blade	0.1	27.3	4.8	6.2	36.8	24.8
sp.	Wild harvest	Blade	0.3	27.6	4.6	7.9	35.2	24.5
sp. B (cult.A)	Cultivated	Blade	0.1	27.9	5.0	6.4	37.6	23.1
sp. B (cult.B)	Cultivated	Blade	0.1	27.7	4.8	6.5	36.5	24.5
sp. B (wild)	Wild harvest	Blade	0.1	28.0	4.8	6.5	36.6	24.0
compressa	Cultivated	Filamentous	0.2	30.1	5.2	5.9	38.3	20.3
flexuosa	Cultivated	Filamentous	0.3	29.0	5.2	5.9	39.4	20.3
prolifera	Cultivated	Filamentous	0.1	30.2	5.3	6.3	38.6	19.6
ralfsii (cult.)	Cultivated	Filamentous	0.2	28.7	4.9	6.7	38.0	21.6
ralfsii (wild)	Wild harvest	Filamentous	0.1	28.8	4.9	6.5	37.6	22.0

[a] Average of duplicates (S.D.<0.01 for N; <0.3 for C, H, S, O, Ash)

App. 7.2.4: Purified ulvan constituent sugar composition (normalised mol%) and total sugar content (µg mg^{-1} sample). Galacturonic acid, glucosamine, and mannose were not detected in any ulvan. Rha = rhamnose; GlcA = glucuronic acid; Xyl = Xylose; IdoA = iduronic acid; Fuc = fucose; Gal = galactose; Glc = glucose; Rib = ribose; Fuc = fucose; Ara = arabinose.

Ulvan Species	Growth Form	Sugars (normalised mol%)[a]									Sugars (µg mg^{-1} sample)[a]									
		Rha	GlcA	Xyl	IdoA	Gal	Glc	Rib	Fuc	Ara	Rha	GlcA	Xyl	IdoA	Gal	Glc	Rib	Fuc	Ara	Total
australis	Blade	51	18	22	7	tr.	tr.	-	tr.	-	251	108	99	43	3	tr.	-	tr.	-	505
rigida	Blade	49	26	6	18	tr.	tr.	-	tr.	-	257	163	27	116	tr.	tr.	-	tr.	-	564
sp.	Blade	47	20	19	10	2	1	1	tr.	-	201	104	73	53	8	7	4	tr.	-	450
sp. B (cult.A)	Blade	51	22	11	15	2	-	-	tr.	-	272	143	52	94	12	-	-	-	-	573
sp. B (cult.B)	Blade	48	31	7	11	2	tr.	1	tr.	-	229	176	30	60	10	4	5	tr.	-	513
sp. B (wild)	Blade	48	26	11	13	1	tr.	tr.	tr.	-	251	163	51	79	6	3	4	tr.	-	558
compressa	Filamentous	47	24	17	7	3	tr.	tr.	tr.	-	267	160	87	46	20	6	4	3	-	593
flexuosa	Filamentous	56	21	15	6	2	tr.	tr.	tr.	tr.	314	142	78	38	12	tr.	1	tr.	tr.	586
prolifera	Filamentous	60	17	15	7	tr.	tr.	-	tr.	-	324	110	75	43	6	tr.	-	5	-	564
ralfsii (cult.)	Filamentous	38	24	16	4	16	tr.	tr.	tr.	tr.	203	155	76	24	94	4	4	3	tr.	563
ralfsii (wild)	Filamentous	43	26	14	6	10	tr.	1	tr.	-	248	180	72	41	62	3	5	2	-	613

[a] Values are the averages of duplicate analyses

Sugars < 1 mol% are considered trace (tr.)

Sugars < 1 µg mg^{-1} are considered trace (tr.)

"-" = not detected

App. 7.2.5: Crude ulvan constituent sugar composition (normalised mol%) and total sugar content (µg mg^{-1} sample). Galacturonic acid, glucosamine, and mannose were not detected in any ulvan. Rha = rhamnose; GlcA = glucuronic acid; Xyl = Xylose; IdoA = iduronic acid; Fuc = fucose; Gal = galactose; Glc = glucose; Rib = ribose; Fuc = fucose; Ara = arabinose.

Ulvan Species	Growth Form	Sugars (normalised mol%)[a]									Sugars (µg mg^{-1} sample)[a]									
		Rha	GlcA	Xyl	IdoA	Gal	Glc	Rib	Fuc	Ara	Rha	GlcA	Xyl	IdoA	Gal	Glc	Rib	Fuc	Ara	Total
australis	Blade	n.d.[e]	n.d.	n.d.	n.d.	n.d.	n.d.	n.d.	n.d.	n.d.	n.d.	n.d.	n.d.	n.d.	n.d.	n.d.	n.d.	n.d.	n.d.	n.d.
rigida	Blade	n.d.	n.d.	n.d.	n.d.	n.d.	n.d.	n.d.	n.d.	n.d.	n.d.	n.d.	n.d.	n.d.	n.d.	n.d.	n.d.	n.d.	n.d.	n.d.
sp.	Blade	48	20	16	10	2	3	-	tr.	-	203	103	62	52	10	14	-	0	-	444
sp. B (cult.A)	Blade	49	21	10	15	2	3	-	tr.	-	218	112	42	83	8	13	-	0	-	477
sp. B (cult.B)	Blade	48	31	6	10	3	3	-	tr.	-	149	115	17	38	9	11	-	0	-	339
sp. B (wild)	Blade	48	25	9	12	2	2	2	-	-	301	190	51	89	11	14	14	-	-	669
compressa	Filamentous	46	23	14	6	4	7	-	1	-	215	129	60	33	19	36	-	3	-	495
flexuosa	Filamentous	n.d.	n.d.	n.d.	n.d.	n.d.	n.d.	n.d.	n.d.	n.d.	n.d.	n.d.	n.d.	n.d.	n.d.	n.d.	n.d.	n.d.	n.d.	n.d.
prolifera	Filamentous	57	15	12	6	3	3	-	2	-	258	80	49	31	13	13	-	7	-	452
ralfsii (cult.)	Filamentous	39	25	14	3	15	5	-	tr.	-	171	130	55	17	71	23	-	2	-	470
ralfsii (wild)	Filamentous	n.d.	n.d.	n.d.	n.d.	n.d.	n.d.	n.d.	n.d.	n.d.	n.d.	n.d.	n.d.	n.d.	n.d.	n.d.	n.d.	n.d.	n.d.	n.d.

[a] Values are the averages of duplicate analyses

Sugars < 1 mol% are considered trace (tr.)

Sugars < 1 µg mg^{-1} are considered trace (tr.)

"-" = not detected

[e] n.d. = not determined; sample unavailable for analysis.

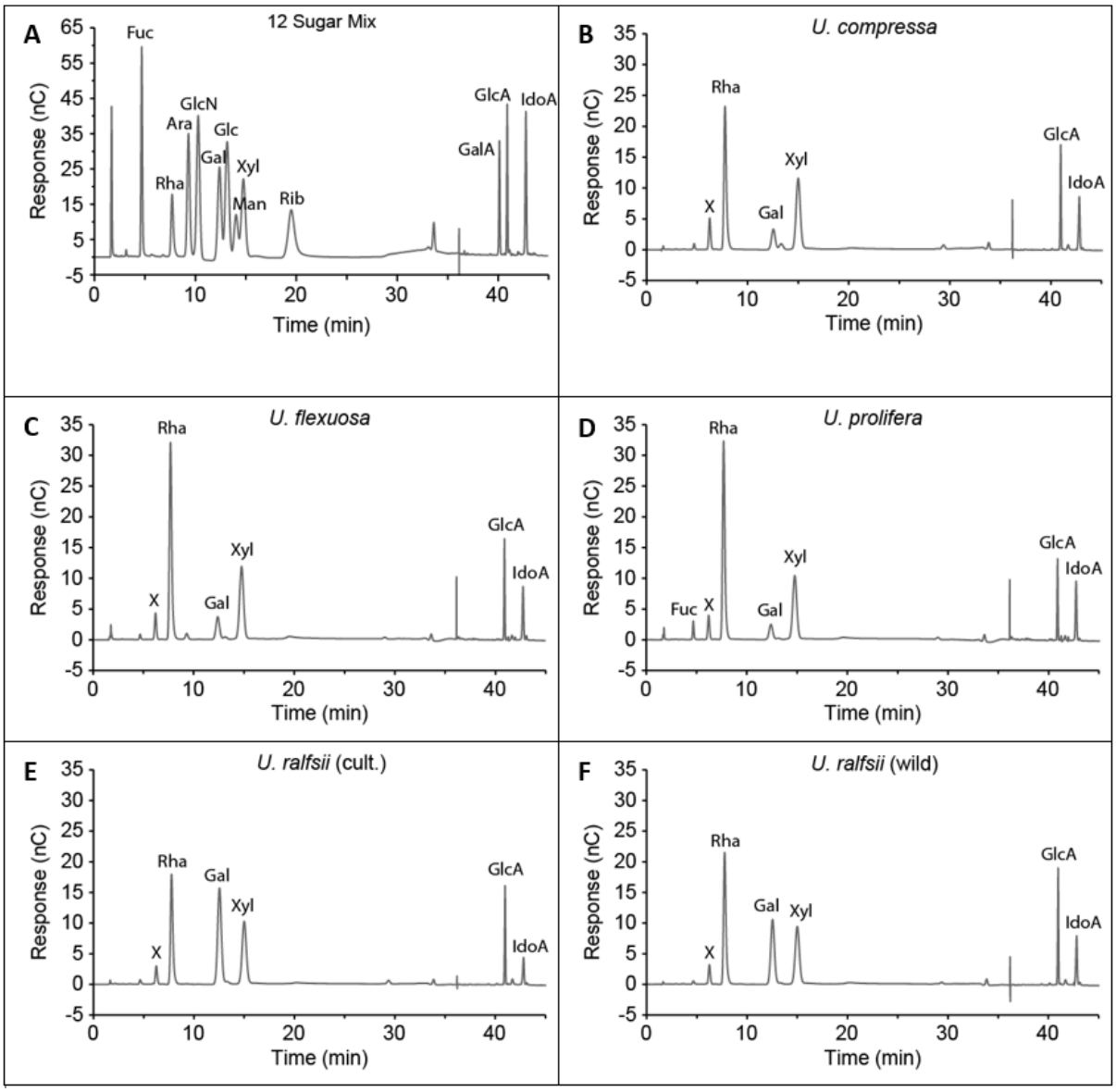

App. 7.2.6: HPAEC-PAD chromatograms for (**A**) a 12 sugar monosaccharide standard mix and purified ulvans from *Ulva* (**B**) *compressa*, (**C**) *flexuosa*, (**D**) *prolifera*, (**E**) *ralfsii* (cult.), (**F**) *ralfsii* (wild). A consistent unknown peak that did not match a known standard has been labelled "X". Rha = rhamnose; GlcA = glucuronic acid; Xyl = Xylose; IdoA = iduronic acid; Fuc = fucose; Gal = galactose; Glc = glucose; Rib = ribose; Fuc = fucose; Ara = arabinose; GlcN = glucosamine; Man = mannose; GalA = galacturonic acid.

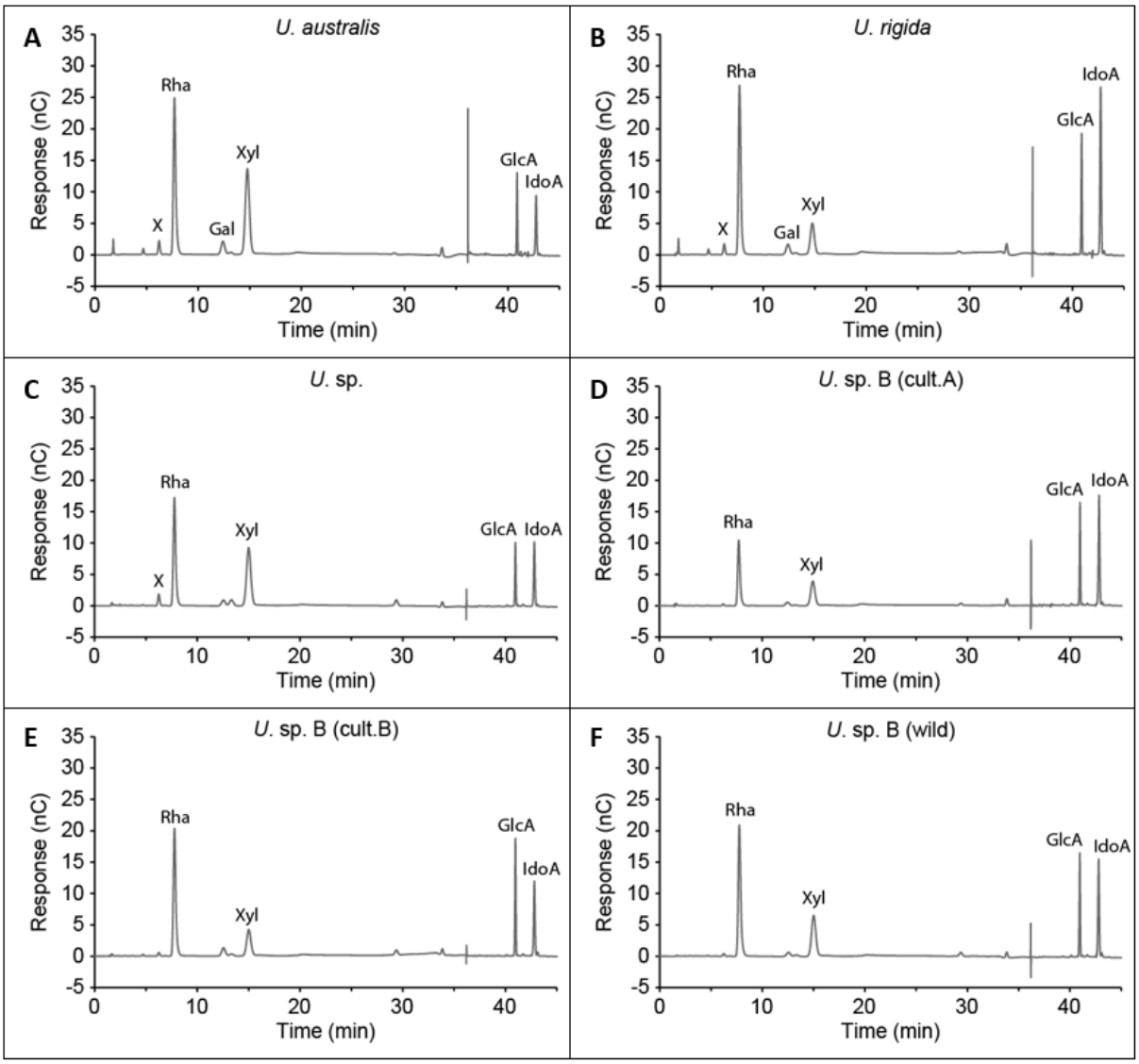

App. 7.2.7: HPAEC-PAD chromatograms for purified ulvans from *Ulva* (**A**) *australis*, (**B**) *rigida*, (**C**) sp., (**D**) sp. B (cult.A), (**E**) sp. B (cult.B), (**F**) sp. B (wild). A consistent unknown peak that did not match a known standard has been labelled "X". Rha = rhamnose; GlcA = glucuronic acid; Xyl = Xylose; IdoA = iduronic acid; Fuc = fucose; Gal = galactose; Glc = glucose; Rib = ribose; Fuc = fucose; Ara = arabinose; GlcN = glucosamine; Man = mannose; GalA = galacturonic acid.

App. 7.2.8: FTIR adsorption wavenumber assignments of the important bonds for ulvan.

Assignment	**Wavenumber (cm^{-1})**	**References**
V_{as} C=O	1650-1600	Robic, Bertrand, Sassi, Lerat, & Lahaye, 2009; Yaich *et al.*, 2017
V_s C=O	1425-1400	Robic, Bertrand, Sassi, Lerat, & Lahaye, 2009; Yaich *et al.*, 2017
V_{as} S=O	1260-1215	Pengzhan *et al.*, 2003; Ray & Lahaye, 1995; Yaich *et al.*, 2017
C-O-H, C-O-C	1055	Pengzhan *et al.*, 2003; Robic, Bertrand*, et al.*, 2009; Zhang *et al.*, 2010
C-O-S	850-835; 795-785	Pengzhan *et al.*, 2003; Ray & Lahaye, 1995; Yaich *et al.*, 2017

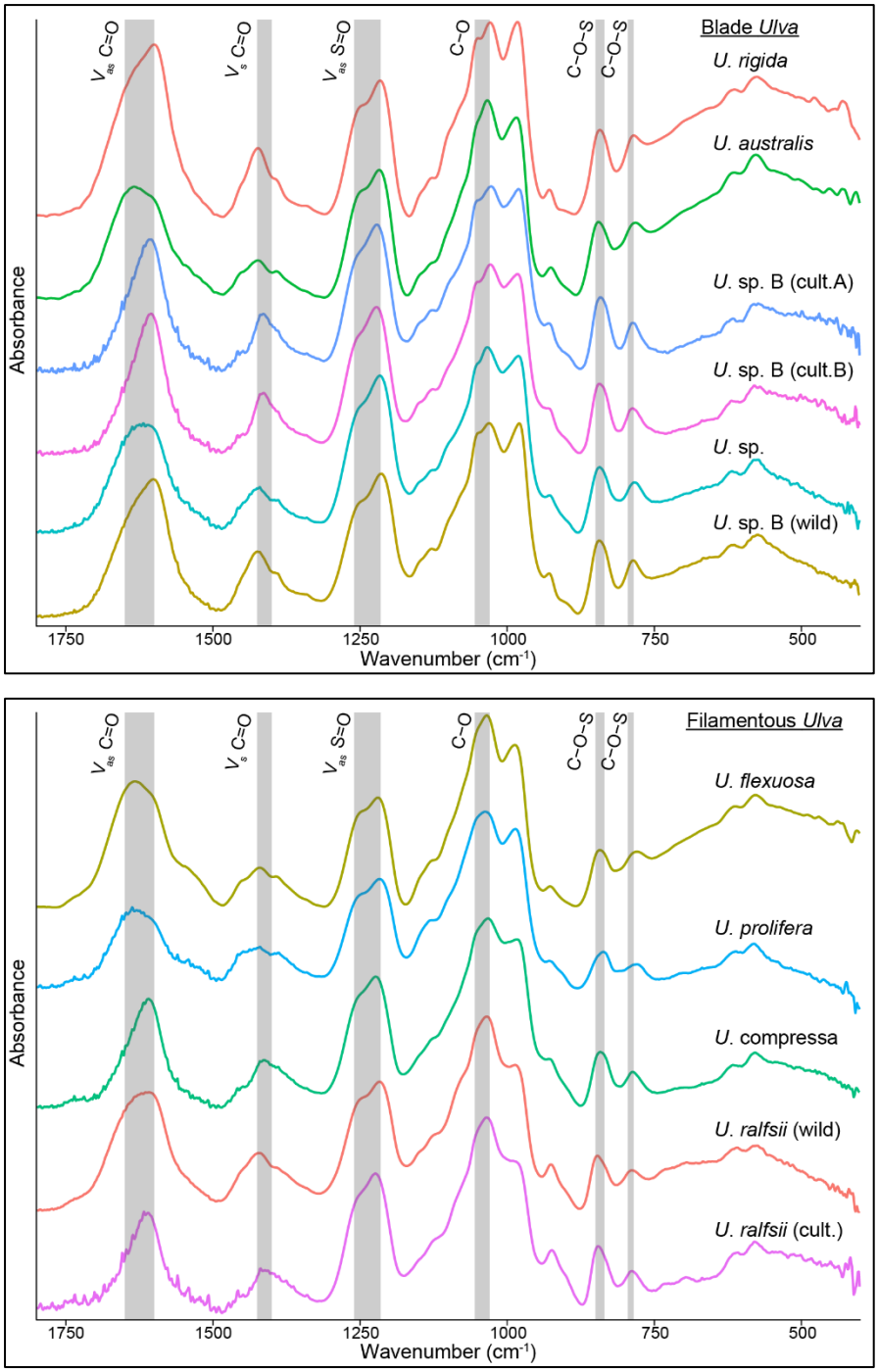

App. 7.2.9: FTIR spectroscopy of purified ulvans isolated from blade (top) and filamentous (bottom) species of *Ulva* in the spectral region of 1800-400 cm^{-1}. Literature defined regions of ulvan fingerprint region overlaid – see App. 7.2.8 (above) and section 3.2.4.1of paper for details.

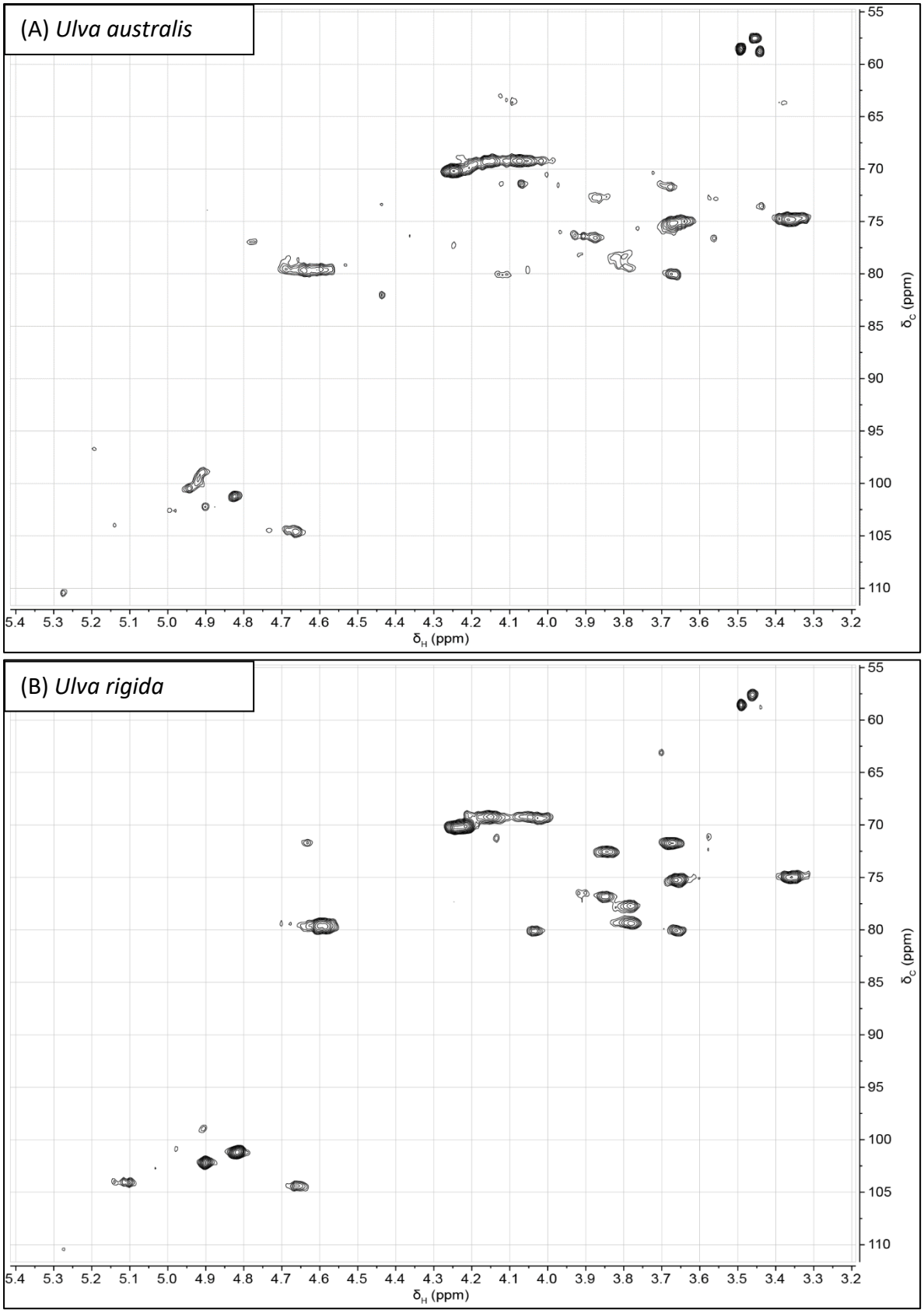

App. 7.2.10: ^{1}H-^{13}C HSQC spectra of purified ulvan isolated from (A) *Ulva australis* and (B) *Ulva rigida*. Chemical shifts relative to acetone at 31.45 and 2.225 ppm for ^{13}C and ^{1}H, respectively.

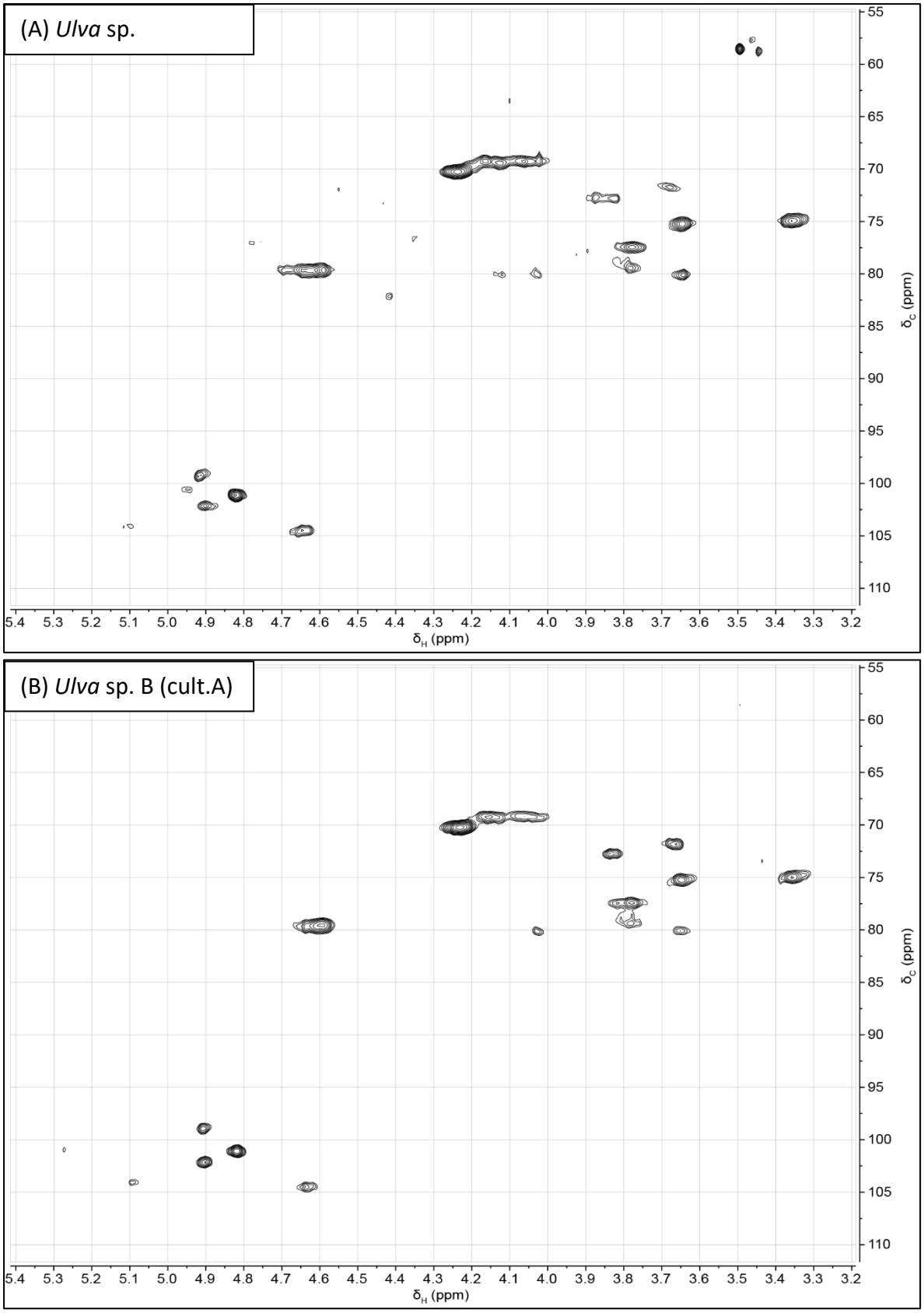

App. 7.2.11: ^{1}H-^{13}C HSQC spectra of purified ulvan isolated from (A) *Ulva* sp. and (B) *Ulva* sp. B (cult.A). Chemical shifts relative to acetone at 31.45 and 2.225 ppm for ^{13}C and ^{1}H, respectively.

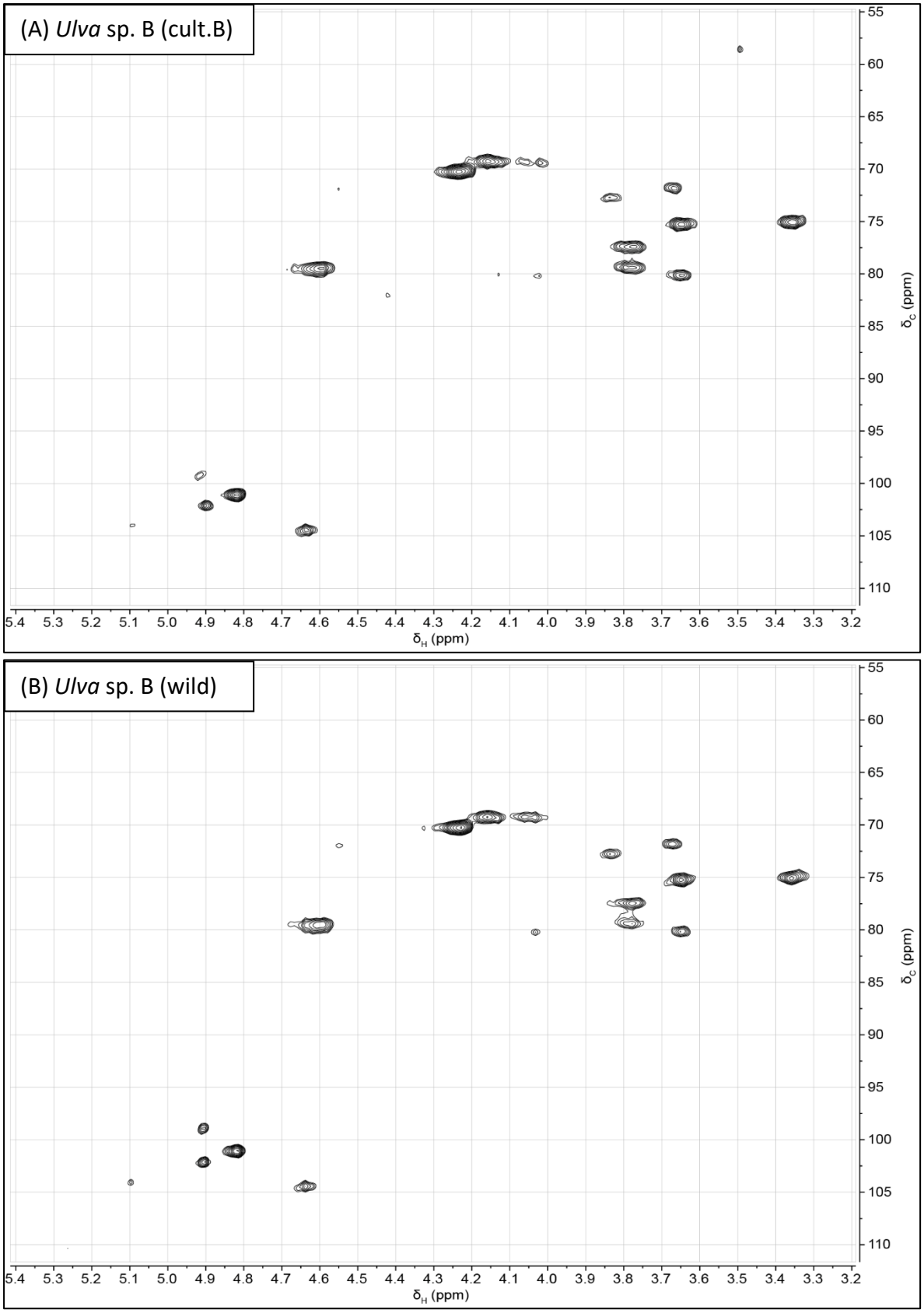

App. 7.2.12: ^{1}H-^{13}C HSQC spectra of purified ulvan isolated from (A) *Ulva* sp. B (cult.A) and (B) *Ulva* sp. B (wild). Chemical shifts relative to acetone at 31.45 and 2.225 ppm for ^{13}C and ^{1}H, respectively.

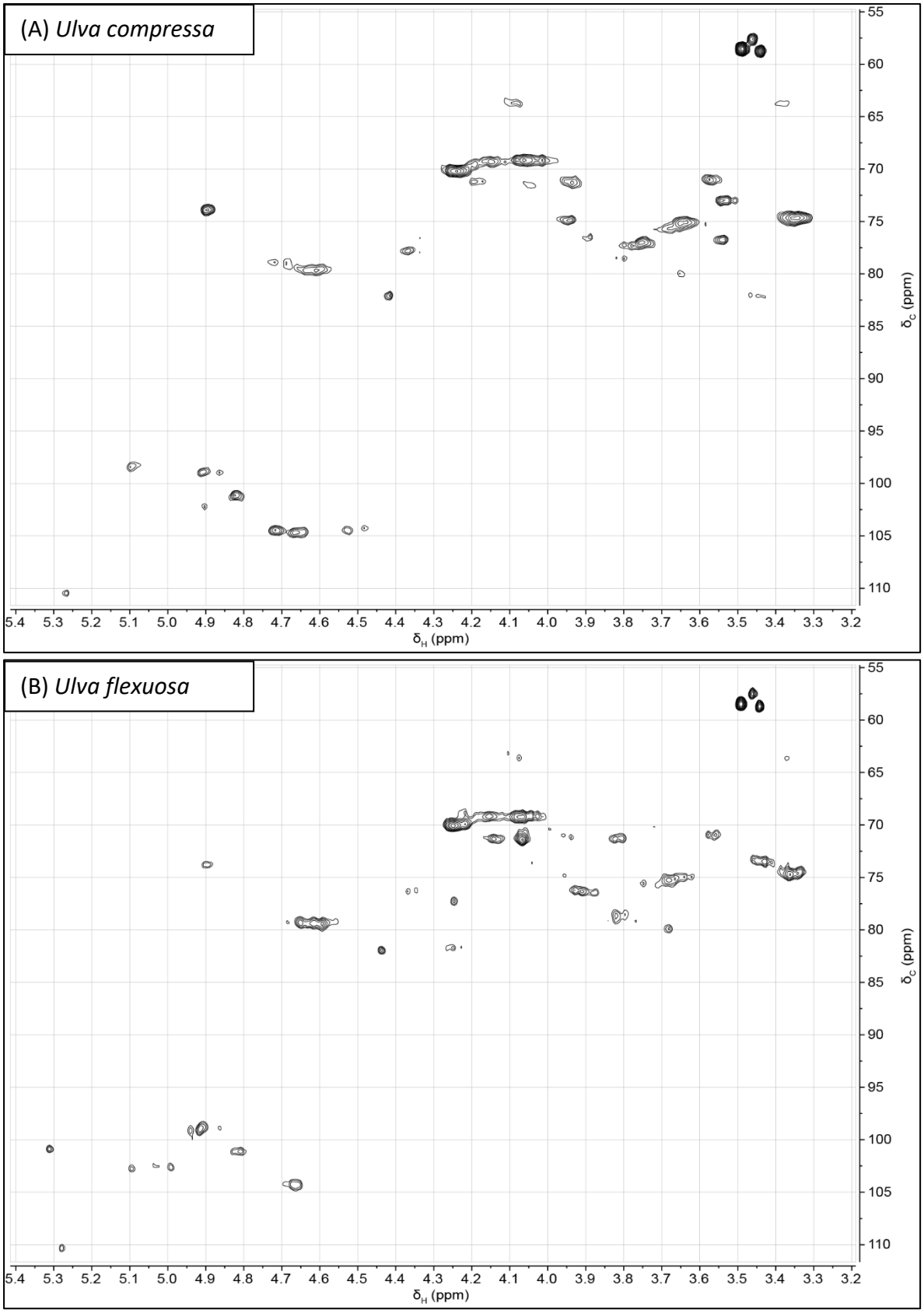

App. 7.2.13: ^{1}H-^{13}C HSQC spectra of purified ulvan isolated from (A) *Ulva compressa* and (B) *Ulva flexuosa*. Chemical shifts relative to acetone at 31.45 and 2.225 ppm for ^{13}C and ^{1}H, respectively.

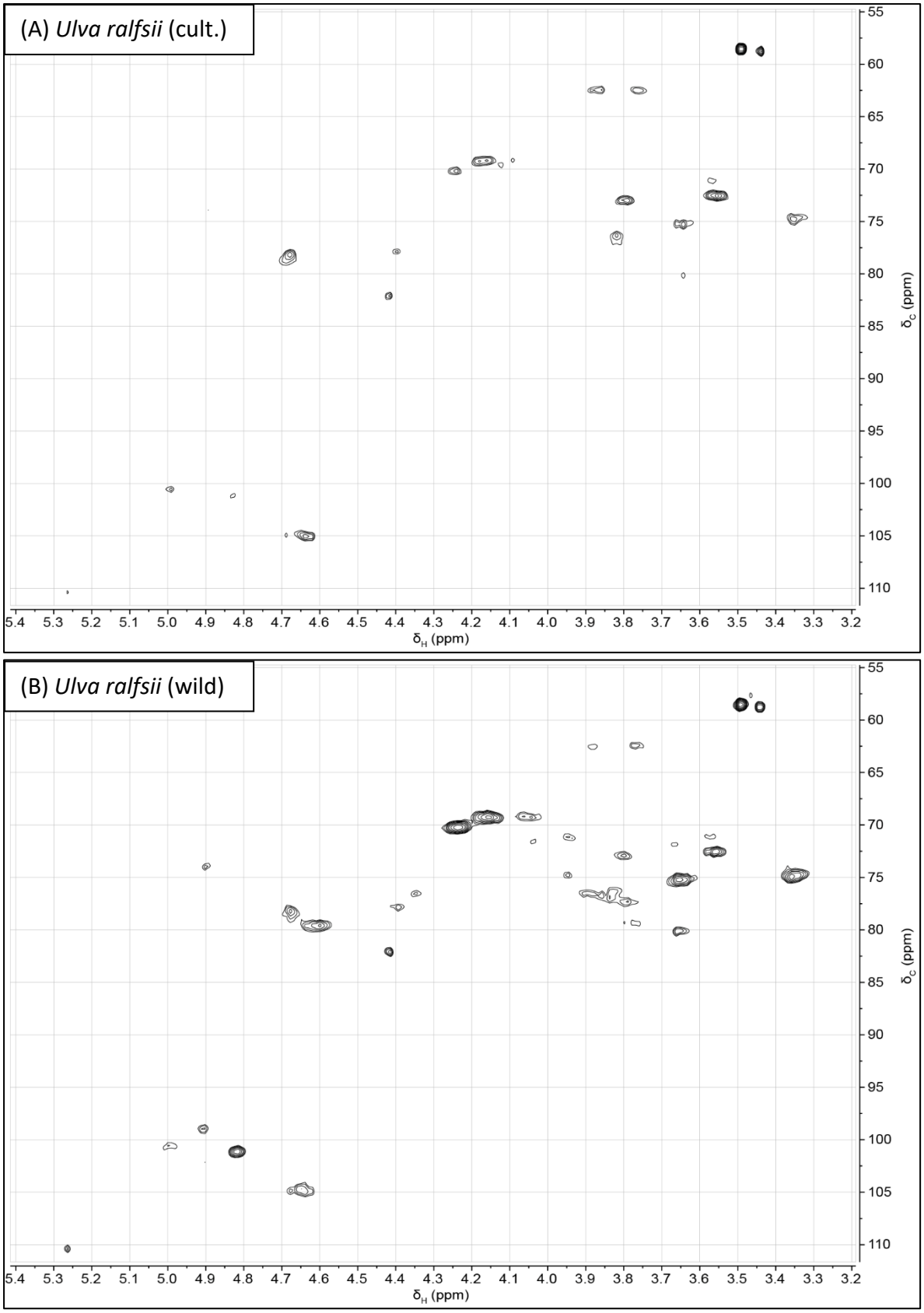

App. 7.2.14: ^{1}H-^{13}C HSQC spectra of purified ulvan isolated from (A) *Ulva ralfsii* (cult.) and (B) *Ulva ralfsii* (wild). Chemical shifts relative to acetone at 31.45 and 2.225 ppm for ^{13}C and ^{1}H, respectively.

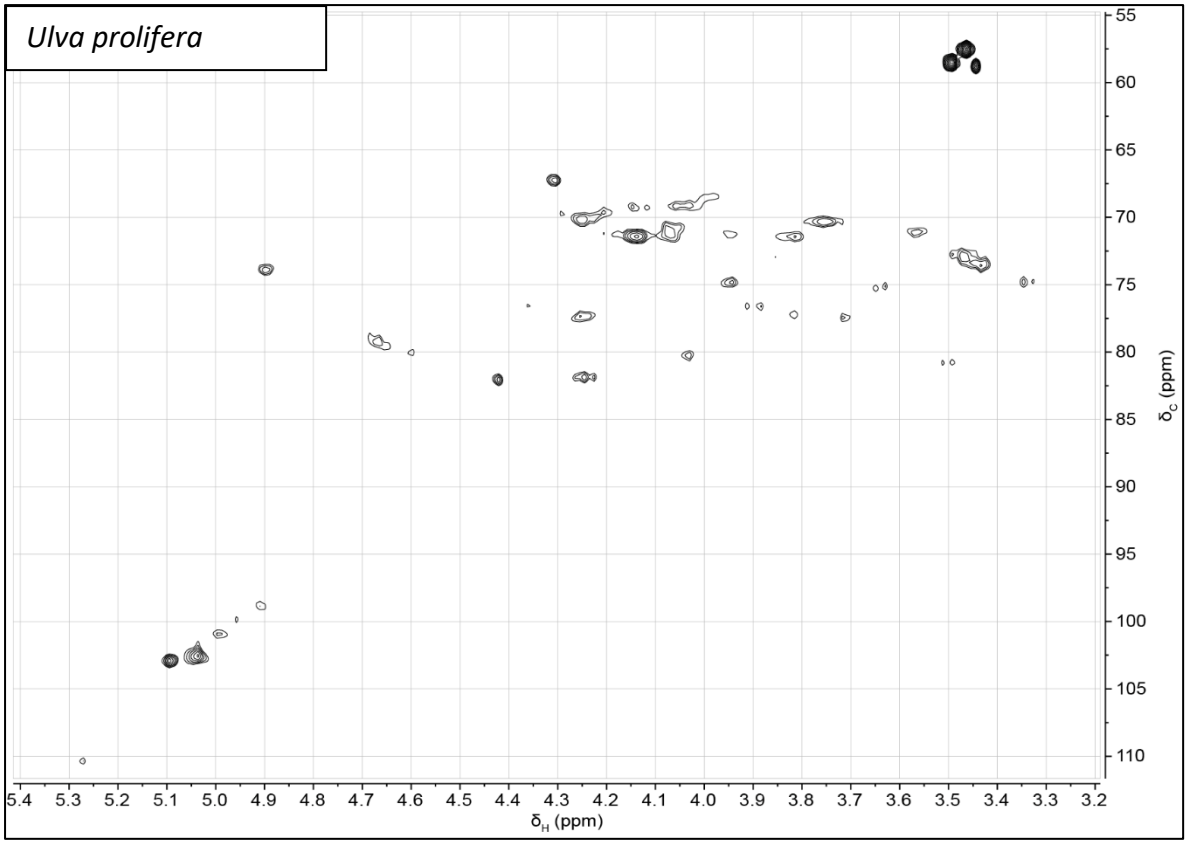

App. 7.2.15: ^{1}H-^{13}C HSQC spectra of purified ulvan isolated from *Ulva prolifera*. Chemical shifts relative to acetone at 31.45 and 2.225 ppm for ^{13}C and ^{1}H, respectively.

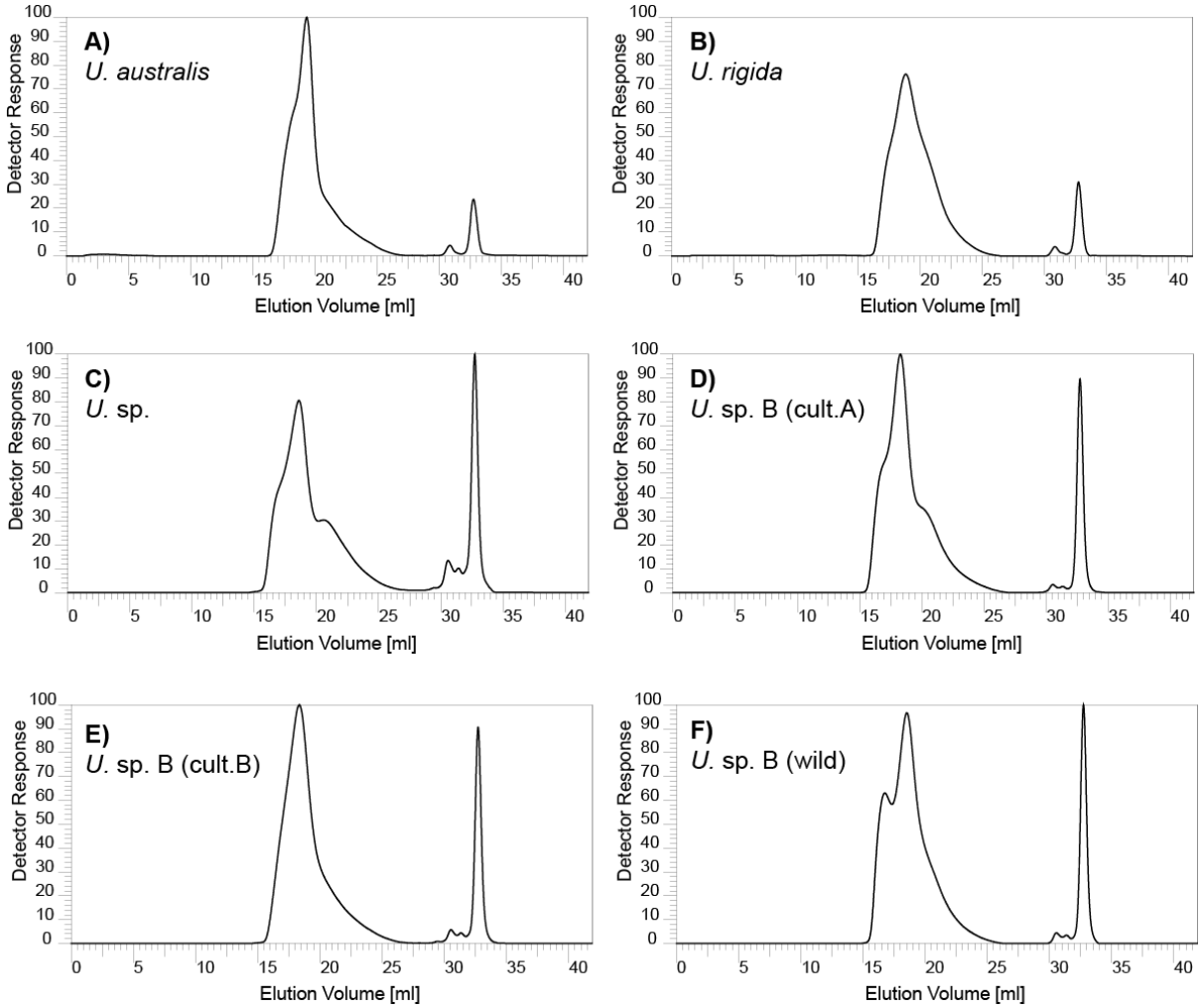

App. 7.2.16: RI traces from SEC-MALLS on purified ulvans from blade species. Chromatography system total volume (V_t) of 32 mL and void volume (V_0) of 15 mL.

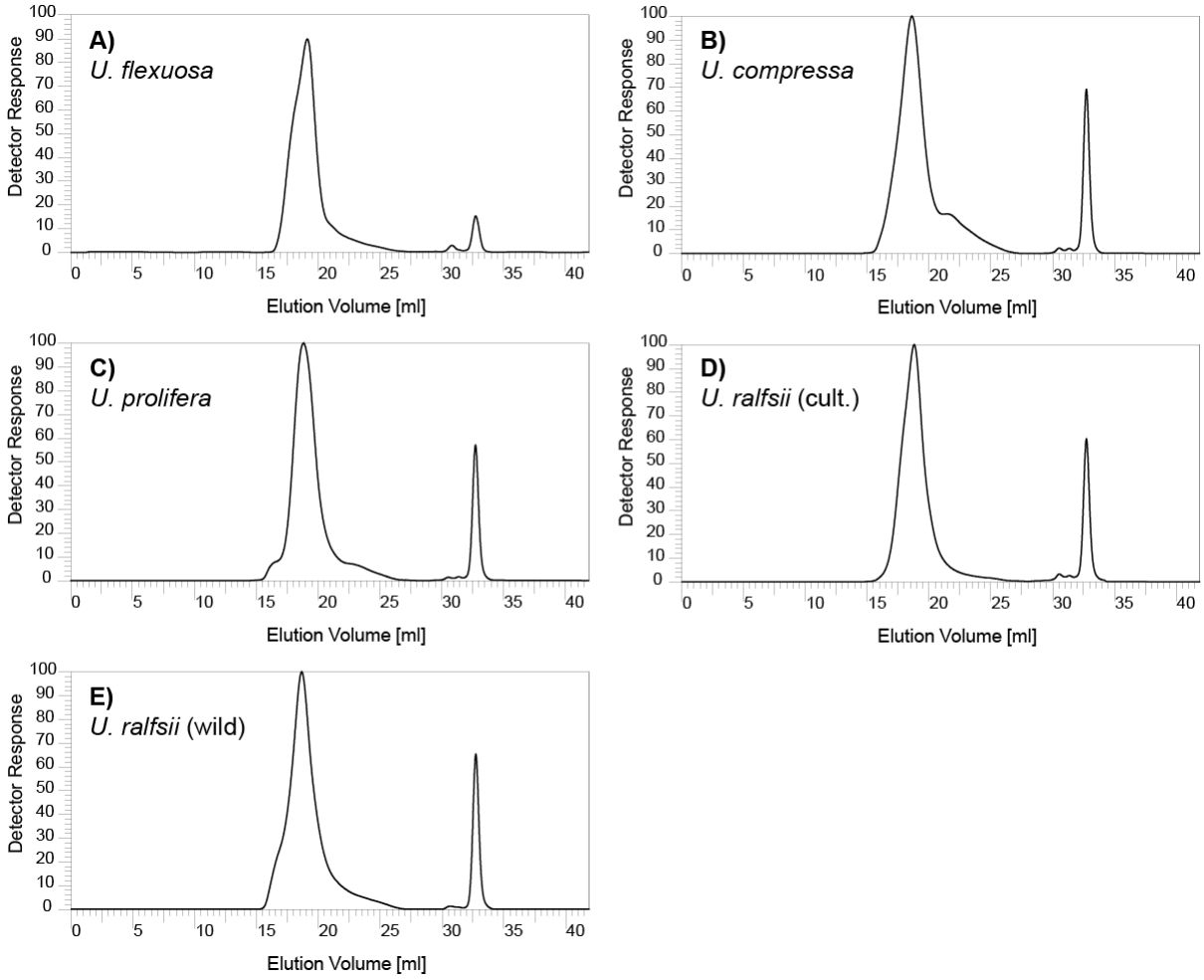

App. 7.2.17: RI traces from SEC-MALLS on purified ulvans from filamentous species. Chromatography system total volume (V_t) of 32 mL and void volume (V_0) of 15 mL.

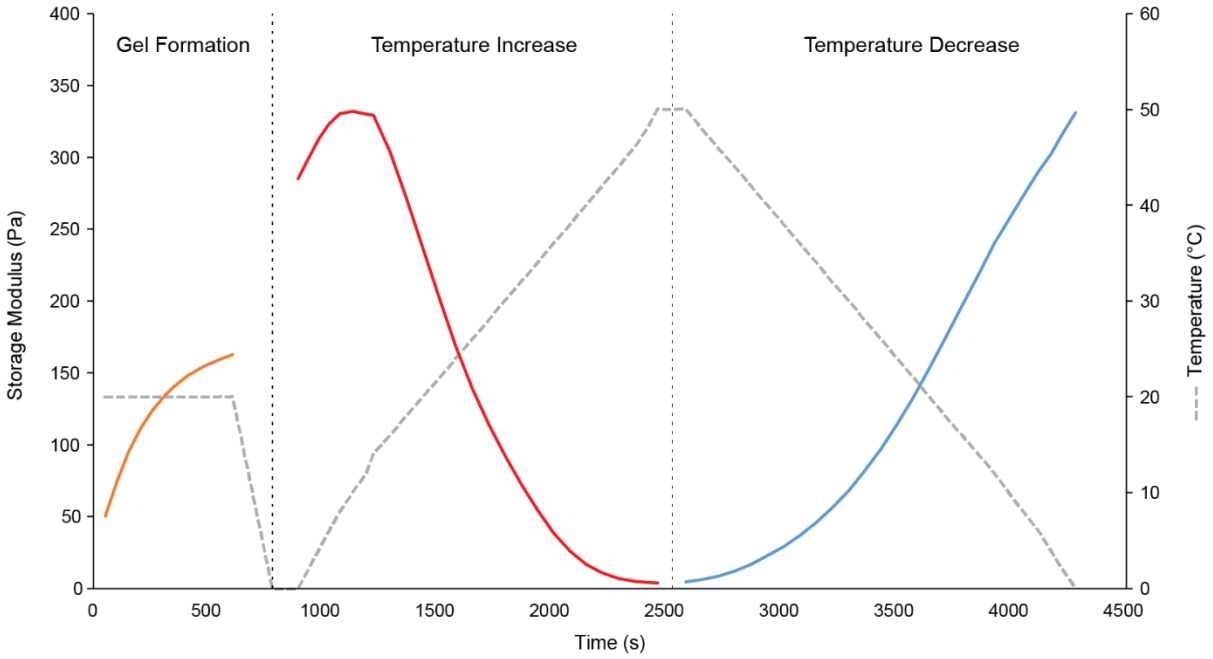

App. 7.2.18: The thermal reversibility of crude ulvan from *Ulva prolifera*. The storage modulus (left y-axis) is shown in solid coloured lines progressing through formation of the gel (orange), a linear temperature increase from 0 to 50 °C (red) and linear temperature decrease from 50 back to 0 °C. The temperature (right y-axis) through the experiment duration is displayed in the dashed grey line.

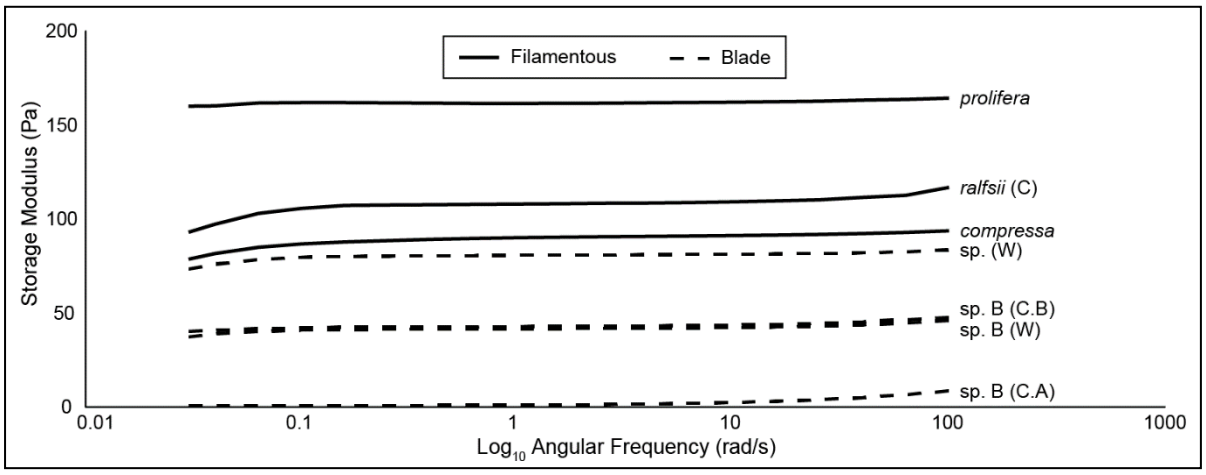

App. 7.2.19: Storage modulus (gel strength) of crude ulvans in response to a range of rheometer angular frequencies (deformation). Solid lines and dashed lines represent ulvans from filamentous and blade *Ulva* species, respectively.

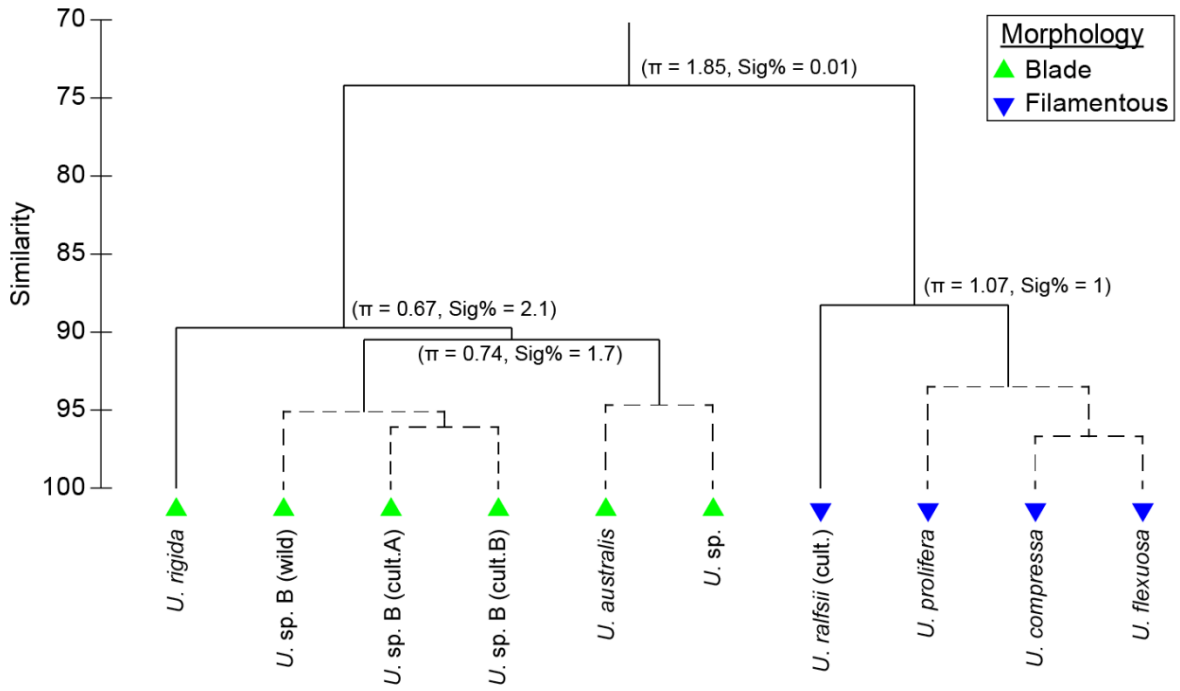

App. 7.2.20: Complete linkage cluster analysis of ulvan data set used to produce MDS and run PERMANOVA on. Square-root transformed data were analysed in a Bray-Curtis similarity matrix. SIMPROF test (20,000 permutations for mean; 9999 permutations for simulation; significance level: 5 %) found several significant clusters as indicated by solid lines. Pi statistic and significance % are present at dividing of a significant cluster. Dashed lines indicate non-significant clusters.

App. 7.2.21: Correlation matrix of ulvan rheological properties and possibly related composition metrics. Correlations performed on mol% constituent sugars and % w/w sulfur and sulfate. Red indicates significant Pearson's correlation with alpha of 0.05. Data for *Ulva ralfsii* (wild) have been removed as the storage modulus of this ulvan is an outlier and skews the correlations (see App. 7.2.22 below).

	Storage modulus	Viscosity	Mw	Mn	Rha	GlcA	Xyl	IdoA	Gal	Protein	Sulfur	Sulfate
Storage mod.	1.0											
Viscosity	-0.4	1.0										
Mw	0.8	-0.3	1.0									
Mn	0.8	-0.3	0.9	1.0								
Rha	-0.1	-0.2	-0.3	-0.2	1.0							
GlcA	-0.3	0.6	-0.1	-0.1	-0.5	1.0						
Xyl	0.4	-0.6	0.4	0.3	0.0	-0.8	1.0					
IdoA	-0.8	0.5	-0.8	-0.8	0.0	0.4	-0.7	1.0				
Gal	0.7	0.0	0.8	0.7	-0.7	0.2	0.1	-0.5	1.0			
Protein	0.2	-0.5	0.5	0.5	0.1	-0.4	0.6	-0.5	0.1	1.0		
Sulfur	-0.2	-0.0	-0.3	-0.4	-0.3	-0.2	0.4	-0.0	0.1	0.0	1.0	
Sulfate	-0.6	-0.0	-0.6	-0.8	0.2	-0.2	0.2	0.4	-0.5	-0.0	0.6	1.0

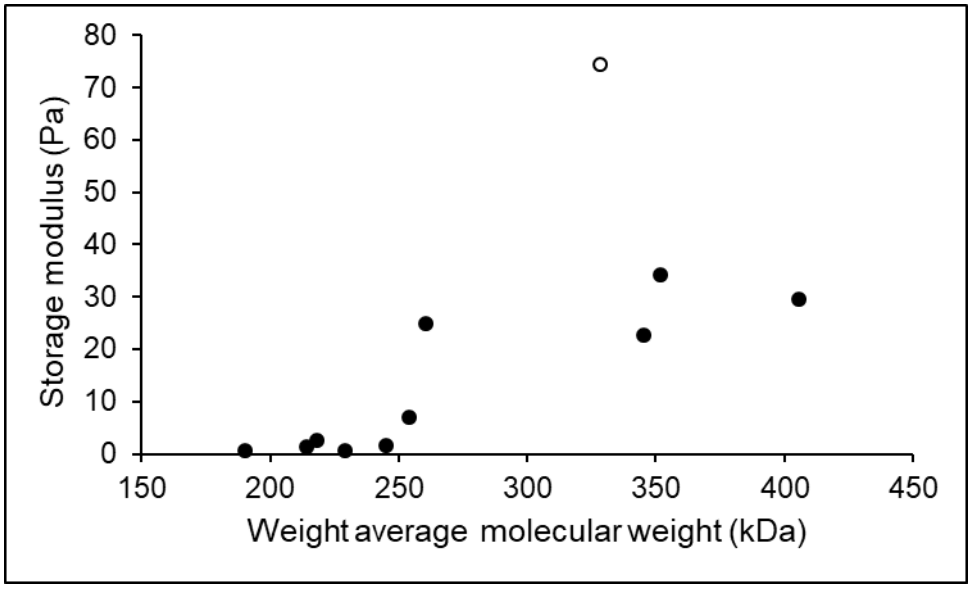

App. 7.2.22: Scatter plot of storage modulus (gel strength) and weight average molecular weight (Mw) of purified ulvans. The storage modulus of ulvan from *Ulva ralfsii* (wild), the open circle, is considered an outlier and excluded from the correlation analysis.

7.3 Chapter 5 supporting information

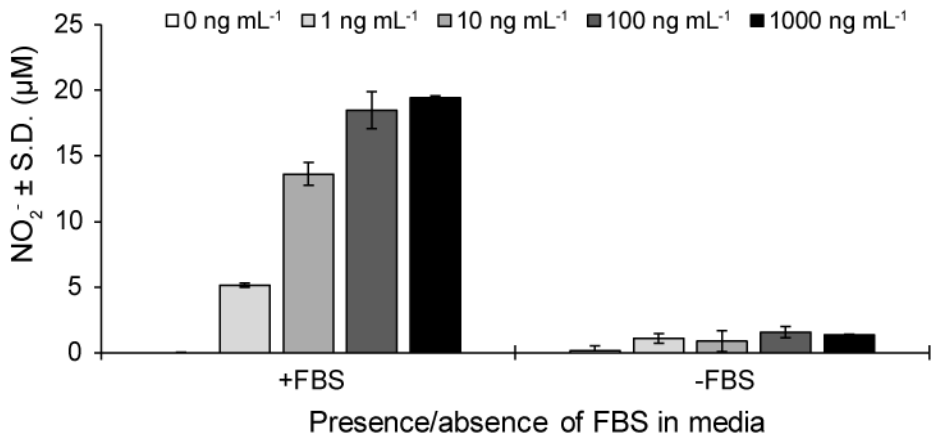

App. 7.3.1: The concentration of NO_2^- secreted into cell culture media in response to a range of lipopolysaccharide (LPS) concentrations (0, 1, 10, 100, 1000 ng mL^{-1}) in the presence or absence of foetal bovine serum (FBS) in the culture media during the assay. RAW264.7 cells seeded at $3x10^5$ cells mL^{-1} in 24-well plates; cells incubated in 100 % humidity and 5 % CO_2 for 16 h to allow for adherence and 24 h following addition of LPS; Dulbecco's modified eagle medium (DMEM) with HEPES buffer and pen/strep with or without 10 % FBS used as media. NO_2^- concentration measured by Griess reagent with absorbance at 540 nm.

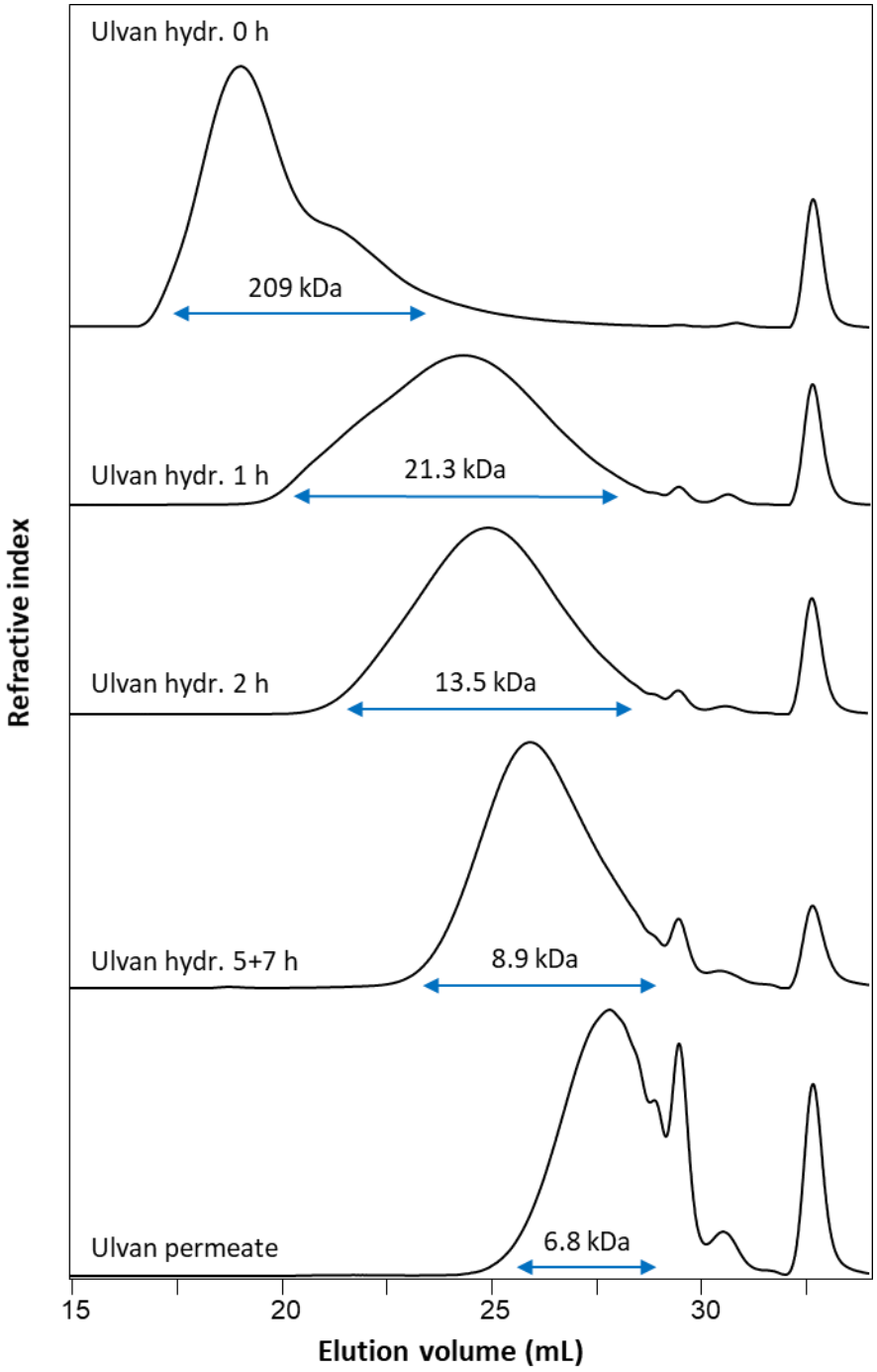

App. 7.3.2: SEC-HPLC-RI chromatograms of the native ulvan, partially hydrolysed fractions and the permeate showing the weight average molecular weights determined by MALLS.

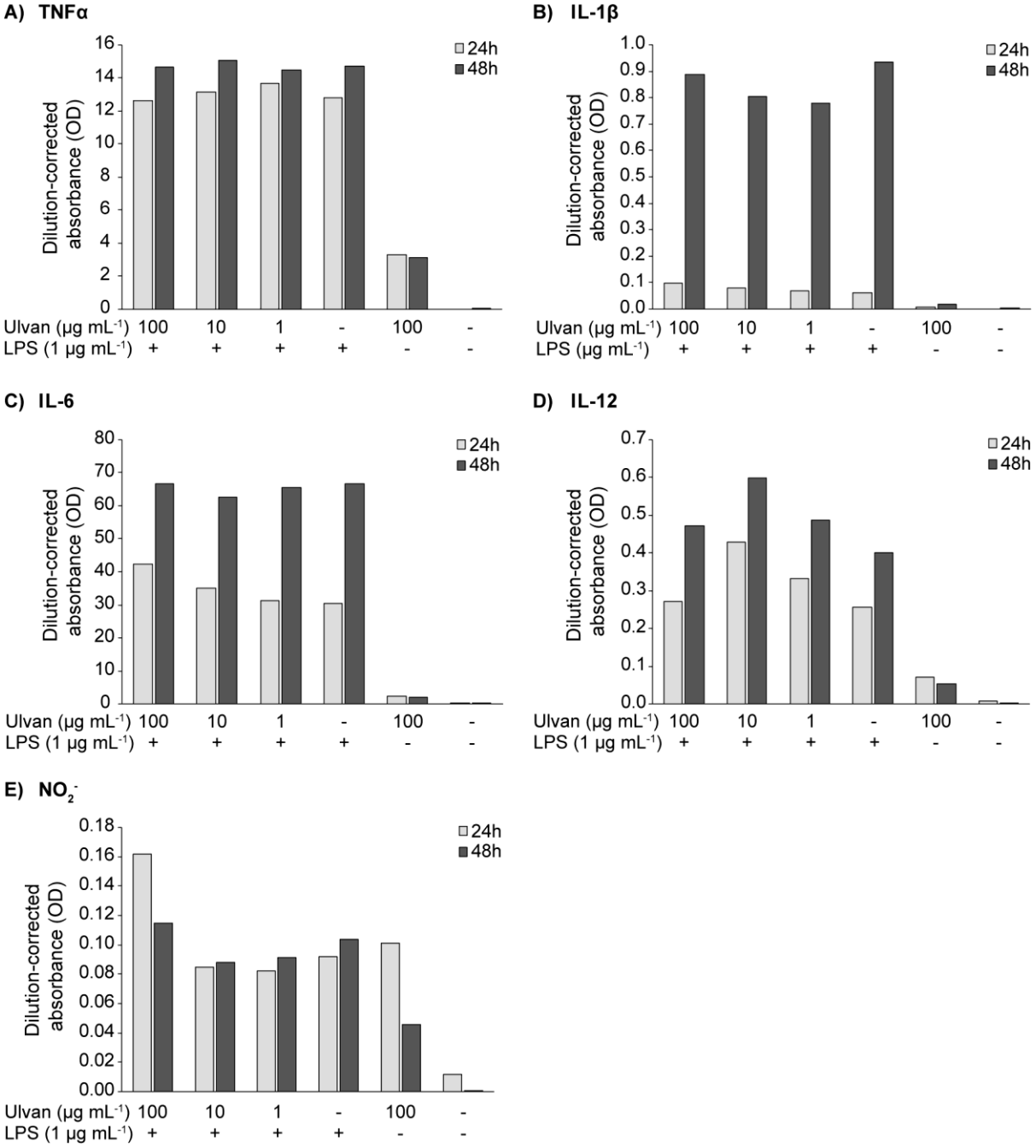

App. 7.3.3: Cytokines secreted into RAW264.7 supernatant following exposure to ulvan of varying concentrations (-, 1, 10 or 100 µg mL^{-1}) in the presence (+) or absence (-) of 1 µg mL^{-1} of LPS for 24 and 48 hours. Absorbance for TNFα **(A)**, IL-1β **(B)**, IL-6 **(C)** and IL-12 **(D)** were determined by enzyme-linked immunosorbent assay (ELISA); absorbance for NO_2^- **(E)** determined by addition of Griess reagent. Absorbance presented as dilution-corrected units (i.e. absorbance multiplied by the dilution factor of the supernatant required to enable spectrophotometric analysis). RAW264.7 cells seeded at $3x10^5$ cells mL^{-1} in 96-well plates; cells incubated in 100 % humidity and 5 % CO_2 for 16 h to allow for

adherence and 24 or 48 h following addition of ulvan and LPS; Dulbecco's modified eagle medium (DMEM) with HEPES buffer, pen/strep and 10 % foetal bovine serum (FBS) used as media.

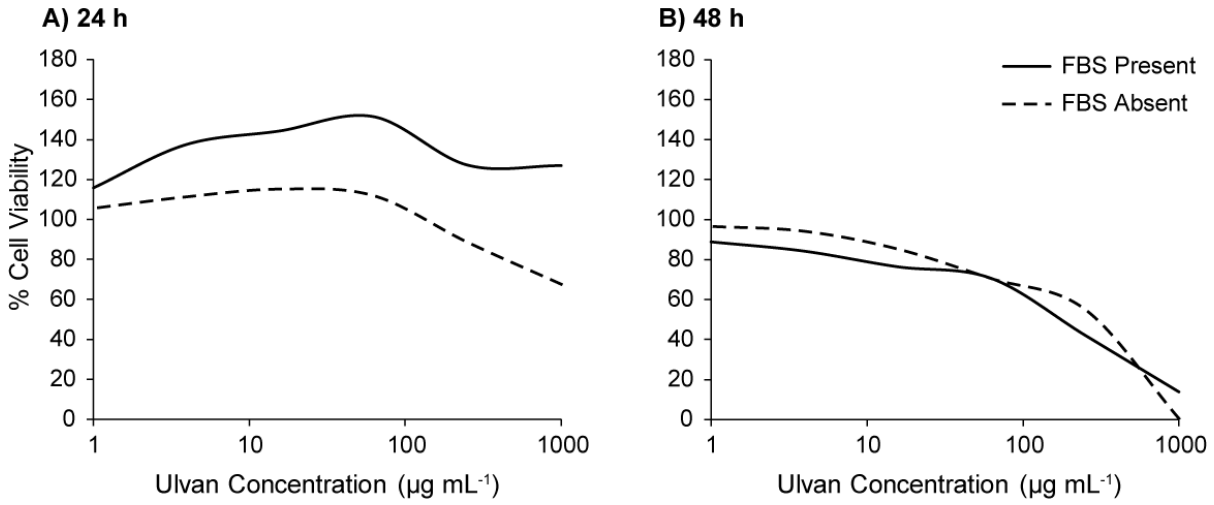

App. 7.3.4: The effect of foetal bovine serum (FBS) during cytotoxic assessment of ulvan on RAW264.7 cells. Cell proliferation was measured after incubation with U209 ulvan at concentrations of 1-1000 µg mL^{-1} in the presence or absence of 10 % FBS for (A) 24 h and (B) 48 h. It was concluded that FBS was required for accurate ulvan cytotoxicity data, and that a dose-dependent increase in cytotoxic effect of high concentration ulvan through time was present.

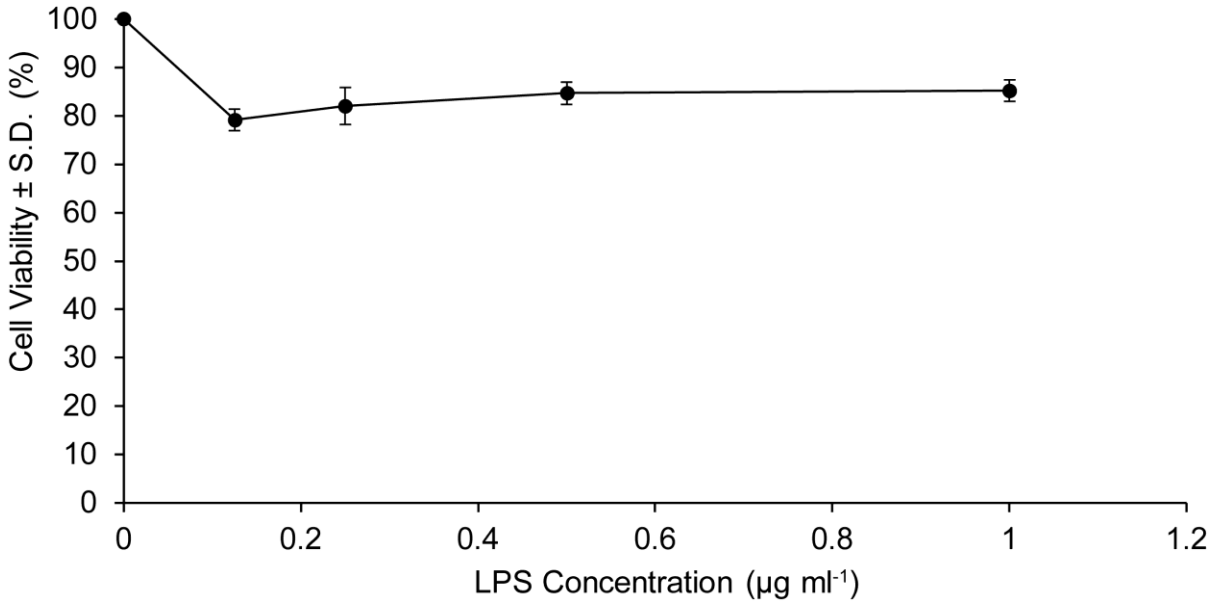

App. 7.3.5: The effect of LPS on the viability of RAW264.7 cells. RAW264.7 cells were seeded in 24 well plates at a density of $5x10^5$ cells/well and allowed to adhere for 17 h before 0, 0.125, 0.25, 0.5 or 1 µg mL^{-1} LPS was added and cells were incubated for a further 24 h. Cells were cultured in Dulbecco's modified eagle medium (DMEM) with HEPES buffer and pen/strep. Cell proliferation was measured using 10 % PrestoBlue reagent following 60 min incubation.

7.4 Chapter 2 publication

Title: Ulvan: A systematic review of extraction, composition and function

Journal: Algal Research 39:101422

DOI: https://doi.org/10.1016/j.algal.2019.101422

Published: 01/05/2019

Scopus citations as of 16/04/2021: 67

Notes: This publication is the second most cited paper in Algal Research published in the last 4 years

Algal Research 39 (2019) 101422

Contents lists available at ScienceDirect

Algal Research

journal homepage: www.elsevier.com/locate/algal

Review article

Ulvan: A systematic review of extraction, composition and function

Joel T. Kidgell[a,*], Marie Magnusson[b], Rocky de Nys[a], Christopher R.K. Glasson[b]

[a] MACRO – The Centre for Macroalgal Resources and Biotechnology, College of Science and Engineering, James Cook University, Townsville, Australia
[b] School of Science, University of Waikato, Tauranga, New Zealand

ARTICLE INFO

Keywords:
Biotechnology
Green algae
Bioactivity
Sulfated polysaccharides
Seaweed

ABSTRACT

Species of green macroalgae (Chlorophyta) of the genus *Ulva* are edible seaweeds with a range of health promoting bioactive components. *Ulva* is high in dietary fibre which promotes gastrointestinal health and is linked to a reduction in the incidence of chronic diseases. The fundamental active constituent of *Ulva* is the soluble fibre ulvan, a gelling sulfated polysaccharide with biological activities including immunomodulating, antiviral, antioxidant, antihyperlipidemic and anticancer. Ulvan also has the capacity to modulate cellular signalling processes in both plant and animal systems leading to beneficial effects on productivity and health. Consequently, ulvan is of significant interest as a constituent in human health, agricultural, and biomaterial products. This comprehensive systematic review investigates and recommends acid extraction, ultrafiltration, sugar constituent and molecular weight analysis for the extraction, purification, and characterisation of ulvan, respectively. The biological activities of ulvans are then critically reviewed.

1. Introduction

Species of green seaweed from the genus *Ulva* have high growth rates and productivities across diverse geo-climatic conditions, with highly exploitable biochemical profiles [1–4]. As a consequence, species of *Ulva* can result in the formation of problematic "green tides" [5–9]. Therefore, they are well suited for cultivation, in particular for use in the bioremediation of nutrient rich wastewater from intensive land-based aquaculture [10–12]. Importantly, cultivation, as opposed to natural harvesting, can produce a high-quality monoculture of *Ulva* biomass, which can then generate high-quality bioproducts of consistent composition. One of the major bioproducts of interest from *Ulva* is the sulfated polysaccharide known as ulvan.

Ulvan is a cell wall polysaccharide that contributes from 9 to 36% dry weight of the biomass of *Ulva* and is mainly composed of sulfated rhamnose, uronic acids (glucuronic acid and iduronic acid) and xylose [13–21]. Species of *Ulva* have three other cell wall polysaccharides (cellulose, xyloglucan, and glucuronan), which with ulvan collectively account for up to 45% of the dry weight biomass [22]. Like ulvan, xyloglucan and glucuronan are also soluble polysaccharides but are only relatively minor constituents of the cell wall polysaccharides [14,23–25]. Interestingly, of the four cell wall polysaccharides present within *Ulva*, ulvan is the only one to contain both rhamnose and iduronic acid [16]. Rhamnose is of interest for its effect on biosynthetic pathways in the dermis [26–28] and on plant immunity [29–31]. Uronic acids (glucuronic and iduronic acids) and their sulfate esters are important constituents in mammalian glycosaminoglycans (GAGs) (e.g., heparin, heparan sulphate, and dermatan sulfate). Like GAGs, ulvan has a repeating disaccharide structure predominantly comprised of an uronic acid linked to a sulfated neutral sugar and is, therefore, a candidate for the modulation of processes and functions carried out by mammalian polysaccharides [16,32,33]. In this regard, ulvan has potential applications in biomaterial science (wound dressings, tissue engineering, biofilm prevention, and excipients), nutraceuticals (antiviral, antioxidant, antihyperlipidemic, anticancer and immunostimulatory), functional foods and agriculture, as outlined in reviews by Venkatesan *et al.* [34], Cunha and Grenha [35], Alves *et al.* [36], Lahaye and Robic [13], and Wijesekara *et al.* [37]. The biological activities of polysaccharides, including ulvan, are directly related to their chemical structure. It is, therefore, important to understand how extraction, isolation and purification procedures affect the chemical structure of the extracted polysaccharide, and as a consequence its biological activity.

This review evaluates research on ulvan with a focus on extraction and purification methods, and its biological activity and potential applications. In preparing this comprehensive, systematic review, a meta-analysis was conducted on publications identified from the search string "(Ulvan* OR ((sulfate* OR sulphate*) AND polysaccharide* AND (Ulva OR Enteromorpha)))" through Scopus and Web of Science on 13th of December 2017 (see supplementary material for methods and

* Corresponding author.
E-mail address: joel.kidgell@my.jcu.edu.au (J.T. Kidgell).

https://doi.org/10.1016/j.algal.2019.101422
Received 27 September 2018; Received in revised form 15 January 2019; Accepted 16 January 2019

full access to metadata). This analysis provides a summary of the chemical structures of ulvans from different sources and the methods used to assess them, as well as providing the biological activity of ulvan, and, where possible, their relative efficacies and mechanisms of action. As a consequence, the review is divided into two major sections. Section 2 describes in detail the chemistry of ulvan, providing an overview of its physicochemical properties, extraction and purification techniques and recommended characterisation for biological activity studies. Section 3 then provides an overview of the biological activities of ulvans with a focus on the mechanistic and structural features involved. Note that in line with current nomenclature convention *Enteromorpha* is referred to as *Ulva* throughout the review [38].

2. Chemistry of ulvans

2.1. Chemical structure of ulvans

The macromolecular properties (e.g., conformation) of polysaccharides are influenced by their primary structure, which is determined by their sugar constituents and the order in which they occur, their glycosidic linkages, degree of branching, molecular weights, and the presence of functional groups, such as sulfate esters, methyl ethers, amides and amines. These structural features then determine the physicochemical properties and the biological activities of the polysaccharide. In this regard, ulvans are polyanionic heteropolysaccharides with sugar compositions that are predominantly rhamnose (45.0 mol%), glucuronic acid (22.5 mol%), iduronic acid (5.0 mol%), and xylose (9.6 mol%) (Median values, see Table 1). There is, however, a broad range in the composition of ulvan sugars reported for rhamnose (5.0–92.2 mol%), glucuronic acid (2.6–52.0 mol%), iduronic acid (0.6–15.3 mol%) and xylose (0.0–38.0 mol%) (Table 1; Fig. S2). The composition of ulvan depends on the source species, eco-physiology, and processing procedures used to prepare both biomass and ulvan (see Table 1). Compositional variation due to eco-physiological factors can then be magnified by different extraction and analytical techniques. Other monosaccharides are often reported in compositional data (e.g., glucose, galactose, arabinose, and mannose), however, their presence as a component of/or contaminant of ulvan is unclear.

The ulvan backbone is most commonly made up of α- and β-(1,4)-linked monosaccharides (rhamnose, xylose, glucuronic acid and iduronic acid) with characteristic repeating disaccharide units. [13,80–82]. The two major disaccharide repeating units are aldobiuronic acids, referred to as ulvanobiuronic acid (types A and B); minor disaccharide aldobioses, referred to as ulvanobioses (type U), are also found in ulvan (Fig. 1). Type A and B are far more common than U [13]. Ulvanobiuronic acid type A_{3s}, one of the most common disaccharide units, consists of β-D-glucuronic acid (1,4)-linked to α-L-rhamnose 3-sulfate, while in type B_{3s} α-L-iduronic acid (a C-5 epimer of glucuronic acid) is (1,4)-linked to α-L-rhamnose 3-sulfate [13,80,81,83]. Ulvanobiose U_{3s} consists of β-D-xylose (1,4)-linked to α-L-rhamnose 3-sulfate, while type $U_{2's,3s}$ consists of β-D-xylose 2-sulfate (1,4)-linked to α-L-rhamnose 3-sulfate [13,81]. While (1,4)-glycosidic linkages are the predominant bonds, (1,2)- and (1,3)-glycosidic linkages also occur [24,81]. In this regard, minor branching has been associated with glucuronic acid (1,2)-linked to the rhamnose residue of the ulvanobiuronic acid type A_{3s} [13,24]. However, there are indications that greater diversity in the structure of ulvan is likely [57,84]. For structural comparisons, a useful list of fully characterised ulvan oligosaccharides can be found in [13,24].

The conformation of ulvan in solutions is in part determined by composition and has been described using both molecular modelling and empirical evidence. Predictions of the conformation of ulvan using molecular modelling are impeded by the limited knowledge of the sequencing of the polysaccharide backbone, beyond the presence of its repeating disaccharide units, and the few longer oligosaccharides described [13,24,81,84,85]. However, theoretical calculations have determined that domains with repetitive sequences of any of the major disaccharide units (e.g., chains of A_{3s} or B_{3s}) can adopt secondary helical structures [41]. In practice the conformation of ulvan in solution is pH dependent and is also influenced by the presence of counter-ions. Due to the relative hydrophobicity of rhamnose and its overall effect on the solubility of ulvan in neutral and low pH aqueous solutions, ulvan folds into a condensed bead-like conformation [86]. In the presence of salts (e.g., NaCl) these beads aggregate. The bead conformation of ulvan reduces its intermolecular interactions resulting in the low viscosity of its solutions, as well as influencing gel strength and activity. In contrast, in high pH solutions (~13) ulvan has a more open conformation increasing the intermolecular interactions that give higher viscosities and greater gel strengths. The influence of pH over the solution properties of ulvans is a convenient mechanism by which to fine-tune its rheology to suit specific applications. Further discussion of gelling properties can be found in Lahaye and Robic [13].

While the mole ratio of constituent sugars in ulvan from a particular source and batch are defined, the molecular structure can be altered through depolymerisation and removal or addition of functional groups (e.g., sulfate esters). In this regard, molecular weights (1 - > 2000 kDa, Fig. 2b, d, f) and degree of sulfation (2.3–40%, Fig. S3) of ulvan extracts vary widely and have a large influence on physicochemical properties and biological activities. These structural features are also relatively easily manipulated and provide convenient methods for the investigation of structure-function relationships. Depolymerisation can be achieved through chemical [28,71,87–89] and enzymatic hydrolysis with ulvan lyases [23,77,90,91]. The degree of sulfation can be altered by addition of sulfate esters [49,92,93] or removal of sulfate esters by solvolysis of the ulvan pyridinium salt [55,72,94,95] or through base hydrolysis [91]. Charge can be altered through manipulation of the degree of sulfation and by derivatisation of the carboxylic acids groups (e.g., esterification and amide formation) [96,97]. Both the charge and the mole ratio of constituent sugars can be varied by reduction of glucuronic acid and iduronic acid to glucose and idose, respectively [94]. Indeed, covalent cross-linking groups can also be added to enhance gel formation and gel strength [98,99].

2.2. Extraction of ulvan

The quantitative yield and the quality of ulvan can vary significantly depending on the applied extraction and purification processes, the source of the biomass (species (Table 2), source as wild or cultivated, location) [36], storage of collected biomass, and pre-extraction processing [100]. In this regard, extraction conditions vary widely in the literature, as does the yield and quality of ulvan produced (Table 2, Fig. S3). The choice of extraction conditions is generally based around the physicochemical properties of the ulvan molecule and its specific interactions with other components of the plant cell wall [77]. Less consideration is given to the capacity for the extraction conditions to degrade ulvan or co-extract impurities such as proteins, other polysaccharides (starch, cellulose, xyloglucan, and glucuronan), and to a lesser extent lipids and pigments. Depending on the intended application of the ulvan extract, co-extraction of impurities can lead to more intensive down-stream purification procedures. We use three criteria to determine optimal conditions for the extraction of ulvan: 1. High yield; 2. High selectivity; and 3. Low degradation (i.e. ulvan is extracted without extensive hydrolysis). To address these criteria, we review the physicochemical properties of the predominant macromolecules in *Ulva*, and then review the literature and provide recommendations on the best practices for the extraction of ulvan, focusing on applications.

The extraction yield of ulvan is affected by the properties of the biomass and its pre-treatment, extraction temperature, extractants, extractant to biomass ratio, biomass particle size, and duration of extraction (Fig. 2a-f). The physicochemical properties of ulvan that influence its extraction yield include its relatively low solubility in

Table 1
Ulvan monosaccharide composition (median, minimum, and maximum in mol%) for each species of *Ulva* (1954–2018). Only Median reported where $n = 1$. For additional detail, see supplementary data set, sheet 2 "Meta-Table", and search by the "In-text reference" column.

Species	Rhamnose			Glucuronic acid			Xylose			Iduronic acid			Glucose			Galactose			Uronic acids			Reference
	Median	Min	Max	Median	Min	Max	Median	Min	Max	Median	Min	Max	Median	Min	Max	Median	Min	Max	Median	Min	Max	
U. arasakii	33.2						11.0												46.7			[39]*
U. armoricana	51.6	41.9	60.0	21.3	15.2	27.5	7.5	3.7	10.1	7.0	3.8	15.3	10.0	0.0	26.2	3.1	1.0	5.1	13.4	12.6	16.5	[32,40]*, [41,42]
U. clathrata	10.7			4.0												4.8						[43]
U. compressa	13.0	5.0	62.0				17.0	15.0	35.0				40.0	5.7	70.0	9.0	4.0	15.0	18.3			[44,45]*, [46]
U. conglobata	67.8	57.0	72.3	6.0			1.5	1.0	20.0				17.1	12.0	22.0	2.4	1.2	5.0				[47,48]
U. fasciata	57.4	8.2	92.2	14.7			26.1	1.5	36.3				7.7	0.7	22.8	1.9	1.6	2.2				[49–55]
U. gigantea	42.1			15.4			28.8			3.6			7.9			2.3						[56]
U. intestinalis	37.2	30.2	61.0				10.9	8.5	14.2				40.0	2.3	48.4	11.4	7.7	15.8				[57,58]
U. lactuca	33.5	8.2	60.8	22.5	2.6	52.0	7.3	0.0	35.4	6.0	5.0	6.0	28.6	2.0	87.2	1.6	0.0	1.9	16.8	16.8	47.1	[59,60]*, [61,62,63]*, [64]
U. linza	61.6	60.7	62.5	22.6	17.2	27.9	10.5	9.6	11.3				10.9									[65]
U. meridionalis	39.0						17.0						6.0			6.0			28.0			[66]*
U. ohnoi	47.1	41.1	53.1	28.6	27.8	29.4	5.5	5.3	5.7	8.8	7.4	10.1	2.5	1.5	3.5	2.6	1.2	4.0				[4]
U. olivascens	53.8			16.7			15.1			3.8			7.6			3.0						[32]
U. pertusa[a]	25.3	15.2	80.7	27.0			7.7	2.7	21.0				4.7	1.0	27.4	0.0						[48,67–69]
U. prolifera	67.8	57.1	87.6				3.8	2.4	8.8				31.9	3.6	67.8	4.0						[70,71]
U. rigida	26.9	10.7	58.3	31.7	19.0	37.0	10.8	4.3	38.0	6.0	2.5	7.0	7.6	1.6	46.1	0.9	0.3	1.7	18.3	10.3	46.0	[14,32], [72]*, [73]*, [74,75], [76]*
U. rotundata	46.8	7.2	55.0	22.5	15.0	28.9	15.0	4.4	25.0	4.0	0.6	9.0	5.3	0.0	62.8	3.0	0.0	4.5				[32,42,77]
U. scandinavica	42.2			11.6			9.6			4.0			30.7			2.0						[32]
U. sp.	33.0	27.9	54.8	13.4	11.3	21.5	12.4	1.7	16.9	3.7	3.3	5.9	5.6	0.1	38.1	1.0	0.0	2.1				[32,78,79]
U. spp.	28.2						3.2						5.9			1.3			19.3			[20]*
Pooled total[b]	45.0	5.0	92.2	22.5	2.6	52.0	9.6	0.0	38.0	5.0	0.6	15.3	9.5	0.0	87.2	2.1	0.0	15.8	17.1	10.3	47.1	$n = 44$

*Content of uronic acids was determined by colourimetric assay.
[a] *pertusa* is currently regarded as a synonym of *australis*.
[b] Ulvan composition pooled across species.

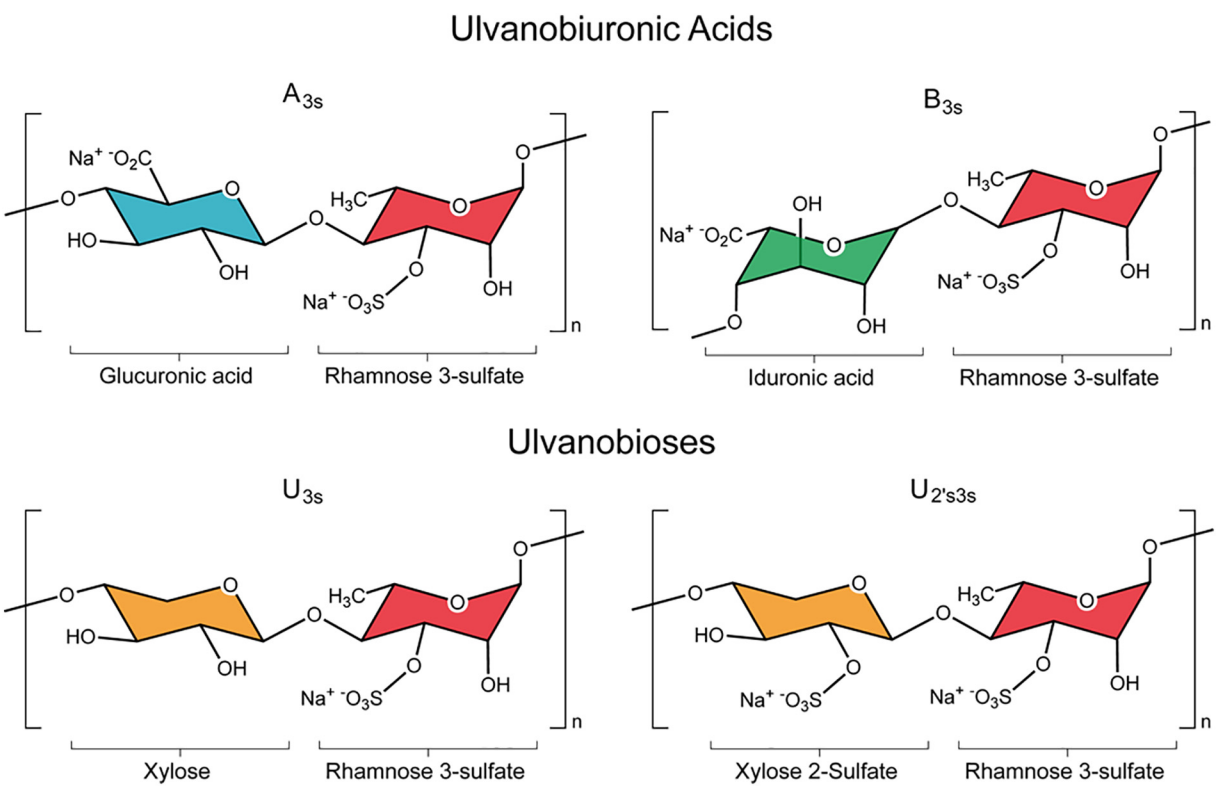

Fig. 1. Nomenclature and structure of the major repeating disaccharide units that comprise ulvan. Ulvanobiuronic acid A_{3s} contains glucuronic acid (blue) attached to rhamnose 3-sulfate (red), while the similar B_{3s} also contains rhamnose 3-sulfate but has iduronic acid (green) in the place of glucuronic acid. Ulvanobioses are comprised of rhamnose 3-sulfate attached to xylose (orange). Xylose can contain a sulfate group, as seen in $U_{2's,3s}$. (For interpretation of the references to colour in this figure legend, the reader is referred to the web version of this article.)

aqueous conditions and its stabilisation in the plant cell wall, predominantly through its interaction with divalent cations (e.g., Ca^{2+}), borate, hydrogen bonding, and entanglement [77]. The solubility of ulvan and its intermolecular interaction are pH dependent [86]. Extraction solutions at pH > pKa of both uronic acids (~3.28) and sulfate esters (~2.0) promote a high charge density on ulvan and theoretically an increase in its solubility. Conversely, extraction solutions at pH < pKa of both uronic acids and sulfate esters theoretically reduce its solubility. In practice, the bead-like conformation of ulvan leads to formation of aggregates at neutral to acid pH, and these aggregates disperse at pH < pKa of the uronic acids allowing for greater solubility of ulvan [77]. The solubility of glucuronan, a homopolysaccharide consisting of repeating (1,4)-linked glucuronic acids, is also pH dependent with expected enhancement in its solubility above the pKa of glucuronic acid. In this regard, both glucuronan and xyloglucan are more soluble in alkaline solutions. The solubility of water soluble protein is also pH dependent. Extraction solutions with pH equal to the isoelectric point (pI) of the protein result in its reduced aqueous solubility. In this regard, the pI for aqueous and alkaline soluble proteins from macroalgae is generally between pH 3–4 [159]. However, lower pI values for soluble proteins from *Ulva* (pI = 2.25) occur [160]. Given these physicochemical properties of macromolecules in *Ulva*, an informed decision of extraction conditions can be made to enhance the efficiency and selectivity of ulvan extraction, while limiting degradation.

Extraction yield can vary significantly between populations of *Ulva* due to eco-physiological variation (light, temperature) [42], and, therefore, comparisons of extraction yields should be evaluated on a single harvest of biomass. In terms of biomass pre-treatment, the reduction of salt in the biomass by warm water extraction enhances the extraction efficiency of ulvan [4]. The mechanism here is twofold, the reduction of salt reduces the aggregation properties of ulvan, and osmotic shock increases the exposure of cell wall components to the extractant. Other pre-treatments, such as pigment and lipid removal, have no effect on either extraction efficiency or the quality of ulvan extracted and for this reason are considered unnecessary, unless they are targeted products. Finally, to increase the interaction of extractant and biomass cell wall, and, therefore, enhance extraction efficiency, biomass is dried and finely milled.

The solubility of ulvan in aqueous solutions is enhanced by extraction at high temperatures (80–90 °C). The temperature is usually capped below the boiling point of water for convenience and to prevent higher temperatures promoting degradation (e.g., depolymerisation and desulfation) [161]. However, high temperature extractions in water generally have low extraction yields due to the interactions of ulvan with other cell wall components [77]. As a result, extractants, such as chelators and acids, are used to overcome the structural integrity of the plant cell wall, thus, enhancing the extraction efficiency of ulvan. Chelators, such as oxalates and EDTA, remove divalent cations (e.g., Ca^{2+}) that promote the cross-linking of ulvan in the cell wall. Extractions using chelators are generally conducted at or near neutral pH and at high temperatures (80–90 °C). Reported yields vary widely (see Fig. 2), but the extraction efficiency (and selectivity) is improved when the pH is adjusted to 4.5 [77]. In this regard, extractions in strong acid (e.g., HCl; Fig. 2) generally produce higher extraction yields [4,77,162]. Mechanistically, extractions at pH below the pK_a of glucuronic acids disperse ulvan aggregates, facilitating its extraction. Notably, high temperatures (80–90 °C) are still required to facilitate high extraction efficiencies at low pH, however, isolation methods influence yields (see Section 2.4). Extraction pH also plays a significant role in the selectivity of ulvan over other macromolecules, as discussed above.

The physicochemical properties of the macromolecular constituents of *Ulva* support extraction pH as an important factor in the selectivity of the extraction process for ulvan. At pH below the pKa of uronic acids (~3.28) the extraction of ulvan is enhanced (see rationale above), and

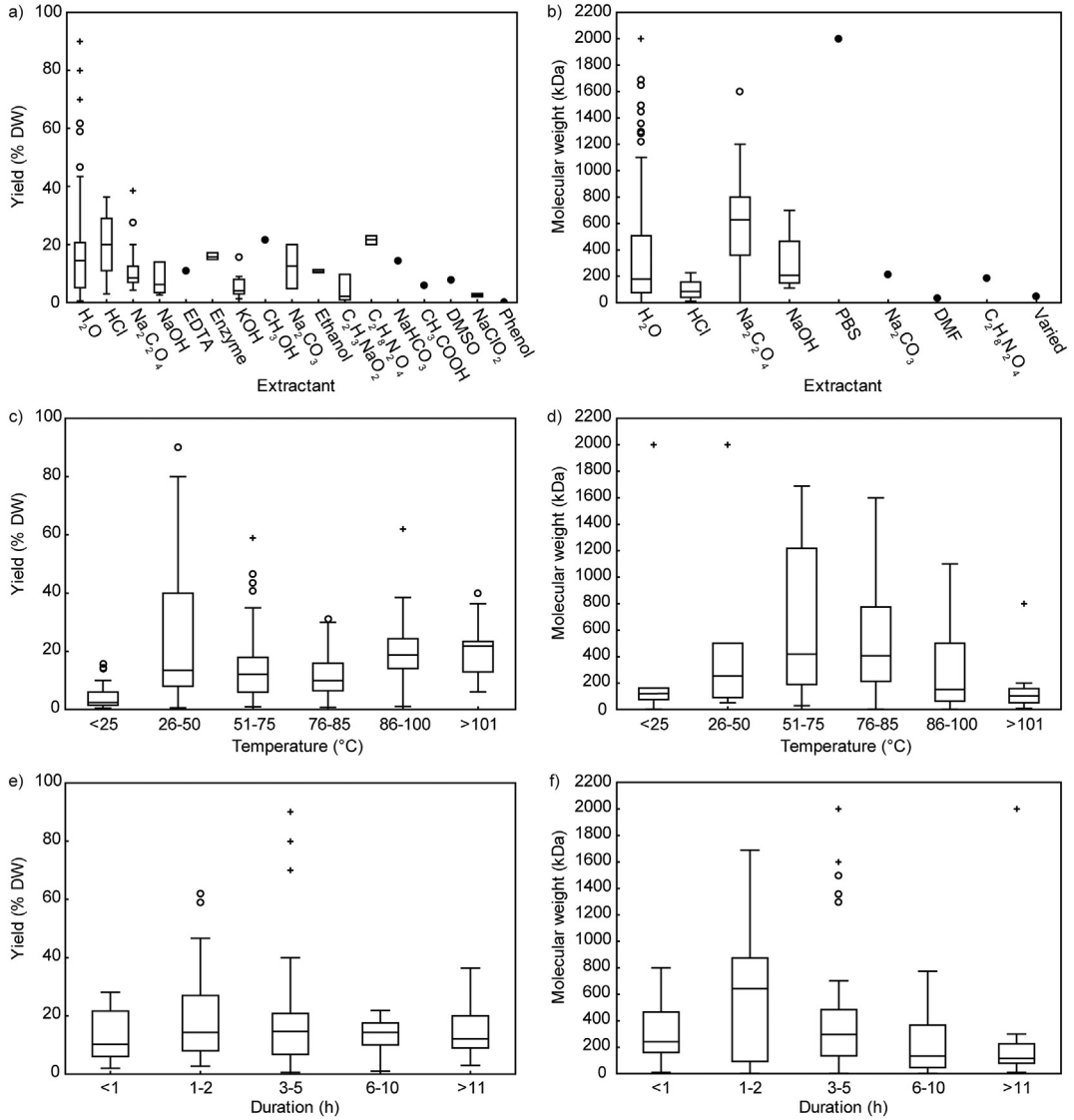

Fig. 2. Box plots of the median and variability in ulvan yield (a,c,e) and average molecular weight (b,d,f) resulting from extractant applied (a,b), temperature (c,d) and duration (e,f) of the extraction procedure. Yield is presented as % of dry weight; average molecular weight in kDa. "PBS" = Phosphate buffered saline; "DMF" = anhydrous *N*,*N*-dimethylformamide; "Varied" = multiple extractants. Boxes represent the interquartile range (IQR) with the mean as a line within the box; whiskers represent the limits of non-outlier data; open circles are outliers, calculated by ± 1.5*IQR; crosses are extreme values, calculated by ± 3*IQR; closed circles represent values for which $n = 1$.

the solubilities of other macromolecules, such as glucuronan, xyloglucan, and soluble protein, are minimised [4,77,133,162]. For example, HCl extracts of fresh *U. ohnoi* had superior selectivity for ulvan (306–333 μg rhamnose/mg extract) over protein (4–7 μg protein/mg extract), when compared with sodium oxalated extracts (114–162 μg rhamnose/mg extract and 41–59 μg protein/mg extract) [4]. The selectivity for ulvan over other polysaccharides can also be inferred by comparing the molar ratios between rhamnose (an ulvan specific monosaccharide), and uronic acids or xylose (both of which are constituents of multiple polysaccharides) of extracts obtained using different extractants [4,77]. For example, ulvan extracted from *Ulva ohnoi* had a molar ratio of 1:0.71 for rhamnose to uronic acids when HCl was used as the extractant, and 1:0.88 when oxalate was used as the extractant, demonstrating increased co-extraction of glucuronan in the latter [4]. Similarly, the mole ratio of rhamnose to uronic acids for ulvan extracted from *Ulva rotundata* with 0.05 M HCl (pH 1.3) was 1:0.83 compared to 1:0.99 when extracted with 0.02 M ammonium oxalate (adjusted to pH 4.6) [77]. These latter studies indicate a quantitative measure of selectivity can be provided using pH, resulting in a more accurate composition of the ulvan attained. It is, however, important to note that while selectivity for ulvan over other macromolecules was enhanced at low pH, significant degradation of its structure also occurred.

Degradation of the structure of ulvan during the extraction procedure may reduce or enhance its functionality depending on the intended application. For this review, we focus on the versatility of the ulvan extract, and as ulvan can be readily degraded after its extraction using chemical and enzymatic approaches (see above), an ulvan sample with minimal degradation is considered the most versatile product. There are two structural features that are most susceptible to degradation during the extraction of ulvan; its degree of polymerisation and degree of sulfation. In this regard, depolymerisation of the polysaccharide is more facile than desulfation of the polysaccharide under the range of extraction conditions used to extract ulvan. Extraction parameters that influence the degree of depolymerisation include pH, temperature, and duration (Fig. 2d, f). In this regard, high temperature (80–90 °C) extractions at low pH (~1.3–1.5) lead to significantly higher levels of depolymerisation than extractions at higher pH (with or

Table 2
Ulvan extract median, minimum, and maximum yield (% algal dry weight) and composition (% w/w) for each species of *Ulva* (1954–2018). Only Median reported where $n = 1$. For additional detail, see Supplementary data set, sheet 2 "Meta-Table", and search by the "In-text reference" column.

Species	Yield			Total carbohydrate			Protein			Ash			Sulfate			Reference
	Median	Min	Max	Median	Min	Max	Median	Min	Max	Median	Min	Max	Median	Min	Max	
U. arasakii				54.9	54.9	54.9							0.4			[39]
U. armoricana	40.0	7.0	90.0	48.7	31.2	78.0	7.3	1.5	13.9	17.0	2.9	18.6	14.4	2.7	19.1	[32,40,42,101–104]
U. clathrata	6.8	0.6	61.9	31.3	26.7	44.6	8.2	0.4	15.3	19.0			10.6	5.6	35.8	[43,105–108]
U. compressa	9.0	0.7	23.0	42.0	23.5	54.0	12.0	8.0	27.8	19.2	10.0	40.0	6.7	3.0	13.0	[44–46,104,105,109]
U. conglobata	1.1	0.9	1.3				3.9	3.8	4.5	16.3	15.4	18.5	23.2	11.9	35.2	[47,48,110]
U. fasciata	13.0	0.5	40.0	48.8	1.4	84.7	4.2	0.2	11.8	14.9	12.4	20.9	18.6	2.3	27.5	[49–55,105,111–114]
U. flexuosa	2.7															[115]
U. gigantea				79.6			5.8						11.9			[32]
U. intestinalis	12.0	2.2	59.1	39.0	4.9	92.2	5.1	0.0	15.0	21.6	12.5	29.4	29.8	2.9	40.0	[57,116–124]
U. lactuca	16.6	1.0	36.4	37.7	4.5	84.1	2.9	0.0	33.1	15.7	0.8	47.2	14.3	5.8	32.2	[15,59,60,62–64,91,105,109,111,125–139]
U. linza	9.8	6.5	15.1	51.0	47.9	60.0	1.9	0.5	3.2				17.7	12.5	21.3	[65,87,140–143]
U. meridionalis	18.7						6.8	4.0	9.5	12.9			10.0			[66,95]
U. ohnoi	6.3	4.3	8.2	54.7	42.3	67.0	2.8	0.4	5.1	25.9	23.3	28.5	14.1	11.5	15.7	[4,144]
U. olivascens				63.4			4.9	4.9	4.9				13.8			[32]
U. pertusa[a]	22.5	1.9	43.4	60.7	33.4	72.3	3.4	1.4	4.8	26.3	22.6	29.9	17.1	11.6	24.0	[48,67–69,83,84,93,97,110,143,145–147]
U. prolifera	20.3	0.6	46.7	56.1	49.2	93.3	1.9	0.0	13.9				16.8	7.7	22.0	[70,71,110,148–153]
U. reticulata	4.5	1.2	8.3	35.7	20.1	46.1	10.1	9.4	20.8	19.5	19.3	19.7	14.6	10.1	17.8	[73,105,111,154,155]
U. rigida	10.9	1.3	38.5	59.5	39.8	75.6	10.0	0.2	25.9	18.1	8.1	25.0	19.8	14.3	37.3	[14,32,73,76,82,88,111]
U. rotundata	8.0	0.1	27.5	35.9	22.3	70.8	12.6	1.0	35.5				11.4	2.4	17.3	[32,42,77,100,156]
U. scandinavica				56.3									13.1			[32]
U. sp.	9.7	5.0	14.4	72.0	25.6	91.9	7.8	4.0	11.6	20.8	6.6	23.0	13.9	7.8	18.5	[28,32,78,79,85,157,158]
U. spp.	12.2	12.2	12.2	41.7			4.3	4.3	4.3	23.7			15.8			[20]
Pooled total[b]	12.0	0.1	90.0	46.1	1.4	93.3	6.6	0.0	35.5	17.1	0.8	47.2	15.5	0.4	40.0	

[a] *pertusa* is currently regarded as a synonym of *australis*.
[b] Ulvan yield and composition pooled across species.

without an added extractant) [4,77,125,133]. However, small changes in pH, temperature, and duration all have a significant effect on the degree of depolymerisation [77,125,133,161]. For example, ulvan was extracted from *U. lactuca* using a factorial experimental design that varied temperature (80 °C or 90 °C), pH (pH 1.5 or 2), and time (1 − 3h) [133]. The harshest extraction condition (90 °C at pH 1.5 for 3 h) resulted in higher yield at the cost of significantly greater depolymerisation than the milder extraction (80 °C at pH 2 for 1 h). Furthermore, at pH 1.5 for 1 and 2 h, significantly higher depolymerisation occurred for extractions conducted at 90 °C than at 80 °C, but a higher yield was also obtained. The same temperature dependence was present for 2 and 3 h extractions at pH 2.

The combination of extraction temperature, solvent pH and extraction duration interact to influence extraction yield and quality (e.g., purity and molecular integrity). Higher extraction temperatures enable greater solubilisation of ulvan (Fig. 2c), low pH improves the selectivity for ulvan, and increased extraction duration can increase ulvan yield. However, compromises must be made to protect the integrity of the ulvan structure. For example, while high temperature results in higher yields, a combination of high temperature, low pH and long extraction duration lead to significant depolymerisation (Fig. 2d, f). However, small adjustments in pH have a large influence on depolymerisation, while small changes in temperature do not. Therefore, using the data available in the literature the following extraction conditions are recommended based on the criteria listed above: 1. High extraction yield; 2. High selectivity; and 3. Low degradation:

- Temperature: 80–90 °C
- pH range: 2–4.5
- Duration: 1–3 h

2.3. Isolation and purification

Methods for the isolation and purification of ulvan vary significantly and are linked to both the availability of resources and the focus of the study. Here we regard isolation as the separation of the extract from residual biomass and the removal of solvent, and purification as the separation of ulvan from other solutes (e.g., salts and other macromolecules). In practice, these steps are not mutually exclusive. It is also important to note that isolation and purification methods influence the physicochemical properties and biological activities of ulvan. We briefly review commonly used methods for the isolation and purification of ulvan that yield two desirable outcomes: 1. High recovery, and 2. Pure product. Methods for the isolation and purification, both chemical and enzymatic, of polysaccharides have been comprehensively reviewed [163]; our focus is to briefly review commonly used isolation and purification methods for ulvan, and comment on their effectiveness.

Following the extraction of ulvan, the extract is separated from the residual biomass by filtration and/or centrifugation prior to the isolation of ulvan by precipitation, evaporation, or concentration by ultrafiltration followed by lyophilisation. For industry, spray drying is another efficient process [38]. Precipitation of ulvan with ethanol is by far the most common isolation method used in the laboratory. Typically, addition of ethanol (e.g. 70–96%) to a concentrated extract is adequate to precipitate ulvan, while ethanol-soluble compounds, such as pigments and metabolites, remain in solution [164]. Although ethanol precipitation is a convenient method, it is limited by the low solubility of salts and higher solubility of low molecular weight ulvan in ethanol-water mixtures. Precipitation methods are also particularly difficult to replicate and in the absence of dialysis or ultrafiltration can lead to high levels of salt in the ulvan extracts [59,133]. Consequently, precipitation can lead to incorrect interpretations of yields, physicochemical properties, and biological activities. Efficient desalting of ulvan extracts can be achieved by dialysis, ultrafiltration, or even chromatography.

Dialysis and ultrafiltration allow for the reduction (removal) of excess salts and small molecules contaminating ulvan extracts. Dialysis is highly effective in the removal of excess salt from analytical samples and for other applications that require very low residual ash. Ultrafiltration is generally employed as a two-step process; concentration (volume reduction) followed by diafiltration (washing or buffer exchange). Both dialysis tubing and membrane filters for ultrafiltration are available with a variety of pore sizes (or molecular weight cut-off (MWCO)). The range of MWCO's used for ulvan generally fall between 3.6 and 12 kDa [92,111]. For dialysis, pore size selection is based around the retention of ulvan, however, for ultrafiltration pore size selection is based on both the retention of ulvan and the rate of permeate flow (which decreases as pore size decreases). The latter extends the time associated with the ultrafiltration processes. The balance between ulvan retention and time efficiency is optimised at ~10 kDa MWCO [4,100,125].

Given the high level of impurities in many ulvan extracts, it is surprising that chromatographic techniques are not applied more widely for purification prior to characterising the physicochemical properties and biological activities of ulvan. In this regard, the polyanionic and polydisperse nature of ulvan lends itself to anion-exchange chromatography (AEC) and size-exclusion chromatography (SEC), respectively. AEC is effective for the removal of proteins and neutral polysaccharide impurities from ulvan samples. Both weak anion-exchangers (e.g., diethylaminoethyl (DEAE) or tertiary amine functionalised media) [25,111] and strong anion-exchangers (e.g., quaternary (Q) amine functionalised media) [77] have been successfully employed to purify ulvan. SEC is widely used as an analytical technique for determining molecular weights and molecular weight distributions (see Section 2.4), however, it has wider applications. For example, SEC can be used to fractionate oligosaccharides and polysaccharides for the elucidation of fine structure [23], and to generate size classes for structure-function relationships [29,165]. With regards to the former, SEC has been used to fractionate ulvan oligosaccharides for fine structure analysis using NMR techniques [81]. A large range of size exclusion media is available targeting different molecular size ranges. Media commonly used for purification of ulvan samples are Sepharose CL-6B [29], Sephacryl S-400/HR [165], Sephacryl S-1000 [166], and Sephadex G-200 [46].

In summary, ideally the choice of extraction techniques will limit the co-extraction of macromolecular impurities (see Section 2.2) and reduce the necessity for intensive purification techniques. However, due to salt content (introduced by extractants and inherent in marine species) and similarities in the physical properties of ulvan and contaminating polysaccharides and proteins, purification is necessary. In general, salt is the most significant impurity and is most effectively removed by dialysis or ultrafiltration techniques. Depending on the extraction process employed, protein may also need to be actively removed, either by chemical or enzymatic approaches [36,163], or using chromatographic techniques. The latter is more reproducible and allows for highly purified fractions of ulvan. In practice, a strategic selection of extraction procedures, and isolation and purification procedures should be made based on the available resources. For example, in a resource limited situation one might select a more selective acid extraction, concentrate by evaporation, purify using dialysis, and isolate by precipitation. In a resource rich situation, a selective acid extraction is ideal, although a less selective extraction process can be tolerated, with concentration and diafiltration with ultrafiltration. Subsequent purification by anion-exchange chromatography, and lyophilisation or spray drying to isolate the purified ulvan can be applied.

2.4. Characterisation

In general, the elucidation of polysaccharide structures is often complicated by the presence of multiple monosaccharide constituents, which may include neutral, acidic and amino sugars, a variety of glycosidic linkages, high molecular weights, branching of constituent

sugars, a variable degree of sulfation and substitution patterns, and complex macromolecular properties (e.g., aggregation). The presence of contaminating polysaccharides further complicates structural elucidation of a particular polysaccharide. Therefore, it is important to start with as pure a sample as possible, and even then full structural elucidation is challenging - 'Structural characterisation' is a more fitting term. Adequate structural characterisation of an ulvan sample is essential for interpreting its physicochemical properties and biological activities. To achieve this a measurement of composition (e.g., total carbohydrate content, protein content and ash) and the identifying structural features of ulvan (e.g., sugar composition, glycosidic linkages, degree of sulfation) are required. Comprehensive reviews of the techniques used to elucidate the chemical structure and macromolecular properties of bioactive polysaccharides are provided elsewhere [167–169]. In this review we focus on the methods used to characterise ulvan and propose the minimum analysis and characterisation required to progress beyond bioprospecting.

The analysis of the chemical structure of ulvan is fundamentally based on the quantitative determination of the major constituent monosaccharides (rhamnose, xylose, glucuronic acid and iduronic acid) and degree of sulfation. The latter is most commonly carried out using a turbidimetric assay [170] but can be measured using ion chromatography, high performance liquid chromatography (HPLC) coupled with conductivity [20], elemental analysis, or Fourier transform infrared spectroscopy (FTIR) [171]. Constituent monosaccharides are predominantly quantified using chromatography techniques, in particular gas chromatography (GC) [20,47,49,59,72], HPLC [70,95], and high-performance anion-exchange chromatography (HPAEC) [4,32]. Depending on the chromatographic technique employed the sample is subjected to pre-treatments. Primarily, accurate quantification of constituent monosaccharides requires complete hydrolysis of ulvan. However, due to the resistance of the aldobiuronic glycosidic linkage to hydrolysis [16,17,172], and the susceptibility of rhamnose, glucuronic acid, iduronic acid and xylose to degradation in concentrated strong acids (e.g., Saeman hydrolysis) [173,174], traditional acid hydrolysis methods, such as with trifluoroacetic acid (TFA), are both ineffective and degradative. A traditional acid hydrolysis will not cleave all of the aldobiuronic linkages and as a result the neutral and uronic acid residues involved in these linkages will not be detected. As ulvan is predominately comprised of repeating aldobiuronic acid disaccharides, a traditional acid hydrolysis will inaccurately characterise ulvan. However, hydrolysis of ulvan using traditional methods is ubiquitous in the literature. A two-step hydrolysis in methanolic HCl followed by aqueous trifluoroacetic acid is an effective alternative to reduce the hydrolysis-induced damage to constituent monosaccharides [4,175]. A chemo-enzymatic degradation involving hydrolysis with a mild acid followed by β-D-glucuronidase cleavage of aldobiuronic acid is also an effective solution [13,16]. Both HPLC [70,87,95] and HPAEC [4,32] methods are used to quantify the monosaccharides in the hydrolysis samples without further derivatisation. HPLC methods generally provide less resolution than HPAEC methods [176], but both allow the assessment of the effectiveness of the hydrolysis method employed [175]. HPAEC-PAD (pulsed amperometric detection) of methanolic-HCl/TFA hydrolysates also has the major advantage of separating and quantifying acidic and neutral sugars (and amino sugars) in a single run, without further derivatisation [175]. GC analysis requires that the constituent sugars be converted to volatile derivatives, such as alditol acetates [20,49,72,83] and trimethylsilyl (TMS) ethers [59]. For the former, reduction of monosaccharide C1-aldehyde is conducted prior to the preparation of alditol acetate. In general, C6-carboxylic acids are not reduced under the conditions employed to reduce aldehydes and, therefore, are not converted to alditol acetates. However, GC–MS analysis of alditol acetates, prepared from ulvan hydrolysates that included the pre-hydrolysis reduction of C6-carboxylic acids with sodium borodeuteride (NaBD4) to generate 6,6′-dideuterio-sugars, allows for the determination of the total uronic acid content [169]. Studies that do not include this conversion generally measure uronic acid content using colourimetric assays [177,178]. Alternatively, TMS ethers of sugars can be prepared using reagents such as *N*,*O*-bis(trimethylsilyl)trifluoroacetamide, allowing for the quantification of both neutral and acidic sugars [59]. However, TMS derivatisation of un-reduced sugar residues can yield several peaks in the GC chromatogram corresponding to different pyranose anomers, which complicates interpretation. A solution to this problem is to follow the preparation of alditol acetate derivatives with reduction to the alditol prior to preparation of the TMS derivative. For sample preparation, HPAEC methods (e.g., HPAEC-PAD) provide the simplest and most comprehensive route for sugar constituent analysis; however, excellent results can also be obtained using either GC or HPLC methods.

While sugar constituents are important in determining the physicochemical properties and biological activities of a polysaccharide, glycosidic linkages and functional group substitution patterns, and sugar sequence are arguably more important. Glycosidic linkage (methylation) analysis is generally conducted using GC–MS methods [25,168,179] and provides information on the linkage positions and substitution patterns of constituent sugars. Briefly, methylation analysis involves the preparation of partially methylated alditol acetates followed by quantitative analysis using GC–MS. To achieve this effectively, the uronic acid components of ulvan are reduced prior to the methylation step [168,169]. Determination of glycosidic linkages and sugar sequence can then be achieved using 2D NMR techniques on hydrolysed ulvan fragments (disaccharides and oligosaccharides) [24,167,180–182]. In many cases, ^{1}H and ^{13}C resonances characteristic of ulvan structures (e.g., repeat disaccharide units) can be assigned by comparison with published data [4,49,77,84,128,183,184]. In addition, the anomeric configuration and position of substituents (e.g., sulfate groups) can be inferred by location of both ^{1}H and ^{13}C resonances [167,181].

The physicochemical properties and biological activities of polysaccharides are also fundamentally linked to molecular weight. Therefore, a measure of average molecular weight (MW) and molecular weight distribution (MWD) is integral to the characterisation of polysaccharides. In this regard, size exclusion chromatographic (SEC) methods are the most commonly employed as they allow a measure of both MW and MWDs. Firstly, as a minimum requirement for the determination of average MW and MWD's, SEC is coupled to a concentration dependent (CD) detector, most commonly refractive index and UV. For ulvan, calibration of these setups is usually achieved with narrow polydispersity polymer standards (e.g., dextrans [28,68,69,88,133,145], pullulans [59,161,185] and polyethylene oxides [61]). However, due to difference in the macromolecular properties, commonly used calibration standards are unlikely to yield accurate results, and accurate measurements of ulvan (and other complex polymers) MW and MWDs require online molecular weight detectors (e.g., multiangle laser light scattering (MALLS) and viscosity (VISC)) [4,57,61,86,128]. Both SEC-MALLS and SEC-VISC also allow analysis of macromolecular properties, such as aggregation behaviour [86,186]. Comprehensive reviews on the theory and variety of detection methods in SEC analysis are provided by [186,187].

These methods for the characterisation of ulvan can represent a significant investment in both equipment and experimental time. However, high-throughput determination of the composition of ulvan extracts is desirable in some applications (e.g., bioprospecting studies, ulvan composition comparisons, and for quality control in industry) and requires an alternative approach. The rapid determination of ulvan in samples is commonly carried out using colorimetric assays that probe sugar constituents (e.g., uronic acids, rhamnose, and xylose) and protein content [188,189], and a turbidimetric assay for determination of sulfate ester content [170]. Common and relatively accurate colorimetric methods for uronic acid determination include the carbazole/sulfuric acid [177] and sulfamate/*m*-hydroxydiphenyl techniques [178]. However, due to a lack of specificity for targeted sugars,

chemical colorimetric methods for quantitative measurements of neutral sugars (e.g., rhamnose and xylose) are hampered by interference. In this regard, highly specific enzymatic assays for monosaccharides typically present in ulvan including rhamnose [190], xylose [191] and uronic acids [192] are available. However, to gain an understanding of composition multiple characterisation assays are necessary resulting in little time savings. In this regard, a truly high-throughput method would require only a single measurement on an un-degraded sample with minimal preparation.

Chemometric methods coupled with spectral analysis, such as IR, Raman, NIR, and NMR, are effective for the rapid (single measurement) compositional analysis of polysaccharides [171,193]. For example, FT-IR spectra in the range of 1770–600 cm^{-1} coupled with the multivariate analysis method of partial least squares (PLS) analysis was used to develop calibrated FT-IR-PLS-models that allowed the sulfate content and the content of the major monosaccharides in ulvan hydrolysates to be determined [171]. The key ulvan spectral features used for the development of FT-IR-PLS-models were the uronic acid carboxylic groups (1650–1600 cm-1 (ν_{asym} C═O); 1425–1400 cm^{-1} (ν_{sym} C═O)) [171,183], sulfate ester groups (1260–1215 cm^{-1} (ν_{asy} S═O); 850–835 cm^{-1} and 795–785 cm^{-1} (C-O-S)) [25,83,183], and the glycosidic linkage between the two major sugars, rhamnose and glucuronic acid (1055–1030 cm-1 (C-O-C)) [171]. While, the broader application of the FT-IR-PLS-models for ulvans is untested, this analytical approach represents a rapid characterisation method for ulvan.

Ulvan has a broad range of biological activities; however, the characterisation of ulvan is often of low resolution leading to uncertainty in the origin of the activities tested. At the research level total characterisation methods are essential in understanding structure-activity relationships. The minimum characterisation data recommended is sugar constituent analysis (preferably suitable for the detection of neutral and acidic sugars), molecular weight analysis, and measures of contaminants, such as protein and ash. To obtain further insight into structure-activity relationships, glycosidic linkage analysis should also be conducted. In the next section we review the biological activities of ulvans and comment on the structural attributes that influence its efficacy.

3. Biological activities of ulvans

3.1. Overview

Ulvan has demonstrated significant biological activities in both animal and plant systems in in vitro and in vivo studies (Table 3). In animals, sulfated polysaccharides, such as free glycosaminoglycans (GAGs) and proteoglycans (protein linked GAGs), are intricately involved in a broad range of biological processes and have significant structural similarities with ulvan [194,195]. Therefore, the capacity of ulvan to mimic GAGs is a logical link. Sulfated polysaccharides are absent in terrestrial plants and the rationale for the biological activity of ulvans towards plants is less clear; however, ulvan has structural similarities with plant rhamnogalacturonans [196] and rhamnolipids from phytopathogenic bacteria [197], providing an insight to its activity. Importantly, the structural features of ulvan (e.g., molecular weight, degree of sulfation, sulfation pattern, constituent sugars, linkages, isomers, and degree of branching) influence its bioactivity. Therefore, ulvan obtained from different species of *Ulva*, and species from different environments, display significantly varied bioactivity profiles. We review the biological activities attributed specifically to ulvan, focusing on activities with potential biomedical applications and the developing body of technologies in plant physiology, horticulture, and agriculture.

3.2. Cytotoxicity

Cytotoxicity of supplements, nutraceuticals, therapeutic agents or adjuvants, and biomedical materials is a critical consideration for product development, including a natural product such as ulvan. In this regard, the cytotoxicity of ulvan has been investigated by dosing a range of macrophage cell lines (e.g., RAW 264.7, J774A.1, and peritoneal) [57,67,70,124], gut cells (e.g., IPEC-1) [101,102,224], fibroblast cells (e.g., mouse C3H [L929]) [225], Vero cells [207], Swiss mice and Wistar rats [129]. Ulvan is largely non-toxic, with ulvan fractions from *U. pertusa* [57,67], *U. intestinalis* [122,124], *U. armoricana* [101,102], *U. lactuca* [129,225,226], *U. clathrata* [107], *U. compressa* [199] and *U. prolifera* [70,227] having > 50% cell viability for cell cultures dosed with ≥500 μg/ml of sample.

3.3. Immunomodulating activity

Molecules that influence the immune system are known as immunomodulators and often act by influencing inflammation. The inflammatory effects of ulvan have been investigated in vitro using macrophage cell types (e.g., RAW 264.7, mouse peritoneal [122], J77A.1 [124] and fish head kidney [223]), tissues (e.g., intestinal epithelial cells [101,102]), and in vivo using animal models (e.g., Wistar rats [209], mice [147,218], and chickens [228]). Inflammation is dependent on cytokine production and is largely the result of the activation of NF-kB (a protein complex that controls transcription) by pathogen-associated molecular patterns (PAMPs) on toll-like receptors (TLRs) [102,229,230]. Lipopolysaccharides (LPS) on the cell wall of gram-negative bacteria are potent activators of TLRs and are the most commonly employed PAMP class in immunomodulation studies. Activated NF-kB induces transcription of genes coding for cytokines, thus, initiating an inflammatory response [229]. Evaluation of the influence of ulvan on inflammation has been conducted using a number of probes, including signalling molecules (e.g., cytokines; TNF-α, IL1, IL2, IL6, IL10, IL12, CXCL1, CXCL12, CXCL14 and CCL22), active metabolites (e.g., PGE2, NO, HOCl), immunoglobulins (e.g., IgM, ICAM and VCAM-1), enzymes (e.g., COX-2, iNOS-2, HO-1 and MPO) and transcription related molecules (e.g., NF-kB, mRNA) [57,67,70,72,101,122,124,144,218,227]. A pro-inflammatory response is initiated by immune cells (e.g., macrophages) through the release of cytokines (e.g., IL-1, IL-2 IL-6, IL-18, IL-12, prostaglandin E2 (PGE2), and tumour necrosis factor alpha ([TNF]-α)) [231]. Anti-inflammatory cytokines, such as IL-4, IL-10, IL-11, and IL-13, can inhibit the release of pro-inflammatory cytokines to prevent damage from excessive macrophage activation. This simplistic representation of the roles of immune cells and cytokines is useful but cytokine activity is complicated, involving multiple effects and interacting pathways [231].

Macrophage cells (e.g., RAW 264.7, mouse peritoneal, J77A.1, and fish head kidney) are often used to study the effect that ulvan (and other bio-actives) have on the inflammatory response [57,67,72,74,118,122,124,144,227]. For example, RAW264.7 cells exposed to 50 μg/ml of purified ulvan from *U. intestinalis* upregulated the production of pro-inflammatory cytokines (TNF-α, IL-1β, IL-6, and IL-12), the anti-inflammatory cytokine IL-10 and enzymes (e.g., iNOS and COX-2) and their products (e.g., NO and PGE_2); a response of equivalent magnitude to the LPS (1 μg/ml) positive control [57]. Importantly IL-10 inhibits pro-inflammatory cytokines (including, TNF-α, IL-1β, IL-6, and IL-12), which might act to limit any potential harmful repercussions from an over-stimulated inflammatory response. Ulvan isolated from *U. pertusa* [67] *U. rigida* [72,227] and *U. prolifera* [70] also activate RAW 264.7 cells, upregulating the production of cytokines (e.g., TNF-α, IL-1β, IL-6, IL10), enzymes (e.g., iNOS and COX-2) and their products (e.g., NO and PGE2). Consistent with RAW 264.7, macrophage J774A.1 cells treated with 200 μg/ml crude ulvan extracted from *U. intestinalis* stimulated the production of pro-inflammatory cytokines TNF-α and IL-1β to a similar degree as the LPS (1 μg/ml) positive control [124]. A similar pro-inflammatory response was also recorded when peritoneal macrophages from male ICR mice were treated with crude ulvan (100–400 μg/ml) from *U. intestinalis* [122]. Ulvan

Table 3
Ulvan bioactivities for each species of *Ulva* reported in publications that also detailed the extraction procedure and/or characterisation of the polysaccharide (1954–2018). For additional detail, see supplementary data set, sheet 2 "Meta-Table", and search by the "In-text reference" column.

Species	Bioactive						Other		
	Anti-coagulant	Immunomodulating	Anti-cancer	Antioxidant	Anti-viral	Antihyperlipidemic	Biomaterial	Plant defence	Various[b]
U. arasakii									
U. armoricana		[101,102]		[40]	[40]			[103]	[101,104]
U. clathrata	[43,65,105]	[108]			[107]				[198]
U. compressa	[105]				[199]		[200]		[104,198]
U. conglobata	[47]								
U. fasciata	[55,105,201]	[202,203]	[53,113]	[52,53,112,113,204]		[202,203,205]		[49–51,206]	[54,114]
U. flexuosa									
U. gigantea									
U. intestinalis		[57,118,121,122,124]	[58,119,121,122]	[116–118,124]	[116,207]	[116]			[208]
U. lactuca	[60,105,137]	[127,129,209]	[128,137,139,209,210]	[64,126,127,131,137,139,204,209,211,212]	[62,127,137]	[211,213]	[61,214]	[91,106]	[134,135,138,208,215]
U. linza	[142]	[87]		[87,142,143]					[140,141]
U. meridionalis									
U. nematoidea	[216]								
U. ohnoi		[144]							
U. olivascens									
U. pertusa[a]		[67,147]	[67]	[68,69,97,143]	[147]	[68,69,83,93,145,146]			[99,217]
U. prolifera		[70,218]	[70]	[71,149,151,153]		[152,219]			[148,220,221]
U. reticulata	[105]			[222]					[155]
U. rigida		[72,223]		[88]			[76]		
U. rotundata							[200]		[198]
U. scandinavica									
U. sp.	[158]	[223]							[28,79]
U. spp.								[29]	
Total publications	11	21	13	31	9	14	4	8	20

[a] *pertusa* is currently regarded as a synonym of *australis*.
[b] Various bioactive properties not otherwise listed on the table. See supplementary data set in for details.

from *U. ohnoi* also stimulated head kidney macrophages from *Solea senegalensis* (sole fish) [144]. Overall, ulvans induce a pro-inflammatory response in animal macrophages with potential for application in animal and human supplements as non-specific immunostimulants.

The effect of ulvan on the immune response has also been investigated in fish [74,144], porcine (pig) intestinal epithelial cells [101,102], rats [129,209], mice [122,129,218,232] and chickens [228]. Despite the range of organisms assessed and extraction techniques applied, ulvan is consistently reported to increase mRNA expression [74,101,102] and promote the release of immunomodulating cytokines or enzymes [144,209,218]. For example, a porcine intestinal epithelial (IPEC-1) cell line treated with purified low molecular weight (4.4 kDa) ulvan (5–500 μg/ml) from *U. armoricana* increased the mRNA and the protein expression of cytokines (e.g., CCL20, IL-8 and TNF-α) [102]. In mechanistic studies conducted by incubating human embryonic kidney (HEK) 293 cells with ulvan (500 μg/ml), ulvan primarily stimulated TLR4, with a subsequent increase in Akt phosphorylation, which activates NF-kB leading to the production of inflammatory cytokines. A similar response was recorded for LPS-treated (100 ng/ml) cells. Increased production of NF-kB was also reported in thymus and spleens of mice (Kunming) treated with ulvan from *U. prolifera* [218]. These mechanistic insights are an important consideration in the development of new supplement (nutraceutical or therapeutic) products for animal and human use.

The immunomodulating activity and potency of ulvan varies significantly between studies of the same species, and between different species. While there is evidence that this variability is due to structural features, some is related to sample purity. In this regard, a significant increase in the potency of the immunomodulatory activity of ulvan from *U. intestinalis* occurs following purification of a crude extract [57,122,124]. However, the structural features of ulvan (e.g., molecular weight and sulfation) also influence potency. For example, the molecular weight of purified ulvan extracted from *U. pertusa* is an important determinant for RAW 264.7 macrophage activation, with higher molecular weight fractions (1450 kDa and 1690 kDa) leading to > 2-fold increase in macrophage activation compared to a lower molecular weight fraction (365 kDa) [67]. An even more pronounced decrease in head kidney macrophages stimulation was measured for low molecular weight (5.92 kDa) ulvan from *U. ohnoi* over high molecular weight ulvan (698 kDa) [144]. However, a study with ulvan from *U. intestinalis* gave contradictory results with a lower molecular weight sample (28.7 kDa) having significantly higher immunomodulatory activity than a higher molecular weight sample (87.2 kDa). This highlights the importance of the interaction of the structural features of ulvan, such as the molecular weight and degree of sulfation, in determining bioactivity [57]. Although molecular weight is considered a major factor affecting immunomodulatory activity, there is also an effect of the degree of sulfation between the high (24.5%w/w) and low (6.25% w/w) molecular weight samples [57]. The level of sulfation is often positively correlated with activity in ulvan and related sulfated polysaccharides (e.g., λ-carrageenan and fucoidan). For example, de-sulfation (partial sulfate ester removal) of ulvan from *U. rigida* resulted in an ~50% reduction in its immunomodulatory effect on RAW 264.7 macrophages [72] and Turbot peritoneal leucocytes [74], when compared to native ulvan. So far, the studies that have investigated the influence of the structural features of ulvan on its effect on inflammation show that structure-activity correlations are species specific and further studies investigating the structure-activity relationships of ulvans across species are required to elucidate the key structural features driving activity. The latter informs the selection of species for cultivation extraction procedures and post-extraction modifications, with a focus of enhancing activity as a non-specific immunomodulatory agent.

3.4. Antioxidant activity

Reactive oxygen species (ROS) and reactive nitrogen species (RNS) are constantly formed in vivo in living tissue by aerobic biogenesis or by oxidative enzymes (e.g., in response to foreign organisms) [233,234]. These highly reactive species attack all major classes of biomolecules, including lipids, DNA, proteins, and sugars. Oxidative stress has been implicated in a host of disorders including inflammatory diseases, neurodegenerative diseases, cancer, cardiovascular diseases, and aging processes. The body has several endogenous enzymatic antioxidant systems to overcome excessive ROS/RNS-mediated damage, including superoxide dismutase (SOD), catalase (CAT), glutathione peroxidase (GSH-Px), glutathione reductase and glucose-6-dehydrogenase, and non-enzymatic antioxidants including glutathione, uric acid, lipoic acid, NADPH, coenzyme Q, albumin, and bilirubin [235]. There are also exogenous antioxidants, including vitamins C and E, carotenoids, phenolic compounds, and trace elements (e.g., zinc and selenium) that play an essential role as antioxidants in living organisms. Food-based protein and polysaccharides also contribute to the antioxidant capacity of organisms, by acting as exogenous antioxidants and enhancing endogenous antioxidants [236]. In this regard, the antioxidant capacity of ulvan is mediated by radical scavenging and subsequent inhibition of lipid peroxidation, and the enhancement of antioxidant enzyme (e.g., SOD, CAT and GSH-Px) activities.

The exogenous anti-oxidant capacity of ulvan has been extensively assessed with in vitro assays using 1,1-diphenyl-2-picryl hydrazil (DPPH) radical scavenging, superoxide scavenging, ferric reducing antioxidant power (FRAP), hydroxyl radical scavenging, and lipid peroxide inhibition. Sulfate content and molecular weight have a significant effect on the anti-oxidant effect of sulfated polysaccharides from macroalgae [37]. In this regard, chemically over-sulfated (32.8% w/w sulfate) ulvan from *U. pertusa* had ~90% hydroxyl radical scavenging at 2.0 mg/ml compared to ~45% at 2.0 mg/ml of native ulvan (19.5% w/w sulfate) [92]. Similarly, radical scavenging is higher for over-sulfated ulvan from *U. linza* compared to its native form [237]. Low molecular weight ulvan also has higher antioxidant capacity relative to higher molecular weight fractions [87,88]. For example, a negative correlation was recorded between hydroxyl radical scavenging (~50–90%) and the molecular weight of ulvan (18.2–100.5 kDa) [87]. This correlation may not be a general trend [183], however, and highlights that comparative extraction conditions, purification protocols, and test protocols are necessary before concluding an overall and consistent structure-activity trend for the anti-oxidant activity of ulvan.

Although ulvan has direct ROS/RNS scavenging activity, it is its capacity to enhance the expression of the enzymatic components of the endogenous antioxidant system that affect animal health the most by ameliorating the propagation of diseases relating to oxidation. Determination of the antioxidant effects of ulvan in vivo has been made by measuring enzymatic antioxidant activities (e.g., SOD, CAT, and GSH-Px) and oxidation products (e.g., malondialdehyde (MDA) as a product of the peroxidation of polyunsaturated fatty acids; GSSH; oxidised glutathione). In this regard, ulvan from *U. lactuca* [135,139,209], *U. pertusa* [68,228,238], *U. armoricana* [102], *U. fasciata* [202,203] and *U. prolifera* [218] mitigate the production of oxidation products and enhance antioxidant enzyme activity in vitro and in vivo. For example, treatment of hyperlipidemic Kunming mice with ulvan from *U. pertusa* resulted in a reduction of MDA (29.2%) and increases in SOD (35.4%) and CAT (43.6%) relative to untreated mice [68]. Interestingly, a fraction with a molecular weight of 83 kDa exhibited higher antioxidant activity than higher molecular weight fractions (e.g., 190 kDa and 201 kDa). These findings were corroborated in a study of the effect of ulvan on egg quality and the health of laying hens [239]. Hens fed a diet supplemented with 1% ulvan showed significantly reduced serum MDA levels and increases in CAT and SOD. Ulvan treated hen groups also had increased levels of cytokines IL-6 and IFN-γ indicative of the close link between the expression of antioxidant enzymes and immune system responses. A single study demonstrated that oversulfated ulvan from *U. pertusa* had a greater capacity to influence antioxidant defence system markers (e.g., MDA, SOD, GSH-Px and CAT) in hyperlipidemic

rats relative to native ulvan [238]. Tentatively, ulvans with high sulfate content and lower molecular weights are most effective at ameliorating oxidative stress in vivo.

The mechanistic rationale for these findings is generally due to radical scavenging activity [69,135,139,238]. However, the capacity for exogenous antioxidants to significantly contribute to radical scavenging in vivo and, therefore, act as an antioxidant endogenously, has been questioned [236]. Furthermore, it was suggested that food-derived antioxidants, like ulvan, act by influencing signalling pathways that lead to the expression of the enzymes involved in the antioxidant defence system. Notably, phytochemicals, including ulvan [68,238], porphyrin [240], and fucoidan [241], have demonstrated their capacity to regulate antioxidant enzyme expression [242]. Ulvan is most likely to enhance antioxidant enzyme activity by activating the transcription enzymes (e.g., Nrf2, NF-kB, AP-1, AP-2, Sp1 and C/EBP) involved in the expression of antioxidant enzymes [236,243]. For example, ulvan from *U. armoricana* stimulates the TLR4 receptor in vitro, which results in the activation of NF-kB and the subsequent upregulation of TNF-α [102], a cytokine that modulates the expression of SOD [243]. However, further research on the mechanism(s) by which ulvan influences the expression of antioxidant enzymes is required to identify the signalling pathway(s) involved. In summary, the capacity of ulvans to boost the endogenous antioxidant system protects the body against toxic oxidation products that cause disease, such as chronic inflammation and cancer.

3.5. Anticancer

The development of cancer is a multistep process initiated by endogenous and exogenous factors, which often lead to oxidative attack on DNA, resulting in mutations that disrupt the normal regulatory pathways between cell proliferation, differentiation, and apoptosis [244]. There are a growing number of studies showing that ulvan acts as an anti-proliferation agent and promotes apoptosis in cancerous cells. Ulvan from *U. lactuca* [94,128,137,139,210], *U. intestinalis* [58,119,122,245], *U. pertusa* [67], *U. prolifera* [70], U. *tubulosa* [246] and *U. fasciata* [53,113] all demonstrate anticancer activities for a range of cancer models with murine sarcoma cancer cell line S180 [122], human cancer cell lines (e.g., HepG2 (hepatocellular carcinoma) [94,119,128,137,210], MCF7 (human breast cancer) [128,246], HeLa (cervical cancer) [128], AGS (human gastric carcinoma) [67,70], MKN45 (human gastric cancer) [113], HT-29 (human colon carcinoma) [94,210], HCT-116 (human colon carcinoma), Caco-2 (human colon carcinoma) [94,210], DLD1 (human colon carcinoma) [53,70,113]) and some cancers in animal models (e.g., rats [58,139,209], mice [122]). However, no clinical human trials have yet been conducted.

The anticancer activity of ulvan from different sources is highly variable. For example, ulvan from *U. lactuca* has significant cytotoxic activity against a number of human cancer cell lines including HepG2 (hepatocellular carcinoma), MCF7 (breast cancer), and HeLa (cervical cancer) [128]. Ulvan at a concentration of 100 μg/ml reduced the in vitro cell viability of all three cancer cell lines to 0%. Although a mechanism of action was not proposed, similar studies of anti-tumour effects of ulvan on HepG2 and MCF-7 cell-lines noted the increased expression of the pro-apoptotic tumour suppressor p53, and reduced expression of anti-apoptotic protein Bcl-2, supporting the conclusion that ulvan promotes programmed cell death (apoptosis) [119,209,210]. The antiproliferation activity of ulvan from *U. lactuca* also reduces levels of proliferating cell nuclear antigen (PCNA) in rat hepatocytes which is indicative of the reduced DNA replication associated with lower proliferation [139]. It is also important to note that many studies have registered only very low to moderate cytotoxic activity relative to traditional chemotherapy drugs [58,67,70,113,122]. For example, ulvan from *U. prolifera* only had low anticancer activity on human gastric carcinoma (AGS) and human colon cancer (DLD-1) cell lines, with dose dependent inhibition of AGS cell proliferation of 10–26% with concentrations of 200–1000 μg/ml [70]. These results do not necessarily preclude the relevance of ulvan in anticancer therapies. For example, ulvan from *U. intestinalis* also had no cytotoxic effects on sarcoma 180 tumour cells in vitro at 50–800 μg/ml, but reduced sarcoma 180 tumour weight in vivo by 61–71% in mice dosed with 100–400 mg/kg [122]. In combination with the latter, important immune organs (e.g., thymus and spleen) were enlarged in ulvan treated mice, supporting the suggestion that the antitumour activity of this polysaccharide originates from its immunomodulatory activity. In summary, the anticancer activity of ulvan appears to operate through one or more of a number of pathways, including the promotion of cancer cell apoptosis, reduction in cancer cell proliferation, and stimulation the innate immune response. Furthermore, the pathways affected are dependent on the source and/or structure of the ulvan.

There are preliminary results suggesting that both molecular weight and degree of sulfation influence the anticancer activity of ulvan [53,58,70,94]. However, at this point there are no conclusive interpretations that can be made with respect to the effect of the structure of ulvan on its anticancer activity. The generally low anti-proliferation activity of ulvan means that ulvan is unlikely to replace established chemotherapy drugs but might find application as a co-treatment, due to its broad-spectrum chemopreventative activities (e.g., immunomodulatory, antioxidant, and anticancer) [209,247]. There are also interesting potential applications for ulvan in cancer therapy. For example, as nanoparticle drug delivery systems for hydrophobic antitumour drugs [248], selenium enriched polysaccharide-protein complexes for cancer treatment [249], and pH responsive polysaccharide nanosystems that inhibit angiogenesis [250]. However, before ulvan can find applications as a co-treatment or adjunct in anticancer technologies, there is a need to ascertain the bioavailability of ulvan and whether ulvan influences the efficacy of traditional chemotherapy drugs in combination therapies.

3.6. Anticoagulant activity

The coagulation cascade is activated by two pathways, the intrinsic and extrinsic pathway, both culminating in the production of thrombin through a final, common pathway [229]. Briefly, this process involves the progressive activation and amplification of serine proteases (e.g., XIII, XII, XI, IX, X and VII) and glycoproteins, collectively termed “factors”, present within the blood. The intrinsic activation pathway is initiated when factor XII is activated by contact with an anionic surface, while activation of the extrinsic pathway occurs when factor XIII binds with tissue factor (a transmembrane receptor) released from damaged cells. Both intrinsic and extrinsic pathways lead to the activation of factor X, mobilising the common pathway and catalysing the conversion of prothrombin to thrombin, and subsequently soluble fibrinogen to insoluble fibrin that facilitates a clot. Anticoagulant compounds can inhibit all three of the above-mentioned pathways. For example, ulvan generally inhibits coagulation through the intrinsic and/or common pathways [47,60,65,93,142,180,201,216,251], while heparin can inhibit intrinsic, extrinsic, and common pathways. Mechanistic details regarding the anticoagulant activity of ulvans, and other potential anticoagulants, are commonly elucidated using three tests, the activated partial thromboplastin time (aPTT), thrombin time (TT) and prothrombin time (PT), which determine if inhibition acts on the intrinsic and/or common pathways, common pathway, and extrinsic pathway, respectively.

Ulvan extracts from *U. clathrata* [93], *U. lactuca* [60,105], *U. prolifera* [251], *U. fasciata* [105,201], *U. nematoidea* [216] *U. conglobata* [47], *U. linza* [65,142], *U. reticulata* [105] and *Capsosiphon fulvescens* [180] have demonstrated anticoagulant activity. For example, ulvan from *U. linza* led to a 3.3–6.2-fold increase in aPTT times relative to normal clotting times, and is dependent on the degree of sulfation and molecular weight [142]. With regards to the latter, a hydrolysed ulvan sample (MW = 11 kDa; SO^{3-} = 20.1%) increased aPTT by 63% compared to the native ulvan extract (MW = 108 kDa; SO^{3-} = 21.3%),

while oversulfation of the hydrolysed sample (SO^{3-} = 34.4%) led to a further 20% increase in aPTT. While similar structure-activity relationships occur for TT, there is minimal PT activity reported. However, data from a study aiming to optimise the enzymatic extraction of ulvan from *U. prolifera* with the intent to optimise anticoagulant activity demonstrated an interaction between degree of sulfation and molecular weight [251]. Namely, increasing sulfation led to high anticoagulant activity until a molecular weight threshold (< 200 kDa) was reached, after which there was a complete loss of activity [251]. In summary, the anticoagulant activity of ulvan is dependent on degree of sulfation and molecular weight [43,47,65,142,251], with a higher degree of sulfation enhancing anticoagulant activity. The relationship between molecular weight and anticoagulant activity remains unclear, and this may also be dependent on the source of the ulvan.

The potency of the anticoagulant activity of ulvan is dependent on species and ecophysiological factors, which directly affect the structure of ulvan [47,65]. The anticoagulant activities for ulvan isolated from different biomass sources are between ~2–40 times less active than heparin. For example, one of the better performers was a highly sulfated ulvan fraction (SO^{3-} = 35.2%) isolated from *U. conglobata* [47]. This sample at 2 μg/ml yielded a 2.5-fold increase in aPTT compared to a 6.2-fold increase in aPTT for 2 μg/ml of heparin. While the latter highlights the potential of ulvan as an anticoagulant, the overall efficacy of ulvan relative to commercial drugs, like heparin, is less than these previous results indicate, as it only acts on two of the three coagulation pathways. This does not diminish the relevance of the anticoagulant activity of ulvan or its capacity to be used in the preparation of anticoagulants. For example, ulvan acts on the intrinsic pathway, which activates multiple pro-inflammatory, pro-coagulant, and immunomodulating pathways [252].

3.7. Antihyperlipidemic

The human body has a sophisticated lipoprotein transport system that utilises triglyceride (TG) rich very low-density lipoprotein-cholesterol (VLDL) to shuttle fatty acids to adipocytes and muscle, resulting in cholesterol rich low-density lipoprotein-cholesterol (LDL-C) that distributes cholesterol for steroidogenesis and cell membranes [253]. Excess cholesterol is transported back to the liver by high-density lipoprotein-cholesterol (HDL-C) for recycling or conversion to bile acids (BA) followed by its removal from the body. Imbalances in the lipoprotein transport system are linked to metabolic syndrome. Patients with metabolic syndrome are often hyperlipidaemic, a condition characterised by abnormally high blood levels of lipid(s) and lipoprotein(s), which can lead to cardiovascular diseases, such as coronary artery disease and atherosclerosis. Importantly, the consumption of macroalgae and the associated sulfated polysaccharides, including ulvan, has demonstrated antihyperlipidemic activity in vivo [254–256].

To measure the antihyperlipidemic activity of foods and supplements, such as sulfated polysaccharides, the serum total cholesterol (TC), TG, HDL-C and LDL-C of hyperlipidemic rat and mice models are commonly assessed [83,93,145,146,202,211,257]. Using these parameters ulvan from *U. pertusa* [68,69,83,93,145,146,238,257,258], *U. fasciata* [116,202,203,205], *U. lactuca* [211,213], *U. prolifera* [152,219] and *Monostroma nitidum* [259] have significant antihyperlipidemic activity, reducing or maintaining low levels of TC, TG, LDL-C, and increasing or maintaining a high level of HDL-C. Both molecular weight and degree of sulfation influence this activity. For example, Wistar rats fed a high starch feed supplemented with native ulvan (151.6 kDa) from *U. pertusa* had significant reductions in serum TC (45%) and LDL-C (54%), with no significant effect on TG and HDL-C compared to control rats fed the same high starch diet [145]. However, rats fed high starch diets with low molecular weight ulvan (28.2 kDa) showed no effect on either TC or LDL-C but significantly reduced TG (78%) and raised HDL-C (61%) relative to control fed rats, the mechanisms of which are discussed below [68]. There is some early evidence that a higher degree of sulfation may enhance the antihyperlipidemic activity [257]. For example, the serum TC of female rats treated with native ulvan (SO^{3-} = 22.5%) at 250 mg/kg was reduced by 28%, while treatment with oversulfated ulvan (SO^{3-} = 40.6%) reduced serum TC by 44% relative to the hyperlipidemic control group [257]. Derivatisation of native ulvan (e.g., acetylation) also influences antihyperlipidemic activity [146]. However, interactions between the degree of substitution and molecular weight are unclear and need to be understood to optimise structures that affect higher antihyperlipidemic activity.

The effect of molecular weight on the parameters used to assess antihyperlipidemic activity supports the conclusion that several mechanisms are operating in parallel. It has been proposed that reduction in serum TC and LDL-C in ulvan supplemented hyperlipidemic rats results in LDL-C conversion to bile acid in the liver followed by excretion [145]. This is further supported by an increase in faecal bile acid concentrations in ulvan supplemented hyperlipidemic rats. In contrast, supplementation of hyperlipidemic rats with lower molecular weight ulvan (28.2 kDa) had no effect on either TC or LDL-C but had elevated faecal bile acids and reduced TG and raised HDL-C relative to control fed rats [145], suggesting that other mechanisms, such as the upregulation of the synthesis of cholesterol in the liver, are also important. Treatment of lipid-loaded hepatocytes with an ulvan-like polysaccharide from *Monostroma nitidum* resulted in lower lipid concentrations accompanied with downregulation of the cholesterol synthesis gene for 3-hydroxy-3-methyl-glutaryl-CoA (HMG-CoA) reductase, upregulation of the cholesterol catabolism gene for cholesterol-7-α-hydroxylase (CYP7A1), and LDL uptake gene for LDL-receptor [259]. To corroborate these results, reduced serum TC concentrations measured in ulvan (*U. prolifera*) treated rats downregulated HMG-CoA reductase and the cholesterol regulating transcription factor sterol regulatory element binding protein 2 (SREBP-2) [219]. In a later study, reduced serum TG concentrations measured in ulvan treated rats were accompanied by downregulation of acetyl-CoA carboxylase (ACC) and its regulating transcription factor, SREBP-1c (regulates fatty acid synthesis) [260]. In theory, structurally different ulvan fractions may influence the regulatory genes (SREBP-1c and SREBP-2) to varying degrees, helping to explain the contradictory results obtained by Pengzhan *et al.* [145]. Evidence for another alternative or additional mechanism suggests that antioxidant effects may contribute to the antihyperlipidemic effects of polysaccharides [261,262]. In this mechanism, molecules with high antioxidant capacity (or those that can upregulate the endogenous antioxidant system) limit lipid oxidation by ROS, which leads to the accumulation of cholesterol due to changes in its biosynthesis and metabolism. In summary, the antihyperlipidemic activity of ulvan appears to operate by multiple mechanisms in parallel, the balance of which depends on the structural features of ulvan. This provides opportunity to optimise antihyperlipidemic supplements for more targeted applications.

3.8. Anti-viral

Viral treatments target the multiple steps in the viral replication cycles, which may be broadly thought of as entry, replication, shedding, and latency. Sulfated polysaccharides derived from marine algae, including ulvan, have promising antiviral activities [263–265]. Ulvans from *U. compressa* [199,266] *U. lactuca* [62,127,137], *U. clathrata* [107], *U. intestinalis* [207], *U. armoricana* [40] and *U. pertusa* [147] all have antiviral activity. The antiviral activity of ulvan extends to the enveloped viruses of herpes simplex virus (HSV) [40,199,266], Newcastle disease virus (NDV) [107], Japanese encephalitis virus (JEV) [127], dengue virus (DENV) [127], yellow fever virus (YFV) [127], West Nile virus (WNV) [127], influenza (H1N1) [62], avian influenza virus (AIV) [147] and measles virus (MeV) [207]. Examination of the antiviral activity of ulvan has been conducted in vitro using human larynx epithelial carcinoma cells (Hep-2) [199], African green monkey cells (Vero) [40,107,137,207], canine kidney cells (MDCK) [62], and in

vivo models using mice [127,147].

The antiviral effects of native ulvans against viral targets (measured as 50% Inhibitory Concentration (IC_{50}), the concentration of ulvan required to inhibit viral yield by 50%) are mixed ranging from weak (IC_{50} > 150 μg/ml [62,199]) to significant (IC_{50} = 0.1–30 μg/ml [107,127,207]). There are some interesting results supporting the use of ulvan in antiviral therapies. Ulvan from *U. clathrata* is an effective anti-viral for NDV, a fatal virus found in chickens causing large anthropogenic food losses [107]. Treatment with ulvan provided a concentration-dependent inhibition of NDV entry into Vero cells with an IC_{50} of 0.1 μg/ml. The activity was related to inhibition of an entry protein known as NDV fusion protein F. Although ulvan from *U. pertusa* had only moderate antiviral activity (40% inhibition at 100 μg/ml) against AIV-H9N2, it had a beneficial effect in a test relevant to immunisation [147], where AIV-H9N2 vaccination combined with ulvan treatment (50 mg/kg) led to an ~100% increase in antibody titre relative to the vaccination alone. This effect was attributed to the enhancement of the humoral immune response, due to the immunomodulatory effects of ulvan.

Variations in the antiviral activity of ulvan from different sources indicate a significant effect of structure; however, there are only a limited number of studies that probe the antiviral activity of ulvan and, consequently, the understanding of its structure-activity relationships is limited. However, the required structural features of ulvan are essentially similar to other sulfated polysaccharide antivirals, where activity is optimised by a high degree of sulfation and high molecular weight [264,267]. In this regard, treatment of HSV infected Hep-2 cells with a highly sulfated (SO^{3-} = 22%) ulvan fraction from *U. compressa* resulted in 100% HSV inhibition at 100 μg/ml and had an IC_{50} of 28.2μg/ml, compared to 153 μg/ml for native ulvan (SO^{3-} = 6%) [199]. Furthermore, ulvan with higher molecular weights (34 kDa) had 2–5 times the antiviral activity of low molecular weight ulvan (< 5 kDa). However, further studies are required to verify the generality of these results. In summary, the investigation of ulvan as an antiviral is in its infancy and at this point ulvan has variable antiviral activity against specific targets, with promise as an immunostimulant co-treatment for vaccinations.

3.9. Plant defence

More recently ulvans have been found to also influence the signalling pathways involved in plant immunity. The effect that ulvans have on plant immunity has been investigated in vitro with cell cultures (e.g., wheat and rice) [50] and in vivo with various non-cropping (e.g., thale cress) and cropping (e.g., apples, beans, wheat and barley) plant species [29,49–51,91,268–272]. Ulvan from *U. fasciata* [49–51,268,271,272], *U. lactuca* [91,269] and *U. armoricana* [29,270] all enhance the inducible defences of plants, a phenomenon known as “priming”. Inducible plant defences operate by the initial recognition of microbe/pathogen-associated molecular patterns (MAMPs/PAMPs), or elicitors, by plant cell membrane bound pattern-recognition receptors (PRRs), known as MAMP/PAMP-triggered immunity (MTI/PTI). Plants also have resistance (R) genes that encode cytoplasmic receptors that recognise pathogen effector molecules designed to suppress PTI, known as effector-triggered immunity (ETI) [273,274]. Plant immune responses downstream of MTI/PTI and ETI include the production of pathogenesis-related proteins that hydrolyse pathogen cell wall constituents, plant cell wall fortification through synthesis of lignin and callose, and the production of antimicrobial secondary metabolites [275,276]. An additional response unique to ETI is the hypersensitive response (HR), which is instigated by a pulse in the production of reactive oxygen species (ROS), triggering localised cell death at the site of infection. MTI/PTI and ETI also trigger systemic acquired resistance (SAR), where the defence alert is transferred from the site of pathogen ingress to distal plant tissues leading to an alert (or primed) state that is more responsive to subsequent pathogen attacks [277]. These plant immune responses are orchestrated by a complex balance of phytohormones (e.g., salicylic acid, jasmonic acid, ethylene and abscisic acid, cytokinins, auxins, brassinosteroids, and gibberellins) dependent on the identity of the pathogen and its trophic lifestyle (i.e., biotrophic vs. necrotrophic) [274]. Therefore, a great deal of information can be found by studying how the balance of molecules involved in the plant immune response are affected by treatment with potential priming agents, such as ulvan.

The effect of ulvan treatment on plant immunity has been investigated using pathogen and plant base measures including pathogen growth and development, plant health measures, such as growth, spotting and wilting, and molecular probes/profiles, such as hormones, proteins, and DNA. Ulvan from *U. fasciata* inhibits a key stage (appressoria differentiation) in the pathogenic cycle of the anthracnose causing fungi *Colletotrichum gloeosporioides* [268]. Consistent with a priming effect in vivo, tests on ulvan pre-treatment on apple leaves reduced disease severity by as much as 50% over control plants. Similar results were obtained when ulvan (from *U. fasciata*) treated *Arabidopsis thaliana* (thale cress) was inoculated with either *Alternaria brassicicola* (black spot fungi) or *Colletotrichum higginsianum* (anthracnose fungi) [49]. Interestingly, the degree of sulfation did not influence pathogenesis. However in another study, desulfation of ulvan from *U. lactuca* significantly reduced its capacity to induce the production of the defence enzyme, phenylalanine ammonia-lyase (PAL) [91]. In this study, a > 2-fold increase in the activity of PAL occurred when tomato plants were treated with ulvan oligomers relative to native ulvan [91]. Increased PAL activity was accompanied by an increase in salicylic acid. Therefore, in this case induction of SAR appears to be salicylic acid dependent. However, a study using transcriptomics combined with hormone profiling and enzyme activity measurements found that ulvan from *U. armoricana* induced plant immunity via the jasmonic acid signalling pathway in *Medicago truncatula* (Fabaceae), *Nicotianae tabacum* (Solanaceae), and *Arabidopsis thaliana* (Brassicaceae) [29]. Salicylic acid concentrations were unaffected by ulvan treatment, while jasmonic acid concentrations increased relative to control plants. Furthermore, the mode of action of ulvan was verified by its capacity to induce the expression of jasmonic acid-dependent genes (e.g., PDF1.2 defensin and lipoxygenase NtLOX1 promoter), while failing to induce the expression of salicylic acid-dependent genes (e.g., PR1a and PR5). Regardless of the signalling pathways responsible, ulvan demonstrates significant activity as a bio-elicitor and capacity to act as a priming agent enhancing both plant health and productivity.

According to the current understanding of plant immunity the capacity of ulvan to elicit plant defences requires that it is first recognised by the plant (either directly or indirectly), probably during primary signalling events (e.g., PTI or ETI). Therefore, the assumption that ulvan has analogous structural features to existing MAMPs/PAMPs is a logical conclusion and molecules that have structural similarities with ulvan such as plant rhamnogalacturonan I and rhamnolipids from phytopathogenic bacteria [196,197] also trigger defence responses. Typically, these latter examples contain rhamnose and uronic acids (but not sulfate esters), and these moieties may be important for ulvans activity. Notably, the presence of rhamnose (in ulvan) was required to induce immune defence responses in tomato plants, while glucuronic acid (in glucuronan) had no effect [91]. In terms of molecular weight, tomato plants treated with ulvan oligomers had up to twice the PAL activity than control plants. Conclusions regarding the degree of sulfation remain unclear, with one report indicative of a positive correlation and another indicative of no effect. Clearly the optimisation of ulvan products for use as bio-elicitors is in its infancy; however, its capacity to elicit plant immune responses is promising for reducing agricultural reliance on traditional pesticide treatments.

4. Conclusion

Research into the structural and biological properties of ulvan

remain in its early stages relative to those of the other marine-derived sulfated polysaccharides carrageenan and fucoidan. However, ulvan has the potential to find widespread application, including in agriculture, human health, and biomaterials. General trends in physicochemical properties and biological activities of ulvan relative to its structural features remain ambiguous, and this is due to the limited number of systematic studies on the structure-function properties of highly refined and well characterised ulvan against highly defined target activities. Additionally, the pharmacokinetics and bioavailability of such a complicated macromolecule will require thorough investigation prior to any application in a therapeutic capacity. The structurally distinct features of ulvans across biomass sources also contributes to this ambiguity and highlights the need for a focus on highly characterised refined ulvan of a single origin, or refining process. This will then clarify the structural requirements for specific biological activities, supporting informed decisions about the selection of species for cultivation and processing for specific target applications.

Acknowledgements

The authors acknowledge James Cook University for providing a PhD scholarship to Joel Kidgell. This research is part of the Pacific Biotechnology (previously MBD Industries Ltd) Research and Development program for the Integrated Production of Macroalgae.

Declaration of Interest

Declarations of interest: none. No conflicts, informed consent, human or animal rights applicable.

Author Contributions

All authors contributed to the conception and design of the review, interpretation of the meta-data, drafting of the article and revising it critically for important intellectual content. All authors approve of the final version to be submitted.

Appendix A. Supplementary data

Supplementary data to this article can be found online at https://doi.org/10.1016/j.algal.2019.101422.

References

[1] A.R. Angell, L. Mata, R. de Nys, N.A. Paul, Variation in amino acid content and its relationship to nitrogen content and growth rate in *Ulva ohnoi* (Chlorophyta), J. Phycol. 50 (2014) 216–226.
[2] L. Mata, M. Magnusson, N.A. Paul, R. de Nys, The intensive land-based production of the green seaweeds *Derbesia tenuissima* and *Ulva ohnoi*: biomass and bioproducts, J. Appl. Phycol. 28 (2016) 365–375.
[3] M. Magnusson, C. Carl, L. Mata, R. de Nys, N.A. Paul, Seaweed salt from *Ulva*: a novel first step in a cascading biorefinery model, Algal Res. 16 (2016) 308–316.
[4] C.R.K. Glasson, I.M. Sims, S.M. Carnachan, R. de Nys, M. Magnusson, A cascading biorefinery process targeting sulfated polysaccharides (ulvan) from *Ulva ohnoi*, Algal Res. 27 (2017) 383–391.
[5] J. Blomster, S. Back, D.P. Fewer, M. Kiirikki, A. Lehvo, C.A. Maggs, M.J. Stanhope, Novel morphology in *Enteromorpha* (Ulvophyceae) forming green tides, Am. J. Bot. 89 (2002) 1756–1763.
[6] G. Coat, P. Dion, M.C. Noailles, B. de Reviers, J.M. Fontaine, Y. Berger-Perrot, S. Loiseaux-de Goer, *Ulva armoricana* (Ulvales, Chlorophyta) from the coasts of Brittany (France). II. Nuclear rDNA ITS sequence analysis, Eur. J. Phycol. 33 (1998) 81–86.
[7] M. Hiraoka, S. Shimada, M. Uenosono, M. Masuda, A new green-tide-forming alga, *Ulva ohnoi* Hiraoka et Shimada sp. nov. (Ulvales, Ulvophyceae) from Japan, Phycol. Res. 52 (2004) 17–29.
[8] F. Kong, Y. Mao, F. Cui, X. Zhang, Z. Gao, Morphology and molecular identification of *Ulva* forming green tides in Qingdao, China, J. Ocean Univ. China 10 (2011) 73–79.
[9] D.B. Largo, J. Sembrano, M. Hiraoka, M. Ohno, Taxonomic and ecological profile of 'green tide' species of *Ulva* (Ulvales, Chlorophyta) in central Philippines, Hydrobiologia 512 (2004) 247–253.
[10] R.J. Lawton, L. Mata, R. de Nys, N.A. Paul, Algal bioremediation of waste waters from land-based aquaculture using *Ulva*: selecting target species and strains, PLoS One 8 (2013) e77344.
[11] P.H. de Paula Silva, S. McBride, R. de Nys, N.A. Paul, Integrating filamentous 'green tide' algae into tropical pond-based aquaculture, Aquaculture 284 (2008) 74–80.
[12] A.E. Nardelli, V.G. Chiozzini, E.S. Braga, F. Chow, Integrated multi-trophic farming system between the green seaweed *Ulva lactuca*, mussel, and fish: a production and bioremediation solution, J. Appl. Phycol. (2018), https://doi.org/10.1007/s10811-018-1581-4.
[13] M. Lahaye, A. Robic, Structure and functional properties of ulvan, a polysaccharide from green seaweeds, Biomacromolecules 8 (2007) 1765–1774.
[14] B. Ray, M. Lahaye, Cell-wall polysaccharides from the marine green alga *Ulva* "*rigida*" (ulvales, chlorophyta). Extraction and chemical composition, Carbohydr. Res. 274 (1995) 251–261.
[15] J.W.E. Brading, M.M.T. Georg-Plant, D.M. Hardy, The polysaccharide from the alga *Ulva lactuca*. Purification, hydrolysis, and methylation of the polysaccharide, Journal of the Chemical Society (Resumed) (1954) 319–324.
[16] B. Quemener, M. Lahaye, C. Bobin-Dubigeon, Sugar determination in ulvans by a chemical-enzymatic method coupled to high performance anion exchange chromatography, J. Appl. Phycol. 9 (1997) 179–188.
[17] J.P. McKinnell, E. Percival, The acid polysaccharide from the green seaweed, *Ulva lactuca*, J. Chem. Soc. (1962) 2082–2084 Resumed.
[18] A.F. Abdel-Fattah, M. Edrees, A study on the polysaccharide content of *Ulva lactuca* L, Qualitas Plantarum et Materiae Vegetabiles 22 (1972) 15–22.
[19] C.C. Gosselin, A. Holt, P.A. Lowe, Polysaccharides of *Enteromorpha* species, Journal of the Chemical Society (Resumed) (1964) 5877–5880.
[20] M. Lahaye, M.A.V. Axelos, Gelling properties of water-soluble polysaccharides from proliferating marine green seaweeds (*Ulva* spp.), Carbohydr. Polym. 22 (1993) 261–265.
[21] E. Percival, J.K. Wold, The acid polysaccharide from the green seaweed *Ulva lactuca*. Part II. The site of the ester sulphate, J. Chem. Soc. (1963) 5459 Resumed.
[22] M. Lahaye, B. Kaeffer, Seaweed dietary fibres: structure, physico-chemical and biological properties relevant to intestinal physiology, Sci. Aliment. 17 (1997) 563–584.
[23] M. Lahaye, M. Brunel, E. Bonnin, Fine chemical structure analysis of oligosaccharides produced by an ulvan-lyase degradation of the water-soluble cell-wall polysaccharides from *Ulva* sp. (Ulvales, Chlorophyta), Carbohydr. Res. 304 (1997) 325–333.
[24] M. Lahaye, B. Ray, Cell-wall polysaccharides from the marine green alga *Ulva* "*rigida*" (Ulvales, Chlorophyta) - NMR analysis of ulvan oligosaccharides, Carbohydr. Res. 283 (1996) 161–173.
[25] B. Ray, M. Lahaye, Cell-wall polysaccharides from the marine green alga *Ulva* "*rigida*" (Ulvales, Chlorophyta). Chemical structure of ulvan, Carbohydr. Res. 274 (1995) 313–318.
[26] E. Andrès, J. Molinari, G. Péterszegi, B. Mariko, E. Ruszova, V. Velebny, G. Faury, L. Robert, Pharmacological properties of rhamnose-rich polysaccharides, potential interest in age-dependent alterations of connectives tissues, Pathol. Biol. 54 (2006) 420–425.
[27] G. Faury, E. Ruszova, J. Molinari, B. Mariko, S. Raveaud, V. Velebny, L. Robert, The α-L-Rhamnose recognizing lectin site of human dermal fibroblasts functions as a signal transducer: modulation of Ca^{2+} fluxes and gene expression, Biochim. Biophys. Acta, 1780 (2008) 1388–1394.
[28] A. Adrien, A. Bonnet, D. Dufour, S. Baudouin, T. Maugard, N. Bridiau, Pilot production of ulvans from *Ulva* sp. and their effects on hyaluronan and collagen production in cultured dermal fibroblasts, Carbohydr. Polym. 157 (2017) 1306–1314.
[29] V. Jaulneau, C. Lafitte, C. Jacquet, S. Fournier, S. Salamagne, X. Briand, M.T. Esquerre-Tugaye, B. Dumas, Ulvan, a sulfated polysaccharide from green algae, activates plant immunity through the jasmonic acid signaling pathway, J. Biomed. Biotechnol. 2010 (2010) 1–11.
[30] S. Trouvelot, M.-C. Héloir, B. Poinssot, A. Gauthier, F. Paris, C. Guillier, M. Combier, L. Trdá, X. Daire, M. Adrian, Carbohydrates in plant immunity and plant protection: roles and potential application as foliar sprays, Front. Plant Sci. 5 (2014) 592.
[31] M.J. Stadnik, M.B. de Freitas, Algal polysaccharides as source of plant resistance inducers, Tropical Plant Pathology 39 (2014) 111–118.
[32] M. Lahaye, E.A.C. Cimadevilla, R. Kuhlenkamp, B. Quemener, V. Lognoné, P. Dion, Chemical composition and 13C NMR spectroscopic characterisation of ulvans from *Ulva* (Ulvales, Chlorophyta), J. Appl. Phycol. 11 (1999) 1–7.
[33] L.-A. Fransson, G.O. Aspinall (Ed.), Mammalian Glycosaminoglycans, The Polysaccharides Academic Press, New York, 1985, pp. 338–415.
[34] J. Venkatesan, B. Lowe, S. Anil, P. Manivasagan, A.A.A. Kheraif, K.-H. Kang, S.-K. Kim, Seaweed polysaccharides and their potential biomedical applications, Starch - Stärke 67 (2015) 381–390.
[35] L. Cunha, A. Grenha, Sulfated seaweed polysaccharides as multifunctional materials in drug delivery applications, Marine Drugs 14 (2016).
[36] A. Alves, R.A. Sousa, R.L. Reis, A practical perspective on ulvan extracted from green algae, J. Appl. Phycol. 25 (2013) 407–424.
[37] I. Wijesekara, R. Pangestuti, S.K. Kim, Biological activities and potential health benefits of sulfated polysaccharides derived from marine algae, Carbohydr. Polym. 84 (2011) 14–21.
[38] J. Barbosa, S. Borges, M. Amorim, M.J. Pereira, A. Oliveira, M.E. Pintado, P. Teixeira, Comparison of spray drying, freeze drying and convective hot air drying for the production of a probiotic orange powder, J. Funct. Foods 17 (2015) 340–351.

[39] M.f. Lai, C.F. Li, C.y. Li, Characterization and thermal behavior of six sulphated polysaccharides from seaweeds, Top. Catal. 8 (1994) 215–232.

[40] K. Hardouin, G. Bedoux, A.-S. Burlot, C. Donnay-Moreno, J.-P. Bergé, P. Nyvall-Collén, N. Bourgougnon, Enzyme-assisted extraction (EAE) for the production of antiviral and antioxidant extracts from the green seaweed *Ulva armoricana* (Ulvales, Ulvophyceae), Algal Res. 16 (2016) 233–239.

[41] G. Paradossi, F. Cavalieri, E. Chiessi, A conformational study on the algal polysaccharide ulvan, Macromolecules 35 (2002) 6404–6411.

[42] A. Robic, J.F. Sassi, P. Dion, Y. Lerat, M. Lahaye, Seasonal variability of physicochemical and rheological properties of ulvan in two *Ulva* species (chlorophyta) from the Brittany coast, J. Phycol. 45 (2009) 962–973.

[43] X.H. Qi, W.J. Mao, Y. Gao, Y. Chen, Y.L. Chen, C.Q. Zhao, N. Li, C.Y. Wang, M.X. Yan, C. Lin, J.M. Shan, Chemical characteristic of an anticoagulant-active sulfated polysaccharide from *Enteromorpha clathrata*, Carbohydr. Polym. 90 (2012) 1804–1810.

[44] K. Chattopadhyay, P. Mandal, P. Lerouge, A. Driouich, P. Ghosal, B. Ray, Sulphated polysaccharides from Indian samples of *Enteromorpha compressa* (Ulvales, Chlorophyta): isolation and structural features, Food Chem. 104 (2007) 928–935.

[45] J.P. McKinnell, E. Percival, Structural investigations on the water-soluble polysaccharide of the green seaweed *Enteromorpha compressa*, Journal of the Chemical Society (Resumed) (1962) 3141–3148.

[46] B. Ray, Polysaccharides from *Enteromorpha compressa*: isolation, purification and structural features, Carbohydr. Polym. 66 (2006) 408–416.

[47] W. Mao, X. Zang, Y. Li, H. Zhang, Sulfated polysaccharides from marine green algae *Ulva conglobata* and their anticoagulant activity, J. Appl. Phycol. 18 (2006) 9–14.

[48] M. Yamamoto, H. Imai, K. Mita, Y. Tadokoro, Physicochemical characterization of sulfated polysaccharides from green seaweeds: *Ulva pertusa* and *Ulva conglobata*, Agric. Biol. Chem. 44 (1980) 723–729.

[49] M.B. de Freitas, L.G. Ferreira, C. Hawerroth, M.E.R. Duarte, M.D. Noseda, M.J. Stadnik, Ulvans induce resistance against plant pathogenic fungi independently of their sulfation degree, Carbohydr. Polym. 133 (2015) 384–390.

[50] R. Paulert, D. Ebbinghaus, C. Urlass, B.M. Moerschbacher, Priming of the oxidative burst in rice and wheat cell cultures by ulvan, a polysaccharide from green macroalgae, and enhanced resistance against powdery mildew in wheat and barley plants, Plant Pathol. 59 (2010) 634–642.

[51] R. Paulert, V. Talamini, J.E.F. Cassolato, M.E.R. Duarte, M.D. Noseda, A. Smania, M.J. Stadnik, Effects of sulfated polysaccharide and alcoholic extracts from green seaweed *Ulva fasciata* on anthracnose severity and growth of common bean (*Phaseolus vulgaris* L.), Journal of Plant Diseases and Protection 116 (2009) 263–270.

[52] P. Shao, M. Chen, Y.P. Pei, P.L. Sun, In vitro antioxidant activities of different sulfated polysaccharides from chlorophytan seaweeds *Ulva fasciata*, Int. J. Biol. Macromol. 59 (2013) 295–300.

[53] P. Shao, Y. Pei, Z. Fang, P. Sun, Effects of partial desulfation on antioxidant and inhibition of DLD cancer cell of *Ulva fasciata* polysaccharide, Int. J. Biol. Macromol. 65 (2014) 307–313.

[54] P. Shao, M.P. Qin, L.F. Han, P.L. Sun, Rheology and characteristics of sulfated polysaccharides from chlorophytan seaweeds *Ulva fasciata*, Carbohydr. Polym. 113 (2014) 365–372.

[55] M.M. de Carvalho, R.A. de Freitas, D.R.B. Ducatti, L.G. Ferreira, A.G. Gonçalves, F.G. Colodi, E. Mazepa, E.M. Aranha, M.D. Noseda, M.E.R. Duarte, Modification of ulvans via periodate-chlorite oxidation: chemical characterization and anticoagulant activity, Carbohydr. Polym. 197 (2018) 631–640.

[56] P. Chandika, S.C. Ko, W.K. Jung, Marine-derived biological macromolecule-based biomaterials for wound healing and skin tissue regeneration, Int. J. Biol. Macromol. 77 (2015) 24–35.

[57] M. Tabarsa, S. You, E.H. Dabaghian, U. Surayot, Water-soluble polysaccharides from *Ulva intestinalis*: molecular properties, structural elucidation and immunomodulatory activities, J. Food Drug Anal. 26 (2) (2018) 599–608.

[58] A.A. Matloub, H.A. Aglan, S.S. Mohamed El Souda, M.E. Aboutabl, A.S. Maghraby, H.H. Ahmed, Influence of bioactive sulfated polysaccharide-protein complexes on hepatocarcinogenesis, angiogenesis and immunomodulatory activities, Asian Pac J Trop Med 9 (2016) 1200–1211.

[59] C. Costa, A. Alves, P.R. Pinto, R.A. Sousa, E.A. Borges da Silva, R.L. Reis, A.E. Rodrigues, Characterization of ulvan extracts to assess the effect of different steps in the extraction procedure, Carbohydr. Polym. 88 (2012) 537–546.

[60] A. Adrien, D. Dufour, S. Baudouin, T. Maugard, N. Bridiau, Evaluation of the anticoagulant potential of polysaccharide-rich fractions extracted from macroalgae, Nat. Prod. Res. 31 (2017) 2126–2136.

[61] A.A.A. Barros, A. Alves, C. Nunes, M.A. Coimbra, R.A. Pires, R.L. Reis, Carboxymethylation of ulvan and chitosan and their use as polymeric components of bone cements, Acta Biomater. 9 (2013) 9086–9097.

[62] G. Jiao, G. Yu, W. Wang, X. Zhao, J. Zhang, S.H. Ewart, Properties of polysaccharides in several seaweeds from Atlantic Canada and their potential anti-influenza viral activities, J. Ocean Univ. China 11 (2012) 205–212.

[63] H. Tian, X. Yin, Q. Zeng, L. Zhu, J. Chen, Isolation, structure, and surfactant properties of polysaccharides from *Ulva lactuca* L. from South China Sea, Int. J. Biol. Macromol. 79 (2015) 577–582.

[64] Y. Yuan, X. Xu, C. Jing, P. Zou, C. Zhang, Y. Li, Microwave assisted hydrothermal extraction of polysaccharides from *Ulva prolifera*: functional properties and bioactivities, Carbohydr. Polym. 181 (2018) 902–910.

[65] X.H. Qi, W.J. Mao, Y. Chen, Y.L. Chen, C.Q. Zhao, N. Li, C.Y. Wang, Chemical characteristics and anticoagulant activities of two sulfated polysaccharides from *Enteromorpha linza* (Chlorophyta), J. Ocean Univ. China 12 (2013) 175–182.

[66] A. Onda, S. Onda, M. Koike, K. Yanagisawa, S. Tsubaki, M. Hiraoka, Catalytic hydrolysis of polysaccharides derived from fast-growing green macroalgae, ChemCatChem 9 (2017) 2638–2641.

[67] M. Tabarsa, J.H. Han, C.Y. Kim, S.G. You, Molecular characteristics and immunomodulatory activities of water-soluble sulfated polysaccharides from *Ulva pertusa*, J. Med. Food 15 (2012) 135–144.

[68] W. Li, N. Jiang, B. Li, M. Wan, X. Chang, H. Liu, L. Zhang, S. Yin, H. Qi, S. Liu, Antioxidant activity of purified ulvan in hyperlipidemic mice, Int. J. Biol. Macromol. 113 (2018) 971–975.

[69] W. Li, K. Wang, N. Jiang, X. Liu, M. Wan, X. Chang, D. Liu, H. Qi, S. Liu, Antioxidant and antihyperlipidemic activities of purified polysaccharides from *Ulva pertusa*, J. Appl. Phycol. 30 (4) (2018) 2619–2627.

[70] M. Cho, C. Yang, S.M. Kim, S. You, Molecular characterization and biological activities of water-soluble sulfated polysaccharides from *Enteromorpha prolifera*, Food Sci. Biotechnol. 19 (2010) 525–533.

[71] M.J. Shi, X. Wei, J. Xu, B.J. Chen, D.Y. Zhao, S. Cui, T. Zhou, Carboxymethylated degraded polysaccharides from *Enteromorpha prolifera*: preparation and in vitro antioxidant activity, Food Chem. 215 (2017) 76–83.

[72] J.M. Leiro, R. Castro, J.A. Arranz, J. Lamas, Immunomodulating activities of acidic sulphated polysaccharides obtained from the seaweed *Ulva rigida* C. Agardh, Int. Immunopharmacol. 7 (2007) 879–888.

[73] M. Lahaye, J.-L. Gomez-Pinchetti, M.J. del Rio, G. Garcia-Reina, Natural decoloration, composition and increase in dietary fibre content of an edible marine algae, *Ulva rigida* (Chlorophyta), grown under different nitrogen conditions, J. Sci. Food Agric. 68 (1995) 99–104.

[74] R. Castro, M.C. Piazzon, I. Zarra, J. Leiro, M. Noya, J. Lamas, Stimulation of turbot phagocytes by *Ulva rigida* C. Agardh polysaccharides, Aquaculture 254 (2006) 9–20.

[75] R. Pezoa-Conte, A. Leyton, A. Baccini, M.C. Ravanal, P. Mäki-Arvela, H. Grénman, C. Xu, S. Willför, M.E. Lienqueo, J.P. Mikkola, Aqueous extraction of the sulfated polysaccharide Ulvan from the green alga *Ulva rigida* - kinetics and modeling, Bioenergy Research 10 (2017) 915–928.

[76] G. Toskas, R.D. Hund, E. Laourine, C. Cherif, V. Smyrniotopoulos, V. Roussis, Nanofibers based on polysaccharides from the green seaweed *Ulva rigida*, Carbohydr. Polym. 84 (2011) 1093–1102.

[77] A. Robic, C. Rondeau-Mouro, J.F. Sassi, Y. Lerat, M. Lahaye, Structure and interactions of ulvan in the cell wall of the marine green algae *Ulva rotundata* (Ulvales, Chlorophyceae), Carbohydr. Polym. 77 (2009) 206–216.

[78] C. Bobin-Dubigeon, M. Lahaye, F. Guillon, J.-L. Barry, D.J. Gallant, Factors limiting the biodegradation of *Ulva* sp cell-wall polysaccharides, J. Sci. Food Agric. 75 (1997) 341–351.

[79] N. Violle, P. Rozan, H. Demais, P. Nyvall Collen, J.F. Bisson, Evaluation of the antidepressant- and anxiolytic-like effects of a hydrophilic extract from the green seaweed *Ulva* sp. in rats, Nutr. Neurosci. (2017) 1–9.

[80] E. Percival, R.H. McDowell, Chemistry and Enzymology of Marine Algal Polysaccharides, Academic Press, London, 1967.

[81] M. Lahaye, NMR spectroscopic characterisation of oligosaccharides from two *Ulva rigida* ulvan samples (Ulvales, Chlorophyta) degraded by a lyase, Carbohydr. Res. 314 (1998) 1–12.

[82] G. Paradossi, F. Cavalieri, L. Pizzoferrato, A.M. Liquori, A physico-chemical study on the polysaccharide ulvan from hot water extraction of the macroalga *Ulva*, Int. J. Biol. Macromol. 25 (1999) 309–315.

[83] Y. Pengzhan, Z. Quanbin, L. Ning, X. Zuhong, W. Yanmei, L. Zhi, en, Polysaccharides from *Ulva pertusa* (Chlorophyta) and preliminary studies on their antihyperlipidemia activity, J. Appl. Phycol. 15 (2003) 21–27.

[84] M. Tako, M. Tamanaha, Y. Tamashiro, S. Uechi, Structure of ulvan isolated from the edible green seaweed, *Ulva pertusa*, Adv. Biosci. Biotechnol. 6 (2015) 645–655.

[85] M. Lahaye, F. Inizan, J. Vigouroux, NMR analysis of the chemical structure of ulvan and of ulvan-boron complex formation, Carbohydr. Polym. 36 (1998) 239–249.

[86] A. Robic, C. Gaillard, J.F. Sassi, Y. Lerat, M. Lahaye, Ultrastructure of ulvan: a polysaccharide from green seaweeds, Biopolymers 91 (2009) 652–664.

[87] Z. Zhang, X. Wang, M. Zhao, S. Yu, H. Qi, The immunological and antioxidant activities of polysaccharides extracted from *Enteromorpha linza*, Int. J. Biol. Macromol. 57 (2013) 45–49.

[88] H. Qi, T. Zhao, Q. Zhang, Z. Li, Z. Zhao, R. Xing, Antioxidant activity of different molecular weight sulfated polysaccharides from *Ulva pertusa* Kjellm (Chlorophyta), J. Appl. Phycol. 17 (2005) 527–534.

[89] Y. Pengzhan, Z. Quanbin, Z. Hong, N. Xizhen, L. Zhien, Preparation of polysaccharides in different molecular weights from *Ulva pertusa* Kjellm (Chorophyta), Chin. J. Oceanol. Limnol. 22 (2004) 381–385.

[90] L. Reisky, C. Stanetty, M.D. Mihovilovic, T. Schweder, J.-H. Hehemann, U.T. Bornscheuer, Biochemical characterization of an ulvan lyase from the marine flavobacterium *Formosa agariphila* KMM 3901T, Appl. Microbiol. Biotechnol. 102 (16) (2018) 6987–6996.

[91] C. El Modafar, M. Elgadda, R. El Boutachfaiti, E. Abouraicha, N. Zehhar, E. Petit, Z. El Alaoui-Talibi, B. Courtois, J. Courtois, Induction of natural defence accompanied by salicylic acid-dependant systemic acquired resistance in tomato seedlings in response to bioelicitors isolated from green algae, Sci. Hortic. 138 (2012) 55–63.

[92] H. Qi, Q. Zhang, T. Zhao, R. Chen, H. Zhang, X. Niu, Z. Li, Antioxidant activity of different sulfate content derivatives of polysaccharide extracted from *Ulva pertusa* (Chlorophyta) in vitro, Int. J. Biol. Macromol. 37 (2005) 195–199.

[93] H. Qi, L. Huang, X. Liu, D. Liu, Q. Zhang, S. Liu, Antihyperlipidemic activity of high sulfate content derivative of polysaccharide extracted from *Ulva pertusa* (Chlorophyta), Carbohydr. Polym. 87 (2012) 1637–1640.

[94] B. Kaeffer, C. Benard, M. Lahaye, H.M. Blottiere, C. Cherbut, Biological properties of ulvan, a new source of green seaweed sulfated polysaccharides, on cultured normal and cancerous colonic epithelial cells, Planta Med. 65 (1999) 527–531.

[95] S. Tsubaki, M. Hiraoka, S. Hadano, H. Nishimura, K. Kashimura, T. Mitani, Functional group dependent dielectric properties of sulfated hydrocolloids extracted from green macroalgal biomass, Carbohydr. Polym. 107 (2014) 192–197.

[96] H.M. Qi, Q.B. Zhang, T.T. Zhao, R.G. Hu, K. Zhang, Z. Li, In vitro antioxidant activity of acetylated and benzoylated derivatives of polysaccharide extracted from *Ulva pertusa* (Chlorophyta), Bioorg. Med. Chem. Lett. 16 (2006) 2441–2445.

[97] H.M. Qi, X.L. Liu, J. Ma, Q.B. Zhang, Z.E. Li, In vitro antioxidant activity of acetylated derivatives of polysaccharide extracted from *Ulva pertusa* (Cholorophta), Journal of Medicinal Plants Research 4 (2010) 2445–2451.

[98] A. Morelli, M. Betti, D. Puppi, C. Bartoli, M. Gazzarri, F. Chiellini, Enzymatically crosslinked ulvan hydrogels as injectable systems for cell delivery, Macromol. Chem. Phys. 217 (2016) 581–590.

[99] K. Kanno, T. Tanigawa, Y. Fujita, N. Ohnaka, Y. Kubo, K. Yoshida, K. Kojima, K. Nakata, M. Shimohara, Adsorbents for apheresis prepared from polysaccharides of algae that threaten ecosystem services, Chem. Biodivers. 11 (2014) 1140–1150.

[100] A. Robic, J.F. Sassi, M. Lahaye, Impact of stabilization treatments of the green seaweed *Ulva rotundata* (Chlorophyta) on the extraction yield, the physico-chemical and rheological properties of ulvan, Carbohydr. Polym. 74 (2008) 344–352.

[101] M. Berri, C. Slugocki, M. Olivier, E. Helloin, I. Jacques, H. Salmon, H. Demais, M. Le Goff, P.N. Collen, Marine-sulfated polysaccharides extract of *Ulva armoricana* green algae exhibits an antimicrobial activity and stimulates cytokine expression by intestinal epithelial cells, J. Appl. Phycol. 28 (2016) 2999–3008.

[102] M. Berri, M. Olivier, S. Holbert, J. Dupont, H. Demais, M. Le Goff, P.N. Collen, Ulvan from *Ulva armoricana* (Chlorophyta) activates the PI3K/Akt signalling pathway via TLR4 to induce intestinal cytokine production, Algal Res. 28 (2017) 39–47.

[103] V. Jaulneau, C. Lafitte, M.F. Corio-Costet, M.J. Stadnik, S. Salamagne, X. Briand, M.T. Esquerré-Tugayé, B. Dumas, An *Ulva armoricana* extract protects plants against three powdery mildew pathogens, Eur. J. Plant Pathol. 131 (2011) 393–401.

[104] V. Gadenne, L. Lebrun, T. Jouenne, P. Thebault, Role of molecular properties of ulvans on their ability to elaborate antiadhesive surfaces, J. Biomed. Mater. Res. A 103 (2015) 1021–1028.

[105] M. Shanmugam, B.K. Ramavat, K.H. Mody, R.M. Oza, A. Tewari, Distribution of heparinoid-active sulphated polysaccharides in some Indian marine green algae, Indian Journal of Marine Sciences 30 (2001) 222–227.

[106] R.M. Hernandez-Herrera, G. Virgen-Calleros, M. Ruiz-Lopez, J. Zanudo-Hernandez, J.P. Delano-Frier, C. Sanchez-Hernandez, Extracts from green and brown seaweeds protect tomato (*Solanum lycopersicum*) against the necrotrophic fungus *Alternaria solani*, J. Appl. Phycol. 26 (2014) 1607–1614.

[107] J.A. Aguilar-Briseño, L.E. Cruz-Suarez, J.F. Sassi, D. Ricque-Marie, P. Zapata-Benavides, E. Mendoza-Gamboa, C. Rodríguez-Padilla, L.M. Trejo-Avila, Sulphated polysaccharides from *Ulva clathrata* and *Cladosiphon okamuranus* seaweeds both inhibit viral attachment/entry and cell-cell fusion, in NDV infection, Marine Drugs 13 (2015) 697–712.

[108] P. del Rocío Quezada-Rodríguez, E.J. Fajer-Ávila, The dietary effect of ulvan from *Ulva clathrata* on hematological-immunological parameters and growth of tilapia (*Oreochromis niloticus*), J. Appl. Phycol. 29 (2017) 423–431.

[109] M. Lahaye, D. Jegou, Chemical and physical-chemical characteristics of dietary fibres from *Ulva lactuca* (L.) Thuret and *Enteromorpha compressa* (L.) Grev, J. Appl. Phycol. 5 (1993) 195.

[110] M. Yamamoto, Physicochemical studies on sulfated polysaccharides extracted from seaweeds at various temperatures, Agric. Biol. Chem. 44 (1980) 589–593.

[111] A.K. Siddhanta, A.M. Goswami, B.K. Ramavat, K.H. Mody, O.P. Mairh, Water soluble polysaccharides of marine algal species of *Ulva* (Ulvales, Chlorophyta) of Indian waters, Indian Journal of Marine Sciences 30 (2001) 166–172.

[112] G.M. Jose, M. Kurup, In vitro antioxidant properties of edible marine algae *Sargassum swartzii*, *Ulva fasciata* and *Chaetomorpha antennina* of Kerala coast, Pharmaceutical Bioprocessing 4 (2016) 100–108.

[113] P. Shao, X. Chen, P. Sun, In vitro antioxidant and antitumor activities of different sulfated polysaccharides isolated from three algae, Int. J. Biol. Macromol. 62 (2013) 155–161.

[114] P. Shao, J. Shao, L. Han, R. Lv, P. Sun, Separation, preliminary characterization, and moisture-preserving activity of polysaccharides from *Ulva fasciata*, Int. J. Biol. Macromol. 72 (2015) 924–930.

[115] R. Pankiewicz, B. Łęska, B. Messyasz, J. Fabrowska, M. Sołoducha, M. Pikosz, First isolation of polysaccharidic ulvans from the cell walls of freshwater algae, Algal Res. 19 (2016) 348–354.

[116] A.A. Matloub, S.S.M. Elsouda, W.M. El-Senousy, M. Hamed, H. Aly, S.A. Ali, R.S. Mohammed, K. Mahmoud, S. El-Hallouty, N.A. Ibrahim, N.A. Awad, H.M. El-Rafaie, In vitro antiviral, cytotoxic, antioxidant and hypolipidemic activites of polysaccharide isolated from marine algae, International Journal of Pharmacognosy and Phytochemical Research 7 (2015) 1099–1111.

[117] N. Peasura, N. Laohakunjit, O. Kerdchoechuen, S. Wanlapa, Characteristics and antioxidant of *Ulva intestinalis* sulphated polysaccharides extracted with different solvents, Int. J. Biol. Macromol. 81 (2015) 912–919.

[118] F. Rahimi, M. Tabarsa, M. Rezaei, Ulvan from green algae *Ulva intestinalis*: optimization of ultrasound-assisted extraction and antioxidant activity, J. Appl. Phycol. 28 (2016) 2979–2990.

[119] X.X. Wang, Y. Chen, J.J. Wang, Z.X. Liu, S.G. Zhao, Antitumor activity of a sulfated polysaccharide from *Enteromorpha intestinalis* targeted against hepatoma through mitochondrial pathway, Tumor Biol. 35 (2014) 1641–1647.

[120] H.J. Alipour, M. Rezaei, B. Shabanpour, M. Tabarsa, Effects of sulfated polysaccharides from green alga *Ulva intestinalis* on physicochemical properties and microstructure of silver carp surimi, Food Hydrocoll. 74 (2018) 87–96.

[121] L.L. Jiao, P. Jiang, L.P. Zhang, M.J. Wu, Antitumor and immunomodulating activity of polysaccharides from *Enteromorpha intestinalis*, Biotechnol. Bioprocess Eng. 15 (2010) 421–428.

[122] L.L. Jiao, X. Li, T.B. Li, P. Jiang, L.X. Zhang, M.J. Wu, L.P. Zhang, Characterization and anti-tumor activity of alkali-extracted polysaccharide from *Enteromorpha intestinalis*, Int. Immunopharmacol. 9 (2009) 324–329.

[123] B. de Reviers, A. Leproux, Characterization of polysaccharides from *Enteromorpha intestinalis* (L.) link, chlorophyta, Carbohydr. Polym. 22 (1993) 253–259.

[124] N. Peasura, N. Laohakunjit, O. Kerdchoechuen, P. Vongsawasdi, L.K. Chao, Assessment of biochemical and immunomodulatory activity of sulphated polysaccharides from *Ulva intestinalis*, Int. J. Biol. Macromol. 91 (2016) 269–277.

[125] H. Yaich, H. Garna, S. Besbes, J.-P. Barthélemy, M. Paquot, C. Blecker, H. Attia, Impact of extraction procedures on the chemical, rheological and textural properties of ulvan from *Ulva lactuca* of Tunisia coast, Food Hydrocoll. 40 (2014) 53–63.

[126] O.A. Al-Amoudi, H.H. Mutawie, A.V. Patel, G. Blunden, Chemical composition and antioxidant activities of Jeddah corniche algae, Saudi Arabia, Saudi Journal of Biological Sciences 16 (2009) 23–29.

[127] Y.H. Chiu, Y.L. Chan, T.L. Li, C.J. Wu, Inhibition of Japanese encephalitis virus infection by the sulfated polysaccharide extracts from *Ulva lactuca*, Mar. Biotechnol. 14 (2012) 468–478.

[128] T.T.T. Thanh, T.M.T. Quach, T.N. Nguyen, D.V. Luong, M.L. Bui, T.T.V. Tran, Structure and cytotoxic activity of ulvan extracted from green seaweed *Ulva lactuca*, Int. J. Biol. Macromol. 93 (2016) 695–702.

[129] I.W.F. de Araújo, J.A.G. Rodrigues, A.L.G. Quinderé, J.D.F.T. Silva, G.D.F. Maciel, N.A. Ribeiro, E. de Sousa Oliveira Vanderlei, K.A. Ribeiro, H.V. Chaves, K.M.A. Pereira, M.M. Bezerra, N.M.B. Benevides, Analgesic and anti-inflammatory actions on bradykinin route of a polysulfated fraction from alga *Ulva lactuca*, Int. J. Biol. Macromol. 92 (2016) 820–830.

[130] T.K. Gajaria, P. Suthar, R.S. Baghel, N.B. Balar, P. Sharnagat, V.A. Mantri, C.R.K. Reddy, Integration of protein extraction with a stream of byproducts from marine macroalgae: a model forms the basis for marine bioeconomy, Bioresour. Technol. 243 (2017) 867–873.

[131] J. He, Y. Xu, H. Chen, P. Sun, Extraction, structural characterization, and potential antioxidant activity of the polysaccharides from four seaweeds, Int. J. Mol. Sci. 17 (2016).

[132] D.G. Medcalf, T. Lionel, J.H. Brannon, J.R. Scott, Seasonal variation in the mucilaginous polysaccharides from *Ulva lactuca*, Bot. Mar. 18 (1975) 67–70.

[133] H. Yaich, H. Garna, S. Besbes, M. Paquot, C. Blecker, H. Attia, Effect of extraction conditions on the yield and purity of ulvan extracted from *Ulva lactuca*, Food Hydrocoll. 31 (2013) 375–382.

[134] A. Haug, The influence of borate and calcium on the gel formation of a sulfated polysaccharide from *Ulva lactuca*, Acta Chemica Scandinavica. Series B: Organic Chemistry and Biochemistry 30 (1976) 562–566.

[135] A. Sathivel, Balavinayagamani, B.R. Hanumantha Rao, T. Devaki, Sulfated polysaccharide isolated from *Ulva lactuca* attenuates D-galactosamine induced DNA fragmentation and necrosis during liver damage in rats, Pharm. Biol., 52 (2014) 498–505.

[136] A. Alves, R.A. Sousa, R.L. Reis, Processing of degradable ulvan 3D porous structures for biomedical applications, J. Biomed. Mater. Res. A 101 (2013) 998–1006.

[137] H.H. Abd El-Baky, F.K. El Baz, G.S. El Baroty, Potential biological properties of sulphated polysaccharides extracted from the macroalgae *Ulva lactuca* L, Academic Journal of Cancer Research 2 (2009) 1–11.

[138] T. Devaki, A. Sathivel, H.R. BalajiRaghavendran, Stabilization of mitochondrial and microsomal function by polysaccharide of *Ulva lactuca* on D-Galactosamine induced hepatitis in rats, Chem. Biol. Interact. 177 (2009) 83–88.

[139] U.K. Hussein, H.M. Mahmoud, A.G. Farrag, A. Bishayee, Chemoprevention of diethylnitrosamine-initiated and phenobarbital-promoted hepatocarcinogenesis in rats by sulfated polysaccharides and aqueous extract of *Ulva lactuca*, Integrative Cancer Therapies 14 (2015) 525–545.

[140] J. Wang, W.H. Jin, Y. Hou, X.Z. Niu, H. Zhang, Q.B. Zhang, Chemical composition and moisture-absorption/retention ability of polysaccharides extracted from five algae, Int. J. Biol. Macromol. 57 (2013) 26–29.

[141] H.A. Badr, K. Takahashi, R. Kawakami, Y. Oyama, K. Yokoigawa, K. Kanemaru, Screening and analysis of edible seaweeds in the ability to adsorb Shiga toxin, Eur. Food Res. Technol. 243 (2017) 2147–2153.

[142] X.M. Wang, Z.S. Zhang, Z.Y. Yao, M.X. Zhao, H.M. Qi, Sulfation, anticoagulant and antioxidant activities of polysaccharide from green algae *Enteromorpha linza*, Int. J. Biol. Macromol. 58 (2013) 225–230.

[143] Z.S. Zhang, F. Wang, X.M. Wang, X.L. Liu, Y. Hou, Q.B. Zhang, Extraction of the polysaccharides from five algae and their potential antioxidant activity in vitro, Carbohydr. Polym. 82 (2010) 118–121.

[144] C. Fernández-Díaz, O. Coste, E.J. Malta, Polymer chitosan nanoparticles functionalized with *Ulva ohnoi* extracts boost in vitro ulvan immunostimulant effect in Solea senegalensis macrophages, Algal Res. 26 (2017) 135–142.

[145] Y. Pengzhan, L. Ning, L. Xiguang, Z. Gefei, Z. Quanbin, L. Pengcheng, Antihyperlipidemic effects of different molecular weight sulfated polysaccharides from *Ulva pertusa* (Chlorophyta), Pharmacol. Res. 48 (2003) 543–549.

[146] H.M. Qi, X.L. Liu, J.B. Zhang, Y. Duan, X.L. Wang, Q.B. Zhang, Synthesis and antihyperlipidemic activity of acetylated derivative of ulvan from *Ulva pertusa*, Int. J. Biol. Macromol. 50 (2012) 270–272.

[147] L. Song, X. Chen, X. Liu, F. Zhang, L. Hu, Y. Yue, K. Li, P. Li, Characterization and comparison of the structural features, immune-modulatory and anti-avian influenza virus activities conferred by three algal sulfated polysaccharides, Marine

Drugs (2016) 14.
[148] C. Cai, Z. Guo, Y. Yang, Z. Geng, L. Tang, M. Zhao, Y. Qiu, Y. Chen, P. He, Inhibition of hydrogen peroxide induced injuring on human skin fibroblast by *Ulva prolifera* polysaccharide, Int. J. Biol. Macromol. 91 (2016) 241–247.
[149] B. Li, S. Liu, R. Xing, K.C. Li, R.F. Li, Y.K. Qin, X.Q. Wang, Z.H. Wei, P.C. Li, Degradation of sulfated polysaccharides from *Enteromorpha prolifera* and their antioxidant activities, Carbohydr. Polym. 92 (2013) 1991–1996.
[150] Y. Yu, Y.P. Li, C.Y. Du, H.J. Mou, P. Wang, Compositional and structural characteristics of sulfated polysaccharide from *Enteromorpha prolifera*, Carbohydr. Polym. 165 (2017) 221–228.
[151] J.X. Li, Z. Chi, L.J. Yu, F. Jiang, C.G. Liu, Sulfated modification, characterization, and antioxidant and moisture absorption/retention activities of a soluble neutral polysaccharide from *Enteromorpha prolifera*, Int. J. Biol. Macromol. 105 (2017) 1544–1553.
[152] Z.L. Teng, L. Qian, Y. Zhou, Hypolipidemic activity of the polysaccharides from *Enteromorpha prolifera*, Int. J. Biol. Macromol. 62 (2013) 254–256.
[153] J. Xu, L.L. Xu, Q.W. Zhou, S.X. Hao, T. Zhou, H.J. Xie, Isolation, purification, and antioxidant activities of degraded polysaccharides from *Enteromorpha prolifera*, Int. J. Biol. Macromol. 81 (2015) 1026–1030.
[154] Q.T.M. Thu, T.H. Bang, N.T. Nu, D.V. Luong, B.M. Ly, T.T.T. Van, T.T.T. Thuy, Structural determination of ulvan from green seaweed *Ulva reticulata* collected at central coast of Vietnam, Chem. Lett. 44 (2015) 788–790.
[155] T.T.V. Tran, H.B. Truong, N.H.V. Tran, T.M.T. Quach, T.N. Nguyen, M.L. Bui, Y. Yuguchi, T.T.T. Thanh, Structure, conformation in aqueous solution and antimicrobial activity of ulvan extracted from green seaweed *Ulva reticulata*, Nat. Prod. Res. (2017) 1–6.
[156] P.N. Collén, J.F. Sassi, H. Rogniaux, H. Marfaing, W. Helbert, Ulvan lyases isolated from the flavobacteria *Persicivirga ulvanivorans* are the first members of a new polysaccharide lyase family, J. Biol. Chem. 286 (2011) 42063–42071.
[157] A. Alves, S.G. Caridade, J.F. Mano, R.A. Sousa, R.L. Reis, Extraction and physicochemical characterization of a versatile biodegradable polysaccharide obtained from green algae, Carbohydr. Res. 345 (2010) 2194–2200.
[158] V.C. Padmanaban, K.P. Prashant, M.V. Ranjith, T. Aswani, M.T. Aswani, Comparative analysis of anti-coagulant potential of marine macro algae, Int J Pharm Pharm Sci 5 (2013) 334–337.
[159] P.A. Harnedy, R.J. FitzGerald, Extraction and enrichment of protein from red and green macroalgae, Methods Mol. Biol. 1308 (2015) 103–108.
[160] A.R. Angell, N.A. Paul, R. de Nys, A comparison of protocols for isolating and concentrating protein from the green seaweed *Ulva ohnoi*, J. Appl. Phycol. 29 (2017) 1011–1026.
[161] S. Tsubaki, K. Oono, M. Hiraoka, A. Onda, T. Mitani, Microwave-assisted hydrothermal extraction of sulfated polysaccharides from *Ulva* spp. and *Monostroma latissimum*, Food Chem. 210 (2016) 311–316.
[162] E. Hernández-Garibay, J.A. Zertuche-González, I. Pacheco-Ruíz, Isolation and chemical characterization of algal polysaccharides from the green seaweed *Ulva clathrata* (Roth) C. Agardh, J. Appl. Phycol. 23 (2011) 537–542.
[163] L. Shi, Bioactivities, isolation and purification methods of polysaccharides from natural products: a review, Int. J. Biol. Macromol. 92 (2016) 37–48.
[164] A. Béress, O. Wassermann, T. Bruhn, L. Béress, E.N. Kraiselburd, L.V. Gonzalez, G.E. de Motta, P.I. Chavez, A new procedure for the isolation of anti-HIV compounds (polysaccharides and polyphenols) from the marine alga *Fucus vesiculosus*, J. Nat. Prod. 56 (1993) 478–488.
[165] H.-J. Zhang, W.-J. Mao, F. Fang, H.-Y. Li, H.-H. Sun, Y. Chen, X.-H. Qi, Chemical characteristics and anticoagulant activities of a sulfated polysaccharide and its fragments from *Monostroma latissimum*, Carbohydr. Polym. 71 (2008) 428–434.
[166] P. Ghosh, U. Adhikari, P.K. Ghosal, C.A. Pujol, M.J. Carlucci, E.B. Damonte, B. Ray, In vitro anti-herpetic activity of sulfated polysaccharide fractions from *Caulerpa racemosa*, Phytochemistry 65 (2004) 3151–3157.
[167] L. Yang, L.-M. Zhang, Chemical structural and chain conformational characterization of some bioactive polysaccharides isolated from natural sources, Carbohydr. Polym. 76 (2009) 349–361.
[168] I.M. Sims, S.M. Carnachan, T.J. Bell, S.F.R. Hinkley, Methylation analysis of polysaccharides: technical advice, Carbohydr. Polym. 188 (2018) 1–7.
[169] F.A. Pettolino, C. Walsh, G.B. Fincher, A. Bacic, Determining the polysaccharide composition of plant cell walls, Nat. Protoc. 7 (2012) 1590–1607.
[170] J.S. Craigie, Z.C. Wen, J.P. van der Meer, Interspecific, intraspecific and nutritionally-determined variations in the composition of agars from *Gracilaria* spp, Bot. Mar. (1984) 55.
[171] A. Robic, D. Bertrand, J.F. Sassi, Y. Lerat, M. Lahaye, Determination of the chemical composition of ulvan, a cell wall polysaccharide from *Ulva* spp. (Ulvales, Chlorophyta) by FT-IR and chemometrics, J. Appl. Phycol. 21 (2009) 451–456.
[172] J.N. BeMiller, Acid-catalyzed hydrolysis of glycosides, Adv. Carbohydr. Chem. Biochem. 22 (1967) 25–108.
[173] L.A. Fransson, L. Roden, M.L. Spach, Automated ion-exchange chromatography of uronic acids and uronic acid containing oligosaccharides, Anal. Biochem. 23 (1968) 317–330.
[174] H.E. Conrad, The acid lability of the glycosidic bonds of L-iduronic acid residues in glycosaminoglycans, The Biochemical journal 191 (1980) 355–363.
[175] G.A. De Ruiter, H.A. Schols, A.G.J. Voragen, F.M. Rombouts, Carbohydrate analysis of water-soluble uronic acid-containing polysaccharides with high-performance anion-exchange chromatography using methanolysis combined with TFA hydrolysis is superior to four other methods, Anal. Biochem. 207 (1992) 176–185.
[176] D.W. Templeton, M. Quinn, S. Van Wychen, D. Hyman, L.M.L. Laurens, Separation and quantification of microalgal carbohydrates, J. Chromatogr. A 1270 (2012) 225–234.
[177] B. Radhakrishnamurthy, G.S. Berenson, Effect of temperature and time of heating on the carbazole reaction of uronic acids and acid mucopolysaccharides, Anal. Chem. 35 (1963) 1316–1318.
[178] N. Blumenkrantz, G. Asboe-Hansen, New method for quantitative determination of uronic acids, Anal. Biochem. 54 (1973) 484–489.
[179] J.E. Cassolato, M.D. Noseda, C.A. Pujol, F.M. Pellizzari, E.B. Damonte, M.E. Duarte, Chemical structure and antiviral activity of the sulfated heterorhamnan isolated from the green seaweed *Gayralia oxysperma*, Carbohydr. Res. 343 (2008) 3085–3095.
[180] A. Synytsya, D.J. Choi, R. Pohl, Y.S. Na, P. Capek, E. Lattová, T. Taubner, J.W. Choi, C.W. Lee, J.K. Park, W.J. Kim, S.M. Kim, J. Lee, Y.I. Park, Structural features and anti-coagulant activity of the sulphated polysaccharide SPS-CF from a green alga *Capsosiphon fulvescens*, Mar. Biotechnol. 17 (2015) 718–735.
[181] J.Ø. Duus, C.H. Gotfredsen, K. Bock, Carbohydrate structural determination by NMR spectroscopy: modern methods and limitations, Chem. Rev. 100 (2000) 4589–4614.
[182] H.N. Cheng, T.G. Neiss, Solution NMR spectroscopy of food polysaccharides, Polym. Rev. 52 (2012) 81–114.
[183] H. Yaich, A.B. Amira, F. Abbes, M. Bouaziz, S. Besbes, A. Richel, C. Blecker, H. Attia, H. Garna, Effect of extraction procedures on structural, thermal and antioxidant properties of ulvan from *Ulva lactuca* collected in Monastir coast, Int. J. Biol. Macromol. 105 (Pt 2) (2017) 1430–1439.
[184] M. Kopel, W. Helbert, Y. Belnik, V. Buravenkov, A. Herman, E. Banin, New family of ulvan lyases identified in three isolates from the alteromonadales order, J. Biol. Chem. 291 (2016) 5871–5878.
[185] A. Morelli, M. Betti, D. Puppi, F. Chiellini, Design, preparation and characterization of ulvan based thermosensitive hydrogels, Carbohydr. Polym. 136 (2016) 1108–1117.
[186] A.M. Striegel, Multiple detection in size-exclusion chromatography of macromolecules, Anal. Chem. 77 (2005) 104 A–113 A.
[187] L.K. Kostanski, D.M. Keller, A.E. Hamielec, Size-exclusion chromatography—a review of calibration methodologies, J. Biochem. Biophys. Methods 58 (2004) 159–186.
[188] M.M. Bradford, A rapid and sensitive method for the quantitation of microgram quantities of protein utilizing the principle of protein-dye binding, Anal. Biochem. 72 (1976) 248–254.
[189] O.H. Lowry, N.J. Rosebrough, A.L. Farr, R.J. Randall, Protein measurement with the Folin phenol reagent, J. Biol. Chem. 193 (1951) 265–275.
[190] F. Pittner, P.L. Turecek, The application of immobilized α-L-rhamnosidase and L-rhamnosedehydrogenase in the analysis of L-rhamnose and α-L-rhamnosides, Appl. Biochem. Biotechnol. 16 (1987) 15–24.
[191] Z. Gong, W. Zhou, H. Shen, Z. Yang, G. Wang, Z. Zuo, Y. Hou, Z.K. Zhao, Co-fermentation of acetate and sugars facilitating microbial lipid production on acetate-rich biomass hydrolysates, Bioresour. Technol. 207 (2016) 102–108.
[192] T.S. Moon, S.-H. Yoon, M.-J. Tsang Mui Ching, A.M. Lanza, K.L.J. Prather, Enzymatic assay of D-glucuronate using uronate dehydrogenase, Anal. Biochem. 392 (2009) 183–185.
[193] T. Salomonsen, H.M. Jensen, D. Stenbæk, S.B. Engelsen, Chemometric prediction of alginate monomer composition: a comparative spectroscopic study using IR, Raman, NIR and NMR, Carbohydr. Polym. 72 (2008) 730–739.
[194] T.M. Handel, Z. Johnson, S.E. Crown, E.K. Lau, A.E. Proudfoot, Regulation of protein function by glycosaminoglycans–as exemplified by chemokines, Annu. Rev. Biochem. 74 (2005) 385–410.
[195] D. Scharnweber, L. Hubner, S. Rother, U. Hempel, U. Anderegg, S.A. Samsonov, M.T. Pisabarro, L. Hofbauer, M. Schnabelrauch, S. Franz, J. Simon, V. Hintze, Glycosaminoglycan derivatives: promising candidates for the design of functional biomaterials, J. Mater. Sci. Mater. Med. 26 (2015) 232.
[196] A.L. Varnier, L. Sanchez, P. Vatsa, L. Boudesocque, A. Garcia-Brugger, F. Rabenoelina, A. Sorokin, J.H. Renault, S. Kauffmann, A. Pugin, C. Clement, F. Baillieul, S. Dorey, Bacterial rhamnolipids are novel MAMPs conferring resistance to *Botrytis cinerea* in grapevine, Plant Cell Environ. 32 (2009) 178–193.
[197] P. Vatsa, L. Sanchez, C. Clement, F. Baillieul, S. Dorey, Rhamnolipid biosurfactants as new players in animal and plant defense against microbes, Int. J. Mol. Sci. 11 (2010) 5095–5108.
[198] S. Bigot, G. Louarn, N. Kébir, F. Burel, Click grafting of seaweed polysaccharides onto PVC surfaces using an ionic liquid as solvent and catalyst, Carbohydr. Polym. 98 (2013) 1644–1649.
[199] N. Lopes, S. Ray, S.F. Espada, W.A. Bomfim, B. Ray, L.C. Faccin-Galhardi, R.E.C. Linhares, C. Nozawa, Green seaweed *Enteromorpha compressa* (Chlorophyta, Ulvaceae) derived sulphated polysaccharides inhibit herpes simplex virus, Int. J. Biol. Macromol. 102 (2017) 605–612.
[200] V. Gadenne, L. Lebrun, T. Jouenne, P. Thebault, Antiadhesive activity of ulvan polysaccharides covalently immobilized onto titanium surface, Colloids Surf. B: Biointerfaces 112 (2013) 229–236.
[201] C. Faggio, M. Pagano, A. Dottore, G. Genovese, M. Morabito, Evaluation of anticoagulant activity of two algal polysaccharides, Nat. Prod. Res. 30 (2016) 1934–1937.
[202] M.Z. Rizk, H.F. Aly, A.A. Matloub, G.I. Fouad, The anti-hypercholesterolemic effect of ulvan polysaccharide extracted from the green alga *Ulva fasciata* on aged hypercholesterolemic rats, Asian Journal of Pharmaceutical and Clinical Research (2016) 9.
[203] M.Z. Rizk, M. El-Sherbiny, I.H. Borai, M.K. Ezz, H.F. Aly, A.A. Matloub, A.E.R. Farrag, G.I. Fouad, Sulphated polysaccharides (SPS) from the green alga *ulva fasciata* extract modulates liver and kidney function in high fat diet-induced hypercholesterolemic rats, Int J Pharm Pharm Sci 8 (2016) 43–55.
[204] A. Tariq, M. Athar, J. Ara, V. Sultana, S. Ehteshamul-Haque, M. Ahmad, Biochemical evaluation of antioxidant activity in extracts and polysaccharide

fractions of seaweeds, Global Journal of Environmental Science and Management 1 (2015) 47–62.
[205] I.H. Borai, M.K. Ezz, M.Z. Rizk, M. El-Sherbiny, A.A. Matloub, H.F. Aly, G.I. Fouad, Hypolipidemic and anti-atherogenic effect of sulphated polysaccharides from the green alga *Ulva fasciata*, International Journal of Pharmaceutical Sciences Review and Research 31 (2015) 1–12.
[206] L. Araújo, M.J. Stadnik, L.C. Borsato, R.M. Valdebenito-Sanhueza, Potassium phosphite and ulvan in the control of 'Gala' leaf spot on apple, Tropical Plant Pathology 33 (2008) 148–152.
[207] K. Morán-Santibañez, L.E. Cruz-Suárez, D. Ricque-Marie, D. Robledo, Y. Freile-Pelegrín, M.A. Peña-Hernández, C. Rodríguez-Padilla, L.M. Trejo-Avila, Synergistic effects of sulfated polysaccharides from Mexican seaweeds against measles virus, Biomed. Res. Int. 2016 (2016).
[208] J. Spavieri, M. Kaiser, R. Casey, S. Hingley-Wilson, A. Lalvani, G. Blunden, D. Tasdemir, Antiprotozoal, antimycobacterial and cytotoxic potential of some british green algae, Phytother. Res. 24 (2010) 1095–1098.
[209] G.E.F. Abd-Ellatef, O.M. Ahmed, E.S. Abdel-Reheim, A.H.Z. Abdel-Hamid, *Ulva lactuca* polysaccharides prevent Wistar rat breast carcinogenesis through the augmentation of apoptosis, enhancement of antioxidant defense system, and suppression of inflammation, Breast Cancer: Targets and Therapy 9 (2017) 67–83.
[210] O.M. Ahmed, R.R. Ahmed, Anti-proliferative and apoptotic efficacies of ulvan polysaccharides against different types of carcinoma cells in vitro and in vivo, Journal of Cancer Science and Therapy 6 (2014) 202–208.
[211] S. Hassan, S.A. El-Twab, M. Hetta, B. Mahmoud, Improvement of lipid profile and antioxidant of hypercholesterolemic albino rats by polysaccharides extracted from the green alga *Ulva lactuca* Linnaeus, Saudi Journal of Biological Sciences 18 (2011) 333–340.
[212] H.M. Mahmoud, U.L. Hussein, U.L. Hussein, Suppression of N-nitrosodiethylamine induced oxidative renal toxicity by sulphated polysaccharide and aqueous extract of *Ulva lactuca* in rats, Int J Pharm Pharm Sci 6 (2014) 248–253.
[213] A. Sathivel, H.R.B. Raghavendran, P. Srinivasan, T. Devaki, Anti-peroxidative and anti-hyperlipidemic nature of *Ulva lactuca* crude polysaccharide on D-Galactosamine induced hepatitis in rats, Food Chem. Toxicol. 46 (2008) 3262–3267.
[214] A. Alves, E.D. Pinho, N.M. Neves, R.A. Sousa, R.L. Reis, Processing ulvan into 2D structures: cross-linked ulvan membranes as new biomaterials for drug delivery applications, Int. J. Pharm. 426 (2012) 76–81.
[215] S.S. Alam, H.A.M. Abd El-Kader, A.H. Abd El-Rahim, S.M. Hamed, A.A. Saber, The protective role of *Ulva lactuca* against genotoxic and biochemical effects induced by γ-irradiation in rats, International Journal of Pharmaceutical Sciences Review and Research 37 (2016) 40–48.
[216] G. Guerra-Rivas, C.M. Gomez-Gutierrez, G. Alarcon-Arteaga, I.E. Soria-Mercado, N.E. Ayala-Sanchez, Screening for anticoagulant activity in marine algae from the northwest Mexican Pacific coast, J. Appl. Phycol. 23 (2011) 495–503.
[217] J.M. Shi, C.L. Cheng, H.T. Zhao, J. Jing, N. Gong, W.H. Lu, In vivo anti-radiation activities of the *Ulva pertusa* polysaccharides and polysaccharide-iron(III) complex, Int. J. Biol. Macromol. 60 (2013) 341–346.
[218] J. Wei, S. Wang, G. Liu, D. Pei, Y. Liu, Y. Liu, D. Di, Polysaccharides from *Enteromorpha prolifera* enhance the immunity of normal mice, Int. J. Biol. Macromol. 64 (2014) 1–5.
[219] R. Ren, J. Gong, Y. Zhao, X. Zhuang, Y. Ye, W. Lin, Sulfated polysaccharides from *Enteromorpha prolifera* suppress SREBP-2 and HMG-CoA reductase expression and attenuate non-alcoholic fatty liver disease induced by a high-fat diet, Food and Function 8 (2017) 1899–1904.
[220] W.T. Lin, W.X. Wang, D.D. Liao, D.M. Chen, P.P. Zhu, G.X. Cai, A. Kiyoshi, Polysaccharides from *Enteromorpha prolifera* improve glucose metabolism in diabetic rats, Journal of Diabetes Research 2015 (2015) 1–12 (Article ID: 675201).
[221] Q. Kong, S.Y. Dong, J. Gao, C.Y. Jiang, In vitro fermentation of sulfated polysaccharides from *E. prolifera* and *L. japonica* by human fecal microbiota, Int. J. Biol. Macromol. 91 (2016) 867–871.
[222] H. Balaji Raghavendra Rao, A. Sathivel, T. Devaki, Antihepatotoxic nature of *Ulva reticulata* (Chlorophyceae) on acetaminophen-induced hepatoxicity in experimental rats, J. Med. Food 7 (2004) 495–497.
[223] R. Castro, I. Zarra, J. Lamas, Water-soluble seaweed extracts modulate the respiratory burst activity of turbot phagocytes, Aquaculture 229 (2004) 67–78.
[224] M. Roselli, M.S. Britti, I. Le Huërou-Luron, H. Marfaing, W.Y. Zhu, E. Mengheri, Effect of different plant extracts and natural substances (PENS) against membrane damage induced by enterotoxigenic Escherichia coli K88 in pig intestinal cells, Toxicol. in Vitro 21 (2007) 224–229.
[225] A. Alves, R.A. Sousa, R.L. Reis, In vitro cytotoxicity assessment of ulvan, a polysaccharide extracted from green algae, Phytother. Res. 27 (2013) 1143–1148.
[226] M. Alves, C. Dore, A.J.G. Castro, M.S. do Nascimento, A.K.M. Cruz, E.M. Soriano, N.M.B. Benevides, E.L. Leite, Antioxidant, cytotoxic and hemolytic effects of sulfated galactans from edible red alga Hypnea musciformis, J. Appl. Phycol. 24 (2012) 1217–1227.
[227] J.-K. Kim, M.L. Cho, S. Karnjanapratum, I.-S. Shin, S.G. You, In vitro and in vivo immunomodulatory activity of sulfated polysaccharides from *Enteromorpha prolifera*, Int. J. Biol. Macromol. 49 (2011) 1051–1058.
[228] J.K. Hong, M.H. Bong, J.C. Park, H.K. Moon, D.W. Kim, S.C. Lee, J.H. Lee, Antioxidant and immunomodulatory effects of *Ulva pertusa* Kjellman on broiler chickens, Journal of Animal Science and Technology 53 (2011) 419–428.
[229] H.P. Rang, J.M. Ritter, R.J. Flower, G. Henderson, Rang & Dale's Pharmacology, Churchill Livingstone, 2016.
[230] P.N. Moynagh, Toll-like receptor signalling pathways as key targets for mediating the anti-inflammatory and immunosuppressive effects of glucocorticoids, J. Endocrinol. 179 (2003) 139–144.
[231] J.M. Cavaillon, Pro-versus anti-inflammatory cytokines: myth or reality, Cell. Mol. Biol. 47 (2001) 695–702.
[232] C. Zhu, S. Zhang, C. Song, Y. Zhang, Q. Ling, P.R. Hoffmann, J. Li, T. Chen, W. Zheng, Z. Huang, Selenium nanoparticles decorated with *Ulva lactuca* polysaccharide potentially attenuate colitis by inhibiting NF-κB mediated hyper inflammation, Journal of Nanobiotechnology 15 (2017) 20.
[233] E. Birben, U.M. Sahiner, C. Sackesen, S. Erzurum, O. Kalayci, Oxidative stress and antioxidant defense, World Allergy Organization Journal 5 (2012) 9–19.
[234] S.B. Nimse, D. Pal, Free radicals, natural antioxidants, and their reaction mechanisms, RSC Adv. 5 (2015) 27986–28006.
[235] J. Bouayed, T. Bohn, Exogenous antioxidants–double-edged swords in cellular redox state: health beneficial effects at physiologic doses versus deleterious effects at high doses, Oxidative Med. Cell. Longev. 3 (2010) 228–237.
[236] H.J. Forman, K.J. Davies, F. Ursini, How do nutritional antioxidants really work: nucleophilic tone and para-hormesis versus free radical scavenging in vivo, Free Radic. Biol. Med. 66 (2014) 24–35.
[237] Z.S. Zhang, X.M. Wang, S.C. Yu, L. Yin, M.X. Zhao, Z.P. Han, Synthesized oversulfated and acetylated derivatives of polysaccharide extracted from *Enteromorpha linza* and their potential antioxidant activity, Int. J. Biol. Macromol. 49 (2011) 1012–1015.
[238] H.M. Qi, Y.L. Sun, Antioxidant activity of high sulfate content derivative of ulvan in hyperlipidemic rats, Int. J. Biol. Macromol. 76 (2015) 326–329.
[239] Q. Li, J. Luo, C. Wang, W. Tai, H. Wang, X. Zhang, K. Liu, Y. Jia, X. Lyv, L. Wang, H. He, Ulvan extracted from green seaweeds as new natural additives in diets for laying hens, J. Appl. Phycol. 30 (2018) 2017–2027.
[240] Q. Zhang, N. Li, G. Zhou, X. Lu, Z. Xu, Z. Li, In vivo antioxidant activity of polysaccharide fraction from *Porphyra haitanesis* (Rhodephyta) in aging mice, Pharmacol. Res. 48 (2003) 151–155.
[241] A.R. Phull, S.J. Kim, Fucoidan as bio-functional molecule: insights into the anti-inflammatory potential and associated molecular mechanisms, J. Funct. Foods 38 (2017) 415–426.
[242] X.G. Lei, J.H. Zhu, W.H. Cheng, Y. Bao, Y.S. Ho, A.R. Reddi, A. Holmgren, E.S. Arner, Paradoxical roles of antioxidant enzymes: basic mechanisms and health implications, Physiol. Rev. 96 (2016) 307–364.
[243] L. Miao, D.K. St Clair, Regulation of superoxide dismutase genes: implications in disease, Free Radic. Biol. Med. 47 (2009) 344–356.
[244] M. Valko, M. Izakovic, M. Mazur, C.J. Rhodes, J. Telser, Role of oxygen radicals in DNA damage and cancer incidence, Mol. Cell. Biochem. 266 (2004) 37–56.
[245] A.A. Matloub, A.H. Salama, H.A. Aglan, M.M. AbouSamra, S.S.M. ElSouda, H.H. Ahmed, Exploiting bilosomes for delivering bioactive polysaccharide isolated from *Enteromorpha intestinalis* for hacking hepatocellular carcinoma, Drug Dev. Ind. Pharm. 44 (2018) 523–534.
[246] Z. Hu, P. Hong, Y. Cheng, M. Liao, S. Li, Polysaccharides from *Enteromorpha tubulosa*: optimization of extraction and cytotoxicity, Journal of Food Processing and Preservation 42 (2018) e13373.
[247] C. Gerhauser, A. Alt, E. Heiss, A. Gamal-Eldeen, K. Klimo, J. Knauft, I. Neumann, H.R. Scherf, N. Frank, H. Bartsch, H. Becker, Cancer chemopreventive activity of Xanthohumol, a natural product derived from hop, Mol. Cancer Ther. 1 (2002) 959–969.
[248] J. Li, F. Jiang, Z. Chi, D. Han, L. Yu, C. Liu, Development of *Enteromorpha prolifera* polysaccharide-based nanoparticles for delivery of curcumin to cancer cells, Int. J. Biol. Macromol. 112 (2018) 413–421.
[249] X. Sun, Y. Zhong, H. Luo, Y. Yang, Selenium-containing polysaccharide-protein complex in Se-enriched *Ulva fasciata* induces mitochondria-mediated apoptosis in A549 human lung cancer cells, Marine Drugs 15 (2017).
[250] F. Yang, X. Fang, W. Jiang, T. Chen, Bioresponsive cancer-targeted polysaccharide nanosystem to inhibit angiogenesis, Int. J. Nanomedicine 12 (2017) 7419–7431.
[251] J. Cui, Y. Li, S. Wang, Y. Chi, H. Hwang, P. Wang, Directional preparation of anticoagulant-active sulfated polysaccharides from *Enteromorpha prolifera* using artificial neural networks, Sci. Rep. 8 (2018) 3062.
[252] A.T. Long, E. Kenne, R. Jung, T.A. Fuchs, T. Renné, Contact system revisited: an interface between inflammation, coagulation, and innate immunity, J. Thromb. Haemost. 14 (2016) 427–437.
[253] C.H. Lee, P. Olson, R.M. Evans, Minireview: lipid metabolism, metabolic diseases, and peroxisome proliferator-activated receptors, Endocrinology 144 (2003) 2201–2207.
[254] S. Mohamed, S.N. Hashim, H.A. Rahman, Seaweeds: a sustainable functional food for complementary and alternative therapy, Trends Food Sci. Technol. 23 (2012) 83–96.
[255] L. Wang, X. Wang, H. Wu, R. Liu, Overview on biological activities and molecular characteristics of sulfated polysaccharides from marine green algae in recent years, Marine Drugs 12 (2014) 4984–5020.
[256] G. Jiao, G. Yu, J. Zhang, H.S. Ewart, Chemical structures and bioactivities of sulfated polysaccharides from marine algae, Marine Drugs 9 (2011) 196–233.
[257] H. Qi, J. Sheng, The antihyperlipidemic mechanism of high sulfate content ulvan in rats, Marine Drugs 13 (2015) 3407–3421.
[258] H. Qi, X. Liu, K. Wang, D. Liu, L. Huang, S. Liu, Q. Zhang, Subchronic toxicity study of ulvan from *Ulva pertusa* (Chlorophyta) in Wistar rats, Food Chem. Toxicol. 62 (2013) 573–578.
[259] M.H. Hoang, J.-Y. Kim, J.H. Lee, S. You, S.-J. Lee, Antioxidative, hypolipidemic, and anti-inflammatory activities of sulfated polysaccharides from *Monostroma nitidum*, Food Sci. Biotechnol. 24 (2015) 199–205.
[260] R. Ren, J. Gong, Y. Zhao, X. Zhuang, Y. Ye, F. Huang, W. Lin, Sulfated polysaccharide from *Enteromorpha prolifera* suppresses SREBP-1c and ACC expression to lower serum triglycerides in high-fat diet-induced hyperlipidaemic rats, J. Funct. Foods 40 (2018) 722–728.

[261] L. Gesquière, N. Loreau, A. Minnich, J. Davignon, D. Blache, Oxidative stress leads to cholesterol accumulation in vascular smooth muscle cells, Free Radic. Biol. Med. 27 (1999) 134–145.
[262] M.M. Ali, F.G. Agha, Amelioration of streptozotocin-induced diabetes mellitus, oxidative stress and dyslipidemia in rats by tomato extract lycopene, Scand. J. Clin. Lab. Invest. 69 (2009) 371–379.
[263] Q. Shi, A. Wang, Z. Lu, C. Qin, J. Hu, J. Yin, Overview on the antiviral activities and mechanisms of marine polysaccharides from seaweeds, Carbohydr. Res. 453-454 (2017) 1–9.
[264] M. Witvrouw, E. De Clercq, Sulfated polysaccharides extracted from sea algae as potential antiviral drugs, General Pharmacology: The Vascular System 29 (1997) 497–511.
[265] E.B. Damonte, M.C. Matulewicz, A.S. Cerezo, Sulfated seaweed polysaccharides as antiviral agents, Curr. Med. Chem. 11 (2004) 2399–2419.
[266] J.B. Lee, K. Hayashi, M. Maeda, T. Hayashi, Antiherpetic activities of sulfated polysaccharides from green algae, Planta Med. 70 (2004) 813–817.
[267] T. Ghosh, K. Chattopadhyay, M. Marschall, P. Karmakar, P. Mandal, B. Ray, Focus on antivirally active sulfated polysaccharides: from structure-activity analysis to clinical evaluation, Glycobiology 19 (2009) 2–15.
[268] L. Araujo, A.E. Goncalves, M.J. Stadnik, Ulvan effect on conidial germination and appressoria formation of *Colletotrichum gloeosporioides*, Phytoparasitica 42 (2014) 631–640.
[269] L.G. Castellanos-Barriga, F. Santacruz-Ruvalcaba, G. Hernández-Carmona, E. Ramírez-Briones, R.M. Hernández-Herrera, Effect of seaweed liquid extracts from *Ulva lactuca* on seedling growth of mung bean (*Vigna radiata*), J. Appl. Phycol. 29 (2017) 2479–2488.
[270] S. Cluzet, C. Torregrosa, C. Jacquet, C. Lafitte, J. Fournier, L. Mercier, S. Salamagne, X. Briand, M.-T. Esquerré-Tugayé, B. Dumas, Gene expression profiling and protection of *Medicago truncatula* against a fungal infection in response to an elicitor from green algae *Ulva* spp, Plant Cell Environ. 27 (2004) 917–928.
[271] D.Z. Delgado, M.B. de Freitas, M.J. Stadnik, Effectiveness of saccharin and ulvan as resistance inducers against rust and angular leaf spot in bean plants (*Phaseolus vulgaris*), Crop Prot. 47 (2013) 67–73.
[272] M.B. de Freitas, M.J. Stadnik, Race-specific and ulvan-induced defense responses in bean (*Phaseolus vulgaris*) against *Colletotrichum lindemuthianum*, Physiol. Mol. Plant Pathol. 78 (2012) 8–13.
[273] J.D.G. Jones, J.L. Dangl, The plant immune system, Nature 444 (2006) 323.
[274] A. Robert-Seilaniantz, M. Grant, J.D.G. Jones, Hormone crosstalk in plant disease and defense: more than just jasmonate-salicylate antagonism, Annu. Rev. Phytopathol. 49 (2011) 317–343.
[275] C.M. Pieterse, A. Leon-Reyes, S. Van der Ent, S.C. Van Wees, Networking by small-molecule hormones in plant immunity, Nat. Chem. Biol. 5 (2009) 308–316.
[276] L. Burketova, L. Trda, P.G. Ott, O. Valentova, Bio-based resistance inducers for sustainable plant protection against pathogens, Biotechnol. Adv. 33 (2015) 994–1004.
[277] U. Conrath, G.J. Beckers, V. Flors, P. Garcia-Agustin, G. Jakab, F. Mauch, M.A. Newman, C.M. Pieterse, B. Poinssot, M.J. Pozo, A. Pugin, U. Schaffrath, J. Ton, D. Wendehenne, L. Zimmerli, B. Mauch-Mani, Priming: getting ready for battle, Mol. Plant-Microbe Interact. 19 (2006) 1062–1071.

7.5 Chapter 3 publication

Title: Are all ulvans equal? A comparative assessment of the chemical and gelling properties of ulvan from blade and filamentous *Ulva*

Journal: Carbohydrate Polymers 264:118010

DOI: https://doi.org/10.1016/j.carbpol.2021.118010

Published: 02/04/2021

Scopus citations as of 16/04/2021: 0

Carbohydrate Polymers 264 (2021) 118010

Contents lists available at ScienceDirect

Carbohydrate Polymers

journal homepage: www.elsevier.com/locate/carbpol

Are all ulvans equal? A comparative assessment of the chemical and gelling properties of ulvan from blade and filamentous *Ulva*

Joel T. Kidgell [a,*], Susan M. Carnachan [b], Marie Magnusson [c], Rebecca J. Lawton [c], Ian M. Sims [b], Simon F.R. Hinkley [b], Rocky de Nys [a], Christopher R.K. Glasson [c]

[a] MACRO – The Centre for Macroalgal Resources and Biotechnology, College of Science and Engineering, James Cook University, Townsville, 4811, Australia
[b] The Ferrier Research Institute, Victoria University of Wellington, Wellington, 6012, New Zealand
[c] Environmental Research Institute, School of Science, University of Waikato, Tauranga, 3110, New Zealand

ARTICLE INFO

Keywords:
Seaweed
Ulva
Sulfated polysaccharide
Ulvan
Rheology
Multivariate analysis

ABSTRACT

Green seaweeds of the genus *Ulva* are rich in the bioactive sulfated polysaccharide ulvan. Herein we characterise ulvan from *Ulva* species collected from the Bay of Plenty, Aotearoa New Zealand. Using standardised procedures, we quantified, characterised, and compared ulvans from blade (*U. australis*, *U. rigida*, *U.* sp. B, and *Ulva* sp.) and filamentous (*U. flexuosa*, *U. compressa*, *U. prolifera*, and *U. ralfsii*) *Ulva* species. There were distinct differences in composition and structure of ulvans between morphologies. Ulvan isolated from blade species had higher yields (14.0–19.3 %) and iduronic acid content (IdoA = 7–18 mol%), and lower molecular weight (Mw = 190–254 kDa) and storage moduli (G' = 0.1–6.6 Pa) than filamentous species (yield = 7.2–14.6 %; IdoA = 4–7 mol%; Mw = 260–406 kDa; G' = 22.7–74.2 Pa). These results highlight the variability of the physicochemical properties of ulvan from different *Ulva* sources, and identifies a morphology-based division within the genus *Ulva*.

1. Introduction

Green seaweeds of the genus *Ulva* occur in two distinct morphologies: a flat sheet-like blade form (occasionally in thin ribbons) and a tubular filamentous form (Fig. 1). Filamentous species of *Ulva* were historically considered a separate genus, *Enteromorpha*, until genetic barcoding concluded that these two genera were not distinct evolutionary entities and were, therefore, consolidated into a single genus, *Ulva* (Hayden et al., 2003). Both morphologies flourish under high nutrient conditions, resulting in blooms or 'green tides' in extreme cases (Ye et al., 2011). Rapid and resilient growth make species of *Ulva* ideal candidates for the bioremediation of nutrient-rich wastewater, such as that produced by land-based aquaculture of shellfish and finfish (Bolton, Robertson-Andersson, Shuuluka, & Kandjengo, 2009; Lawton, Mata, de Nys, & Paul, 2013; Nardelli, Chiozzini, Braga, & Chow, 2019). Applied at a large scale, *Ulva* bioremediation produces a high-quality monoculture of biomass with a biochemical profile that is suitable for the development of valuable bio-products (Glasson, Sims, Carnachan, de Nys, & Magnusson, 2017). Notably, both blade and filamentous *Ulva* are established food products sold as "Aosa" and "Aonori", respectively (Holdt & Kraan, 2011; McHugh, 2003; Ohno, 1993). A key feature of *Ulva* is the high content of soluble fibre, predominantly as the cell wall sulfated polysaccharide ulvan, with desirable biological activities and rheological properties (Alves, Sousa, & Reis, 2013; Kidgell, Magnusson, de Nys, & Glasson, 2019; Lahaye & Robic, 2007).

Ulvan is a heterogeneous rhamnose-rich sulfated polysaccharide that forms weak gels (Haug, 1976; Lahaye & Axelos, 1993). The polysaccharide is characterised by repeat disaccharides of 3-sulfated rhamnose 1,4-linked to either glucuronic acid (ulvanobiouronic acid, A_{3s}), iduronic acid (ulvanobiouronic acid, B_{3s}), or xylose (ulvanobioses, U_{3s}) (Lahaye & Robic, 2007). These assignments, and indeed the majority of research on ulvan, has been conducted on species with the blade morphology (see: Alves et al. (2013); Kidgell et al. (2019); Lahaye and Robic (2007)), while research into the detailed structure of ulvans from filamentous species of *Ulva* is lacking (notable exceptions include: Chattopadhyay et al., 2007; Qi, Huang et al., 2012; Qi, Mao et al., 2012; Tabarsa, You, Dabaghian, & Surayot, 2018; Yu, Li, Du, Mou, & Wang, 2017). In particular, publications characterising ulvans from

* Corresponding author.
E-mail addresses: joel.kidgell@my.jcu.edu.au (J.T. Kidgell), susie.carnachan@vuw.ac.nz (S.M. Carnachan), marie.magnusson@waikato.ac.nz (M. Magnusson), rebecca.lawton@waikato.ac.nz (R.J. Lawton), ian.sims@vuw.ac.nz (I.M. Sims), simon.hinkley@vuw.ac.nz (S.F.R. Hinkley), rocky.denys@jcu.edu.au (R. de Nys), christopher.glasson@waikato.ac.nz (C.R.K. Glasson).

https://doi.org/10.1016/j.carbpol.2021.118010
Received 28 January 2021; Received in revised form 10 March 2021; Accepted 27 March 2021
Available online 2 April 2021

filamentous species of *Ulva* rarely quantify iduronic acid content (Zhong et al., 2020), limiting the extent to which the composition of these ulvans can be compared to those from blade species or between filamentous species (Kidgell et al., 2019). In any case, the structure and composition of ulvan, that is, the constituent sugars, the molecular weight and dispersity, the degree of sulfation, and the content of ulvan within individual *Ulva* samples, varies substantially in the literature (Kidgell et al., 2019).

Variation in the composition and structure of ulvans is due to biological (e.g. *Ulva* species (Shanmugam, Ramavat, Mody, Oza, & Tewari, 2001), holobiont (microbial) community structure (Singh & Reddy, 2014)), environmental (e.g. location (Lahaye et al., 1999), seasonal (Robic, Sassi, Dion, Lerat, & Lahaye, 2009)), and methodological factors (Glasson et al., 2017; Kidgell et al., 2019; Robic, Sassi, & Lahaye, 2008; Yaich et al., 2013). These sources of variation in turn influence the bioactivity and physical properties (e.g. rheology) of the extracted polysaccharide. While the natural variations due to biological and environmental factors are difficult to control, except through controlled cultivation, variability due to methodology can be minimised through the use of standardised procedures. Therefore, the current study used an optimised extraction protocol (Glasson et al., 2019), industry-standard analytical techniques (Pettolino, Walsh, Fincher, & Bacic, 2012) and an optimised rheology protocol (Lahaye & Axelos, 1993; Lahaye, Ray, Baumberger, Quemener, & Axelos, 1996) to compare the yield, composition and structure, and rheological properties of ulvan from *Ulva* species collected and/or cultivated in the Bay of Plenty, Aotearoa New Zealand. Our working hypothesis was that; as ulvan is a structural polysaccharide, the physicochemical properties of ulvan will differ between structurally distinct *Ulva* morphologies.

This study was conducted with the broader aim of selecting target species of *Ulva* for cultivation based on the physicochemical properties of the bioactive polysaccharide ulvan. To achieve this goal, the physicochemical properties of ulvan isolated from different *Ulva* species and morphologies were compared. We determined the yield, constituent sugars, content of sulfate esters, molecular weight distribution, and the rheological properties of ulvans from blade (*U. australis*, *U. rigida*, *U.* sp. B and *U.* sp.) and filamentous (*U. compressa*, *U. flexuosa*, *U. prolifera*, and *U. ralfsii*) *Ulva* species. FTIR and NMR spectroscopy were used to confirm the presence of characteristic ulvan functionality and disaccharides, respectively. Multivariate techniques were then applied to distinguish groupings of similar ulvans based on physicochemical properties of the ulvan from different species and morphologies.

2. Methods

2.1. Materials

The following were purchased from Sigma-Aldrich: glucuronic acid (>98 %, #G5269), sodium tetraborate (99.998 %, #229946), *m*-hydroxydiphenyl (85 %, #262250), concentrated sulfuric acid (ACS, 95–98 %, #258105), boric acid (#B6768), calcium chloride (>99 %, #223506), sodium nitrate (>99.0 %, #S5506), sodium azide (>99 %, #S2002), methanolic HCl (#90964), L-fucose (#F2252), L-rhamnose (#3875), L-arabinose (#10839), D-galactose (#0750), D-glucose (#8270), D-glucosamine (#G4875), D-mannose (#2069), D-xylose (#95729), D-ribose (#7500), D-galacturonic acid (#73960), and D-glucuronic acid (#5269). Other reagents were sourced as follows: trifluoroacetic acid (Synthesis grade, Scharlau, Spain, #AC31420100), sodium chloride (AJAX FineChem, Thermo Fisher Scientific, New Zealand, #AJA465), sodium hydroxide (50 % w/w, Fisher Scientific, Thermo Fisher Scientific, New Zealand, #SS254), anhydrous sodium acetate (Carlo Erba, France, #366377), deuterium oxide (99.9 %, Cambridge Isotope Laboratories, USA, #DLM-4), and L-iduronic acid (Carbosynth, UK, #MI08102).

2.2. Extraction and purification of ulvan

2.2.1. Algae collection & cultivation

Nine morphologically distinct blade and filamentous *Ulva* samples were collected between October 2018 and April 2019 from the Bay of Plenty region, Aotearoa New Zealand (37°42'S, 176°18'E; Fig. S1; See online dataset for details) under Ministry for Primary Industries University of Waikato Special Permit 560. Samples were identified to species level by DNA barcoding by Lawton et al. (Lawton, Sutherland, Glasson, & Magnusson, 2021), and found to consist of seven distinct species (*Ulva australis*, *U. rigida*, *U.* sp. B, *U. compressa*, *U. flexuosa*, *U. prolifera*, *U. ralfsii* [syn. *U.* sp. 5]) and one sample that did not amplify successfully so is referred to as "*Ulva* sp.".

The nine *Ulva* samples were cleaned of epiphytes and rinsed in salt water before being cultivated or extracted. Cultivation was attempted on all nine *Ulva* samples to increase biomass for ulvan extraction, however, *Ulva* sp. was unable to be cultivated. Three of the *Ulva* samples (*U.* sp. B, *U.* sp., *U. ralfsii*) had sufficient wild harvested biomass to extract ulvan after some biomass was taken for cultivation. *Ulva* was cultivated as reported previously (Lawton, Sutherland, Glasson, & Magnusson, 2021). Briefly, cultivation was carried out in 20 L buckets at a density of 1 g fresh weight L^{-1} and a temperature of 18–20°C in sea water with the addition of F/2 nutrients (Cell-Hi F2P, Varicon Aqua Solutions UK, 0.1 g L^{-1}) under bright white LED (1200 mm J Series T8 LED tubes producing 1800 lm of 4000−4500 K light) lights on a cycle of 12 h/12 h light/dark. Biomass was harvested every 7 days and spun to remove excess water. After restocking, excess biomass was frozen at −18 °C until a sufficient supply was produced for ulvan extraction. Frozen biomass was freeze-dried, milled using a domestic blender, and stored over silica gel until extraction.

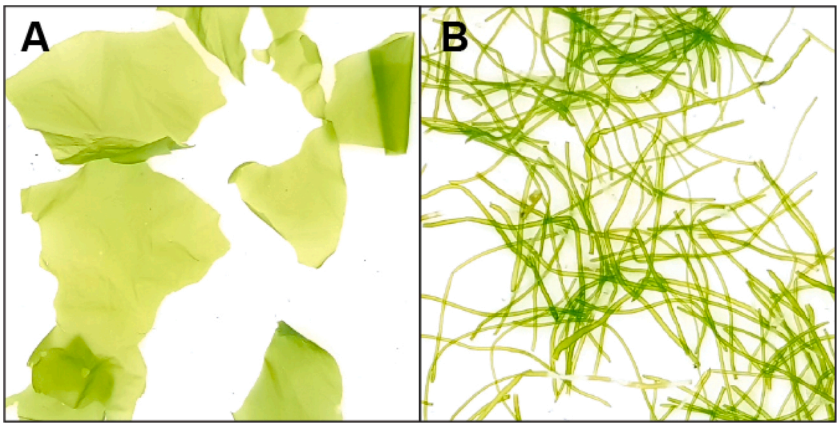

Fig. 1. Characteristic blade (**A**) and filamentous (**B**) morphologies of *Ulva* collected from the Bay of Plenty, Aotearoa New Zealand.

Table 1
Purified ulvan composition: details of the *Ulva* biomass from which ulvan was extracted and purified, the yield (of purified ulvan) obtained, the sulfate and protein content and the ratio of rhamnose to the sum of glucuronic acid, iduronic acid and xylose.

Ulva details			Yield	Composition		
Ulva species	Biomass source	Morphology	Ulvan (% dw)[a]	$\%SO_4^{2-}$[b]	%Protein [c]	[Rha] : [GlcA + IdoA + Xyl][d]
australis	Cultivated	Blade	6.5	16.9 ± 1.1	0.8	1.0
rigida	Cultivated	Blade	5.7	15.2 ± 0.3	0.6	1.1
sp.	Wild harvest	Blade	6.3	16.5 ± 0.7	1.3	1.0
sp. B (cult.A)	Cultivated	Blade	9.5	9.9 ± 0.9	0.7	1.0
sp. B (cult.B)	Cultivated	Blade	8.3	10.4 ± 0.5	0.5	1.1
sp. B (wild)	Wild harvest	Blade	8.0	13.1 ± 1.1	0.3	1.0
compressa	Cultivated	Filamentous	3.3	7.5 ± 0.8	1.2	1.0
flexuosa	Cultivated	Filamentous	7.3	12.2 ± 0.5	1.5	1.3
prolifera	Cultivated	Filamentous	6.6	9.4 ± 0.5	0.7	1.5
ralfsii (cult.)	Cultivated	Filamentous	4.1	7.7 ± 0.4	0.9	0.9
ralfsii (wild)	Wild harvest	Filamentous	4.3	9.8 ± 0.4	0.7	0.9

[a] % dry weight (dw) biomass.
[b] Average of triplicate (±S.D.).
[c] Estimated from conversion factor of 5 (%N x 5).
[d] Ratio of mol% of rhamnose to sum of glucuronic acid, iduronic acid and xylose.

2.2.2. Ulvan extraction

Ulvan was extracted using an optimised extraction procedure (Glasson et al., 2019). A stirred suspension of milled *Ulva* biomass (40 g dry weight) in dilute H_2SO_4 (1 L, pH 2.92) was heated at 90 °C for 90 min. The extract was then separated from the biomass by filtration through 50 μm mesh followed by centrifugation (20 min, 3000 *g*) to remove ultrafine particulate material prior to neutralisation with 2 M NaOH. The extract was then concentrated (10×) by ultrafiltration (ÄKTA flux 6 fitted with a Xampler 10,000 Da NMWC cartridge filter), diafiltered with Type 1 water until the permeate conductivity was ≤20 μS cm^{-1} and freeze dried to yield "crude ulvan" (Table S1).

These crude ulvans containing residual protein and other polysaccharides were characterised in the same manner as the purified ulvan (Table S1). However, four samples (*U. ralfsii* (wild), *U. rigida, U. australis*, and *U. flexuosa)* had insufficient quantities of crude ulvan for characterisation of both crude and purified material. Therefore, only the characterisation of the purified ulvans is explored in detail in the results and discussion.

2.2.3. Purification & fractionation

Crude ulvan was dissolved overnight in Type 1 water at a concentration of 1 % w/w and filtered by vacuum filtration (Filtech, 453) prior to purification by anion exchange chromatography (AEC) using an ÄKTA pure 150 L coupled with a single wavelength (280 nm) UV detector and fraction collector. The ulvan solution was loaded onto an equilibrated (Type 1 water, 5 column volumes (CV); 2 M NaCl, 5 CV; Type 1 water, 5 CV) XK 50/30 column (GE Healthcare Life Sciences) packed with Q Sepharose XL media (bed height =24.5 cm). The column was eluted using a stepwise gradient of NaCl (0 M, 2 CV; 0–1 M, 4 CV; 1–2 M, 1.2 CV; 2 M, 3 CV) at a flow rate of 20 mL min^{-1}. A chromatogram was produced by colorimetric analysis of collected fractions (13 mL) for uronic acid using the *m*-hydroxybiphenyl method with glucuronic acid as standard (van den Hoogen et al., 1998). Fractions containing uronic acid that did not overlap the major peak in the UV trace (attributed to protein and other chromophore containing impurities) were pooled and concentrated by diafiltration with Type 1 water (ÄKTA flux 6 system fitted with a 10,000 Da NMWC filter, UFP-10-E-4 × 2 MA) until permeate conductivity was <5 μS cm^{-1} and then freeze dried to yield "purified ulvan".

Ulvan was successfully extracted and purified from eight cultivated samples and from the wild harvested biomass of three samples (*U.* sp. B, *U.* sp., *U. ralfsii*), resulting in a total of eleven purified ulvans (Table 1). *Ulva* sp. B and *U. ralfsii* both had ulvans extracted and purified from wild harvested and cultivated biomass (Table 1). Two of the *Ulva* samples collected and cultivated were later identified as *U.* sp. B, so were named "*U.* sp. B (cult.A)" and "*U.* sp. B (cult.B)".

2.3. Chemical composition

2.3.1. Elemental characterisation

Elemental analysis (% C, H, N, S; n = 1) and ash content (% w/w) of ulvans were measured commercially by OEA labs (www.oealabs.com, Callington, UK). Percent oxygen was calculated as % O = 100 – Σ(C, H, N, S, ash), where C, H, N, S, and ash are expressed as a percentage of the total mass. Sulfate content was measured using the turbidimetric assay (Craigie, Wen, & van der Meer, 1984). Protein content was estimated from the N content using the nitrogen-to-protein conversion factor of 5 (% N x 5) (Angell, Mata, de Nys, & Paul, 2016).

2.3.2. Constituent sugar composition

Constituent sugar composition was determined by high-performance anion-exchange chromatography with pulsed amperometric detection (HPAEC-PAD) after hydrolysis of the polysaccharides to their component monosaccharides based the methodology of Nep et al. (2016), but with a modified eluant gradient. This methodology was based on the protocol optimised by de Ruiter, Schols, Voragen, and Rombouts (1992) for the analysis of water-soluble uronic acid-containing polysaccharides. Briefly, samples (1 mg) were hydrolysed in duplicate with methanolic HCl (3 M, 500 μL, 80 °C, 18 h), followed by aqueous trifluoroacetic acid (TFA, 2.5 M, 500 μL, 120 °C, 1 h). The resulting hydrolysates were dried, redissolved in Type 1 water (1 mL), and diluted to 50 μg mL^{-1}. Aliquots (20 μL) of the hydrolysates were analysed on a CarboPac PA-1 (4 × 250 mm) column equilibrated in 20 mM NaOH and eluted with a simultaneous gradient of NaOH (20 mM from 0 to 25 min, 20–100 mM from 25−30 min, 100–200 mM from 30 to 50 min, then held to 60 min) and NaOAc (0 mM until 30 min, 0–500 mM from 30 to 50 min, 500–1000 mM from 50 to 52 min, then held until 60 min) at 30 °C and a flow rate of 1 mL min^{-1}. The sugars were identified from their elution times relative to a standard sugar mix (L-fucose, L-rhamnose, L-arabinose, D-galactose, D-glucose, D-glucosamine, D-mannose, D-xylose, D-ribose, D-galacturonic acid, D-glucuronic acid, and L-iduronic acid), quantified from response calibration curves of each sugar and expressed as μg of the anhydro-sugar (as this is the form of sugar present in a polysaccharide) per mg of sample; the normalised mol% of each anhydro-sugar was also calculated.

2.4. Structural characterisation

2.4.1. NMR & FTIR spectroscopy

Samples of ulvan were dissolved in D_2O at 25 mg mL^{-1}. Acetone (0.4

% v/v) was added as an internal standard to all samples and assigned as the reference peak (31.45 ppm for ^{13}C and 2.225 ppm for ^{1}H). NMR data was collected on a Bruker Avance III 500 operating at a proton frequency of 499.843 MHz running Topspin 2.1 software. Data was collected on a Bruker two channel 5-mm broadband observe nuclei probe (31P-109 Ag) equipped with actively shielded Z-axis gradient coil (303 K). Proton NMR spectra were recorded with a spectral width of 20 ppm, 65,536 complex data points, 30-degree excitation pulse, each with a 1-second delay time and an acquisition time of 3.18 s. Heteronuclear single quantum coherence (HSQC) experiments were carried out using pulse programs supplied with the Bruker manual. The superimposed HSQC plots were calibrated by standardising the intensity of the acetone (0.4 % v/v) added as an internal standard resonance between ulvan spectra. Spectra were processed with a standard exponential weighting function of 0.3 Hz line broadening prior to Fourier transformation. NMR spectra were analysed and processed in Mestranova (Ver. 14.1.1).

FTIR spectra of ulvans were recorded on a Shimadzu IRSpirit with a QATR-detector between wavenumbers 400 and 4000 cm^{-1} with an average of 32 scans. Data were processed in LabSolutions IR software using the built-in smoothing function followed by ATR correction, baseline correction and normalisation around the significant peaks for C—O stretching (~1050 cm^{-1}).

2.4.2. Molecular weight

Molecular weight distributions were determined using size-exclusion chromatography coupled with multi-angle laser light scattering (SEC-MALLS). Samples (5 mg mL^{-1} in 0.1 M $NaNO_3$) were dissolved by heating at 80 °C and then standing at room temperature overnight (~20 h). Soluble material was separated on three columns (TSK-Gel $G5000PW_{XL}$, $G4000PW_{XL}$, and $G3000PW_{XL}$, 300 × 7.8 mm, Tosoh Corp., Tokyo, Japan) connected in series, with a void volume (V_0) of 15 mL and total volume (V_t) of 32 mL, eluting with 0.1 M $NaNO_3$ with 0.02 % NaN_3 (0.5 mL min^{-1}, 60 °C). The eluted material was detected using a variable wavelength detector (280 nm), an SDL7000 MALLS detector (PSS Polymer Standards Service GmbH, Mainz, Germany) and a refractive index monitor. Weight-average molecular weight (Mw), number-average molecular weight (Mn), and dispersity (Đ) were calculated using Win GPC Unichrom software (v8.2.1, PSS Polymer Standards Service) using a refractive index increment, dn/dc, of 0.146 mL g^{-1} (Robic et al., 2008). The angular dependence of light scattering was fitted using a linear Debye plot and molecular weight data fitted using linear regression.

2.5. Rheology

Gelling properties of ulvan from *Ulva* species were determined through dynamic rheological measurements performed using a TA Instruments DHR-1 single-head hybrid rheometer with a temperature-controlled Peltier plate and a steel cone geometry (60 mm diameter, 1° angle). Rheological data were collected using TA TRIOS software (ver. 4.3.0.38388). Experiments were conducted at 20 °C with a solvent trap over the geometry to reduce evaporation. Viscosity was measured on a 2 % w/v ulvan solutions (prior to addition of gel-inducing reagents) with a logarithmic flow sweep using a shear rate range of 500 to 1 s^{-1}. For the gelling experiments, the 2 % ulvan solution was pH-adjusted to 7.5 and heated to 75 °C prior to addition of $CaCl_2$ and H_3BO_3 to final concentrations of 7 and 33 mM, respectively, resulting in a final ulvan concentration of 1.6 % (Lahaye & Axelos, 1993; Lahaye, Ray, Baumberger, Quemener, & Axelos, 1996). To prevent the gel from forming prior to starting measurements, H_3BO_3 was added immediately prior to transferring the ulvan solution to the rheometer plate, and the plate was held at 40 °C while the rheometer geometry (rotating at 1 rad s^{-1}) was lowered onto the ulvan solution. Finally, the geometry movement was stopped, the solvent trap was added, and the temperature adjusted to 20 °C prior to beginning any experiments.

The linear viscoelastic region (LVR) was determined with a constant angular frequency of 1 rad s^{-1} across a displacement of 5×10^{-5} to 0.5 rad and indicated that ulvan gels could not withstand an oscillation displacement (strain) greater than 0.01 rad. A displacement of 0.003 rad was selected for subsequent experiments. Ulvan gel formation was monitored by recording the storage modulus resulting from a constant angular frequency of 1 rad s^{-1} with a displacement of 0.003 rad for 30 min. Mechanical spectra (storage and loss moduli, tan δ, complex viscosity) were recorded once gel formation was complete using a constant strain of 0.003 rad displacement over an angular frequency range of 0.03 to 100 rad s^{-1}, a range which maintained a raw phase angle of ≤175° and therefore did not allow inertial forces to dominate the measurements.

2.6. Data & statistical analysis

The effect of the morphology of *Ulva* on chemical and rheological properties of the extracted ulvan was analysed with a one-factor permutational analysis of variance (PERMANOVA) (Anderson, Gorley, & Clarke, 2008). Morphology was treated as a fixed factor. The PERMANOVA was conducted with 9,999 unrestricted permutations and type III sum of squares. Homogeneity of multivariate dispersions was confirmed with the PERMDISP function. Complete linkage cluster analysis was performed with an associated SIMPROF test using a significance level of 5 %, 20,000 permutations to generate the mean profile, and 9,999 permutations to calculate the statistic. Permutational statistical analyses were performed in Primer v6 (Primer-E Ltd., UK) using a Bray-Curtis similarity matrix on square-root transformed data. Correlation matrices were produced in Statistica for Windows (Ver. 12, Statsoft Inc.). Figures were generated using relevant specialised software listed above, R, or Microsoft Excel 2016 and prepared for publication in Adobe Illustrator (Ver. 24).

3. Results and discussion

The physicochemical properties of eleven ulvans isolated and purified from either blade (*U. australis*, *U. rigida*, *U.* sp. B, and *Ulva* sp.) or filamentous (*U. flexuosa*, *U. compressa*, *U. prolifera*, and *U. ralfsii*) *Ulva* species were assessed. The composition of characteristic ulvan sugars (rhamnose, xylose, glucuronic acid, and iduronic acid) conformed to the expected stoichiometry (~1:1 for [Rha]:[GlcA + IdoA + Xyl]) for all ulvans, except those from *U. flexuosa* (1.3:1) and *U. prolifera* (1.5:1), which had 56 and 60 mol% rhamnose, respectively. In general, blade species of *Ulva* had higher yields of ulvan (14.0–19.3 %) containing a higher iduronic acid content (IdoA = 7−18 mol%), lower average molecular weights (M_w = 190−254 kDa), and lower storage moduli (i.e. gel strength, G' = 0.1–6.6 Pa) than ulvan isolated from filamentous species (yield = 7.2–14.6 %; IdoA = 4−7 mol%; M_w = 260−406 kDa; G' = 22.7–74.2 Pa). The above compositional, structural, and rheological data were assessed in a multivariate context which identified a significant difference between ulvans isolated from filamentous and blade species of *Ulva* (PERMANOVA, pseudo-$F_{1,9}$ = 18.0, $p < 0.005$). The current research highlights the variability of the composition and structure of ulvans from different *Ulva* species, and confirms our hypothesis that the physicochemical properties of ulvans differ between *Ulva* morphologies.

3.1. Yield and composition

There are very few studies in the literature that systematically assess the yield and composition of ulvan from a range of *Ulva* species (notable exceptions include: Shanmugam et al. (2001) and Lahaye et al. (1999)), and none that systematically compare ulvans isolated from blade and filamentous morphologies. In this regard, an average yield of 13.4 ± 4.3 % w/w ulvan was extracted from the *Ulva* biomass (Table S1), with an average recovery after purification of 48.3 ± 7.1 % w/w (Table 1). In general, higher yields of purified ulvans were recorded for blade species

(7.4 ± 1.4 %) than for filamentous species (5.1 ± 1.7 %) (Table 1). The crude yields of ulvan (16.5 ± 2.0 % for blade species and 9.8 ± 3.1 % for filamentous species; Table S1) fall within the range of median crude yields (median 12.0, interquartile range = 6.0–20.0) reported in a recent meta-analysis of ulvans (Kidgell et al., 2019), and indicate that blade *Ulva* species have higher contents of ulvan compared to filamentous species. The elemental composition of the ulvans was consistent with previous reports (Tables S1, S2) (Glasson et al., 2017; Kidgell et al., 2020; Shanmugam et al., 2001). Ulvans isolated from blade species had a higher content of sulfate esters than filamentous species with 13.7 ± 2.9 % compared to 9.3 ± 1.8 %, respectively. The degree of sulfation in ulvan has previously been correlated with anticoagulant (Wang, Zhang, Yao, Zhao, & Qi, 2013), antihyperlipidemic (Qi & Sheng, 2015), and anti-viral (Lopes et al., 2017) activity. These results suggest that ulvans isolated from blade and filamentous species of *Ulva* may have different bioactivities (Leiro, Castro, Arranz, & Lamas, 2007; Qi, Huang et al., 2012; Qi, Mao et al., 2012; Shao, Pei, Fang, & Sun, 2014; Wang et al., 2013). The degree of sulfation is also likely to affect the solution properties of ulvan (e.g. rheology) (Lahaye, Ray, Baumberger, Quemener, & Axelos, 1996). Importantly, the protein content of the ulvans in this study is low and there is negligible difference in protein content between samples from blade (0.7 ± 0.3 %) and filamentous (1.0 ± 0.4 %) *Ulva* species, as this is another factor that could drive rheological differences (Robic, Sassi et al., 2009).

The constituent sugar compositions of all purified ulvans broadly conformed to the literature definition of ulvan (Kidgell et al., 2019; Lahaye & Robic, 2007). The ulvans were comprised of 38–60 mol% rhamnose, 17–31 mol% glucuronic acid, 6–22 mol% xylose and 4–18 mol% iduronic acid (Fig. 2, Table S3, Figs. S2, S3). Additionally, a large proportion of galactose (10–16 mol%) was present in ulvans from *U. ralfsii*, and as a minor component in all other ulvans (Tables S3, S4). Notably, ulvans from filamentous species had a lower proportion of acidic to neutral monosaccharides (~0.4:1) compared to those isolated from blade species (~0.6:1). Of particular note is the low proportion of iduronic acid in ulvans isolated from filamentous species (6 ± 1 mol%) relative to ulvans isolated from blade species (12 ± 4 mol%) (Fig. 2). Within this study, ulvan from *U. rigida* had the highest iduronic acid content with 18 mol%, closely followed by ulvans from *U.* sp. B with 11–15 mol% (Fig. 2). An iduronic acid content of 18 mol% (116 μg mg^{-1}; Table S3) is the highest recorded for ulvan in the literature to date (Kidgell et al., 2019). High contents of iduronic acid in ulvans extracted from other blade *Ulva* species, *U. armoricana* (15 mol% (Paradossi, Cavalieri, & Chiessi, 2002) and ~11 mol% (Robic, Sassi et al., 2009)), and *U. ohnoi* (10 mol% (Glasson et al., 2017)) have also been reported. While the effect that iduronic acid content has on ulvan and its function as a cell wall polysaccharide is unclear, high contents are associated with *Ulva* species with blade morphology.

There were several ulvans with sugar compositions that substantially deviate from median literature values (Kidgell et al., 2019). Specifically, ulvans isolated from *U. flexuosa* and *U. prolifera* had high proportions of rhamnose (56 and 60 mol%, respectively), and ulvans from *U. ralfsii* contained high proportions of galactose (10 and 16 mol%) (Fig. 2, Tables S3, S4). The high content of rhamnose in *U. flexuosa* and *U. prolifera* is an interesting result as ulvan is considered to be comprised of rhamnose-containing disaccharides (Lahaye & Robic, 2007). Based on this assumption, the ratio of rhamnose to the sum of glucuronic acid, iduronic acid and xylose (i.e. Rha:[GlcA + IdoA + Xyl]) is theoretically 1:1. Indeed, this ratio is consistent for almost all of the ulvans in this study (ranging from 0.9 to 1.1:1), however, ulvans from *U. flexuosa* and *U. prolifera* had ratios of 1.3:1 and 1.5:1, respectively (Table 1). The excess rhamnose present in these samples may exist as repeat units interspaced between conventional disaccharides, as branching chains, or possibly as a separate repeating rhamnan, related to those found in green seaweeds of the order Ulotrichales, *Gayralia oxsperma* and *Monostroma latissimum* (Cassolato et al., 2008; Lee, Yamagaki, Maeda, & Nakanishi, 1998; Li et al., 2011). Interestingly, despite the high proportions of galactose found in ulvans from filamentous *U. ralfsii*, the Rha:[GlcA + IdoA + Xyl] ratio for both was 0.9:1 (Table 1). A ratio that is also consistent with galactose being either interspaced between the conventional disaccharides of ulvan, as branching chains, or as part of a separate galactan (Castro et al., 2009; Farias et al., 2008). Further structural investigation via linkage analysis and NMR is required to ascertain the origin of the excess rhamnose and high galactose detected in the sugar analysis of ulvans from *U. flexuosa* and *U. prolifera*, and *U. ralfsii*, respectively.

3.2. Structure and rheology

3.2.1. NMR spectroscopy

The ^{1}H and ^{1}H-^{13}C HSQC spectra of purified ulvans from blade and filamentous species of *Ulva* suggest structural differences between the morphologies (Figs. 3–5). Ulvans from blade species have fewer and

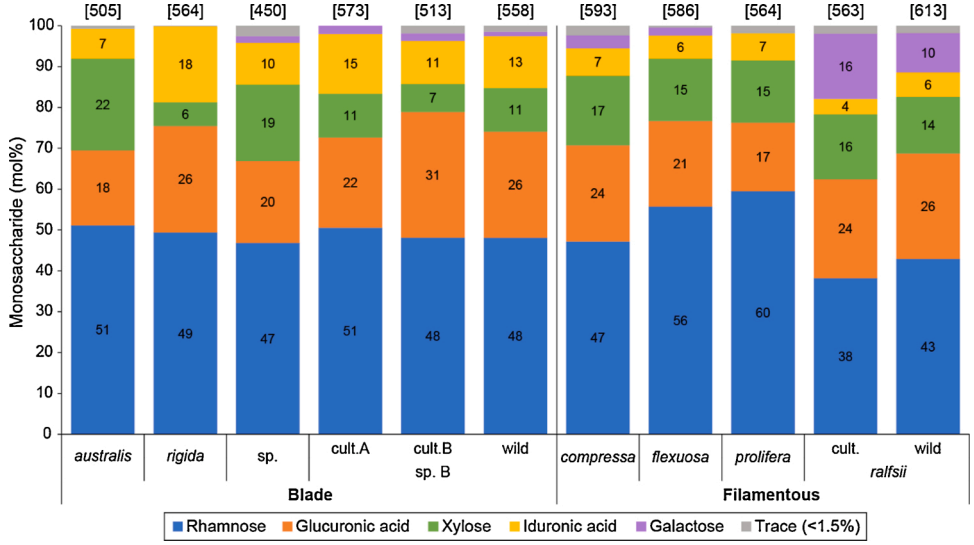

Fig. 2. Constituent monosaccharide composition (mol%) of purified ulvans, categorised by *Ulva* morphology, species, and, for *U.* sp. B and *U. ralfsii*, biomass source. For visual clarity, monosaccharides less than 1.5 mol% were grouped as 'Trace' – full data in Table S3. The total sugar content (μg mg^{-1}) of each ulvan is presented at the top of the respective column in square brackets [].

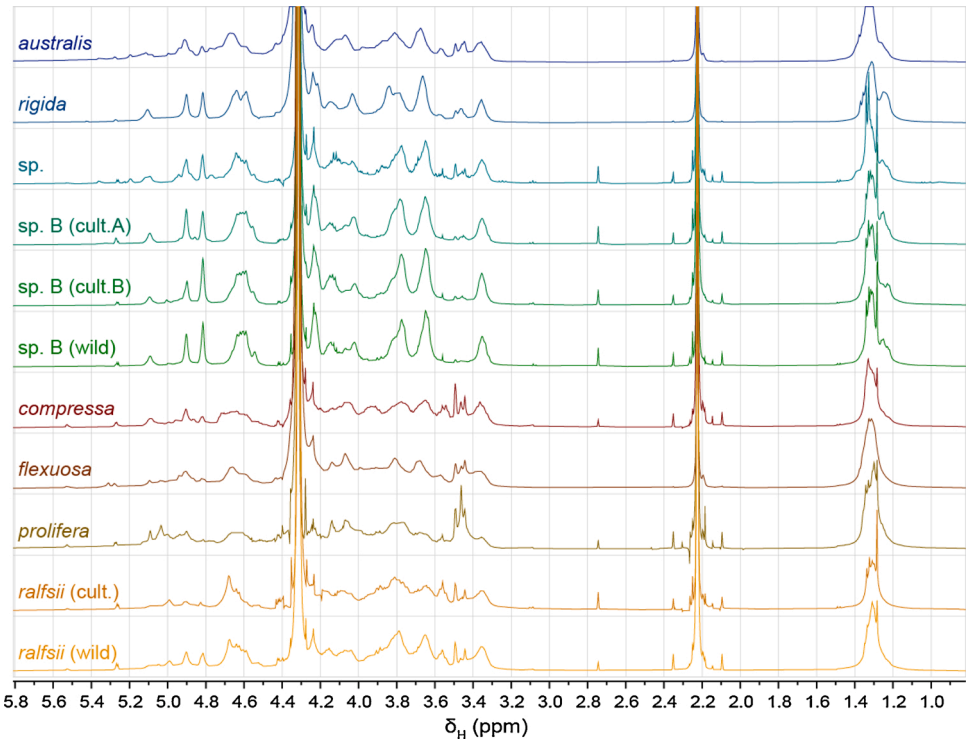

Fig. 3. ^{1}H spectrum of purified ulvans from blade (blue-green) and filamentous (red-yellow) *Ulva* species. Chemical shifts relative to acetone (2.225 ppm).

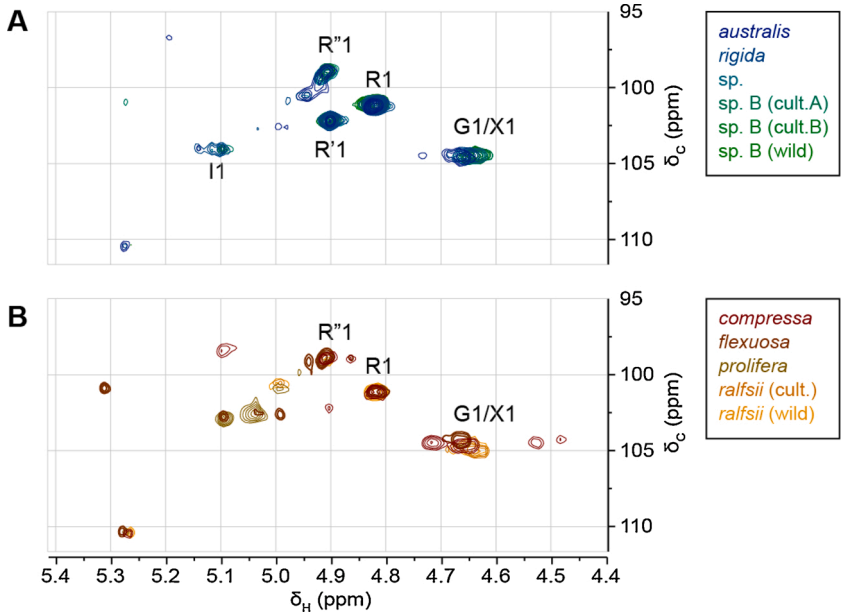

Fig. 4. The anomeric region of superimposed ^{1}H-^{13}C HSQC spectra highlighting the structural difference of ulvans from (**A**) blade and (**B**) filamentous *Ulva* species. Chemical shifts relative to acetone at 31.45 and 2.225 ppm for ^{13}C and ^{1}H, respectively. Labels and numbers correspond to carbon/proton coupling pair of ulvan units outlined in Table 2.

more highly resolved peaks compared to ulvans from filamentous species. This pattern in the 1H NMR may be explained by ulvans isolated from blade species of Ulva containing a high proportion of repeating saccharide structural-moieties, while ulvans from filamentous species are more heterogeneous in structure displaying greater signal complexity (Fig. 3). Almost all the peaks from ulvans of blade species can be identified by comparison with the literature (Table 2). Within the anomeric region (^{13}C ~95–105 ppm/^{1}H ~4.6–5.1, ppm), there are resonances consistent with A_{3S} and U_{3S} disaccharides in ulvans from both blade and filamentous species (Fig. 4, Table 2). Resonances for B_{3S} disaccharides are also detected in ulvans from blade species (Fig. 4A), but not in the spectra of ulvans from filamentous species (Fig. 4B). A lack of anomeric resonances associated with the B_{3S} disaccharide is consistent with the lower content of iduronic acid detected in ulvans from filamentous species (See Section 3.1). Individual HSQC plots further support the constituent sugar analysis (Figs. S5–10). For example, strong resonances are detected for R"1 and R'1 for ulvans high in xylose (*U. australis*, Fig. S5A) and iduronic acid (*U. rigida*, Fig. S5B),

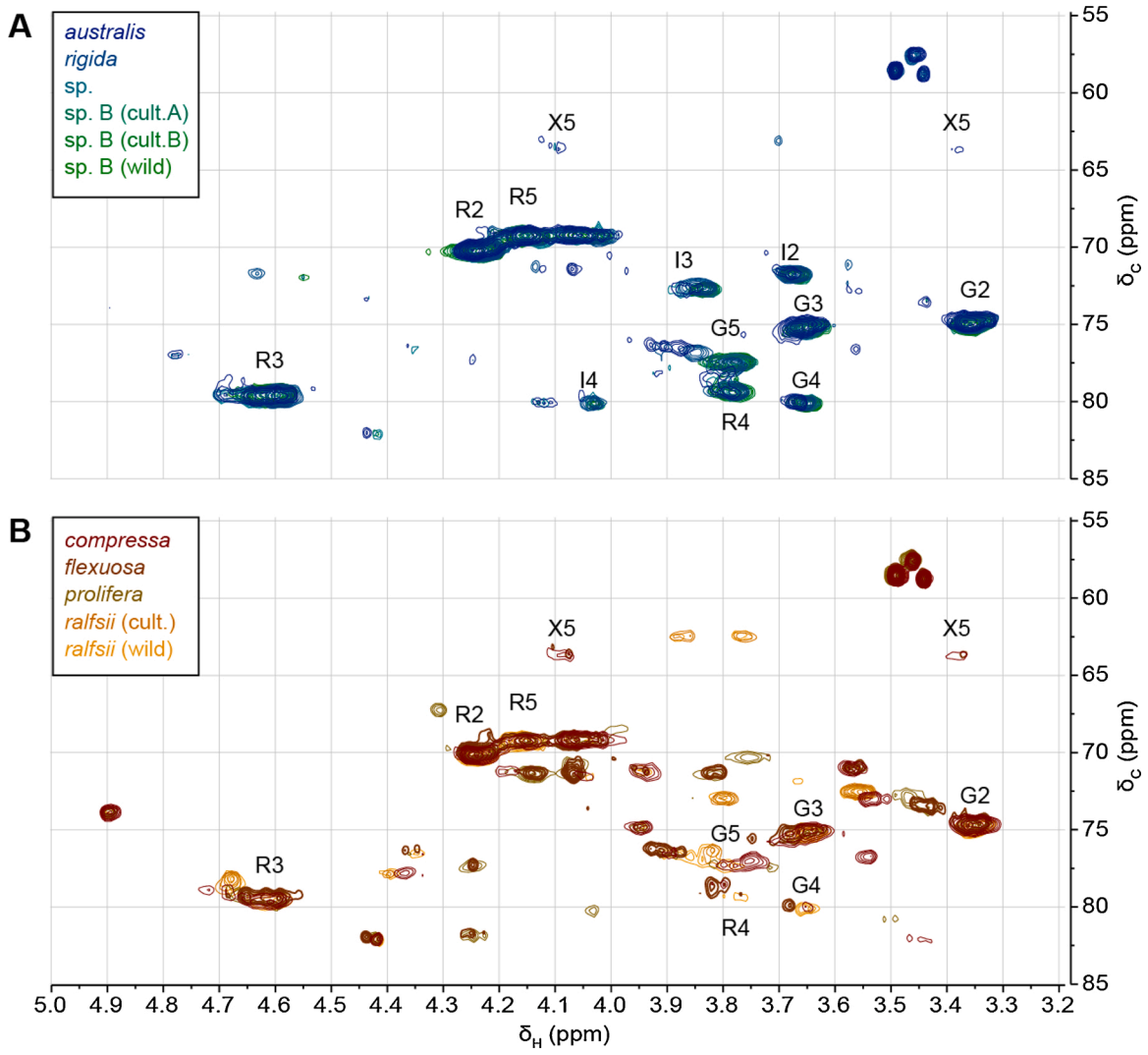

Fig. 5. Non-anomeric region of superimposed ^{1}H-^{13}C HSQC spectra highlighting the structural difference of ulvans from (**A**) blade and (**B**) filamentous *Ulva* species. Chemical shifts relative to acetone at 31.45 and 2.225 ppm for ^{13}C and ^{1}H, respectively. Labels and numbers correspond to carbon/proton coupling pair of ulvan units outlined in Table 2 – note that many resonances from B_{3S} and U_{3S} overlap with A_{3S} so are not specifically listed.

Table 2
Ulvan disaccharide units, assigned labels, and approximate chemical shifts based on references indicated; rounded chemical shift values are given as peaks from different ulvans vary.

Diads[a]	Units	Label	Chemical shift (ppm)[b]						Reference
			C1/H1	C2/H2	C3/H3	C4/H4	C5/H5	C6/H6	
A_{3S}	[→4)-*β*-D-GlcpA-(1→	G	104.5/ 4.65	75.0/ 3.35	75.0/ 3.65	80.0/ 3.65	77.0/ 3.80	–	de Carvalho et al. (2018), de Freitas et al. (2015), Lahaye, Inizan, and Vigouroux (1998)
	4)-*α*-L-Rhap3S-(1→]	R	101.0/ 4.80	70.0/ 4.25	79.0/ 4.60	79.0/ 3.80	69.0/ 4.15	18.0/ 1.30	de Carvalho et al. (2018), de Freitas et al. (2015), Lahaye et al. (1998)
B_{3S}	[→4)-*β*-D-IdopA-(1→	I	104.0/ 5.10	72.0/ 3.70	73.0/ 3.85	80.0/ 4.00	–	–	de Carvalho et al. (2018), Lahaye et al. (1998)
	4)-*α*-L-Rhap3S-(1→]	R'	102.0/ 4.90	70.0/ 4.25[c]	79.0/ 4.60[c]	79.0/ 3.80[c]	69.0/ 4.15[c]	–	Adrien et al. (2017), de Carvalho et al. (2018), Lahaye et al. (1998)
U_{3S}	[→4)-*β*-D-Xyl-(1→	X	104.5/ 4.65	75.0/ 3.35[d]	75.0/ 3.65[d]	75.0/ 3.65[d]	64.0/ 3.40 64.0/ 4.10	–	de Carvalho et al. (2018), de Freitas et al. (2015), Lahaye et al. (1998)
	4)-*α*-L-Rhap3S-(1→]	R"	99.0/ 4.90	70.0/ 4.25[c]	79.0/ 4.60[c]	79.0/ 3.80[c]	69.0/ 4.15[c]	–	de Carvalho et al. (2018), de Freitas et al. (2015), Lahaye et al. (1998)

[a] Nomenclature for disaccharide units follows (Lahaye & Robic, 2007).
[b] Chemical shifts relative to acetone at 31.45 and 2.225 ppm for ^{13}C and ^{1}H, respectively.
[c] Resonance peaks overlap with R.
[d] Resonance peaks overlap with G.

respectively. There are also a series of unassigned resonances detected in ulvans isolated from filamentous species in the region of ^{13}C 100−103 ppm/^{1}H 5.0–5.1 ppm that are absent in those isolated from blade species (Fig. 4, Table 2). Some of these resonances could result from deshielding of the xylose or glucuronic acid anomeric carbons due to the presence of a 2-sulfate (Lahaye et al., 1999), however, further research is required for conclusive assignment. The greater complexity in resonances of ulvans isolated from filamentous species is also detected in the non-anomeric region.

Within the non-anomeric region of the ^{1}H-^{13}C HSQC, the resonances for the A_{3S} and U_{3S} disaccharides can be identified in the spectra of ulvans from both blade and filamentous species of *Ulva* (Table 2). Similar to the anomeric region, resonances for the B_{3S} disaccharide are detected in ulvans from blade species (Fig. 5A) yet are not detected for ulvans from filamentous species (Fig. 5B). Furthermore, a series of resonances between ^{13}C 70-75 ppm/^{1}H 3.4–3.6 ppm are present in the spectra of ulvans from filamentous but not blade species, and do not appear to be identified in the ulvan literature. In the spectra of the galactose-rich ulvans isolated from *U. ralfsii* there are two unidentified resonances at ^{13}C 62.5/^{1}H 3.75 ppm and ^{13}C 62.5/^{1}H 3.85 ppm (Fig. 5B; S9). These resonances are in a region similar to previous assignments made for the C6/H6,6' for a galactan isolated from a green alga (Farias et al., 2008) and a sea urchin (Castro et al., 2009). In addition there are three resonances centred at ~^{13}C 57/^{1}H 3.4 ppm that are more intense in ulvans isolated from filamentous species than blade species (Fig. 5). These resonances likely correspond to a methoxy substituent on one of the sugars, such as 3-O-Me rhamnose (Gosselin, Holt, & Lowe, 1964; McKinnell & Percival, 1962; Ogawa, Yamaura, & Maruyama, 1997). The greater complexity of resonances throughout the ^{1}H-^{13}C HSQC NMR for ulvans isolated from filamentous species supports a higher level of structural complexity in these polysaccharides. However, further structural investigation via linkage analysis is required to elucidate the structural differences between ulvans isolated from blade and filamentous species of *Ulva*.

3.2.2. FTIR spectroscopy

Ulvan has a unique FTIR fingerprint region in the range of 1770−600 cm^{-1} due to the presence of absorptions by carboxylic groups (V_{as} C═O, 1650−1600cm^{-1}; V_s CO, 1425−1400 cm^{-}═^{1}) (Robic, Bertrand, Sassi, Lerat, & Lahaye, 2009; Yaich et al., 2017), sulfate ester groups (V_{as} S═O, 1260−1215 cm^{-1}; COS, 850−835 cm——$^{-1}$ and 795−785 cm^{-1}) (Pengzhan et al., 2003; Ray & Lahaye, 1995; Yaich et al., 2017), and sugar ring side groups and glycosidic linkages (C—OH, COC, ~1055 cm^{-}———^{1}) (Pengzhan et al., 2003; Robic, Bertrand et al., 2009; Zhang et al., 2010). The ulvans assessed in this study consistently displayed absorption profiles characteristic of ulvan within the above-mentioned fingerprint region, with minor variations between ulvans detected (Fig. S4, Table S5). In general, the intensities of the sulfate ester (C—OS, 850−835 cm—$^{-1}$ and 795−785 cm^{-1}) absorptions (relative to absorptions not related to these groups) were higher for ulvans isolated from blade species than ulvans from filamentous species. This pattern is consistent with the higher content of sulfate esters in ulvans from blade species of *Ulva* (See Section 3.1). The absorption pattern in the region commonly associated with glycosidic linkages and other pyranose vibrational modes (~1160−900 cm^{-1}) differed between ulvans isolated from blade and filamentous species of *Ulva*. Specifically, the absorbance at ~980 cm^{-1} had a lower intensity relative to the absorbance at ~1040 cm^{-1} in ulvans isolated from filamentous *Ulva*. While the absorption band at 980 cm^{-1} remains unassigned, the feature corresponds with a lower content of sulfate esters in filamentous samples relative to blade samples and thus may arise due to a vibrational mode associated with the presence of sulfate esters. Indeed, desulfation of ulvan isolated from *U. rigida* also resulted in the disappearance of this peak in two independent studies (Castro et al., 2006; Ray & Lahaye, 1995). However, such an assignment needs further confirmation.

3.2.3. Molecular weight

It is difficult to compare molecular weight profiles of polysaccharides between studies as each step leading to quantification (e.g. biomass collection/cultivation/pre-treatment, extraction, isolation, and measurement method employed) affects the molecular weight measured (de Reviers & Leproux, 1993; Glasson et al., 2017; Robic, Sassi et al., 2009; Robic et al., 2008; Shanmugam et al., 2001; Yaich et al., 2014). For example, in a study where ulvans were extracted from a single source of *U. ohnoi* (a blade species) using different biorefinery pre-treatments and extractants, the weight average molecular weight (M_w) of the isolated ulvan varied from 10.5–312 kDa (Glasson et al., 2017). Other studies have reported widely varying molecular weights for ulvans (e.g. 2000 kDa from blade *U. armoricana* (Hardouin et al., 2016), 194 kDa from filamentous *U. intestinalis* (Tabarsa et al., 2018), and 1218 kDa from filamentous *U. prolifera* (Cho, Yang, Kim, & You, 2010)). The use of standardised protocols such as those employed in the current study overcome the issues of extraction and measurement variability, producing ulvans that only differ on the basis of source biomass (i.e. species/morphology/wild harvest/cultivation).

The M_w of purified ulvans assessed in the current study ranged from 190 to 406 kDa, with ulvans from filamentous species (338 ± 52 kDa) being approximately 50 % larger than those from blade species (225 ± 23 kDa). (Table 3, Figs. S11, S12). Similarly, the number average molecular weight (M_n) of ulvans from filamentous species (216 ± 27 kDa) was over double that of ulvans from blade species (102 ± 24 kDa; Table 3). Variation in molecular weight was detected for ulvans extracted from different biomass sources (cultivated vs. wild harvest) of the same *Ulva* species. Ulvans isolated from blade *U.* sp. B only had a minor variation of 36 kDa (218−254 kDa) while ulvans from filamentous *U. ralfsii* varied by 78 kDa (328−406 kDa). The ulvans with highest molecular weight from both species were isolated from the cultivated biomass. This variation highlights the importance of species selection and cultivation conditions on the quality of ulvan products.

3.2.4. Rheology

Ulvan polysaccharides are capable of forming a weak gel with a storage modulus (i.e. gel strength, G') ranging from 5−600 Pa (Lahaye & Axelos, 1993; Lahaye, Ray, Baumberger, Quemener, & Axelos, 1996; Robic, Sassi et al., 2009; Sari-Chmayssem et al., 2019; Yaich et al., 2014). The ulvan gels formed in this study were prepared using a standardised method at pH 7.5 with a final concentration of ulvan, $CaCl_2$ and H_3BO_3 of 1.6 % w/v, 7 mM, and 33 mM, respectively. Under these conditions the ulvans that formed stronger gels did so rapidly on addition of the boric acid at room temperature, impeding accurate measurements. To overcome this issue, we exploited the thermoreversilibility of the ulvan gels (Fig. S13) (Lahaye, Ray, Baumberger, Quemener, & Axelos, 1996; Qiao et al., 2016; Shao, Qin, Han, & Sun, 2014; Yaich et al., 2014) by adding boric acid to the ulvan solution while heated to 75 °C and maintained the Peltier plate at 40 °C while the geometry was lowered into position for measurement. Using this approach, ulvans isolated from filamentous species of *Ulva* consistently produced gels with a higher storage modulus (G' = 22.7–74.2 Pa) compared to ulvans isolated from blade species (G' = 0.1–6.6 Pa) (Fig. 6, Table 3). It should be noted that the storage modulus of the ulvan isolated from *Ulva ralfsii* (wild) of 74.2 ± 2.6 Pa is greater than three standard deviations from the storage moduli of other ulvans and so was considered an outlier and excluded from further analysis.

Gels formed by ulvans from filamentous species (G' = 27.8 ± 5.1 Pa, excluding *U. ralfsii* (wild)) held their shape and resisted light pressure, while the gels formed by ulvans from blade species (G' = 1.8 ± 2.5 Pa) were akin to highly viscous liquids. Indeed, half of the gels formed by ulvans from blade species of *Ulva* had a tan δ > 1, indicating that the gel was more viscous than elastic and could not be considered a gel (Table 3). The higher content of sulfate in ulvans isolated from blade *Ulva* species could potentially impede intramolecular interactions resulting in lower storage moduli compared to ulvans from filamentous

Table 3
Purified ulvan molecular weight and rheological properties: details of the *Ulva* biomass from which ulvan was extracted, the weight average (M_w) and number average (M_n) molecular weight, dispersity (Đ), the storage modulus and tan δ of the ulvan gel, and the viscosity of a 2 % w/v ulvan solution.

Ulva details		Molecular Weight			Rheology		
Ulva species	Morphology	M_w (kDa)	M_n (kDa)	Đ	Storage Modulus (Pa)[a]	Tan δ	Viscosity (mPa s^{-1})[b]
australis	Blade	214	82	2.6	0.4 ± 0.1	1.6	8
rigida	Blade	190	66	2.9	0.1 ± 0.0	4.3	10
sp.	Blade	245	104	2.4	1.3 ± 0.2	0.8	9
sp. B (cult.A)	Blade	218	126	1.7	0.1 ± 0.0	3.8	14
sp. B (cult.B)	Blade	254	114	2.2	2.2 ± 0.1	0.7	13
sp. B (wild)	Blade	229	120	1.2	6.6 ± 1.4	0.3	14
compressa	Filamentous	346	208	1.7	22.7 ± 2.0	0.1	7
flexuosa	Filamentous	352	218	1.6	34.2 ± 1.8	<0.1	10
prolifera	Filamentous	260	185	1.4	24.9 ± 3.1	0.1	7
ralfsii (cult.)	Filamentous	406	259	1.6	29.5 ± 4.2	0.1	10
ralfsii (wild)	Filamentous	328	210	1.6	74.2 ± 2.6	<0.1	9

[a] Average of triplicate values (±SD) recorded at an angular frequency of 10 rad s^{-1}.
[b] Value recorded at a shear rate of 100 s^{-1}.

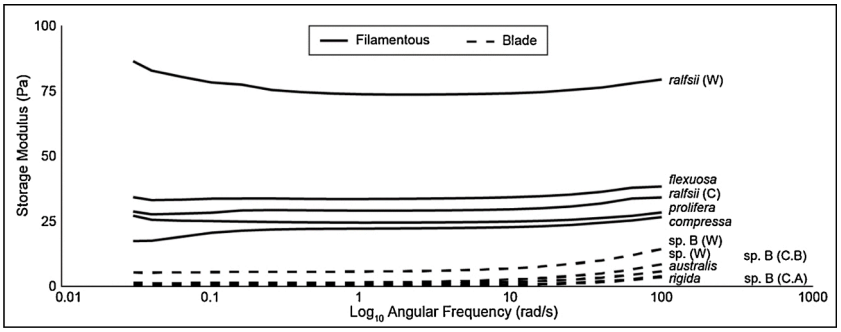

Fig. 6. Storage modulus (gel strength) of purified ulvans in response to a range of rheometer angular frequencies (deformation). Solid lines and dashed lines represent ulvans from filamentous and blade *Ulva* species, respectively. "W" and "C" following a species name indicates whether the biomass was wild harvested or cultivated, respectively; see Table 3 for further details.

species. However, the relationship between ulvan gel formation and sulfate content is unclear and requires further research. Robic, Sassi et al. (2009) found that the gels formed by ulvans varied substantially (G' = 5–600 Pa) when assessing ulvans isolated from different batches of wild harvested *U. rotundata* and *U. armoricana*. The authors attributed the variation in storage moduli to the proportion of high molecular weight ulvan, but also acknowledged that the presence of protein (which ranged from 1.2 to 16.4 % in the ulvans assessed) amplified the storage modulus of the resulting gel. In other studies where the protein content is <5 %, the maximum recorded storage modulus is 250 Pa, but is more consistently below 100 Pa (Lahaye & Axelos, 1993; Sari-Chmayssem et al., 2019; Yaich et al., 2014). Yaich et al. (2014) also reported a decrease in storage modulus with a decrease in molecular weight of ulvans with <5 % protein, as was observed in the current study. Thus, the storage moduli of ulvan gels recorded in the current study (0.1–34.2 Pa) may be at the low end of the reported range for ulvan (G' = 5–600 Pa) due, in part, to low protein content (i.e. high purity of ulvan). In support of this hypothesis is the higher storage moduli of gels formed by crude ulvans, which had higher protein content than purified counterparts (Table S1; Fig. S14). However, crude ulvans also had higher molecular weights than purified ulvans. Further research into the relationship between the storage modulus of ulvan gels, molecular

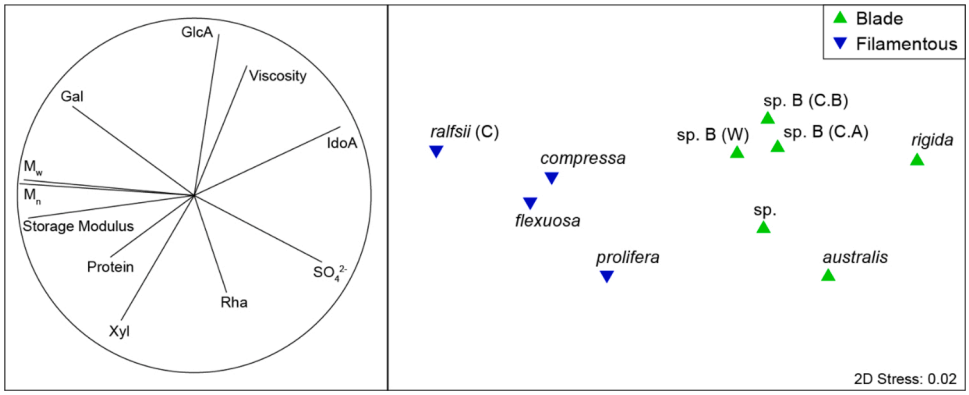

Fig. 7. Multidimensional scaling (MDS) from a square-root transformed Bray-Curtis similarity matrix of the chemical characteristics of the ten ulvans (excluding *U. ralfsii* (wild) as an outlier). Pearson correlation vectors (left plot) influence the distribution of data points (right plot). "W" and "C" following a species name indicates whether the biomass was wild harvested or cultivated, respectively; see Table 3 for further details.

weight, and protein is needed.

3.3. Multivariate synthesis of results

When the composition, structure, and rheological data are considered as a whole, ulvans isolated from blade *Ulva* species are significantly different (pseudo-$F_{1,9} = 18.0$, $p < 0.005$) (Fig. 7) from ulvans isolated from filamentous *Ulva* species. The multivariate dispersions of ulvans from blade and filamentous *Ulva* species did not significantly differ (pseudo-$F_{1,9} = 0.444$, $p = 0.556$), indicating that the significant PERMANOVA result above is due to a difference in ulvans from the two *Ulva* morphologies and not heterogeneous multivariate dispersity of the groups. Ulvans from filamentous and blade species separate on the MDS plot (Fig. 7) due predominantly to the strong positive correlation of large molecular weight and high storage modulus of ulvans of filamentous species, and the high iduronic acid and sulfate content of ulvans from blade species (Table S6). The clustering of ulvans from different morphologies was also significant with 25 % dissimilarity between the two clusters (SIMPROF, $\pi = 1.85$, $p = 0.01$; Fig. S15). The content of glucuronic acid, rhamnose and xylose, and the viscosity of ulvan solutions all had very little effect on the significant distinction of ulvans between *Ulva* morphologies (Fig. 7). The blade and filamentous species analysed here are dispersed throughout the *Ulva* phylogenetic tree (Hayden et al., 2003), and the ulvan physicochemical properties do not reflect the phylogenetic relationship between species. For example, while the physicochemical properties of the ulvans from filamentous *U. compressa* and *U. flexuosa* cause these species to tightly cluster on the MDS plot, these two species are more distantly related phylogenetically than filamentous *U. compressa* and blade *U. australis* (Lawton, Sutherland, Glasson, & Magnusson, 2021), which are widely dispersed on the MDS plot. These findings demonstrate that morphology is driving the significant difference in ulvans and not phylogeny.

The storage modulus of ulvan is strongly positively correlated ($r^2 = 0.9$) with molecular weight (both M_w and M_n), and strongly negatively correlated with iduronic acid ($r^2 = -0.8$) (Table S6). And, in turn, iduronic acid content is strongly negatively correlated with molecular weight ($r^2 = -0.8$). A correlation between molecular weight and storage modulus is intuitive, where an increase in the size of a gel-forming polymer will result in an increase in gel strength due to an increase in intermolecular interactions (Yaich et al., 2014). The correlation of iduronic acid, molecular weight, and storage modulus is somewhat more complicated. Iduronic acid is notoriously acid labile (Conrad, 1980) and its presence in a polysaccharide may contribute to the lower M_w of ulvans due to greater rates of depolymerisation during extraction. In contrast, however, is the principal that the glycosidic linkage of uronic acid to neutral residues is highly acid resistant and the presence of these linkages reduces depolymerisation (BeMiller, 1967). How the acid lability of iduronic acid as a monosaccharide relates to the acid-resistance of its glycosidic linkage is unclear. Iduronic acid also possesses a high degree of conformational freedom (Casu, Petitou, Provasoli, & Sinaÿ, 1988; Hsieh, Thieker, Guerrini, Woods, & Liu, 2016) relative to other monosaccharides (Rees, Morris, Thorn, & Madden, 1982), which may lead to polysaccharide conformations that impede gel formation. Consistent with this hypothesis, ulvans are known to form microbead structures, where the polysaccharide folds back on itself and rolls up into little balls (de Carvalho et al., 2020; Robic, Gaillard, Sassi, Lerat, & Lahaye, 2009). A spherical structure limits the exposed functional areas of the polymer, impeding the strong intramolecular interactions required for high gel strengths, especially given the proposed weak ionic cross-linking mechanism of ulvan gel formation (Lahaye, Ray, Baumberger, Quemener, & Axelos, 1996). Furthermore, models of oligomers of repeat B_{3S} disaccharides (IdoA-Rha3S) have a more helical folded arrangement compared to the more linear structure of oligomers of repeat A_{3S} disaccharides (GlcA-Rha3S) (de Carvalho et al., 2020; Paradossi et al., 2002). The helical arrangement would further limit intramolecular interactions of ulvans rich in B_{3S} disaccharides. Therefore, the sequence and arrangement of disaccharide repeating units in ulvan will likely have a great impact on the gelling capacity of the polymer. Indeed, these studies and our results suggest that the gelling properties of ulvan is diminished in ulvans with high proportions of the B_{3S} disaccharide.

4. Conclusion

The multivariate analysis identified an *Ulva* morphology-based division in the physicochemical properties of isolated ulvans, thus confirming our original hypothesis. The data are compelling when assessed in a multivariate context, which is appropriate as the composition and structure of ulvans drive their rheological properties. Although further validation with ulvans from other species is required to generalise this pattern more broadly, the identification of a morphology-based distinction in ulvan is an important step forward in ulvan research. Not only in characterisation of the under-studied ulvans from filamentous species of *Ulva*, but also in the application of ulvan isolated from cultivated *Ulva* biomass. This research identifies a potential to select an *Ulva* morphology for cultivation to target a desirable property or activity in the resulting ulvan. For example, in the context of this study, ulvan from *U. ralfsii* would be suited for rheological applications. However, further understanding of the structure-activity relationships between ulvans isolated from different species and morphologies are required for species selection based on favourable biological activities. In closing, there is a clear disparity in ulvans from blade and filamentous species of *Ulva*, demonstrating the importance of considering morphology in the selection of *Ulva* species for cultivation with respect to the biotechnical applications of ulvan.

CRediT authorship contribution statement

Joel T. Kidgell: Conceptualisation, investigation, data curation, visualisation, writing – original draft. **Susan M. Carnachan:** Investigation, supervision, writing – original draft. **Marie Magnusson:** Conceptualisation, resources, funding, writing – review and editing. **Rebecca Lawton:** Investigation (algal cultivation), writing – original draft. **Ian M. Sims:** Investigation, writing – original draft. **Simon F.R. Hinkley:** Resources, supervision, writing – review and editing. **Rocky de Nys:** Conceptualisation, resources, funding, supervision, writing – review and editing. **Christopher R.K. Glasson:** Conceptualisation, investigation, supervision, methodology, writing – original draft.

Acknowledgments

The authors would like to thank Peter Randrup for his assistance with sample collection, *Ulva* cultivation and photos, Ari Brandenburg for her assistance in the laboratory work, and Andrew Lewis for his assistance in performing the NMR experiments. We would also like to acknowledge James Cook University and the Australian Government for providing a Research Training Program Scholarship to Joel Kidgell. This research is part of the Entrepreneurial Universities Macroalgal Biotechnologies Programme, jointly funded by the University of Waikato and the Tertiary Education Commission.

Appendix A. Supplementary data

Supplementary material related to this article can be found, in the online version, at doi:https://doi.org/10.1016/j.carbpol.2021.118010.

References

Adrien, A., Bonnet, A., Dufour, D., Baudouin, S., Maugard, T., & Bridiau, N. (2017). Pilot production of ulvans from *Ulva* sp. and their effects on hyaluronan and collagen production in cultured dermal fibroblasts. *Carbohydrate Polymers, 157*, 1306–1314.

Alves, A., Sousa, R. A., & Reis, R. L. (2013). A practical perspective on ulvan extracted from green algae. *Journal of Applied Phycology, 25*(2), 407–424.

Anderson, M. J., Gorley, R. N., & Clarke, R. K. (2008). *Permanova+ for Primer: Guide to software and statistical methods*.

Angell, A. R., Mata, L., de Nys, R., & Paul, N. A. (2016). The protein content of seaweeds: A universal nitrogen-to-protein conversion factor of five. *Journal of Applied Phycology, 28*(1), 511–524.

BeMiller, J. N. (1967). Acid-catalyzed hydrolysis of glycosides. *Advances in Carbohydrate Chemistry and Biochemistry, 22*, 25–108.

Bolton, J. J., Robertson-Andersson, D. V., Shuuluka, D., & Kandjengo, L. (2009). Growing Ulva (Chlorophyta) in integrated systems as a commercial crop for abalone feed in South Africa: A SWOT analysis. *Journal of Applied Phycology, 21*(5), 575–583.

Cassolato, J. E., Noseda, M. D., Pujol, C. A., Pellizzari, F. M., Damonte, E. B., & Duarte, M. E. (2008). Chemical structure and antiviral activity of the sulfated heterorhamnan isolated from the green seaweed *Gayralia oxysperma*. *Carbohydrate Research, 343*(18), 3085–3095.

Castro, M. O., Pomin, V. H., Santos, L. L., Vilela-Silva, A. C., Hirohashi, N., Pol-Fachin, L., et al. (2009). A unique 2-sulfated {beta}-galactan from the egg jelly of the sea urchin Glyptocidaris crenularis: Conformation flexibility versus induction of the sperm acrosome reaction. *The Journal of Biological Chemistry, 284*(28), 18790–18800.

Castro, R., Piazzon, M. C., Zarra, I., Leiro, J., Noya, M., & Lamas, J. (2006). Stimulation of turbot phagocytes by *Ulva rigida* C. Agardh polysaccharides. *Aquaculture, 254*(1), 9–20.

Casu, B., Petitou, M., Provasoli, M., & Sinaÿ, P. (1988). Conformational flexibility: A new concept for explaining binding and biological properties of iduronic acid-containing glycosaminoglycans. *Trends in Biochemical Sciences, 13*(6), 221–225.

Chattopadhyay, K., Mandal, P., Lerouge, P., Driouich, A., Ghosal, P., & Ray, B. (2007). Sulphated polysaccharides from Indian samples of *Enteromorpha compressa* (Ulvales, Chlorophyta): Isolation and structural features. *Food Chemistry, 104*(3), 928–935.

Cho, M., Yang, C., Kim, S. M., & You, S. (2010). Molecular characterization and biological activities of water-soluble sulfated polysaccharides from *Enteromorpha prolifera*. *Food Science and Biotechnology, 19*(2), 525–533.

Conrad, H. E. (1980). The acid lability of the glycosidic bonds of L-iduronic acid residues in glycosaminoglycans. *The Biochemical Journal, 191*(2), 355–363.

Craigie, J. S., Wen, Z. C., & van der Meer, J. P. (1984). Interspecific, intraspecific and nutritionally-determined variations in the composition of agars from *Gracilaria* spp. *Botanica Marina, 27*, 55.

de Carvalho, M. M., de Freitas, R. A., Ducatti, D. R. B., Ferreira, L. G., Gonçalves, A. G., Colodi, F. G., et al. (2018). Modification of ulvans via periodate-chlorite oxidation: Chemical characterization and anticoagulant activity. *Carbohydrate Polymers, 197*, 631–640.

de Carvalho, M. M., Noseda, M. D., Dallagnol, J. C. C., Ferreira, L. G., Ducatti, D. R. B., Gonçalves, A. G., et al. (2020). Conformational analysis of ulvans from *Ulva fasciata* and their anticoagulant polycarboxylic derivatives. *International Journal of Biological Macromolecules, 162*, 599–608.

de Freitas, M. B., Ferreira, L. G., Hawerroth, C., Duarte, M. E. R., Noseda, M. D., & Stadnik, M. J. (2015). Ulvans induce resistance against plant pathogenic fungi independently of their sulfation degree. *Carbohydrate Polymers, 133*, 384–390.

de Reviers, B., & Leproux, A. (1993). Characterization of polysaccharides from *Enteromorpha intestinalis* (L.) link, chlorophyta. *Carbohydrate Polymers, 22*(4), 253–259.

de Ruiter, G. A., Schols, H. A., Voragen, A. G. J., & Rombouts, F. M. (1992). Carbohydrate analysis of water-soluble uronic acid-containing polysaccharides with high-performance anion-exchange chromatography using methanolysis combined with TFA hydrolysis is superior to four other methods. *Analytical Biochemistry, 207*(1), 176–185.

Farias, E., Pomin, V., Valente, A., Nader, H., Rocha, H., & Mourão, P. (2008). A preponderantly 4-sulfated, 3-linked galactan from the green alga *Codium isthmocladum*. *Glycobiology, 18*, 250–259.

Glasson, C. R. K., Donnet, L., Angell, A., Vucko, M. J., Lorbeer, A. J., Vamvounis, G., et al. (2019). Multiple response optimisation of the aqueous extraction of high quality ulvan from *Ulva ohnoi*. *Bioresource Technology Reports, 7*.

Glasson, C. R. K., Sims, I. M., Carnachan, S. M., de Nys, R., & Magnusson, M. (2017). A cascading biorefinery process targeting sulfated polysaccharides (ulvan) from *Ulva ohnoi*. *Algal Research, 27*, 383–391.

Gosselin, C. C., Holt, A., & Lowe, P. A. (1964). Polysaccharides of *Enteromorpha* species. *Journal of the Chemical Society (Resumed)*, 5877–5880.

Hardouin, K., Bedoux, G., Burlot, A.-S., Donnay-Moreno, C., Bergé, J.-P., Nyvall-Collén, P., et al. (2016). Enzyme-assisted extraction (EAE) for the production of antiviral and antioxidant extracts from the green seaweed *Ulva armoricana* (Ulvales, Ulvophyceae). *Algal Research, 16*, 233–239.

Haug, A. (1976). The influence of borate and calcium on the gel formation of a sulfated polysaccharide from *Ulva lactuca*. *Acta Chemica Scandinavica. Series B: Organic Chemistry and Biochemistry, 30*(6), 562–566.

Hayden, H. S., Blomster, J., Maggs, C. A., Silva, P. C., Stanhope, M. J., & Waaland, J. R. (2003). Linnaeus was right all along: *Ulva* and *Enteromorpha* are not distinct genera. *European Journal of Phycology, 38*(3), 277–294.

Holdt, S. L., & Kraan, S. (2011). Bioactive compounds in seaweed: Functional food applications and legislation. *Journal of Applied Phycology, 23*(3), 543–597.

Hsieh, P.-H., Thieker, D. F., Guerrini, M., Woods, R. J., & Liu, J. (2016). Uncovering the relationship between sulphation patterns and conformation of iduronic acid in Heparan sulphate. *Scientific Reports, 6*(1), 29602.

Kidgell, J. T., Glasson, C. R. K., Magnusson, M., Vamvounis, G., Sims, I. M., Carnachan, S. M., et al. (2020). The molecular weight of ulvan affects the in vitro inflammatory response of a murine macrophage. *International Journal of Biological Macromolecules, 150*, 839–848.

Kidgell, J. T., Magnusson, M., de Nys, R., & Glasson, C. R. K. (2019). Ulvan: A systematic review of extraction, composition and function. *Algal Research, 39*, Article 101422.

Lahaye, M., & Axelos, M. A. V. (1993). Gelling properties of water-soluble polysaccharides from proliferating marine green seaweeds (*Ulva* spp.). *Carbohydrate Polymers, 22*(4), 261–265.

Lahaye, M., & Robic, A. (2007). Structure and functional properties of ulvan, a polysaccharide from green seaweeds. *Biomacromolecules, 8*(6), 1765–1774.

Lahaye, M., Cimadevilla, E. A. C., Kuhlenkamp, R., Quemener, B., Lognoné, V., & Dion, P. (1999). Chemical composition and 13C NMR spectroscopic characterisation of ulvans from *Ulva* (Ulvales, Chlorophyta). *Journal of Applied Phycology, 11*(1), 1–7.

Lahaye, M., Inizan, F., & Vigouroux, J. (1998). NMR analysis of the chemical structure of ulvan and of ulvan-boron complex formation. *Carbohydrate Polymers, 36*(2-3), 239–249.

Lahaye, M., Ray, B., Baumberger, S., Quemener, B., & Axelos, M. A. V. (1996). Chemical characterisation and gelling properties of cell wall polysaccharides from species of *Ulva* (Ulvales, Chlorophyta). *Hydrobiologia, 326*(1), 473–480.

Lawton, R. J., Mata, L., de Nys, R., & Paul, N. A. (2013). Algal bioremediation of waste waters from land-based aquaculture using *Ulva*: Selecting target species and strains. *PloS One, 8*(10), Article e77344.

Lawton, R. J., Sutherland, J. E., Glasson, C. R. K., & Magnusson, M. (2021). Selection of temperate *Ulva* species and strains for land-based cultivation and biomass applications. *Algal Research*. Submitted for publication.

Lee, J. B., Yamagaki, T., Maeda, M., & Nakanishi, H. (1998). Rhamnan sulfate from cell walls of *Monostroma latissimum*. *Phytochemistry, 48*(6), 921–925.

Leiro, J. M., Castro, R., Arranz, J. A., & Lamas, J. (2007). Immunomodulating activities of acidic sulphated polysaccharides obtained from the seaweed *Ulva rigida* C. Agardh. *International Immunopharmacology, 7*(7), 879–888.

Li, H., Mao, W., Zhang, X., Qi, X., Chen, Y., Chen, Y., et al. (2011). Structural characterization of an anticoagulant-active sulfated polysaccharide isolated from green alga *Monostroma latissimum*. *Carbohydrate Polymers, 85*(2), 394–400.

Lopes, N., Ray, S., Espada, S. F., Bomfim, W. A., Ray, B., Faccin-Galhardi, L. C., et al. (2017). Green seaweed *Enteromorpha compressa* (Chlorophyta, Ulvaceae) derived sulphated polysaccharides inhibit herpes simplex virus. *International Journal of Biological Macromolecules, 102*, 605–612.

McHugh, D. J. (2003). *A guide to the seaweed industry*. FAO Fisheries Technical Paper. No. 441 (p. 105). Rome: FAO.

Nardelli, A. E., Chiozzini, V. G., Braga, E. S., & Chow, F. (2019). Integrated multi-trophic farming system between the green seaweed *Ulva lactuca*, mussel, and fish: A production and bioremediation solution. *Journal of Applied Phycology, 31*, 847–856. https://doi.org/10.1007/s10811-018-1581-4

McKinnell, J. P., & Percival, E. (1962). The acid polysaccharide from the Green Seaweed, *Ulva lactuca*. *Journal of the Chemical Society*, 2082–2084 (Resumed)(0).

Nep, E. I., Carnachan, S. M., Ngwuluka, N. C., Kontogiorgos, V., Morris, G. A., Sims, I. M., et al. (2016). Structural characterisation and rheological properties of a polysaccharide from sesame leaves (*Sesamum radiatum* Schumach. & Thonn.). *Carbohydrate Polymers, 152*, 541–547.

Ogawa, K., Yamaura, M., & Maruyama, I. (1997). Isolation and identification of 2-O-methyl-l-rhamnose and 3-O-methyl-l-rhamnose as constituents of an acidic polysaccharide of *Chlorella vulgaris*. *Bioscience, Biotechnology, and Biochemistry, 61*(3), 539–540.

Ohno, M. (1993). Cultivation of the green algae *Monostroma* and *Enteromorpha* "*Aonori*". In M. Ohno, & A. T. Critchley (Eds.), *Seaweed cultivation and marine ranching* (pp. 7–16). Jokocuka: Japan International Cooperation Agency.

Paradossi, G., Cavalieri, F., & Chiessi, E. (2002). A conformational study on the algal polysaccharide ulvan. *Macromolecules, 35*(16), 6404–6411.

Pengzhan, Y., Quanbin, Z., Ning, L., Zuhong, X., Yanmei, W., & Zhi'en, L. (2003). Polysaccharides from *Ulva pertusa* (Chlorophyta) and preliminary studies on their antihyperlipidemia activity. *Journal of Applied Phycology, 15*(1), 21–27.

Pettolino, F. A., Walsh, C., Fincher, G. B., & Bacic, A. (2012). Determining the polysaccharide composition of plant cell walls. *Nature Protocols, 7*(9), 1590–1607.

Qi, H., & Sheng, J. (2015). The antihyperlipidemic mechanism of high sulfate content ulvan in rats. *Marine Drugs, 13*(6), 3407–3421.

Qi, H., Huang, L., Liu, X., Liu, D., Zhang, Q., & Liu, S. (2012). Antihyperlipidemic activity of high sulfate content derivative of polysaccharide extracted from *Ulva pertusa* (Chlorophyta). *Carbohydrate Polymers, 87*(2), 1637–1640.

Qi, X. H., Mao, W. J., Gao, Y., Chen, Y., Chen, Y. L., Zhao, C. Q., et al. (2012). Chemical characteristic of an anticoagulant-active sulfated polysaccharide from *Enteromorpha clathrata*. *Carbohydrate Polymers, 90*(4), 1804–1810.

Qiao, L. K., Li, Y. P., Chi, Y. Z., Ji, Y. L., Gao, Y., Hwang, H. M., et al. (2016). Rheological properties, gelling behavior and texture characteristics of polysaccharide from *Enteromorpha prolifera*. *Carbohydrate Polymers, 136*, 1307–1314.

Ray, B., & Lahaye, M. (1995). Cell-wall polysaccharides from the marine green alga *Ulva* "*rigida*" (Ulvales, Chlorophyta). Chemical structure of ulvan. *Carbohydrate Research, 274*, 313–318.

Rees, D. A., Morris, E. R., Thorn, D., & Madden, J. K. (1982). Shapes and interactions of carbohydrate chains. In G. O. Aspinall (Ed.), *The polysaccharides* (pp. 195–290). New York: Academic Press.

Robic, A., Sassi, J. F., & Lahaye, M. (2008). Impact of stabilization treatments of the green seaweed *Ulva rotundata* (Chlorophyta) on the extraction yield, the physico-chemical and rheological properties of ulvan. *Carbohydrate Polymers, 74*(3), 344–352.

Robic, A., Bertrand, D., Sassi, J. F., Lerat, Y., & Lahaye, M. (2009). Determination of the chemical composition of ulvan, a cell wall polysaccharide from *Ulva* spp. (Ulvales, Chlorophyta) by FT-IR and chemometrics. *Journal of Applied Phycology, 21*(4), 451–456.

Robic, A., Gaillard, C., Sassi, J. F., Lerat, Y., & Lahaye, M. (2009). Ultrastructure of ulvan: A polysaccharide from green seaweeds. *Biopolymers, 91*(8), 652–664.

Robic, A., Sassi, J. F., Dion, P., Lerat, Y., & Lahaye, M. (2009). Seasonal variability of physicochemical and rheological properties of ulvan in two *Ulva* species (chlorophyta) from the Brittany coast. *Journal of Phycology, 45*(4), 962–973.

Sari-Chmayssem, N., Taha, S., Mawlawi, H., Guégan, J.-P., Jeftić, J., & Benvegnu, T. (2019). Extracted ulvans from green algae *Ulva linza* of Lebanese origin and amphiphilic derivatives: Evaluation of their physico-chemical and rheological properties. *Journal of Applied Phycology, 31*(3), 1931–1946.

Shanmugam, M., Ramavat, B. K., Mody, K. H., Oza, R. M., & Tewari, A. (2001). Distribution of heparinoid-active sulphated polysaccharides in some Indian marine green algae. *Indian Journal of Marine Sciences, 30*(4), 222–227.

Shao, P., Pei, Y., Fang, Z., & Sun, P. (2014). Effects of partial desulfation on antioxidant and inhibition of DLD cancer cell of Ulva fasciata polysaccharide. *International Journal of Biological Macromolecules, 65*, 307–313.

Shao, P., Qin, M. P., Han, L. F., & Sun, P. L. (2014). Rheology and characteristics of sulfated polysaccharides from chlorophytan seaweeds *Ulva fasciata*. *Carbohydrate Polymers, 113*, 365–372.

Singh, R. P., & Reddy, C. R. K. (2014). Seaweed–microbial interactions: Key functions of seaweed-associated bacteria. *FEMS Microbiology Ecology, 88*(2), 213–230.

Tabarsa, M., You, S., Dabaghian, E. H., & Surayot, U. (2018). Water-soluble polysaccharides from *Ulva intestinalis*: Molecular properties, structural elucidation and immunomodulatory activities. *Journal of Food and Drug Analysis, 26*(2), 599–608.

van den Hoogen, B. M., van Weeren, P. R., Lopes-Cardozo, M., van Golde, L. M., Barneveld, A., & van de Lest, C. H. (1998). A microtiter plate assay for the determination of uronic acids. *Analytical Biochemistry, 257*(2), 107–111.

Wang, X. M., Zhang, Z. S., Yao, Z. Y., Zhao, M. X., & Qi, H. M. (2013). Sulfation, anticoagulant and antioxidant activities of polysaccharide from green algae *Enteromorpha linza*. *International Journal of Biological Macromolecules, 58*, 225–230.

Yaich, H., Amira, A. B., Abbes, F., Bouaziz, M., Besbes, S., Richel, A., et al. (2017). Effect of extraction procedures on structural, thermal and antioxidant properties of ulvan from *Ulva lactuca* collected in Monastir coast. *International Journal of Biological Macromolecules, 105*(Pt 2), 1430–1439.

Yaich, H., Garna, H., Besbes, S., Barthélemy, J.-P., Paquot, M., Blecker, C., et al. (2014). Impact of extraction procedures on the chemical, rheological and textural properties of ulvan from *Ulva lactuca* of Tunisia coast. *Food Hydrocolloids, 40*, 53–63.

Yaich, H., Garna, H., Besbes, S., Paquot, M., Blecker, C., & Attia, H. (2013). Effect of extraction conditions on the yield and purity of ulvan extracted from *Ulva lactuca*. *Food Hydrocolloids, 31*(2), 375–382.

Ye, N.-h., Zhang, X.-w., Mao, Y.-z., Liang, C.-w., Xu, D., Zou, J., et al. (2011). "Green tides" are overwhelming the coastline of our blue planet: Taking the world's largest example. *Ecological Research, 26*(3), 477.

Yu, Y., Li, Y. P., Du, C. Y., Mou, H. J., & Wang, P. (2017). Compositional and structural characteristics of sulfated polysaccharide from *Enteromorpha prolifera*. *Carbohydrate Polymers, 165*, 221–228.

Zhang, Z. S., Wang, F., Wang, X. M., Liu, X. L., Hou, Y., & Zhang, Q. B. (2010). Extraction of the polysaccharides from five algae and their potential antioxidant activity in vitro. *Carbohydrate Polymers, 82*(1), 118–121.

Zhong, R., Wan, X., Wang, D., Zhao, C., Liu, D., Gao, L., et al. (2020). Polysaccharides from marine *Enteromorpha*: Structure and function. *Trends in Food Science & Technology, 99*, 11–20.

7.6 Chapter 5 publication

Title: The molecular weight of ulvan affects the in vitro inflammatory response of a murine macrophage

Journal: International Journal of Biological Macromolecules 150:839-848

DOI: https://doi.org/10.1016/j.carbpol.2021.118010

Published: 01/05/2020

Scopus citations as of 16/04/2021: 2

International Journal of Biological Macromolecules 150 (2020) 839–848

Contents lists available at ScienceDirect

International Journal of Biological Macromolecules

journal homepage: http://www.elsevier.com/locate/ijbiomac

The molecular weight of ulvan affects the *in vitro* inflammatory response of a murine macrophage

Joel T. Kidgell [a,*], Christopher R.K. Glasson [b], Marie Magnusson [b], George Vamvounis [c], Ian M. Sims [d], Susan M. Carnachan [d], Simon F.R. Hinkley [d], Andreas L. Lopata [e,f], Rocky de Nys [a], Aya C. Taki [e,f,g]

[a] MACRO – The Centre for Macroalgal Resources and Biotechnology, College of Science and Engineering, James Cook University, Townsville, Australia
[b] School of Science, University of Waikato, Tauranga, New Zealand
[c] College of Science and Engineering, James Cook University, Townsville, Australia
[d] The Ferrier Research Institute, Victoria University of Wellington, Wellington, New Zealand
[e] Molecular Allergy Research Laboratory, College of Public Health, Medical and Veterinary Sciences, James Cook University, Townsville, Australia
[f] Australian Institute of Tropical Health and Medicine, James Cook University, Townsville, Australia
[g] Faculty of Veterinary and Agricultural Sciences, The University of Melbourne, Parkville, Australia

ARTICLE INFO

Article history:
Received 21 December 2019
Received in revised form 4 February 2020
Accepted 8 February 2020
Available online 10 February 2020

Keywords:
Immunomodulation
Molecular weight
Sulfated polysaccharide

ABSTRACT

Ulvan, a sulfated polysaccharide extracted from the green seaweed genus *Ulva*, has bioactive properties including an immunomodulating capacity. The immunomodulatory capacity of ulvan from *Ulva ohnoi*, however, has not been assessed in detail. We depolymerised purified ulvan from *U. ohnoi* to obtain a range of molecular weight fractions (M_w 7, 9, 13, 21, 209 kDa), which were characterised by constituent sugar analysis, SEC-MALLS, and NMR. Ulvan fractions contained 48.8–54.7 mol% rhamnose, 32.5–35.9 mol% glucuronic acid, 4.5–7.3 mol% iduronic acid, and 3.3–5.6 mol% xylose. ^{1}H and ^{13}C NMR was consistent with hydrolysis occurring at the anomeric centre without further modification to the oligosaccharide structure. The *in vitro* immunomodulatory effect of ulvan fractions was quantified by measuring levels of inflammatory-mediating signalling molecules released from LPS-stimulated RAW264.7 murine macrophages. All ulvan fractions showed no toxicity on RAW264.7 cells at concentrations below 100 μg mL^{-1} over 48 h. Secreted interleukin-10 and prostaglandin E2 demonstrated an anti-inflammatory effect by higher molecular weight ulvan fractions at 100 μg mL^{-1}. To a lesser extent, these fractions also enhanced the LPS-induced inflammation through minor increases of IL-1β and IL-6. This study confirms that ulvan from *U. ohnoi* has a mild *in vitro* immunomodulatory effect.

1. Introduction

Sulfated polysaccharides are complex, bioactive macromolecules featuring sugar residues with sulfate esters [1]. In mammals, sulfated polysaccharides modulate a range of biological functions including blood coagulation, cell adhesion, and cell growth; in addition to contributing structural support to the extracellular matrix and cartilage [2–4]. Sulfated polysaccharides containing the monosaccharide rhamnose induce a host of immunostimulating reactions in human skin [5]. Rhamnose is uncommon in nature; only being found in bacterial exopolysaccharides, plant pectic (non-sulfated) polysaccharides, and ulvan - a sulfated polysaccharide from green marine algae of the genus *Ulva* [6]. Ulvan is composed predominantly of sulfated rhamnose, uronic acids (glucuronic and iduronic), and xylose. Featuring a rare bioactive monosaccharide and exhibiting a wide range of bioactive properties ulvan has potential for human health applications [7–10].

To assess the impact of ulvan on human health, ulvan (or extracts containing ulvan) has been tested for the capacity to alter the inflammatory response both *in vitro* using macrophages (*e.g.* RAW264.7 cells) [11–18] and *in vivo* using animal models [19–21]. *In vitro* assessment of the effect of ulvan on inflammatory responses is often evaluated by quantifying the levels of inflammatory cytokines secreted from macrophages such as interleukin (IL)-1β, 4, 5, 6, 10, 12, 18, and tissue necrosis factor alpha (TNF-α), and other inflammation markers such as prostaglandin E2 (PGE_2) and nitric oxide (NO) [13,18]. Despite the increasing number of reports on the immunomodulating properties of ulvan, little is known about the structure-activity relationships of this class of sulfated polysaccharide. However, molecular weight (M_w) is known to be critical to the efficacy of bioactive polysaccharides [1,4,7,8,18,22]. Ulvan extracts naturally exhibit a high level of polydispersity (which may be exacerbated by the extraction conditions employed) [23], a feature that hinders precise assignment of immunomodulating activity.

* Corresponding author at: Coastal Marine Field Station, 58 Cross Road, Sulphur Point, Tauranga 3110, New Zealand.
E-mail address: joel.kidgell@my.jcu.edu.au (J.T. Kidgell).

https://doi.org/10.1016/j.ijbiomac.2020.02.071
0141-8130/

The aims of this study were, therefore, to elucidate the effect of the molecular weight of purified ulvan, extracted from *Ulva ohnoi*, on the inflammatory response of RAW264.7 murine macrophages. To achieve these aims, we (i) characterised 'native' and depolymerised ulvan from *U. ohnoi*; (ii) assessed toxicity of ulvan on murine macrophages; (iii) assessed the effect of 'native' *U. ohnoi* ulvan on the inflammatory response of murine macrophages; and (iv) assessed the effect that the molecular weight of ulvan has on the inflammatory response of murine macrophages.

2. Methods

2.1. Materials

The following were purchased from Fisher Scientific, Thermo Fisher Scientific, Australia: H_2O_2 (ACS, 30%, #H325) and NaCl (ACS, #S271). The following were purchased from Sigma-Aldrich, Australia: Glucuronic acid (>98%, #G5269), sodium tetraborate (99.998%, #229946), *m*-hydroxydiphenyl (85%, #262250), concentrated sulfuric acid (ACS, 95–98%, #258105), dimethyl sulfoxide (>99.9%, #276855), Na_2CO_3 (ACS, >99.5%, #222321), $NaHCO_3$ (ACS >99.7%, #S6014), K_2SO_4 (>99.0%, #P0772), and sodium nitrite (ACS >97%, #237213). The following were purchased from Sigma-Aldrich, New Zealand: $NaNO_3$ (>99.0%, #S5506), NaN_3 (>99%, #S2002), methanolic HCl (#90964), L-fucose (#F2252), L-rhamnose (#3875), L-arabinose (#10839), D-galactose (#0750), D-glucose (#8270), D-mannose (#2069), D-xylose (#95729), D-ribose (#7500), D-galacturonic acid (#73960), and D-glucuronic acid (#5269). Other reagents were sourced as follows: trifluoroacetic acid (Synthesis grade, Scarlau, Spain, #AC31420100), NaOH (50% w/w, Fisher Scientific, Thermo Fisher Scientific, New Zealand, #SS254), anhydrous NaOAc (Carlo Erba, France, #366377), D_2O (99.9%, Cambridge Isotope Laboratories, USA, #DLM-4), and L-iduronic acid (Carbosynth, UK, #MI08102).

2.2. Ulvan preparation

2.2.1. Algal cultivation & ulvan extraction

Ulva ohnoi (Gen-bank accession number KF195509, strain JCU 1 [24]) was cultivated and supplied by Pacific Biotechnologies ABA facility, a land-based aquaculture facility near Ayr, Queensland, Australia (19°29′S, 147°28′E). Crude ulvan was extracted using a proprietary extraction procedure (Marinova Pty. Ltd.) and purified as described below.

2.2.2. Purification & fractionation

Crude ulvan (2 g L^{-1}) was dissolved in Type 1 water prior to vacuum filtration (Filtech, 453) and diafiltration (ÄKTA flux 6 system fitted with a 10,000 NMWC filter, UFP-10-E-4X2MA) with five volumes of Type 1 water. Protein was separated from the diafiltered retentate *via* anion exchange chromatography (AEC) using an ÄKTA pure 150 L coupled with a single wavelength (280 nm) UV detector. The retentate (400 mL) was loaded onto an equilibrated (Type 1 water, 5 column volumes (CV); 2 M NaCl, 5 CV; Type 1 water, 5 CV) XK 50/30 column (GE Healthcare Life Sciences) packed with Q Sepharose XL media (bed height = 24.5 cm). The column was eluted using a stepwise gradient (0 M NaCl, 2 CV; 0–0.5 M NaCl, 2 CV; 0.5–1 M, 2 CV; 1–1.75 M NaCl, 3 CV; 1.75–2 M NaCl, 5 CV) at a flow rate of 20 mL min^{-1}. A chromatogram was produced by analysing collected fractions (13 mL) for uronic acid colourimetrically using the *m*-phenyl-phenol method with glucuronic acid as standard [25]. Fractions containing uronic acid that did not overlap the major peak in the UV trace (attributed to protein) were pooled and concentrated by diafiltration with Type 1 water until permeate conductivity was <5 μS cm^{-1}. The purified ulvan was recovered *via* lyophilisation – this is referred to as 'native' ulvan.

2.2.3. Ulvan hydrolysis

The hydrolysis method was modified from Zhang et al. [26] so that time was the only variable parameter. Native ulvan solution (1% w/v in Type 1 water) was heated to 50 °C under constant stirring before H_2O_2 was added to a final solution concentration of 2.5% v/v. The hydrolysis reaction was held at 50 °C for 1, 2, 5, or 7 h before being quenched in an ice bath. The cold solution was diafiltered (Amicon Ultra-15, 10 kDa NMWL) with five volumes of Type 1 water prior to recovery by lyophilisation. The permeates from hydrolysed ulvan samples were collected, combined, and lyophilised. The 5 and 7 h treatments were combined due to low yield of hydrolysed ulvan and comparable molecular weight profiles. Table 1 assigns sample labels used throughout the text.

2.3. Chemical characterisation

2.3.1. Elemental characterisation

Elemental analysis (% C, H, N, S; n = 1) and ash content (% w/w) of ulvan samples were measured commercially by OEA labs (www.oealabs.com, Callington, UK). Percent oxygen was calculated as % O = 100 – Σ(C, H, N, S, ash), where C, H, N, S, and ash are expressed as a percentage of the total mass. Sulfate content was quantified by ion chromatography (Metrohm 930 Compact IC Flex fitted with a Metrosep A Supp 5, 150 × 4.0 mm column and a Metrosep RP 2 Guard 3.5 mm guard column) by elution at 0.7 mL min^{-1} with 3.2 mmol L^{-1} Na_2CO_3 and 1.0 mmol L^{-1} $NaHCO_3$ using K_2SO_4 as a standard. Protein content was estimated using the nitrogen-to-protein conversion factor of 5 (% N × 5) [27].

2.3.2. Molecular weight

Molecular weight (M_w) distributions were determined using size-exclusion chromatography coupled with multi-angle laser light scattering (SEC-MALLS). Samples (5 mg mL^{-1} in 0.1 M $NaNO_3$) were dissolved by heating at 80 °C and then standing at room temperature overnight (~20 h). Soluble material was separated on three columns (TSK-Gel $G5000PW_{XL}$, $G4000PW_{XL}$ and $G3000PW_{XL}$, 300 × 7.8 mm, Tosoh Corp., Tokyo, Japan) connected in series, eluted with 0.1 M $NaNO_3$ with 0.02% NaN_3 (0.5 mL min^{-1}, 60 °C). The eluted material was detected using a variable wavelength detector (280 nm), a SDL7000 MALLS detector (PSS Polymer Standards Service GmbH, Mainz, Germany) and a refractive index monitor. The data for molecular weight determination were analysed using Win GPC Unichrom software (v8.2.1, PSS Polymer Standards Service) using a refractive index increment, dn/dc, of 0.146 mL g^{-1} [28].

2.3.3. Constituent sugar composition

Constituent sugar composition was determined by high-performance anion-exchange chromatography with pulsed amperometric detection (HPAEC-PAD) after hydrolysis of the polysaccharides present to their component monosaccharides. Samples (1 mg) were hydrolysed and analysed in duplicate with methanolic HCl (3 M, 500 μL, 80 °C, 18 h), followed by aqueous trifluoroacetic acid (TFA, 2.5 M, 500 μL, 120 °C, 1 h). The resulting hydrolysates were dried and redissolved in Type 1 water (1 mL). An aliquot of hydrolysate was then diluted with Type 1 water (to 50 μg mL^{-1}) and analysed on a CarboPac PA-1 (4 × 250 mm) column equilibrated in 20 mM NaOH

Table 1
Sample labels used through the text for hydrolysed ulvan fractions.

Sample ID	Hydrolysis time (h)
U209	0 (native ulvan)
U21	1
U13	2
U9	5 + 7
U7	Permeate

and eluted with a simultaneous gradient of NaOH and NaOAc at 30 °C and a flow rate of 1 mL min^{-1}. The sugars were identified from their elution times relative to a standard sugar mix, quantified from response calibration curves of each sugar and expressed as μg of the anhydro-sugar (as this is the form of sugar present in a polysaccharide) per mg of sample; the normalised mol % of each anhydro-sugar was also calculated.

2.3.4. NMR spectroscopy

Ulvan samples were dissolved in D_2O at 25 mg mL^{-1}. NMR data was collected on a Bruker Avance III 500 operating at a proton frequency of 499.843 MHz and 125.698 MHz for ^{13}C running Topspin 2.1 software.

Data was collected on a Bruker two channel 5-mm broadband observe nuclei probe (31P-109 Ag) equipped with actively shielded *Z*-axis gradient coil (303*K*). Typical high-power 90°-pulse widths for proton observation were 10.5 μs and 11 μs for ^{13}C. Proton NMR spectra were recorded with a spectral width of 20 ppm, 65,536 complex data points, 30-degree excitation pulse, each with a 1-s delay time and an acquisition time of 3.18 s. The residual solvent peak was assigned as the reference peak for proton NMR. Carbon-13 NMR spectra were recorded using a spectral width of 240 ppm, 65,536 data points, 30-degree excitation pulse, with a 0.5-s recycle delay, an acquisition time of 1.0486 s with low power WALTZ-16 proton composite pulse decoupling (CPD) with power levels corresponding to a proton 90° r.f. pulse width of 68 μs. TMS was defined as 0 ppm for ^{13}C NMR. Spectra were processed with a standard exponential weighting function of 0.3 Hz (1H) or 3 Hz (13C) line broadening prior to Fourier transformation.

2.4. Immunomodulating activity

2.4.1. Cell culture

RAW264.7 murine macrophages were purchased from The European Collection of Authenticated Cell Cultures (ECACC) (Sigma-Aldrich, Australia, #85062803) and maintained in a clean culture of Dulbecco's modified eagle medium (DMEM, #LTS10566016) with GLUTAMAX with the addition of 0.5 M HEPES buffer (HEPES, #83264) (Gibco, Thermo Fisher scientific, Australia) and 10% foetal bovine serum (FBS) (Bovogen, Interpath Services, Australia, #SFBS-FR). Cells were cultured in T75 flasks at 37 °C in an atmosphere of 5% CO_2 with 100% humidity until reaching 80–90% confluence before passage with cell scraper to dislodge cells. RAW264.7 cells were regularly screened for mycoplasma.

2.4.2. Cell viability assay

Toxicity of 2 to 2000 μg mL^{-1} of ulvan fractions was assessed over 48 h. Cells were seeded into a 96-well plate at a density of 3×10^5 cells/well in DMEM supplemented with FBS, HEPES, 100 U penicillin/100 μg mL^{-1} streptomycin (pen/strep) (Gibco, Thermo Fisher scientific, Australia, #LTS15140148), and allowed to adhere for 16 h. Ulvan (dissolved in DMEM containing HEPES and pen/strep) was added through a media change in concentrations from 2 to 2000 μg mL^{-1}. The cells were then incubated for 6, 24 or 48 h. Following incubation, PrestoBlue™ reagent (Invitrogen, Thermofisher scientific, Australia) was added to the wells to 10% v/v. The cells were incubated for a further 60 min before fluorescence was measured (excitation, 544 nm; emission 620 nm) on a BMG POLARstar Omega microplate reader. The relative fluorescence units (RFU) were used to calculate macrophage viability by: viability % = $RFU_t/RFU_c \times 100$, where RFU_t and RFU_c are the intensity of test and control groups, respectively. Ulvan concentrations were log_{10}-transformed, fitted using a variable slope four-parameter equation with the top value constrained to 100% using a least squares (ordinary) fit model in GraphPad Prism (v. 8.1.0).

2.4.3. Lipopolysaccharide (LPS) stimulation assay

The immunomodulating effect of ulvan fractions was assessed in lipopolysaccharide (LPS)-stimulated RAW264.7 cells by measuring the concentrations of secreted cytokines (IL-1β, IL-6, IL-10, IL-12, and TNFα) and PGE_2 in the cell culture supernatant by enzyme-linked immunosorbent assay (ELISA) (Fig. 1). RAW264.7 cells were seeded into 24-well plates at a density of 1×10^5 cells/well in 1000 μL of DMEM supplemented with FBS, HEPES, and pen/strep; cells were allowed to adhere for 16 h. Ulvan fractions (dissolved in DMEM supplemented with FBS, HEPES, pen/strep, and absent phenol red) in concentrations of 1, 10 or 100 μg mL^{-1} were added through a media change. It was determined during optimisation that FBS is required for the successful release of cytokines by LPS-stimulated RAW264.7 cells (Supp. 1). 1 μg mL^{-1} dexamethasone (Sigma-Aldrich, Australia, #D4902) served as a positive control; wells without the addition of ulvan served as negative controls.

Cells were pre-treated with ulvan or dexamethasone for 2 h before LPS from *Escherichia coli* (0111:B4; Sigma-Aldrich, Australia, #L4391) was added to a final concentration of 1 μg mL^{-1}. There were an equal number of wells across all treatments that did not receive LPS-stimulation to act as internal controls. Cells were incubated for 46 h (48 h was necessary for secretion of IL-1β – see Supp. 3B), after which the supernatant was collected and stored at 4 °C. The concentration of cytokines in the cell culture supernatant was analysed using respective ELISA kits within 6 h of separation from cells by following the manufacturer's instructions (Abcam, UK: ab208348, 1:10 dilution; ab197742, 1:2 dilution; ab46103, 1:2 dilution; ab222503, 1:50 dilution; ab136949, 1:1 dilution; ab236717, 1:2 dilution). The optical density (OD) or relative fluorescence units (RFU) for each of the cytokine assays was read on a BMG POLARstar Omega microplate reader at the wavelength recommended by the assay manufacturer.

2.4.4. Nitric oxide assay

Nitric oxide (NO) secretion was estimated through quantification of its decomposition product, nitrite (NO_2^-) (Fig. 1). The concentration of NO_2^- in cell supernatant was determined using the Griess reagent (modified) (Sigma-Aldrich, Australia, #G4410). Cell supernatant collected as outlined in Section 2.4.3 was mixed with equal volumes of Griess reagent (modified). The absorbance was read at 540 nm after 15 min on a BMG POLARstar Omega microplate reader. Concentration of nitrite in cell supernatant was calculated from 0 to 100 μM sodium nitrite standards.

2.5. Data & statistical analysis

Cytokine concentrations were calculated by using either 4-parameter logistic regressions or linear regressions derived from the assay standards. The fit with the highest r^2 value was used. Recorded sample OD values less than three standard deviations of the mean ELISA assay blank OD value were considered to have a concentration of zero. In the rare occurrence that a treatment OD was outside the standard range of the 4-parameter fit, linear regression was used to estimate a corresponding concentration. Prior to statistical analysis, cytokine, PGE_2, and NO_2^- concentrations were normalised to a percent of the respective ulvan-free control for each plate.

The effects of ulvan M_w and concentration on RAW264.7 cells were analysed with two-factor permutational analysis of variance (PERMANOVA) [29]. Molecular weight and ulvan concentration were treated as fixed factors. Cytotoxicity of ulvan on RAW264.7 cells was analysed by a three-factor PERMANOVA with ulvan M_w, ulvan concentration, and exposure time as fixed factors. All analyses were performed in Primer v6 (Primer-E Ltd., UK) using Euclidian distance similarity and 9999 unrestricted permutations of the raw data. *a posteriori* pair–wise comparisons were used to determine the contribution of factors to significant results. Monte Carlo P-values were used in pair-wise comparisons with <100 unique permutations [29].

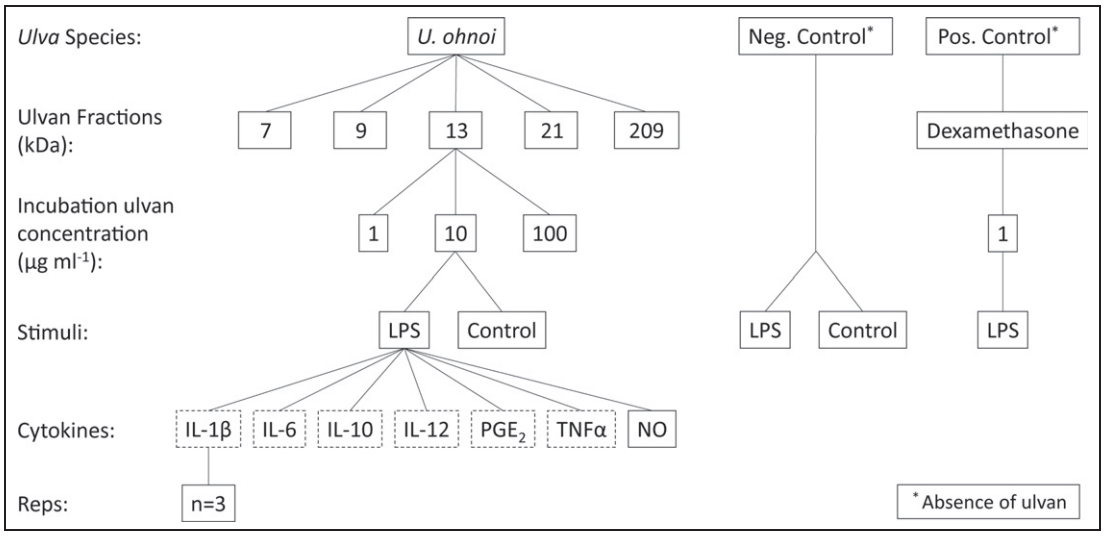

Fig. 1. Experimental design of lipopolysaccharide (LPS) stimulation assay. "Cytokines" collectively refers to cytokines and other immunological markers such as prostaglandin E2 (PGE_2) and nitric oxide (NO). Cytokines with dashed borders were quantified by ELISA; NO was quantified through the Griess test.

3. Results

3.1. Chemical characterisation

3.1.1. Elemental analysis

Ulvan elemental composition, ash, sulfate ester and protein contents are presented in Table 2. The ratio for C, H, O, N, and S are similar between samples, with significantly lower contents of N (and protein) in the chromatographed samples compared to the crude extract (data not shown). Variations in the content of ash account for the absolute content of C, H, O, N, and S. Sulfate content was the same for the native, unhydrolysed sample (U209) and for samples hydrolysed for up to 2 h (U21, U13), reducing after 5 to 7 h of hydrolysis (U9), and higher in crude ulvan (data not shown) and the permeate sample (U7).

3.1.2. Molecular weight

Native ulvan (U209) had a weight average molecular weight (M_w) of 209 kDa (Table 3). Both the weight average molecular weight (M_w) and dispersity of the hydrolysed ulvans decreased with increasing time of hydrolysis (Table 3, Supp. 2).

3.1.3. Constituent sugar composition

The total sugar content of the ulvan fractions ranged from 367 to 486 μg mg^{-1} of sample (Table 4). Native ulvan had the highest total sugar content (486 μg mg^{-1} sample) with the three partially hydrolysed ulvans having similar total sugar contents (453–478 μg mg^{-1} sample). U7 had the lowest total sugar content (367 μg mg^{-1} sample).

The ulvan fractions contained 48.8–54.7 mol% rhamnose, 32.5–35.9 mol% glucuronic acid, 4.5–7.3 mol% iduronic acid, and 3.3–5.6 mol% xylose (Table 5). Smaller amounts of other sugars including fucose, arabinose, galactose, glucose, and mannose were also present in all fractions. U9 had the highest content of rhamnose (54.7 mol %), with the lowest content of xylose (3.3 mol%), glucuronic acid (32.5 mol%), iduronic acid (4.5 mol%), in addition to the highest content of fucose, arabinose, galactose, glucose, and mannose.

3.1.4. NMR spectroscopy

Both ^{13}C and ^{1}H NMR spectra recorded were consistent with data reported for ulvan polysaccharides [9,30–37]. Spectra from native and partially hydrolysed ulvan samples were recorded in D_2O (Fig. 2 and Fig. 3).

The ^{13}C NMR displayed signals characteristic of those reported [37] for anomeric resonances assigned to glucuronic acid (104 ppm) and rhamnose (100 ppm) (Fig. 2). The relative intensity of these resonances was consistent with ulvan predominantly containing the named disaccharide, A_{3s} [-4-GlcA-1,4-Rha(3S)-1-] [38]. Further evidence for this assignment is the uronic acid carboxyl resonance at δ 176 ppm and the rhamnose methyl peak at δ 17 ppm [34]. Intense signals for rhamnose C5, C2, and C3/C4 from A_{3s} are also observed resonating at 68, 69, and 78 ppm, respectively. A strong signal recorded at 74 ppm is consistent with the C3/C2 of glucuronic acid in A_{3s}, with the remaining uronic acid detected at 76 ppm (C5) and 79 ppm (C4) [9,34]. The minor peak at ~71 ppm, readily identified in the U13 spectra, is consistent with overlapping C2/C5 resonances that can be assigned to iduronic acid, indicating the presence of another known ulvan disaccharide, B_{3s} [-4-IdoA-1,4-Rha(3S)-1-] [34,38].

Proton NMR data supports the ^{13}C assignments outlined above (Fig. 3). A strong ^{1}H resonance at δ 1.3 ppm may be attributed to the protons of the rhamnose methyl group (C6). The ^{1}H NMR peaks at 3.3 ppm and 3.7 ppm are consistent with H2 and H3/H4 of glucuronic acid, respectively [9,34]. Proton resonances at 3.8–3.9 ppm are likely a combination of a H4 peak from rhamnose and H5 peak of glucuronic acid [9,34]; these peaks are more highly resolved and separated in the U13 and U7 spectra. The major peak at 4.2 ppm is consistent with the

Table 2
Elemental analysis of native and hydrolysed ulvan. Average %w/w (±S.D., where applicable). Protein content calculated from % N.

Sample ID	%C	%H	%O	%N	%S	%Ash	%Sulfate	%Protein[1]
U209 (native)	25.9	4.8	42.1	0.1	5.5	21.7	16.4 ± 0.5	0.5
U21	26.7	4.8	41.3	0.1	5.7	21.5	16.3 ± 0.7	0.5
U13	26.2	4.9	42.7	0.1	5.4	20.8	16.3 ± 0.6	0.5
U9	29.7	5.0	43.9	0.3	5.9	15.1	13.7 ± 3.8	1.7
U7	26.5	4.2	35.4	0.1	6.3	27.5	22.4 ± 1.7	0.5

[1] Based on % N × 5.

Table 3
The duration of hydrolysis applied to native ulvan, resulting weight average molecular weight (M_w) and dispersity (Đ).

Sample ID	Hydrolysis time (h)	M_w (kDa)	Dispersity (Đ)
U209 (native)	0	208.9	2.2
U21	1	21.3	1.7
U13	2	13.4	1.4
U9	5 + 7	8.9	1.4
U7	Permeate	6.8	1.3

Table 4
Constituent sugar composition and total sugar content (μg mg^{-1} sample) of purified, native ulvan, partially hydrolysed fractions and the permeate.

Sample ID	Sugars (μg mg^{-1} sample)[a]									
	Rha	Xyl	GlcA	IdoA	Fuc	Ara	Gal	Glc	Man	Total
U209 (native)	218.6	22.5	194.0	38.7	0.5	0.2	10.3	1.2	tr.	486.1
U21	223.2	21.9	183.6	36.5	0.5	0.2	10.1	1.5	0.5	478.1
U13	213.1	18.4	176.7	31.7	0.6	0.2	9.9	1.6	0.4	452.6
U9	233.4	12.7	167.1	22.9	2.1	0.6	14.8	4.3	1.7	459.5
U7	178.3	15.1	137.0	29.8	0.1	0.2	4.7	0.7	1.1	367.0

Sugars <0.1 μg mg^{-1} are considered trace (tr.)
[a] Values are the averages of duplicate analyses.

data reported for the H2 of rhamnose, and H5 is recorded resonating at 4.1 ppm [9,34].

3.2. Immunomodulating activity

3.2.1. Ulvan cytotoxicity

All ulvan fractions showed no toxicity on RAW264.7 cells at concentrations below 100 μg mL^{-1} over 48 h (Fig. 4). The cytotoxic effect of U9, U13, U21, and U209 increased with time for concentrations >100 μg mL^{-1}, while the lowest M_w ulvan, U7, showed no cytotoxicity at any concentration up to 48 h (Fig. 4A, B, C). This deviation in cytotoxicity with ulvan M_w, ulvan concentration and exposure time produced a significant three-way interaction (pseudo-$F_{88,360} = 13.15$ $P < 0.01$).

After 6 h, >100 μg mL^{-1} of ulvan induced cell proliferation, with up to 33% increase in cell viability induced by 2000 μg mL^{-1} of U209 (Fig. 4A). After 24 h, all ulvan fractions decreased cell viability at higher concentrations, except for U7. The lowest 24 h viability observed was 75% by 500 μg mL^{-1} of U21 and U209 ulvan (Fig. 4B). With the exception of U7, the reduction in cell viability by ulvan became pronounced ≥100 μg mL^{-1} (Fig. 4C). 500 μg mL^{-1} of ulvan was sufficient to reduce cell viability to 70% for U9 and to 50% for larger M_w ulvans (U12, U21, and U209); these reduced viabilities respectively remained at 70% and 50% up to the highest concentration of ulvan tested (2000 μg mL^{-1}). The dose-dependent increase in cytotoxic effect of high concentration (100–500 μg mL^{-1}) ulvan through time was also confirmed during pilot assays (Supp. 4). The presence of 1 μg mL^{-1} LPS had low toxicity to RAW264.7 cell (85% viable at 24 h) (Supp. 5), therefore this concentration was selected for further experiments.

3.2.2. Effect of ulvan in modulating inflammatory response

3.2.2.1. Inflammatory cytokines. High concentration of the two highest M_w fractions consistently resulted in the greatest levels of IL-1β, IL-6, IL-10 and IL-12 from RAW264.7 cells (Fig. 5A–D). For IL-10, each concentration of U21 and U209 (1, 10, and 100 μg mL^{-1}) produced significantly higher levels of IL-10 compared to ulvan-absent controls (pseudo-$F_{13,42} = 4.28$, $P < 0.001$), while the lower M_w fractions resulted in no change or a reduction in levels of IL-10 (Fig. 5A).

Table 5
Constituent sugar composition (normalised mol%) of purified, native ulvan, partially hydrolysed fractions and the permeate.

Sample ID	Sugars (normalised mol%)[a]								
	Rha	Xyl	GlcA	IdoA	Fuc	Ara	Gal	Glc	Man
U209 (native)	48.8	5.6	35.9	7.2	0.1	0.1	2.1	0.2	tr.
U21	50.5	5.5	34.5	6.9	0.1	tr.	2.1	0.3	0.1
U13	51.0	4.9	35.1	6.3	0.1	0.1	2.1	0.3	0.1
U9	54.7	3.3	32.5	4.5	0.5	0.1	3.1	0.9	0.4
U7	52.5	4.9	33.5	7.3	tr.	0.1	1.2	0.2	0.3

Sugars <0.1 mol% are considered trace (tr.)
[a] Values are the averages of duplicate analyses.

High M_w ulvan fractions at high concentrations increased the secretion of IL-1β, IL-6, and IL-12 above that of ulvan-absent controls. The level of IL-1β was increased by 44 and 32% in treatments with 100 μg mL^{-1} of U13 and U209, respectively (Fig. 5B) (pseudo-$F_{13,46} = 15.52$, $P < 0.001$). Additionally, 100 μg mL^{-1} of U209 also increased the level of IL-6 by 7% - the only treatment to significantly increase the level of IL-6 above the ulvan-absent control (Fig. 5C) (pseudo-$F_{13,46} = 12.88$, $P < 0.001$). As with IL-6, significantly more IL-12 was produced in treatments with 100 μg mL^{-1} of U13 and U21 (pseudo-$F_{13,46} = 7.95$, $P < 0.001$). However, lower concentrations of high M_w ulvan also increased IL-12 levels (Fig. 5D).

Low concentrations of ulvan, often combined with low molecular weights, resulted in the lowest levels of cytokine production. For example, IL-10 was reduced by 59 and 55% from 1 μg mL^{-1} of U7 and U9, respectively (Fig. 5A) (pseudo-$F_{13,42} = 4.28$, $P < 0.001$). Levels of IL-6 were also reduced by low concentrations: by 10–15% for U13, U21, and U209 (pseudo-$F_{13,46} = 12.88$, $P < 0.001$) (Fig. 5C). Contrary to IL-6 and IL-10, the lowest level of IL-1β (13% lower than the ulvan-absent control) was at a high concentration (100 μg mL^{-1}) of low M_w ulvan (U7) (Fig. 5B) (pseudo-$F_{13,46} = 15.52$, $P < 0.001$).

Dexamethasone (1 μg mL^{-1}) significantly reduced the level of IL-1β, IL-6, and IL-12 to a greater extent than any ulvan treatment (Fig. 5B–D). Conversely, dexamethasone significantly increased IL-10 level by 40% (Fig. 5A). These effects of dexamethasone are consistent with the literature [39,40]. Basal expression (cytokine levels in the absence of LPS) of IL-1β, IL-6, and IL-12 were, on average, 98%, 99%, and 98% lower than LPS-treated cells, respectively. Further, basal IL-10 levels were 35% lower, on average, in the absence of LPS compared to LPS treated cells and showed no effect of M_w or concentration.

TNFα was released in concentrations far exceeding that recorded during optimisation trials (Supp. 3). The levels of TNFα for all LPS treatments in the LPS stimulation assay were above the OD detection limit for the microplate reader, resulting in unusuable data. No basal TNFα levels were recorded.

3.2.2.2. PGE_2 and NO_2^-. The levels of PGE_2 were consistently reduced when ulvan was applied to RAW264.7 cells stimulated by LPS; further reductions occurred at higher concentrations of ulvan (Fig. 6A). A dose-dependent reduction in PGE_2 occurred when averaged across ulvan molecular weights (pseudo-$F_{3,45} = 8.21$, $P < 0.001$), culminating with 100 μg mL^{-1} of U9, U21, and U209 inducing reductions of 24, 29, and 39%, respectively. The proportional reduction in PGE_2 induced by 100 μg mL^{-1} of U209 (39%) was very close to the 42% reduction induced by 1 μg mL^{-1} of dexamethasone. In contrast, lower concentrations of ulvan resulted in reduced concentrations of nitrite (NO_2^-), on average (Fig. 6B). 1 and 10 μg mL^{-1} of ulvan resulted in significantly lower nitrite levels compared to either ulvan-absent controls or 100 μg mL^{-1} of ulvan (pseudo-$F_{3,46} = 7.18$, $P < 0.001$). There was no significant difference between 100 μg mL^{-1} of ulvan and the ulvan-absent controls.

Dexamethasone (1 μg mL^{-1}) significantly reduced secretion of PGE_2, but had no significant effect on nitrite secretion. On average, dexamethasone produced significantly less PGE_2 than 9, 13 and 21 kDa ulvan (pseudo-$F_{5,45} = 3.39$, $P < 0.05$). The nitrite level in the absence of LPS was on average 84% lower than LPS treatments. However, in the absence of LPS the nitrite level was 2–8 times higher from 100 μg mL^{-1} of 9, 13, 21 and 209 kDa ulvan compared to any other respective concentration. No PGE_2 was detected in the absence of LPS.

4. Discussion

Ulvan from *Ulva ohnoi* was depolymerised into fractions of 7, 9, 13, 21, and 209 kDa (named U7, U9, U13, U21, and U209, respectively). These fractions were chemically characterised and their cytotoxic and immunomodulating effect on RAW264.7 murine macrophages

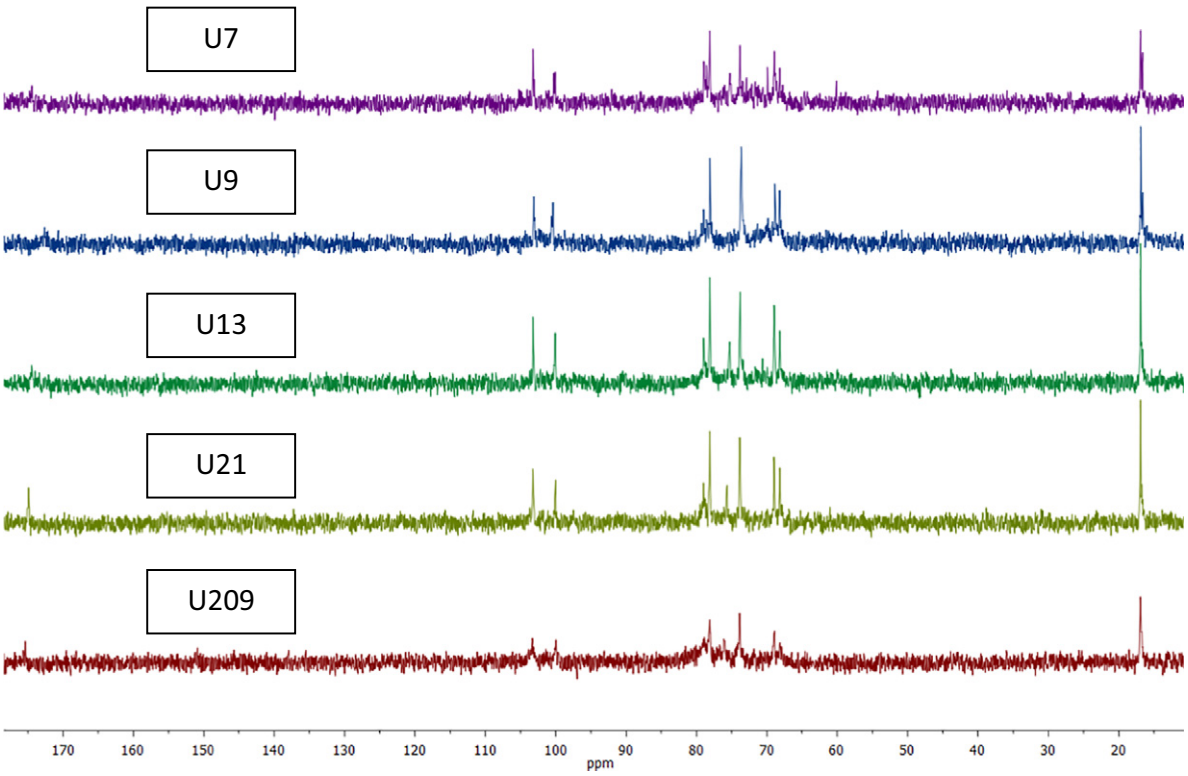

Fig. 2. ^{13}C NMR data of native and hydrolysed ulvan samples (25 mg mL^{-1}, D_2O, 25 °C, 125 MHz).

assessed. No ulvan fraction showed toxicity to RAW264.7 cells at concentrations up to 100 μg mL^{-1} over 48 h. Higher molecular weight fractions of ulvan elicited a greater immunomodulatory response at 100 μg mL^{-1} (by increasing IL-10, IL-1β and IL-6, and decreasing PGE2) compared to lower M_w ulvan fractions. Ulvan extracted from *Ulva ohnoi* is non-cytotoxic and has a mild immunomodulating capacity.

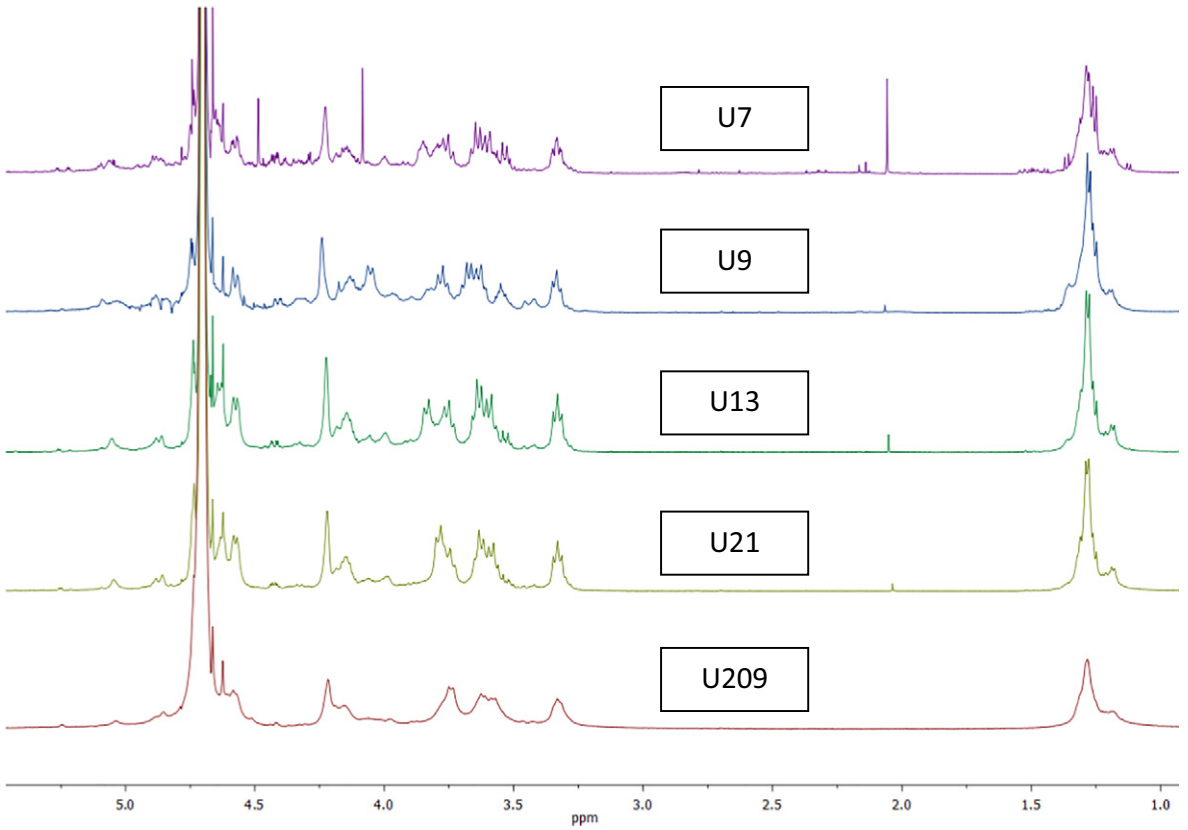

Fig. 3. ^{1}H NMR data of native and hydrolysed ulvan samples (25 mg mL^{-1}, D_2O, 25 °C, 500 MHz, HDO peak not suppressed).

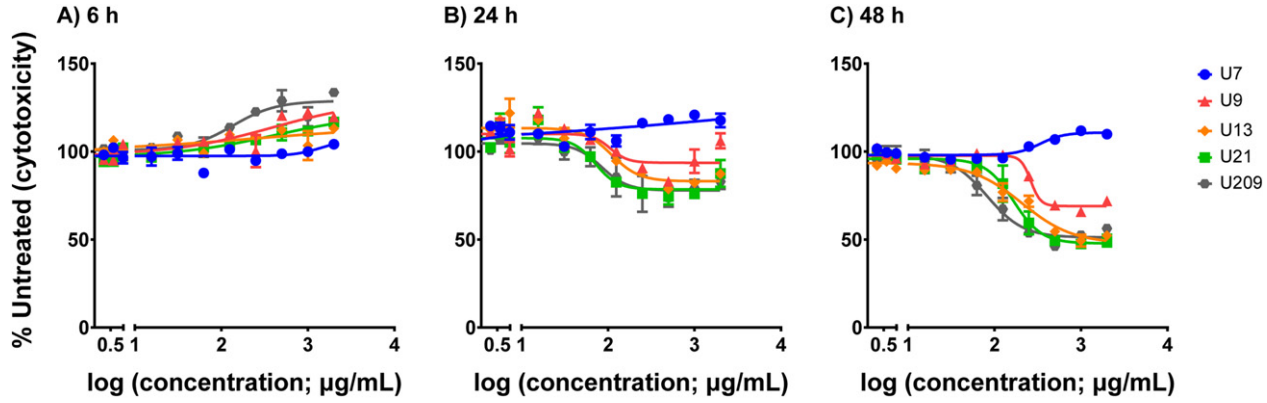

Fig. 4. Effect of ulvan fractions on RAW264.7 cell viability. Cell proliferation was measured after incubation with ulvan of differing molecular weights (U7, U9, U13, U21, and U209) at concentrations of 2–2000 µg mL^{-1} for (A) 6 h, (B) 24 h and (C) 48 h.

4.1. Chemical characterisation

Minor variation in elemental composition, ash, and sulfate ester content confirmed only small changes in the composition between ulvan fractions. The ash content for ulvan fractions ranged from 15 to 21% ash for U9-U209, while U7 had an ash content of 27%. The latter was due to the ulvan being analysed and tested without desalting. The sulfate ester content ranged from 13.7–22.4%, which is consistent with previously analysed ulvan from *U. ohnoi* (7.1 to 15.7%) [30,41] and the median from the ulvan literature (15.5%) [7]. Depolymerisation had no effect on sulfate ester content for ulvan hydrolysed for 0–2 h (U209, U21, and U13), however a lower content was measured for U9 which was hydrolysed for 5–7 h. The apparent low sulfate content detected for U9 could be a result of the high variability in the sulfate measurement. In support of this, the S content for U9-U209 is consistent, reinforcing no change in sulfate ester content in ulvan fractions over the full 0–7 h hydrolysis period.

Chemical depolymerisation of ulvan with H_2O_2 was the chosen method as it has been used to selectively depolymerise related algal sulfated polysaccharides [26,41]. In this study, SEC-MALLS measurements confirmed that H_2O_2 successfully depolymerised native ulvan affording five different molecular weight fractions ranging from 7 to 209 kDa, depending on the duration of treatment. ^{1}H and ^{13}C NMR spectra of the fractions were both dominated by resonances consistent with ulvan samples that were rich in the disaccharide A_{3s} [-4-GlcA-1,4-Rha(3S)-1-]. The extent to which the spectra from the native and hydrolysed ulvan variants overlap in both ^{1}H and ^{13}C NMR indicate that the only major chemical modification observed was depolymerisation at the anomeric centre. However, further chemical characterisation of these fractions detected minor differences in composition; in particular, small variations in the amount of labile constituent sugars were detected.

Constituent sugar analysis confirmed that the native, sulfated polysaccharide extracted here from *U. ohnoi* and its hydrolysed products

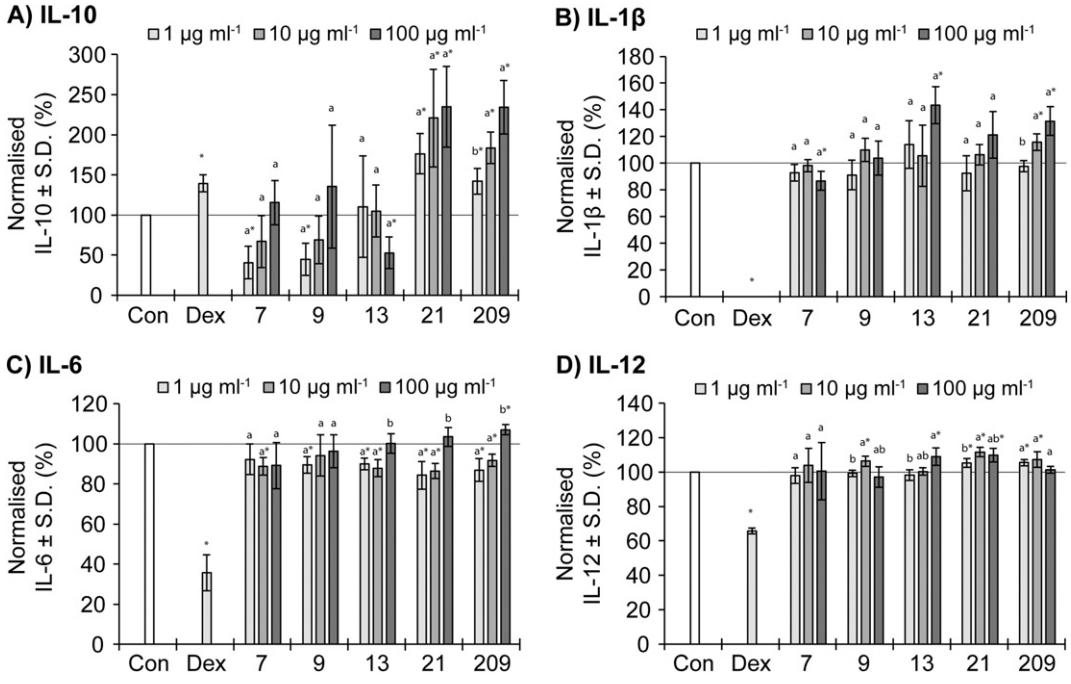

Fig. 5. Percent normalised concentrations of interleukins (IL) (A) IL-10, (B) IL-1β, (C) IL-6, and (D) IL-12 (±S.D., n = 3) measured in RAW264.7 cell supernatant following exposure to ulvan of differing molecular weights (7, 9, 13, 21, 209 kDa) at 1, 10 and 100 µg mL^{-1} in the presence of 1 µg mL^{-1} LPS. 1 µg mL^{-1} Dexamethasone (Dex) used as a positive control. Control (Con) contained 1 µg mL^{-1} LPS in the absence of ulvan or dexamethasone. Superscript letters (a, b) indicate significant difference between concentrations within a molecular weight fraction; Asterisk (*) indicates significant difference from control.

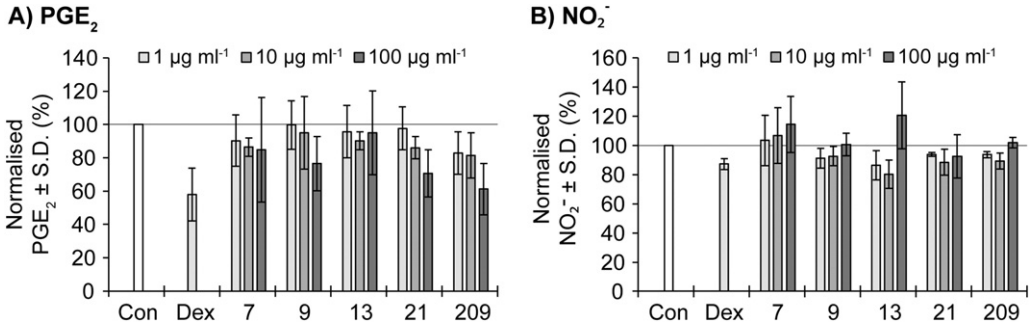

Fig. 6. Percent normalised concentration of (A) prostaglandin E2 (PGE_2) and (B) nitrite (NO_2^-) (±S.D., n = 3) measured in RAW264.7 cell supernatant following exposure to ulvan of differing molecular weights (7, 9, 13, 21, 209 kDa) at 1, 10 and 100 μg mL^{-1} in the presence of 1 μg mL^{-1} LPS. Nitrite measured with Griess reagent using $NaNO_2$ (0–100 μM) as standard. 1 μg mL^{-1} Dexamethasone (Dex) used as a positive control. Control (Con) contained 1 μg mL^{-1} LPS in the absence of ulvan or dexamethasone. Statistical analysis not possible due to lack of interaction between ulvan concentration and M_w.

were consistent with the broader literature definition of ulvan [7,30]. Furthermore, a high content of both rhamnose and glucuronic acid confirmed the NMR finding that ulvan from *U. ohnoi* is rich in the disaccharide A_{3s} [-4-GlcA-1,4-Rha(3S)-1-]. However, sugar constituent analysis also detected incremental degradation of xylose and iduronic acid, with concomitant increase in the content of rhamnose, as the duration of hydrolysis was increased. This is consistent with previous reports that xylose and iduronic acid are the most labile of the ulvan constituents [42]. The small changes in rhamnose and glucuronic acid (the two major constituent sugars) indicate only minor variations in constituent sugars between fractions, particularly relative to the differences in molecular weight.

Thus, in terms of cytotoxicity and immunomodulation, the composition of ulvan is considered to be equal between hydrolysed fractions. Differences in the bioactivity of these fractions are therefore interpreted on the basis of concentration and molecular weight.

4.2. Cytotoxicity and immunomodulating activity

All ulvan M_w fractions showed no cytotoxic effects on RAW264.7 cells after 48 h of exposure with <100 μg mL^{-1}. Furthermore, for all fractions, cell viability was only reduced to 50% with a 5- to 20-fold increase in ulvan concentration. These results are consistent with previous cytotoxic assessments of ulvan-containing extracts on murine macrophages and cancer cells [13–17]. In the present study, the lowest M_w ulvan (U7) displayed no cytotoxicity over 48 h (up to and including the highest concentration tested, 2000 μg mL^{-1}) and instead increased cell proliferation by 10%; by 18% from the same concentration over 24 h. A similar 20% increase in cell proliferation is also observed for the lowest molecular weight ulvan fraction (29 kDa) from *U. intestinalis* [16]. The low cytotoxicity of all ulvan M_w fractions allowed the immunomodulation capacity of ulvan to be assessed on RAW264.7 cells with an upper concentration limit of 100 μg mL^{-1}. Additionally, as neither 100 μg mL^{-1} ulvan nor 1 μg mL^{-1} LPS are significantly toxic to RAW264.7 cells, differences in cytokine release are interpreted on the basis ulvan concentration and molecular weight.

Immunomodulatory effects have been reported for ulvan samples from *U. armoricana* [43,44], *U. clathrata* [45], *U. fasciata* [46,47], *U. intestinalis* [12,14,16,48], *U. lactuca* [19,49,50], *U. linza* [51], *U. ohnoi* [41], *U. australis* [15,21], *U. prolifera* [17,20], and *U. rigida* [18,52]. In this study, ulvan from *U. ohnoi* had immunomodulatory effects on RAW264.7 cells that were both concentration dependent and influenced by M_w.

Increased levels of IL-10 and IL-1β, and to a lesser extent IL-6 and IL-12, were observed at high concentrations of the high molecular weight fractions (U21 and U209), a response that is consistent with the literature [13–15,18,48]. IL-10, a predominately anti-inflammatory cytokine that inhibits cytokine production and down-regulates inflammation, had the largest magnitude of change, increasing by 135% from the treatment of U209 at 100 μg mL^{-1}, suggesting an anti-inflammatory effect of ulvan. PGE_2 is a principal protagonist in the inflammatory response due to its hyperalgesic, pyrogenic, and potent vasodilator capacities [53]. The dose-dependent reduction of PGE_2 levels below the control (up to 40% reduction with 100 μg mL^{-1} of U209) also suggests an anti-inflammatory response. The reduction in PGE_2 is particularly notable as in a similar study on RAW264.7 cells, ulvan from *U. rigida* stimulated a dose-dependent increase in PGE_2 levels from <10 pg mL^{-1} up to ~270 pg mL^{-1} (a 2700% increase) in treatments of 0 to 100 μg mL^{-1} of polysaccharide [18]. However, increased levels of the pro-inflammatory cytokines IL-1β, IL-6, and IL-12 detected in the current study contradict the anti-inflammatory response of IL-10 and PGE_2. The precise immunomodulatory nature of ulvan *in vivo* cannot be conclusively predicted from this study alone, however, these *in vitro* results support previous findings that ulvan possesses immunomodulating activity [13–16,18].

Although the mechanism of interaction between ulvan and LPS on RAW264.7 cells cannot be determined from the current data, molecular weight evidently plays a role in the cytotoxicity and immunomodulating capacity of ulvan. However, the apparent effect of ulvan M_w in the literature is contradictory, with some studies finding comparatively enhanced immunomodulating activity from higher M_w ulvan [13,15,41] while others found comparatively higher activity with lower M_w ulvan [12,14,16]. Due to the wide range of M_w reported, and methods of determining immunomodulating activity, it is difficult to directly compare these studies. It is important to note that while these studies did use similar dose concentrations of ulvan, they did not study the effect of ulvan M_w in isolation; variation in the proportions of constituent sugars, proteins, and sulfate esters could affect immunomodulating activity. In the current study, we did assess the effect of ulvan M_w in isolation, having shown that all the ulvan fractions had similar chemical compositions. The fact that the native (*i.e.* unhydrolysed) ulvan had the greatest immunomodulating effect is ideal for future studies and potential future commercial applications as minimal processing reduces production costs and time.

The mild immunomodulating activity and enhanced cell proliferation effects of ulvan, coupled with the capacity of mammalian skin fibroblast and keratinocyte cells to directly recognise and respond to rhamnose [5,54,55], suggest that ulvan may be applicable for topical treatments (*e.g.* wound dressing). However, while the *in vitro* results presented here are encouraging, *in vivo* assessment of ulvan will provide a more complete picture of ulvan immunomodulatory effects, and related anti-cancer [33,56], antioxidant [22,51], and antihyperlipidemic [57–59] effects.

5. Conclusion

We assessed the influence of the molecular weight of ulvan, extracted from *Ulva ohnoi*, on cytotoxicity and immunomodulatory activity. Ulvan M_w and concentration interacted to influence the cytotoxicity in RAW264.7 murine macrophages, and level of signalling molecules released. Depolymerisation appears to make the ulvan more benign; the unhydrolysed 'native' ulvan was the most bio-active, particularly at

high concentrations. However, low molecular weight ulvan enhanced cell proliferation with little to no detectable immunomodulation activity. To summarise, due to the promotion of cell viability, low cytotoxicity at low concentrations, a moderate immunomodulating activity, and innate capacity to interact with human skin immunomodulatory cells, ulvan has multiple characteristics ideal for applications targeting the treatment of dermal diseases and wounds.

CRediT authorship contribution statement

Joel T. Kidgell: Conceptualization, Investigation, Data curation, Formal analysis, Visualization, Writing - original draft, Writing - review & editing. **Christopher R.K. Glasson:** Conceptualization, Methodology, Writing - original draft, Writing - review & editing. **Marie Magnusson:** Conceptualization, Resources, Writing - review & editing. **George Vamvounis:** Investigation. **Ian M. Sims:** Investigation, Writing - original draft. **Susan M. Carnachan:** Investigation, Writing - original draft. **Simon F.R. Hinkley:** Investigation, Writing - original draft. **Andreas L. Lopata:** Conceptualization, Resources, Supervision. **Rocky de Nys:** Conceptualization, Resources, Supervision, Writing - review & editing. **Aya C. Taki:** Conceptualization, Methodology, Writing - original draft, Writing - review & editing.

Declaration of competing interest

The authors declare there are no conflicts of interest, and no informed consent, human or animal right are applicable to this research.

Acknowledgments

The authors would like to thank Maria Martinez, Joel Lenton, Kunal Pratap, and Sandip Kamath for their assistance in the laboratory and acknowledge James Cook University for providing a PhD scholarship to Joel Kidgell. This research is funded, in part, by Pacific Biotechnologies, Australia (previously MBD Industries Ltd.) as part of the Research and Development program for the Integrated Production of Macroalgae. This work was also financially supported by an Innovation Connections grant (No. ICG000136) from the Australian Government.

Appendix A. Supplementary data

Supplementary data to this article can be found online at https://doi.org/10.1016/j.ijbiomac.2020.02.071.

References

[1] I. Wijesekara, R. Pangestuti, S.K. Kim, Biological activities and potential health benefits of sulfated polysaccharides derived from marine algae, Carbohydr. Polym. 84 (1) (2011) 14–21.
[2] T.N. Wight, M.G. Kinsella, E.E. Qwarnstrom, The role of proteoglycans in cell adhesion, migration and proliferation, Curr. Opin. Cell Biol. 4 (5) (1992) 793–801.
[3] C. Blondin, E. Fischer, C. Boisson-Vidal, M.D. Kazatchkine, J. Jozefonvicz, Inhibition of complement activation by natural sulfated polysaccharides (fucans) from brown seaweed, Mol. Immunol. 31 (4) (1994) 247–253.
[4] Z. Shriver, I. Capila, G. Venkataraman, R. Sasisekharan, Heparin and heparan sulfate: analyzing structure and microheterogeneity, Handb. Exp. Pharmacol. 207 (2012) 159–176.
[5] E. Andrès, J. Molinari, G. Péterszegi, B. Mariko, E. Ruszova, V. Velebny, G. Faury, L. Robert, Pharmacological properties of rhamnose-rich polysaccharides, potential interest in age-dependent alterations of connectives tissues, Pathol. Biol. 54 (7) (2006) 420–425.
[6] M. Lahaye, B. Ray, Cell-wall polysaccharides from the marine green alga *Ulva* "*rigida*" (Ulvales, Chlorophyta) - NMR analysis of ulvan oligosaccharides, Carbohydr. Res. 283 (1996) 161–173.
[7] J.T. Kidgell, M. Magnusson, R. de Nys, C.R.K. Glasson, Ulvan: a systematic review of extraction, composition and function, Algal Res. 39 (2019), 101422.
[8] G. Jiao, G. Yu, J. Zhang, H.S. Ewart, Chemical structures and bioactivities of sulfated polysaccharides from marine algae, Marine Drugs 9 (2) (2011) 196–233.
[9] M. Lahaye, A. Robic, Structure and functional properties of ulvan, a polysaccharide from green seaweeds, Biomacromolecules 8 (6) (2007) 1765–1774.
[10] A. Alves, R.A. Sousa, R.L. Reis, A practical perspective on ulvan extracted from green algae, J. Appl. Phycol. 25 (2) (2013) 407–424.
[11] J.M. Leiro, M. Varela, M.C. Piazzon, J.A. Arranz, M. Noya, J. Lamas, The anti-inflammatory activity of the polyphenol resveratrol may be partially related to inhibition of tumour necrosis factor-α (TNF-α) pre-mRNA splicing, Mol. Immunol. 47 (5) (2010) 1114–1120.
[12] L.L. Jiao, P. Jiang, L.P. Zhang, M.J. Wu, Antitumor and immunomodulating activity of polysaccharides from *Enteromorpha intestinalis*, Biotechnol. Bioprocess Eng. 15 (3) (2010) 421–428.
[13] J.-K. Kim, M.L. Cho, S. Karnjanapratum, I.-S. Shin, S.G. You, In vitro and in vivo immunomodulatory activity of sulfated polysaccharides from *Enteromorpha prolifera*, Int. J. Biol. Macromol. 49 (5) (2011) 1051–1058.
[14] N. Peasura, N. Laohakunjit, O. Kerdchoechuen, P. Vongsawasdi, L.K. Chao, Assessment of biochemical and immunomodulatory activity of sulphated polysaccharides from *Ulva intestinalis*, Int. J. Biol. Macromol. 91 (2016) 269–277.
[15] M. Tabarsa, J.H. Han, C.Y. Kim, S.G. You, Molecular characteristics and immunomodulatory activities of water-soluble sulfated polysaccharides from *Ulva pertusa*, J. Med. Food 15 (2) (2012) 135–144.
[16] M. Tabarsa, S. You, E.H. Dabaghian, U. Surayot, Water-soluble polysaccharides from *Ulva intestinalis*: molecular properties, structural elucidation and immunomodulatory activities, J. Food Drug Anal. 26 (2) (2018) 599–608.
[17] M. Cho, C. Yang, S.M. Kim, S. You, Molecular characterization and biological activities of water-soluble sulfated polysaccharides from *Enteromorpha prolifera*, Food Sci. Biotechnol. 19 (2) (2010) 525–533.
[18] J.M. Leiro, R. Castro, J.A. Arranz, J. Lamas, Immunomodulating activities of acidic sulphated polysaccharides obtained from the seaweed *Ulva rigida* C. Agardh, Int. Immunopharmacol. 7 (7) (2007) 879–888.
[19] G.E.F. Abd-Ellatef, O.M. Ahmed, E.S. Abdel-Reheim, A.H.Z. Abdel-Hamid, *Ulva lactuca* polysaccharides prevent Wistar rat breast carcinogenesis through the augmentation of apoptosis, enhancement of antioxidant defense system, and suppression of inflammation, Breast Cancer: Targets and Therapy 9 (2017) 67–83.
[20] J. Wei, S. Wang, G. Liu, D. Pei, Y. Liu, Y. Liu, D. Di, Polysaccharides from *Enteromorpha prolifera* enhance the immunity of normal mice, Int. J. Biol. Macromol. 64 (2014) 1–5.
[21] L. Song, X. Chen, X. Liu, F. Zhang, L. Hu, Y. Yue, K. Li, P. Li, Characterization and comparison of the structural features, immune-modulatory and anti-avian influenza virus activities conferred by three algal sulfated polysaccharides, Marine Drugs 14 (1) (2016).
[22] H. Qi, T. Zhao, Q. Zhang, Z. Li, Z. Zhao, R. Xing, Antioxidant activity of different molecular weight sulfated polysaccharides from *Ulva pertusa* Kjellm (Chlorophyta), J. Appl. Phycol. 17 (6) (2005) 527–534.
[23] C.R.K. Glasson, L. Donnet, A. Angell, M.J. Vucko, A.J. Lorbeer, G. Vamvounis, R. de Nys, M. Magnusson, Multiple response optimisation of the aqueous extraction of high quality ulvan from Ulva ohnoi, Bioresource Technology Reports 7 (2019).
[24] R.J. Lawton, L. Mata, R. de Nys, N.A. Paul, Algal bioremediation of waste waters from land-based aquaculture using Ulva: selecting target species and strains, PLoS One 8 (10) (2013), e77344.
[25] B.M. van den Hoogen, P.R. van Weeren, M. Lopes-Cardozo, L.M. van Golde, A. Barneveld, C.H. van de Lest, A microtiter plate assay for the determination of uronic acids, Anal. Biochem. 257 (2) (1998) 107–111.
[26] H.-J. Zhang, W.-J. Mao, F. Fang, H.-Y. Li, H.-H. Sun, Y. Chen, X.-H. Qi, Chemical characteristics and anticoagulant activities of a sulfated polysaccharide and its fragments from *Monostroma latissimum*, Carbohydr. Polym. 71 (3) (2008) 428–434.
[27] A.R. Angell, L. Mata, R. de Nys, N.A. Paul, The protein content of seaweeds: a universal nitrogen-to-protein conversion factor of five, J. Appl. Phycol. 28 (1) (2016) 511–524.
[28] A. Robic, J.F. Sassi, M. Lahaye, Impact of stabilization treatments of the green seaweed *Ulva rotundata* (Chlorophyta) on the extraction yield, the physico-chemical and rheological properties of ulvan, Carbohydr. Polym. 74 (3) (2008) 344–352.
[29] M.J. Anderson, R.N. Gorley, R.K. Clarke, Permanova+ for Primer: Guide to Software and Statistical Methods, 2008.
[30] C.R.K. Glasson, I.M. Sims, S.M. Carnachan, R. de Nys, M. Magnusson, A cascading biorefinery process targeting sulfated polysaccharides (ulvan) from *Ulva ohnoi*, Algal Res. 27 (2017) 383–391.
[31] C. Costa, A. Alves, P.R. Pinto, R.A. Sousa, E.A. Borges da Silva, R.L. Reis, A.E. Rodrigues, Characterization of ulvan extracts to assess the effect of different steps in the extraction procedure, Carbohydr. Polym. 88 (2) (2012) 537–546.
[32] M. Lahaye, J.-L. Gomez-Pinchetti, M.J. del Rio, G. Garcia-Reina, Natural decoloration, composition and increase in dietary fibre content of an edible marine algae, *Ulva rigida* (Chlorophyta), grown under different nitrogen conditions, J. Sci. Food Agric. 68 (1) (1995) 99–104.
[33] T.T.T. Thanh, T.M.T. Quach, T.N. Nguyen, D.V. Luong, M.L. Bui, T.T.V. Tran, Structure and cytotoxic activity of ulvan extracted from green seaweed *Ulva lactuca*, Int. J. Biol. Macromol. 93 ((2016) 695–702.
[34] T.T.V. Tran, B.T. Huy, H.B. Truong, M.L. Bui, T.T.T. Thanh, D.Q. Dao, Structure analysis of sulfated polysaccharides extracted from green seaweed Ulva lactuca: experimental and density functional theory studies, Chem. Mon. (2018) 1–9.
[35] A. Robic, C. Rondeau-Mouro, J.F. Sassi, Y. Lerat, M. Lahaye, Structure and interactions of ulvan in the cell wall of the marine green algae *Ulva rotundata* (Ulvales, Chlorophyceae), Carbohydr. Polym. 77 (2) (2009) 206–216.
[36] A. Robic, C. Gaillard, J.F. Sassi, Y. Lerat, M. Lahaye, Ultrastructure of ulvan: a polysaccharide from green seaweeds, Biopolymers 91 (8) (2009) 652–664.
[37] M. Tabarsa, S.J. Lee, S. You, Structural analysis of immunostimulating sulfated polysaccharides from Ulva pertusa, Carbohydr. Res. 361 (2012) 141–147.
[38] M. Lahaye, F. Inizan, J. Vigouroux, NMR analysis of the chemical structure of ulvan and of ulvan-boron complex formation, Carbohydr. Polym. 36 (2–3) (1998) 239–249.
[39] K. Gewert, U. Svensson, K. Andersson, E. Holst, R. Sundler, Dexamethasone differentially regulates cytokine transcription and translation in macrophages responding to bacteria or okadaic acid, Cell. Signal. 11 (9) (1999) 665–670.

[40] D. Franchimont, H. Martens, M.T. Hagelstein, E. Louis, W. Dewe, G.P. Chrousos, J. Belaiche, V. Geenen, Tumor necrosis factor alpha decreases, and interleukin-10 increases, the sensitivity of human monocytes to dexamethasone: potential regulation of the glucocorticoid receptor, J. Clin. Endocrinol. Metab. 84 (8) (1999) 2834–2839.
[41] C. Fernández-Díaz, O. Coste, E.J. Malta, Polymer chitosan nanoparticles functionalized with *Ulva ohnoi* extracts boost in vitro ulvan immunostimulant effect in Solea senegalensis macrophages, Algal Res. 26 (2017) 135–142.
[42] B. Quemener, M. Lahaye, C. Bobin-Dubigeon, Sugar determination in ulvans by a chemical-enzymatic method coupled to high performance anion exchange chromatography, J. Appl. Phycol. 9 (2) (1997) 179–188.
[43] M. Berri, C. Slugocki, M. Olivier, E. Helloin, I. Jacques, H. Salmon, H. Demais, M. Le Goff, P.N. Collen, Marine-sulfated polysaccharides extract of *Ulva armoricana* green algae exhibits an antimicrobial activity and stimulates cytokine expression by intestinal epithelial cells, J. Appl. Phycol. 28 (5) (2016) 2999–3008.
[44] M. Berri, M. Olivier, S. Holbert, J. Dupont, H. Demais, M. Le Goff, P.N. Collen, Ulvan from *Ulva armoricana* (Chlorophyta) activates the PI3K/Akt signalling pathway via TLR4 to induce intestinal cytokine production, Algal Res. 28 (2017) 39–47.
[45] P. del Rocío Quezada-Rodríguez, E.J. Fajer-Ávila, The dietary effect of ulvan from *Ulva clathrata* on hematological-immunological parameters and growth of tilapia (*Oreochromis niloticus*), J. Appl. Phycol. 29 (1) (2017) 423–431.
[46] M.Z. Rizk, H.F. Aly, A.A. Matloub, G.I. Fouad, The anti-hypercholesterolemic effect of ulvan polysaccharide extracted from the green alga *Ulva fasciata* on aged hypercholesterolemic rats, Asian Journal of Pharmaceutical and Clinical Research 9 (3) (2016).
[47] M.Z. Rizk, M. El-Sherbiny, I.H. Borai, M.K. Ezz, H.F. Aly, A.A. Matloub, A.E.R. Farrag, G.I. Fouad, Sulphated polysaccharides (SPS) from the green alga *ulva fasciata* extract modulates liver and kidney function in high fat diet-induced hypercholesterolemic rats, Int J Pharm Pharm Sci 8 (6) (2016) 43–55.
[48] L.L. Jiao, X. Li, T.B. Li, P. Jiang, L.X. Zhang, M.J. Wu, L.P. Zhang, Characterization and anti-tumor activity of alkali-extracted polysaccharide from *Enteromorpha intestinalis*, Int. Immunopharmacol. 9 (3) (2009) 324–329.
[49] Y.H. Chiu, Y.L. Chan, T.L. Li, C.J. Wu, Inhibition of japanese encephalitis virus infection by the sulfated polysaccharide extracts from *Ulva lactuca*, Mar. Biotechnol. 14 (4) (2012) 468–478.
[50] I.W.F. de Araújo, J.A.G. Rodrigues, A.L.G. Quinderé, J.D.F.T. Silva, G.D.F. Maciel, N.A. Ribeiro, E. de Sousa Oliveira Vanderlei, K.A. Ribeiro, H.V. Chaves, K.M.A. Pereira, M.M. Bezerra, N.M.B. Benevides, Analgesic and anti-inflammatory actions on bradykinin route of a polysulfated fraction from alga *Ulva lactuca*, Int. J. Biol. Macromol. 92 (2016) 820–830.
[51] Z. Zhang, X. Wang, M. Zhao, S. Yu, H. Qi, The immunological and antioxidant activities of polysaccharides extracted from *Enteromorpha linza*, Int. J. Biol. Macromol. 57 (2013) 45–49.
[52] R. Castro, I. Zarra, J. Lamas, Water-soluble seaweed extracts modulate the respiratory burst activity of turbot phagocytes, Aquaculture 229 (1) (2004) 67–78.
[53] H.P. Rang, J.M. Ritter, R.J. Flower, G. Henderson, Rang & Dale's Pharmacology, Churchill Livingstone, 2016.
[54] D. Cerdan, C. Grillon, M. Monsigny, G. Redziniak, C. Kieda, Human keratinocyte membrane lectins: characterization and modulation of their expression by cytokines, Biol. Cell. 73 (1) (1991) 35–42.
[55] B. Condaminet, G. Redziniak, M. Monsigny, C. Kieda, Ultraviolet rays induced expression of lectins on the surface of a squamous carcinoma keratinocyte cell line, Exp. Cell Res. 232 (2) (1997) 216–224.
[56] U.K. Hussein, H.M. Mahmoud, A.G. Farrag, A. Bishayee, Chemoprevention of diethylnitrosamine-initiated and phenobarbital-promoted hepatocarcinogenesis in rats by sulfated polysaccharides and aqueous extract of *Ulva lactuca*, Integrative Cancer Therapies 14 (6) (2015) 525–545.
[57] S.A. Kumar, M. Magnusson, L.C. Ward, N.A. Paul, L. Brown, Seaweed supplements normalise metabolic, cardiovascular and liver responses in high-carbohydrate, high-fat fed rats, Mar Drugs 13 (2) (2015) 788–805.
[58] Y. Pengzhan, L. Ning, L. Xiguang, Z. Gefei, Z. Quanbin, L. Pengcheng, Antihyperlipidemic effects of different molecular weight sulfated polysaccharides from *Ulva pertusa* (Chlorophyta), Pharmacol. Res. 48 (6) (2003) 543–549.
[59] W. Li, K. Wang, N. Jiang, X. Liu, M. Wan, X. Chang, D. Liu, H. Qi, S. Liu, Antioxidant and antihyperlipidemic activities of purified polysaccharides from *Ulva pertusa*, J. Appl. Phycol. 30 (4) (2018) 2619–2627.